# Schafer

# *Space Based Laser Support*

**February 1999**

Prepared by:

*Schafer Corporation*
*1901 N. Fort Myer Drive*
*Suite 800*
*Arlington, VA 22209*
*703/558-7900*

**Task Report - Naval Research Laboratory**
**Contract N00014-97-D-2014/001**

19990409 081

**This Document Contains Missing**
**Page/s That Are Unavailable In**
**The Original Document**

3.1.1-4 Photo.

# TABLE OF CONTENTS

# TABLE OF CONTENTS (CONTINUED)

## LIST OF APPENDICES

# LIST OF APPENDICES (CONTINUED)

# LIST OF TABLES

# LIST OF FIGURES

# LIST OF FIGURES (CONTINUED)

# 1.0 INTRODUCTION

This report summarizes efforts in support of the BMDO/AFSMC Space Based Laser program. The first major work section was in support of BMDO. Another series of major efforts supported AF SMC. These efforts were broad in nature and reflect changing priorities during the report period. Section titles reflect the majority of work performed, but there is overlap among sections. The final major section was in support of the NSWC ABCS program, within the BMDO SBL technology base. Schafer was supported by subcontractors, including Photon Research Associates (PRA) and the University of Illinois Urbana-Champagne (UIUC). Subcontractor reports will be referred to appropriately in the body of the main report, but will be included in their entirety as Appendices. Some of the work reported is classified and will be contained in a separate classified Appendix. A small proprietary Appendix is also included under separate cover. Finally, some of the efforts were competition sensitive to either of the contractor teams during the SBL Concept Definition Studies (CDS). Due to the restrictions imposed by the competition, these efforts are reported only in summary.

# 2.0 BMDO SUPPORT

## Summary of Activities

BMDO activities included analyses in support of Bifocal, electric lasers, and SBL effectiveness and technology surveys and briefing preparation for deployable optics, electric lasers, lethality, LASSOS, etc. Continuing activities such as the Year 2000 software issue continued at a low level. Planning support was provided. A briefing was prepared summarizing the history of relays, analyses on cost, and low power usage of relays for Lt. Col. Mark Nelson to present at the LASSOS meeting in Albuquerque, NM.

The development and coordination of draft interim Security Classification Guidance for the SBLRD program continued. An update of the Test and Experiment Activity Summary data sheets has begun.

ASAT analysis and briefing support were provided to the customer. The analysis looked at the differing capabilities of alternate levels of deployment of the SBL and the SBLRD. The analysis was summarized in a briefing that was given to Lt. Col. Jay Airis of Air Force Space Command. Additional study may be required by the customer to support a more detailed briefing. A briefing describing tasks funded by BMDO to support launch vehicle component technologies was assembled and delivered to the customer. The briefing is also under review and will be given shortly.

A number of issues have been raised concerning the effects of various non-modeled conditions on the performance of the SBL. The first set of these includes effects which can cause asymmetries in the coverage of the SBL constellation. These asymmetries are important when calculating geometric filling and numbers of platforms. The issues include: 1) sun/moon within ~5 degrees of target as viewed from SBL (exact value will be input), 2) specular reflection off target, earth, clouds, 3) sun/moonlit background, 4) SBL moving in/out of the terminator. These effects have not been included in ISAAC analysis in recent years. The necessary portions of the ISAAC code are being reviewed for accuracy and will be updated as needed during the analysis. Inclusion of advanced missile types is also needed to perform SBL sizing analyses. ETA-T, a missile trajectory generating program (FORTRAN, part of the ISAAC suite), is being modified to provide for the inclusion of revised missile types. In the process, the code is being updated and improved in efficiency.

Transition activities to provide information to ANSER (the new BMDO SETA) began. These activities during late July involved meetings with BMDO to discuss transition issues. Many of the technical activities that were in progress will be terminated. Analyses in support of Bifocal are complete. Support for the electric laser technology assessment has been stopped. The assessment of lightweight and deployable optics is being completed (a summary briefing will be prepared, although no further assessment work is planned). Continuing activities such as the Year 2000 software issue will be handled by ANSER.

2

Sample optimization analyses for various SBL constellations vs. various threats were discussed with BMDO. These analyses included roughly 216,000 data points, each data point being a full engagement of the missile threat by the full constellation. The range of parametric analysis included two lethalities, various number of platforms, orbital altitudes, and ring structures. Each engagement is simulated for 216 war start times, to ensure adequate sampling of the temporal changes in coverage. Recent improvements in code automation have significantly reduced the amount of analyst time required for such analyses, making such detailed analysis practical for essentially any parametric variation.

Support was provided to an ancillary mission meeting at another government facility. TMD performance estimates from older sources were compiled and given to BMDO. Further work on supporting analyses for lethality issues was performed.

Meetings at BMDO in support of the SBL Test facility site selection process were attended. Briefing material on SBL life cycle cost for the POM submission process in response to requests from BMDO/TOD were prepared.

A briefing on lightweight and deployable large optics was developed for BMDO. The effort surveyed the various large optics contractors to determine the state of the art, and reviewed the competition sensitive CDS study reports to determine what was currently proposed for both the operational SBL and the RD (or IFX). The effort also developed an initial set of requirements for the proposed beam expander and discussed the issues associated with new technology development. A parametric study of system requirements as a function of output power, wavelength, and diameter was completed, showing that beam control and resulting beam expander requirements grow exceptionally difficult as larger, shorter wavelength systems are proposed

The BMDO/SMC technology meeting was supported. All of the key SBL technologies were reviewed, including a large deployable optics presentation prepared by Schafer and Aerospace In preparation for the AFSMC/BMDO technical interchange meeting, a list of program risks was compiled to identify technical areas of interest. The following items are risks identified by a prime or from Schafer risk lists developed and maintained for BMDO (denoted as GG in table below). The items have been grouped by categories and technical points of contact within the SBL community are indicated The people list is not exhaustive.

| Category/Item | Prime or GG List | Person | Comment |
| --- | --- | --- | --- |
| LASER | | | |
| Autonomous Alignment | P/GG | Golnik, Tyson | Critical to all areas |
| Resonator design and fabrication | P/GG | Zajac, Swain | Widely different issues for the two concepts. |
| HYLTE performance and fabrication | P/GG | Graves, Zajac | Needs to be accelerated |

| Category/Item | Prime or GG List | Person | Comment |
|---|---|---|---|
| RSES | P/GG | Zajac, Patton | Ignored for years, these issues will bite us in the weight budget (big time) |
| Coating survivability | P/GG | Skolnik | Longer term issue. We need a separate flight experiment for long duration. |
| Reverse wave suppression | P/GG | Golnik | Still no consensus on whether this is important or not. |
| Uncooled PME | GG | Heckert | Lack of detail in designs in this area continues to be a worry. This hurt us badly in Alpha and could again in the RD. The primes seem to want to ignore it again. |
| Startup transients | GG | Heckert | An issue that may not make it on the list, but is of concern for operational system performance. |
| Ignition | GG | Zajac | Hand waving by TRW has made everyone complacent, but this is still far from over as an issue. |
| GGA regenerative cooling | GG | Heckert | The Alpha design doesn't work, and HYLTE is harder to cool. |
| GGA cavity isolation | GG | Heckert | A potential major issue (preventing laser gas from entering the resonator). |
| Microgravity figure of optics | GG | Golnik | Particularly for annular resonators, we have no experience with microgravity. |
| BEAM CONTROL / BEX | | | |
| Autonomous Alignment | P/GG | Golnik | As above. This should really be a system issue, but the laser and beam control people never seem to be able to work it in combination. |
| Deployable Large Optics | P/GG | Golnik | Major research effort is needed to even show proof of concept. |
| Lightweight Large Optic | P/GG | Skolnik, Golnik | Thermal performance is an issue, as well as the usual fabrication and test issues. |
| Beam control performance (jitter and WFE) | P/GG | Swain, Golnik | We still have not gotten anywhere near the performance that people quote in their error budgets. |

4

| Category/Item | Prime or GG List | Person | Comment |
|---|---|---|---|
| PM phasing | P/GG | Skolnik | Never done. May require auxiliary equipment not in weight budgets. Could drive system performance, yet ignored in scalability arguments. |
| Aperture Sharing Element | P/GG | Lieto, Skolnik | Despite contractor claims, this is a major concern and should be demonstrated at high power within the next year if we are to move out in a shared aperture design. |
| BEX structural control | P/GG | Skolnik, Wells | Another major issue with the potential to dominate system performance. Ever since LODE, we have had trouble figuring out how to even simulate the major issues, and have never tested them. |
| Off-axis pointing and calibration | P/GG | Golnik, Thomas | A much harder task than is generally known, and a problem waiting for a solution in all of the current designs. |
| Beam director gimbal and isolator | P/GG | Skolnik, Wells | If we try to do this in the RD, the structural issues become even more complex. |
| Uncooled PME | GG | Golnik | Although not as complicated a problem as in the resonator, diffractive effects have been poorly understood in ALI. |
| OPE deployable sun shade | P | ? | This is a new concept, if adopted, and has serious structural implications. |
| Coating survivability | P/GG | Skolnik, Lieto | For the PM, in particular. As we go to larger PM sizes and more open architectures, this gets worse. |
| Microgravity figure of optics | GG | Skolnik | What happens to the DM and PM? |
| HOE fabrication scaling | GG | Skolnik | Dependent on segment size, but even at LAMP sizes, we have lost much of the capability. |
| UDM reliability | GG | Skolnik, Swain, Demers | We have never flown anything like it. |
| PM coating | GG | Skolnik, Lieto | Depending on size of segments, we may not have the capability. |

| Category/Item | Prime or GG List | Person | Comment |
|---|---|---|---|
| Telescope metrology | GG | Jacoby, Golnik | The part of ALI that has yet to be demonstrated, this is another "forgotten" area that is critical to performance. |
| IR focal plane coolers | GG | Skolnik, Demers | As with the trackers, jitter/vibration becomes more of an issue as budgets get tighter. |
| Beam walk control | GG | Swain, Skolnik | Hard to sense, hard to correct, may cause beam control problems due to misregistration. |
| **ATP** | | | |
| Fire Control | P | Wolfe, Gurski, Nelson | Sequencing of events, handovers, functionality, performance. |
| Autonomous Alignment | P/GG | Golnik | The forgotten part of the system. The ATP is getting more complex all the time, and alignment becomes more of an issue. |
| Illuminator | P/GG | Wolfe, Gurski, Nelson | Reliability, power, vibration, all still concerns. |
| Active tracking | P/GG | Wolfe, Gurski, Nelson | How well does it work? Can the error budgets be achieved? |
| Space vehicle pointing | P/GG | Wolfe, Gurski, Nelson | How accurate must it point, and what are the dynamics? |
| Boresight | GG | Wolfe, Gurski, Nelson | Shared aperture doesn't magically solve this, although the primes claim it does. |
| Target acquisition | GG | Wolfe, Gurski, Nelson | Different targets, backgrounds, etc. Models have been simplistic to date. |
| HF stray light rejection in IR focal planes | GG | Wolfe, Gurski, Nelson | Relevant whether we have shared or separate aperture. |
| IR focal plane coolers | GG | Wolfe, Gurski, Nelson | As jitter budgets get smaller, vibration may become a major issue. |
| **INT & TEST** | | | |
| Ground test feasibility | GG | Loomis, Mail | High power beam control remains an issue. Also, no one has come up with a feasible way of testing the tracker. |

| Category/Item | Prime or GG List | Person | Comment |
|---|---|---|---|
| PM testing gravity effects | GG | Loomis, Mail | This can be a major issue with the potential for large lightweight deployable optics. |
| **LAUNCH** | | | |
| Payload integration | GG | Loomis | Possibly the most complex ever attempted. |
| Booster availability | GG | Zajac | Heavy-lift (~45,000 lbs.) will definitely be required |
| **OTHER** | | | |
| Human in the loop response | P | Vieceli | More for the operational system than the RD. |
| System weight | GG | Loomis, Golnik | We have somehow managed to squeeze much more brightness out of much less weight. Also, weight margins are low or negative for the RD. |
| Software reliability | GG | Mail | Particularly testing of the software. |
| Lethality | GG | Harada, Golnik, Skolnik | Many issues, including that the AFRL numbers given to the contractors were unreasonably high. |
| Flight computer hardware and software | P/GG | Mail | We have made the assumption that the necessary processors will be available, which may not be true. |
| Spacecraft charging | GG | Silvaggio | The laser community hasn't worried much about this. I don't know if the spacecraft people still consider it an issue, |
| Spacecraft thermal management | GG | Loomis | This is a major concern and neither prime seems to be paying much attention. |
| Solar array torques | GG | Wells | Usually ignored until too late (as in Hubble) |
| Eye safety | | Golnik | If we talk about moving to 1.3 um devices, we need to understand what happens to the 80% of the power that doesn't hit the target. |
| Cost | | Mail | Impacts many of the technical issues. |
| RD performance | | Harada, Vieceli, Golnik | The RD performance envelope is shrinking and we need to understand why. |

There are additional issues which apply to the operational system. Other issues were discussed in the SBL technology meeting (7-8 October 1998). The technology interface meeting provided the desired "frank and open" interchange, with the primary exception being the lack of any defense of their choices by the hardware contractors. The key technology areas had the following primary issues (brief answers to the issues are indicated parenthetically with more detail to follow). Issues which remain competition sensitive have been omitted.

Laser Device: Should the uncooled resonator be completed and installed on Alpha? (Consensus seemed to be that this was the best baseline plan) Should the HYLTE nozzle become the baseline technology for all future activities? (Jury is still out depending on the HYLTE tests and on a fair comparison between best operating conditions, which will be different for the two nozzles) Are there other technologies which should be considered? (Yes, but funding has always been the issue and will remain so) What is the current state of Alpha and HYWND technology and how does it compare to HYLTE? (Slightly confused because of the available free fluorine issue, but probably less than the 30% advantage for HYLTE and perhaps equal!) Why have the hardware contractors made the choices they did and what are the associated issues? (Choices seem to be driven by issues outside of the laser device, but no consensus was reached in the absence of the contractors.)

Beam Control: {Most critical issue deleted because of competition} How good does the beam control system need to be? (Much better than the current state of the art, and perhaps improbably so if we go to very large apertures and shorter wavelengths) What is the next step with ALI? (Complete the planned low power testing, make the system as good as it can reasonably be, and then confirm with high power tests) What should be done with the SBS program? (Complete it or drop it, but don't keep it barely alive.) Alignment and calibration, although the largest single contributor to the error budgets, was not a significant topic of discussion at the meeting,

Large Optics How large and lightweight an optic can reasonably be built? (as yet unknown, but growing exceptionally difficult after 8 meters and perhaps impossibly difficult after 12 meters Weights of under 50 kg/m$^2$ for the primary mirror (only!!) grow increasingly difficult, with 20 kg/m$^2$ unlikely to be achievable ) What is the state of the art of deployable optics? (None have been built, and the technology developed for radio-wave telescopes is questionable for optical telescopes. A basic technology program is absolutely essential before committing to a baseline depending on the technology.) Have the contractors or the government considered all of the related issues of thermal control, sunshades, launch loads, HOEs, dynamic phasing, coatings, microgravity effects, etc. in sufficient detail to provide confidence in a technology path? (No!!) Does the current weight scaling story make sense? (No. The weights appear to be arbitrarily constrained to fit the launch vehicle and not reasonably arrived at by a balanced consideration of technologies )

Test and Evaluation Have the contractors paid adequate attention to testing issues and their influence on the design? (No. Two examples: a beam control approach which cannot be

8

tested until on orbit, and large, lightweight, deployable optics, which require exceptional new facilities and which still may not be testable on the ground).

Spacecraft and launch  What are the launch loads and have they been considered in the concepts for other subsystems?  (The loads seem to be estimated to first order, but have not been much of a consideration in any of the concepts)  Is the weight budget reasonable?  (Attempts to make the RD/IFX fit on a medium-lift vehicle , or the operational system fit on an EELV-heavy seem to lack any reasonable basis).

# 3.0 SMC SUPPORT

## Summary of Activities

Most of the recent efforts have concentrated on the evaluation of the contractor's BVRs and preparation of resulting assessment documentation. Details of the process are competition sensitive and have been provided directly to SMC. Supported SMC/ADE SE, Laser -Beam Control IPTs at numerous internal reviews regarding RFP preparation, evaluation criteria, Technical Issues, weekly staff meetings. Supported SCG Working Group for Laser/Beam Control IPT and Test IPT Leads. Attended TRW and LMA interchange meetings. Participated in BVR evaluations.

A technical evaluation of the proposed contractor CDS follow-on tasks was provided.

Work continued on an assessment of SBL operational system performance against a reference NMD threat. The analysis concentrated on optimization of the SBL constellation, with brightness, number of platforms, number of rings, inclination, and error budgets being free parameters. Initial conclusions are being developed into a presentation which will be given to SMC in October. Cost scaling is also being developed as part of an overall plan to determine the functional form of the optimization trade space, and to determine the optimum SBL configuration and its variation as a function of the level of technology available to the future designers of an operational constellation.

Support to ALI/ALO activities continued, including a series of data review sessions. Recent results show that the ALI beam control system has nearly met its goals, and will meet its goals with continued improvements in calibration and alignment planned during upcoming low power testing.

Efforts to understand the SBL NMD architecture and costs continued. It has been many years since the SBL cost and performance models were integrated, and past models to do so are now archaic. Many recent scaling analyses have assumed that technology is available to provide arbitrary performance without any direct cost penalty. While clearly inadequate, such an approach has been necessary because of the complexity of both the cost and performance models. A new approach to synthesize a useful combined approach has been started. There are no results as yet.

Efforts in support of the ALI/ALO data review meetings continued .This effort is a detailed attempt to understand both laser device and beam control performance in recent high power tests. Initial data show that the system performance is approaching the original program goals.

Technology planning efforts in support of SMC continued. Efforts included review of large optics and vibrational disturbances. A variety of cost and schedule summaries have been reviewed.

Support was provided to the ALO data review, held 19 November at Aerospace. TRW presented a summary of data from many lasing tests in a comprehensive review of Alpha lasing performance. Efforts under this task included several Schafer personnel working with TRW to understand the significance of the test data. There have been a total of 19 lasing tests, with 5 in 1998.

TRW reached several conclusions. The laser has performed reliably, and output quality has improved, primarily due to reductions in water coolant flow rates and the corresponding reductions in optical disturbances. The performance of the facility vacuum system has been degrading over time as the equipment ages. Several problems have been found in support equipment. Measurement of laser cavity pressures indicates that lasing performance is not yet affected, but some repairs are required. Alpha laser power has decreased over the last 7 tests. The decrease has not been monotonic. TRW suspects coating degradation and misalignment. The Alpha coatings were designed for a three year lifetime when they were fabricated (c. 1986). The Alpha flow rates were recently discovered to be different from what TRW thought. Due to a calibration error, significantly higher $NF_3$ was flowing, resulting in an oxidizer-rich mixture. The effective reaction temperature was cooler than predicted, and the power lower. The output beam has a large static phase structure, which is correctable but not ideal. This performance is consistent with the Alpha design philosophy, which relied on the beam control system to correct low spatial frequency errors. Some of the aberrations do not correspond with predictions, and further investigation is needed to understand the sources of the errors. There is some suggestion of an aging-related problem with the annular molybdenum heat exchangers (no longer a baseline for future systems). The phase error seems to grow for the first 0.5 seconds of lasing. TRW has theorized that thermal distortion is the root cause, but if that were the case, the distortion could be expected to continue to grow.

The Alpha beam jitter has been reduced to below the ALI goal, with most of the reduction coming from coolant flow reductions. The next logical step in improved performance is to fabricate and install an uncooled resonator. TRW has recommended an ALO program with four phases maintenance and upgrades to the facility, improved and additional diagnostics, low power testing to assess optical performance, and high power tests to confirm flow conditions and alignment. Such a program seems to be a logical next step.

A variety of ALI and ALO contractual issues were addressed in support of SMC. Review of proposed technical activities continued, with comparison to past similar program efforts. Provided support to BMDO (Bob Frey) and SMC (Capt. Norris) in the negotiations of the ALI POOO95 contract modifications. This included development of a spreadsheet that evaluated the labor hours, material and subcontracts proposed by LMA as well as attending the fact-finding and negotiations meetings and telecons. Attended an ALO proposal briefing by TRW to SMC. This effort would be the follow-on activity to the current ALO effort. Participated in a government evaluation session. Participated in the ALI weekly schedule telecons. Monitored the progress of the test activity and provided advise to SMC as appropriate. Participated in ALO Monthly Business meeting by Telecon. Participated in ALI Monthly Business meeting. At a meeting set up by Julie Norris, met with her (and Angela Spaith) replacements (Manny Casipit, Todd Weist, Marc Herrera to discuss continued support requirements. At the request of Manny Casipit,

11

attended the visit of Gen. Tattini to CTS. Participated in the briefing the SBL hardware and facilities. Monitored activity at CTS for the ALI BCT low power test series. Attended a meeting hosted by SMC (Capt. Todd Wiest) to review a proposal presented by TRW on follow-on ALO activity for FY 99. TRW presented a series of logic diagrams that resulted from the analysis of the last several high power tests and presented a number of facility upgrades, optical system upgrades, low and high power tests. A Technical Evaluation of this proposal has been requested by SMC to aid them in determining the correct program to put on contract. Reviewed and provided comments to Capt. Manny Casipit with regard to the GFE list submitted by LMA for the follow-on ALI activity for FY 99. Reviewed and provided comments to Capt. Manny Casipit with regard to the ALI DCO 337. Developed a draft integrated test schedule for the ALO and ALI activity for FY 99 at CTS. Submitted to SMC for there use. Provided Capt. Julie Norris a high power test history of the uncooled optics for inclusion in the ROMA report. Attended a meeting hosted by SMC on the capability of Lincoln Labs to support SMC in a variety of areas. Attended the monthly LODTM management meeting at LLNL.

Technical activities under this task included support to continuing ALI/ALO test and planning activities. A briefing was prepared to describe ALI status to the SBL Independent Review Team. Planning meetings continued as part of the effort to understand past test data and develop appropriate recommendations for further testing and data reduction. Test reports for the ALI 317 and 318 series were received and will be reviewed.

## Recent SBL History and Status

During the past two years, the Air force (SMC/ADE) has assumed management responsibility as the executing agent for the SBL program. Through Congressional adds from FY96-FY99, congress is intent on funding a near term (2006-2008) SBL flight demonstration. The current SBL FY99 budget is $167.8M (58.8 BMDO + 35.0 AF + 74.0 Congressional Add), with a promise of additional (2000-2005) BMDO and AF POM funding totaling $140M/yr. The objectives of the Integrated Fight Experiment (IFX) are to 1) validate SBL as a viable option for missile defense by destroying a boosting target from Space and 2) to obtain performance data an integrated high power laser system operation in space including long range precision acquisition, tracking and pointing (ATP) and adjunct mission feasibility. Although the AF and BMDO developed a strategy to pursue a 2008 launch, near term POM funding constraints imposed by OSD extended the program to a launch in 2014. Congressional criticism of this approach prompted increased CSAF involvement and support for a more aggressive schedule (~2012 launch) OSD has approved the more aggressive approach, but the actual launch date remains in a state of flux pending final fiscal and programmatic guidance, and pending agreement between OSD and Congress. To date, a plan acceptable to all stakeholders has failed to materialize.

During FY98, two teams, LMA and TRW/Boeing each performed 6 month, $10M, baseline validations (Concept Definition Studies, CDS) of competitive IFX designs to assess future system needs and "traceable" demonstrations. The "baseline" IFX systems (and several options thereof) that developed from these studies differed drastically from the former BMDO baseline SBL RD design (4M meter monolithic primary mirror and Alpha derived cylindrical HF chemical laser). These new designs were driven by technology "traceability" to a higher

brightness operational system. In turn, the new operational system design was driven by 1) a much harder threat – hence the need for a higher brightness system and 2) the requirement that the operational system be launched on a programmed launch vehicle, i.e. the EELV series. These constraints imposed severe weight and diameter limitations, and thus conflict with the need for higher brightness systems. Hence, the contractors were forced to propose advanced technology solutions (e.g., deployable optics, phase conjugation, etc) in order to simultaneously meet launch and brightness requirements. Traceability thus drove configuration of the IFX, rather than trying to keep the demonstration as simple as possible and to do it as soon as possible. Thus, current IFX designs are somewhat unbalanced and are higher risk. The CDS efforts were extended by a bridge of $5M each to keep both contractor teams going through Jan 99. Each contractor proposed a series of risk reductions, analyses, and design activities to be conducted in the Oct 98– Jan 99 time frame

The technology programs continued in FY98. There were five high power tests at CTS, three ALO (HI907, HL908A, HL908B) and two ALI tests (HL430, HL440). The three ALO tests to characterize the Alpha laser included two rear cone alignment scans to determine power and beam quality sensitivity to rear cone misalignment. The ALI tests involved end-to-end traceable beam control at high power of the outgoing wavefront sensor system, full bandwidth operation of an uncooled fast steering mirror, and the first successful test of the uncooled deformable mirror. The High Altitude Balloon Experiment (HABE) completed integration of the acquisition and tracking payload and initiated passive tracking experiments of scaled rockets. Finally, HYLTE completed a series of tests on a water cooled module, and is fabricating a self cooled module for testing in FY99.

As stated earlier, Congressional expectations call for a laser in space, a lethal demonstration, an integrated ground test with the required facility, and a demonstration in the 2006-2008 time frame. The Congressional actions taken included SBL budget plus-ups of $50M in FY96, 70M in FY97, and 98M in FY98. The POM funding for SBL during those years was a nominal $30M/yr. In addition, the Congress provided impetus to BMDO to increase the SBL budget to $60M/yr and to the Air Force to create a new line at $35M/yr. (More recently, there has been an agreement between BMDO and AF to provide $140M/yr total for SBL.) In FY99, Congress added $74M to the SBL budget.

The FY99 program currently consists of three basic parts: 1) on-going technology development (ALI, ALO HYLTE, HABE, ABCS, Uncooled Resonator, APEX), 2) Architecture and Affordability Studies, and 3) The Integrated Flight Experiment (IFX). The technology programs are really a continuation of BMDO efforts under new or novated Air Force contracts. The Navy and Army, continue to execute ABCS, HYLTE, and APEX under Air Force direction. The Architecture and Affordability Study was initiated this past year as a response to a Dr. Gansler (USDA&T) inquiry about how the IFX fits into an overall plan for acquisition of an operational SBL system. The study is to be used to define a S & T long term investment strategy, as well as to address the multi mission capabilities of each of the defined architectures (i.e. overall system affordability). Two studies will be awarded to the contractor teams at a level of ~ $8M for a 12 month period. Award of Phase I (~$1M) is in early January 99 as a continuation of the CDS contracts; Phase II (~$7M each) as a letter contract to each team in February 99. Phase I (~2

months) consists of interaction with Government study team, researching past studies, developing a Phase II concept analysis plan, and developing a Phase II proposal. Phase I products are system requirements (prioritized missions, performance thresholds, and top level system constrains), architecture evaluation methodology, and mission scenarios. Phase II will be a more detailed study of the necked down architecture possibilities and concludes with a report detailing incremental cost and performance trades for each architecture. The study is headed by a General Officers Steering Panel (GOSP) which is supported by an Action Officers Panel (0-6 level). The GOSP consists of general officers and high ranking civilians from AF organizations, BMDO, JTAMDO, and NSSA. Study leaders are BMDO/TOR and SMC/ADE. Small working groups support the study. They are Mission Definition, Cost, Technology Validation, and Related Efforts (countermeasures, lethality, M&S IPT). A Integration IPT integrates results of these working groups and reports to the study leaders. The study leaders then seek concurrence from the GOSP. The GOSP provides a link to strategic planners, and reviews and approves assumptions, missions, measures of effectiveness, concepts, and final architecture selection.

In parallel with the architecture studies, SMC/ADE has initiated a lethality program which is executed by AFRL/DEPE, and is overseen by an SMC Lethality Working Group. The FY99 funding total is $3.3M including $1.5M for SBL specific targets (composites) and $1.8M for SBL/ABL "synergy". A program plan has been generated by AFRL that will look at both in-house testing and other facilities for $2.7\mu m$ tests (CTS, WSMR).

The IFX status is in a state of flux. During the past year both contractor teams, LMC and TRW/Boeing, developed competitive concepts for an IFX. As stated previously, these designs were driven by launch vehicle constraints and high brightness operational system traceability requirements They both departed considerably from the BMDO SBLRD balanced construct of an Alpha derived laser, and a 4M telescope which was developed by the LMA/TRW team under the Zenith Star Program. The current efforts were conducted in a highly competition sensitive environment in which the government was to select a single contractor to peruse detailed design, fabrication, and testing of the IFX. After pursuing this acquisition strategy for the past year, and after several meetings with high ranking AF, BMDO, and OSD officials, the strategy was recently changed to once again "encourage" the formation of a "Community Team". This team is to be patterned after the NASP Joint Venture (JV) approach which combined five competing contractors under a single JV contract to demonstrate the technology and a design for a subscale single stage to orbit aerospace plane. NASP technology at the time lagged far behind SBL maturity today, and the NASP JV never produced a hardware product. Also, the JV and was directed by a large government program office which had direct communication with each of the 5 participating companies. The award of the IFX JV contract is on hold pending approval by BMDO, AF, OSD, and the Congress.

The following sections of this report discuss technical details of each of the areas the where Schafer Corporation has recent made contributions to the SBL program during the execution of this contract In addition, specific briefings, program plans, review memoranda, and technical papers are presented in the appendices.

14

## 3.1    ALI/ALO/UCR

This task report includes support to both BMDO and SMC for the Alpha LAMP Integration (ALI) program, the Alpha Laser Optimization (ALO) program and the Uncooled Resonator (UCR) program. This report is organized to provide a description of the technical activity on each of the three programs followed by a discussion on the programmatic activity. Since the ALO and ALI programs are very interrelated, Schafer Corp. has been instrumental in developing plans for integrated test activity at CTS. Section 3.1.7 provides a description of the planning activity for 1999 and a schedule of these activities. Schafer Corp. provided technical advice initially to BMDO and continued this support as the contract activity was transferred to SMC.

### 3.1.1    Alpha LAMP Integration (ALI)

**3.1.1.1 Uncooled Deformable Mirror (UDM) Fabrication** – The ALI UDM was fabricated by Xinetics, Inc. under contract to Lockheed Martin Missiles and Space and coated by Lohnstar Optics. The UDM is a single crystal silicon optic similar to the ALI uncooled turning flats; however, the face sheet thickness is a few millimeters whereas the turning flats are two inches thick. Additionally, 241 actuators are mounted to the UDM optic face sheet to provide wave front control. These actuators are epoxied to the face sheet as well as the mounting structure. Very low absorption (VLA) coating performance is very dependent on application temperature. Therefore, temperature control for the various processes is extremely critical to achieve a successful coating while not degrading the actuator bonds joints. Several coating runs were performed with witness samples followed by two different pathfinder mirrors before committing to the actual optic. A number of coating runs was needed to perfect the coating process.

**3.1.1.2 SDA Wave Front Sensor (WFS) Fabrication** – The SDA WFS was fabricated in 1997 and shipped to the Capistrano Test Site (CTS) for integration and checkout prior to the UDM high power test. Initially, an acceptance test was performed on the SDA WFS after arrival at CTS prior to installing on the SDA bench and this acceptance test activity was continued during the installation on the SDA bench in the TCA. A hardware incompatibility was discovered between the SDA WFS centroid processor and the incoming data stream that was traced to a short clock pulse. This problem was corrected by installing new programmable integrated circuits that provided a longer clock pulse.

**3.1.1.3 UDM Integration & Test** – As a result of the Experiment IIB data analysis, a number of hardware improvements were identified. These improvements were addressed and resolved in preparation for the UDM high power test. An algorithm error was discovered in the centroid processor that incorrectly averaged negative values in the centroiding algorithm causing the centroids to "hop" around. This error was corrected which resulted in much smoother centroids. A diagnostic to measure return energy into the Alpha laser was designed, fabricated, installed and calibrated. A low power test series identified as TS-336 was planned as a precursor to the high power test HL 440. Initially, the test plan called for two TS-336 tests to be performed

to establish confidence that the high power test would be successful. Schafer Corp. actively participated in the day – day planning and in the weekly schedule status reviews. Schafer Corp. was an integral part of the decision process as the test anomalies occurred and made recommendations to LMA and SMC for implementation of corrective action.

**3.1.1.4** A number of hardware anomalies occurred which required several test runs of the 336 series. These included the discovery and elimination of data corruption between the Wavefront Jitter Control Processor (WJCP) and the UDM Console. Another anomaly identified was the inability of the UDM electronics to respond to the full bandwidth of the UDM. Changes in these electronics resolved this problem. Cracks were discovered in the OWS X Focal Plane Array (FPA) and resoldering was required. Corrections to the timing pulse between the simulated OWS data and actual data was required. Also, KG-95 Data Encryption Links were required to be installed and checked out to satisfy security requirements.

**3.1.1.5** A plan to reduce the jitter induced by the water coolant flow in the Alpha resonator optics and the Power Management Equipment (PME) was implemented in TS-336. Flow reductions of 60% and 80% were initially planned to determine that these reduced flow rates would significantly reduce the mechanically induced noise to acceptable levels. By reducing the jitter noise, performance models predict significant performance improvement in the ALI Beam Control System without compromising the integrity of the optics and PME coolant circuits.

**3.1.1.6** HL 440 was successfully conducted on 9 June 1998. The UDM performed flawlessly with no damage to the thin face sheet optic. The ALI Beam Control System performed better than prediction and close to the original goals established for the ALI program. The test ran for the planned full duration of 5.0 seconds with 4.5 seconds of closed loop performance. The Alpha near field intensity was well filled and well centered. The reduction in coolant flow reduced the induced jitter and had no adverse affect on the resonator optics performance. Hardware anomalies and schedule conflicts with other test programs occurred which caused several test delays prior to the completion of the test. An optical transmitter problem occurred in the optical link between the WFCP and the UDM that caused a test reschedule. An abort occurred due to an over temperature and under pressure in the Thiokol #3 engine steam generator.

**3.1.1.7** **Beam Control Test (BCT)** – Initially, planning called for the follow on program to ALI to be a demonstration of various autonomous alignment approaches for the SBL Readiness Demonstrator (SBL RD). The ALI Autonomous Alignment program was redefined as a Beam Control Test (BCT). The BCT consisted of a series of low power test that would demonstrate the hardware enhancements identified during the initial ALI Phase I program. These hardware enhancements included: a) remote capability to capture the Low Energy Laser (LEL) beam as it enters the Test Chamber Assembly (TCA), b) replace the far-field camera in the Center of Curvature Figure Sensor (CoCFS), c) provide LAMP figure data to the Master Control Center (MCC), d) remotely position the CoCFS from the MCC, and e) use Holographic Optical Elements (HOE) spots to maintain LAMP segment pointing. The BCT tests were defined in an update to the ALI Test Plan and consisted of the following tests:

**3.1.1.8 TS-317 – Beam Control Alignment Test.** The purpose of TS-317 was to demonstrate enhancement of the alignment capability of the ALI Beam Control Test (BCT) hardware, including the implementation of the following upgrades:

- Far Field Reference Beam (FFRB) improvements
- Alignment Annulus Assembly (AAA) improvements
- Calibration and Alignment Assembly (CAA) visibility improvements
- System Diagnostics Assembly (SDA) Wavefront Sensor (WFS) input to Optical test system (OTS) computers
- SDA Far Field Camera (FFC) inputs to OTS computers

**3.1.1.9 TS-318 – Beam Control Characterization (Ambient) Test.** The purpose of TS-318 was to determine the limits of correctability of both the Fast Steering Mirror (FSM) and the Deformable Mirror (DM). Hardware and software enhancements including an aberration generator, UDM diagnostics, and OWS focal plane array sensitivity equalization were made to the ALI system for TS-318.

**3.1.1.10 TS-319 – Beam Control Characterization (Vacuum) Test.** The purpose of TS-319 was to determine the limits of correctability of both the Fast Steering Mirror (FSM) and the Deformable Mirror (DM) in a vacuum environment in a test configuration similar to TS-318.

**3.1.1.11 TS-337 – Jitter Reduction Characterization.** The purpose of this test series was to identify jitter reduction enhancements and to characterize these reductions. Further reduction of PME and Optics induced jitter was demonstrated during this test series.

**3.1.1.12 TS-338 – High Power Beam Control Simulation at Low Power.** The purpose of this test was to demonstrate all enhancements were operable at low power and demonstrate the Beam Control System will meet performance requirements.

**3.1.1.13 TS-339 – Precision Beam Control Test.** The purpose of this test was to demonstrate performance of the beam control with an absolute measurement of performance. This absolute measurement will utilize the AAA as the reference and measure FSM and DM performance relative to the AAA rather than the OWS.

**3.1.1.14 Resonator Optics Material Assessment (ROMA)** – Work on the ROMA program was primarily focused on bringing the Large Optics Diamond Turning Machine (LODTM) back to an operational status, qualifying at least two vendors for coating the uncooled resonator optics and publishing a final report to document all the prior years technical activity. LODTM was recalibrated and achieved a laser periodic error of less the 0.2 micro inches. An uncorrectable spindle error of less than 2 micro inches was identified. Two vendors (LPO and Star Optics) were on contract to develop competing design approaches and perform VLA coating risk reduction tasks in preparation for a down select of a coating vendor for the resonator optics. This activity was completed and the data provided to TRW to support continued effort on the Uncooled Resonator program discussed in subsequent paragraphs. The ROMA final report was issued by LMA. Due to higher priority business, the ROMA Final Report publication was delayed several months. Schafer personnel reviewed and assessed the final report, provided inputs for additional information and recommended approved to SMC.

### 3.1.2 Alpha Laser Optimization (ALO)

#### 3.1.2.1 High Power Test.

**3.1.2.2 ALO Power Investigation Team.** Schafer Corp. was an integral team member of the ALO Power Investigation Team. As a result of the apparent low power output of the ALI high power tests, this team was formed to review all past test data in conjunction with the current test data to ascertain the potential causes of the low out-coupled power.

**3.1.2.3 HL 907 High Power Test.** HL 907 was conducted on 28 Jan 1998. This test consisted of two flow conditions, and an array of diagnostics to establish the Alpha performance re-baselining. The test ran the planned duration of 6.0 seconds. Flow condition 1 was the Alpha nominal case (reduced NF3 flow) and flow condition 2 was the original Alpha design flow condition. Schafer personnel were an integral part of the test operations actively participating in the Test Readiness Review (TRR) and monitored the progress of the test as it proceeded through the countdown sequence. Schafer personnel provided support to the test director and during the management status reviews. Additionally, Schafer was a member of the test data review team and supported the HL 907 data review.

**3.1.2.4 CTS Facility Maintenance.** Schafer personnel monitored the facility and optics maintenance and upgrades performed by TRW at CTS. Schafer reviewed plans for repair of the Alpha Probe Laser (APL), the Alignment Unit (AU), the precision metrology capability and various diagnostic components. Schafer personnel reviewed plans for installation of an IDA Far Field Camera as a new diagnostic for HL 907.

**3.1.2.5 HL 908.** Schafer personnel actively reviewed the planning for HL 908 and provided recommended changes to the test configuration. HL 908 was a two-configuration test of the rear cone alignment. HL 908A was performed on 23 July 1998 and HL 908B was performed on 30 July 1998. A number of diagnostic changes were made to improve the test data. These included modification of the AU control software to perform the rear cone scan for the test as well as design and integration of a new Total Power Calorimeter (TPC) P(t) sensor. Another sensor was added which provided a through ASM 1 jitter diagnostic measurement.

**3.1.2.6 ALO Data Review.** Schafer personnel participated in an exhaustive review of the test results of the more recent Alpha high power tests. This review focused primarily on the results of ALO HL 905, 906, 907, and 908 as well as the ALI tests HL 410, 420, 430 and 440. The focus of this effort was to address the issue of apparent declining output power, alignment irregularities, incomplete mode filling and other observed test inconsistencies or anomalies. Assessment of the test results as well as a re-evaluation of the predictions of various design models was performed. The anomalies were identified and potential causes were identified and ranked. A plan of action was developed which identified the hardware and facility enhancements required to confirm the cause of and / or correct each anomaly. A series of low and high power were also proposed to demonstrate the enhanced performance at the completion of the hardware enhancements.

### 3.1.3 Uncooled Resonator (UCR)

**3.1.3 1 Design Activity.** Schafer personnel reviewed and provided technical inputs to BMDO and SMC on the uncooled resonator special study. This included attending and participating in various design and readiness reviews such as the SCSi Annular Resonator Optic Braze Readiness Review (BRR).

**3.1.3.2 Fabrication Activity.** Schafer personnel reviewed the progress of the uncooled resonator hardware fabrication throughout the report period. Significant progress has been made in the machining of the optics structural components. Final machining of the precision match machining of the Annular Resonator Optic (ARO) segments is nearing completion with the finalization of the machining and cleaning processes. The effort to tune the cast silicon carbide CTE to that of silicon made significant progress. Material samples were produced and will be tested. A number of braze materials were assessed in a matrix to determine the optimum material for an inner cone to tangent flange bond as well as various mounting inserts. An Inner Cone Assembly (ICA) pathfinder braze is planned in early January 1999. The braze fixtures are complete through stress relief ready for final machining. A SCSi-workpiece cleaning process has been finalized which will leave machined parts free of contaminants and stains.

**3.1.3.3 LODTM Activity.** Schafer personnel attended the monthly Large Optics Diamond Turning Machine (LODTM) technical progress and status meeting at Lawrence Livermore National Laboratory (LLNL) and provided technical assessment to BMDO and SMC. Schafer personnel reviewed the preparation of the copper clad aluminum Reflaxicon Conical Test Article (RCTA). The results of the diamond turning of the aluminum RCTA were extremely good and indicated the LODTM is operating at or better than when the original Alpha optics were fabricated. Schafer personnel reviewed the results of the silicon diamond turning parameter assessment study performed by LLNL and provided recommended follow-on activity to achieve the desired results. A cutting fluid containment system for use on LODTM is in the design process

### 3.1.4 Alpha LAMP Integration (ALI)

**3.1.4.1 Business Meeting Support** – Schafer Corp. provided support to the monthly ALI business meetings. This support included a review and assessment of the technical, schedule and cost progress of the ALI contract. As new work was added or changed, Schafer provided technical support in the development of Statements of Work (SOW), Justification and Authorization (J&A) and Contract Data Requirements Lists (CDRLs). Schafer personnel provided recommended changes to the ALI Autonomous Alignment activity to convert it to the Beam Control Test (BCT) low power test activity. These changes were reflected in an updated SOW.

**3.1.4.2 Proposal Evaluations** – A Technical Evaluation of the ALI Fab & Ops Restoration proposal was performed by a team of Schafer personnel. A detailed spreadsheet and assessment was provided to BMDO for subsequent fact-finding and negotiations. Due to

continuing funding fluctuations and technical delays in the UDM activity, subsequent updates of the evaluation spreadsheet was provided as updates to the LMA proposal was provided. An evaluation of the LMA proposal in response to PO0095 issued by BMDO was performed by Schafer Corp. and submitted to SMC. Additional evaluations of PO0098 and PO0099 were performed by Schafer Corp. and submitted to SMC.

**3.1.4.3 Negotiation Support** – Schafer Corp. provided support to SMC and BMDO during the negotiations of the Uncooled DM activity, PO0095, PO0098 and PO0099 contract modifications. Support was also provided to the ALI Experiment closeout activity. A list of government furnished equipment was reviewed and disposition recommendations were made to SMC.

### 3.1.5 Alpha Laser Optimization (ALO)

**3.1.5.1 Business Meeting Support** - Schafer provided support to the monthly ALI business meetings. This support included a review and assessment of the technical, schedule and cost progress of the ALI contract. As new work was added or changed, Schafer provided technical support in the development of Statements of Work (SOW), Justification and Authorization (J&A) and Contract Data Requirements Lists (CDRLs).

**3.1.5.2 Proposal Evaluations** - Schafer personnel provided detailed analysis and evaluation of the TRW CLIN 0007 proposal update. A spreadsheet of resources (technical hours, material, travel and ODC dollars) was provided to SMC to support fact-finding and negotiations.

**3.1.5.3 Negotiation Support** – Schafer personnel provided technical support to BMDO to complete the contract definitization of TRW ALO CLIN 0001, CLIN 0006 and CLIN 0007.

### 3.1.6 Uncooled Resonator (UCR)

**3.1.6.1 Proposal Evaluations** – Schafer personnel performed a technical evaluation of the TRW Uncooled Resonator (UCR) special study CLIN 0004 proposal for the uncooled resonator activity A detailed spreadsheet and assessment was provided to SMC to support fact-finding and negotiation. Also, a set of spreadsheet analyses was provided for TRW CLIN 0008 UCR facility proposal and the CLIN 0009 UCR three phrase hardware proposal. Schafer personnel provided an evaluation of the critical small vendors and subcontractors developed as a part of the uncooled resonator activity to SMC. These vendors included McCarter Machine, Eagle Machine, Silicon Crystals and Xinetics Inc.

**3.1.6.2 Negotiation Support** – Schafer personnel assisted the SMC project office during the fact-finding and negotiations of the TRW UCR special study, the CLIN 0008 facility proposal and the CLIN 0009 hardware proposal.

**3.1.6.3 LLNL Support** – Schafer personnel reviewed the LLNL proposed resource allocation of the LODTM support to TRW and provided recommended changes to this allocation. Schafer personnel participated in the fact-finding discussions and in baselining the LLNL effort for

20

FY 98. Schafer personnel validated the cost of two HVAC chillers installed by LLNL to preclude temperature fluctuations in the LODTM.

### 3.1.7 Integrated Test Schedule Activity

**3.1.7.1** Tentative plans for FY 99 have been developed which include a series of ALI tests initially using a high power Beam Profile Generator (BPG) that will provide the capability to exercise the ALI Beam Control System through a wide range of parameters. This test series will establish range of performance for the critical parameters that can not be achieved in high power testing. After the BPG has been designed, fabricated, integrated and checked out, a series of low power tests will be performed to validate the parameter performance and provide simulations of high power test conditions. A high power test is planned to demonstrate the Beam Control System performance and the completion of these low power tests. In parallel, plans call for the ALO program to establish a baseline run condition based on the results of the ALO data review discussed above. A number of facility and hardware enhancements will be performed and a series of low power tests will be performed to validate the enhancements followed by a series of high power tests. The last ALO test will be jointly conducted with the ALI program. An integrated test schedule was developed by Schafer personnel that incorporated the ALI and ALO programs together.

### 3.1.8 HF Technology Maturity Panel

Schafer (Dr. Lawrence Zajac) participated in the HF Maturity Panel sponsored by SMC to evaluate the state of readiness of the HF laser for utility in an NMD role. In particular, the objective of the panel review was to determine the near-term potential of HF technology for a space experiment. As part of this evaluation, the panel members were asked to provide responses to five questions. Dr. Zajac's response to these questions, which also reflects the consensus of the panel, are as follows:

**Question 1)** **Is the HF laser sufficiently mature to commit to a MW class SBL demonstration in space?**

The short answer is **Yes**

The long answer: To assess the maturity of the HF laser (or any other), the 2 key functions of the laser should be separated and evaluated independently. These 2 functions are: gain generation and beam generation. When properly designed, operated, and combined the hardware functions as a laser.

Gain Generator:

**The HF Gain Generator Maturity Level is Equivalent to the Maturity Level of Rocket Engines**

21

The functions of the gain generator part of the HF chemical laser are virtually identical to that of a chemical rocket engine in terms of both hardware design and the aerodynamic/thermodynamic/structural analysis required to support the design. The components comprising the two devices (rockets and gain generators) have similar names and functions; reactant (propellant) storage tanks, valves, flow control devices, injectors, combustion chambers, and subsonic/supersonic nozzles. The design, fabrication, and operation of HF chemical lasers draws heavily from rocket engine experience. Current geometries for the HF gain generator (linear and cylindrical) have parallel rocket geometries (Aerospike and Bell). The analytical models used to design HF gain generators have parallel rocket engine analytical models. The performance of both can be approximated analytically but must be verified empirically and the computer models "anchored" to the empirical data. Both are scaled from smaller devices that experimentally verify performance and design features. Both are "self cooled" and expel the bulk of the heat generated by the chemical reaction in the exhaust products.

## The Performance of the HF Laser Gain Generator At the MW Level is Repeatable and Reliable

All HF and DF lasers tested have reliably produced repeatable macroscopic (power) performance levels providing:

(1) The gain generator hardware remains structurally and thermally stable, and
(2) The "facility" provides repeatable, clean reactant flows and a repeatable operational environment

All failures to achieve repeatable and reliable gain generator performance can be traced to problems caused by one or both of the above caveats. SIGMA experienced thermal/structural problems which degraded performance over time. MADS experienced secondary blade "plugging" leading to hardware damage due to contaminated (dirty) secondary flows. A similar problem is believed to have caused the secondary blade damage in ALPHA. Pumping system problems have plagued ALPHA and is a major factor in reliable ALPHA performance.

MW level HF gain generators have demonstrated repeatable and reliable performance when the above two conditions are met. The linear device, MIRACL, has operated as a laser for over 3500 seconds The cylindrical device, ALPHA, has operated for about 50 seconds. .Although the current ALPHA design is not at thermal equilibrium during the lasing period, the combustor and cavity conditions are repeatable —— and the power should also be.

The "problems" experienced with HF gain generators are not related to the physics of the HF laser. They are problems which can be rectified by improvements in hardware thermal/structural design and proper facility design and maintenance.

## Space is the Natural Environment of the HF Gain Generator

Efficient chemical laser operation (HF, DF, or COIL) requires the production of "gain" to occur in near vacuum conditions. To test on the ground, this then requires vacuum chambers to

contain the gain region and ejectors or pumps to raise the gain region pressure some 50 fold to exhaust to the ambient atmosphere. For virtually all HF devices that have been tested (sub-scale, full-scale, linear, and cylindrical) vacuum chamber and pumping problems have contributed negatively to HF device performance and reliability.

The vacuum of space provides a "natural" operating environment for the HF gain generator --- eliminating the need for special vacuum enclosures and pressure recovery systems. Space operation, of course, presents unique operational issues of it's own --- reliable and remote ignition, reactant storage, supply, and regulation, and the electronics to control the ignition and reactant flows. These are, however, the same operational functions that are successfully dealt with in space with rocket engine operation. Like the rocket engine, no special preparation of the reactants is required for the HF gain generator. Just open the valves, ignite, and it's operating.

The ground environment is, in reality, a very hostile environment for current chemical lasers. While the facilities to operate ground based lasers are accessible and therefore maintainable, the contaminating and oxidizing effect of the environment itself increases the need for continuous maintenance.

Beam Generator.

**The Maturity Level of Optical Resonators for MW HF Beam Generation Has Been Demonstrated**

The generation of a laser beam requires an optical system (resonator) to be properly designed to match and be aligned to the gain generator. (This function is not unique to the HF laser; it is required for all lasers.) This has been successfully done numerous times on linear devices with powers ranging from 10's of kW to several MW (MIRACL). The analysis, scaling, design, and fabrication techniques of the optical components for linear HF beam generation is understood and has been successfully repeated for new devices. Uncooled optical components have been designed, fabricated, and successfully tested at MW power levels.

**The Maturity Level Of Cylindrical Resonators is Less Mature Than Linear Resonators**

While SIGMA was intended to be the gain generator for the first cylindrical resonator demonstration, thermal/structural problems precluded this demonstration. ALPHA was thus the first, and to date only, laser test of a cylindrical resonator coupled with a cylindrical gain generator. With only one design that has been fabricated and tested, the understanding of cylindrical resonator design and performance must be considered to be at a somewhat lower level of "maturity" level than linear resonators. More data is needed to increase the maturity level; however.......

## The Overarching Performance Uncertainty of Cylindrical Resonators - Mode Control - Has been Successfully Demonstrated

The overriding concern at the time of the design of the cylindrical gain generator and resonator for the ALPHA laser was whether or not any cylindrical resonator design could achieve single mode operation comparable to linear resonator configurations. We tend to forget this objective and the fact that mode control has been successfully demonstrated on ALPHA, thus raising the maturity level of cylindrical lasers from paper theory to hardware reality. Once mode control is achieved, the remaining performance concerns are similar to those of linear resonators - figure control, thermal distortion, jitter, coating integrity, extraction efficiency, and alignment. These issues have been successfully resolved in linear resonator configurations and there is no known technical reason why they can't be successfully resolved with a cylindrical resonator configuration. In fact, the ALPHA resonator performance with respect to these issues is reasonably well understood and comparable to linear configurations with one exception - alignment. More on this later.

## Components and Functions Similar to HF Beam Generators Have Been Demonstrated in Space

Optical systems have been deployed and successfully operated in the space environment. They have survived launch loads, have been remotely aligned in space, and the coatings, optics, and electronic components required for operation have survived the space environment. In principle, there is no known reason why the optical resonator for HF beam generation, using similar if not identical components, could not be deployed and operated.

## Question 2)  Are HF Laser Models and Codes Consistent with Alpha Performance Results?

Yes . . .and no.

### HF Laser Models and Codes Are Consistent with Alpha Results at the Nominal Operating Point

Cylindrical resonator codes a priori predicted, e.g., mode control, circumferential intensity distributions, and alignment sensitivities. Furthermore, Alpha performance data can be correlated with subscale data and with coupled cylindrical resonator / gain generator models such as CROQ at the now "nominal" operating condition (e.g. test 902 etc). The codes qualitatively correlate with total power, the power per lasing line, and the contributors to WFE (or BQ) such as intrinsic beam quality, thermal distortion, and jitter. Precise quantitative correlation has not been achieved, possibly because of code physics deficiencies (unlikely), variability in operation/alignment (likely), imprecise code inputs and/or boundary conditions (possibly), or imprecise measurements due to the need to measure very small (WFE) and very large (power) parameters (very likely). Also, the codes do not predict "off nominal" performance (e.g. test 430). Whether the latter is a weakness of the codes or the data is distorted by faulty facility operation is still TBD.

24

## Engineering Codes Failed to Predict Critical Alpha System Performance Parameters

Consistent with the SIGMA experience, the codes that failed badly in ALPHA were the engineering codes; not HF laser physics codes. Particularly, those used to predict the thermal profiles of the primary blades; but also those used to predict ejector performance. There is a lesson here.

### Question 3) Are Additional Alpha Tests Required to Provide Sufficient Confidence in HF Laser Models and Codes to Allow a SBLRD to be Designed with Moderate Risk.

(If NASA had applied this criteria of code confidence and design risk to the F1 in the 60's, Armstrong could still be waiting for a ride.)

**More Alpha Tests are Required to Verify Consistent Performance and to Obtain Design Data for the Flight Hardware.**

As a minimum, these are:

- **Verification of Beam Control and WFE Correction**

The performance of the uncooled DM and FSM together with the ALI beam control system is a pre-requisite to the SBLRD design. To proceed to a design without these data and concept verification would be foolish.

- **Verification of a Precise and Remote Alignment System**

The alignment of the cylindrical resonator is complicated by the need to simultaneously align the resonator with itself and with the cylindrical gain generator. The alignment approach on ALPHA is currently dependent upon the skills and judgment of key individuals. Precise, absolute, and repeatable alignment to a fixed point in space is not being achieved (and probably can't be) with the current techniques. This contributes to the uncertainty of the accuracy and the repeatability of all measurements. It also is a pre-requisite to a SBLRD design.

- **Performance at Off-Nominal Flow Conditions**

To the extent the facility performance allows, the Alpha device needs to be tested at carefully selected flow conditions to determine beam generator performance in terms of both out-coupled power and WFE (BQ) for this "fixed" resonator. These parameters must be correlated with the codes to the extent that trends, if not absolutes, can accurately be predicted. (This may require additional small signal gain measurements on the AVM.) These data will be required to determine if there is a "better" flow condition and provide the design information for a new gain generator/resonator configuration optimized for this better flow condition. Even if a new nozzle configuration is chosen, these data are critical, in my opinion, to learning how to properly design a new resonator to efficiently couple the resonator "mode" to the gain generator "mode".

25

- **Demonstrate Repeatable Performance at SBLRD Operating Conditions**

This will require development of a precise and repeatable alignment technique to remove this uncertainty to performance repeatability. It may also require installation of additional and/or improved diagnostics for parameter measurement. It will certainly require test intervals shorter than what we've had to date.

## Question 4) Is a New Test Laser Required to Provide Sufficient Confidence in HF Laser Models and Codes to Allow a SBLRD to be Designed with Moderate Risk.

### No, a New Test Laser is Not Required if HYWN is the SBLRD Nozzle Concept

If the current ALPHA nozzle design can be redesigned to achieve more rapid thermal equilibration at safe material temperatures and if a specific power can be realized that satisfies mission run time, target lethality, and launch vehicle weight requirements, there is no need to change for the flight laser. (The requirement for "traceability" to a nozzle concept that <u>may</u> be used 20 years hence is a red herring.) These are 2 big ifs; but definitely within the realm of probability

### Maybe Not, if ALPHA Data Can be Applied to Design a New Resonator for A New Flight Laser

If the tests recommended in 3) are performed and if the codes can be used to correlate sub-scale data with full scale data for the HEXDARR resonator, a new laser could be designed for the SBLRD with sufficient confidence. Again, 2 big ifs. But, ALPHA was designed with no HF cylindrical data and performs reasonably close to performance levels predicted by resonator codes and sub-scale data Linear devices have been scaled from sub-scale data to high powers in one step - NACL and MIRACL for example. (But a second generation of either would undoubtedly have performed better.) There is risk, but it has been done.

### To Minimize Cost and Schedule, A New Test Laser Must Also be Designed for Flight

If a new nozzle concept can be shown to have significantly higher performance so that the weight savings more than off-sets the engineering and manufacturing risks - then go for it. This new test laser must be designed for flight; otherwise two lasers must be built - one to test and one to fly.

## Question 5) What Features Are Required of an HF Laser Risk Reduction Plan to Provide Confidence that a SBLRD Will be Successful?

### A Plan that Includes the Tests Listed in 3) Above

### Fabrication and Performance Testing of an Uncooled Resonator

and

## Ground Testing to Verify Flight Hardware Performance

Schafer also presented a brief review of the SIGMA program at the panel discussions. The charts are included below.

**_Schafer_**      SIGMA

---

- <u>Program Objective</u>
  - Design/Fabricate/Test, At Scale, A Cylindrical Laser With Performance Suitable For Airborne Laser Application Using A SOA DF* Nozzle Concept

- <u>Performance Goals</u>
  - Specific Power      -   100 Kj/Kg With $NF_3$
  - Nozzle Power Flux   -   310 $W/cm^2$
  - Pressure Recovery   -   200 Torr (Passive)
  - "Good" Media Quality -   1.02 (?)
  - "High" Cycle Life

- Goals Derived From Conceptual Design Of DF* Airborne Laser

**_Schafer_**      SIGMA - Program Start (Circa 1976)

---

- Major Issues/Concerns-
  - Pressure Recovery - Diffuser/Facility
    - Vaned Diffuser Start Performance
    - Only Linear (No Cylindrical) Vaned Diffuser Data

  - Blade Fabrication
    - Few (< 6?) Produced

  - Thermal/Structural Integrity Of Blades/Baffles
    - Little Margin - Believed To Be Satisfactory

  - Media Quality - Spacer Pad Issue

  - Combustion Wave Ignition - Multiple Chamber Ignition
    - Open Air Tests Successfully Completed

  - Laser Performance ($\sigma/\delta$)
    - Cylindrical Sector Tests Verified Scalability From Linear Device

---

**Schafer** SIGMA - Program Conclusion (Circa 1983)

- Significant Findings
  - Cylindrical Vaned Diffuser Performance - Acceptable
    - After Facility Mods To Provide Start Performance

  - Blades Experienced Thermal/Structural and Debonding Problems
    - Blade Degradation Was Significant Contributor to Reduced Laser Performance

  - Media Quality - Met Goal

  - Combustion Wave Ignition Performance - Acceptable

  - Laser Performance - Matched Predictions
    - Before Blade Degradation


**Schafer** SIGMA - In Retrospect

- Problems Experienced Were Caused By:
  - Pushing SOA Envelope In Nozzle Performance/Fabricability
  - The Necessity To Replicate Operational Environment On Ground
  - The Desire To Achieve Operational System Performance Goals

- Problems Were <u>Not</u> Caused by SIGMA Being An HF*/DF* Laser Device

**Schafer** — Lessons Learned - My Opinion
Applicable To SBLRD

- Carefully Define and Focus On Most Important Program Objectives
  - Traceability/Scalability To Today's Vision Of An Operational Concept Must Be Considered - But Not Be An Overarching Objective
  - The ABL Concept Of 1978 Is Not The ABL Concept Of 1998

- Do Not Stray Too Far From The SOA In Data, Performance, And Fabricability
  - Do What You Really Know How To Do

- Provide Margin - Then Provide Some More
  - Failure To Achieve Projected Performance Can Lead To More Costly Solution(s) - Or Program Failure

**Schafer** — HF*/DF* Laser Maturity

- Every 100KW · HF*.DF* Laser Built And Operated Has Performed As Expected Relative To Sub-Scale Data
  - They Are Scalable - (In Closed Cavity Performance)

- HF* DF* Devices Must Be Tested At Scale
  - To Verify Outcoupled Performance vs Projections
  - To Verify Thermal/Structural Characteristics
  - To Verify Fabricability

- Most Problems Experienced In HF* DF* Laser Operation And Reliability Are Have Been Caused By Need To Replicate Operational Environment
- The Natural Environment Of This Laser Is Space

### 3.1.8.1 Maturity Panel Data Review

During the panel review, TRW presented a review of the ALPHA program and data. The Schafer position at that time was that issues related to what was believed to be poor performance by the ALPHA device could be a result of the operating conditions. In particular, it appeared from the analysis of the data that there was a rather substantial effect of fluorine available on extracted power; an effect that significantly larger than would have been expected. Subsequent to the panel review, TRW discovered that there was an error in the fluorine flowrate calibration and that, indeed, the fluorine available flow was about 20% higher than desired. A report of the analysis of the ALPHA flow conditions is provided below.

The amount of available fluorine for producing acceptable levels of power for the Alpha device at CTS will be discussed. The available fluorine is produced using a proprietary Schafer program that takes into account the temperature and pressure of the combustion fluids and the heat transfer from the Gain Generator during the combustion process. The program allows for the transient behavior of the Alpha system to be examined.

The sonic venturi meter temperatures and pressures were used to produce the flow rates of $NF_3$, $D_2$ and He. These flow rates were produced using the actual values of $C_d$ and the throat area of each sonic venturi meter, in addition to the pipe diameter at the inlet to the sonic venturi meter (Table 3.1-1). These values and mnemonics were supplied to Schafer by TRW and are assumed to be correct in this study. With these sonic venturi meters characterized, the actual flow rates of $NF_3$, $D_2$ and He were produced. These flow rates were constructed by using the appropriate stagnation temperatures and pressures along with the real gas behavior of these gases through the sonic venturi meters. The results of this procedure produced $NF_3$ over 2% higher than those reported by TRW, while the $D_2$ and He mass flow rates were less than 1% higher using the Schafer methodology.

#### Table 3.1-1: Sonic Venturi Data (from TRW)

| Venturi | Designation | Orifice Diameter (in) | $C_dA$ (in$^2$) | Line Size ID (in) |
|---|---|---|---|---|
| Oxidizer ($NF_3$) | NF-F-008 | 1.268 | 1.2470 | 2.9 ( 3" sch 80) |
| $D_2$ | D$_2$-F-161 | 0.505 | 0.1955 | 1.5 (1.5" sch 80) |
| Combustion He | He-F-198 | 0.892 | 0.6179 | 2.9 (3" sch 80) |
| Cavity H$_2$ | H$_2$-F-110 | 0.786 | 0.4741 | 2.9 (3" sch 80) |

The data used to obtain the necessary pressures and temperature were compiled from archival test data. In general, the data were taken at 10 seconds, where it was assumed that the flows should be near their steady state values. Table 3.1-2 through Table 3.1-4 shows the pressure, temperature and mnemonic used for the evaluation of the flow rate for each test.

**Table 3.1-2: NF₃ Pressures and Temperatures (From TRW Data)**

| TEST | NF₃ | | TNFUS (R) |
| | PNFUS (PSIA) | TNFUS (K) | |
| --- | --- | --- | --- |
| 601 | 389.51 | 286.40 | 515.52 |
| 701A | 387.50 | 287.90 | 518.22 |
| 901 | 392.88 | 295.50 | 531.90 |
| 902 | 393.18 | 290.80 | 523.44 |
| 903 | 392.15 | 289.60 | 521.28 |
| 904 | 394.14 | 296.30 | 533.34 |
| 905 | 392.53 | 289.80 | 521.64 |
| 440 | 387.70 | 285.50 | 513.90 |
| 907A | 384.64 | 279.10 | 502.38 |
| 907B | 414.50 | 278.00 | 500.40 |
| 908A | 389.35 | 287.50 | 517.50 |
| 908B | 393.56 | 289.90 | 521.82 |

**Table 3.1-3: D₂ Pressures and Temperatures (From TRW Data)**

| TEST | D₂ | | TD2US (R) |
| | PD2US (PSIA) | TD2US (K) | |
| --- | --- | --- | --- |
| 601 | 666.50 | 294.10 | 529.38 |
| 701A | 670.23 | 295.90 | 532.62 |
| 901 | 675.63 | 300.10 | 540.18 |
| 902 | 669.14 | 295.00 | 531.00 |
| 903 | 673.26 | 300.80 | 541.44 |
| 904 | 677.84 | 305.20 | 549.36 |
| 905 | 677.62 | 301.60 | 542.88 |
| 440 | 664.70 | 293.80 | 528.84 |
| 907A | 668.18 | 290.60 | 523.08 |
| 907B | 662.31 | 290.70 | 523.26 |
| 908A | 666.45 | 295.60 | 532.08 |
| 908B | 671.40 | 299.60 | 539.28 |
| | | | |

32

**Table 3.1-4: Combustion Helium Pressures and Temperatures (From TRW Data)**

| | COMBUTION He | | |
| --- | --- | --- | --- |
| TEST | PHPUS (PSIA) | THPUS (K) | THPUS (R) |
| 601 | 1017.24 | 285.60 | 514.08 |
| 701A | 1033.50 | 296.00 | 532.80 |
| 701B | 1265.50 | 294.30 | 529.74 |
| 901 | 1040.50 | 300.00 | 540.00 |
| 902 | 1030.10 | 294.60 | 530.28 |
| 903 | 1038.15 | 299.40 | 538.92 |
| 904 | 1052.96 | 306.80 | 552.24 |
| 905 | 1040.09 | 299.60 | 539.28 |
| 440 | 1031.90 | 294.90 | 530.82 |
| 907A | 1028.86 | 291.50 | 524.70 |
| 907B | 1027.89 | 291.10 | 523.98 |
| 908A | 1035.78 | 296.40 | 533.52 |
| 908B | 1043.16 | 300.90 | 541.62 |

**Table 3.1-5: NF$_3$ Stagnation Temperatures, Pressures and Corrected Mass Flow Rates**

| | NF$_3$ | | REAL C* | MASS FLOW RATE | MASS FLOW RATE |
| --- | --- | --- | --- | --- | --- |
| TEST | P$_{STAGNATION}$ (PSIA) | T$_{STAGNATION}$ (R) | FT/SEC | lb$_m$/sec | g/sec |
| 601 | 392 62 | 516.50 | 882.56 | 17.85 | 8095.96 |
| 701A | 390 60 | 519.20 | 886.21 | 17.68 | 8021.01 |
| 901 | 396 02 | 532.91 | 902.31 | 17.61 | 7987.27 |
| 902 | 396 33 | 524.43 | 891.96 | 17.83 | 8086.12 |
| 903 | 395.29 | 522.27 | 889.42 | 17.83 | 8087.97 |
| 904 | 397.29 | 534.35 | 903.90 | 17.63 | 7998.79 |
| 905 | 395 67 | 522.63 | 889.82 | 17.84 | 8092.17 |
| 440 | 390.80 | 514.88 | 880.78 | 17.80 | 8074.63 |
| 907A | 387.72 | 503.33 | 866.42 | 17.95 | 8143.67 |
| 907B | 417.82 | 501.35 | 859.45 | 19.50 | 8847.04 |
| 908A | 392 46 | 518.48 | 885.07 | 17.79 | 8069.69 |
| 908B | 396.71 | 522.81 | 889.92 | 17.89 | 8112.49 |

Table 3.1-5 through Table 3.1-7 shows the actual stagnation temperatures and pressures for the various tests examined. In addition, the corrected mass flow rates, which were produced by using the real gas properties for these fluids, are also shown in Table 3.1-5 through Table3.1-7.

**Table 3.1-6: D₂ Stagnation Temperatures, Pressures and Corrected Mass Flow Rates**

| D₂ | | | REAL C* | MASS FLOW RATE | MASS FLOW RATE |
|---|---|---|---|---|---|
| TEST | P$_{STAGNATION}$ (PSIA) | T$_{STAGNATION}$ (R) | FT/SEC | lb$_m$/sec | g/sec |
| 601 | 668 43 | 529.82 | 3753.90 | 1.120 | 507.815 |
| 701A | 672.17 | 533.07 | 3765.00 | 1.122 | 509.152 |
| 901 | 677.59 | 540.63 | 3790.40 | 1.124 | 509.815 |
| 902 | 671.08 | 531.44 | 3759.50 | 1.122 | 509.067 |
| 903 | 675.21 | 541.89 | 3794.60 | 1.119 | 507.464 |
| 904 | 679 80 | 549.82 | 3820.90 | 1.119 | 507.400 |
| 905 | 679.581 | 543.33 | 3799.50 | 1.125 | 510.092 |
| 440 | 666 63 | 529.28 | 3752.00 | 1.117 | 506.700 |
| 907A | 670 12 | 523.52 | 3732.50 | 1.129 | 512.014 |
| 907B | 664 23 | 523.70 | 3733.00 | 1.119 | 507.448 |
| 908A | 668 38 | 532.53 | 3763.00 | 1.117 | 506.549 |
| 908B | 673.34 | 539.73 | 3787.30 | 1.118 | 507.037 |

**Table 3.1-7: Combustion Helium Stagnation Temperatures, Pressures and Corrected Mass Flow Rates**

| COMBUTION He | | | REAL C* | MASS FLOW RATE | MASS FLOW RATE |
|---|---|---|---|---|---|
| TEST | P$_{STAGNATION}$ (PSIA) | T$_{STAGNATION}$ (R) | FT/SEC | lb$_m$/sec | g/sec |
| 601 | 1019 59 | 514.55 | 3512.60 | 5.768 | 2616.274 |
| 701A | 1035 89 | 533.29 | 3575.30 | 5.757 | 2611.479 |
| 901 | 1042 90 | 540.49 | 3599.20 | 5.758 | 2611.708 |
| 902 | 1032 48 | 530.77 | 3566.90 | 5.752 | 2609.017 |
| 903 | 1040 55 | 539.41 | 3595.60 | 5.751 | 2608.418 |
| 904 | 1055 39 | 552.75 | 3639.40 | 5.762 | 2613.789 |
| 905 | 1042 49 | 539.77 | 3596.80 | 5.759 | 2612.421 |
| 440 | 1034 28 | 531.31 | 3568.80 | 5.759 | 2612.185 |
| 907A | 1031 24 | 525.184 | 3548.40 | 5.775 | 2619.463 |
| 907B | 1030 26 | 524.46 | 3546.00 | 5.773 | 2618.764 |
| 908A | 1038 17 | 534.01 | 3577.80 | 5.766 | 2615.411 |
| 908B | 1045 57 | 542.12 | 3604.60 | 5.764 | 2614.462 |

34

It should be noted that the $D_2$ mass flow rate appearing in Table 3.1-6 represents the total mass flow of $D_2$ delivered to the Alpha device. This mass flow rate, however, is not the amount used in the combustion process. Approximately 14% of this total $D_2$ mass flow rate is diverted to the base purge of the nozzles. Thus, only 86% of the total $D_2$ mass flow rate is used for combustion and, since this study is only interested in the combustion process, this reduced $D_2$ mass flow rate is used for evaluation.

## Discussion and Results

Having produced the corrected mass flow rates using the real gas properties for $NF_3$, $D_2$ and He, it is now possible to employ these flow rates in the Schafer proprietary program. The following are the results of this effort.

The data reported by TRW show the $NF_3$ mass flow rates to be precisely defined by two values corresponding to what was believed to be 92% and 100% flow rates. The data that is shown in Table 3.1-5 dispute this premise. Figure 3.1-1 clearly illustrates the variations in the $NF_3$ mass flow rates as produced in this study.

CORRECTED NF₃ MASS FLOW RATE USING STAGNATION CONDITIONS AND THE ACTUAL SONIC VENTURI
C_D AND THROAT AREA VALUES
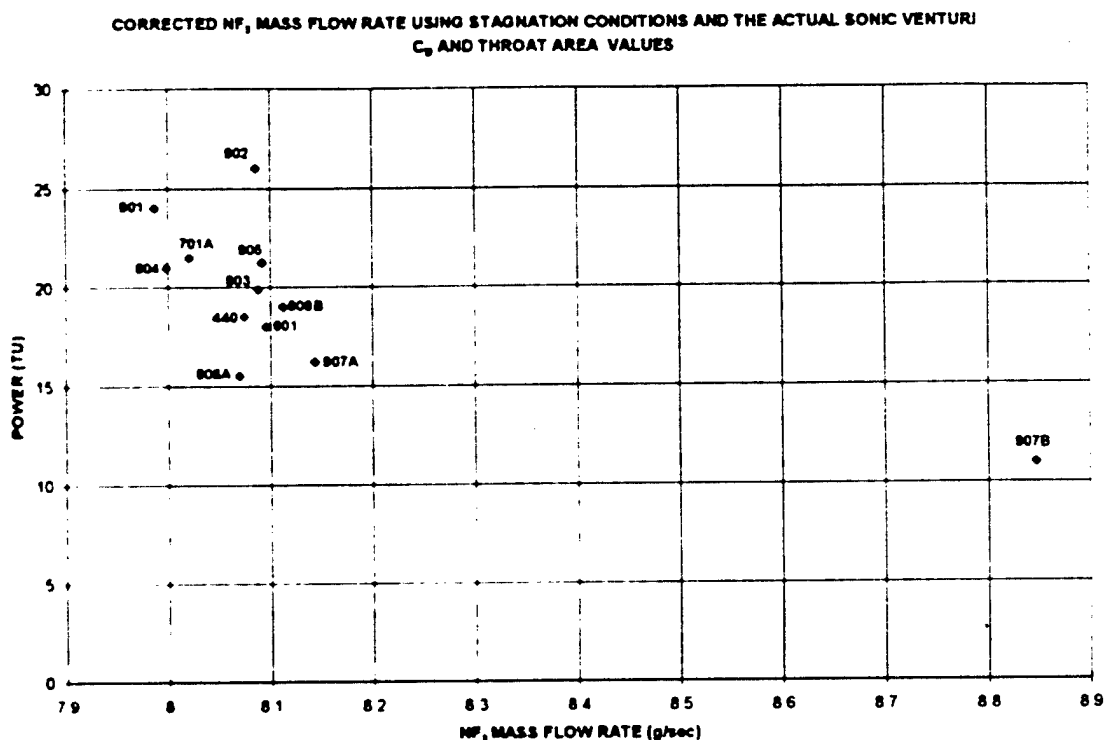


**Figure 3.1-1: NF₃ Mass Flow Rates Produced for the Tests Examined in This Study**

The mass flow rates produced above were used as the inputs to the Schafer transient flow rate program. Table 3.1-8 shows the results of this effort. The test number, time at which the data were extracted, available fluorine and the TPC power are reported in Table 3.1-8.

Table 3-1-8: Available Fluorine and Power for Each Test Examined

| TEST | AVAILABLE F (mol/sec) | APPROXIMATE POWER MEASURED BY THE TOTAL POWER CALORIMETER (TU) |
|---|---|---|
| 601 (10 sec) | 114.2 | 18.00 |
| 701A (9.4 sec) | 112.1 | 21.50 |
| 901 (10.2 sec) | 111.5 | 24.00 |
| 902 (10 sec) | 113.9 | 26.00 |
| 903 (10 sec) | 113.9 | 19.90 |
| 904 (10 sec) | 111.9 | 21.00 |
| 905 (10 sec) | 113.9 | 21.25 |
| 440 (10 sec) | 113.7 | 18.50 |
| 907A (TO 10 sec) | 114.8 | 16.20 |
| 907B (13 sec) | 125.4 | 11.00 |
| 908A (10 sec) | 113.6 | 15.50 |
| 908B (10 sec) | 114.4 | 19.00 |



AVAILABLE FLUORINE USING CORRECTED OXIDIZER AND FUEL FLOW RATES AND THE ALPHA TRANSIENT MODEL WITH TOTAL POWER CALORIMETER FOR POWER MEASUREMENTS
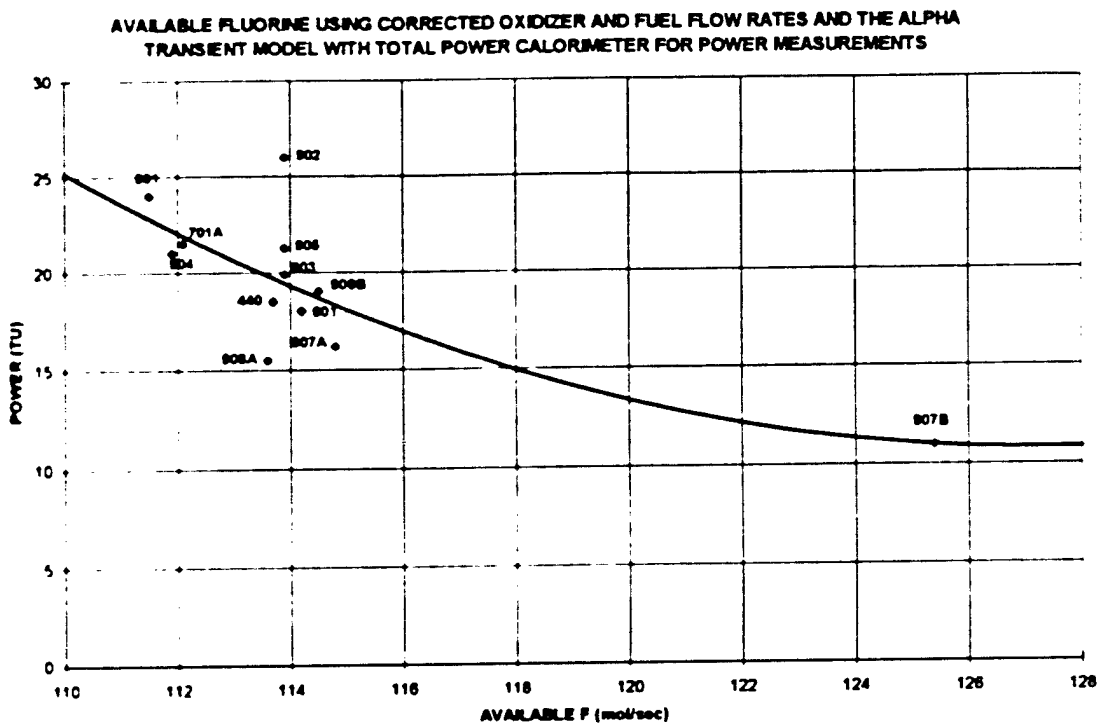
Figure 3.1-2: Available Fluorine

A graphical depiction of the data in Table 3.1-8 may be seen in Figure 3.1-2. Also shown in Figure 3.1-2 is a second order curve fit to the data. From the examination of this figure, it is clear that the available fluorine was not constant during the different tests, but actually varied significantly.

36

Perhaps a more applicable presentation of the data may be seen in Figure 3.1-3, where $\dot{m}_{fluorine}/A$ is depicted as the independent variable. The data used to produce Figure 3.1-3 were generated by converting moles of fluorine to grams of fluorine by multiplying by the atomic weight. This value was then divided by the nozzle bank exit area through which this available fluorine flows. The nozzle bank exit area is taken to be constant and equal to 67,420 $cm^2$).
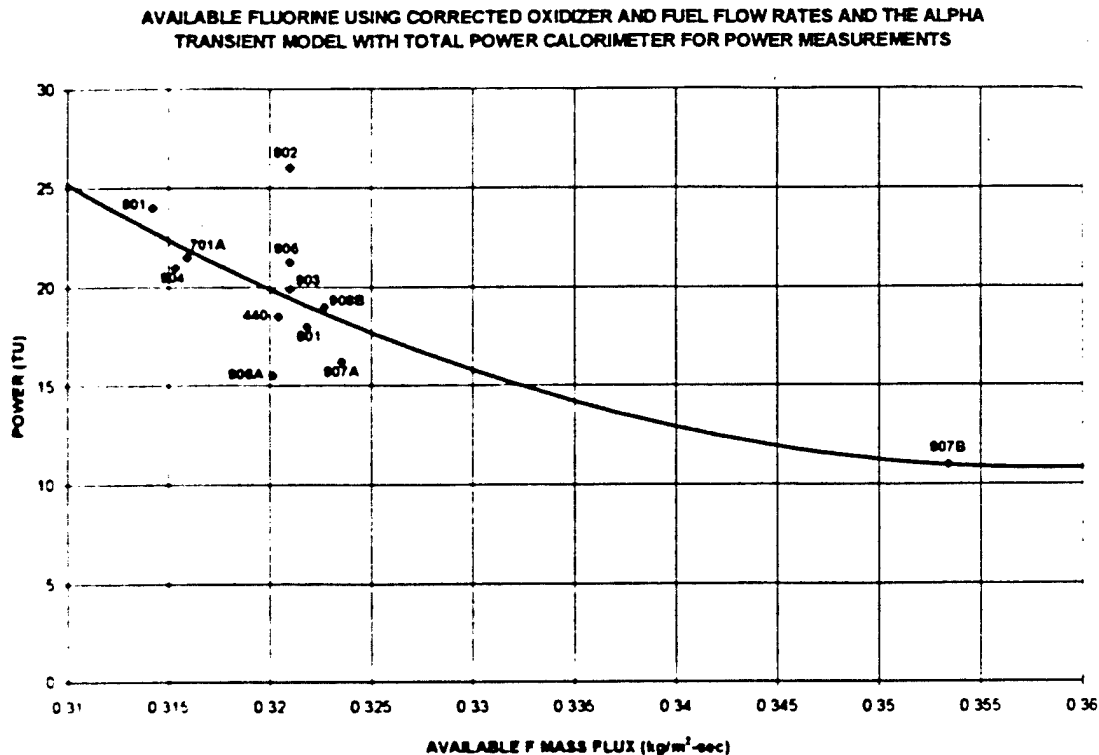


Figure 3.1-3: Available Fluorine Mass Flux

The error associated with the measurements of the $NF_3$, $D_2$ and He mass flow rates was shown to be quite substantial. Table 3.1-9 gives the expected error in these measurements as reported by TRW. For the evaluation of the error associated with the available fluorine produced during this study, the maximum error related to these three flow rates was used. A parametric evaluation was performed to produce the maximum possible error in the available fluorine for Test 902 and Test 908A. Figure 3.1-4 is the results of this parametric study.

Table 3.1- 9: Error Associated with the Combustor Mass Flow Rates

| Measurement | Precision of Measurement | Uncertainty in Results | Maximum Error |
|---|---|---|---|
| NF₃ Mass Flow Rate | 1.0 % | 1.5 % | 2.5 % |
| D₂ Mass Flow Rate | 1.0 % | 3.0 % | 4.0 % |
| He Mass Flow Rate | 1.0 % | 1.5 % | 2.5 % |

37

**AVAILABLE FLUORINE USING CORRECTED OXIDIZER AND FUEL FLOW RATES AND THE ALPHA TRANSIENT MODEL WITH TOTAL POWER CALORIMETER FOR POWER MEASUREMENTS**
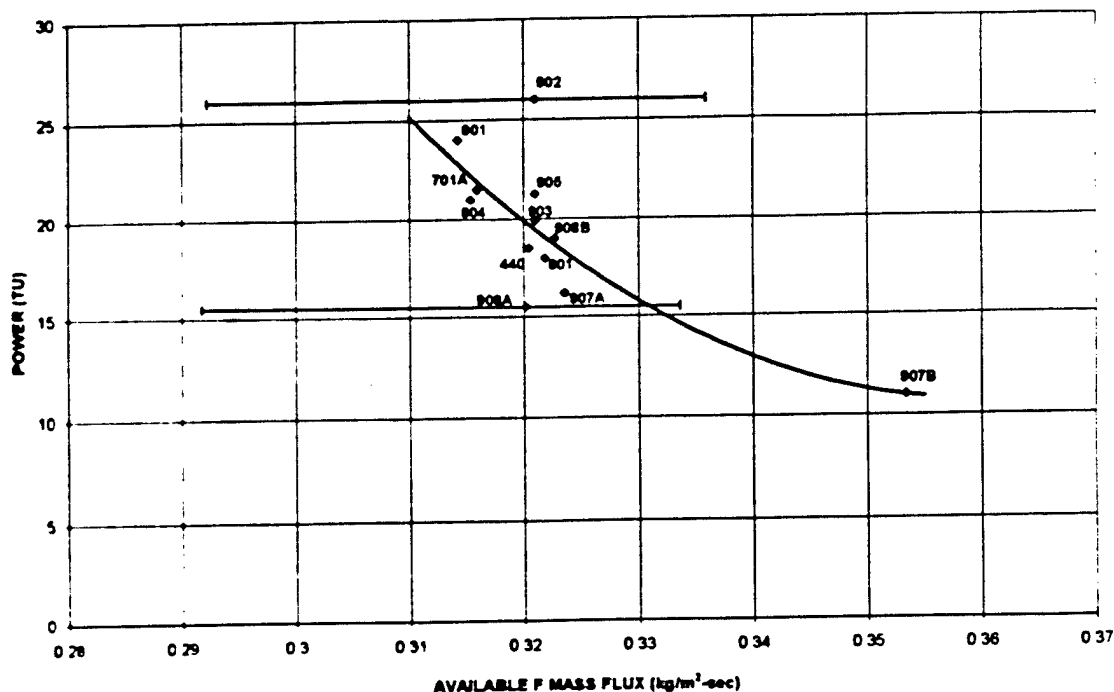
**Figure 3.1-4: Available Fluorine Mass Flux and Associated Errors**

The error associated with Test 902 proved to be the larger of the two tests examined. A positive error of 4.65% in available fluorine was generated when the $NF_3$ mass flow rate was increased by 2.5%, the $D_2$ mass flow rate was left unchanged and the He mass flow rate was decreased by 2.5%. A negative error of 8.96% in available fluorine was produced when the $NF_3$ mass flow rate was decreased by 2.5%, the $D_2$ mass flow rate was increased by 4% and the He mass flow rate was increased by 2.5%. Test 908A showed a 4.21% increase in available fluorine when the $NF_3$ mass flow rate was increased by 2.5%, the $D_2$ mass flow rate was left unchanged and the He mass flow rate was decreased by 2.5%. When the $NF_3$ mass flow rate was decreased by 2.5%, the $D_2$ mass flow rate was increased by 4% and the He mass flow rate was increased by 2.5%, Test 908A showed a decrease in available fluorine of 8.87%.

As a verification of the above results, it was determined that an evaluation of the combustion equations would be prudent. From the basic combustion equations for a $NF_3/D_2$ system that uses He as the diluent, one may write;

$$aD_2 + bNF_3 + cHe \rightarrow 2aDF + \frac{1}{2}bN_2 + \alpha(3b - 2a)F + \frac{1}{2}(3b - 2a)(1 - \alpha)F_2 + cHe$$

38
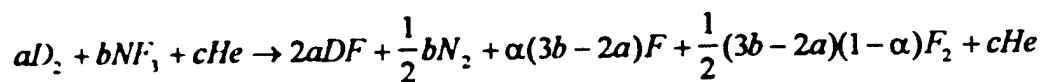
Noting that $a = \dfrac{\dot{m}_{D_2}}{4}$, $b = \dfrac{\dot{m}_{NF_3}}{71}$ and that c is defined by the diluent ratio and not important for this verification of the above results, Table 3.1-10 can be generated assuming the dissociation fraction of fluorine is $\alpha = 0.95$. As seen in Table 3.1-10, the results produced by the chemical combustion balance are in reasonable agreement with the more accurate transient model program.

**Table 3.1-10: Calculated $\dfrac{\dot{m}_F}{A}$ Using Corrected Mass Flow Rates and $\alpha = 0.95$**

| | NF3 | D2 | | | | | | | $\dfrac{\dot{m}_r}{A}$ |
|---|---|---|---|---|---|---|---|---|---|
| TEST | MASS FLOW RATE | MASS FLOW RATE | | | | | | | CALCU-LATED |
| | g/sec | g/sec | B | A | 3/2B-A | OF F2 | 3B-2A | OF F | |
| 601 | 8095.963404 | 436.721153 | 114.03 | 109.18 | 61.86 | 117.54 | 123.72 | 2233.19 | 0.331 |
| 701A | 8021.013091 | 437.870468 | 112.97 | 109.47 | 59.99 | 113.98 | 119.98 | 2165.65 | 0.321 |
| 701B | 9983.170630 | 535.583549 | 140.61 | 133.90 | 77.02 | 146.33 | 154.03 | 2780.28 | 0.412 |
| 901 | 7987.269075 | 438.440491 | 112.50 | 109.61 | 59.13 | 112.36 | 118.27 | 2134.77 | 0.317 |
| 902 | 8086.120410 | 437.797902 | 113.89 | 109.45 | 61.38 | 116.63 | 122.77 | 2215.96 | 0.329 |
| 903 | 8087.969279 | 436.418933 | 113.92 | 109.10 | 61.77 | 117.36 | 123.54 | 2229.82 | 0.331 |
| 904 | 7998.789917 | 436.363378 | 112.66 | 109.09 | 59.90 | 113.81 | 119.80 | 2162.31 | 0.321 |
| 905 | 8092.167357 | 438.678692 | 113.97 | 109.67 | 61.29 | 116.45 | 122.58 | 2212.63 | 0.328 |
| 440 | 8074.627958 | 435.762268 | 113.73 | 108.94 | 61.65 | 117.14 | 123.30 | 2225.57 | 0.330 |
| 907A | 8143.669533 | 440.332184 | 114.70 | 110.08 | 61.97 | 117.74 | 123.93 | 2236.98 | 0.332 |
| 907B | 8847.041889 | 436.405380 | 124.61 | 109.10 | 77.81 | 147.84 | 155.62 | 2808.87 | 0.417 |
| 908A | 8069.687619 | 435.632354 | 113.66 | 108.91 | 61.58 | 117.00 | 123.16 | 2222.98 | 0.330 |
| 908B | 8112.489531 | 436.052120 | 114.26 | 109.01 | 62.38 | 118.52 | 124.76 | 2251.83 | 0.334 |

## Conclusions

Several conclusions can be drawn from this study:

To properly evaluate the mass flow rates of $NF_3$, $D_2$ and He, the actual $C_d$, throat area and inside diameter of the upstream line size is needed. With this information, the stagnation temperature and pressure must be employed to produce a $C^*$, or the equivalent, to account for the real gas properties of the flow.

The $NF_3$ mass flow rates were shown to vary more significantly than indicated by TRW.

As a result of this $NF_3$ mass flow rate variation, the available fluorine was also seen to vary. The data indicate that lower $NF_3$ mass flows rate produce more available fluorine and measured TPC power.

Using the maximum errors associated with the NF₃, D₂ and He mass flow rates, a large error in available fluorine was shown to exist for Test 902 and Test 908A. This vast error in available fluorine indicates the need to accurately measure the $NF_3$, $D_2$ and He mass flow rates.

### 3.1.9 Presentations and Reports

Schafer has provided support in producing a variety of program briefings and reports. Many of the briefings were based on materials originally developed for BMDO. An example is the ACC briefing (Appendix 3.1-1). Other examples are included in Appendixes 3.1-2, 3, 4, 5 and 6.

### 3.2 SMC Site Selection

**Summary of Activities**

An effort was undertaken to provide information to Mr. Tom Craven (US Army SMDC) for the purpose of completing the environmental assessment of the four finalist SBL Test Facility sites. The information covers the Description of Proposed Action and Alternatives, socioeconomic parameters, transportation, hazardous materials and waste management, utilities, health and safety, noise, and air quality. A meeting was held with Mr. Craven to clarify the nature of the needed data and agree on the approach for the data collection. Information is being gathered from various documents and knowledgeable individuals with environmental backgrounds. It is anticipated that a final draft of the report will be delivered on July 17, 1998. It is further anticipated that one or more iterations of this data will be required as the specifics of the Environmental Assessment is written. Support was provided to SMC at several hardware contractor interchange meetings and site visits to identify and evaluate alternative facility development concepts. Support was also provided in the review of the CDS Baseline Validation Reports submitted by the hardware contractors.

Continued data collection activity in support of the SBL laser test facility environmental assessment (EA) through a series of meetings with SBL contractors and subcontractors. Reviewed current SBL design efforts and cost estimating approaches. Participated in several meetings and telecons with staff from Army Space and Missile Defense Center (SMDC) to coordinate the collection of and format for the EA data required by SMDC to complete their EA report.

Attended reviews and technical interchange meetings with AF/SMC contractors regarding progress on the Concept Definition Studies, providing feedback and comments about the approach being taken in the test and evaluation areas as well as facility design concepts. Provided additional input for the SMC contractor Baseline Validation Reports.

Continued data collection activity in support of the SBL laser test facility environmental assessment (EA) through a series of meetings with SBL contractors and subcontractors. Reviewed current SBL design efforts and cost estimating approaches. Supported a cost review meeting on operational system costs.

### 3.2.1 Introduction

In this section, two main topics will be covered:

Support to the process of selecting and qualifying a site for the SBL Laser Test Facility (LTF). Cost analysis performed in support of program planning efforts for the SBL.

### 3.2.2 Laser Test Facility Support

The Space Based Laser test requirements cannot be met using any existing test facilities. Therefore a new Laser Test Facility (LTF) must be constructed at a site suitable for its operation and consistent with applicable policy, regulations and directives. During the this period, Schafer contributed to the LTF development process in two principal ways. First was the participation on a governments-led site selection team which developed selection criteria, surveyed available sites, pared the list of candidates down to a final four, performed a survey of each of the four preferred sites

Second, Schafer assisted in the creation of a environmental assessment of the candidate sites by providing environment-related data and information on the anticipated design, construction and operation of the LTF. These efforts are reported in the following sections.

### 3.2.2.1 Laser Test Facility Site Selection

The process used in this effort is described below. The policy level screening criteria employed to reduce the original list of thousands of candidate sites down to the final four is shown as Appendix 3.2-1. Detailed criteria were employed to rank the final four and this information was presented to BMDO management. However, a re-direction of the SBL development program occurred just prior to the actual selection of the site, and therefore final selection is being held in abeyance at this writing. The elements that went into the selection process however are still considered applicable and will be reviewed and updated as the decision process goes forward.

A key element of the SBL program is the test facility required to perform critical pre-launch tests of the laser in its high performance mode and of the integrated system operating with full functionality. At present, there is no existing facility at which these tests can be performed. Thus the decision was made to build a new facility dedicated to the task. Further, it was decided that the facility will accommodate not only the requirements of the Readiness Demonstrator, but also be compatible with the anticipated needs of the EMD program and the production phase of the SBL system. The central requirements for the LTF are focussed on achieving three main objectives of the SBL program. The first is to carry out the unique testing required to ensure that the operation of the SBL prior to launch. The second is to subject the SBL system to the environmental conditions expected during launch and subsequent operation in orbit, that is, environmental testing. The third objective is to have an efficient facility for the manufacture of the SBL operational systems, once to development phase of the program is complete.

To do so, a three phase construction plan has been developed. In the first phase, all the site preparation, building construction, renovation and test support equipment installation will be provided for acceptance testing of the laser payload element and the integration and high performance testing of the SBLRD space system. This phase of the LTF will consist of the performance test facility, a small remote control center for operations during high energy laser testing and an administrative building for routine office space. In this phase the environmental testing will be done at another location (the location of which has not been decided at this point), for performing various tests of the system's tolerance to conditions expected during launch and while in orbit. Dedicated environmental test facilities are not going to be built during the first phase as a cost saving measure. The size of the SBLRD system is such that existing facilities will accommodate it, and air transport options are available which will allow the system to be taken from the LTF to the environmental test site and from there to the launch site.

The next phase of the program will commence following the successful completion of the SBLRD. As the program enters EMD, additional facilities will be required. The EMD system is expected to be considerably larger than that of RD. This will necessitate an enlargement of the performance test facility, both to accommodate the larger physical dimensions of the system, but also to provide for added pressure recovery system capacity required for the more powerful laser element. The design of the phase one facility will allow for the effective installation of the new equipment without extensive modification to the building structures themselves.

Also in the next phase will be the addition of dedicated environmental test facilities. These facilities are needed for two key reasons. First, the EMD system is too large for effective testing in any currently available facilities. Secondly, it is not feasible to transport the EMD system by air. Therefore, any movement from the performance test facility to an environmental test area would have to take place using barge transport. The time involved and the risk incurred by having to rotate the system from vertical to horizontal and back again, militate against any concept other than a relative co-location of these various facilities. By having the environmental test facilities nearby to the performance test chamber, these problems are eliminated. Transport vehicles can cover the relatively short distances involved while carrying the spacecraft in its vertical orientation, thus eliminating any requirement for rotation. This was the origin of the campus concept for the LTF installation.

The second reason is the need to have room for the production facilities. As the program moves from EMD to production, significant space will be required to handle the payload elements as they are manufactured at various contractors sites. The major elements will be shipped to the LTF for integration and testing, as they had been in the EMD phase. But in production, there will be many more units with which to cope. Processing concepts have been developed which envision an assembly line of major elements moving through each of the necessary steps of integration and assembly, test, further integration, further test, and finally shipment to the launch site. With the production rates anticipated, it will be necessary to have multiple stations for these integration and test functions to be performed. This in turn will require more and larger facilities which must be accommodated on the campus.

In summary, the need for this site to closely tied to the development and production program and its unique attributes. The success of the SBL program and its ultimate capability for

fulfilling a major nation defense policy role, rests in large part on the successful development and operation of the SBL Test Facility.

During this contract year, Schafer participated on a team comprised of government and industry personnel actively involved in the selection of a site for construction of a high energy LTF. The site selection process used by the SBL Program Office to determine a site for the Laser Test Facility, is based an established and approved BMDO Directive. In preparation for the selection of the LTF, the criteria for the selection of the facility site had to be developed. The criteria development was conducted in accordance with the unique requirements of the SBL program, national defense policy guidance and the provisions of applicable DoD regulations and directives

The selection process began with the examination of program goals which were clearly defined and closely tied to the integrated testing requirements established by a team of technical experts comprised of both industry and government personnel. Schafer led the team of technical experts with the assistance of Lockheed Martin, in identifying and establishing the integrated test requirements that would support the development and testing of a space operational system. The team examined areas including: 1) gravitational effects on vertical and horizontal testing of a laser payload element, 2) performance capability achievable for both high power optical beam performance and for acquisition tracking and pointing, 3) detailed end-to-end system performance modeling that could be calibrated and validated in a series of sub-element, element, multi-element and integrated space vehicle tests on the ground which would provide traceability to on-orbit performance, 4) structural dynamics and vibration as a driver in performance error budgets and the physical vibration isolation required in the LTF and 5) the development of a structural vibration/dynamics risk reduction/mitigation plan to assure proper development of sub-element, element, multi-element and integrated space vehicle test plans.

Based on the program goals and test requirements, the facility requirements were then defined A search of existing test facilities and a study of potential modifications, to existing facilities, was completed to ensure no duplication of effort with a test facility, in order to save the government time and money. With the facility requirements and the program operational requirements identified, the development of site selection criteria began. This was a collective effort achieved by the Army Corps of Engineers along with the Space Based Laser Program Office, Lockheed Martin, SciCom, Schafer and other government and industry representatives involved in the siting analysis process. LTF siting criteria assumptions, exclusionary and evaluative criteria were all established. The criteria was prioritized and assigned weights and defined measures. The Army Corps of Engineers then applied the narrowing and exclusionary criteria to a database run of potential sites within the United States. A list of potential sites was generated meeting minimum requirements. A table top evaluation was completed applying the evaluative criteria to screen out marginal sites. The top four sites were determined from this list. The top two sites from DoD, and NASA were then chosen as sites that deemed worthy of a physical inspection Letters were sent to the appropriate agencies requesting permission to examine the sites. A physical site inspection and took place during January 1998 at four sites: Cape Canaveral Air Station, Kennedy Space Center, Redstone Arsenal, and Stennis Space Flight Center. The final site selection will be based on: 1. Siting Analysis, 2. Environmental Analysis, 3. Economic Analysis, 4. Executive and Congressional Guidance.

### 3.2.2.2 Laser Test Facility Environmental Assessment Support

A key criterion in the section of an LTF site is the environmental consequences related to its construction and operation. The environmental aspects of the project have several direct and indirect effects. First is the environmental impact itself. This program, as all others of similar scope, must meet the requirements set forth in various National Environmental Protection Act (NEPA) regulations, as well as similar and related regulations, title and statutes of the state, regional and local jurisdictions. Indirect effects of environmental considerations are the impact on cost and schedule required for documentation of compliance, obtaining requisite permits, and the development, approval and implementation of any necessary mitigation and remediation measures.

In order to fully evaluate the environmental implications of the LTF and to determine whether such implication might bear upon the final site selection, an environmental assessment (EA) for each of the sites was ordered to be performed. The basis for such and EA is usually the preliminary design documentation for the project. However, owing to the competitive nature of the acquisition process in place during this period, the designers were not available for consultation. Therefore, it was decided that the preferred approach for conducting the EA would be for Schafer personnel to collect the necessary data and information, and to make it available to the agency responsible for the EA itself. In this instance, the Army Space and Missile Defense Center (SMDC) was designated as the office with primary responsibility for the EA. In support of SMDC, Schafer worked from a Data Needs Document prepared by the Center. Based on these data needs, design, construction and operational information was developed using existing non-competitive contractor information where available and employing engineering judgement and analysis where is was not. In this section of the report, the data needs fulfillment process is discussed

A key aspect of the EA data collection process is the issue of establishing the baseline design With the re-direction of the program management and objectives, the previous design efforts of the Zenith Star (ZS) program were at first believed to be obsolescent. However, since it became clear that no new design of comparable maturity was likely t be available in a timely fashion, it was determined that even though the former baseline design might differ somewhat from whatever the final design evolves to, the similarities would far out-weigh the differences, and that either would stand as well for the purposes of the EA. With that approach adopted, the EA data collection was conducted based on the ZS parameters.

The EA data needs were spelled out in a document from SMDC and formatted as shown in Appendix 3.2-2. As seen in this attachment, each question is answered in respect to the phase of the program in which the impact might be realized. It is recognized that the most important impacts will be those associated with the initial construction, but the EA must cover all phases of the program. Also noted in the report are the sources for the information provided. Here again, the constraint on information availability made it impact. Since the contractors which had done the original design were involved in a competitive procurement, the best data sources were not permitted to provide the necessary information. For this reason, it was necessary to seek design data from contractors whose familiarity was at a second or third remove from the original design. Even the documentation from the ZS baseline was unavailable or outdated. In such cases, the priority was placed on using a conservative approach in establishing the expected impact. If it was not known whether the construction process would use 20 or 30 acres for waste water

44

containment, the 30 acre value was selected. In all cases, a conservative but representative number was used.

The data need information requests were categorized as follows:

Design and Construction

Socio-Economic

Transportation

Utilities

Hazardous Materials

Health and Safety

Air Quality

The information provided in response to these data requests in shown in Appendix 3.2-2 and will not be further expanded in this section. However the context of responses and the source of the information are discussed in turn.

### Design and Construction

Detailed design information was never developed for the ZS LTF. Preliminary work was completed but not documented. Therefore the information offered in response to the data request relied heavily on the engineering judgement and experience of two organizations: FSEC, Inc. and Black and Veatch, Inc. FSEC had done a considerable amount of work in facilities similar to the anticipated LTF design, where Black and Veatch has considerable experience with program of similar construction scope. Discussions with senior staff members from both companies was invaluable. Some use was made of relevant documentation from older ZS design activities, as well as the experience of Schafer staff members who had worked on the design and operation of the laser test facility at Capistrano Test Site (CTS) at San Juan Capistrano.

In all cases the answers provided were based on their experience and best commercial practice. The construction estimates were based on the assumption of a "green grass" starting point. That is, a case where no advantage was assumed taken of existing buildings, roadways, utilities or other elements of infrastructure. This assumption does not have a markedly different impact from one LTF candidate site to another. In general, the will each require almost completely new construction.

### Socio-Economic

There were only two general areas of concern in this category, construction and operation, both of which arise from consideration of the number of people that the LTF program will bring into the area. To get an estimate of these numbers, reliance made placed on the experience of Black and Veatch with construction jobs of similar scope. From this source the numbers of workers was estimated. The cost of the employment, possibly affecting the local economy, was made using planning factors obtained from Air Force estimating standards.

Estimates of the number of people required for operation was based on previous work reported by Lockheed-Martin during the ZS program. The income for this staff was estimated using cost parameters representation of similar work forces at existing facilities.

45

## Transportation

This category addresses the question of how much road traffic will be associated with the construction and operation of the site. Construction estimates were based on Black and Veatch experience, whereas operational vehicular traffic was estimated from experience at CTS.

## Utilities

Information of the utilities required for the LTF were based on discussions with FSEC, which provided the data relevant to ground support equipment operation, and TRW staff at CTS which provided information on the utilities consumption for a facility with representative infrastructure

## Hazardous Materials

This part of the data needs request was the most difficult to respond to. Most of the specifics of the operating conditions of the high energy laser itself are tied to design choices that have yet to be made  Still it was necessary to provide representative data and information, so reliance was placed on previous analyses that addresses some aspects of the problem. Principally the information was taken from older Lockheed-Martin reports on facility requirements, pressure recovery system operation and discussions with senior Schafer staff members. The result is felt to be within the broad objectives of the data requirement, but does suffer from inconsistencies of design and operational specifics. It is anticipated that this topic may have to be reviewed and revised in the current year's program.

## Health and Safety

The health and safety questions on the LTF refer mainly to the possible impact the facility would have on the public, should there be an accident or other crisis. The specifics of the response were based on preliminary design concepts from the ZS program and discussions with engineers and analysts involved in the project. Further information was obtained from staff at CTS for aspects of the LTF that are expected to be similar to the CTS operation. A notable omission from the response is the calculation of the Explosive Safety-Quantity Distance (ESQD) for handling of explosive materials. This calculation is within the purview of the Corps of Engineers and is expected to be supplied by that organization.

## Air Quality

Air quality questions stem from two principal concerns. First is the emission from construction vehicles and equipment during the construction process. Second is the emission from the LTF itself during operation. The latter category includes both the laser test-related emission and the non-laser emission from vehicles and equipment.

In answering these questions, information was obtained primarily from Black and Veatch (regarding construction) and CTS staff (regarding operation). All of the information provided must be viewed in the same context as previously stated, in that specifics which rely on detailed design have been foregone in favor of conservative engineering estimates.  As with the consideration of hazardous materials, the questions about air quality may have to undergo additional analysis in the coming year.

### 3.2.3 Cost Analysis Support

See Appendix 3.2-3.

## 3.3 SMC Modeling and Simulation

Attended TRW and LMA interchange meetings. Supported government team M&S meetings. Provided listing of past SBL analyses to Sparta. Evaluating NMD constellation sizing for a parametric set of powers and diameters to determine the performance against the new missile in a salvo. Participated in BVR evaluations. Development of an automated SBL error budget has begun, as part of the overall activity to review system engineering issues. The computer program, written primarily in Visual Basic, is designed to be flexible and provide a system engineering tool for analyses of critical measurable parameters of the SBL system and subsystems. The modular design allows for top-down system performance parameter allocations, bottom-up performance parameter assessment, and a wide range of performance parameter comparisons based upon realistic technology limits and predicted technology enhancements. This tool is necessary because existing spreadsheet tools are nearing the end of their usefulness as design issues become more complicated.

Measures of Effectiveness and Measures of Performance for an SBL system are being developed, in response to an action from a previous M&S meeting. A "function line" (similar to a time line) has been created that provides an outline of the functional steps required for a measure of SBL success. Attaching the hardware constraints and quantifying the inputs to the "function line" is the next step.

Attended TRW and LMA interchange meetings. A revised white paper on TMD performance was submitted to Brown. Work on a paper describing SBL history was begun. Analysis of the BVR error budgets is continuing. Support to a variety of internal SMC meetings was provided. Most of this activity is competition sensitive and had been separately reported.

Attended TRW and LMA interchange meetings. Analysis of brightness budgets from the first BVRs was completed and reported. Preparation for upcoming M&S meetings was begun. Lethality support continued including discussions of low-irradiance lethality issues.

Attended TRW and LMA interchange meetings. M&S meetings/telecons were supported. A number of planning activities in support of the SMC FY 99 plan were completed. These activities are confidential to SMC and cannot be reported in detail. Results of the analyses were discussed and further analysis plans are being developed.

System engineering support was provided, both in planning support and a variety of technical issues. The scaling of SBL performance as a function of primary mirror aperture size, laser wavelength, and laser power was analyzed. The results of the analysis show that "brightness saturation" occurs if beam control system performance cannot be improved in (quadratic) proportion to increasing beam diameter and decreasing wavelength. The theoretical brightness

curve should never be used for scaling analysis without the inclusion of wavefront error and jitter terms.

Support for the modeling and analysis activity continued, in preparation for the M&S meeting scheduled for early December in Colorado Springs. The effort includes evaluation of trends in system performance, with varying brightness, power, primary mirror diameter, lethality, and jitter, to provide a complete set of performance results for costing analysis. This analysis is for NMD and for the latest missile type. Two different lethality models were used. The AFRL model uses somewhat higher fluence, and kill times increase exponentially at lower irradiances. The Howie model uses lower fluence and kill time increases more linearly at lower irradiance. There are major differences in system performance for the two lethalities. The Schafer analysis uses 216 war start times for each "battle". This sampling density is critical to determine when coverage gaps appear. The more detailed analyses continue to show what simpler studies have suggested: low jitter is required for brighter, more capable systems.

A series of system architecture analyses were produced to evaluate sizing for an SBL constellation. Trends in system performance were evaluated considering brightness, power, diameter, lethality, and jitter. System performance was then correlated to cost to address the issue of affordability.

The software being used to perform this evaluation is the ISAAC Suite, which is a set of programs taking performance evaluation of an SBL constellation from beginning to end. It includes modules that produce threat sets, performs constellation design, calculates m-on-n scenarios, produces graphics, and evaluates the resulting output.

The overall approach used to perform constellation-sizing analyses is to specify a set of inputs to ISAAC, using ISAAC to calculate the performance of each constellation, optimize the constellation design for a single inclination, and iterate on complex constellation designs with multiple inclinations to minimize the number of satellites required for different latitude regions of coverage. The optimized performance results are then correlated with cost to address affordability.

### 3.3.1 Systems Analysis

In the past two years the technical direction philosophy of the SBL program has been revised to emphasize technologies that support far-term objectives rather than the near-term objectives of the previous approach. In this context far-term objectives refer to those associated with high hardness strategic threats and near term objectives refer to those associated with lower hardness theater threats. The near-term approach was always traceable and scalable to a far-term system, however, major program revisions are associated with the planned space experiment, now referred to as the Integrated Flight Experiment or IFX, and the initial operational capability (IOC) platform. Previously, the IFX was directly linked to a near-term IOC and the lower hardness theater threat; now the IFX will be linked to a far-term IOC and the higher hardness strategic threat

System level analysis performed to guide this change of direction is reported here. Since the near-term approach was always traceable and scalable to far-term objectives, the technologies associated with the far-term were already recognized and the revised technical direction occurred smoothly. A briefing which documents the **SBL Growth Path** and the required top-level system parameters was prepared and presented at SMC. The briefing is summarized below and included as Appendix 3.3-1.

As the SBL program emphasis shifted from near-term to far-term threats, there arose a concern associated with the hardness of far-term threats. Near-term threats are much better understood, so the concern was the degree to which the uncertainty in the far-term hardness would disrupt the far-term system designs of the conceptual design study(CDS) contractors. A briefing which documents the impact of **Far-term SBL Lethality** uncertainty on the top-level SBL system parameters was prepared and presented at SMC. The briefing is summarized below and included as Appendix 3.3-2.

Also, as the SBL program emphasis shifted to strategic threats, a concern arose regarding the SBL system applicability to theater threats, which have a much more stressing time-line because of the much shorter boost-phase time. A briefing which documents the **Theater Missile Defense(TMD) Time-line** and the **Feasibility** of a far-term SBL system for this application was prepared and presented at SMC. The briefing is summarized below and included as Appendix 3.3-3

As ballistic missile technology, including hardened composite materials, proliferates, the SBL system counter-countermeasure approaches include: (1)increased platform brightness and agility, all other parameters fixed; (2)increased number of platforms in the battle, which amounts to increasing the total number of platforms at fixed altitude and brightness in order to maintain coverage, and (3)decreased range, which amounts to increasing the total number of platforms at fixed brightness and decreasing altitude in order to maintain coverage. Previous cost studies have shown that approaches (2) and (3), which do not require a non-recurring cost investment in technology development, are ultimately not cost-effective because of the large recurring cost component associated with increased platform number. Ultimately, when technology scalability limits are reached, approaches (2) and (3) become necessary, however, by invoking approach (1) now the required technologies will be available when needed.

Acknowledging the limits of power scaling, increased brightness can best be achieved with increased diameter projection apertures and the required line-of-sight stabilization(jitter reduction) and with reduced beam divergence associated with shorter laser wavelength and reduced wave-front error. Invoking these factors leads to the conclusion that 12 to 20 meter diameter beam directors and wavelengths of about 1 micron are required to address far-term threats.

The principal conclusion of this study is that, regardless of the lethality assumption, the technology development goals associated with large deployable apertures in the 12 to 20 meter range are appropriate to address far-term threats. The difference between the two assumptions can be accounted for with platform number: for example, under the more stressing assumption,

40 platforms are required and under the less stressing assumption 30 platforms, with all other top level parameters the same.

In this study a detailed pre-engagement time-line for SBL activation is determined. The results show that with reasonable time allocations for pre-engagement functions, a total pre-engagement time delay of 10 seconds is a conservative estimate. With this pre-engagement time delay, model calculations show that for a far-term hardness TMD threat a baseline NMD system is effective for TMD threats with ranges as short as 150km.

### 3.3.2 HF, DF, Overtone

#### Basic Operation

As with all lasers, chemical lasers consist of a gain generator and a resonator. The gain generator produces a region of flowing gas where the chemical laser molecules exist in an excited state The resonator provides optical feedback which allows initially-random fluorescent emission to build into stimulated emission and thus lasing. A simple analogy is the fluorescent light bulb, where gas molecules are excited by electric discharge. The emitted light is omnidirectional. If the gas mixture and characteristics were carefully controlled, and resonator mirrors added at each end of the fluorescent bulb, a laser would result, with the laser energy coming out of the end, rather than the side, of the bulb.

HF, DF, and Overtone lasers are all very similar (many aspects identical). In all three types, an oxidizer, either fluorine or a donor (usually $NF_3$), is burned in a combustor with hydrogen or deuterium An HF laser uses deuterium as the combustor fuel, while a DF laser uses hydrogen Use of the "opposite" isotope prevents the formation of ground state molecules in the combustor, which would prevent lasing by their high absorption. The combustion process results in thermally excited free fluorine ions. These ions are expanded through a nozzle and mixed with a secondary flow of hydrogen (for HF) or deuterium (for DF). Further chemical reactions form $HF^*$ or $DF^*$ (the excited states of the molecules). The overtone laser versions of either HF or DF are identical The overtone lasing is achieved through control of the optical properties of the resonator (more below).

As in any laser, a "population inversion" is necessary for lasing. In chemical lasers of this type, the vibrational/rotational energy levels of the molecule are excited. There are three sets of states that are important: the ground state, the first excited state and the second excited state. Each excited state has a number of sub-levels corresponding to the structural modes of the molecule The population of excited states must be "inverted" in order for lasing to occur. This means that more molecules exist in the second excited state than the first, and more in the first than in the ground state. The lasing wavelength is determined by the energy difference between the excited states. Lasing can take place when molecules are stimulated to emit radiation between the second and first states (the 2-1 transition), the first and ground states (the 1-0 transition), or between the second and ground states (the 2-0 or "overtone" transition). Other higher or more complex transitions are possible, but are not efficient. The most probable energy path is the 2-1, then 1-0 transition. Unless such a path is suppressed, the overtone transition will not lase. HF

50

and DF lasers differ only in that the energy difference for the transitions is slightly smaller in DF, resulting in longer wavelength emissions.

As with all lasers, a resonator must be used to provide sufficient feedback for lasing to start. Gains for the 2-1 and 1-0 transitions are generally much higher than the gain for the overtone transition. The overtone laser uses a set of resonator mirrors which are highly absorptive for the fundamental wavelengths, and highly reflective for the overtone. The additional loss introduced into the 2-1 and 1-0 transitions keeps them below the lasing threshold. The laser then runs on the 2-0 transition. Both HF and DF can be run on their overtone lines, although most work to date has been with HF overtone.

HF and DF lasers produce gain on a number of transitions simultaneously, and usually have sufficient energy to run on 4-8 wavelengths at the same time. The table at the end shows typical operating wavelengths (information used in the table courtesy of Jeannette Betts from TRW). Note that there are potential differences in wavelength depending on measurement technique, and accuracies in the table may not be as good as the number of significant figures might indicate. The gain distribution is not uniform in the downstream, or flow, direction. Different transitions have peak gains closer to the nozzle exit plane, and others further. In general, the higher number transitions have peak gain closer to the nozzle exit. The location of the resonator optical axis thus has significant impact on which lines lase, and shorter or longer wavelengths may run as a result.

### Differences and Relative Performance

The simplest difference is the output wavelength. All HF/DF lasers operate on several lasing wavelengths simultaneously (except when "line selected"). The approximate average wavelength of the HF laser is 2.8 um. The approximate wavelength of the DF laser is 3.8 um. The overtone wavelengths of each are nearly half of the fundamental (HF at 1.3 um, DF at 1.8 um) The wavelengths of the overtone transitions are determined by the energy difference between the second excited state and the ground state. The first excited state is not quite midway between, so the wavelengths do not have an exact factor of two relationship. The DF overtone has not been of much interest. The overtone laser (either version) generally is less efficient than the fundamental because some energy is lost and less overall energy can be extracted. Some experts believe that an overtone efficiency of 80% of the fundamental can be achieved. Most operating lasers to date have achieved the 40-60% range. If perfect optical operation can be achieved, the wavelength advantage for the overtone means that "breakeven" is at about 25% efficiency Actual efficiency comparisons must be done on a weight basis and are much more complex. There is no study to date that shows a detailed comparison between an overtone and a fundamental system, all other factors being held at equal technology levels.

There should be no significant difference in performance between HF and DF lasers on a watt/pound of system weight basis. The overtone version of either laser should operate at roughly 60% (i.e., about 1.67 times as heavy per watt of output). Brightness performance is much more complicated and driven by many optical technologies. The chart below (Figure 3.3-1) shows relative brightness of the four types of lasers as a function of the system wavefront error.

51

The three vertical lines show experimental results (left-most), current goal (middle) and projected operational system performance (right-most). At projected performance levels performance differences are relatively small, with HF and HF OT nearly the same, and the other two about 10% (DF OT) and 30% (DF) less bright. The engineering difficulty of achieving OT performance is significantly larger than achieving Fundamental performance due to the relative lack of maturity of the OT devices.
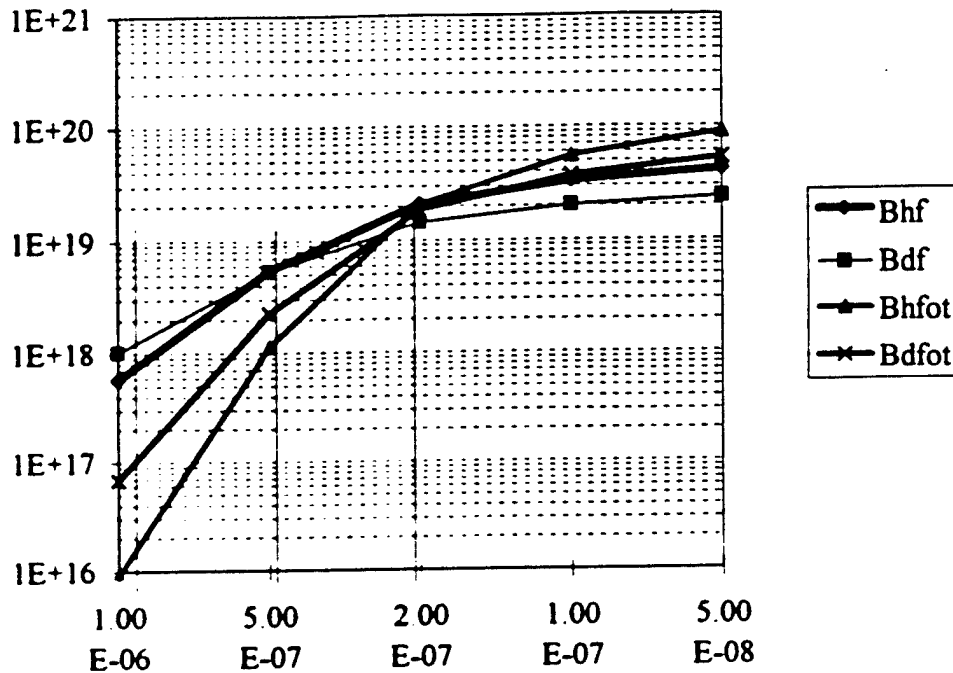


**Figure 3.3-1. Brightness vs. wavelength**

**Line Selection**

HF or DF lasers can be made to run on fewer wavelengths either by using gratings to preferentially reflect certain wavelengths, or by coating mirrors with narrow band coatings which suppress unwanted lines. Energy transfer through the various excited states follows pathways determined by quantum selection rules. Selecting a single wavelength will not efficiently extract energy, since much of the energy will be "stuck" in other excited states until the gas flow removes those molecules from the lasing region. Efficient operation on a smaller number of lines is possible, and such experiments have been conducted at the University of Illinois.

**Atmospheric Transmission**

Just as molecular lasers emit light, molecules that are in resonance with that light will absorb it (in addition, scatter, turbulence, and other effects play a major role). Water vapor has a

52

complex molecular absorption profile that is strongly absorbing over the range from about 1.35 um to about 1.5 um, from 1.8um to 2.0 um, and from 2.5 um to 3.5 um. As with any molecular absorber, absorption can vary by orders of magnitude over very narrow changes in wavelength, even within generally absorbing regions. Both HF overtone and DF propagate well through the atmosphere, while HF fundamental propagates poorly. These general statements must be modified by looking at particular lasing lines under specific atmospheric conditions. On a very dry winter night, at least one HF fundamental wavelength may penetrate to the ground from space. During a rainstorm, no wavelength may penetrate to the ground (although the mechanism may be scattering rather than absorption). For system engineering purposes, we tend to use a single absorption per kilometer number to represent some average condition for each wavelength.

Atmospheric transmission must consider both the path through the atmosphere and the conditions over that path. Transmission to the ground may also not be needed for many applications. Absorption is highly non-linear with path length, and is greatly reduced with altitude. If we want to kill a missile at first opportunity, it may still be several kilometers above the ground by the time it can be prosecuted. A cruise missile, on the other hand, may be only a few hundred meters above the ground.

**Typical Operating Wavelengths**

The table below shows typical operating wavelengths. More detailed information for a few lines is shown subsequently.

| Laser Transition | Wavelength |
|---|---|
| HF overtone (2-0 transition) | |
| P(2) | 1.3045 |
| P(3) | 1.3126 |
| P(4) | 1.3212 |
| P(5) | 1.3305 |
| P(6) | 1.3404 |
| P(7) | 1.3510 |
| P(8) | 1.3622 |
| P(9) | 1.3737 |
| HF fundamental | |
| $P_1(5)$ | 2.672653 |
| $P_1(6)$ | 2.707523 |
| $P_1(7)$ | 2.744129 |
| $P_1(8)$ | 2.782643 |
| $P_1(9)$ | 2.823137 |
| $P_2(3)$ | 2.727504 |
| $P_2(4)$ | 2.760466 |
| $P_2(5)$ | 2.79525 |
| $P_2(6)$ | 2.831923 |
| $P_2(7)$ | 2.870551 |

| | |
|---|---|
| P$_2$(8) | 2.911212 |
| P$_2$(9) | 2.953986 |
| P$_2$(10) | 2.998959 |
| DF fundamental | |
| P$_1$(7) | 3.6449 |
| P$_1$(8) | 3.6789 |
| P$_1$(9) | 3.7142 |
| P$_1$(10) | 3.7508 |
| P$_1$(11) | 3.7887 |
| P$_2$(7) | 3.7648 |
| P$_2$(8) | 3.8001 |
| P$_2$(9) | 3.8369 |
| P$_2$(10) | 3.8749 |
| P$_2$(11) | 3.9144 |
| DF overtone | Not available (around 1.8um) |

The table below shows HF OT line measurements. Bill Jeffers at Helios measured 2 unspecified lines to accuracies of 0.2 cm$^{-1}$, or wavelength accuracies of about +/- 0.00004 μm. This is sufficient accuracy to compare with the McDonnell Douglas water vapor absorption cell measurements, but not sufficient to make precise arguments for those lines near the edge of a water vapor resonance. Several of the lines are clearly too far from resonance for absorption to be a major issue

| Wavelength designator | Wavelength | Wavenumber | Transmission 1.2 km to space |
|---|---|---|---|
| Iodine | 1.315246 | 7603.1385 | .93 |
| P3 | 1.31256 | 7618.71 | .90 |
| P4 | 1.32122-6* | 7568.33,7568.76* | .88,.84 |
| P5 | 1.33052, 1.330499 | 7515.86, 7515.98 | .72, .26 |
| P6 | 1.3404 | 7460 46 | .37 |
| P7 | 1.30957 | 7402.16 | .01 |
| P8 | 1.362166 | 7341.25 | 0 |

*measured vs calculated. Measurement technique is unknown, perhaps absorption spectroscopy.

The only two available (of the probable four) MacDac data sets is also attached, as are a series of FASCODE runs which match the data reasonably well, although with lower resolution. There are gaps in the wavenumbers/wavelengths covered (the working notes found are clearly incomplete) Some of the measured OT spectra indicate that the higher lines run. These generally have poorer transmission. The x$_c$ data show that if the optical axis is moved downstream, the shorter wavelengths tend to run. Assuming that the efficiency is available, we would clearly like to run at as short a wavelength as possible. Lee Sentman (UIUC) has also made some progress in line selection that may be of use.

### 3.3.3 SBL Disturbance Spectrum

An issue was raised as to the validity of the SBL disturbance spectrum in the AMSD specification. The disturbance spectrum in the specification seemed very familiar. Many of its characteristics were similar or identical to the output jitter spectra estimations for the SBL operational system (low frequencies) and the ALI output spectrum (higher frequencies). The units (acceleration) were also puzzling. The original disturbance spectra were expressed as PSDs in $\mu$ $rad^2$/Hz, an appropriate set of units for a jitter spectrum. The low frequency disturbances were generated by estimates (from analytical models) of turbulent flow in the reactant supply pipes and from gain generator disturbances. The higher frequency (above 50Hz), were the result of mirror vibration due to coolant flow. The coolant flow disturbances will not exist in future SBLs because of the advances in uncooled optics.

Schafer (Golnik) spoke with a number of people in the AF SMC SPO to try to determine the origin of the information. The only one who seemed to remember sending any information to AFRL was Kevin Zondervan (Aerospace). He recalled sending information from ALI/ALO which is consistent with the jitter spectrum. He did not recall ever seeing an acceleration spectrum.

I also spoke at length with Jim Wells of the Schafer LA office. Jim was a key person, while at TRW, in developing the disturbance estimates. He has recommended a program to develop better disturbance estimates, and has commented that there were errors in some of the old estimates, which should thus be considered suspect.

The expected SBL on-board disturbances will likely come from several primary sources: reactant flow in the storage and feed system; combustion in the laser; reactant flow through the EMA and unbalanced exhaust forces; "ringing" of the spacecraft due to induced slewing motions; rotational frequencies of CMGs (if used); thermal effects on the structures; on-board mechanisms (power conditioning, etc.); and optical control elements (fast steering mirrors). These disturbances will be isolated from the spacecraft if they are large. The primary mirror assembly will be further isolated from the spacecraft (passively or dynamically). The calculation of the expected disturbance at the attachment points of the PM, for example, is thus very difficult to calculate We do not have a structural model of an SBL which can be used. I caution against overly-conservative estimates that make the PM design job very difficult. At the same time, a disturbance "floor" is very difficult to determine. More SBL design work is necessary, but is not in the near-term plan.

### 3.3.4 SBL Technical Briefings

Schafer developed a plan which could be used to reduce the number of analyses needed to develop a full study of possible SBL architectures. The plan was described in a briefing, which is included below. Other briefings are included in Appendix 3.3-4.

**Schafer**

## Architecture Study Neck-down Plan

Gary Golnik
Schafer Corporation
20 January 1999

10 January 1999                    CONFID                                    1

- General Considerations
  - Although the number of possible permutations is high, many trades are independent, and thus the number of realistic permutations is very limited
  - For those permutations that must be studied, limit analyses should be used instead of parametric analyses
  - Further constraints due to policy, launch, or ancillary missions only increase cost; develop the lowest cost approach and then determine cost increases due to changes
  - Certain "design details" are independent of permutations and can be pursued in parallel
  - A number of independent trades should be pursued in parallel
- Approach is divided into three major sections:
  - Determine "policy envelope"
  - Develop individual platforms' characteristics
  - Determine constellation performance and cost
- Final task in neck-down phase should be development of specification for contractors

19 January 1999　　　　　　　　　　OOWP02　　　　　　　　　　2

---

**Schafer**　　　Trade Space/Methodology (1)



19 January 1999　　　　　　　　　　OOWP02　　　　　　　　　　3

57

*Schafer*
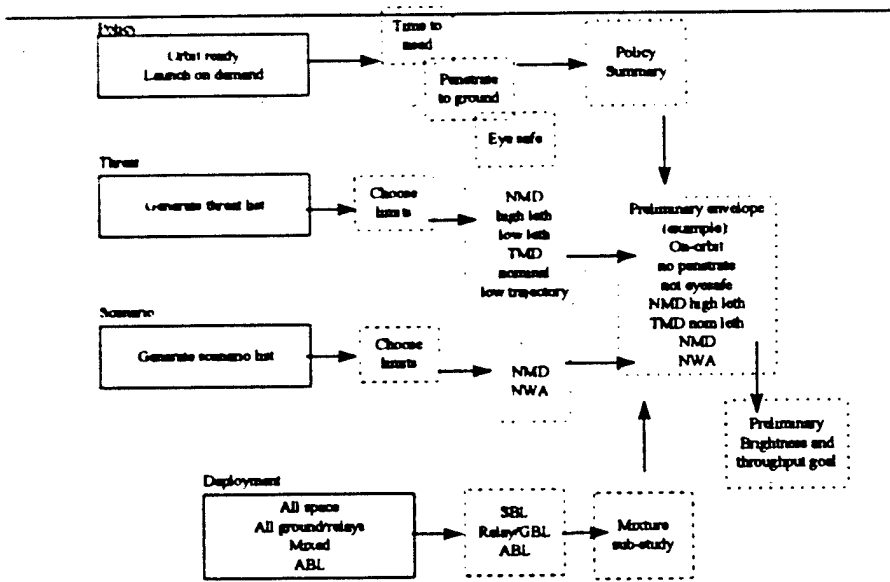
Possible Systems
SBL Only
GBL only
Hybrid
ABL-augmented

Hybrid: Needs FMs for
geometric coverage, then
add SBLs and GBLs until
lowest cost solution is
achieved

FM - Fighting Mirror

☐
Monocle Relay or High SBL

SBL or FM    SBL or FM

○            ○ ◇ GBL

Target  Target
SBL or FM    ○○    ○○    SBL or FM
SBL or FM    SBL or FM

○
Target

SBL or FM    SBL or FM
○            ○

☐
Monocle Relay or High SBL

10 January 1999          OO44P02          4

---

*Schafer*

Preliminary
brightness and
throughput grid

Platform Characteristics

Deployment
SBL
Relay/GBL
ABL
Mix

SBL
Laser
Optics/Beam control
Spacecraft

Effective
brightness vs
weight
cost
cost vs
technology

GBL/Relay
Laser
Optics/Beam control
(Relay/FM Beacon set)
Spacecraft
Uplink

Effective brightness vs
weight (space)
Ground asset complexity
cost
cost vs technology

ABL (from
SPO)

Laser Type Substudy
Sigma, delta limit for space
Scaling power ratio limit

Acceptable
lasers

10 January 1999          OO44P02          5

58

### 3.3.5   System Architecture Analysis

A series of system architecture analyses were produced to evaluate sizing for an SBL constellation. Trends in system performance were evaluated considering brightness, power, diameter, lethality, and jitter. System performance was then correlated to cost to address the issue of affordability. The subject of cost is written up in the costing section of this report. A classified Appendix will be delivered under separate cover.

The software being used to perform this evaluation is the ISAAC Suite, which is a set of programs taking performance evaluation of an SBL constellation from beginning to end. It includes modules that produce threat sets, performs constellation design, calculates m-on-n scenarios, produces graphics, and evaluates the resulting output.

### 3.3.5.1   The ISAAC Suite

The ISAAC Suite consists of a set of programs that provide the tools to perform System architecture analysis. ISAAC, which stands for Integrated Strategic Architecture Analysis Code, is at the heart of this suite. ISAAC is a deterministic, discrete timestep, m-on-n simulation which is used to architecture analysis for varying war start times. It provides rapid exploration of a significant parameter space without sacrificing fidelity to evaluate constellation performance. In

each timestep, the code updates the status and position of each SBL and each target. The code flies out the threat, accounts for all the necessary calculations in the timeline, calculates the brightness and aspect and delivers the required fluence to the target. It performs all the battle management functions and provides deconfliction between the different platforms in the constellation.
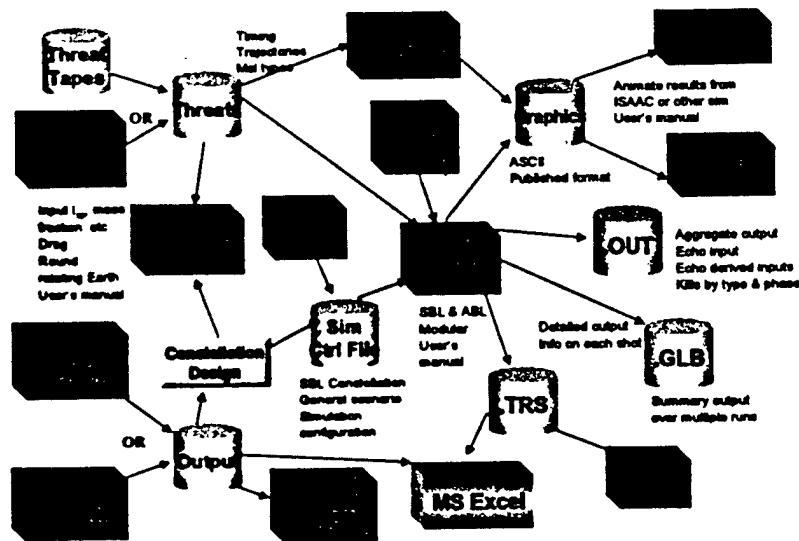


**Figure 3.3-2 :  The ISAAC Suite – Integrated Strategic Architecture Analysis Code**

Figure 3 3-2 shows the general flow in utilizing the various routines in the ISAAC suite. The threat scenarios are either provided on threat tapes or generated by ETA-T, which performs all the flyouts and creates trajectory information based on missile characteristics and location inputs  Constellation design is performed using ETA-S, JACOB and ETA-G.  These programs each provide a different type of output that allows for a thorough review of constellation design for sensor type constellations.  The output can be used as an initial assessment of constellation design for an SBL system  The next step is to run the constellations in ISAAC to determine whether or not that constellation is adequate as an SBL constellation under various threat scenarios  Because of factors such as aspect angle, circles cannot describe coverage so the scenarios must be played out in an architecture program to assure the constellation can handle the threat  ISAAC utilizes input from an atmospheric propagation program called SBLE that accounts for atmospheric losses due to extinction and turbulence.  These losses are mainly a factor in ear limb or across the limb shots.  The output from ISAAC can be utilized to graphically view the scenario.  ESAU is used to create a graphical depiction of the scenarios, which enables the user to visually synthesize the effectiveness of the system and battle management issues.  It will also show any problems with threat flyouts provided to ISAAC.  Output tables are created that are used to evaluate statistics of the scenarios concerning multiple war start times or scenarios

### 3.3.5.2 Approach

The overall approach used to perform constellation-sizing analyses is to generate a threat set of interest, evaluate constellation sizing optimums using Rider's method, and creating a parameter space to investigate depending on this initial assessment. Figure 3.3-3 shows the next series of steps following this initial assessment. At step 1 we specify a set of inputs to ISAAC and then use ISAAC to calculate the performance of each constellation in step 2. These 2 steps are iteratively performed millions of times to evaluate all necessary permutations of the input parameters. This yields a set of results where the minimum number of satellites for each power, diameter, jitter, and lethality trade can be determined by evaluating all possible combinations of the input parameters: altitude, rings, inclination, and phase. We can then determine the optimized constellation design for a single inclination for the threat scenario used. The next step will be to iterate on complex constellation designs with multiple inclinations to minimize the number of satellites required for different latitude regions of coverage. The optimized performance results are then correlated with cost to address affordability.



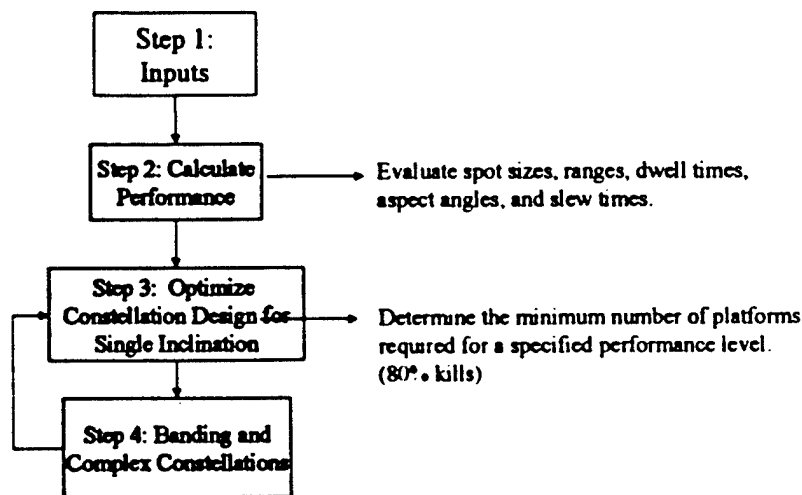Figure 3.3-3— Approach to optimizing constellation design

### Step 1 – Specify the inputs to ISAAC

Step 1 is to specify the inputs to ISAAC. These include parameters associated with the platform brightness, the constellation design and the threats.

The platform brightness is described by

$$B = \frac{\pi PD^2}{4\lambda^2} K_o K_p e^{-(2\pi\delta_l)^2} e^{-(2\pi\delta_b)^2} \frac{1}{\chi^2} \frac{1}{1 + \left(2.22\frac{\sigma_{jl}}{\sigma_d}\right)^2 + \left(2.22\frac{\sigma_{jb}}{\sigma_d}\right)^2 + \left(2.22\frac{\sigma_{jt}}{\sigma_d}\right)^2}$$

**Equation 1: The Brightness Equation**

where the parameters are defined in Table 3.3-1.

**Table 3.3-1: Brightness Equation Parameters**

| equation parameter | name | units | parameter space evaluated |
|---|---|---|---|
| B | Brightness | Watts/sr | (classified) |
| P | Power exiting the laser scraper within the clear aperture | Watts | (classified) |
| D | Diameter of the exit aperture at the primary mirror | meters | 8, 12, 16 |
| $\lambda$ | The power weighted average output wavelength. | meters | $2.83 \times 10^{-6}$ m for the HF laser |
| $K_o$ | The effective brightness reduction term due to obscurations | dimensionless | 0.71 |
| $K_r$ | The fraction of power lost by absorption or scatter in optical components after exiting the laser | dimensionless | 0.98 |
| $\delta_l$ | The wavefront error (RMS $1\sigma$) due to aberrations in the laser after correction by the beam control system | fraction of a wave at the operating wavelength | 0.045 |
| $\delta_b$ | The equivalent wavefront error term for the beam control system. | fraction of a wave at the operating wavelength | 0.05 |
| $\chi$ | This term is allocated to polarization effects, or other non-phase terms that might degrade laser output quality without inducing wavefront error. | dimensionless | 1.02 |

| | | | |
|---|---|---|---|
| $\sigma_{jl}$ | The net corrected jitter (RMS $1\sigma$ single axis) at the scraper, divided by the beam expander magnification. Jitter is defined as any beam tilt motion at temporal frequency greater than or equal to 2 Hertz. | radians | Total jitter of 50, 100, 150, and 200 nrad. |
| $\sigma_{jb}$ | The net corrected jitter ($1\sigma$ single axis) in output space due to the beam control system. | radians | |
| $\sigma_{jt}$ | The net corrected jitter (1s single axis) in output space due to the tracker system. | radians | |
| $\sigma_d$ | The diffraction angle $\lambda/D$. | radians | $\lambda/D$ |

Details on the derivation of this equation as well as related equations can be found in reference[1]  Other parameters not specifically included in the brightness equation but required for input are the boresight drift rate, the boresight offset angle, the settling times, and the slew rates.

The constellation design is specified by: the number of rings in the constellation, the number of satellites per ring, the inclination angle of the constellation, the altitude of the constellation, and the walker number. The parameter space investigated is specified in Table 3.3-2

**Table 3.3-2: Constellation design parameters**

| Name | Parameter Space Investigated |
|---|---|
| Number of rings | 4, 5, 6 |
| Number of satellites per ring | factors providing up 100 total satellites in the constellation |
| Inclination angle | 50-60 deg, though the optimum number was always 54, 55, or 56 for this specific threat |
| Altitude | 600, 700, 800, 900, 1000, 1100, 1200, 1300, 1400, 1500 |
| Walker number | all possible |

The last set of inputs required includes all values associated with the threats. The analysis described in this final report has been performed for a single classified scenario described in the classified appendix.

---

[1] Golnik.G.. memorandum on "Brightness. Far Field Irradiance, Kill Time Equations," 23 July 1996, GG-96B-06a

## Step 2- Calculate Performance

ISAAC is then used to calculate performance for each of the permutations being evaluated in the input matrix. The code evaluates more than 200 war start times across an effective period of the constellation. Figure 3.3-4 shows a sample of the ranges with time of a constellation with 4 rings and 7 satellites in each ring. Each point on each curve represents the range of a satellite to a point at a given latitude and longitude with time. Each narrow sinusoid is the track of a single satellite. Each wide sinusoid signifies a ring of satellites and is represented by a color. The pattern shown in Figure 3.3-4 eventually repeats itself. The averaging period provides a fair representation of coverage with time. Figure 3.3-4 illustrates the need to average over a representative period. Averaging over shorter periods such as 50 minutes would completely miss the sparsest regions of coverage.
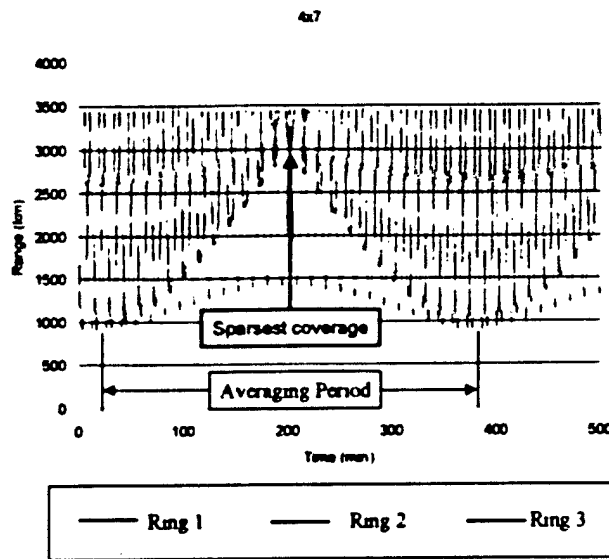


**Figure 3.3-4: Orbital periods of a 4x7 constellation.**

The output from ISAAC can be used to evaluate statistics on spot sizes; engagement ranges, dwell times, starting times of engagement, ending times of engagement, altitudes of engagement, aspect angles of the targets at engagement, fuel usage, slew times, and intensity on target. A sample statistical output is shown Figure 3.3-5.
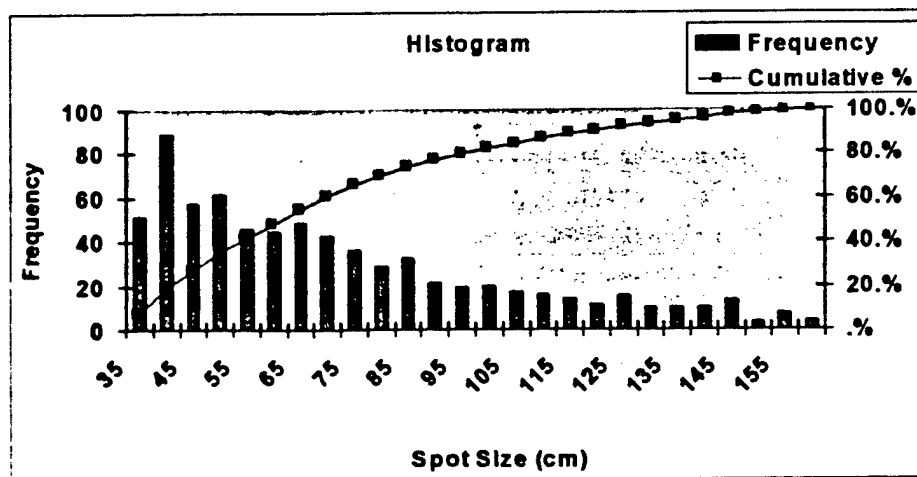
64

**Figure 3.3-5. Example of ISAAC Statistical Output**

## Step 3 – Optimize Constellation Design for Single Inclinations

The next step is to evaluate the large parameter space of results and determine the optimum combination of altitude, inclination angle, phase, and ring number by determining which combination provides the highest average percent of kills for the scenario of interest. In other words, each number combination is evaluated. So if the number of satellites is 20, then 4 rings of 5 satellites and 5 rings of 4 satellites are evaluated. For those 4x5 and 5x4 combinations, altitudes ranging from 600 km to 1500 km were evaluated, inclinations of 54, 55, and 56 degrees were evaluated, and Walker numbers of 0, 1, 2, and 3 for the 4 ring case and of 0, 1, 2, 3, and 4 for the 5 ring case were evaluated. Patterns arising in the average percent of kills output were also evaluated. Definite altitude and inclination angle optimums were present for a particular threat type and scenario. Though patterns were present for phasing and ring number, these tended to be more randomized. Summarily, a significant parameter space needed to be evaluated to optimize the constellation because all phasing possibilities or all ring number possibilities can cause the average percent kills to vary >10%. When effects of the variations are combined, i.e. phasing and number of rings the variations can be >20%.

## Step 4 – Banding and Complex Calculations

Step 4 is to look at constellations comprising multiple inclination angles. This step has not yet been performed in the analysis. Streets of coverage calculations indicate that significantly greater numbers of satellites are required to provide global coverage versus coverage over only mid latitudes. Covering the equator is particularly problematic. "Small" holes open up at the equator for a constellation with optimum coverage in the midlatitude regions. Often the number of satellites must be doubled to close these holes in a simple constellation. Satellite constellations with multiple inclinations may be able to provide global coverage with equal performance using

65

fewer satellites. A simple example would be a constellation that optimizes coverage in the midlatitudes with a single equatorial ring to close the holes around the equator.

## Step 5 – Costing

The affordability issue is addressed by relating costing to performance as shown in Figure 3.3-6. Life cycle cost for each SBL unit is determined for each set of input factors such as power, diameter, wavelength, and jitter. The details of this life cycle cost estimation are covered in the cost section. The outcome of the optimization on performance provides the minimum number of satellites required to achieve a certain level of performance. These numbers can then be used to estimate cost for an entire operational system along with specifics that affects cost such as the number of rings in the constellation. Given a parameter space of power-diameter-jitter combinations for equivalent performance a determination of minimum cost solution for that performance can be made.
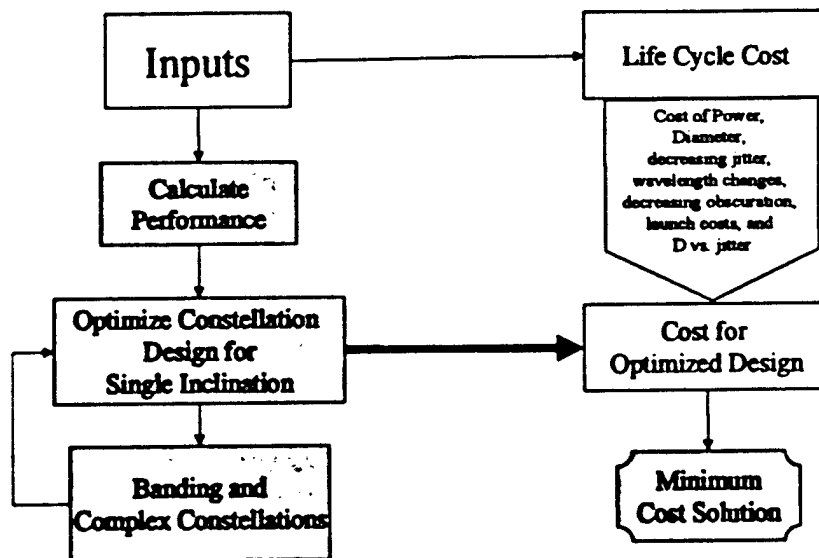


**Figure 3.3-6: Approach to determining affordability**

### 3.3.5.3 Assumptions for Current Analysis

The general categories of assumptions that were made to perform this analysis include; scenario, threat, performance, statistical, and input assumptions. The unclassified assumptions are discussed in this document. Classified information is included in the classified appendix.

## Threat Assumptions

The threat type assumed in this analysis is an NMD missile. There are two lethality estimates associated with this threat that have been used. They are both shown in Figure 3-3.7. One estimate was produced by AFRL and the other by Steade Howie of ARA.

S. Howie estimate                              AFRL estimate
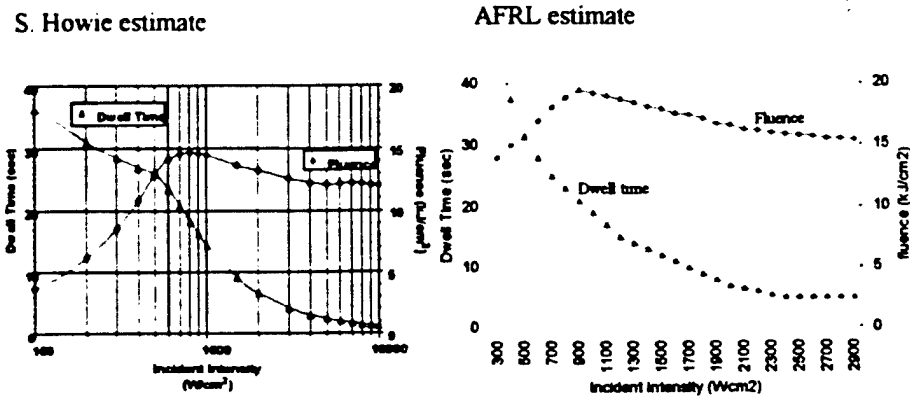


**Figure 3.3-7: Lethality estimates showing fluence and dwell requirements with intensity**

The shapes of the two fluence curves above the intensity 500 W/cm$^2$ are similar though the curves are shifted by about 5 kJ/cm$^2$ with respect to one another. The peak occurs at about 800 W/cm$^2$ in both cases. The most significant differences occur below 500 W/cm$^2$. The S. Howie estimate shows a distinctive knee in the dwell time curve at 500 W/cm$^2$. AFRL's code does not calculate values below 500 W/cm$^2$ and the results for those values have been extrapolated.

## Scenario Assumptions

Multiple missiles are launched from a single location. The launch latitude is around 52° N. Because the runs were performed over a representative period, the results should not change much with longitude.

## Performance Assumptions

Results were reviewed in terms of equivalent performance parametrics. In other words, to assure the comparisons were being made on an equal basis, each constellation was required to have an equivalent average kill performance.

67

A representative period is evaluated in each case. This analysis required that there be no holes in the constellation during the entire period (i.e. Must kill at least 1 missile in boost for every event evaluated.) The reason for this requirement is that an enemy would exploit these holes giving the constellation an effectiveness of zero.

**Statistics Assumptions**

216 war start times were evaluated for each representative period of each constellation design. Though this number may miss holes in the constellation on occasion, the average of this number of war start times should not change much even when evaluating a larger number of war start times

**Input Assumptions**

Input assumptions used have been specified in Table 3.3-1.

### 3.3.5.4 Equivalent Performance Parametric Results

The results of this study are evaluated in terms of equivalent performance. In other words, a constellation of a certain number must have an average performance level of 90%, 80%, or 70% In addition to achieving these performance levels, the constellation could not have any zero kill events indicating the existence of holes in the constellation though it is rare for a constellation to achieve such high average performance levels and have holes in it at the same time

Table 3.3-3, Table 3.3-4 and Table 3.3-5 contain the number of satellites required for various combinations of power, diameter, jitter, and lethality estimate for a 90%, 80%, and 70% average performance of the constellation. The powers increase from P1 to P4. Similarly, the diameters increase from D1 to D3.

Note the large differences in satellites required between the two lethality estimates especially at lower brightness.

## Table 3.3-3

### 90% performance

| Power | Diameter | Steade | | | | AFRL | | | |
|---|---|---|---|---|---|---|---|---|---|
| | | 200 nrad | 150 nrad | 100 nrad | 50 nrad | 200 nrad | 150 nrad | 100 nrad | 50 nrad |
| P1 | D2 | NA | NA | 72 | 54 | NA | NA | NA | NA |
| P1 | D3 | NA | 96 | 60 | 40 | NA | NA | NA | 72 |
| P2 | D1 | NA | 92 | 65 | 54 | NA | NA | NA | NA |
| P2 | D2 | 90 | 60 | 45 | 36 | NA | NA | NA | 60 |
| P2 | D3 | 78 | 56 | 40 | 30 | NA | NA | 64 | 42 |
| P3 | D1 | 60 | 48 | 40 | 36 | NA | 84 | 72 | 60 |
| P3 | D2 | 54 | 40 | 32 | 28 | 100 | 72 | 48 | 36 |
| P3 | D3 | 48 | 36 | 28 | 20 | 88 | 60 | 36 | 25 |
| P4 | D1 | 45 | 40 | 32 | 30 | 84 | 70 | 48 | 45 |
| P4 | D2 | 40 | 32 | 28 | 24 | 68 | 48 | 35 | 25 |
| P4 | D3 | 40 | 30 | 24 | 16 | 66 | 42 | 30 | 20 |

## Table 3.3-4

### 80% performance

| Power | Diameter | Steade | | | | AFRL | | | |
|---|---|---|---|---|---|---|---|---|---|
| | | 200 nrad | 150 nrad | 100 nrad | 50 nrad | 200 nrad | 150 nrad | 100 nrad | 50 nrad |
| P1 | D2 | NA | 100 | 64 | 48 | NA | NA | NA | 92 |
| P1 | D3 | NA | 84 | 48 | 35 | NA | NA | NA | 64 |
| P2 | D1 | 96 | 76 | 54 | 45 | NA | NA | NA | 80 |
| P2 | D2 | 78 | 52 | 40 | 30 | NA | NA | 68 | 48 |
| P2 | D3 | 70 | 48 | 32 | 25 | NA | 92 | 55 | 36 |
| P3 | D1 | 52 | 40 | 35 | 30 | NA | 80 | 60 | 48 |
| P3 | D2 | 42 | 35 | 28 | 24 | 84 | 60 | 40 | 30 |
| P3 | D3 | 40 | 32 | 24 | 16 | 80 | 52 | 30 | 20 |
| P4 | D1 | 40 | 32 | 28 | 25 | 72 | 56 | 40 | 36 |
| P4 | D2 | 35 | 28 | 24 | 18 | 60 | 42 | 30 | 24 |
| P4 | D3 | 32 | 28 | 20 | 15 | 52 | 36 | 24 | 16 |

69

## Table 3.3-5

### 70% performance

| Power | Diameter | Steade | | | | AFRL | | | |
|---|---|---|---|---|---|---|---|---|---|
| | | 200 nrad | 150 nrad | 100 nrad | 50 nrad | 200 nrad | 150 nrad | 100 nrad | 50 nrad |
| P1 | D2 | NA | 88 | 54 | 40 | NA | NA | NA | 76 |
| P1 | D3 | NA | 72 | 42 | 28 | NA | NA | 95 | 54 |
| P2 | D1 | 84 | 60 | 45 | 40 | NA | NA | 100 | 76 |
| P2 | D2 | 68 | 44 | 32 | 28 | NA | 100 | 60 | 40 |
| P2 | D3 | 60 | 40 | 28 | 20 | NA | 84 | 48 | 30 |
| P3 | D1 | 44 | 35 | 28 | 28 | 92 | 70 | 52 | 42 |
| P3 | D2 | 35 | 30 | 24 | 20 | 72 | 56 | 35 | 25 |
| P3 | D3 | 35 | 28 | 20 | 14 | 64 | 44 | 24 | 20 |
| P4 | D1 | 32 | 28 | 24 | 20 | 60 | 48 | 36 | 30 |
| P4 | D2 | 28 | 24 | 20 | 15 | 52 | 35 | 25 | 20 |
| P4 | D3 | 28 | 24 | <18 | 12 | 45 | 32 | <24 | 15 |

## Power with constant D

Figure 3.3-8 shows the number of satellites required for variations in power over lines of constant diameter. Increasing power 1 level from the lowest to the next one up yields a significant different in the number of satellites required and indicates a knee in the curve at this point

70

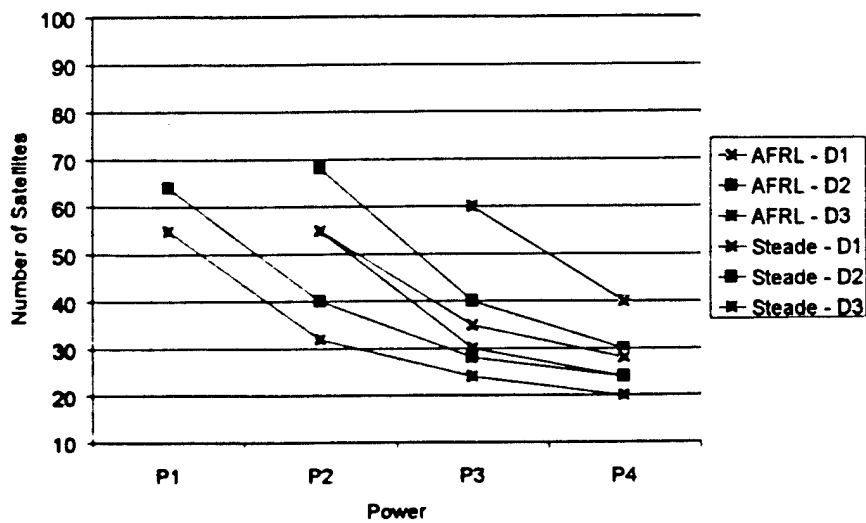**Figure 3.3-8: 100 nrad jitter – 80%**

## Diameter with constant P

Figure 3.3-9 shows the number of satellites required for variations in diameter over lines of constant power. These curves are flatter than the power curves at the jitter level of 100 nrad. The payoff is fairly linear going from one diameter to the next. For lower jitter levels the higher diameters will yield significantly better results.
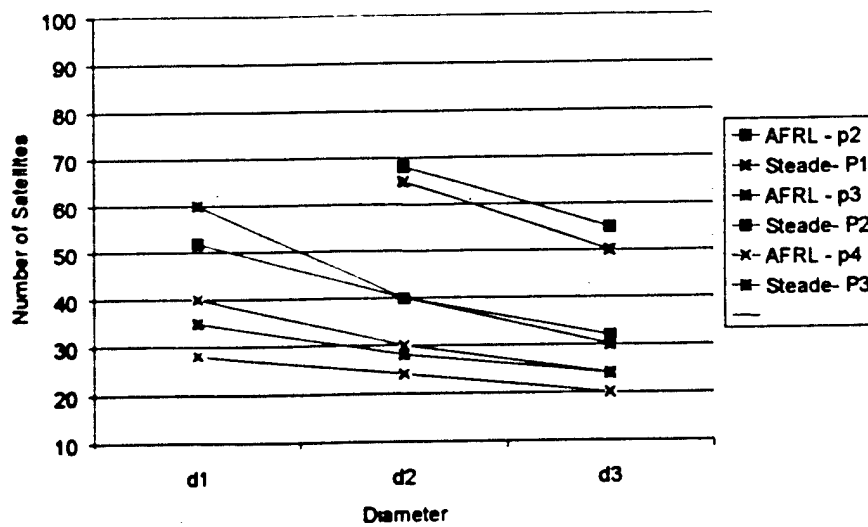
**Figure 3.3-9: 100 nrad – 80% performance**

## Effects of Diameter and Jitter on Performance

Figure 3.3-10 and Figure 3.3-11 illustrate the effects of diameter and jitter on performance. The curves have been grouped in sets of [p1d2, p1d3, p2d1], [p2d2, p2d3, p3d1], and [p3d2, p3d3, p4d1] since these sets yield similar results. Somewhere between 100 nrad and 200 nrad in each of the cases the higher power / low diameter case yields better results than the lower power / high diameter case. This illustrates that if a lower power / large diameter design is chosen, the jitter must be less than 100 nrad to optimize the power diameter trade with weight. Otherwise trading more power for less diameter is a more optimum solution.

72
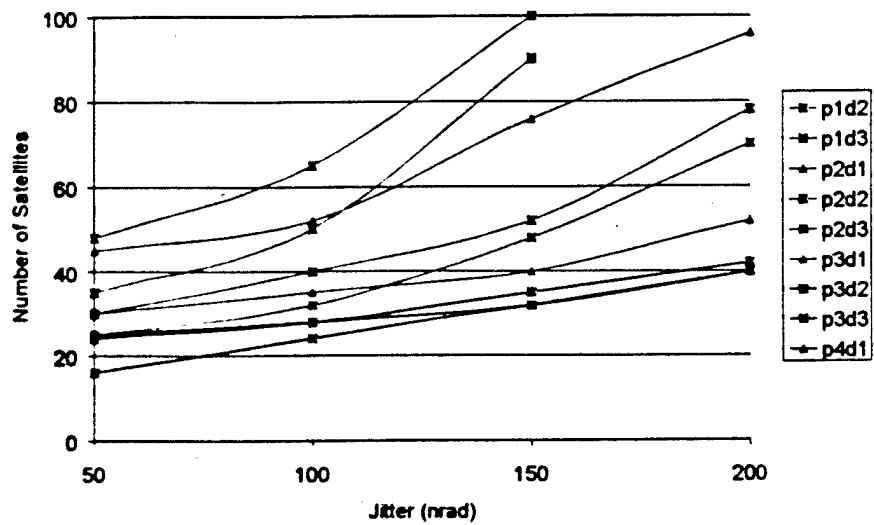
**Figure 3.3-10 : Effect of Diameter and Jitter on Performance**
**Steade Lethality Estimates - 80%**
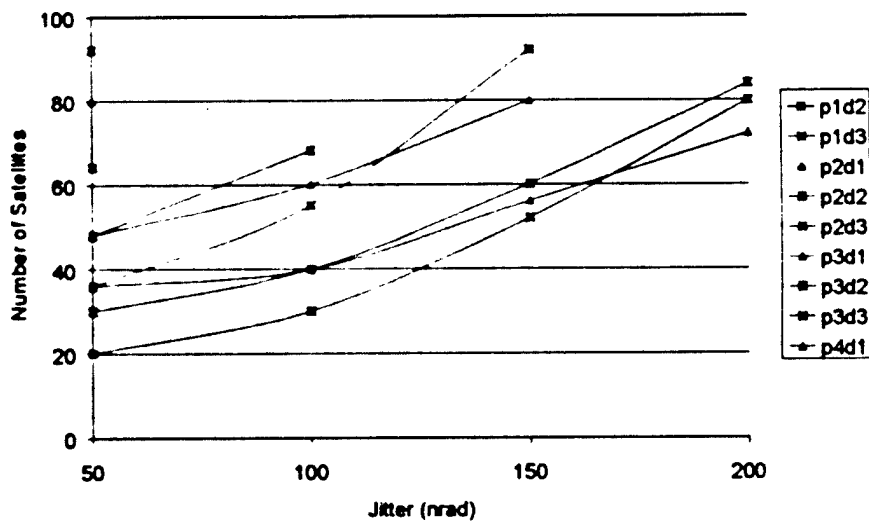


**Figure 3.3-11: Effect of Diameter and Jitter on Performance**
**AFRL Lethality Estimates - 80%**

73

## Performance Curves

Figure 3.3-12 and Figure 3.3-13 and Figure 3.3-14 show performance curves for 3 different sets of powers and diameters. The curves show the number of satellites required to achieve varying average percents of kills for a given lethality and jitter. Lower brightness systems require significant increases in the number of satellites to increase the average percent of kills and jitter. They require drastic increases in numbers with increases in fluence requirements.
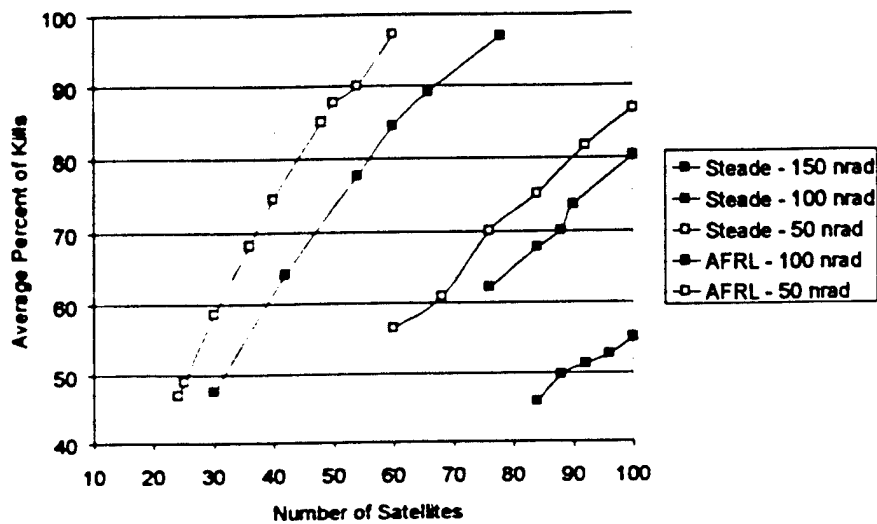


**Figure 3.3-12: P1 D2 performance curve**
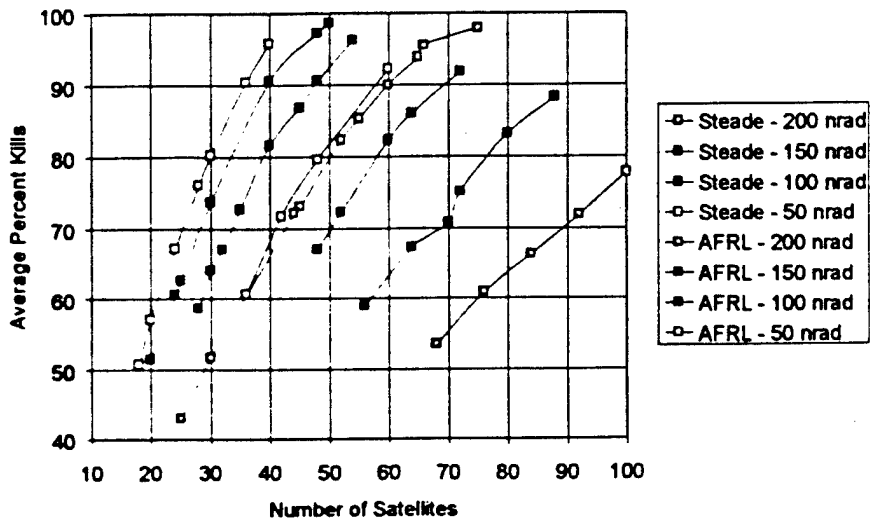
**Figure 3.3-13. P3 D1 performance Curves**
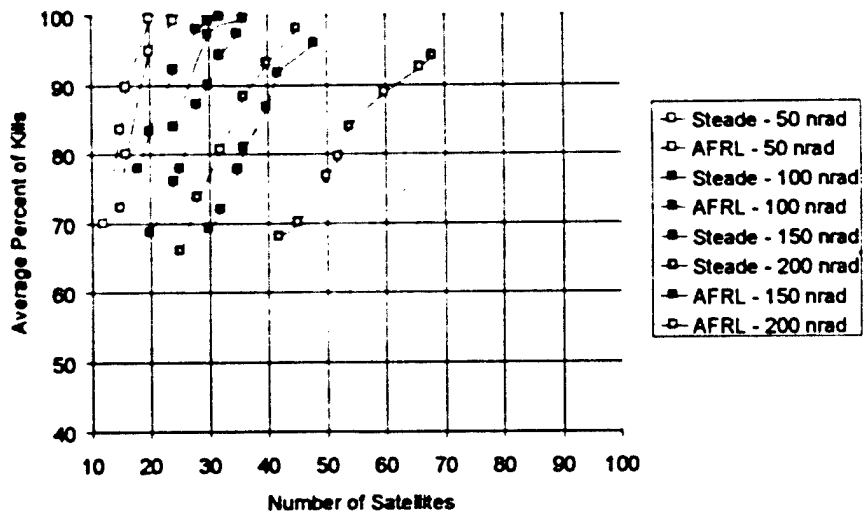


**Figure 3.3-14: P4D3 performance curves**

75

### 3.3.5.5 Summary

The differences in results using the two lethality estimates at a maximum dwell time of 35 seconds, provides the single greatest difference in the number of satellites required, especially at lower brightness.

When considering a weight trade between power and diameter, jitter is an integral part of the design. For the cases studied, designs with jitters greater than 100 nrad favor increasing power rather than continuing to increase diameter. For designs with jitters significantly lower than 100 nrad, increasing diameter clearly adds more benefit than increasing power.

The brightest systems are the most robust in that they require significantly smaller increments of satellite numbers with changes in jitter, fluence requirements, or average percent of kill requirements.

### 3.3.6 Retargeting of Primary Mirrors

A study to determine the effects of retargeting of large, lighten primary mirrors was completed and is attached as Appendix 3.3-5.

### 3.3.7 Brightness Saturation

Quasi-technical arguments have been offered in the past to explain brightness scaling in simple terms. Such arguments include scaling brightness inversely as the square of wavelength and directly as the square of diameter, according to the equation:

$$B = \frac{\pi P D^2}{4 \lambda^2} S^2$$

Such a simplistic approach argues that shorter wavelengths and larger diameters are better (greater power is also better). Unfortunately, the term S in the above equation (the Strehl ratio, or degradation of the laser beam) is also a function of both diameter and wavelength, and generally reduces the brightness with increasing diameter and decreasing wavelength.

Figure 3.3-15 shows the brightness obtained from a more detailed version of the brightness equation (Schafer memorandum GG-96B-06a describes the brightness equation in detail).

76

**Brightness Scaling**
**(Diameter, Wavelength, Power all vary)**

Legend:
- Theoretical Brightness
- Brightness 1 Jitter 50 nanoradians; WFE 0.1 micrometers
- Brightness 2 Jitter 125 nanoradians; WFE 0.2 micrometers
- Brightness 3 Jitter 200 nanoradians; WFE 0.3 micrometers
- Brightness 4 Jitter 275 nanoradians; WFE 0.4 micrometers

Y-axis: Brightness

X-axis: Power, Wavelength, Diameter

**Figure 3.3-15. Brightness Scaling**

The uppermost curve is the theoretical brightness obtained with a perfect beam (Strehl ratio of 1 0)   The horizontal axis shows simultaneously increasing power, diameter, and decreasing wavelength.  For this particular parametric example, the theoretical brightness rapidly increases   Adding two of the primary system errors shows a more realistic behavior.  For 50 nanoradians net system jitter and 0.1 micrometers wavefront error, the second curve from the top of the set is obtained.  Although the trend is similar, the brightness is reduced by a significant amount (~35% at 11 m diameter).   Additional errors are added to obtain the third curve.  Brightness saturation is now present.  By about 14 m diameter, the brightness peaks and then begins to fall   As more errors are added, the peak of the brightness curve shifts to the left (longer wavelength and smaller diameter)   Figure 3.3-16 shows an expanded scale.  The lowest curve shows a brightness peak near 9 m diameter.
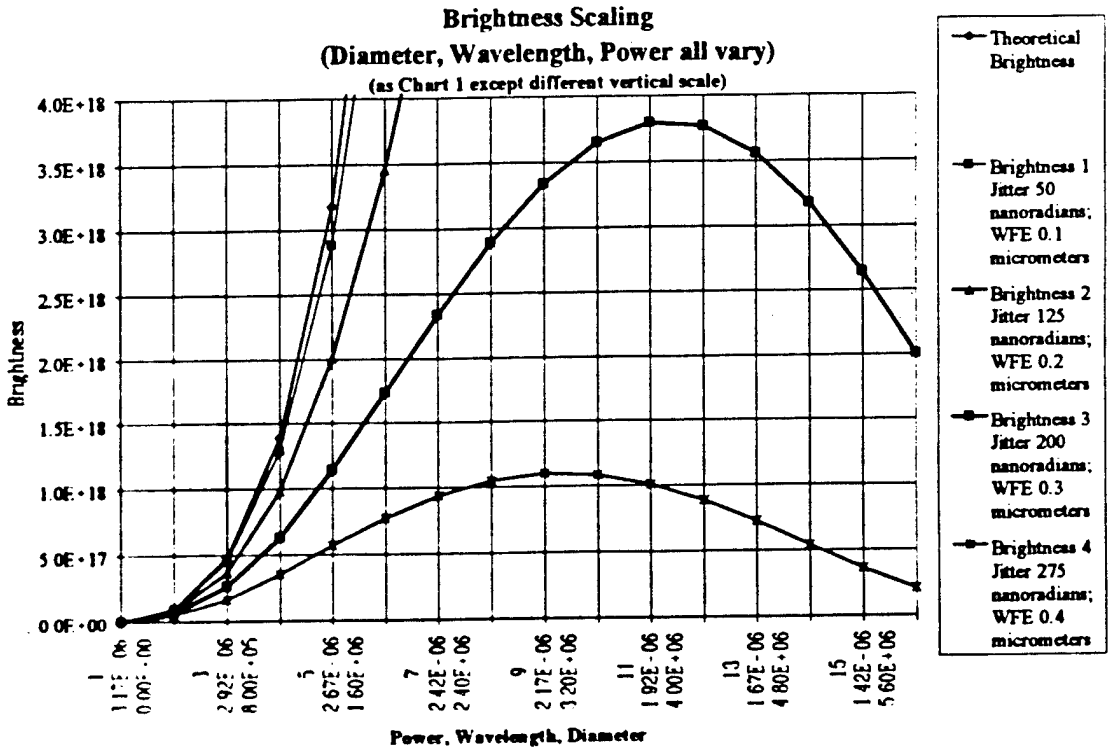
**Figure 3.3-16: Brightness Scaling**

The explanation for this behavior is simple. As the diameter increases, and the wavelength decreases, the spot size of the focussed beam gets very small. Pointing errors move a smaller beam by a more significant amount, and wavefront errors which spread the beam are also more noticeable

There are other effects which are more detailed, but which should not be ignored. As mirrors become larger, they are less rigid for a comparable weight. The mirrors thus have more jitter and wavefront error (if the retarget and settling times are held the same).

For a mirror of more than 10 meters diameter, total system jitter must be less than 100 nanoradians Past error budgets have generally assumed that the uncorrectable portion of the laser jitter, the beam control/large optics jitter, and the track jitter are roughly comparable and uncorrelated This implies that each must be less than about 60 nanoradians. For mirrors of the 16 m class, the overall budget must be about 30 nanoradians, with the three lower tier budgets about 17 nanoradians (WFE reduced similarly). The beam control problem is thus challenging, and will limit the available diameter just as much, if not more, than fabrication technology.

## 3.3.8 Code Development

Code development activities are summarized in Appendices 3.3-6, 7, 8, and 9.

## 3.4    University of Illinois

### Summary of Activities

The UIUC program has always had a dual function: provide research into the physics of chemical laser devices in a very cost-efficient fashion (many thousands of seconds of device run time per thousands of expended dollars), and provide a training ground for graduate students to replace the rapidly dwindling U.S. supply of trained laser physicists. Recent research has concentrated on line selection techniques for chemical lasers, and the effect of modified nozzle techniques on device performance.

HF lasers have a spectrally-rich gain region, and will lase on as many as 4-8 laser lines(wavelengths) simultaneously. Some of the lasing lines are strongly absorbed by water vapor, and thus do not propagate well into the atmosphere. This poor atmospheric propagation results in difficulty in engaging thrusting missiles at altitudes as low as could be achieved without the absorption. Previous research at TRW and UIUC investigated the overtone laser wavelengths (at about 1.3 um). Overtone lasing is still a promising candidate, but suffers from some efficiency penalties and lower gains, increasing the difficulty of resonator design and power extraction. If the number of lasing lines in the fundamental operation (at around 2.7 um) could be restricted to only those lines which have low absorption, both of the goals of good atmospheric penetration and efficient operation could be achieved. Such "line selection" is accomplished by using wavelength-sensitive gratings in the resonator. Physics of the gain region also constrain the paths by which energy is transferred among energy levels of the HF molecules, so arbitrary lines cannot be selected

As part of an investigation of line-selected HF laser performance, a number of experiments have been performed using line selection gratings. Single line off-Littrow performance was measured for Grating 4. The highly efficient Grating 4 put 80.4% to 99.99% of the total power (outcoupled + secondary zero order + primary zero order) in the outcoupled beam. The less efficient Grating 2 placed 45.0% to 51.8% of the total power in the outcoupled beam.

Multiple line selected performance was measured for 18 line combinations, 5 cascade pairs, 8 non-cascade pairs, and 5 triplets. The best performing cascade pairs were $[P_2(6), P_1(7)]$, $[P_2(7), P_1(8)]$ and $[P_2(8), P_1(9)]$ with $[P_2(7), P_1(8)]$ giving almost 25% more power than the other two pairs, 26.3 watts. The best performing non-cascade pair was $[P_2(7), P_1(7)]$, which gave as much power, about 21 watts, as the cascade pairs $[P_2(6), P_1(7)]$ and $[P_2(8), P_1(9)]$. The triplet performance is rather interesting. When the line $P_1(7)$ was added to the non-cascade pair $[P_2(8), P_2(7)]$, the triplet performance was 21.6% larger than the pair performance. However, when the line $P_1(8)$ was added to this same pair, the triplet performance was 58% larger than the pair performance! This suggests that multiple line selected performance is a strong function of the lines that can be lased simultaneously. The possibilities are limited by the grating equation. When $P_1(8)$ was added to the cascade pair $[P_2(8), P_1(9)]$, the triplet performance was 14.7% larger than the pair performance.

Previous studies included Helium film cooling nozzle power as a function of flow rates. For comparison to other laser devices, the data have been presented in terms of the film cooling He (FCHE) mass flow rates and molar flow rates divided by the total primary flow, the secondary $H_2$ flow, the secondary He flow, the total secondary flow, the total (primary + secondary) flow and the total throat area of the nozzle bank. This research is important in understanding the design and performance of the nozzle concepts proposed in the CDS studies.

The performance of the He Film cooling nozzle bank was measured as a function of the mass flow rate of the cooling He. Maximum performance was obtained for a He film flow rate of 0.040gm/s. For larger He film flow rates, the power decreased significantly. By re-optimizing the flow rates, it was possible to recover about 30% of the lost power at the larger He film flow rates. Re-optimizing the flow rates decreased the nozzle blade temperatures. The data are summarized in the appendix. The analysis of the data is on going.

Single line off-Littrow performance was measured for Grating 4. The highly efficient Grating 4 put 80.4% to 99.99% of the total power (outcoupled + secondary zero order + primary zero order) in the outcoupled beam. The less efficient Grating 2 placed 45.0% to 51.8% of the total power in the outcoupled beam.

Multiple line selected performance was measured for 18 line combinations, 5 cascade pairs, 8 non-cascade pairs, and 5 triplets. The best performing cascade pairs were [$P_2(6)$, $P_1(7)$], [$P_2(7)$, $P_1(8)$] and [$P_2(8)$, $P_1(9)$] with [$P_2(7)$, $P_1(8)$] giving almost 25% more power than the other two pairs, 26.3 watts. The best performing non-cascade pair was [$P_2(7)$, $P_1(7)$], which gave as much power, about 21 watts, as the cascade pairs [$P_2(6)$, $P_1(7)$] and [$P_2(8)$, $P_1(9)$]. The only other non-cascade pair that came close to cascade pair performance was [$P_2(8)$, $P_1(7)$] at 18 watts. The triplet performance is rather interesting. When the line $P_1(7)$ was added to the non-cascade pair [$P_2(8)$, $P_2(7)$], the triplet performance was 21.6% larger than the pair performance. However, when the line $P_1(8)$ was added to this same pair, the triplet performance was 58% larger than the pair performance! This suggests that multiple line selected performance is a strong function of the lines that can be lased simultaneously. The possibilities are limited by the grating equation. When $P_1(8)$ was added to the cascade pair [$P_2(8)$, $P_1(9)$], the triplet performance was 14.7% larger than the pair performance. Adding $P_1(6)$ to the pair [$P_2(8)$, $P_1(7)$] increased performance by only 6.1%. Adding $P_1(7)$ to the pair [$P_1(9)$, $P_1(8)$] decreased performance by 2%.

Comparison of the zero order, outcoupled and total (outcoupled + zero order + secondary zero order) powers of the line selected combinations that were measured for both Grating 2 and 4 show that Grating 4 outcoupled power is significantly larger and the zero order power is significantly smaller than that for Grating 2.

The Helium film cooling nozzle power as a function of flow rates was presented in last month's progress letter. For comparison to other laser devices, the data are presented in terms of the film cooling He (FCHE) mass flow rates and molar flow rates divided by the total primary flow, the secondary $H_2$ flow, the secondary He flow, the total secondary flow, the total (primary + secondary) flow and the total throat area of the nozzle bank.

Grating efficiencies were determined from Littrow and off-Littrow single line data. Because Grating 4 is a very good grating, it was necessary to take into account the transmission and absorption/scattering losses of the feedback mirror when grating efficiencies were deduced from the off-Littrow data. For lines whose wave length is shorter than the Blaze wavelength of the grating, the efficiency is greater than 99.8%. For lines whose wave length is longer than the Blaze wavelength of the grating, the efficiency falls off rapidly the farther the wave length is from the Blaze wavelength. The efficiencies deduced from the Littrow and off-Littrow data agree within 0.15% for lines whose wavelength is less than the Blaze wavelength of the grating. The differences between the Littrow and off-Littrow efficiencies increase the longer the wave length is compared to the Blaze wavelength.

These results suggest that if the Blaze wavelength is larger than any of the wavelengths of interest, the grating efficiency for the $P_2$ lines for $J > 4$ would be comparable to that for the lower $J$ lines. This would result in significantly better line selected performance of the peak power $P_2$ lines $J = 6, 7, 8,$ and $9$. A new grating with $\lambda_{Blaze} = 3.4$ or $3.5$ $\mu m$ should be tried.

The HYSIM overtone data were used to determine the values of the Rigrod parameters $g_0L_c$ and $I_{sat}$ that gave the best fit to the data. With these values of $g_0L_c = 0.014$ and $I_{sat} = 14,000$ watts, the Rigrod $P_{IC}$ versus $\sqrt{R_1R_2}$ curve, which can be used to deduce the reflectivity of a mirror, was generated. The HYSIM data with the 4mCC#8/4mCC#10 mirrors was used to determine the reflectivity of the 4mCC#8 mirror. The R, T and A/S characteristics of this mirror are 97.72%, 0.9768%, 1.3032%.

During October, the flow rates for optimum performance of the notched $H_2$ injector nozzle bank were measured and found to be the same as for the HYSIM nozzle. Power, beam size, optical axis location for peak power ($x_c$), and spectra were measured for 24%, 50%, 73%, 93%, and 96% reflectivity outcouplers. The addition of the hydrogen notches had essentially no effect on the performance of the laser. The data were within the ±10% repeatability band of the HYSIM nozzle bank data. Since one of the purposes of the secondary helium injectors is to shield the hydrogen from the fluorine atoms in the primary flow until the hydrogen has reached the nozzle exit plane, there might have been no increase in performance because the helium injectors were not notched. To answer the question, the helium injectors were notched in a similar fashion. Resulting data showed that performance was still essentially unchanged, indicating that notching had little effect on laser performance.

A plot of grating efficiency versus wavelength for grating 4 showed that all efficiencies were reduced sharply for wavelengths exceeding the blaze wavelength. A number of other grating measurements were completed.

During November, measured efficiency data for Gratings 2 and 3 suggested that a grating with a blaze wavelength shorter than any of the wavelengths of interest may have a higher efficiency than that of a grating with a blaze wavelength in the center of the wavelength range of interest. The groove spacing and blaze angle were measured with a HeNe laser for Gratings 2, 3, and 4 for both 0° (right side up) and 180° (upside down) orientation of the grating face. These experiments confirmed that all of the gratings were ruled as specified, 600 lines/mm. The

81

measurements showed that the blaze angles in the 0° orientation for Gratings 3 and 4 were 56.37°, as specified. For the degraded Grating 2, the 0° orientation blaze angle was 21°. In the 180° orientation, the blaze angles for Gratings 2 and 4 were both 33.63° and for Grating 3 was 21°. The corresponding groove vertex angles, which were supposed to be 90°, were 125.37° for Grating 2, 102.63° for Grating 3 and 90° for Grating 4. For the wavelength range of interest, 2.5 to 3.1μm, diffracting into the first order, a blaze angle of 33.63° corresponds to a blaze wavelength of 1.85μm. Since Grating 4 is blazed at 1.85 μm in the 180° position, which is shorter than all wavelengths of interest, single line Littrow performance will be measured with Grating 4 in the 180° position to test the efficiency hypothesis. Other continuing work included setting up the optical layout for the RFG HYSIM experiments, designing the water vapor cell for the line selected intracavity water vapor cell experiments, and experimentally determining the effect of decrease in blaze angle on line selected grating performance. Future plans include measurement of the residual fundamental gain while lasing on the overtone for the 30 cm gain length HYSIM nozzle, and measurement of line selected performance obtained with a water vapor cell as the line selecting element.

An intracavity water vapor cell is being designed to determine if line selection can be obtained by suppressing the gain on lines with poor atmospheric propagation due to high water vapor absorption A mechanical layout was devised with appropriate plumbing to the water vapor cell to monitor and control the cell's pressure, temperature, and humidity. The literature is under review to gain an understanding of water vapor absorption calculations as a function of wavelength and atmospheric conditions. With logarithmic absorption coefficients obtained from Ref (1), the transmission of the vapor cell was calculated as a function of pressure, temperature, relative humidity, and cell length. As a consistency check, these calculations are being compared with computer code results from LOWTRAN 3[1] and the HF absorption tables[2] for beam transmittance at 1 km. Our rotational nonequilibrium computer model is being modified to simulate the effect of an intracavity water vapor cell on the output spectra of the laser.

The full UIUC report is attached in Appendix 3.4-1.

## 3.5    BMDO Support (PRA)

The work accomplished by Photon Research Associates is provided in Appendix 3-5. (provided under separate cover due to proprietary information).

## 3.6    Lethality

This effort provided lethality calculations and support to the lethality process. During the past month, further calculations were performed and a presentation developed for upcoming meetings with AFRL and SMC. There are still some discrepancies between the ARA and AFRL models in the low intensity regime, where ablation is minimal and thermal effects dominate. These analyses have been conducted for a particular composite motor case design of interest to the SBL community.

Support was provided to a meeting at Aerospace with SMC, AFRL (Beraun et al), and Aerospace technical staff. The topic of discussion was the differences between ARA and AFRL analysis. There still appear to be significant differences between models in the low intensity regime (under 500 watts per square centimeter). Considerable discussion of the correct parameters for modeling did not lead to a firm conclusion. Further review of test data obtained at PSI was recommended by Rigby. Brief discussion of the TMD lethality document indicated that the requirements previously given to the CDS contractors were very conservative (perhaps 40% higher than normally used, and as much as 200% higher than some analyses would indicate).

### 3.6.1 General Lethality Issues

A number of issues relating to lethality need to be considered by the lethality working group. Lethality of ballistic missiles is critically important to SBL system performance, since kill time is directly proportional to target lethality. A factor of two difference in lethality is roughly comparable to the difference between an 8 meter diameter SBL primary mirror and a 12 meter mirror. Both absolute lethality and uncertainty in lethality are critical. Lethality is defined as the total accumulated fluence (energy) required to kill the target. The total fluence is calculated by determining the "edge fluence" at a beam diameter which matches the target damage spot size (more below), and integrating that edge fluence over the kill time until the required total fluence is achieved. In a practical sense, heating of the target causes its destruction, so that target temperature is actually the direct measurement. Fluence is more practical to specify for the output of an SBL. Since the fluence at the center of the beam is larger than at the edge, the total deposited energy will always be considerably more than the lethality criteria. That extra energy is "wasted" when specifications are considered, but should result in a faster target kill. Lethality specifications are thus intrinsically conservative.

Past lethality work has concentrated on the "prompt ablation" regime. This region is characterized by high incident energy. The rapid deposition of energy converts the irradiated part of the missile surface rapidly into gas and fragments which are quickly removed from the surface. Very little chemistry takes place, and the surface material is quickly removed. The missile wall gets thinner, without the surrounding region heating up. The heat simply does not have time to diffuse before the material is removed. Failure occurs when the missile wall becomes thin enough that the internal pressure of the underlying tank or combustion chamber causes the wall to rupture

The prompt ablation regime was chosen because the massive Soviet threat of the early 1980's required very bright laser systems. The sheer number of targets required that individual targets be killed in fractions of a second. The irradiance required to deposit sufficient energy in such a short period of time was so high that only ablation needed to be considered.

Current SBL systems are projected to operate at delivered irradiance levels that are much lower than the projected systems of the early 1980's. Depending on the range to target, the irradiance is generally between 80 W/cm$^2$ and 5500 W/cm$^2$ (peak) and about 40-2800 W/cm$^2$ edge, with the higher irradiance at the shorter ranges. These numbers are strictly parametric and can vary widely with specific designs. RD or IFX irradiance is likely to range from 150-600

W/cm$^2$ peak and roughly half that at the edge (larger ranges of irradiance are possible since the design concepts are not mature). Edge irradiance is defined as the irradiance at the diameter associated with the target damage spot size. The damage spot size is determined by the critical crack propagation length for burst. The irradiated spot will begin to fail at the point of highest irradiance (modified by any weak spots in the target).

As delivered irradiance is reduced, chemical reactions at the surface become more important, and the physical effects change from prompt ablation to the thermal regime. In the low irradiance limit, no material is removed and only target heating is important (even at low irradiance levels, accumulated energy raises the surface temperature to the point where material begins to be removed, so the length of time and total deposited energy is also important). In between the two regimes, the material begins to break down. Pyrolosis, the chemical decomposition of the surface by heat, begins. The surface chars, cracks, and gasifies. If oxygen is present (as is the case during boost phase) combustion may take place. Some of the chemical reactions can add heat to the surface. Others remove material and take heat away from the surface As the surface heats, all of the reactions intensify. Since the beam irradiance falls from center to edge, different thermal regimes occur across the beam at different times. When the material becomes thin enough, or sufficiently weakened, the internal pressures cause cracks to form near the center of the beam. The cracks propagate across the damaged area, and the missile bursts Once the process begins, considerable mechanical energy is released, and the results can be spectacular. Pressure bottles mounted to test stands with 1 inch bolts have sheared the bolts during the burst event.

Older, higher brightness systems generally had very large apertures (up to 6 times larger than the RD CoDR baseline) and very small spot sizes. Current projected systems have spot sizes ranging from about 14-180 cm in diameter (calculated from the 50% power point; i.e. full width half max), depending on range and primary mirror size. Current target kill spots range from a few centimeters to about 30 centimeters. The SBL beam is almost always larger than the kill spot, and so overall thermal effects must be considered.

Spot size is important for several reasons. A critical failure length must be reached before cracks can propagate. If the spot is too small, a vent will form, but the missile may not burst. Buckling may also occur if the weakened region can no longer support the load forces. These events are dependent on the ductility of the missile wall material. A ductile material such as some of the duplex stainless steels will bend considerably before failing. A brittle composite material will fail much more suddenly.

## 3.6.2    Coupling

Coupling refers to the fraction of incident laser intensity that is actually absorbed by the target. Almost all surfaces of interest are optically black (good absorbers) in the infrared (2.8 μ m). Data taken at 1.3 μm begins to be effected more by lower absorptance and must be carefully corrected. Essentially any surface becomes a very good absorber as the surface heats and begins to char. Coupling effects are thus of primary concern in the first few seconds of irradiation, and usually have only a small impact on total kill time. They can be of significance in small scale

coupon tests. Some experts have argued that coupling can be low for certain targets. Experimental data has proven them to be incorrect. Coupling at 2.8 μm appears to be excellent (80-95%) for essentially all targets. Coupling is lowest for shorter wavelengths and polished metal surfaces. Very small amounts of surface contamination from oils, dust, water vapor, etc. cause absorption to rise rapidly. Paint is particularly good at increasing coupling. The complex chemistry, as paint burns, rapidly chars the underlying surface, and there is no discernible reduction in coupling throughout the irradiation time.

All materials pass through phase changes at certain temperatures, as pyrolosis ends and the solid material is gasified. This phase change can be seen as a change in the slope of the heating curve. The chemistry associated with this temperature regime is extremely complex, with many reactions occurring simultaneously.

Very limited data is available for the low irradiance regime. In 1994, some 20 test samples were measured at Helios to determine coupling effects. The chart below shows a small sample of the test data taken on small coupon samples at low irradiance. Other limited pressure bottle tests at low irradiance have been cited by AFRL but the references have not yet been made available.
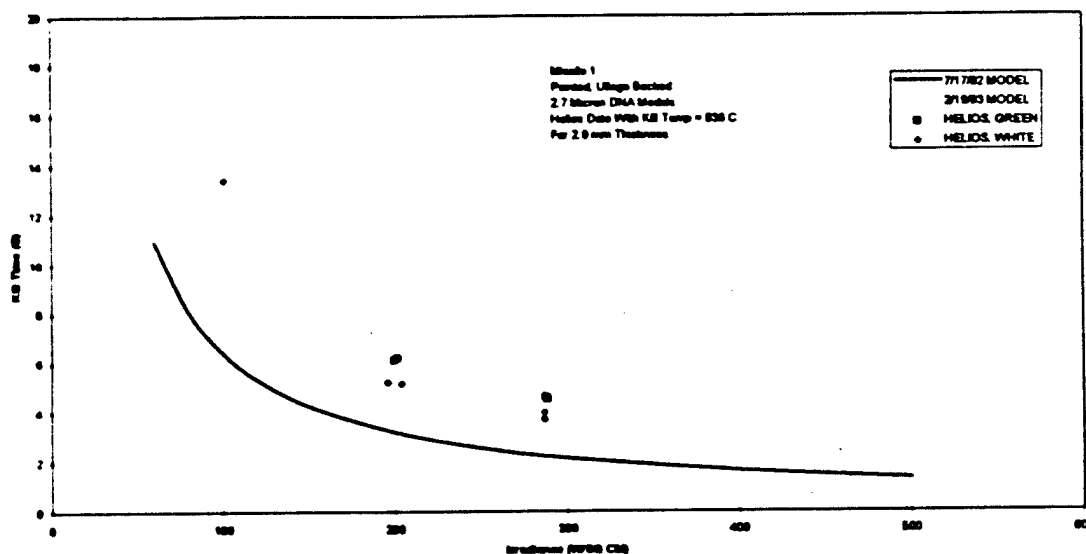


### 3.6.3    Thermal Issues

In the ablation regime (high irradiance, 2-5 KW/cm$^2$ and higher), the thermal effects are negligible and the problem is essential one-dimensional. As material is removed, the wall becomes thinner and eventually fails. In the thermal regime (below 2-5KW/cm$^2$), heat has time to soak into the material. Thermal gradients build up both in the depth of the material and in both transverse directions along the missile wall. As the laser beam heats the surface and its temperature rises, the surface first chars and then gasifies. A maximum temperature is reached which represents a

thermal balance between the incoming radiation and the losses due to material removal, radiation, and conduction/convection. This maximum temperature limits the gradient that can be achieved into the depth of the missile.

### 3.6.4 Material Issues

Missile materials fall into two general types, metals and composites. Most liquid-fuel rockets use metal walls and tanks, and most solid-fuel rockets use composite walls, although there are a few exceptions. When metals are heated, they soften. Material failure is dependent on temperature and material properties, with materials like duplex stainless, which is very ductile, failing at higher temperatures than other materials like aluminum. Composite materials consist of a binder material and embedded fibers. As the composite heats up, the binder material rapidly loses strength, leaving the fibers "floating". As the fibers heat up, they eventually break at a weak point. The fibers, which are heavily stressed, may then contract away from the breakage point. Fibers have also been seen to turn up out of plane, forming hair-like growths which can have significant thermal effects on coupon samples. The combined failure mechanism is dependent on the details of the residual strength of the composite as the binder softens and the fibers break. Significant heating can occur over regions as large as three times the spot sizes quoted above, since the edge irradiance is at the half power point. Since binder materials can soften at temperatures of 200-300 °C (fibers and metal fail at 800 °C or more), many meters of missile length and the entire missile width can lose some fraction of its strength. Experts charged with lethality calculations often assume that missiles are very difficult to kill and maintain integrity and strength under conditions that missile designers would not begin to consider survivable. An integral part of test programs should include direct heating tests to determine strength of materials (laser heating is not required).

### 3.6.5 Test Issues

Past tests have involved small coupons (from a few cm to 10's of cm), pressure vessels (tank-like bottles charged with gas or water), full-size missile sections, and a few actual missile bodies. The only tests conducted with actual thrusting missile stages (locked in place on the ground) were of very limited use due to experimental problems. No tests have been conducted on actual thrusting missiles travelling in the atmosphere.

Coupon tests are subject to large heat losses not representative of the actual engagement of a missile. If the coupon is under-filled by the beam, there are significant conduction losses to the non-irradiated portion. If the coupon is over-filled, measurement of actual incident energy becomes difficult. In both cases, beam profile is a major issue. A perfectly uniform beam is easier to model, but difficult to achieve. Thermocouple measurements can cause heat losses for small samples. Conduction and convection losses are critical. The coupon must be held without providing heat losses through the mounting. Edge losses due to convection and radiation are not representative of an actual missile which is a continuous piece of material. If the experiment is run in a vacuum, convective losses due to air streaming over the surface are minimized, but the effects of air on the thermo-chemistry is removed. If the experiment is run in still air, no material is removed by an air stream as it would be in flight. In composite materials, hair-like structures

formed by the broken tips of the fibers can provide larger radiative heat losses. These effects are not easily scaled to full size missiles where such hairs may form over much larger areas. Calculation of heat losses for coupon samples requires that the temperature measurements be continued after irradiation stops, so that decay rates can be measured. Care must be taken to avoid burnthrough and resulting damage to thermocouples.

Bottle tests are more expensive than coupon tests, but provide additional data. If appropriately scaled, the bottle can properly represent the stresses in an actual missile. Scaling becomes more difficult as the irradiated area increases and size and curvature of the bottle become important. One significant shortcoming of past bottle tests is that the bottle was simply pressurized, so that when a hole formed in the side, the pressure was immediately relieved. Such a test is fine for the prompt ablation regime, since the transition from operating pressure to burst is usually rapid. For a large-spot, thermal regime, the burst characteristics may be significantly different. The best subscale test would include a gas generator inside the bottle that could simulate the combustor pressure of a solid fuel rocket, or the ullage over fluid characteristics of a liquid fuel rocket

High energy laser beams are not very available. A 3 KW/cm$^2$ average irradiance over a 30 cm spot size requires 2.1 MW of power in the spot, and perhaps as much as a 3 MW laser to deliver such energy after beam shaping, etc. The Alpha laser has no effects test capability. MIRACL does  No other lasers in the megawatt class exist. Typical tests have been conducted with much smaller lasers, using smaller spot sizes and scaling the various data for appropriate losses  Beam profile and temporal characteristics must be carefully monitored. The best choice for reasonable power level at reasonable cost is a device in the tens of kilowatts range.

Coupon and bottle samples must be carefully prepared, in sufficient quantities for useful statistical results to be obtained. In some cases, the material properties of the target are not well-known, and a range of samples covering the expected range of target characteristics should be used

A detailed test plan is essential. The test plan should indicate the modeling to be done, the design of the experiment, the number and type of samples, the testing matrix and schedule, the data analysis plan, and the post-test model re-anchoring.

### 3.6.6    Modeling

The AFRL/SAIC models use a scaling law which works well in the prompt ablation regime, but not in the low intensity regime. A 2-D or 3-D finite element model is needed to adequately address the thermal and mechanical effects. This model would ideally be coupled to a temperature-dependent surface chemistry model, which would determine the heat transport and heat losses at the surface where the beam and the material interact. Such models do not exist. Any experiments must be accompanied by predictions of the experiment results prior to the experiments, and re-anchoring of the models after experiments. In a well-designed program, about 25-40% of total program resources should be spent on modeling, with about 60-75% spent on experiments (all other management and overhead proportioned equally).

### 3.6.7 SBL/ABL Issues

There are differences in coupling, spot size, lethality, and aimpoint between the SBL and the ABL which must be carefully considered. Past efforts have shown that if ABL data is used directly for SBL lethality, it results in too conservative a lethality specification. The ABL utilizes a return wave system in order to compensate for the atmosphere. This system tracks a beacon spot placed on the missile. In the past, limits on location of the beacon spot limited the ABL aimpoint choices. In one target of interest, the fuel and the oxidizer tanks were likely aimpoints. The ABL was, at the time, limited to shooting at the lower pressure tank, which was harder to kill because it was less highly-stressed. The SBL had no such limitation. The ABL beam is a shorter wavelength, which does not initially couple to the target as well as the SBL beam. The ABL spot size is smaller and less thermal energy is transmitted to the area surrounding the kill spot. These effects have caused as much as a factor of 2 discrepancy in the projected lethalities, with the ABL being higher, and the SBL having an easier time killing the same target. The differences change with time, analysis, and test data. Another effect not yet fully considered is the initial temperature of the target missile. As the missile flies through the atmosphere, it heats up by a significant amount. AFRL has said that this effect has been included in their analysis, yet the lethality has not been reduced as expected.

### 3.6.8 Funding

BMDO spent roughly $140M on lethality, with about $35M on thermal laser lethality. A renewed lethality program should be entered with reasonable expectations and an understanding of the serious difficulties involved in the subject area.

### 3.6.9 Further Work

The ARA model should be extended to 3D rather than 1D to investigate conduction effects. This effort would take about 2-3 man weeks (at about $6K per man week exclusive of travel).

The PSI and bottle data should be reviewed as a check on what Rigby's (SAIC) analysis claims. ARA and Schafer believe that the energy balance in Rigby's analysis is flawed. Pyrolosis seems to take place later than should happen, and takes significantly more energy than expected. ARA offered the following explanation. The PSI data indicate that as the composite material is pyrolized, charred, and ablated, the individual carbon fibers in the composite break. A combination of the mechanics and material flow outward from the material cause the fibers to stick up from the surface like tiny hairs. Since the fibers present very little surface area, they stop absorbing much incident radiation. They remain hot by soaking up energy from the surface (conduction, radiation, and gas transfer/convection). Since the fibers have relatively large surface area as a function of volume, and high emissivity, they radiate very well. This radiation loss is larger than the parent surface, and plays a large role in the PSI data as well as Rigby's analysis. In a real missile, however, the spot would be much larger. As the fibers toward the center of the spot radiate (in nearly $4\pi$ steradians), their energy is blocked/absorbed either by the parent surface or by the "curtain" of fibers formed by other composite strands at greater diameter. ARA argues

that the effect is primarily an edge effect and is thus large for small spots and small coupon samples, but small in the actual target. A concern with this argument is that the effective radiation will also be determined by the fiber density. If adjacent fibers are far apart, much of the energy radiated at shallow angles will pass over nearby fibers without being trapped. The issue, while complex, is key because the PSI data is being interpreted more pessimistically than the NRL data because of this greater radiative loss.

Getting further data to support either side of the argument will not be easy, since small spot tests are of very limited value, and high power devices are in short supply. The difference between the two analyses is significant in terms of overall system performance.

Further review of the available data by ARA is recommended and would take about 2 man weeks. Although the review is critical, data are actually quite limited.

A review of Scud lethality and a careful review of the AFRL specification are critical to system performance in the TMD scenarios. The AFRL lethality may be as much as 45% higher than the canonical number, and perhaps 250% higher than the "best case". Further data reduction of the Helios data is needed to verify the coupling. The temperature and strain data should be reviewed. Changes in the missile operation should be considered. ARA and Schafer both believe that AFRL analysis continues to be unduly pessimistic for the SBL. Completion of this task would take about 5 man weeks.

Modeling of other targets, and in particular the SS-25, is critical to the question of overall SBL effectiveness against a range of scenarios. Such analysis is best coupled to further ISAAC analysis by Larrene Harada and her Schafer group, and can answer the question of overall SBL effectiveness against the range of targets likely to be of interest. ARA did not provide any estimate of the resources required, since this task is dependent on the number of threats and the level of available detail.

These tasks would take about $100K in total. BMDO has expressed some interest in this work

### 3.6.10  Damage Spot Size

The size of the damage spot is dependent on a number of parameters. The primary structural parameter is the ratio of the internal operating pressure of the missile to the burst pressure. The missile has been considered to be equivalent to a pressurized bottle. The hoop stress is larger than the aerodynamic and vibrational stresses, although there are still some controversies about the details of the dynamics. The pressure ratio for typical missiles is probably in the range of 0.45 to 0.72. Higher ratios provide too small a safety factor, while lower ratios result in a heavy missile with reduced payload.

The attached Excel chart shows typical damage sizes for various composites (Schafer can't guarantee the identification of the composites, and there is considerable difference in the composition even of composites that go by the same name). Material properties of the binder and

fibers vary, and the layup is critically important. The three curves should thus be considered as rough order of magnitude (ROM) representations. The three curves for the composites are read from the left axis. The left axis is the ratio between the operating pressure and the burst pressure. The horizontal axis is the ratio of the damage spot radius to the missile radius. As the pressure ratio increases, the size of the burst spot decreases. For 2m diameter missiles (1 m radius), the axis can be read as damage size in meters. For example, at a pressure ratio of 0.72, the damage spot size varies from about 2cm to about 7 cm (radius) depending on material. At a pressure ratio of 0.45, the radii vary from 4.5 cm to 19 cm. The damage size is independent of the energy needed to damage the missile in the sense that if only the damage spot size were irradiated, the missile would fail. If a larger area is irradiated, the missile will fail somewhat sooner. How soon is a major source of contention within the damage community.

**ROM Damage Radius (various composites)**



Rd/Rr
(Approximate size in m for 2m diameter missile)
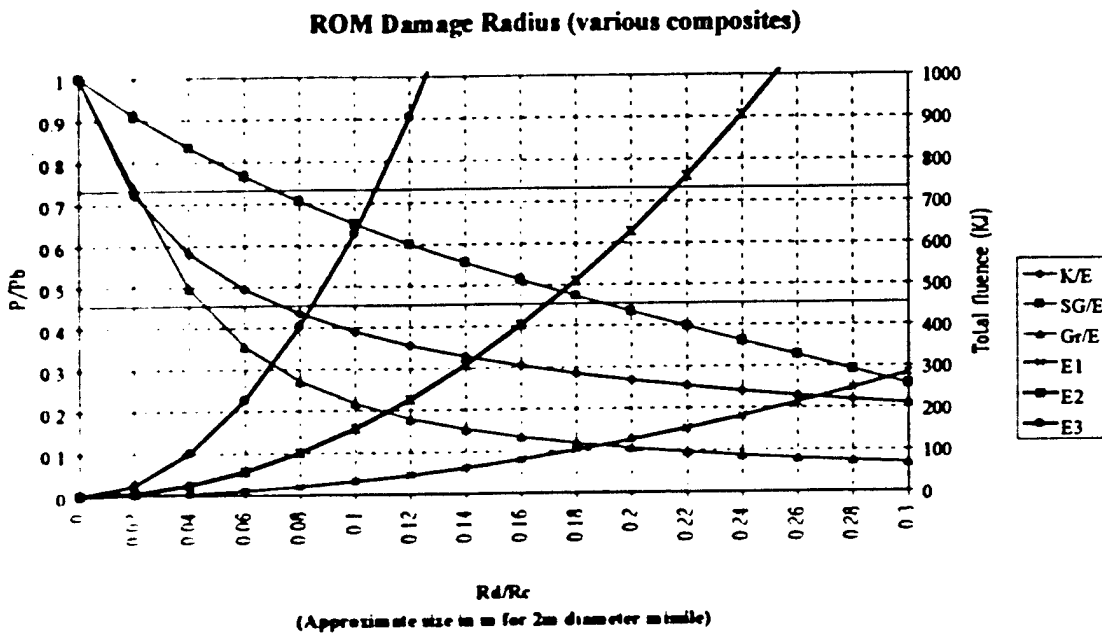
The missiles will almost always be irradiated by large spots (compared to the damage size) because of the large range to the target and diffractive spreading of the beam. For damage testing, there is a conflict between the desire to irradiate large spots to simulate actual engagements, and the limited available power. Under some conditions, the irradiating source must be a laser. Under other conditions a broad band thermal source may be used. In any case, damage tests should be preceded by structural and materials tests to determine the properties of both the virgin material, and the material properties under increased temperature, temperature gradients, and stresses. Sufficient testing must be done to determine statistically valid properties, ensuring that the variation in material and sample preparation does not bias the results.

The required irradiance can be calculated by assuming a damage threshold and assuming uniform irradiation over the damage spot size. The Excel chart shows three other curves (E1, E2

and E3, which were arbitrarily chosen as 1, 5 and 20 KJ/cm$^2$ for this parametric analysis) which should be read to the right-hand axis. These show the required energy in kilojoules. Dividing by the run time yields the required power. For instance, 100KJ deposited over a 100 second laser firing would require a 1 kW laser. The total deposited energy is independent of the rate at which the energy is deposited in a theoretical sense. In practice, losses become more important as the power density drops. We know from past experiments that levels below 100 W/cm$^2$, while important to understand, cause losses from sample edges, conduction, convection, and radiation all to become very significant, decreasing experimental accuracy. Actual laser powers need to be somewhat higher because uniform irradiance cannot be achieved, and times of order ten seconds are more practical experimentally. A laser of about 15 kW represents a good compromise between available power and cost of run time.

How then do we choose appropriate spot sizes and irradiances? As an example, choose a point on the K/E curve (blue with filled diamonds) at pressure ratio of 0.5. The resulting damage spot size ratio is 0.06. Assume that a small (8 inch diameter) pressure bottle is used. The radius is 10.2 cm. The damage spot size is thus 0.06 times 10.2 or 0.61 cm (6mm). The required irradiance must be calculated, since the curves assume a missile size larger than the pressure bottle. The spot area is 1.17 cm$^2$. Assume a desired irradiation of 500 W/cm$^2$, and a desired fluence of 5 KJ/cm$^2$. The required irradiation time is 10 sec and the required laser power is 585 W. For a full scale missile (2m diameter), under the same conditions, the damage spot size is 6 cm. The irradiation time is the same, but the required laser power is 56.5 kW.

Experiments thus become more difficult as the damage threshold rises (roughly as the square of the threshold ratio), and as the target size rises (roughly as the square of the target damage spot size). The goal of the experimental program should be to map the parameter space, in a fashion similar to the Excel chart, where the relevant area is bounded by the upper (purple, filled squares) and lower (red, filled triangles) material curves, and the two black horizontal lines representing pressure ratios. The appropriate sizes in flat samples are determined more by the experimental constraints in trying to match code predictions. Above all, unknown heat losses must be avoided, and all heat losses should be minimized. Location of thermocouples is critical to accurate temperature measurements. Other diagnostics to measure input power and losses are key. Samples have the annoying tendency to vanish (burn through) at higher temperatures (longer irradiation times, higher irradiance), with the attendant loss of instrumentation. Thermocouples also have temperature limits above which they become inaccurate.

The details of a test program must be worked out iteratively with understanding of the various constraints. Practical considerations indicate that a laser of significant power (like VM) is probably required. If a laser is used, it must be at the right wavelength. Some tests can be done with (almost) any thermal source.

Another major variable in this whole process is the test environment (pressure, gas composition, etc.). Static tests in vacuum can have problems with sample material and gases blocking the beam. Static tests in air are subject to the formation of a "chimney" which convects away the exhaust material, but adds oxygen in large quantities to the reactions. Probably the best test would include a well-designed flow nozzle which would simulate actual missile flow

conditions in the atmosphere, with the oxygen partial pressures correct, but the remainder of the flow an inert gas. Many people have had many ideas about the "right" way to do such tests, and the community should discuss the options. The better the test, the more it costs (if that isn't a law of physics, it should be!). The presence or lack of oxygen can be critical, since some of the reactions are exothermic in the presence of oxygen (i.e., the laser is turned off and the temperature keeps rising because the material is burning).

A final note: many of the processes that we need to understand are complicated. We need a valid statistical sample for each type of test, and we should not rush into a test series without the right analysis support and predictions of the physics. Schafer would rather see a test of one hundred small samples which we understand, than a test of 4 small samples and a full scale pressure bottle which we probably won't understand. Scatter in past data has sometimes exceeded 100%! Also, our only two full scale tests (tethered thrusting missile stages) were useless because of experimental failures/conditions.

### 3.6.11 Lethality Meeting (17 November 1998)

The lethality meeting was productive and a consensus seemed to be reached on the key technical issues. The AFRL plan (basic SBL testing) includes all of the key issues which need to be resolved, although most will be resolved later. The key issues associated with each of the eight principal activities are discussed below.

#### Materials

The possible range of composite materials will be very large, and some way of thinning the list will be required. Jorge Beraun indicated that acquisition of foreign materials should be pursued, and that we should look into that quickly, since it can take a long time. The "baseline" design from the intelligence community will be pursued, but we need to have bounding cases which can cover the range of possible material properties.

#### Test Facilities

The critical item in developing a test facility plan is the wavelength and power of the laser required for each of the various tests. There was consensus that testing of composites must be done at the operational wavelength (2.8 um) because of the wavelength dependence of the absorption. Certain of the early tests, which depend only on the heating of materials, can be done with non-laser sources. In between, there will probably be a few disagreements on where the transition to the 2.8 um laser must occur. There was also general agreement that lasers of at least 10KW will be needed, and that many tests will require lasers of several hundred kW. Larger lasers cost more to run, and we need to set up a balanced program which trades the desired number of tests with the costs. The "pit" lasers at AFRL (both $CO_2$ at 10.6 um) will probably be of limited value. Primary candidates seem to be the mid-power laser at WSMR and the VM and NACL lasers at Capistrano. The LHMEL $CO_2$ laser does not seem to be a viable candidate because of the wavelength.

**Test Plan**

The most critical issue in the test plan is to define a logical path to acquire the data needed to develop the models to predict performance. Another key issue is the diagnostics: what will be measured, how will the data be analyzed, and will the uncertainties be small enough for the data to be useful. At low irradiance levels, losses in the system are critical and must be carefully characterized. There has been a particular concern with reradiation as a loss mechanism, due to the complex surface structure of a damaged composite. As we saw in the video, fibers execute large dynamic motions when they fail.

**Data Analysis / Model Validation Plan**

Data without anchored models is of limited use. There are disagreements between models in the low-irradiance regime. A two-dimensional finite element analysis (and perhaps a 3D) are probably necessary to understand the effects in detail and to help anchor current models. Uncertainty in both the test data and the models are to be expected, but we need to reduce the uncertainty as much as possible.

**Test Report**

One failing of some past tests has been a lack of adequate reporting of test data. Test reports must include "raw" data as well as selected data used to produce final conclusions. This raw data should be available in electronic form as well as paper.

**Data Analysis and Model Validation**

The main issue in this task is uncertainty and error bars. The task should include enough statistical analysis to allow us to understand whether the uncertainty is in the experiment, in the models, in the diagnostics, or in the materials themselves.

**Vulnerability Estimate**

Past estimates have been expressed in terms that are difficult for people outside the damage community to use and interpret. The estimates must be clearly described in a way which can be translated into system architecture and design studies without ambiguity.

**Post FY99 Follow-on**

The "Holy Grail" of lethality testing has been a full scale test of an actual thrusting missile (in a ground fixture). The main problem with such a test is the number of things that can go wrong, or at least provide significant uncertainties. We should view such a test not as an end in itself, but as an opportunity to predict the performance/lethality well-enough so that the test can be advertised as a global confirmation of effects, with a reasonably small uncertainty. We are likely to get more advertising from such a test than science. We need to be absolutely certain that

93

we are not going to get unexplainable "bad" results, since such a test tends to stick in the minds of Generals.

## Lethality Plan

Subsequent to the meeting described above, AFRL developed a plan to implement the agreements of the meeting. The plan is excellent overall, with the gaps mainly to be filled in before the various TRR's. AFRL pointed out that they need information on the expected engagements (time of runs to characterize the engagement statistics for the TMD and NMD cases of interest. This engagement, variations in likely irradiance and spot size). Schafer recommends a short series of ISAAC would allow us to determine the best ranges to use and give us a good statistical indication of spot sizes, incidence angles, kill times, etc. These curves could then be used to provide a simpler set of numbers to AFRL.

The manufacturers of the test samples and the constraints given to those manufacturers are critical to the entire process. AFRL plans to review this information prior to procurement, which is appropriate, but Schafer stresses the importance of that review and recommend that the entire working group give it high priority.

On page 10 of the plan, AFRL indicates measurements of optical properties at 2.7, 3.8, and 10 6 $\mu$m, but 1.3$\mu$m is not mentioned. If this omissions was deliberate, we might want to add the extra wavelength (both for COIL and for Overtone HF). A minor point is that the power-weighted HF wavelength is about 2.83$\mu$m rather than 2.7$\mu$m.

One issue not mentioned in the experimental test section was blockage by smoke. To the extent that such blockage is not representative it should be avoided.

The plan points out that the edges of coupon samples are critical. We found in past small coupon testing that the surface area of the edges can be a relatively large fraction of the total surface area Conductive losses to the holder must of course be minimized by use of insulating contacts, but a continuous ring of insulator might be better than small three-point kinematic mounts for some tests Such a holder would minimize radiative and convection losses (if not in vacuum) The holder might also over-constrain the sample, leading to deformation. Energy impinging on the holder can also affect the thermal balance. An aperture in front of the sample and holder, but far enough away to avoid thermal contact might, be appropriate. AFRL has a lot of experience in this area, and may already have an appropriate holder.

In section 3.4.4 of the plan, the list of test facilities does not include Aerospace. If they have a facility, they should be included.

There have been questions in the past about the adequacy of tensile testing due to its one-dimensional nature and the severe dimensional anisotropy of composites. Such tests are still very useful if properly modeled. We might consider if it is possible to do an equivalent two-dimensional laser irradiance test by bending a flat sample over a rounded mandrel, perhaps with a central hole in the mandrel and certainly with an insulator over the mandrel's top.

The lethality model discussion in Section 3.6 of the plan brings to mind past discussions about the adequacy of the various models. Steade Howie would be a good person to have on the working group, or at least at the TRR's. He and Fred Rigby have sufficiently differing views that a discussion between them will generally bring out any points that we might miss.

Section 3.7.3.3 of the plan on test conditions mentions water pressurization of the bottle samples. This test method has caused some contention in the past, with some in the community believing that the conditions of burst and the dynamics during burst are not adequately represented by water-pressurization. The relatively small gas volume bleeds very quickly. One suggestion which may be of interest is to use, for at least a few tests, a gas generator. The metal end caps could be fitted at one end with a generator port, and at the other end with a relief valve. Such an experiment could better match the dynamic pressure profile of a real target. There are obvious experimental and safety constraints, including choice of gases. Again, gas generators are a topic for discussion, not something for which we have a definite answer.

In summary, the program plan is a good one. Schafer at the time did not know the budget situation in sufficient detail to comment on the funding breakouts. The schedule seemed reasonable, although a general caution is that past funding and schedule estimates for any experimental program are often optimistic, and we might expect some shortfalls in the objectives due to unexpected problems. These sorts of problems are independent of the group or facility, and the observation should not be taken as a reflection on AFRL, whose past programs have been well-managed and successful.

## 4.0 ABCS SUPPORT

The ABCS program uses a state of the art beam control brassboard to investigate autonomous alignment techniques necessary for the SBL. In the past year, experiments have concentrated on alignment techniques for the deformable mirror and the secondary mirror of the telescope. Both of these elements are key parts of any of the beam control system concepts being studied under the CDS programs. Previous years' experiments had modified the brassboard to add secondary mirror actuators and to implement the software required for deformable mirror control.

The fundamental technology being developed in ABCS is one of a number of promising candidate approaches for alignment. The portion of the SBL alignment being addressed is "pre-alignment", starting with the system in a state immediately after launch, and aligning the optical system to a precision that is adequate for the fast control systems to be calibrated and to then maintain alignment. The ABCS approach uses a single "far field" camera, combined with a Simplex algorithm. The far field camera uses the image of a star or auxiliary laser, and aligns the optical system by improving the image. This approach has a significant advantage: because all of the light from the star is concentrated in a single point image, the light is used very efficiently and the sensor need not be extremely efficient. Other approaches in the past, and recently proposed, rely on "near field" or collimated beam wavefront sensing. The star source is used as a point source to fill the entire aperture, and the wavefront error is measured over the entire aperture. Several orders of magnitude more light energy is required. Since available stars are of fixed magnitude, the ABCS approach is much more robust. The disadvantage of the approach is that the far field information is less complete. That disadvantage can be overcome by means of the Simplex algorithm, which simultaneously optimizes many degrees of freedom, providing an algorithm which is thus both accurate and light-efficient.

ABCS experiments at Raytheon Optical Systems, Inc. (ROSI, formerly HDOS) have gathered fundamental data about the performance of this approach. These data include sensitivity to noise, the effects of various "merit functions" which provide the core guidance to the algorithm, investigation of actuator hysteresis, and other data which are key to understanding of the approach As a result of the complex interrelationship among the various parameters, the algorithm currently converges at times, and does not at other times. Such phenomena are identical to those found at subscale in earlier subscale experiments, and were handled in those experiments by adjustment of the merit function to avoid regions of low sensitivity (flat areas of the multi-dimensional optimization space). Various techniques were also developed to avoid convergence on localized maxima and to avoid drift due to hysteresis and cumulative buildup of small errors. These techniques have not yet been applied to the ABCS full-scale brassboard.

ROSI has proposed adding a ring resonator to the brassboard to look at the interactions between the resonator alignment and beam control system alignment. Although a valid experiment, more fundamental investigations of the utility of various merit functions are the next logical step. These investigations can be carried out without modification to the current brassboard. Given the current contractual mechanisms, active SMC participation in such

experiments would be required. Such participation could result in rapid technical progress, directly applicable to current concepts, at funding levels less than $500K.

A review meeting was held at ROSI Danbury on 15 October. The ROSI plan for FY 99 work was discussed, but the program path is uncertain because funding has not been allocated by SMC to continue the ROSI effort. Schafer efforts will concentrate on preparing several software packages and technical descriptions of experimental techniques needed for the continuation of the program. Schafer will provide a summary briefing for the new ROSI program manager. Coordination with SMC will continue, with the goal of reaching a final plan for continuation of technology development in automated alignment systems.

The recent ABCS meeting was a good summary of ROSI's position and their plan for renewed experiments. There are two primary issues: current funding does not support ROSI's plan, and there are a number of issues not adequately resolved which should be done before embarking on a new experimental program. ROSI has again moved the brassboard to a new laboratory, near the large vacuum chamber once suggested as the baseline for coating a four meter monolith for the RD. They have again said that this laboratory is not likely to be in demand any time soon (as they did the last time). There was no indication of any problem associated with the move, although they have not rechecked the alignment. At the meeting, ROSI distributed a draft white paper.

The ROSI briefing concentrated on their plans for a resonator alignment experiment which could be added to the existing brassboard in the area used originally for the Helios HF (OT) laser. They have proposed building an 8 inch diameter replica of the Alpha resonator, to be diamond turned by OFC (Keene, NH; formerly Pneumo Precision). This is a change from the previous proposal to use 4 inch diameter optics. The cost difference is apparently not large, but the eight inch version is apparently easier to work with. ROSI did not seem to have a good understanding of the tolerances needed for the resonator optics. As a result, there is some question as to whether the price/delivery/quality of the optics from OFC will be reliable.

ROSI presented a program schedule that calls for experiments in the April-August 1999 period, assuming immediate authorization to purchase hardware (which was not forthcoming). Their proposed price was $565K. The proposed staffing level averaged 1.45 persons, with a peak of 2.9 during the height of the experiments. This is an average cost of $390K per person year. The staffing level is marginally adequate for a reasonable experimental program. ROSI needs to add an optical engineer to the program at least 75% time in order to ensure a more complete program. ROSI's past efforts have been flawed by the lack of sufficient optical expertise internal to their program.

The ROSI resonator design is reasonably good, although the compact leg design lacks an actuated turning flat. Addition of such a flat would make the resonator an exact analog of Alpha and would remove the slight tilts introduced by the actuation of the injected beam splitter (which should not be active). The specification of the inner-to-outer cone errors in the waxicon/reflaxicon was not adequate in the presentation. ROSI admitted that OFC would do a "best effort", but the specifications must be within OFC's capabilities, or the aberrations of the

conics will dominate the alignment aberrations and the experiment will not be representative. OFC does not have metrology capability to verify the individual element specifications, and ROSI did not present a metrology plan.

Performance of the brassboard and the algorithms during the most recent phase of the experiments was not, in Schafer's opinion, adequate to proceed into the next phase. As Bob Tyson and Michelle Thomas have pointed out, there are serious concerns associated with the small dynamic range of the current camera. This small dynamic range can cause convergence difficulties. There are also still concerns associated with repeatability of actuator positioning and sensitivity of the merit function.

We also identified that the merit function used by ROSI (5x5 PIB) is not the best function, and certainly is not appropriate for all degrees of freedom. We recommended the use of different merit functions for SM despace and for SM 5 DOF, and a sequenced approach, switching merit functions as appropriate. We also recommended a 3x3 merit function for DM convergence. ROSI tried one run with such a merit function, but concluded that it was noisy. The conditions of the experiment at the time they performed that test essentially guaranteed a noisy run.

There is insufficient data to determine the exact causes of the dynamic merit function noise (the February 1998 data has not been made available to us for analysis). We have found in our laboratory experiments that the noise sources can typically be reduced or eliminated, since many of them have to do with the details of implementation, and not with fundamental physical noise processes. Further experiments, on more complex hardware, cannot be recommended until these noise sources have been identified and eliminated.

The ROSI ABCS autoalignment white paper begins with an overview of ABCS history and hardware. It next describes the experiment requirements, the control and diagnostic systems, and software. The paper then describes the operating procedure. The operating procedure is correct, but fails to mention the large number of characterizations of the brassboard which must be made prior to successful testing. The experiments must include, and the white paper should describe, merit function noise testing, actuator repeatability tests, various merit functions, camera spot size (both aberrated and aligned), different sequences for convergence, SM single vs. multiple DOF runs, etc.

ROSI's test results section is too short. Preliminary results are presented as if definitive. ROSI indicates that "the secondary mirror 5 DOF Simplex was unable to find this best [alignment] location". After using the two pass technique recommended by Schafer at the start of this phase of ABCS, ROSI showed somewhat improved performance, with occasional failures. Schafer's analysis of system noise indicates that such a result is to be expected, and is a result of experiment conditions having little to do with Simplex. Furthermore, these experiment conditions should be fairly easily improved to allow lower-noise experiments. The DM experiments have a very limited description. This description implies that the experiments had very limited success. A better description would indicate that the experiments are far from complete, and that many more tests, including more careful noise characterization, are necessary before any conclusions can be reached.

The conclusion section is far more critical of the experiments than necessary. All of the noted deficiencies are due to the characteristics of the ROSI experiment. Concluding that "further effort is required in order to make this approach viable for an operational system" indicates that the problem is with the approach. In fact, the experiments were not sufficiently detailed to make such a conclusion with any degree of certainty.

The recommendations section is seriously flawed. It recommends constructing a computer model of the DM Simplex operation to see if the model predicts the observed experiment results. A better approach would be to better characterize the brassboard noise, after improving the camera dynamic range. Implementation of other techniques previously given to ROSI, such as "fluffing" the simplex to avoid convergence to local minima, should also be considered. Schafer already has full models of the ABCS system. Building another is not efficient. The merit function optimization suggested by ROSI has already been done, and provided to them.

ROSI has conducted a good series of experiments, making the most of extremely low staffing levels. The experiments are incomplete. A more systematic approach is needed, including better noise characterization after camera dynamic range upgrades. We should recognize that the last phase of the program has not been successfully completed. Programmatic and contractual issues associated with such a conclusion should be resolved before going on to more complex new experiments. The resonator experiments are critical to SBL alignment. Rushing into such experiments without adequate preparation is unwise.

Work continued at a relatively low level to develop an information package describing the "fluffing" modification to simplex which may be applicable to convergence problems on the ROSI brassboard. ROSI prepared a brief outline of a modified plan which incorporates most of the previous suggestions for amplifying experiments prior to committing to new hardware. A meeting will be held in January to discuss plans for the remainder of the calendar year.

A review of alignment literature from Zenith Star was completed and a package of documentation is on file at Schafer. These documents will be discussed with ROSI and provided on an as-needed basis.

## 4.1    Autoalignment Algorithm Modifications

In order to assist ROSI in the ABCS program, a discussion of the simplex fluffing modification has been prepared. To date, the studies we have performed in a laboratory used algorithms based on the downhill simplex method of Nelder and Mead with few modifications. In the following sections, this method is referred to as the original simplex. A complete discussion of the routine and the code itself can be found in Numerical Recipes[2].

One modification to the original simplex, which showed promise when using computer models of optical system alignment, has not yet been tried in a laboratory environment. The

---

[2] William H. Press et al, Numerical Recipes The Art of Scientific Computing (Cambridge: Cambridge University Press, 1986)

99

procedure is called simplex shape optimization or, more informally, fluffing. In simulations, this enhancement has improved simplex results both by reducing number of iterations and by avoiding convergence to less than optimal solutions. The complete description of the original study can be found in a previous final report[3]. An extract of that discussion is included below in the section on mathematical techniques.


## 4.2 Review of Original Simplex Algorithm

Given that N represents the number of degrees of freedom (DOFs), a simplex is described as the geometrical figure in N-dimensional space consisting of N+1 vertices and all their interconnecting line segments and polygonal faces. For example, if N = 2, the simplex is a triangle Associated with each vertex is a functional value. The goal of the simplex routine is to find the minimum value of the N-dimensional function often called the merit function.

To better understand how this process works to align an optical system, the following associations can be defined. The N degrees of freedom relate to the N controllable mirror motions (e g tilts and translations of each optical surface). Each vertex is defined by a particular set of misalignments of the N mirror positions. In our case, the merit function value is a metric calculated from the far-field intensity distribution resulting from each set of mirror misalignments. Merit functions are chosen such that the best attainable optical quality is achieved when the function value is at the global minimum. Therefore, function minimization refers to the search for the best optical alignment as defined by the quality of the far-field intensity spot.

The minimization process begins with initialization of the N+1 vertices. In our current format, the vertices are placed randomly throughout the N-dimensional space and a merit function value is computed for each. The simplex method then takes a series of steps which iteratively move the current worst vertex (i.e. the worst merit function value) to a location with a better value Most of the steps move the bad vertex along a vector extending from the location of this point through the geometrical midpoint of the opposite "face" of the simplex formed by the remaining vertices (The only exception is the "global contraction" step which is a last resort that gathers all vertices in toward the current best.) The process continues until the vertices converge to a minimum functional value

The original simplex algorithm can converge to a local optimum rather than the global. How often that occurs depends on, among other things, the topography of the N-dimensional merit function being evaluated and the route through N-dimensional space that the simplex follows Since there are limitless choices for the function itself, modifying the simplex algorithm to more wisely select a convergence path is a more useful approach to combating this problem.

---

[3] L.J. Palumbo et al. "Task Order 10. Autoalignment of High Energy Lasers", WJSA-R-94-B-003, 28 January 1994. Contract SDIO84-92-C-0008.

## 4.3 Overview of Simplex Shape Optimization (Fluffing)

Restarting the original simplex process after an initial convergence to a functional minimum and occasionally nudging the simplex during the convergence phase are two common recommendations for avoidance of local solutions. Simplex shape optimization, more simply known as fluffing, falls into a similar category.

The idea behind fluffing is to avoid letting the simplex reduce its scope within the N-dimensional space in which it exists. It was determined that a more efficient search path could be maintained by ensuring that the simplex did not become too "flat" thereby limiting its visibility. In the two dimensional analogy, envision the triangle collapsed to a line. (In N dimensions, a flat simplex has collapsed to a hyperplane defined as an (N-1)-dimensional subspace of the N-dimensional space.) Using only the steps defined by the original simplex algorithm, the vertices are trapped such that they can never escape from this line to explore the second dimension. Although complete collapse to a flat simplex is unlikely, simplexes tending toward flatness are not uncommon.

It was found that maintaining the "roundness" of the simplex helps to improve the convergence characteristics of the algorithm. Given that an equilateral simplex is described as a symmetrical figure in which all sides and all altitudes have equal length and all faces have equal area, the roundness of a simplex is defined as the ratio of its shortest altitude to the altitude of an equilateral simplex with the same volume. At the extremes, the roundness of an equilateral simplex is 1 and that of a flat simplex is 0.

The first stage of this modification to the original simplex procedure is implemented by occasionally computing the roundness of the simplex during convergence. If the roundness value has dropped below a certain threshold, the simplex is reshaped into an equilateral figure enclosing the same volume as the original simplex. In the current incarnation of the method, the new simplex is positioned such that its centroid is located at the same point in space as was the near-flat simplex. At this time, since all the vertices have been redefined, the associated merit function values must be recomputed before the simplex algorithm can resume. With this last point in mind, it is advisable to keep the frequency of the fluffing to a reasonable level. As N increases, repeatedly revisiting all the vertices can be impractical.

## 4.4 Implementation of Simplex Shape Optimization (Fluffing)

The goal of the shape optimization method is to maintain the "roundness" of the simplex in order to maintain optimum visibility throughout the N-dimensional space in which the simplex resides. This is accomplished by occasionally "fluffing" the simplex when it tends toward flatness. This section describes the fluffing algorithm currently implemented in the ABCS laboratory autoalignment code.

The autoalignment module requires a set of parameters which define how the code will run during a particular experiment. Fluffing is controlled by the ninth parameter, MODFLG, which allows two possible settings:

1 = original simplex
2 = activate fluffing

A setting of 1 tells the code to skip any roundness-checking sections while a value of 2 incorporates into the original algorithm the roundness-checking and any subsequent fluffing of the simplex.

Although the formal definition of a perfectly round, or equilateral, simplex assumes all DOFs have the same characteristics, this is not necessarily the case in real systems. The DOFs can vary in engineering units and ranges of motion. Therefore, in order to implement the fluffing method, all DOFs are normalized within the routine. This is necessary since statistics, such as the average simplex altitude, would not make sense if using values with different units or ranges. The normalization is based on input ranges of motion for each DOF. Note that these ranges may not be the full actuator stroke possible, but rather the maximum reasonable values considering detector grid size, far-field spot size, and individual sensitivities.

Two other values control the operation of the fluffing algorithm: roundness threshold and frequency of roundness-checking. As a starting point, the need for fluffing is tested at a frequency of N iterations, where N is the number of DOFs being aligned, and fluffing is executed when roundness falls below the threshold of 0.6. The threshold value stems from the original fluffing study where it was found that the progress of the algorithm slowed considerably whenever the roundness dropped below a value of approximately 0.6. As an additional precaution, no fluff occurs is roundness is below 0.1. Since a fluffed simplex takes on the same volume as the "flat" simplex, a volume approaching zero will contract the vertices into a very small region. However, the value of 0.1 is an arbitrary choice and, since it has not been tested, may require modification based on simulation or experimental results.

Although the original study recommended a roundness-check every 2N iterations, the speed with which other optical models had locked-up in the past suggested the need for more frequent checks. Merely checking roundness is not a time consuming task and, for relatively few DOFs, even if all checks indicated that a fluff was required, the time penalty for revisiting all the vertices would not be excessive. As the number of DOFs increases, however, this issue should be revisited

Briefly, the fluffing process follows the following steps:
Find the centroid of the current simplex, C0
Create a fluffed (equilateral) simplex with one vertex at the origin
Find the centroid of the fluffed simplex
Shift the fluffed simplex such that its centroid is at C0

The details of the mathematics describing this process are discussed below.

After fluffing, the new vertices are checked to ensure they do not exceed the input range limits of each DOF, also referred to as the hard stops. Although this should be a rare occurrence in a well-behaved system, any vertex which violates the restriction is adjusted by setting any errant DOF to its limit. Obviously, the simplex will no longer be equilateral. However, the fluffing process has still acted as a restart or nudge and should still be effective. The final step is to recompute the merit function for each new vertex in preparation for the next simplex iteration.

## 4.5    Vertex Refreshment

Although a necessity after fluffing, periodically reevaluating the merit functions of each vertex is also recommended for any system in which drift, hysteresis, or the occasional unexpected mechanical error can occur during the course of the simplex convergence process. Since the fundamental driver of the simplex algorithm is the location of the best vertex (i.e. the one with the lowest merit function value), an occasional check of the ranking of vertices from best to worst is advisable. Since this step requires revisiting all the vertices, it can be time consuming, so a judicious choice of the frequency with which the process is invoked is needed. At a minimum, we suggest that vertex refreshment be done whenever the simplex algorithm chooses to perform a global contraction. Since the global contraction step completely relies on knowledge of the best vertex, recomputing the merit functions just prior to this step can avoid a misdirected convergence.

Like the fluffing process, this modification to the original algorithm is also controlled by an input parameter, NREFR. If greater than 0, the value assigned to this variable indicates the frequency of vertex refreshment in terms of simplex iterations. For example, a value of 5 would force the routine to recalculate all merit functions every 5 iterations. Setting NREFR = 0 is a flag to perform vertex refreshment only when a global contraction is requested. Any value less than 0 shuts off this option.

## 4.6    Simplex Shape Optimization: Mathematical Techniques

The implementation of simplex shape optimization required the development of mathematical techniques for computing the volume and altitudes of an N-dimensional simplex and for creating an equilateral simplex with a given volume and location. These techniques are described in this section.

### Local Optima and Search Efficiency

Occasionally, for some types of optical systems more than others, we have noticed a tendency for simplex to "hang up" on a local optimum or to get stuck in a region of parameter space where it appears to make very slow progress. There are two different mechanisms that may cause this type of behavior: (1) the algorithm converges to a local optimum because its search space is too small to allow it to "see" the better global optimum; or (2) the simplex collapses nearly to a hyperplane or otherwise gets very small and, therefore, its search space is greatly reduced. In the latter case, it is possible that the algorithm may not be able to see either a global or a local optimum.

In many of these cases, the final alignment state to which the algorithm converges is clearly not optimal. Depending on the complexity of the search terrain in N-dimensional hyperspace (where N is the number of degrees of freedom controlled by the simplex algorithm), the tendency to hang up can occur more or less frequently. Any multidimensional optimization method, including simplex, is capable of exhibiting tendencies to converge to local optima. Indeed, all methods have difficulty distinguishing whether the solution to which they have converged is global or local. The simplex algorithm is known for its ability to avoid local optima; but, given a rugged enough search space, it can also fail in this manner.

## Simplex Restarting

There is a commonly recommended approach for testing whether a particular point to which a multidimensional optimization algorithm has converged is a global or local optimum. That approach is to restart the search in the region around the current solution to see if the algorithm can jump out of a local hole and find a better solution. In the downhill simplex method, this means that one should construct a new simplex by re-initializing the vertices in the region of hyperspace around which the algorithm has converged. Some knowledge of the search space is required so that one may choose an appropriate size for the new simplex to be used to restart the algorithm. Also, it is important to have a means of determining when the algorithm needs to be restarted. We will discuss approaches for this in the following subsections.

## Hyperplanes

There is another potentially pathological problem that, because of its geometrical nature and search methodology, may be unique to the simplex method. This is the possibility of having search space limited by collapse of the simplex vertices into, or nearly into, a *hyperplane*. Recall that a simplex is a geometrical figure defined by the locations of N+1 vertices in the N-dimensional space defined by N controlled DOFs. A hyperplane is an (N-1)-dimensional "flat surface" in the N-dimensional hyperspace, or search space, where the algorithm tries to find an optimum. Just as three points determine a plane in 3-dimensional space, N points determine a hyperplane in N-dimensional space. If the N+1 vertices of the simplex all happen to lie in the same hyperplane (or in an even smaller dimensional space, e.g., a "*hyperline*"), then for all subsequent algorithm steps, the vertices will remain in that hyperplane and thus the search for the optimum will be limited to a flat region of hyperspace. If the optimum state does not happen to lie in that particular hyperplane, then the simplex algorithm will never find it.

If all the simplex vertices lie in a hyperplane, then none of the types of vertex movements allowed by the algorithm can move any vertex out of that hyperplane. Conversely, if the N+1 simplex vertices span N-dimensional hyperspace (i.e., they do not lie in a hyperplane and, thus the simplex has a finite *hypervolume*) then none of the vertex movements allowed by the simplex algorithm can move a given vertex into the hyperplane formed by the other N vertices. Also, one can visualize for small values of N that if the N+1 vertices of a simplex nearly form a hyperplane, then a series of simplex steps can "round out" the simplex hence broadening it search space, thus improving its search efficiency.

If the N+1 simplex vertices all lie close to -- but not exactly in -- a hyperplane, then one of two things may happen as the algorithm proceeds toward convergence. Either the simplex, in a series of standard steps allowed by the algorithm, works its way out of the near hyperplanar shape and resumes an efficient search of problem space, or the simplex tends to limit its search space to points near the hyperplane. The latter option may be stated in other words by saying that a *flat simplex tends to stay flat*. We have found that maintaining the *roundness* of the simplex helps greatly to improve the convergence characteristics of the algorithm.

## Simplex Geometry

Several quantities that characterize the size and shape of an N-dimensional simplex will now be defined and discussed. To streamline the discussion we will usually drop the prefix "hyper" from these quantities; therefore, terms such as hypervolume, hyperarea, hyperspace, and hyperplane will simply be referred to as volume, area, space and plane, respectively. We define in this subsection the terms, simplex volume, volume determinants, areas of simplex faces, partial volumes, simplex altitudes, simplex sides and the concept and properties of equilateral and isosceles-right simplexes. For convenient reference, definitions of these terms and relationships between them are collected in mathematical notation in Figures 4.6-1 through 4.6-4.

## Augmented Simplex Matrix and Adjoint Simplex Matrix

(Examples are shown for a simplex in 5-dimensional space where the coordinate axes are $x, y, z, u,$ and $w$. Subscripts refer to vertices and range from 1 to 6).

**Augmented Simplex Matrix**

$$A = \begin{bmatrix} x_1 & y_1 & z_1 & u_1 & w_1 & 1 \\ x_2 & y_2 & z_2 & u_2 & w_2 & 1 \\ x_3 & y_3 & z_3 & u_3 & w_3 & 1 \\ x_4 & y_4 & z_4 & u_4 & w_4 & 1 \\ x_5 & y_5 & z_5 & u_5 & w_5 & 1 \\ x_6 & y_6 & z_6 & u_6 & w_6 & 1 \end{bmatrix}$$

**Adjoint Simplex Matrix**

$$B = \begin{bmatrix} X_1 & X_2 & X_3 & X_4 & X_5 & X_6 \\ Y_1 & Y_2 & Y_3 & Y_4 & Y_5 & Y_6 \\ Z_1 & Z_2 & Z_3 & Z_4 & Z_5 & Z_6 \\ U_1 & U_2 & U_3 & U_4 & U_5 & U_6 \\ W_1 & W_2 & W_3 & W_4 & W_5 & W_6 \\ P_1 & P_2 & P_3 & P_4 & P_5 & P_6 \end{bmatrix}$$

(Each element of the adjoint simplex matrix is a cofactor of the augmented simplex matrix).

### Simplex Volume Determinant, D, and Volume, V.

$$D = \begin{vmatrix} x_1 & y_1 & z_1 & u_1 & w_1 & 1 \\ x_2 & y_2 & z_2 & u_2 & w_2 & 1 \\ x_3 & y_3 & z_3 & u_3 & w_3 & 1 \\ x_4 & y_4 & z_4 & u_4 & w_4 & 1 \\ x_5 & y_5 & z_5 & u_5 & w_5 & 1 \\ x_6 & y_6 & z_6 & u_6 & w_6 & 1 \end{vmatrix}$$

$$V = \frac{D}{N!} = \frac{D}{6!}$$

### Typical Element of Adjoint Simplex Matrix

$$U_3 = -\begin{bmatrix} x_1 & y_1 & z_1 & w_1 & 1 \\ x_2 & y_2 & z_2 & w_2 & 1 \\ x_4 & y_4 & z_4 & w_4 & 1 \\ x_5 & y_5 & z_5 & w_5 & 1 \\ x_6 & y_6 & z_6 & w_6 & 1 \end{bmatrix}$$

**Figure 4.6-1. Augmented simplex matrix, adjoint simplex matrix and related determinants and cofactors for a simplex in 5 dimensions**

## Hyperarea, A4, of Simplex Face Opposite Vertex 4

$$E_4 = \sqrt{X_4^2 + Y_4^2 + Z_4^2 + U_4^2 + W_4^2} \qquad A_4 = \frac{E_4}{(N-1)!} = \frac{E_4}{5!}$$

## Partial Projected Areas Sum to Zero Across a Row

$$Z_1 + Z_2 + Z_3 + Z_4 + Z_5 + Z_6 = 0$$

## Computation of Simplex Altitudes, H

$$V = \frac{1}{N} H_J A_J \qquad H_J = NV \frac{1}{A_J} = N \times \frac{D}{N!} \times \frac{(N-1)!}{E_J} = \frac{D}{E_J}$$

## Partial Volume Determinants Add Up to Total Volume Determinant

$$P_1 + P_2 + P_3 + P_4 + P_5 + P_6 = D = N! \times V = 6! \times V$$

## Length, L, of a Simplex Side

$$L_{2,5} = \sqrt{(x_2 - x_5)^2 + (y_2 - y_5)^2 + (z_2 - z_5)^2 + (u_2 - u_5)^2 + (w_2 - w_5)^2}$$

## Number of Sides, K, in an N-Dimensional Simplex

$$K(N) = \frac{N(N+1)}{2}$$

**Figure 4.6-2.** Relationships between simplex volumes, face areas, altitudes, and lengths of sides.

## Relationships Between Altitude (H), Length of Side (L) and Volume Determinant (D) for an N-Dimensional Equilateral Simplex

$$H = L\sqrt{\frac{N+1}{2N}} \qquad\qquad L = H\sqrt{\frac{2N}{N+1}}$$

$$D = H^N \sqrt{\left(\frac{N}{N+1}\right)^N (N+1)} \qquad\qquad D = L^N \sqrt{\left(\frac{N+1}{2^N}\right)}$$

$$H = D^{1/N} \sqrt{\left(\frac{N+1}{N}\right)\frac{1}{(N+1)^{1/N}}} \qquad\qquad L = D^{1/N} \sqrt{\frac{2}{(N+1)^{1/N}}}$$

## Augmented Simplex Matrix for an Equilateral Simplex in Five Dimensions (N=5) with One Vertex at the Origin

$$
\begin{bmatrix}
0 & 0 & 0 & 0 & 0 & 1\\
r+q & q & q & q & q & 1\\
q & r+q & q & q & q & 1\\
q & q & r+q & q & q & 1\\
q & q & q & r+q & q & 1\\
q & q & q & q & r+q & 1
\end{bmatrix}
$$

where $r = \dfrac{L}{\sqrt{2}} = H\sqrt{\dfrac{N}{N+1}}$ and $q = L\left(\dfrac{\sqrt{N+1}-1}{\sqrt{2N^2}}\right) = H\dfrac{1}{\sqrt{N}}\left(1 - \dfrac{1}{\sqrt{N+1}}\right)$

Figure 4.6-3. Mathematical relationships for an equilateral simplex

108

## Relationships Between Short Altitude (H), Length of Short Sides (L) and Volume Determinant (D) for an N-Dimensional Isosceles Right Simplex

$$H = L\sqrt{\frac{1}{N}} \qquad\qquad L = H\sqrt{N}$$

$$D = H^N \sqrt{N^N} \qquad\qquad D = L^N$$

$$H = D^{1/N} \sqrt{\frac{1}{N}} \qquad\qquad L = D^{1/N}$$

$$\text{Length of Long Sides} = L\sqrt{2} \qquad \text{Length of Long Altitudes} = L$$

## Augmented Simplex Matrix for an Isosceles Right Simplex in Five Dimensions (N=5) with One Vertex at the Origin

$$
\begin{bmatrix}
0 & 0 & 0 & 0 & 0 & 1 \\
L & 0 & 0 & 0 & 0 & 1 \\
0 & L & 0 & 0 & 0 & 1 \\
0 & 0 & L & 0 & 0 & 1 \\
0 & 0 & 0 & L & 0 & 1 \\
0 & 0 & 0 & 0 & L & 1
\end{bmatrix}
$$

## Roundness of an Isosceles Right Simplex

$$Roundness = \sqrt{\frac{(N+1)^{1/N}}{N+1}} = (N+1)^{\frac{1-N}{2N}}$$

| N= | R= |
|----|--------|
| 2 | 0.7598 |
| 3 | 0.6300 |
| 4 | 0.5469 |
| 5 | |
| | .4884 |
| 6 | |
| | .4445 |

Figure 4.6-4 . Mathematical relationships for an isosceles-right simplex

## Augmented Simplex Matrix and Simplex Volume

A useful entity for describing a simplex and in computing its size and shape is a square matrix which we define as the *augmented simplex matrix*. This is an N+1 by N+1 matrix formed by tabulating the coordinates of the N+1 simplex vertices and appending a column of ones on the right to make the matrix square (see Figure 4.6-1). The coordinates of a given vertex occupy a row; consequently, there are N+1 rows. Much useful information about the size, shape and orientation of an N-dimensional simplex can be obtained from the augmented simplex matrix, its determinant and its inverse. We frequently refer to the augmented simplex matrix simply as matrix A.

The determinant of the augmented simplex matrix is called the *volume determinant*. The volume of the simplex is computed by dividing the volume determinant by N factorial (N!). This can easily be shown to be true for the area of a triangle (N=2) and the volume of a tetrahedron (N=3). We assume that the quantity computed similarly for N > 3 also has meaning as an N-dimensional hypervolume

## Adjoint Simplex Matrix

For every square matrix, P, we can construct another square matrix, Q, called the adjoint of P. The adjoint is the transpose of the matrix of cofactors of the original matrix; obviously, it has the same dimensions If matrix P is nonsingular, then it has an inverse and the adjoint, Q, can be calculated by multiplying the inverse of P by the determinant of P. This method is much more efficient computationally than computing the cofactors directly.

If the vertices of a simplex do not all lie in the same (hyper)plane, then the simplex volume is finite This means that its volume determinant is non-zero, matrix A is nonsingular and, hence, it has an inverse Thus we can compute the inverse of the A, multiply it by its non-zero determinant and obtain a new useful matrix which we refer to as the *adjoint simplex matrix*. The product of the augmented simplex matrix, A, and the adjoint simplex matrix, taken in either order, is the identity matrix times the determinant of A The elements of the adjoint simplex matrix have physical meaning relevant to the size, shape and orientation of the simplex. For brevity, we often refer to the adjoint simplex matrix as matrix B

## Areas of Simplex Faces

Referring to Figure 4.6-1, we note that in matrix A, the rows correspond to vertices and the columns correspond to coordinates. Rows 1, 2, ..., N+1 contain vertices 1, 2, ..., N+1, respectively, while the first N columns, 1, 2, 3, ..., N, contain the x, y, z, ... coordinates. In the adjoint simplex matrix, B, this association is transposed. Here, each of the rows is associated with a given coordinate of N-dimensional space and each of the columns is associated with a particular vertex. The bottom row of matrix B is associated with the right-hand column of ones in matrix A.

**Table 4.6-2 . Comparison of numerical simulations of simplex algorithm convergence with and without simplex shape optimization**

| N | L | Simplex shape optimization strategy | | |
| | | None | From Start | After 1000 Iters |
|---|---|---|---|---|
| 6 | 1 | 646 | 169 | |
| 6 | 2 | 950 | 152 | |
| 6 | 3 | 398 | 164 | |
| 6 | 201 | 193 | 124 | |
| 6 | 202 | 129 | 130 | |
| 6 | 203 | 143 | 142 | |
| 8 | 1 | Fail | 248 | 1346 |
| 8 | 2 | Fail | 232 | 1478 |
| 8 | 3 | Fail | 238 | 1193 |
| 8 | 201 | 1615 | 180 | |
| 8 | 202 | 1229 | 193 | |
| 8 | 203 | 987 | 198 | |
| 10 | 1 | Fail | 393 | 1664 |
| 10 | 2 | Fail | 348 | 1408 |
| 10 | 3 | Fail | 339 | 1468 |
| 10 | 201 | Fail | 234 | 1208 |
| 10 | 202 | Fail | 258 | 1337 |
| 10 | 203 | Fail | 259 | 1337 |
| 16 | 1 | Fail | 1042 | |
| 16 | 2 | Fail | 766 | |
| 16 | 3 | Fail | 639 | |
| 16 | 201 | Fail | 420 | |
| 16 | 202 | Fail | 436 | |
| 16 | 203 | Fail | 467 | |

*COLUMN LABELS:*

$N$ = Number of spatial dimensions or degrees of freedom

$L$ = Length of short side of starting isosceles-right simplex

*Simplex shape optimization strategy:*

*None* No shape optimization

*From Start* Check simplex roundness every 2N iterations. If it has dropped below 0.6. then perform a shape optimization (fluffing) step

*After 1000 Iterations* No shape optimization for first 1000 simplex steps. Then apply strategy as in *From Start*

*CONSTANTS:*

*Merit function:* Negative of N-dimensional distance from optimum point at (100. 100. 100. ...) spatial units  Range = minus infinity to zero

*Stopping criterion:* Merit function of worst vertex > -0.01

*Starting simplex geometry:* Isosceles-right simplex with short sides parallel to the coordinate axes and with the simplex centroid at the origin.

*NOTE:*

"Fail" means that after more than 2000 iterations the algorithm has essentially dug itself into a hole. The simplex has become very flat (typical roundness in range $10^{-3}$ ... $10^{-5}$), and very small compared to its distance to the optimum  The simplex is still progressing toward its goal, but very slowly with a step size is of order $10^{-4}$ to $10^{-6}$ spatial units and shrinking. Often the point at which the small simplex gets stuck is close to the optimum, but clearly further away than the stopping criteria of 0.01 spatial units.

Except for the elements in the bottom row, the values of the elements of the adjoint simplex matrix, B, can be physically interpreted as *partial projected hyperarea determinants*. Note (Figure 4.6-1) that a typical element in B is a cofactor that has the form, including the column of ones, of the determinant of an augmented simplex matrix with one less vertex and one less dimension than the determinant of matrix A. Just as the determinant of matrix A is related to the N-dimensional simplex volume, a single element of matrix B is a volume determinant in (N-1)-dimensional space. Since our viewpoint is in N-dimensional space, we refer to a volume determinant in (N-1)-dimensional space as a *hyperarea determinant* or, more simply as an *area determinant*.

The element in row i, column j of matrix B is proportional to the projection onto the coordinate plane, i, (i.e., the plane perpendicular to coordinate axis, i) of the area of the closed figure formed in an (N-1)-dimensional hyperplane by all the simplex vertices except vertex j. The proportionality factor is $1/(N-1)!$. This closed figure, the face of the simplex opposite vertex j, is referred to as simplex face j. A combination of the partial projected area determinants taken down a column gives a useful geometrical quantity, as we shall now see.

Given a closed figure in a plane oriented arbitrarily in space, we note that its projected area onto a coordinate plane is the actual area of the planar figure times the cosine of the angle between the normal to the plane and the coordinate axis (i.e., the *direction cosine*). We know that the square root of the sum of squares (RSS) of the complete set of direction cosines of a vector is unity. Therefore, we conclude that the RSS of the partial projected area determinants in column j is proportional to the area of simplex face j. This RSS value must not include the last row of the adjoint simplex matrix and it must be divided by $(N-1)!$ to compute the actual hyperarea of simplex face j (See Figure 4.6-2).

Two other interesting N-dimensional geometrical concepts can be derived from the elements of matrix B. First, the direction of the normal to hyperplane j, expressed in terms of direction cosines, can be directly computed by dividing the partial projected area determinants (the individual elements of B) by their RSS taken down column j, for row i = 1 to N. Second, one can see that if matrices B and A are multiplied, in that order, the elements of the last column (except the element in the last row) will all be zero. This, of course, follows from the fact that the product of the two matrices is proportional to the identity matrix. This means that the projected areas of all the simplex faces onto a given coordinate plane add algebraically to zero.

## Simplex Altitudes

*Simplex altitudes* are distances from a given vertex to the face opposite that vertex taken along a line perpendicular to the face. Recall that the area of a triangle is 1/2 the length of the base times the altitude and the volume of a tetrahedron is 1/3 the area of the base times the altitude. Extrapolating to N dimensions, we can state that the volume of a simplex is 1/N times the hyperarea of a face times the altitude dropped from the opposite vertex to that face (See Figure 4.6-2). This holds for any simplex face and its corresponding altitude. Therefore, if we have values for the simplex volume and for the areas of all of its faces, computed as described above, we can use the formula just discussed to compute all of the simplex altitudes. Working out the math, we see that the factors of N, N! and

112

(N-1)! cancel and the altitude is just the volume determinant divided by the RSS of the partial projected area determinants.

We may think of the altitude as a vector. The length of the vector is simply the altitude. The direction of the altitude vector is the direction of the normal to the plane to which the altitude is dropped. A method for specifying this direction in terms of direction cosines was described above.

**Partial Volumes**

The elements of the bottom row of the adjoint simplex matrix can be interpreted as *partial volume determinants*. By examining the cofactor (determinant) that defines the element in row N+1, column j, it can be shown that the value of this element is the volume determinant of a new simplex formed by replacing vertex j of the original simplex by the origin.

The algebraic sum of the elements in the bottom row of matrix B is equal to the volume determinant of the original simplex. This can be seen by noting that the product of matrices A and B is equal to the identity matrix times the simplex volume determinant. In performing this multiplication, we compute the dot product of the bottom row of B and the right-hand column of ones of A to produce a diagonal element whose value is the simplex volume determinant. Of course, forming a dot product of vector, V, with a vector of all ones is equivalent to simply summing the elements of V. From this it can be seen that *if all partial volume determinants have the same sign, then the origin lies inside the simplex.*

**Equilateral Simplex**

Looking ahead to our recommended approach for simplex shape optimization, we have chosen a method for restarting the simplex by periodically reshaping it into what we assume is a nearly optimal shape – *an equilateral simplex*. This is a highly symmetrical simplex in which all sides and all altitudes have equal lengths and in which all faces have equal areas. Figure 4.6-3 presents mathematical relationships between the altitude, side lengths, and volume determinants of an equilateral simplex. The Figure also shows an augmented simplex matrix that illustrates how the locations of the vertices of an equilateral simplex can be computed.

For comparison, we show in Figure 4.6-4 similar mathematical relationships for an *isosceles-right simplex*. This is the N-dimensional analog to an isosceles-right triangle, a well-known two-dimensional figure with two 45-degree angles. An isosceles-right simplex is easy to construct; the relationships between its sides, altitudes and volume are fairly simple. However, for large N, this type of simplex does not have an optimal shape.

**Simplex Flatness and Roundness**

Since we want to detect and avoid flat simplexes, we need some way to define the flatness or, conversely the roundness, of a given simplex. Intuitively, we postulate that a flat simplex has at least one altitude that is significantly smaller than the average. Given the vertex coordinates of a simplex, we can apply the methodology just discussed to quantify simplex size and shape. We may use the elements

113

of the matrix B to compute the areas of all simplex faces and the lengths of the altitudes dropped from each vertex.

We assume that an equilateral simplex provides the algorithm with an optimal (or at least a very good) "view" of search space. Although we have not proven it rigorously, we assume intuitively that an equilateral simplex has the smallest ratio of "perimeter" to volume -- much like a sphere. Therefore we define the term roundness such that an equilateral simplex has a roundness value of unity. Furthermore, we define the *roundness* of an arbitrary simplex to the be *ratio of its shortest altitude to the altitude of an equilateral simplex with the same volume*. Thus, the value of roundness varies from zero to one. For a simplex that has collapsed into a hyperplane, all altitudes are zero and the roundness is also zero. We sometimes use the term *flatness*, which is defined as 1 minus roundness.

## 4.7    Monotonic Merit Functions

Simplex algorithm behavior was investigated mainly with simple merit functions that could be defined similarly for any number of dimensions. Simple forms were chosen to highlight various aspects of algorithm behavior that are independent of merit function topology. These included N-space distance and an N-dimensional Lorentzian -- two very smooth merit functions with only one optimum, i.e., no local optima. These merit functions improve monotonically as one moves in N-dimensional space toward the optimum. A few runs were done with a more complex "optical" merit function to provide a rough search terrain.

The smooth monotonic merit functions were chosen in order to separate pathological algorithm behaviors due only to the nature of the simplex algorithm from those caused by a rough search terrain or local optima. The simplest merit function, *N-dimensional distance*, is defined as the distance between a vertex and a selected (optimum) point in N-space. This merit function is optimized when the distance is zero, i.e., when the vertex is moved to the location of the selected point. N-dimensional distance is computed by taking the square root of the sum of the squares (RSS) of the differences of the individual vertex coordinates and the coordinates of the optimum location. The use of this merit function allows us to study simplex algorithm behavior problems that are due only to simplex size, shape and location and the nature of the simplex algorithm. Most of the work described in this section was done with the N-dimensional distance merit function and, unless otherwise stated, the results presented below pertain to runs done with this merit function. It should be noted that results from runs using an N-dimensional Lorentzian for a merit function showed no significant differences from those using N-dimensional distance.

Some preliminary runs were done with an "optical" merit function that exhibited very rough terrain typical of optical interference phenomenon. This merit function, an analytical expression for the on-axis far-field intensity produced by an array of possibly misaligned rectangular light sources (such as illuminated mirrors), proved difficult for the simplex algorithm to handle. However, the use of simplex shape optimization helped significantly in these numerical experiments too. Since this work was very preliminary, we mention it here for informational purposes only; it will not be discussed further in this report.

114

## 4.8    Initial Runs and Problems Observed

It was expected that the algorithm, in the form as originally described by Nelder and Mead, would be well behaved with a very simple monotonic merit function. However, we were surprised to find that it was easy to create starting conditions that would cause the algorithm to dig itself into a hole that it could not work its way out of. These conditions occurred when all the initial simplex vertices were close together but they were all relatively far away from the optimum. The simplex would often tend to shrink to an even smaller size and thus it would never make its way over to the region of the optimum. A similar problem also occurred for starting simplexes that were large but flat. If the simplex starts out very flat, it tends to stay that way or get even flatter or smaller. Sometimes, a flat simplex would shrink about a point away from the optimum point. This results in the algorithm "getting in a rut" with very bad convergence efficiency.

By contrast, if the size of the starting simplex was large relative to the distance to the optimum and the initial vertices either enclosed the optimum or lay within a few simplex widths of the optimum, then the algorithm usually converged to the optimum with reasonable efficiency.

### Roundness and Shape Optimization

When the simplex gets too flat, its search space becomes limited and the convergence rate of the simplex algorithm is greatly reduced. We have found, by observing the progress of the algorithm, that whenever the simplex roundness dropped below a value of approximately 0.6, the algorithm convergence rate tended to slow considerably. In cases like this, there is a strong tendency for the simplex to get even flatter and also smaller as the algorithm progresses; therefore the algorithm search space can rapidly become very small. This roundness threshold value of 0.6 acts as a useful practical criterion for any number of spatial dimensions (range studied: N = 3...80). Again, it should be emphasized, that this behavior was observed for very *smooth monotonic merit functions*.

### Implementation of Fluffing Operation

We therefore have incorporated into the algorithm a capability for computing and monitoring the simplex size and shape (volume, altitudes, roundness, etc.) and we have also implemented an option to reshape the simplex whenever it gets too flat. In approximate but essential terms, *whenever the roundness drops below 0.6, the simplex is reshaped into an equilateral simplex* and the algorithm is restarted with its new set of vertices. Since we are interested in modifying the shape only, the *volume of the simplex is preserved* while reshaping. We refer to the operation of reshaping a simplex into an equilateral simplex with the same volume as *simplex shape optimization* or, more simply, as *"fluffing"* the simplex

Restarting has traditionally been recommended for practically all types of multi-dimensional optimization methods, including simplex, as a technique for coaxing the algorithm away from a local optimum. For the simplex algorithm, a widely recommended approach is to generate a new simplex in the shape of an isosceles-right simplex with one of its vertices coinciding with the position of the best vertex of the old simplex. The vertex coordinates of an isosceles-right simplex with short sides parallel

to the coordinate axes have a simple mathematical form as shown in Figure 4.6-4 and, therefore, are easy to compute.

However, that same Figure (near the bottom) shows that, for N > 3, an isosceles-right simplex is too flat. Its roundness is less than 0.6, the limit of our roundness criterion. Similarly, we found that a simplex created from *randomly generated vertices* is also very unlikely to exceed the roundness limit, especially for moderate to large values of N. Because isosceles-right simplexes and simplexes with randomly located vertices tend to have roundness values less than 0.6, we have chosen to use an equilateral simplex (with a roundness of 1.0) to restart the algorithm.

### Results of Implementing Shape Optimization

In order to study the effect of simplex shape optimization (fluffing), we performed several numerical simulations in which the shape optimization feature was turned on and off. Some typical and illustrative results are summarized in Table 4.6-1. Simulations were performed with different numbers of DOFs, N, and with large and small starting simplexes. We compared results with no fluffing, with fluffing active, and with fluffing activated after 1000 algorithm steps.

The starting simplex in all cases was an isosceles-right simplex with its vertex coordinates computed as shown in Figure 4.6-4. The simplex was then shifted so that it centroid was located at the origin. The N short sides were parallel to the coordinate axes. All runs used the same merit function: N-dimensional distance from a defined optimum point with coordinates (100, 100, 100, ..., 100) expressed in arbitrary spatial units. Therefore, initially, the simplex centroid was $100 \sqrt{N}$ spatial units away from the optimum. The tabulated results are the number of algorithm iterations required to meet the stopping criterion, which occurred when the merit functions of all the vertices exceeded -0.01, that is, all vertices lay closer than 0.01 spatial units away from the optimum point.

Horizontal lines in the Table separate the runs into groups of three. Within each group, the value of N is constant and the size, L, of the starting simplex varies only slightly; therefore, one would expect that the resulting iteration count would be comparable. The observed variation indicates the "statistical" behavior of the simplex algorithm. The amount of variation within a group is much smaller for the runs where shape optimization is active. This more consistent, or less chaotic, behavior has been observed in practically all simulations (of which those in Table 4.6-1 are a small sample) done with the fluffing enhancement active.

For each N, simulations were performed for three small values of L and three large values of L. For the latter, the starting simplex is large enough such that the N-space distances between the simplex vertices and the optimum point are comparable to the simplex size. This means that if the simplex does not initially contain the optimum point, it has the capability of enclosing it in a few algorithm steps. For large starting simplexes, one might expect that the algorithm will converge reasonably efficiently in its basic form, without help from shape optimization. After all, it has worked very well on many types of problems for years. The Table shows that this is true for N = 6 and L = 201, 202 and 203. In these cases, the combination of adequate starting simplex size and small problem dimensionality is sufficiently favorable that the activation of the fluffing feature improves convergence very little, if at all. For more difficult starting conditions (N = 6, L = 1, 2, 3), with all the vertices clustered around the origin far

from optimum, the unaided algorithm does indeed converge to the right the answer. But, with shape optimization activated, the convergence time decreases on average by about a factor of 4.

For the higher dimensional simulations, N = 8, 10 and 16, the unaided algorithm "fails" in almost all trials. (See the note in Table 4.6-1 for a description of the failure mode.) The only exceptions are the large starting simplex group for N = 8. For these cases, the unaided algorithm converges in all three attempts; however, helped by shape optimization, the convergence rate is improved dramatically (a factor of ~7 if one compares averages of three trials).

For all fifteen runs listed in Table 4.6-1 in which the unaided algorithm failed to converge, the enhanced algorithm was successful. The version enhanced by shape optimization always takes somewhat longer given more difficult starting conditions (small starting simplexes) and it requires more iterations as the number of DOFs, N, increases. The number of iterations required to achieve the stopping criterion shows only a small statistical variation for closely similar initial conditions. Also, it increases nearly, but slightly faster than, linearly with N. The variation is closer to linear for runs with large starting simplexes.

Algorithm behavior for all entries marked "fail" in the Table was practically identical (see the note). After several hundred iterations the simplex size, and hence its motion per step, became smaller by orders of magnitude than the distance the vertices had to move to reach the optimum point. Consequently, the rate of convergence slowed to a crawl. Worse yet, the simplex became flat (roundness value of order 0.00001) and kept getting even smaller and flatter. It was apparent that the algorithm would never converge, although there was clearly no tendency for it to diverge either. The simplex was essentially stuck in one place.

The question arose as to whether the algorithm could be lifted out of that helpless state by using simplex shape optimization. This was tried and the results are indicated in the last column of Table 4.6-1. In these runs, we allowed the algorithm to run for 1000 iterations in which it dug itself deeply into a failed state of the type just described. At that point we activated the fluffing capability and, in 9 out of 9 trials (we did not perform these tests for N = 16), the enhanced algorithm was able to recover in only a few hundred additional steps. The two identical iteration counts of 1337 in the last column of Table 4.6-1 (N = 10) are a coincidence; they are not misprints.

The recovery process was similar in all runs and was interesting to watch. First, a fluffing operation made the simplex perfectly round. Then, as the algorithm progressed, the simplex grew larger. Whenever the simplex started to get flat (and, consequently its rate of growth started to level off), a fluffing operation would force it to be made round again and its rate of growth would be restored. The simplex kept growing at a roughly exponential rate until its size became comparable to the distance in N-dimensional space that it had to travel to reach the optimum point. Then it moved to enclose the optimum point and, finally, shrunk down around that point until convergence was reached. In this shrinking phase, the simplex tended to stay reasonably round by itself; it did not need much help from the shape optimization feature.

117

## 4.9    Summary and Recommendations

We have modified the logic flow of the simplex algorithm by adding a new type of step that the algorithm can take when necessary. The new step is referred to as a simplex shape optimization (or "fluffing") step. It is executed whenever the simplex becomes too flat. This modification greatly enhances the algorithm convergence rate by nudging it out of pathological situations in which its search efficiency is seriously degraded. In essence, the modification consists of monitoring the simplex shape and restarting the algorithm with a new optimally shaped simplex whenever necessary. More specifically, when the roundness value of the simplex decreases below the value 0.6, the algorithm is restarted with an equilateral simplex (which has a roundness of 1). It was found empirically that this roundness value limit of 0.6 applied to any number of degrees of freedom. The roundness, which varies in value from zero to one, is defined as the ratio of the shortest altitude of a given simplex to the altitude of an equilateral simplex with the same volume.

To aid in defining simplex size and shape, we have developed a computationally efficient mathematical formalism based on matrices and determinants to calculate such quantities as simplex volumes, altitudes, and roundness. This formalism also allows us to compute the vertex locations needed to create an equilateral of any size and dimension.

Typical pathological situations that the algorithm can get itself into are not necessarily caused by the algorithm converging to a local optimum. Another type situation, a flat simplex condition, has been seen to occur frequently with smooth monotonic merit functions that have only one global optimum and no local optima. This phenomenon involves the shrinking and flattening of the simplex such that the steps it takes toward the optimum are very tiny and grow even smaller as the iteration count increases. In runs with smooth monotonic merit functions, the flat simplex problem has been observed to occur quite frequently. It has happened for systems with as few as 8 DOFs with challenging starting conditions (small simplex with vertices far away from the global -- and only -- optimum) and for systems with as few as 10 DOFs with good starting conditions.

The results of implementing simplex shape optimization were dramatic. The convergence efficiency and robustness of the simplex algorithm were greatly improved. In *every* simulation we have run, the simplex algorithm with shape optimization activated converged efficiently and consistently. In cases where the algorithm converged both with and without shape optimization activated, either the same or more iterations were required to reach convergence without it. In many runs without shape optimization, the algorithm "hung up" when it degraded into a flat simplex condition. Repeating these runs with the fluffing option activated from the start, or continuing these runs from the degraded state after activating the fluffing feature, always resulted in successful convergence.

Because of the substantial improvements we observed in convergence rate and consistency, we strongly recommend that the simplex shape optimization enhancement described in this section be incorporated into all optimization systems based on the simplex algorithm.

## 5.0    SUMMARY

The following tasks are suggested to develop technologies for key SBL issues. Schafer has concentrated on technology development issues.

### Alignment

Current plans calls for limited funding to support automated alignment activities. Small-scale brassboard activities in the Schafer Chelmsford laboratory are a very efficient way to advance alignment technologies beyond ABCS brassboard plans. A detailed proposal could be prepared, but an effort at 1 person LOE (about $200K) is a sensible precaution which the program should undertake.

### Costs

The current SBL operational system cost, driven by the desire to handle a particular hardened threat, is in danger of reaching a level which will kill support for the program. A revised cost/technical architecture is needed which can bring the program costs back down to affordable levels  This approach must consider technology, threats, and costs. It should identify key cost drivers as a function of threats and technology, and should investigate large numbers of potential architectures in a cost-efficient manner. Schafer has the unique people and tools in place to perform such a special study. This study should be an intensive 3 person effort for 4 months, followed by a 1 person level of effort for an additional 3 months for reporting and briefings. Total cost would be about $300K.

### Architecture envelope

Our current architecture studies are limited, because ISAAC used to be limited in the number of cases which could be run  Advances in code automation have made this tool orders of magnitude faster than older versions or than any comparable tool in the community. A rapid search of parameter space should be conducted to find any "local optima" that have been missed in the past  This task would logically be a precursor to the cost task above, and would involve 2 people for 2 months ($80K).

### Beam control technology

The current SBL operational concept relies on beam control system performance that is considerably better than any performance projected in past studies. No particular breakthroughs are cited. The contractors propose arbitrary beam control performance, which is set at a level just sufficient to achieve the desired brightness, without any explanation of how such technology is to be achieved. If such technology was available today, it would achieve 120 times more brightness than has been demonstrated to date on ALI at high power. This two-order-of-magnitude

improvement in performance would ordinarily require two generations of major high power beam control experiments beyond ALI. A critical study of beam control technology is needed, to determine the true current state of the art, and to define reasonable limits which should be placed on system studies so that the resulting architectures are reasonable projections. This effort would require 3 people working half time over 6 months ($200K).

## Large lightweight optics

There has been an argument for the last 20 years between proponents of active technology and passive technology for large optics. Current concepts may involve combining both approaches, with a passive large mirror coupled with an active beam control system in the compact leg In order to understand the likely contractor approaches, a critical study of the two major approaches should be completed. This can be thought of as a completion of the initial status briefing, but needs to be extended to understand the interaction between the large optics and their integral beam control system. This effort would require 2 people at half time for 9 months ($200K).

## Telescope phasing

The basis for the only successful phasing technology demonstrated to date (early LAMP tests) was the piston interferometer developed by the Schafer Rome operation. One of the few analytic demonstrations of phasing algorithms was the Simplex work done by Bob Tyson a few years ago We have argued in the community that phasing is the key technology required for large deployable optics. We should do first an analytical investigation, then a simple experiment, to demonstrate the feasibility of phasing approaches. This effort is critical prior to setting forth on a telescope development program which is likely to cost of order $100M. Schafer could conduct such an effort for the order of $500K.

## Laser performance

The current approach to the operational system is the HYLTE nozzle. This approach was developed in the early 1980s. There are other, better, nozzle concepts that have been developed. The program should conduct an investigation which looks at the past technologies proposed in MICOM nozzle programs, and develop a program plan for nozzle development as an "advanced technology". This effort would require 2 people working at 25% time for 1 year ($150K).

## System Engineering Handbook

Schafer calls attention to the system engineering handbook proposed, which received high marks from the evaluation team. Since no rights to usage of the proposed approach vested in the government, and since such an approach would produce a technical product which would be uniquely valuable to the community, Schafer suggests separate tasking to prepare such a handbook. This would not be a support task, but would rather produce a handbook of the general quality of the IR&EOS handbook published by SPIE (to which Bob Tyson and Gary Golnik contributed chapters). Such a handbook would provide a lasting legacy for future SBL and DE

120

programs for the next generation. We would follow an approach similar to that taken by ERIM in the above mentioned handbook. Authors are not directly compensated for their time, but receive a small honorarium for their contributions. The task costs support the editorial and production process. Schafer does not have a detailed cost estimate, but suspects that it would be on the order of $500K, depending on whether one of the professional societies (probably SPIE) could be persuaded to be involved.

# Space Based Laser
## ACC Briefing

Space and Missile Systems Center
Advanced Systems
Lt. Col. Weidenheimer
15 Dec 98

# Appendix 3.1-1
# ACC Briefing

# How We Do It

# Agenda

- ## Overview
  - Introduction
  - Single SBL Platform
  - Architecture

- ## SBL Potential for ACC Missions Areas
  - TMD
  - Air & Ground Attack
  - Reconnaissance & Surveillance
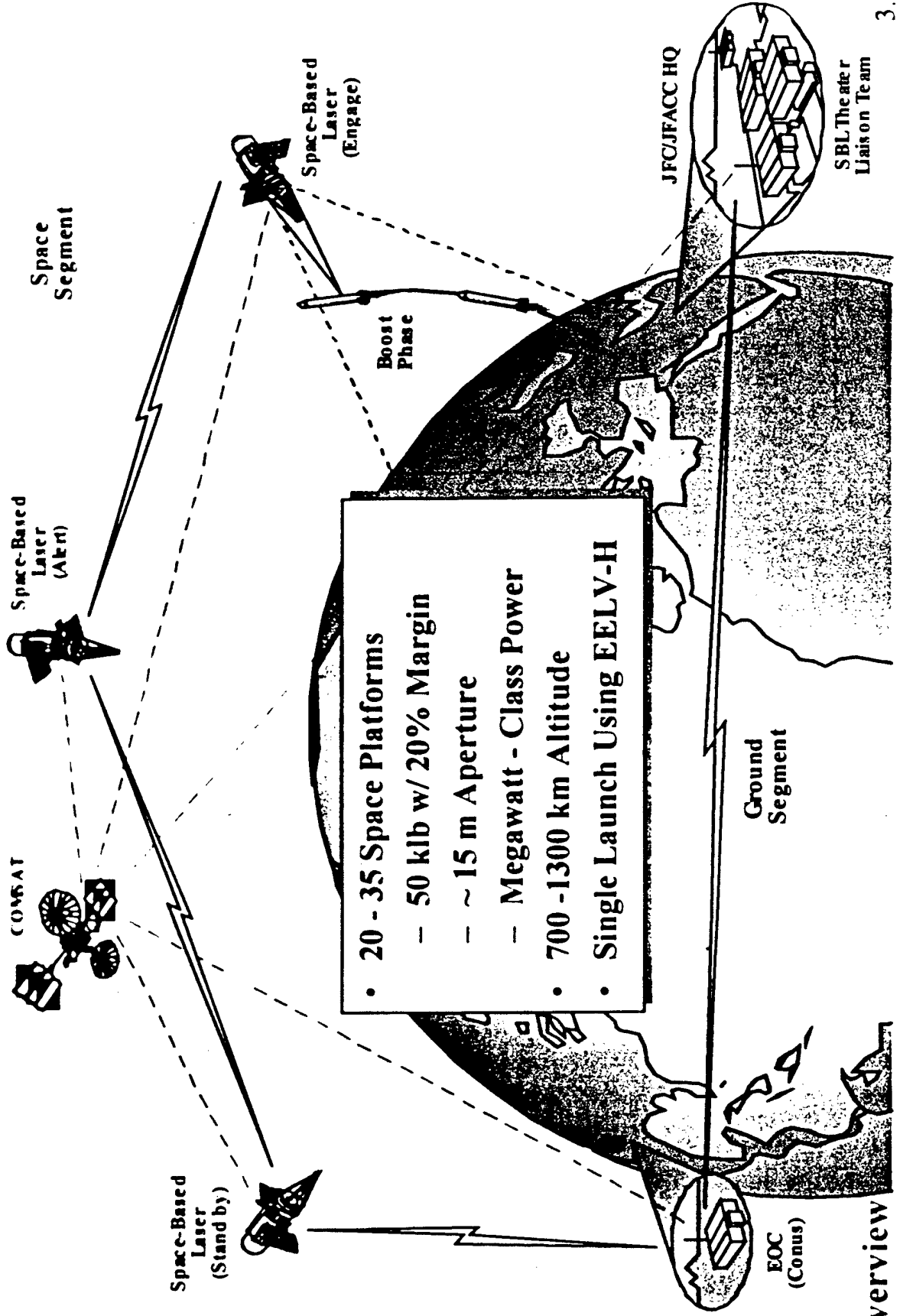
- ## Program Plan

- ## Summary

# Introduction

- **SBL Provides Worldwide Capability For:**

  - **Ballistic Missile Defense**

  - **Counterspace Missions**

  - **Ancillary Missions**

- **SBL Supports Multiple Missions Simultaneously**

- **SBL Will Be Highly Automated, Yet Have Human in Control**

# Space Based Laser System



Space Based Laser (Engage)

Space-Based Laser (Alert)

Space Based Laser (Stand by)

COMBAT

Boost Phase

Space Segment

Ground Segment

- 20 - 35 Space Platforms
  - 50 klb w/ 20% Margin
  - ~ 15 m Aperture
  - Megawatt - Class Power
  - 700 -1300 km Altitude
- Single Launch Using EELV-H

JFC/JFACC HQ

SBL Theater Liaison Team

EOC (Conus)

Overview

# Notional SBL Platform



**Bus (ACS, Comm, Power)**

**Acquisition and Tracking**

**Laser Device/ Doors**

**Reactant Storage**

**Beam Control**

**Beam Expander**

**Secondary Mirror/Outgoing Wavefront Sensor**
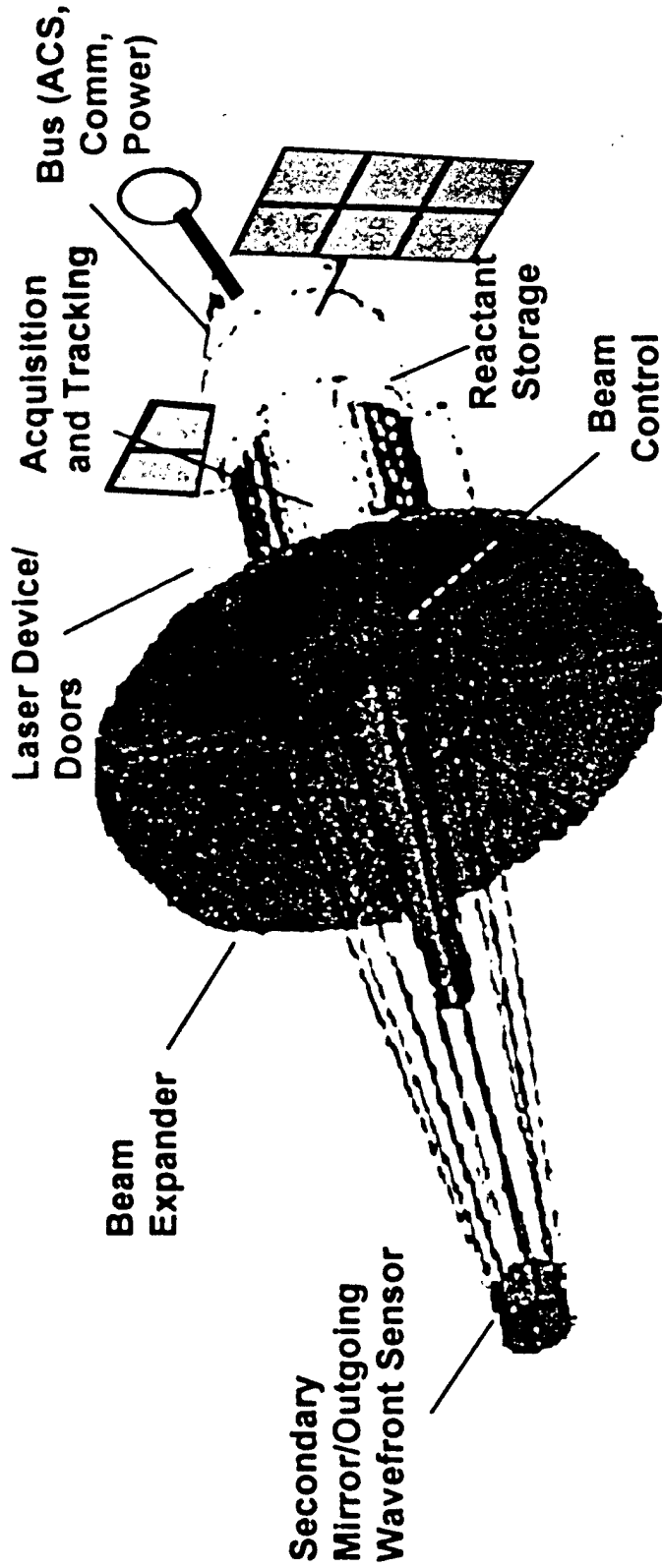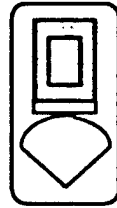
- Size: 4.5 m x 20 m
- Beam Expander Diameter: ~ 15 m
- Mass: ~ 23,000 kg (50,000 lb.)
- Beam Intensity ~1000's Suns (100s - 1000s w/cm$^2$)
- Beam Power ~ Megawatt Class
- 3000+ km range with ~ 100 shots
- 10 - 13 year system lifetime
- On-orbit refueling and maintenance

Overview

# Alpha High Energy Laser

REAR CONE

BEAM COMPACTOR
(OUTER AND INNER CONES) 3.1-1-8

REAR CONE

ANNULAR LASER BEAM

OUTER CONE

SCRAPER CLIPPER

BSM1

SCRAPER

BSM2

INNER CONE

UNCOOLED
SINGLE-CRYSTAL
SILICON MIRRORS

OUTPUT LASER BEAM

Annular Resonator (HEX-DARR)

LASER DEVICE
(SURROUNDED BY ANNULAR RESONATOR)

Overview

# Elements of SBL Beam Control
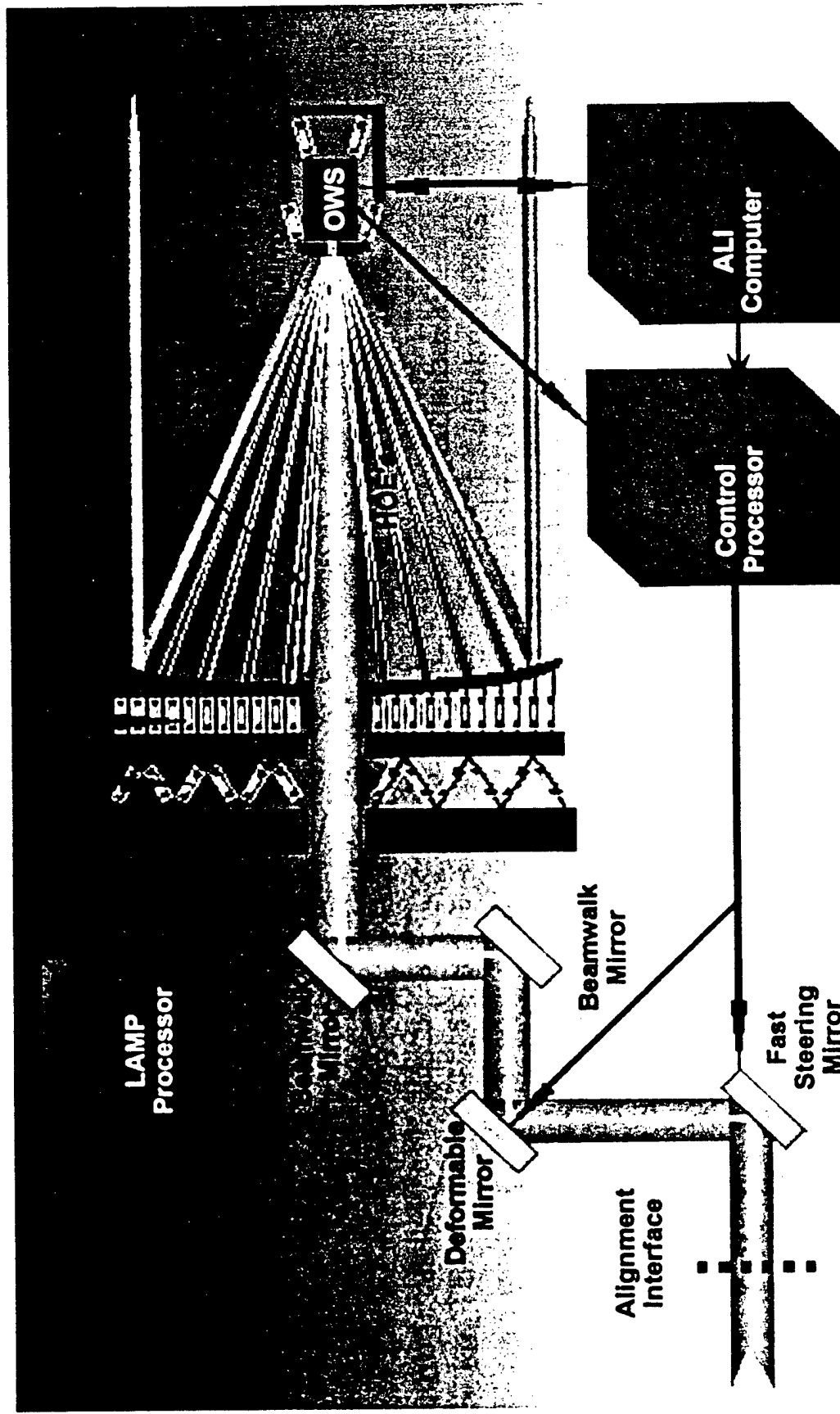
Overview

# Sub-Scale Prototype Primary Mirror
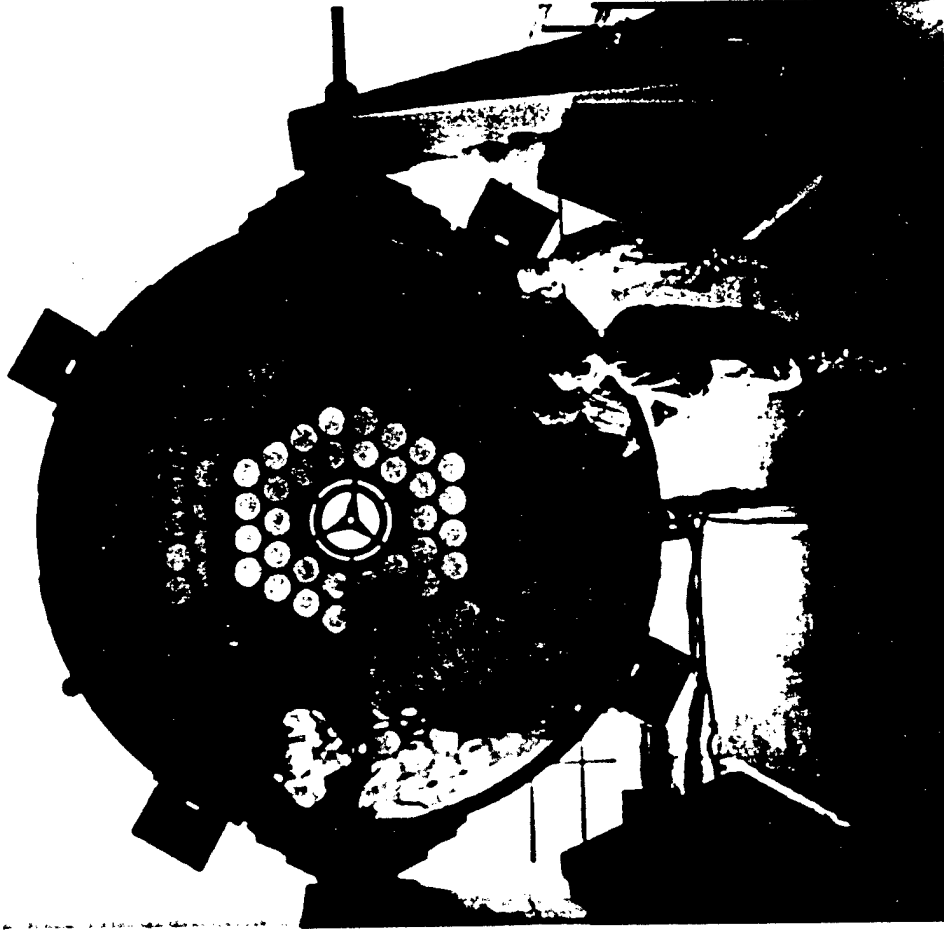


LAMP - Ready for ALI Test
Integrated at CTS with HOE's (1995)

Overview

# Demonstration ATP System

- The ATP System
  Finds the Target,
  Points the Laser
  at the Target, and
  Holds the Laser
  on the Aimpoint
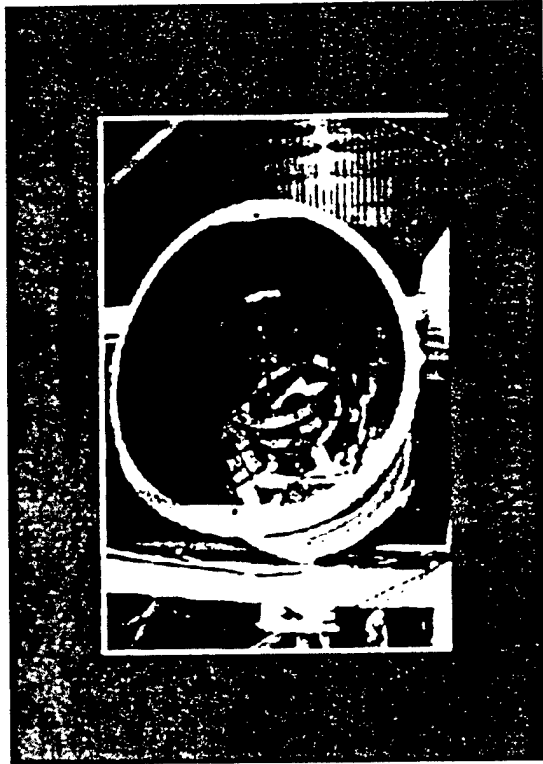
HABE Risk Reduction Program

Acquire  Passive Track  Active Track  Aimpoint Selection
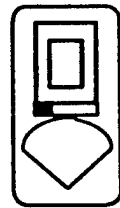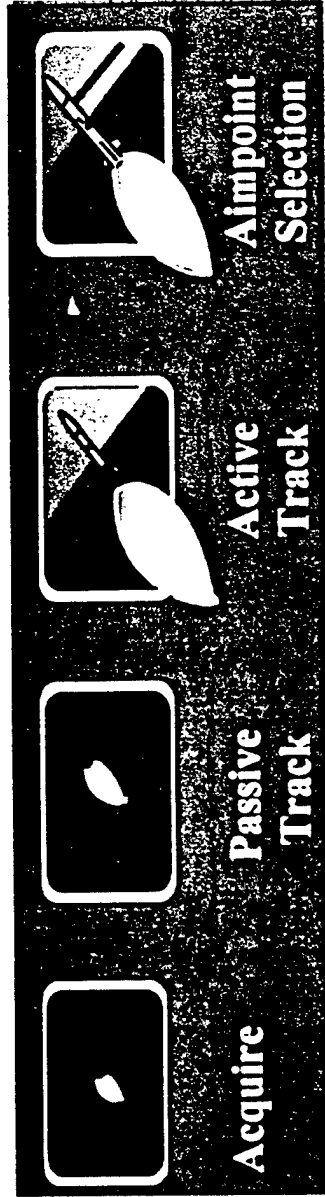
Overview

# Current SBL Test Status

**DEMONSTRATED TECHNOLOGIES**
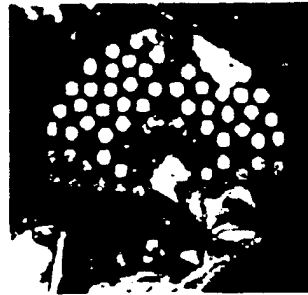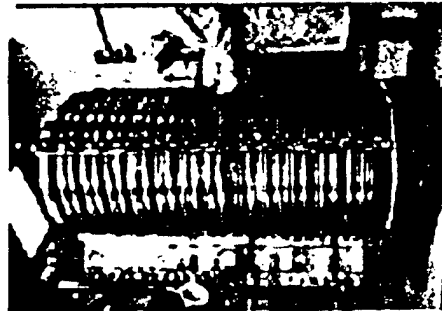
**Large Optics**
(LAMP, 1989)

**Beam Control**
(LODE, 1987)

**Laser**
(ALPHA, 1991)

**INTEGRATION**

Alpha-LAMP Integration (ALI)
End-to-End Weapon Element Testing
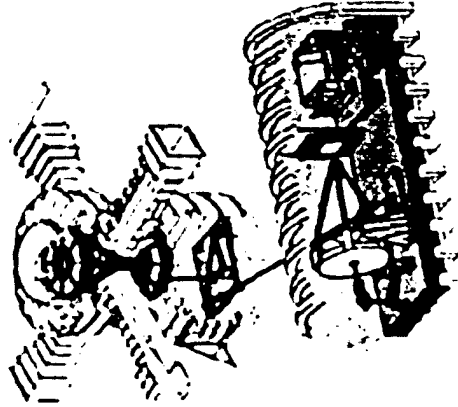
Acquisition, Tracking, Pointing & Fire Control
(High Altitude Balloon Experiment (HABE))

**High Power Laser and Beam Control Tests**

- 14 High Power Tests from May 1990 thru July 1998

Demonstrated Repeatability of Megawatt Level Power Production

- Demonstrated Order of Magnitude Jitter Reduction

- Demonstrated Significant Beam Quality Improvement

- Demonstrated Uncooled Optics Performance

- Demonstrated Open and Closed Loop Beam Control

- Demonstrated Uncooled Deformable Mirror Operation

- Initiated Laser Performance Envelope Sensitivity Testing to Alignment & Flow Conditions

Overview

# ATP-FC Program

**INERTIAL REFERENCE UNIT (1991-94)**

- Near Flight Qualifiable Bassboard
- Reference Beam Jitter < 40 nrad
- Isolation > 90 dB, 1 Hz

**SSLRS (1990-95)**

- Solid State Diode Pumped
- Space Traceable
- 400mJ, 60Hz

**FIRE CONTROL (1985-Present)**
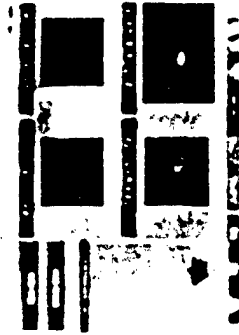
- Plume-to-Hardbody Handover
- Aimpoint Selection
- Integrated Decision Function Simulation

**SPICE (1985-95)**

- Pointing and Disturbance Isolation
- Multi-level Controls Design Tools

**ADAPT (1991-97)**

- ATP System Concept Definition
- Integrated ATP Experiments Design and Execution
- ATP Flight Unit for Star LITE
- ATP Technology Requirements Definition and Demonstration

**RAPID RETARGETING (1982-94)**

- Rapid Retargeting Testbed
- Precision Pointing Testbed
- LOS Stabilization

**HABE (1992-Present)**

- Integrated ATP Testbed
- Autonomous ATP Performance
- High Resolution Target Imagery and Background Phenomenology

**LACE/UVPI (1986-92)**

- Low Power Atmospheric Compensation Demonstrated
- Solid-Rocket Plume UV Signatures Measured UV Backgrounds Measured

**RME (1986-91)**

- Laser Beam Relay via Satellite Mirror
- Weapon Level Beam Stabilization and Pointing

## Overview

3.1-1-13

# Chemical Laser Lethality Demonstration

Titan Booster With Full Simulated Flight Load Destroyed by
MIRACL Laser, September 6, 1985
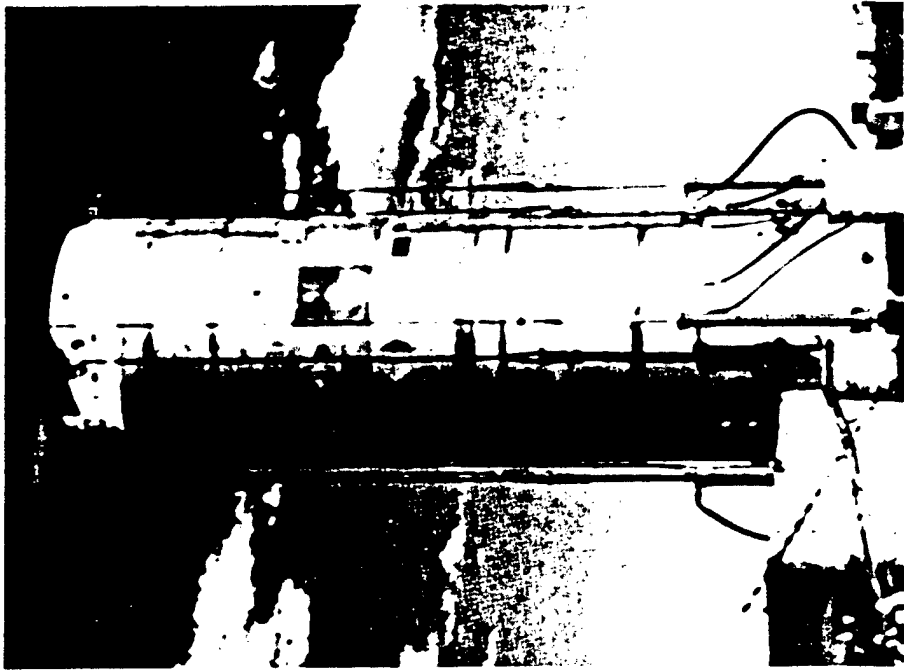
Overview

# Example SBL Coverage for TMD

- **Single Platform Capability**
  - **Altitude: 1300 Km**

Number of 600 km TBMs*

Number of 1000 km TBMs*

Number of 300 km TBMs*

SBL Location

| 3 | 5 | 10 | 16 | 34 | 20 | 11 | 5 |

11 | 19 | 6 | 3

400 km

2500 km

3500 km
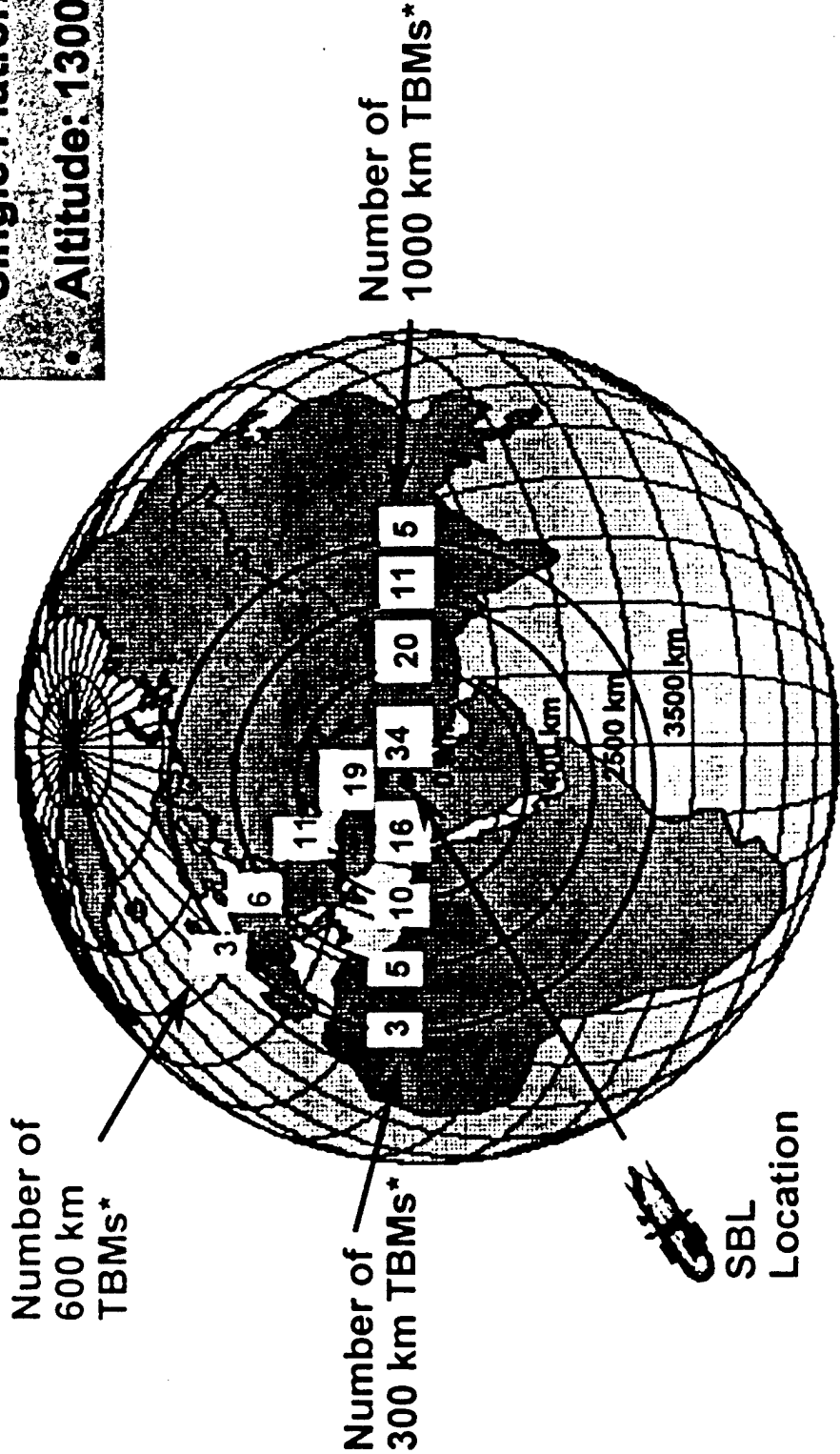
* Missiles are Launched Simultaneously

Overview

3.1-1-15

# SBL Earth Coverage

- – – Airborne Targets: Global Coverage Every Instant
- ⋯⋯ Ground Targets: Global Coverage Every ~90 min

45°
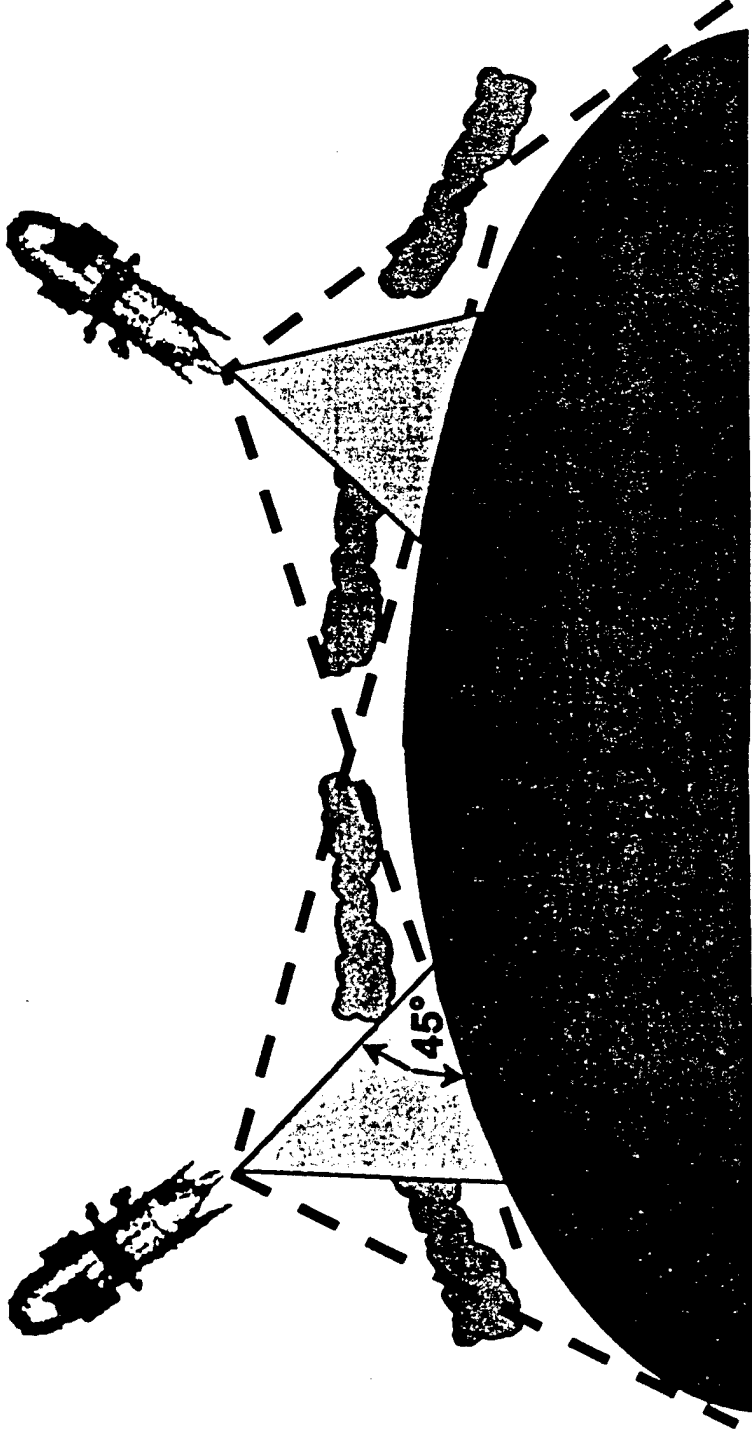
# Coverage for 2 SBL Platforms



Single Platform Coverage
Double COverage
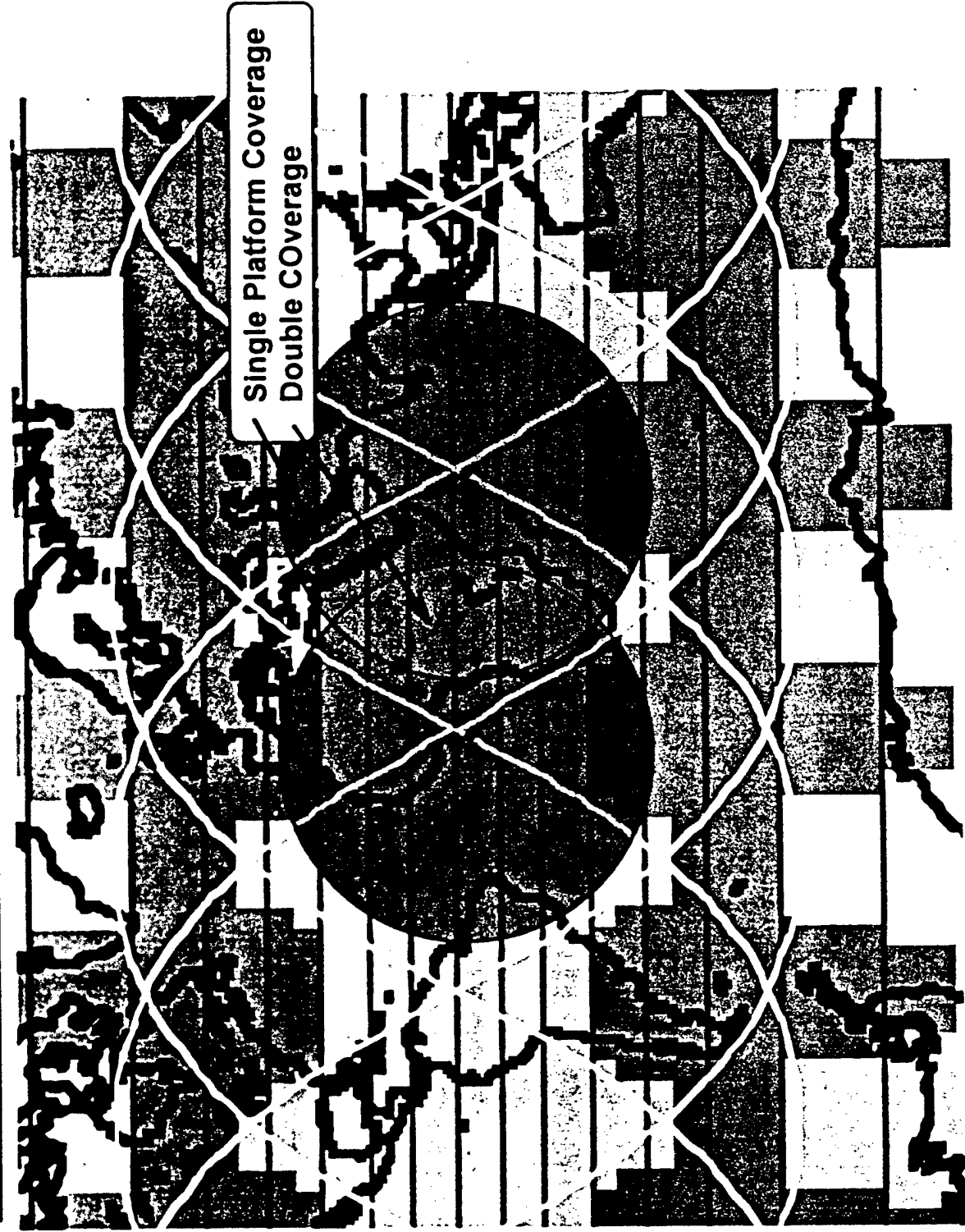
# Example of Instantaneous SBL Coverage

**Coverage Scale:**
**Number of SBLs**
**Covering**

| | |
|---|---|
| 0 | 0 |
| 1 | 1 |
| 2 | 2 |
| 3 | 3 |
| 4 | 4 |
| 5 | 5 |
| 6 | 6 |
| 7 | 7 |
| 8 | 8 |
| 9 | 9 |
| 10 | 10 |
| | 10+ |
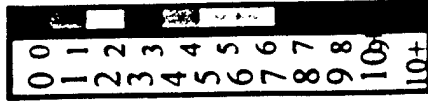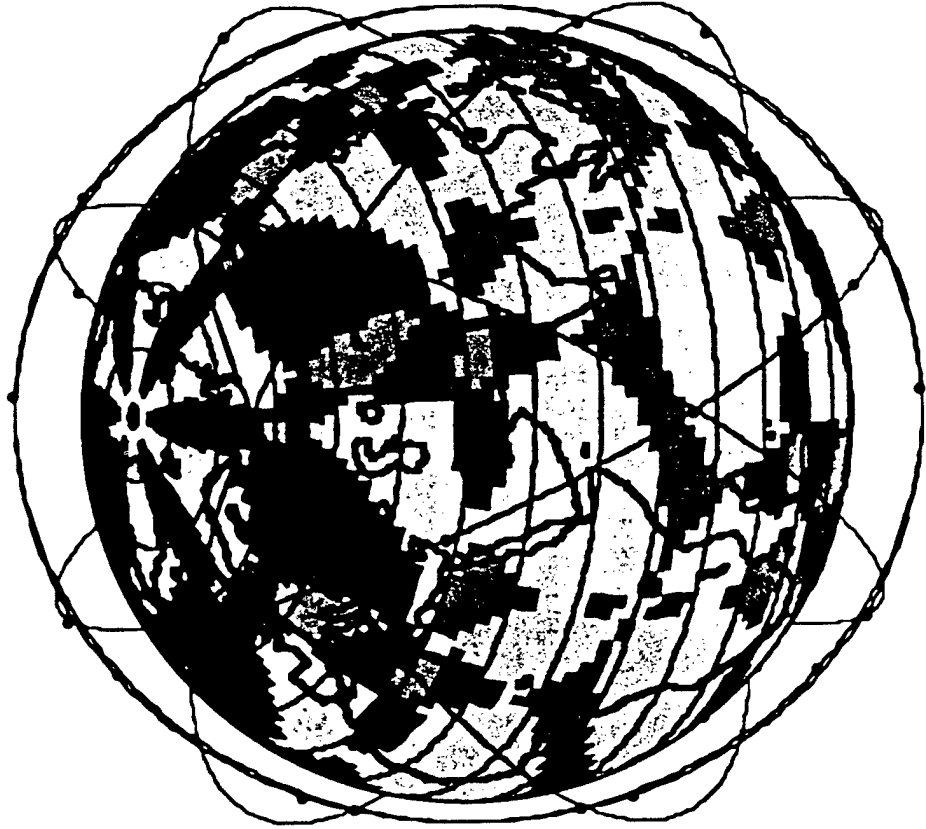
**30 SBLs**
**6x5**
**1100 km alt.**
**62 deg. incl.**



Overview

# Example of SBL Average Coverage

**Coverage Scale:**
**Number of SBLs**
**Covering**

| |
|---|
| 0 |
| 1 |
| 2 |
| 3 |
| 4 |
| 5 |
| 6 |
| 7 |
| 8 |
| 9 |
| 10 |
| 10+ |

**30 SBLs**
**6x5**
**1100 km alt.**
**62 deg. incl.**



Overview
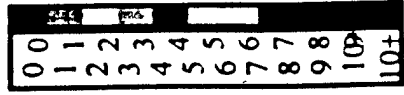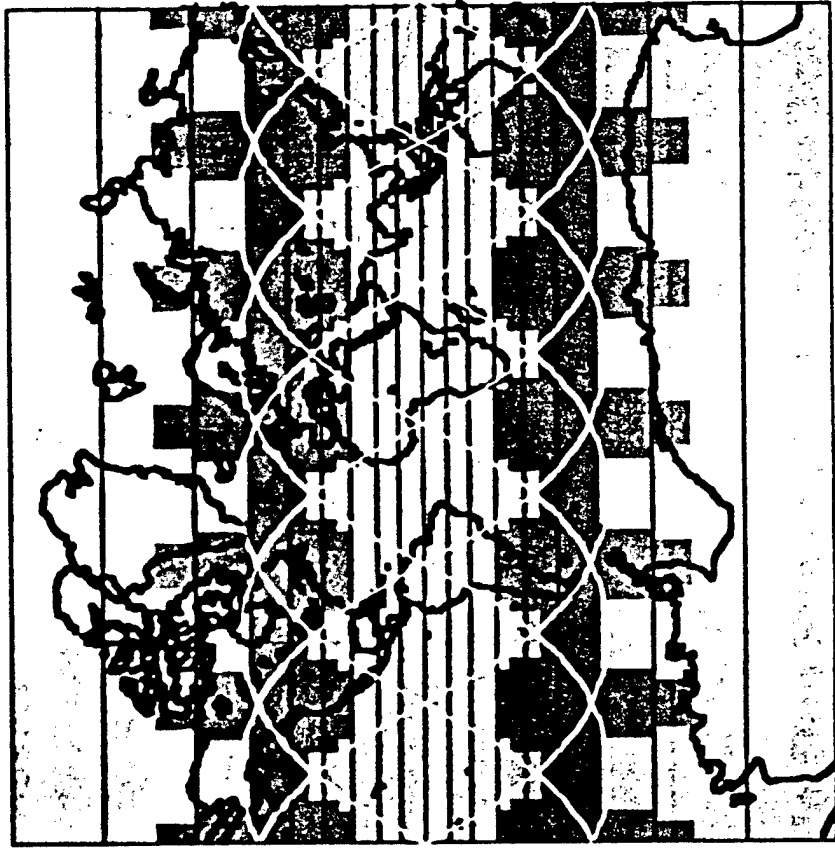
# SBL CONOPS

- ## Primary Missions
  - BMD
  - Protection of On-Orbit Assets
  - Counter Space
- ## Ancillary Capability
  - Surveillance
  - Air/Ground Attack Deterrence
  - Target Designation
  - Hyperspectral Imagery
  - Space Object Tracking and Imagery
  - Environmental Data for Treaty Monitoring
  - Astronomical Data

## C² of Space Weapon Issues
- Timelines
- Human-in-Control
- CONUS vs. Theater Battle Management
- Integration with other assets
- Rules of engagement

Integration with Warning Assets

Remote Operations

Coordination with Theater

# Potential SBL Missions

**Space Superiority**

Satellite Negation/ Protection

NMD

**Precision Employment***

Precision Engagement - Direct Strike

* Requires Transmission Thru Atmosphere

Active and Passive Imaging of Space and Terrestrial Objects

**Information Dominance**

NBC, Winds, Clouds

Geo-Location/ Designation of Ground Objects

TMD

**Air Superiority**

High Altitude Aircraft Negation

**AFSPC Approved SBL CONOPS (15 May 98)**

Overview

# Desert Storm Dependence on Space

## FUNCTIONS / SYSTEMS

**COMMUNICATIONS**
DSCS
UFO/FLTSAT
MILSTAR
COMMERCIAL

**EARLY WARNING**
DSP
GPS NUDET SUBSYSTEM

**NAVIGATION**
TRANSIT
GPS

**WEATHER**
DMSP
NOAA, GOES

## USERS

CINCS
Theater Commanders
Ground Forces (Special Forces, Recon Units, FACs, & SAR)
Naval Forces

Theater Commanders
Ground Forces
Patriot Batteries
Civilians

Naval Forces
Ground Forces (Special Forces, Armored & Artillery Units, & SAR)
Precision Weapons
Airborne Forces

Ground Forces
Naval Forces
Special Forces

## DESERT STORM DEPENDENCE
### (% supplied via space)

90%

40%

80%

50%

**Assurance of Space Asset Availability is Critical**

Overview

# Agenda

- **Overview**
- **SBL Potential for ACC Missions Areas**
  - TMD
  - Air & Ground Attack
  - Reconnaissance & Surveillance
- **Program Plan**
- **Summary**

# SBL Potential for ACC Mission Areas

- ## Theater Missile Defense
  - Boost Phase
  - Midcourse
  - Attack Ops
  - Synergy with Other Systems (ABL, THAAD, etc.)

- ## Reconnaissance & Surveillance (R&S)
  - Air Targets
  - Ground Targets
  - Chem/Bio
  - Weather

- ## Counter Air and Ground Attack
  - Laser Designation
  - HEL Attack

Mission Areas - TMD

# Ballistic Missile Defense-in-Depth

## Operational Situation

- First Day of War
- Forced Entry
- Joint Battle / MRC
- Deterrence
- Operations Other than War
- Rogue/Terrorist

# Leakers versus # Assets

Attack Ops

BPI — SBL, ABL

EXO — THAAD, NTW

ENDO — PAC3, NADS, Hawk
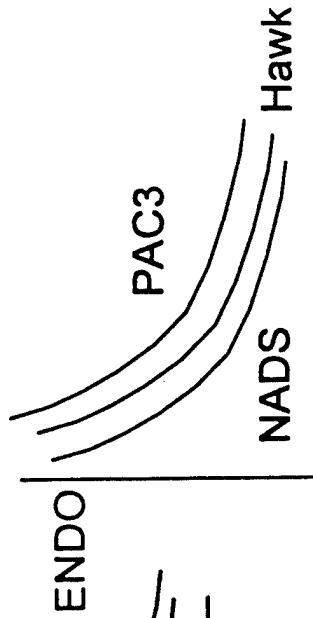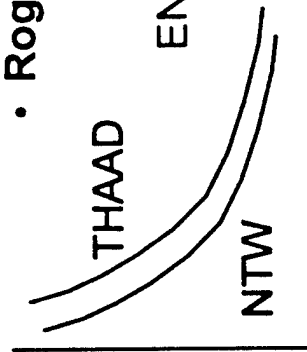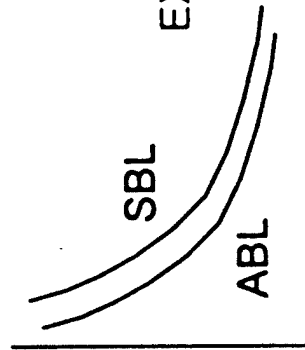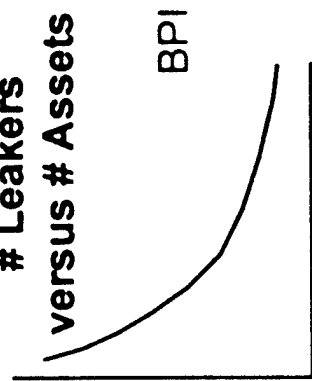
Diminishing Leakers

- **Each System Contributes to Reducing Leakers, But**
- **No One System Can Provide Total TMD Capability**

# TMD Boost-Phase Intercept

Sensor FOV

HEL Beam

Fine Track Beam
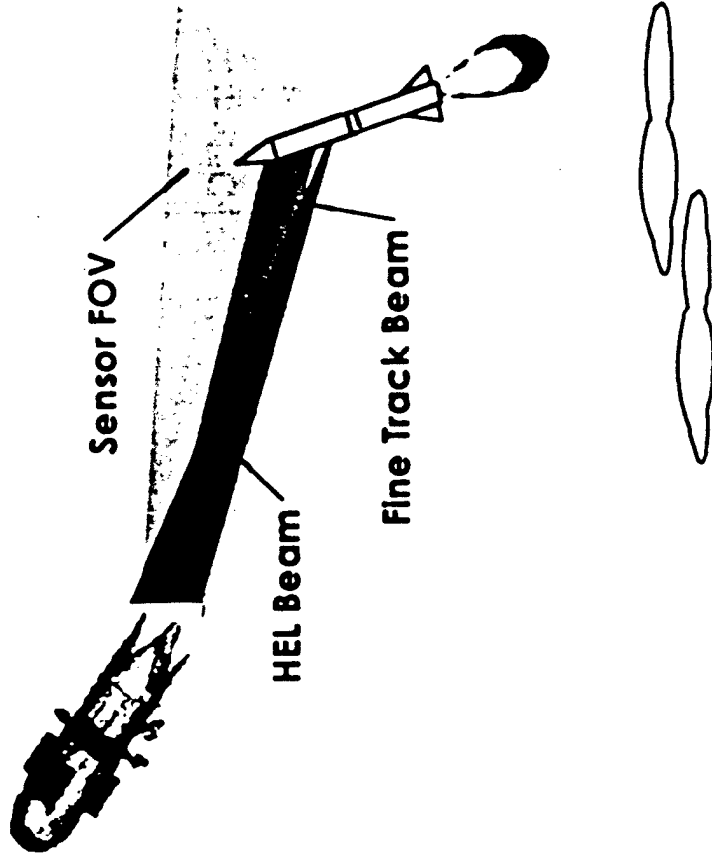
- **POTENTIAL UTILITY**
  - Global BMD Access
  - Continuous Coverage

- **REQUIRED MODIFICATIONS**
  - None, This is the Primary Mission

# Midcourse Interactive Discrimination for Responsive Threats

- **POTENTIAL UTILITY**
  - Precise 3D tracking (<< 1m, 1m/s) and high resolution imaging
  - Passively resolve closely spaced objects
  - Designation or thermal tagging of objects
  - Destructive discrimination of balloons
  - Detect and track TBM warheads
  - Generate target object maps
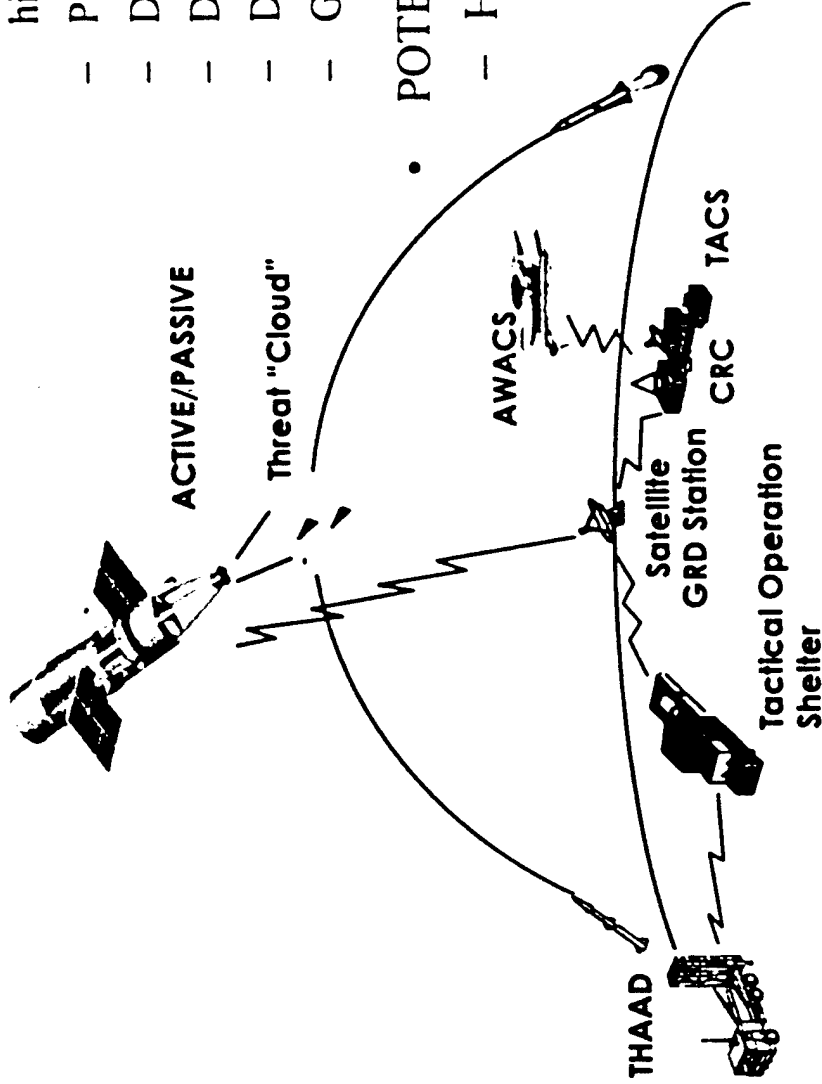
- **POTENTIAL MODIFICATIONS**
  - High (Degree of Difficulty)
    - Flip-in Mirrors
    - Additional Optical Trains/Benches
    - Broadband Mirror Coatings
    - Additional LWIR Sensors / Cyro Coolers
  - Low
    - Additional Software

ACTIVE/PASSIVE

Threat "Cloud"

AWACS

TACS

CRC

Satellite GRD Station

Tactical Operation Shelter

THAAD

*Extend range and capacity by using 8m low power aperture sharing sensors

**Mission Areas – TMID**

9811L022

# Target Designation
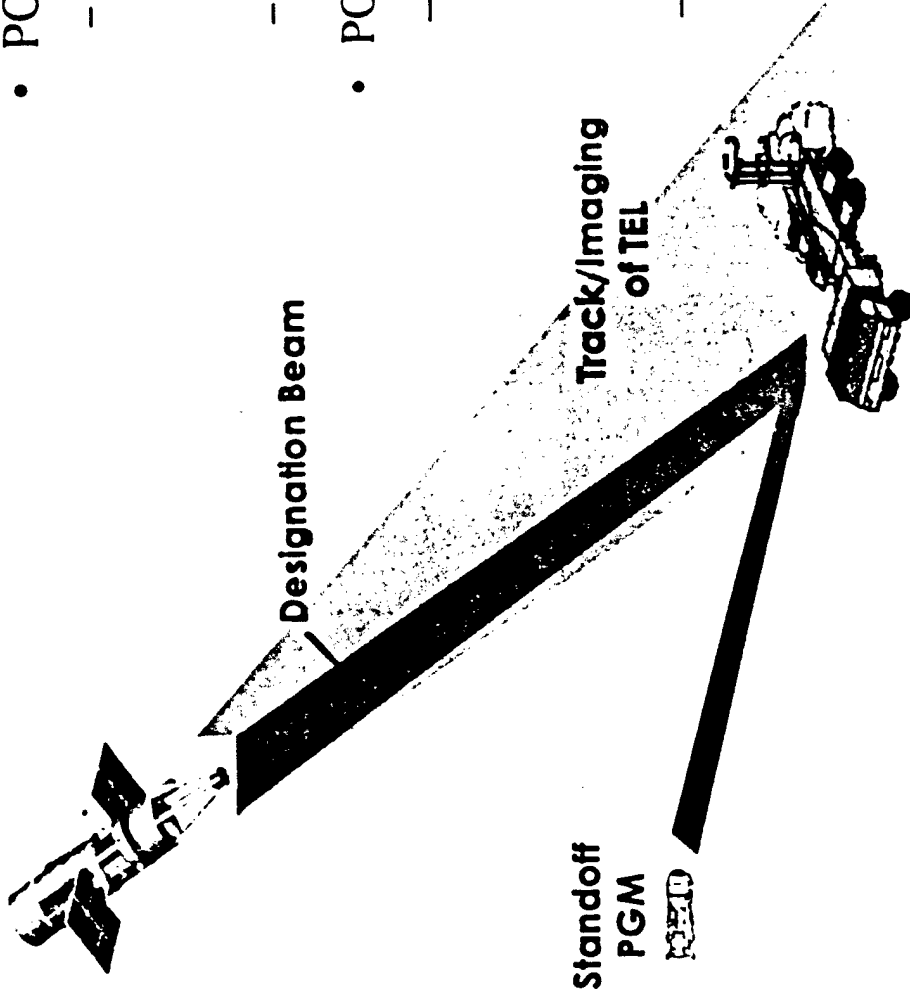
- **POTENTIAL UTILITY**
  - TEL Designation
    - Global Access
    - ~90 min Revisits
  - Covert Attacks

- **POTENTIAL MODIFICATIONS**
  - High (Degree of Difficulty)
    - Flip-in Mirrors
    - Additional Optical Trains/Benches
    - Broadband Mirror Coatings
  - Medium
    - Improved Mirror Figure
    - Additional Sensors and Bus Components
  - Low
    - Additional Software

**Standoff PGM**

**Designation Beam**

**Track/Imaging of TEL**

Mission Areas - TMD

# ID and Designation for Attack Operations

## SINGLE FRAME SIGNAL LEVEL - ONLY CENTRAL REGION OF FOCAL PLANE SHOWN



ACTIVE VISIBLE FLOOD ILLUMINATION

PASSIVE VISIBLE (SOLAR)

PASSIVE SWIR (SOLAR)
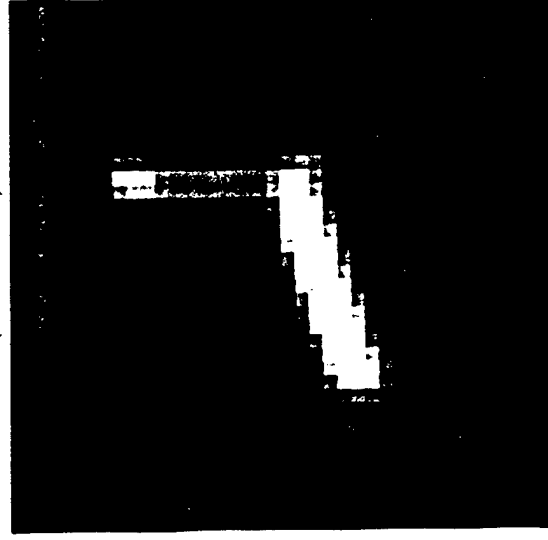
25 m · 25 m · 25 m

Spot size for focused illuminator operating through primary aperture

- 8 m APERTURE OPERATING IN CLEAR WEATHER
- SBL SENSORS PROVIDE REAL TIME IMAGERY, TARGET LOCATION AND DESIGNATION TO ~ 1m
- DESIGN MODIFICATIONS CAN SUPPORT SEARCH RATES > 10 SQ. km/sec

Mission Areas – TMD

# SBL Interoperability in Theater

SATCOMM

NAVIGATION

SURVEILLANCE

ENEMY'S ASAT

TBM THREAT

Leakers or Outside SBL Coverage

LASER GUIDED MUNITIONS
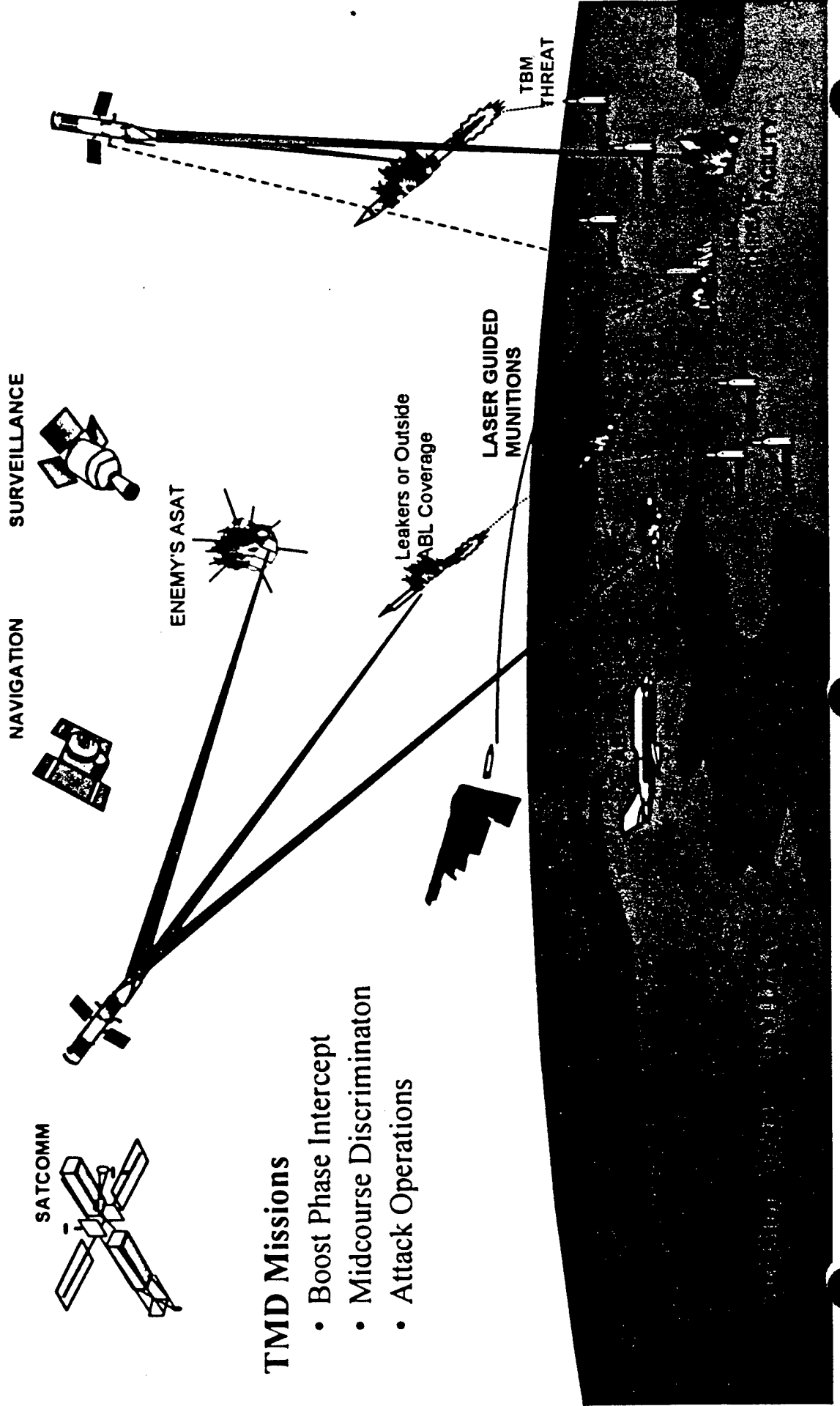
**TMD Missions**

- Boost Phase Intercept
- Midcourse Discriminaton
- Attack Operations
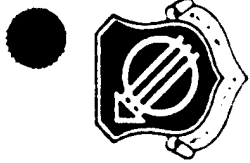
# SBL Potential for ACC Mission Areas

- **Theater Missile Defense**
  - Boost Phase
  - Midcourse
  - Attack Ops
  - Synergy with Other Systems (ABL, THAAD, etc.)

- **Reconnaissance & Surveillance (R&S)**
  - Air Targets
  - Ground Targets
  - Chem/Bio
  - Weather

- **Counter Air and Ground Attack**
  - Laser Designation
  - HEL Attack

Mission Areas - R&S

# Potential Sensor Capability for Operational SBL

| Sensor | Polish/Figure | Resolution (GRD) | Image Resolution Capability ( 8 m Aperture @ 2000 km Range ) |
|---|---|---|---|
| MWIR | IR Quality | 2.4 m | Identify large fighter aircraft<br>Identify tracked vehicles<br>Determine the shape of a submarine bow |
| SWIR | IR Quality | 1.2 cm | Identify radar as vehicle or trailer mounted<br>Identify deployed tactical SSM systems<br>Identify individual railroad cars |
| Visible | IR Quality | 40 cm | Identify fittings & fairings on fighter aircraft<br>Identify ports, ladders, vents on electronics vans<br>Identify individual railroad ties |
| Visible | Visible Quality | 20 cm | Identify rivet lines on bomber aircraft<br>Identify hand-held SAMs<br>Determine windshield wipers on vehicle |

Inherent Capability ⇐

⇒ Achievable Capability

# Air Vehicle Tracking/Imagery

**HIGH ALTITUDE AIRCRAFT**
(Moerately Difficult Functionality)
2m MWIR @ 3000 km    8m Active Vis @ 3000 km

↑
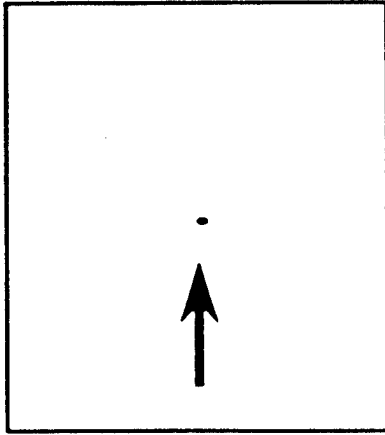
**LOW ALTITUDE CRUISE MISSILE**
(Very Difficult Functionality)
8m Multi-Frame Streak Detection @ 3000 km
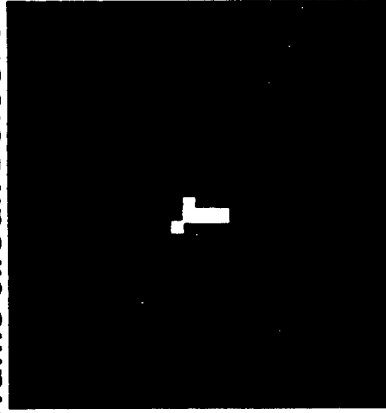
- POTENTIAL UTILITY
  - Air Object ID & Track
  - Global Access
  - Near-Real Time
  - Cruise Missile Search (Requires Maintaining Fence)

- POTENTIAL MODIFICATIONS
  - High (Degree of Difficulty)
    - Flip-in Mirrors
    - Additional Optical Trains/Benches
    - Broadband Mirror Coatings
  - Medium
    - Improved Mirror Figure
    - Additional Sensors and Bus Components
  - Low
    - Additional Software

Mission Areas - R&S

3.1-1-33

# Ground Target Tracking/Imagery

- POTENTIAL UTILITY
  - Global Access
  - ~90 min Revisit
  - Intelligence Data
  - Battle Damage Assessment

- POTENTIAL MODIFICATIONS
  - High (Degree of Difficulty)
    - Flip-in Mirrors
    - Additional Optical Trains/Benches
    - Broadband Mirror Coatings
  - Medium
    - Improved Mirror Figure
    - Additional Sensors and Bus Components
  - Low
    - Additional Software

**8m Passive IR @ 1500 km**

**8m Passive Visible @ 1500 km**

# Regional Reconnaissance and Surveillance

**Hyperspectral Image Over
Yuma Proving Grounds
2500 ft AGL , GSD ~ 1 m
Scaled to 15 m Aperture at 1500 km**
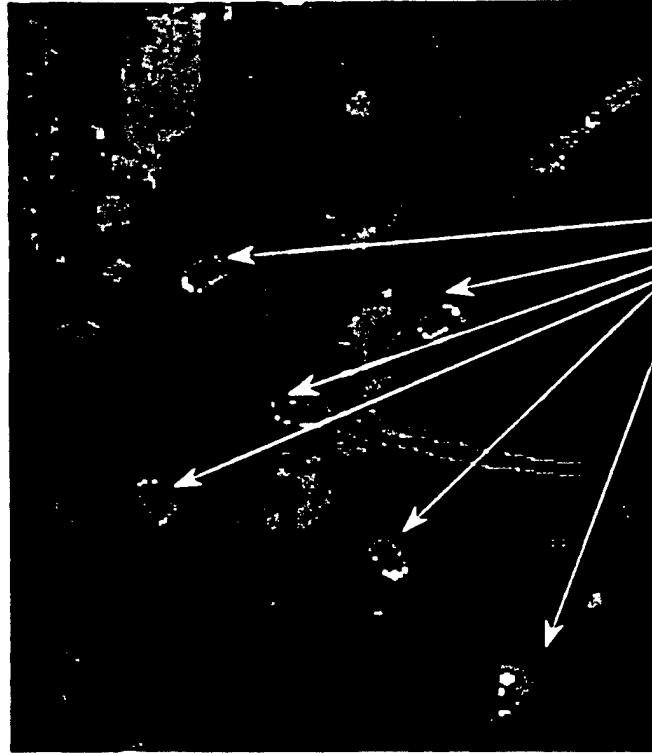


**Desert Pavement    Military Vehicles
Broken Pavement    Vegetation
Sandy Soil**

**Mission Areas - R&S**

- POTENTIAL UTILITY
  - Global Access
  - ~ 90 min Revisit
  - Terrain ID for Ground Forces
  - Intelligence Data
  - Battle Damage Assessment

- POTENTIAL MODIFICATIONS
  - High (Degree of Difficulty)
    - Flip-in Mirrors
    - Additional Optical Trains/Benches
    - Broadband Mirror Coatings
  - Medium
    - Improved Mirror Figure
    - Additional Sensors and Bus Components
  - Low
    - Additional Software

# Chem/Bio Agent Detection/Location

- POTENTIAL UTILITY
  - Global Access
  - ~ 90 min Revisit
  - Treaty Verification
  - Intelligence Data
  - Battle Damage Assessment

- POTENTIAL MODIFICATIONS
  - High (Degree of Difficulty)
    - Lidar
    - Flip-in Mirrors
    - Additional Optical Trains/Benches
    - Broadband Mirror Coatings
  - Medium
    - Improved Mirror Figure
    - Additional Sensors and Bus Components
  - Low
    - Additional Software

**Imaging of Scene**

**Lidar Beam**

**Chemical/Biological Agent Cloud**
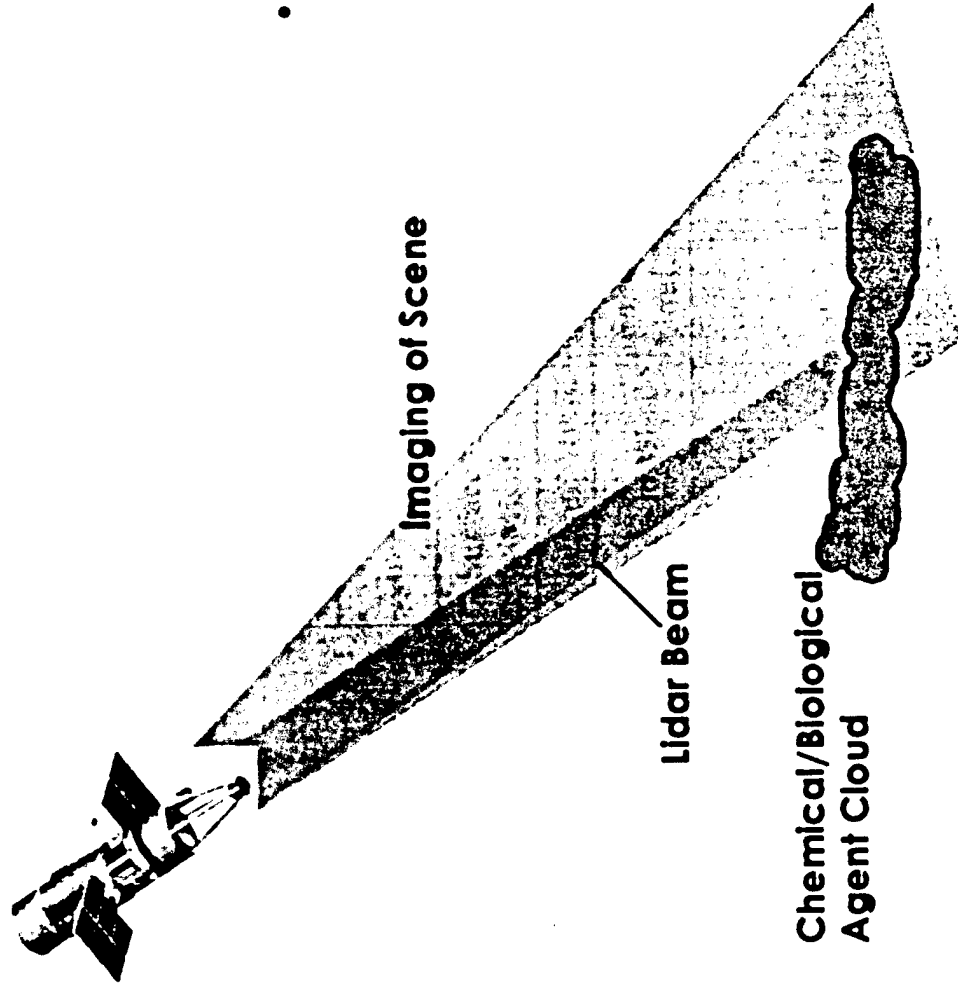
Mission Areas - R&S

# 3D Tropospheric Wind and Cloud Sensing

- POTENTIAL UTILITY
  - Global Wind Monitoring
  - Global Cloud Tops/Bottoms
  - ~ 90 min Revisit
  - Forecasts Improved by a Factor of 5
  - Improved A/C Fuel Efficiency
  - Improved PGM Strikes

- POTENTIAL MODIFICATIONS
  - High (Degree of Difficulty)
    - Lidar
    - Flip-in Mirrors
    - Additional Optical Trains/Benches
    - Broadband Mirror Coatings
  - Medium
    - Improved Mirror Figure
    - Additional Sensors and Bus Components
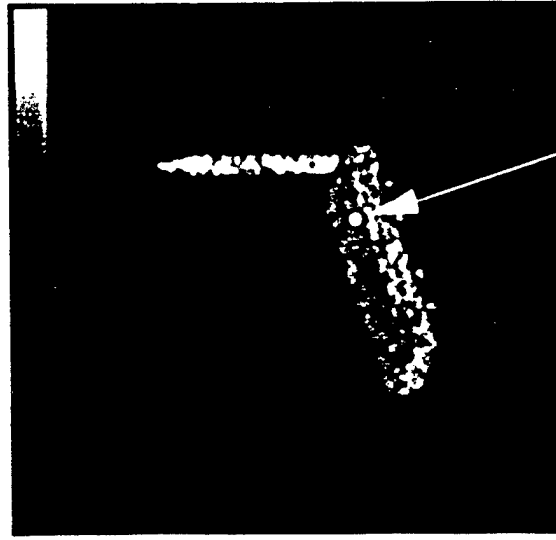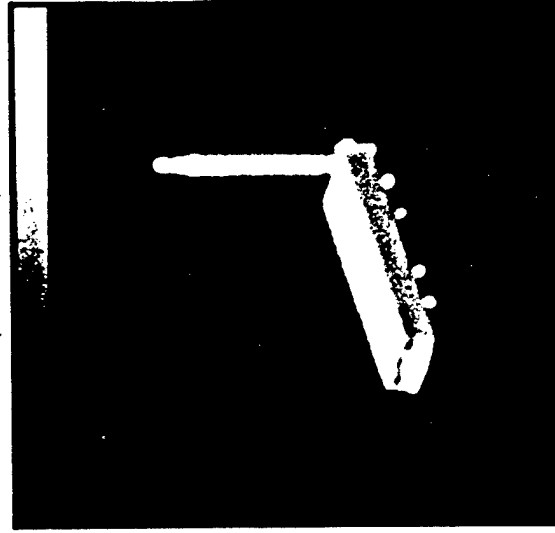  - Low
    - Additional Software

**Lidar Beam**
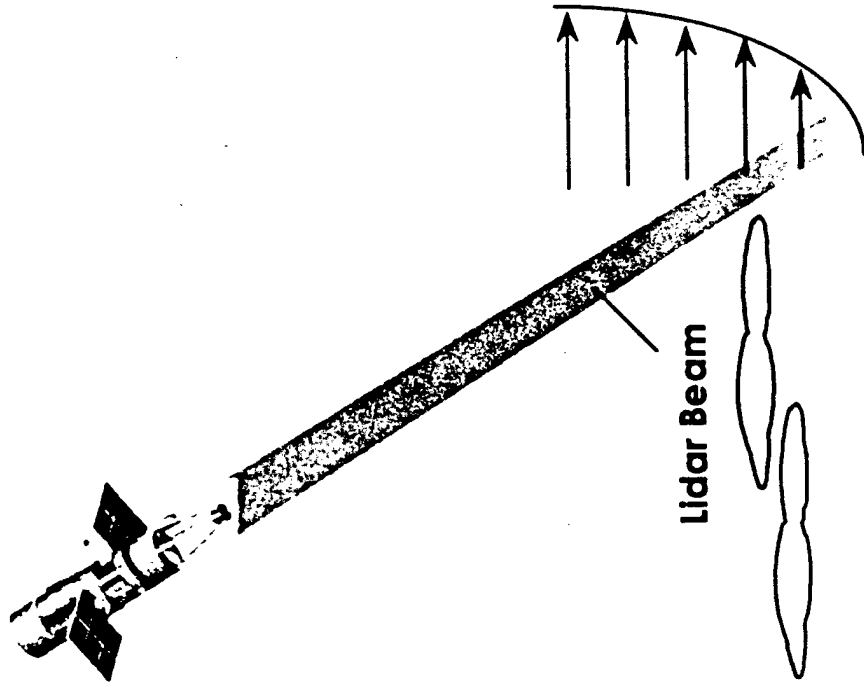
**Mission Areas - R&S**

# SBL Potential for ACC Mission Areas

- ## Theater Missile Defense

  – Boost Phase

  – Midcourse

  – Attack Ops

  – Synergy with Other Systems (ABL, THAAD, etc.)

- ## Reconnaissance & Surveillance (R&S)

  – Air Targets

  – Ground Targets

  – Chem/Bio

  – Weather

- ## Counter Air and Ground Attack

  – Laser Designation

  – HEL Attack

**Mission Areas - Counter Air**

# High Altitude Air Attack

- POTENTIAL UTILITY
  - Target Altitude > ~30,000 ft
  - Global Access
  - Revisits: ~0 min

- POTENTIAL MODIFICATIONS
  - None, Same Capability as Main Mission
  - Assumes Target Localization Cue
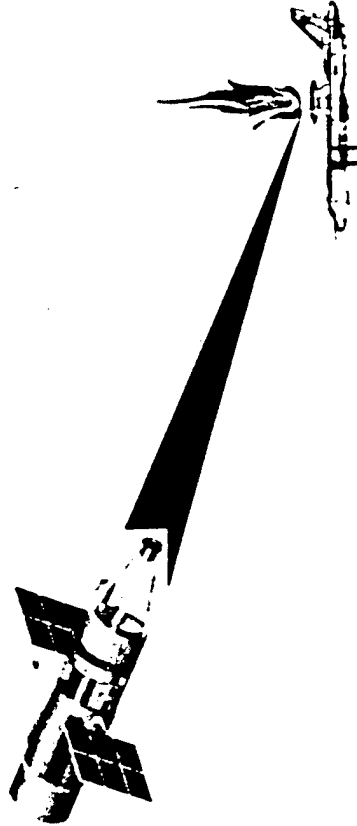
# Low Altitude Air Attack
## and Ground Attack
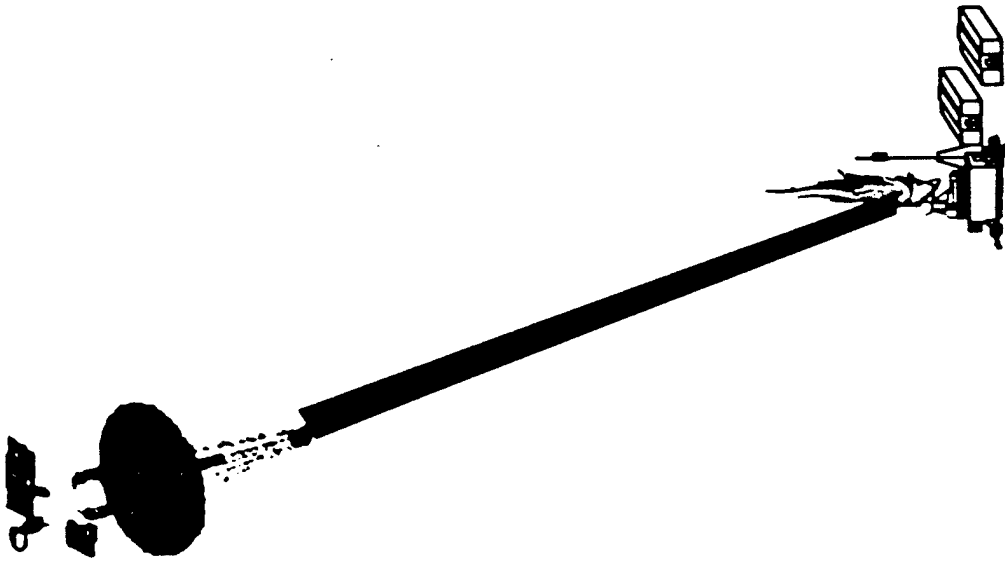
- POTENTIAL UTILITY
  - Requires Near-Perfect Weather Conditions
  - Provides Global Access
  - ~90 min Revisit

- POTENTIAL MODIFICATIONS
  - Very High (Degree of Difficulty)
    - New Laser Baseline for Atmospheric Penetration
  - High
    - Flip-in Mirrors
    - Additional Optical Trains/Benches
    - Broadband Mirror Coatings
  - Medium
    - Additional Sensors and Bus Components
  - Low
    - Additional Software

**Mission Areas - Counter Air**

# HEL Atmospheric Penetration

DF

HF

HF Line Selected

HF Overtone

COIL

Solid State

ICBM Burn Out (off scale)

5 Sec Flight Interval × Burn Out (TBM)

Weather Balloon

Reconnaissance Aircraft

Cloud Break

(8-12km)

AWACS

Fighter

Cruise Missile

Other Land Sites

Mt. Everest

km
30
20
10
0

ft
100,000
66,000
33,000
0
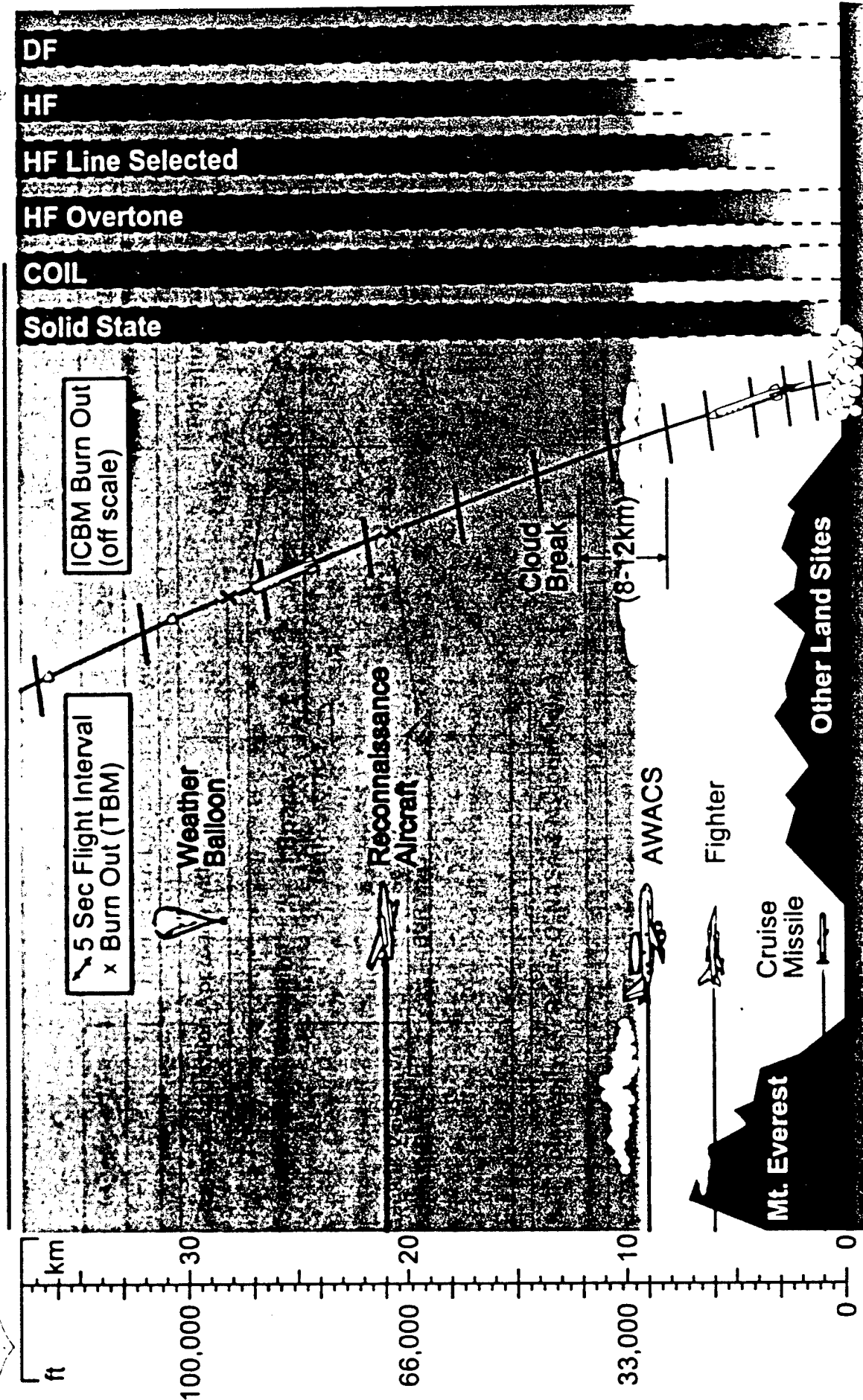
25007

3.1-1-41

# Adjunct Mission Vulnerabilities

| Target | Component | Fluence Damage Criteria (kJ/cm²) |
|--------|-----------|----------------------------------|
| Satellite | Various | Some Components |
| Aircraft | Crew | |
| | Fuel Tank/ | |
| | Control Surface | |
| | Radar | (30-60 kJ/cm²) |
| Cruise Missile | Fuel Tank | |
| Air-Air Missile | Guidance/Control | |
| | Seeker | |
| Surface -Air Missile | Radar | |
| | Guidance/Control | |
| Theater Missile | Fuel Tank | |
| Strategic Missile | Solid Propellant | |
| | Liquid Propellant | |

(axis: 0   5   10   15)
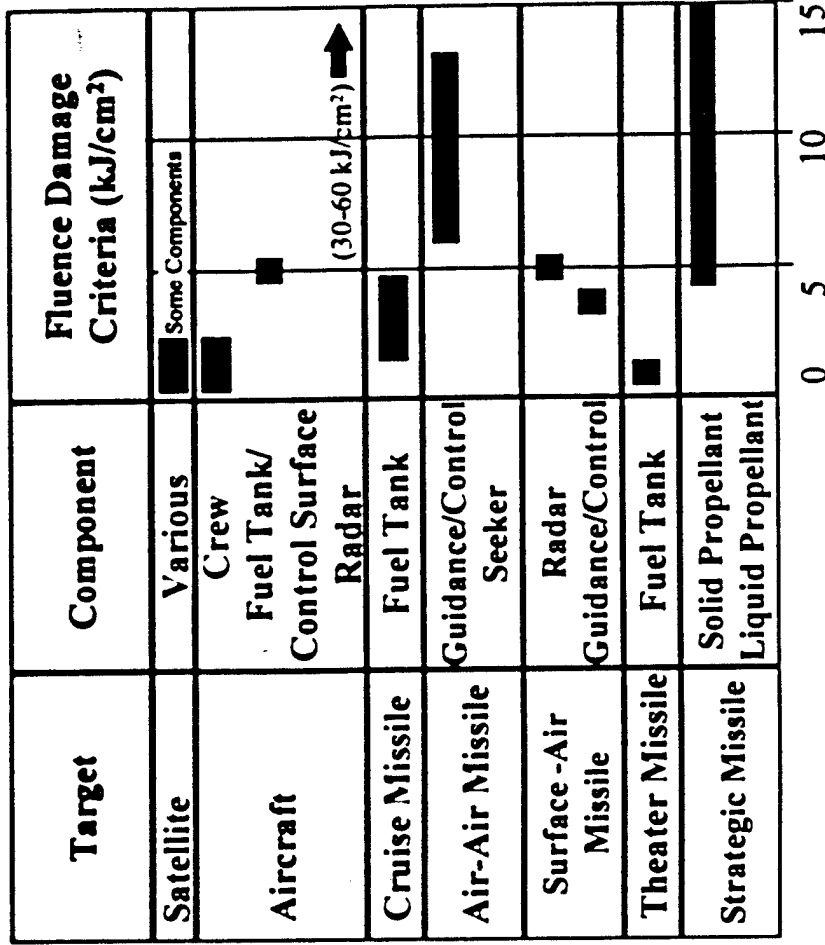
- ## Other Targets for Analysis

  – Supply Depot, Fuel Storage Areas, Electric Transformers, etc...

Mission Areas - Counter Air

# Agenda

- **Overview**
- **SBL Potential for ACC Missions Areas**
  - TMD
  - Reconnaissance & Surveillance
  - Air & Ground Attack
- **Program Plan**
- **Summary**

Program Plan

# Notional Total Program Schedule

MILESTONES
2031 1st Unit
2035 IOC (12)
2038 FOC (30)

| | 2000 | 2010 | 2020 | 2030 | 2040 | 2050 |
|---|---|---|---|---|---|---|

**IPTD** — VIP / CDR Completion

**IFX** — VIP / Mfg / CDR / LAUNCH

**Prototype** — VIP / CDR / Mfg / LAUNCH / PLORBI

**EMD & Prod** — VIP / CDR / Mfg / LAUNCH / MSL / LAUNCHES

**O&S** — O&S

**STF** — Build

**Ops SV Qty** — 1 12 4 6 66 6

Replacement Sats
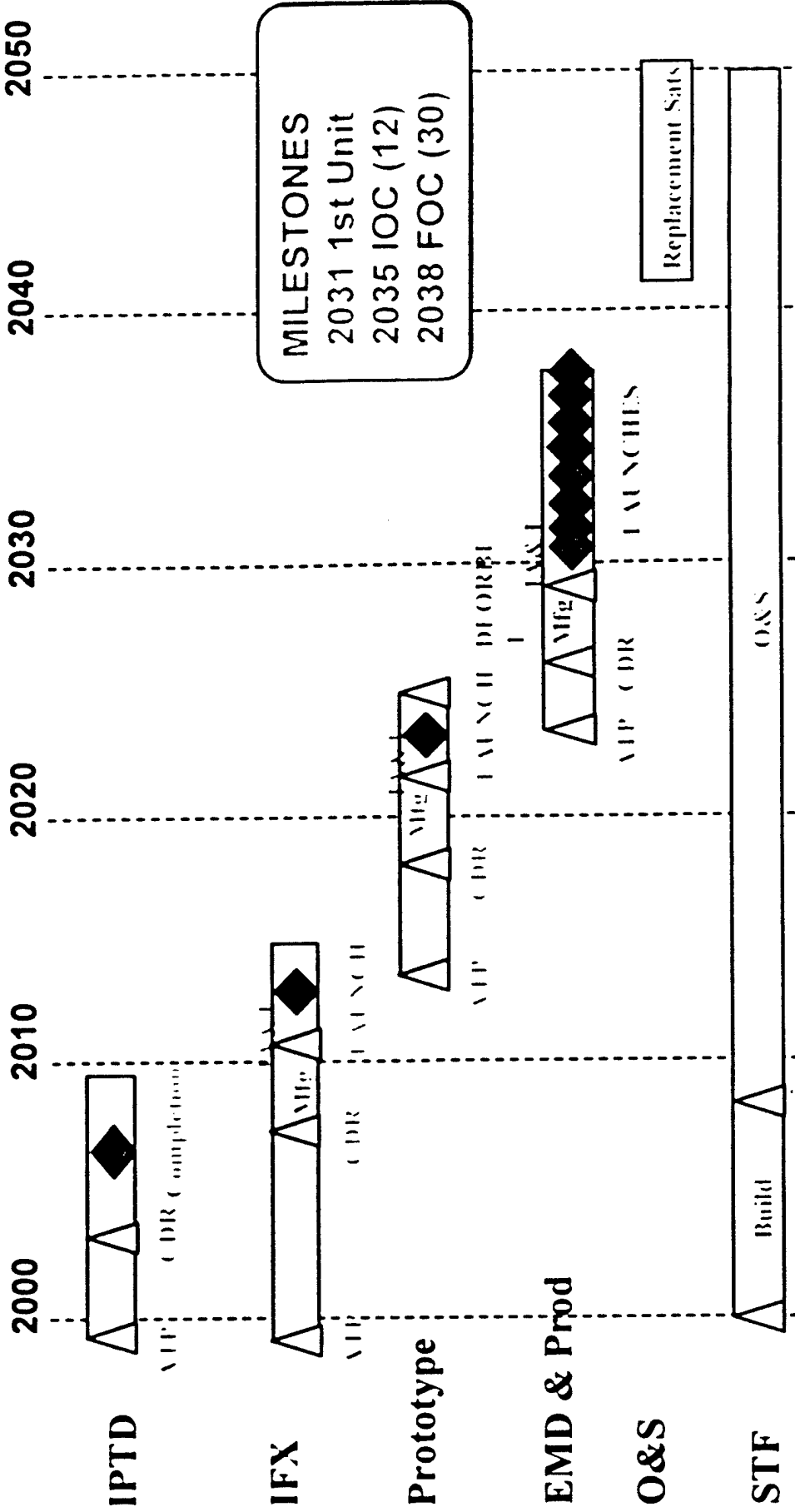
Schedule Reflects No National Imperative
More Rapid Path to Operational System Possible

**Program Plan**

# SBL Challenges for IFX



(Venn diagram of three overlapping circles: "Affordable Funding Profile", "Meaningful Demonstration", and "Congressional Expectations")
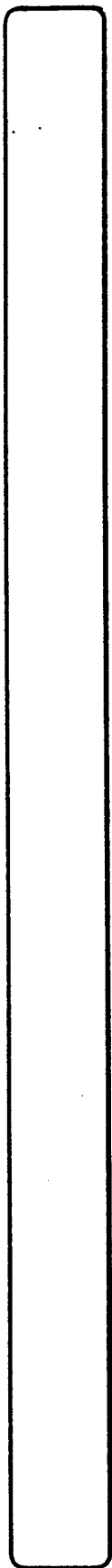
- Affordable
  - Total demonstration costs expected to exceed $2B
  - Currently not fully supported in BMDO or AF POM

- Meaningful
  - Advances State of the Art towards an operational SBL
  - Addresses required research objectives

- Meets Congressional Expectations
  - Space Based Laser
  - Target kill during boost phase
  - Demonstration ASAP
  - Initiation of an integrated laser system test facility
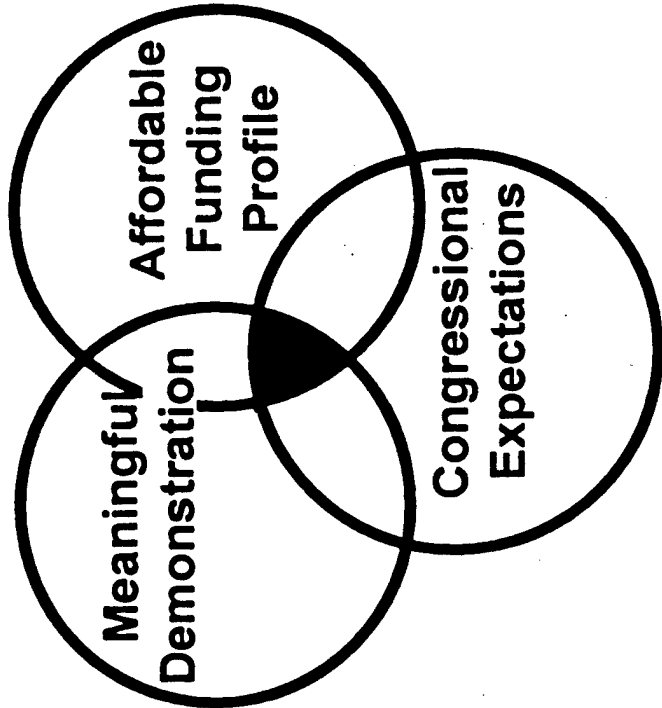
Program Plan

# Outline of SBL IFX Program



Program Plan

3.1-1-46

# Near-Term Plan Overview

| Oct | Nov | Dec | Jan |
|-----|-----|-----|-----|

Brief Lt Gen Lyles & Mrs Druyun

Develop Revised Acquisition Approach with Industry

Potential Start of Procurement with Early Mar 99 Award

Briefing Series to User Community

Space Conference

Senior BMDO/AF Review

Acquisition Approach

Support

Vision

Report to Congress

Aerospace Senior

BVR Mtgs

IRT -3

Brief CSAF, SECAF & OSD

Brief Congress

Baseline Validation Reports (BVR) Review

Engage S&T Community (AFRL, NRO, NASA & National Labs)

Historical & S&T Perspective

On-going SBL Technology Development

General Officer Steering Panel

Dr Hastings' Path to Global Energy Projection Study

Prep

Collect/form Input (and "Consensus" on same) for Arch Study

**Program Plan**

Contractor Architectural Study

3.1-1-47

# SBL Development Path

**DEMONSTRATED TECHNOLOGIES**
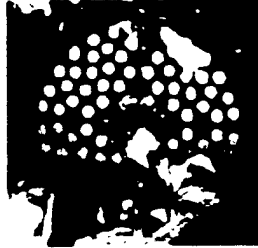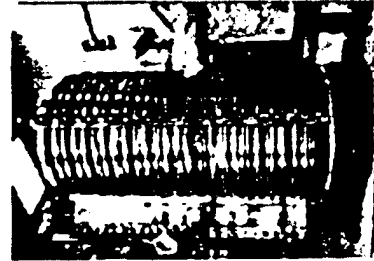
Large Optics
(LAMP, 1989)

Beam Control
(LODE, 1987)

Laser
(ALPHA, 1991)

**INTEGRATION**

Alpha-LAMP Integration (ALI)
End-to-End Weapon Element Testing
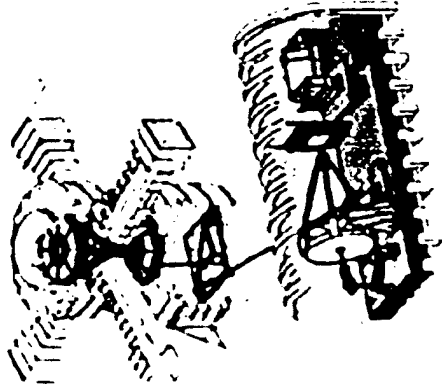
Acquisition, Tracking, Pointing & Fire Control
(High Altitude Balloon Experiment (HABE))

**SYSTEM-LEVEL DEVELOPMENT**

Integrated Ground Test
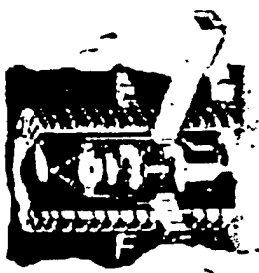
Demonstrator
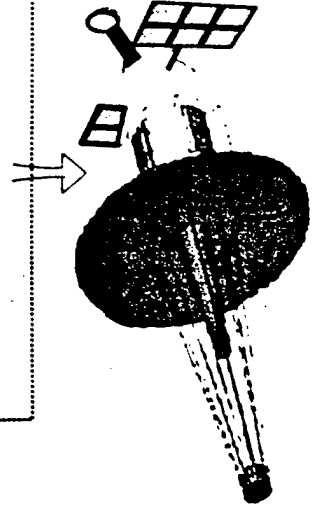
Potential Future
Operational SBL

Program Plan

# Agenda

- **Overview**
- **SBL Potential for ACC Missions Areas**
  - TMD
  - Reconnaissance & Surveillance
  - Air & Ground Attack
- **Program Plan**
- **Summary**

# Summary

- **Space Based Lasers Uniquely Offer Continuous, Global, Boost Phase Intercept**
  - Theater and National Missile Defense with One System
  - Highly Effective Versus Threat Trends

- **Deployed Space Based Lasers Provide Numerous Ancillary Missions**
  - Space Control, Earth/Space Imagery, Aircraft/Cruise Missile Defense

- **Space Based Laser Technology is Rapidly Maturing**
  - All Subsystems Demonstrated in Scaleable, Traceable Hardware
  - Significant Progress in High Power Integrated Demonstrations

- **Next Step to the Operational System Is an Integrated Flight Experiment**

- **Space Based Lasers can be Ready for Deployment in the Next 20 Years**

# Kill Range Determination

- TYPE OF TARGET   "Softer is Better"

- OUTPUT POWER   "More is Better"

- LASER SPOT SIZE ON TARGET   "Smaller is Better (to a point)"

  - Larger Aperture Diameter Makes Smaller Spot

  - Shorter Laser Wavelength Makes Smaller Spot

  - Correcting Aberrations and Jitter Makes Smaller Spot

- WEAPON DWELL TIME   "Longer is Better"

  - However Long Dwells Expend Chemical Magazine and Reduce Shot Rate

  - Available Dwell Time is Limited by Target Flight Time

- RANGE OF ATP and BEAM CONTROL SYSTEM   "You Can't Kill It if You Can't See It"

# LIST OF ACRONYMS

| | | |
|---|---|---|
| ABL | - | Airborne Laser |
| ALI | - | Alpha LAMP Integration |
| ALO | - | Alpha Laser Optimization |
| ALPHA | - | Megawatt Class Laser at Capistrano Test Site |
| ATP | - | Acquisition, Tracking & Pointing; also Authority to Proceed |
| BC | - | Beam Control |
| BEX | - | Beam Expander |
| BMDO | - | Ballistic Missile Defense Organization |
| BSM | - | Beam Steering Mirror |
| BPI | - | Boost Phase Intercept |
| CTS | - | Capistrano Test Site |
| DM | - | Deformable Mirror |
| FPA | - | Focal Plane Array |
| FSM | - | Fast Steering Mirror |
| GRD | - | Ground Resolution Distance |

# LIST OF ACRONYMS (cont.)

| | | |
|---|---|---|
| GSD | - | Ground Spatial Distance |
| HABE | - | High Altitude Balloon Experiment |
| HF | - | Hydrogen Fluoride |
| HOE | - | Holographic Optical Element |
| IFX | - | Integrated Flight Experiment |
| LAMP | - | Large Advanced Mirror Program |
| LODE | - | Large Optics Demonstration Experiment |
| MWIR | - | Mid Wave Infrared |
| NADS | - | Navy Area Defense System |
| NGST | - | Next Generation Space Telescope |
| NIIRS | - | National Imagery Interpretation Rating System |
| NMD | - | National Missile Defense |
| NTW | - | Navy Theater Wide |
| OWS | - | Outgoing Wavefront Sensor |
| SBL | - | Space Based Laser |
| SBLRD | - | Space Based Laser Readiness Demonstrator |

# LIST OF ACRONYMS (cont.)

SM     -     Secondary Mirror

SWIR     -     Short Wave Infrared

THAAD     -     Theater High Altitude Area Defense

TF     -     Turning Flat

TMD     -     Theater Missile Defense

VM     -     Verification Module

# Backups

# FY98 Technical Progress Highlights

- ## Five high power tests at CTS

  - Three ALO tests to characterize Alpha (HL907, HL908A, HL908B)
    - On-going analysis of data is enhancing understanding of Alpha
    - Facilitation and design of an uncooled resonator initiated
  - Two ALI tests to evaluate SBL beam control approach (HL430, HL440)
    - First high power, end-to-end demonstration of traceable beam control
    - New uncooled deformable mirror (UDM) survived and operated
    - Fast steering mirror operated at full bandwidth

- ## High Altitude Balloon Experiment

  - Acquisition and tracking payload integration and test completed
  - Initiation of passive tracking experiments vs scaled target rockets

- ## HYLTE water cooled module test series completed

  - Provided data for projecting HYLTE gain generator performance
    - Potential for ~20 to 30% performance improvement
  - Building self-cooled HYLTE module for testing in FY99
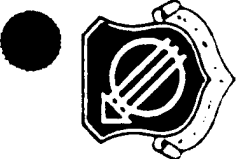
# Hydrogen Fluoride Chemical Laser

**Laser Beam**
2.7 µm wavelength

**Combustor**

**Makes atomic fluorine from easily stored reactants**

NF$_3$

D$_2$

H$_2$

F

**Chemical reaction creates excited Hydrogen fluoride**

$F + H_2 = HF^* + H$
(32 kcal/mole)

HF*

**Exhaust Gases**
HF
Other Gases
Waste Heat

**Optical Resonator**
Converts HF* energy into laser beam

Overview
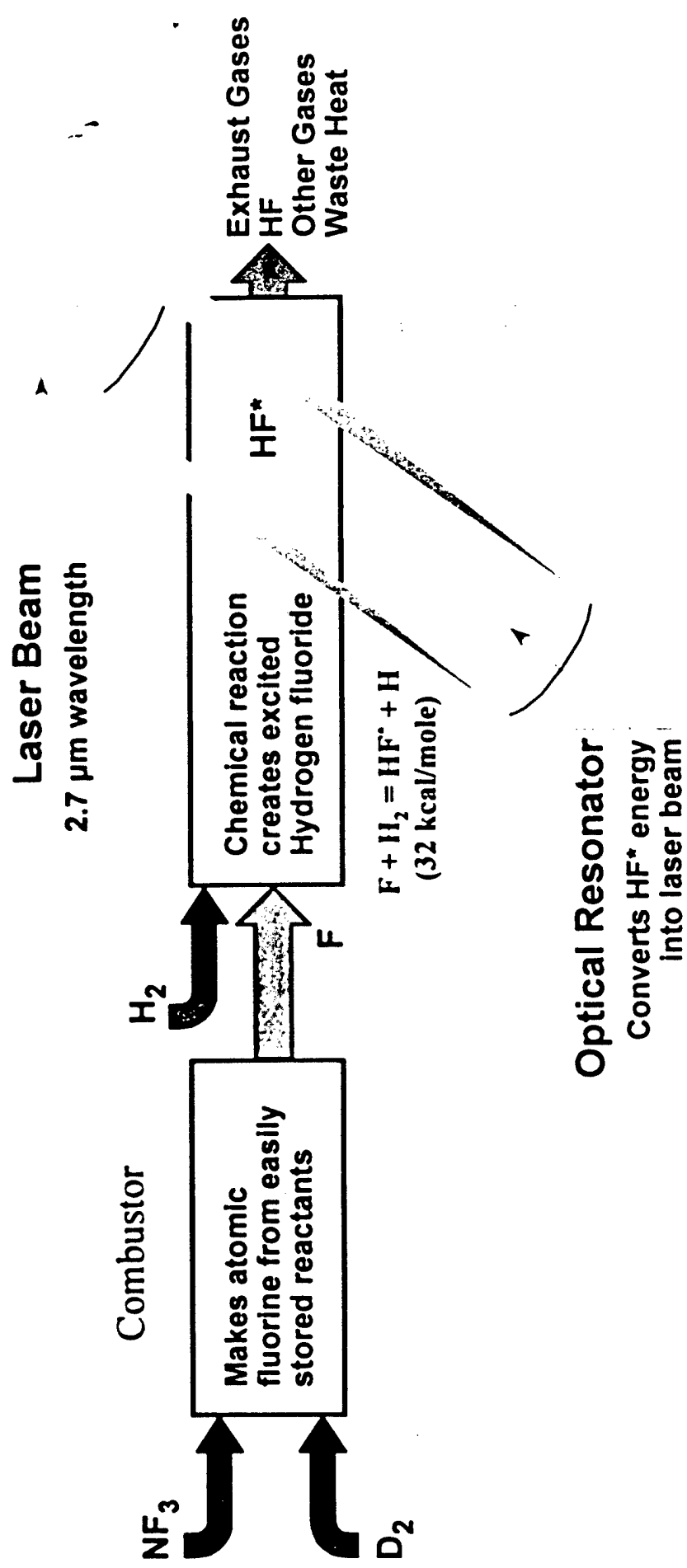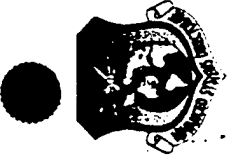
# Potential SBL Aircraft Detection Capability

**Surveillance Sensor**

**Single Frame**
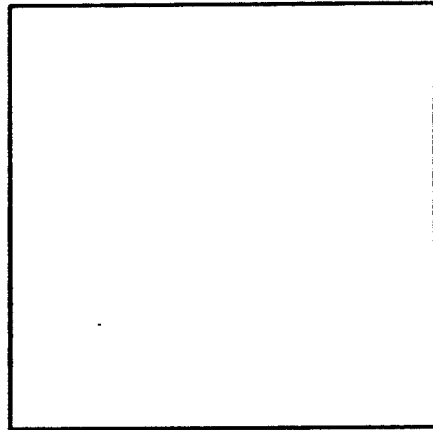
**Processed Image**

Thresholded Image

15 Km Footprint
(30 m Pixels)

15 Km Footprint
(30 m Pixels)
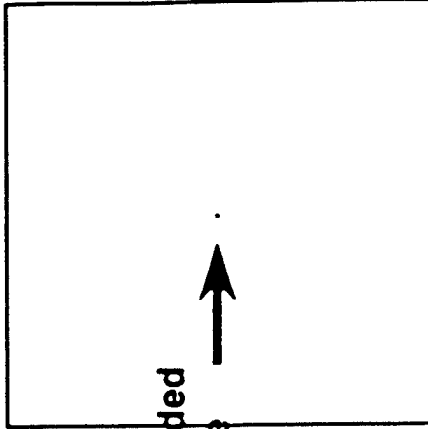
High
Altitude
Aircraft

**Fine Tracker Sensor**

120m

- 3000 km Slant Range
- 4.3 Micron Band
- 2 m Surveillance Sensor
- 8 m Fine Track Sensor

SBL Sensors Can Be Adapted to Detect High Aircraft
Over Large Areas and Image Them for Identification
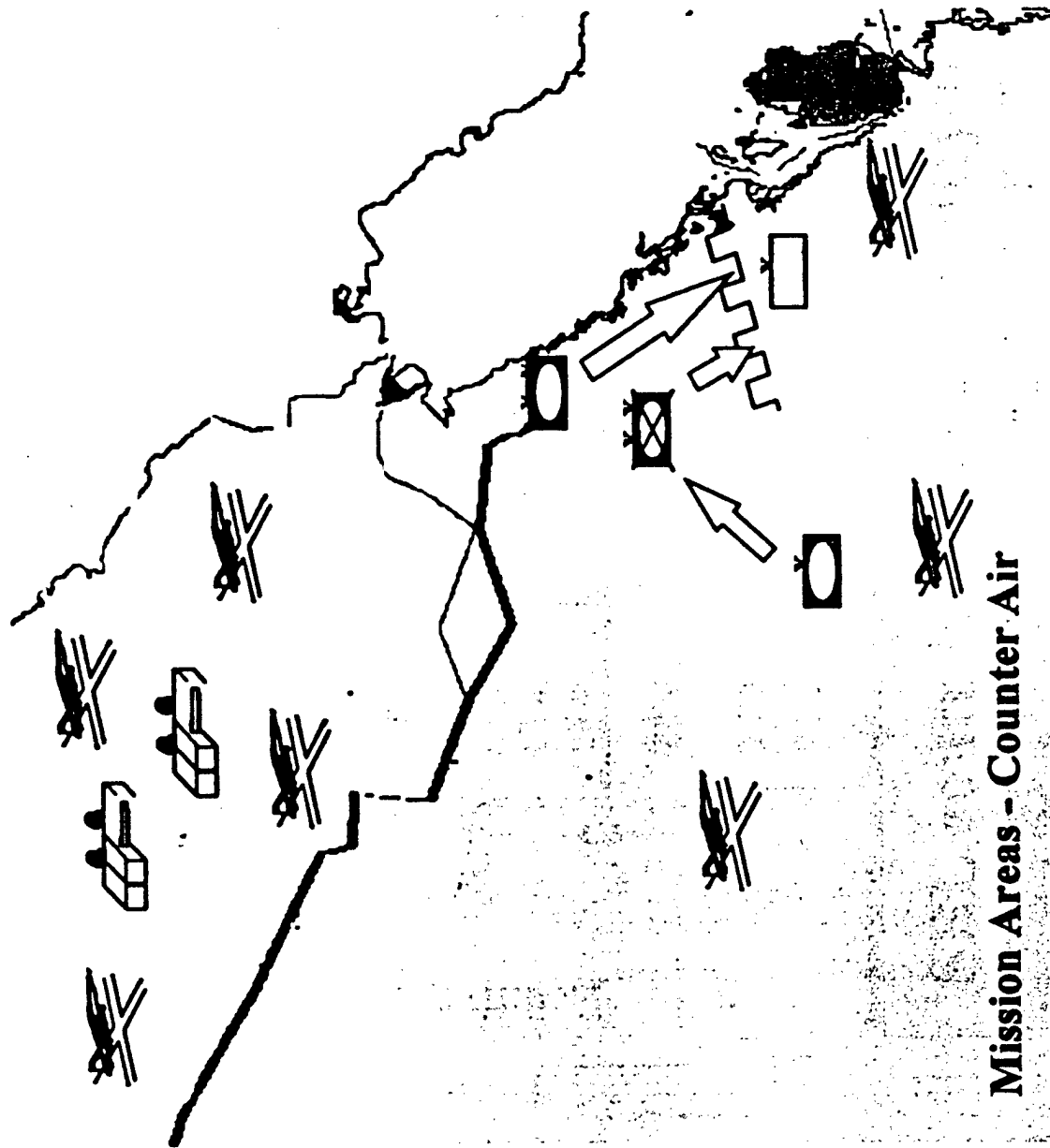
**Mission Areas - R&S**

3.1-1-58

# Force Laydown

**Iraqi Forces**
1 Armored Division
1 Mechanized Division
4 Air Defense Squadrons
2 Ground Attack Squadrons
4 SA-10 Batteries
3 TBM Regiments
2 SPOT Satellites

**US/Allied Forces**
1 Saudi Armored Brigade
1 US Armored Brigade
1 Attack Helicopter Battalion
4 US Ground Attack Squadrons
2 US Air Superiority Squadrons
2 Saudi Air Superiority Squadrons
Naval Task Force
  - 1 Aircraft Carrier
  - 3 TLAM Ships
1 JSTARS
1 AWACS
3 ISR Satellites

**Mission Areas - Counter Air**
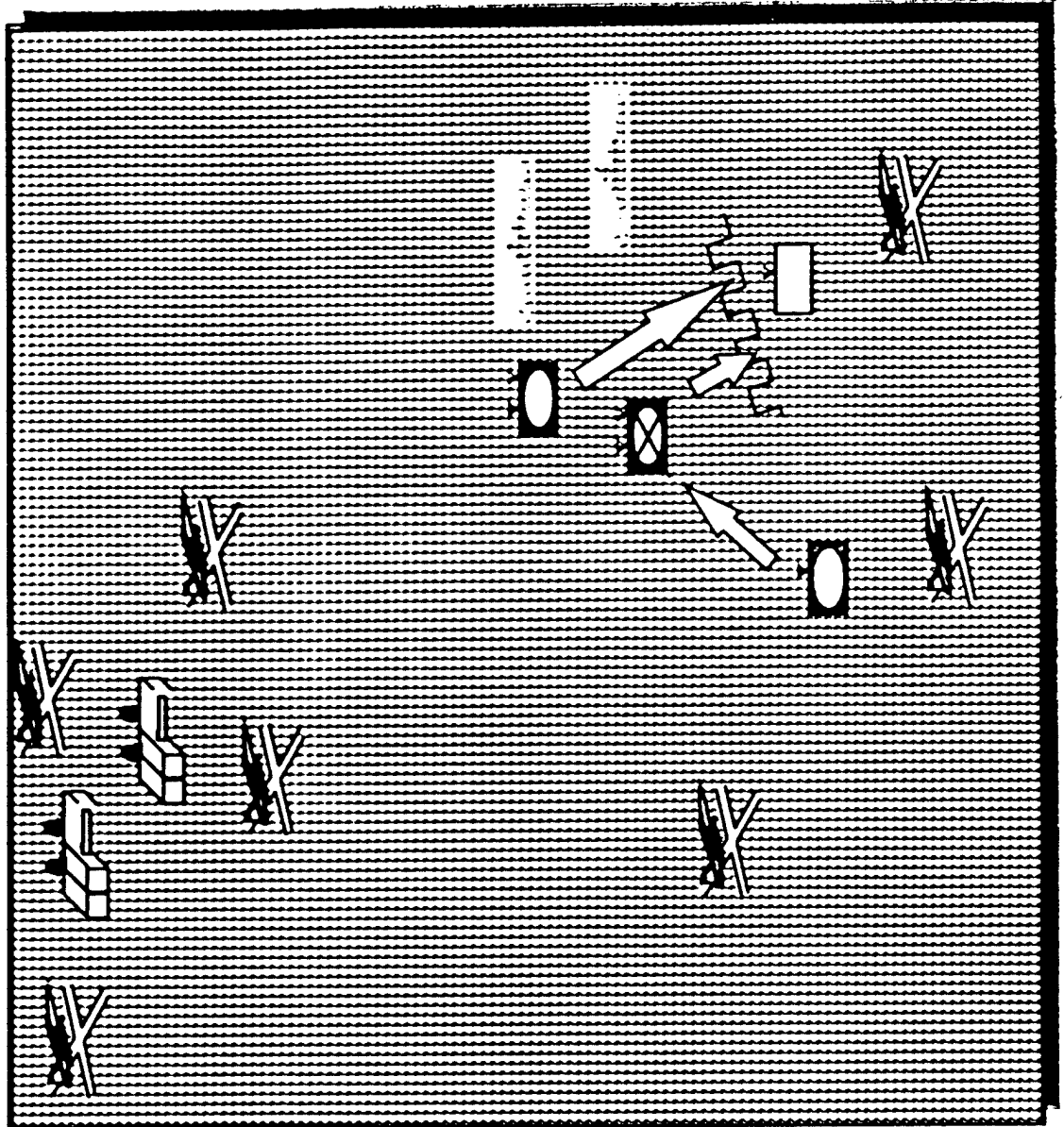
3.1-1-59

# Force Laydown

**Iraqi Forces**
- 1 Armored Division
- 1 Mechanized Division
- 4 Air Defense Squadrons
- 2 Ground Attack Squadrons
- 4 SA-10 Batteries
- 3 TBM Regiments
- 2 SPOT Satellites

**US/Allied Forces**
- 1 Saudi Armored Brigade
- 1 US Armored Brigade
- 1 Attack Helicopter Battalion
- 4 US Ground Attack Squadrons
- 2 US Air Superiority Squadrons
- 2 Saudi Air Superiority Squadrons
- Naval Task Force
  - 1 Aircraft Carrier
  - 3 TLAM Ships
- 1 JSTARS
- 1 AWACS
- 3 ISR Satellites

# Laser Designator Results for TBM TEL Attrition
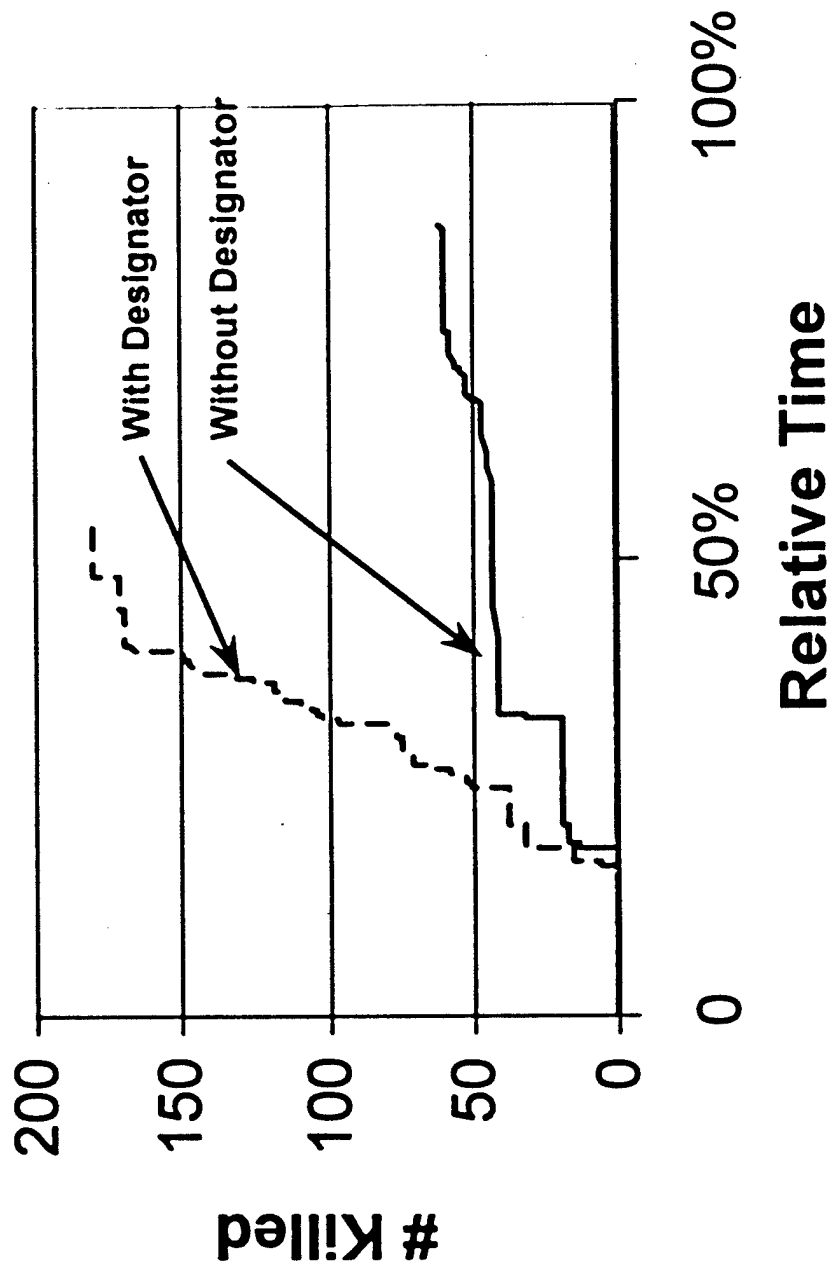


In clear weather, SBL greatly increases attrition of TBM TELs

# SEAS Scenario Emulation - Red
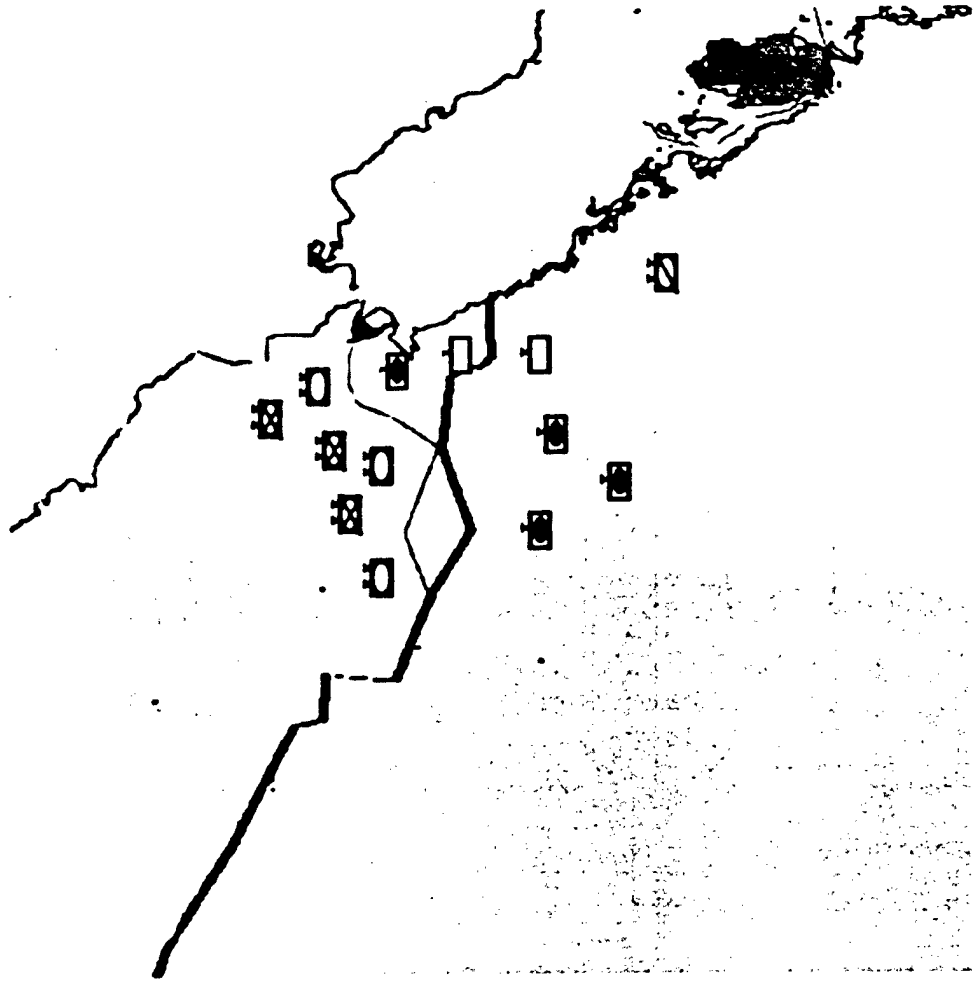
# SEAS Scenario Emulation - Blue
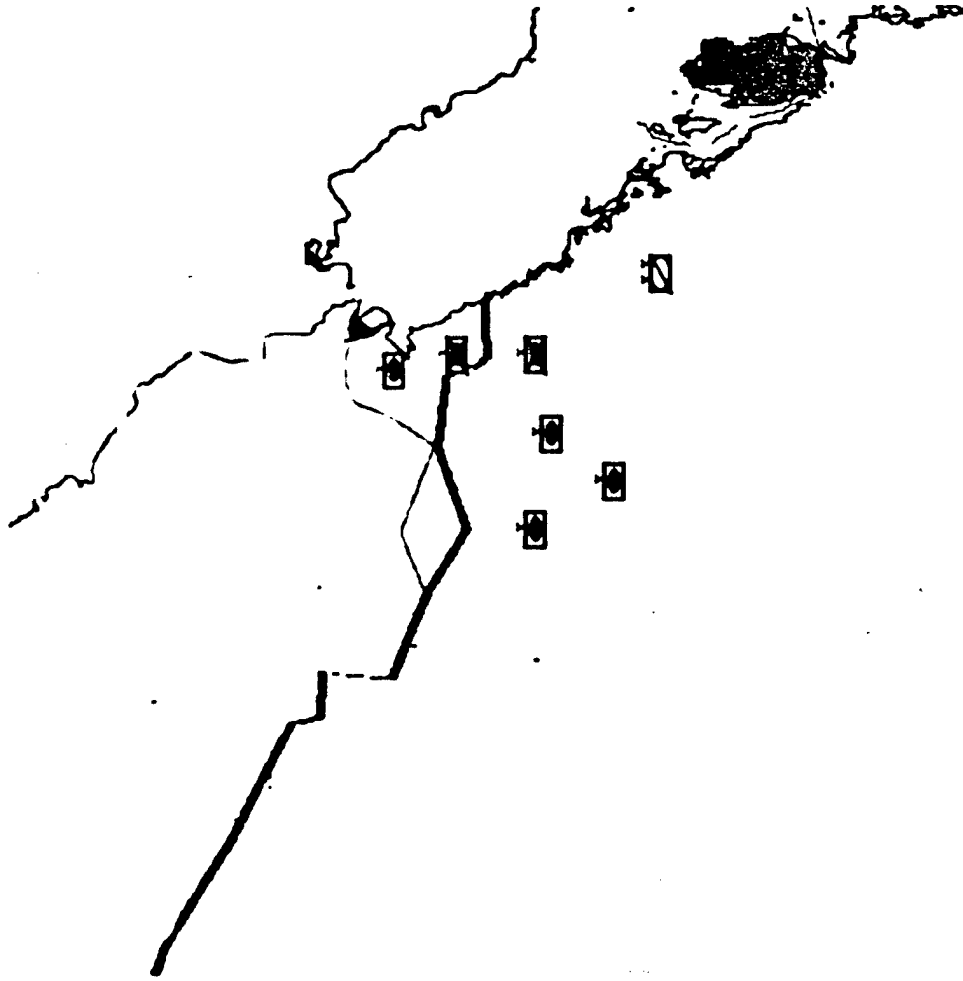
| Units | SEAS Objects |
|---|---|
| 6 Armored/Mech Brigades | 200 M1A1s<br>100 M3A2s<br>24 M109A6s |
| 1 Armored Cav Division | 100 M1A2s<br>50 M3A2s<br>24 M109A6s<br>24 AH-64Ds<br>24 RAH-66 |
| 2 Air Superiority Squadrons | 30 F-22s |
| 2 Ground Attack Squadrons | 15 F-16s<br>15 F-117s<br>10 B-1s |
| 1 Carrier Battle Group | 10 F-18Es<br>3 TLAM Ships |
| ISR | Provided |
| Space S&TW | SBIRS High/Low |

# National Imagery Interpretation Rating System Scale

**NIIRS 0 -- GRD N/A**
No interpretation of imagery
Obscurations, degradation, poor resolution

**NIIRS 1 -- GRD > 9 m**
Detect medium port facility
Distinguish taxiways and runways (large airport)

**NIIRS 2 -- 4.5 < GRD < 9 m**
Detect large hangars
Detect military training areas
Detect large buildings

**NIIRS 3 -- 2.5 < GRD < 4.5 m**
Identify large aircraft
Identify a large surface ship in port
Detect trains on railroad tracks

**NIIRS 4 -- 1.2 < GRD < 2.5 m**
Identify large fighter aircraft
Identify tracked vehicles
Determine the shape of a submarine bow

**NIIRS 5 -- 0.75 < GRD < 1.2 m**
Identify radar as vehicle or trailer mounted
Identify deployed tactical SSM systems
Identify individual railroad cars

**NIIRS 6 -- 40 < GRD < 75 cm**
Distinguish between small/large helicopters
Distinguish between SAM airframes
Distinguish between sedans and station wagons

**NIIRS 7 -- 20 < GRD < 40 cm**
Identify fittings and fairings on fighter aircraft
Identify ports, ladders, vents on electronics vans
Identify individual railroad ties

**NIIRS 8 -- 10 < GRD < 20 cm**
Identify rivet lines on bomber aircraft
Identify a hand-held SAM
Identify windshield wipers on a vehicle

**NIIRS 9 -- GRD < 10 cm**
Differentiate cross/straight-slot aircraft fasteners
Identify missile screws and bolts on components
Identify vehicle registration numbers on trucks

# Time to Achieve Air Supremacy
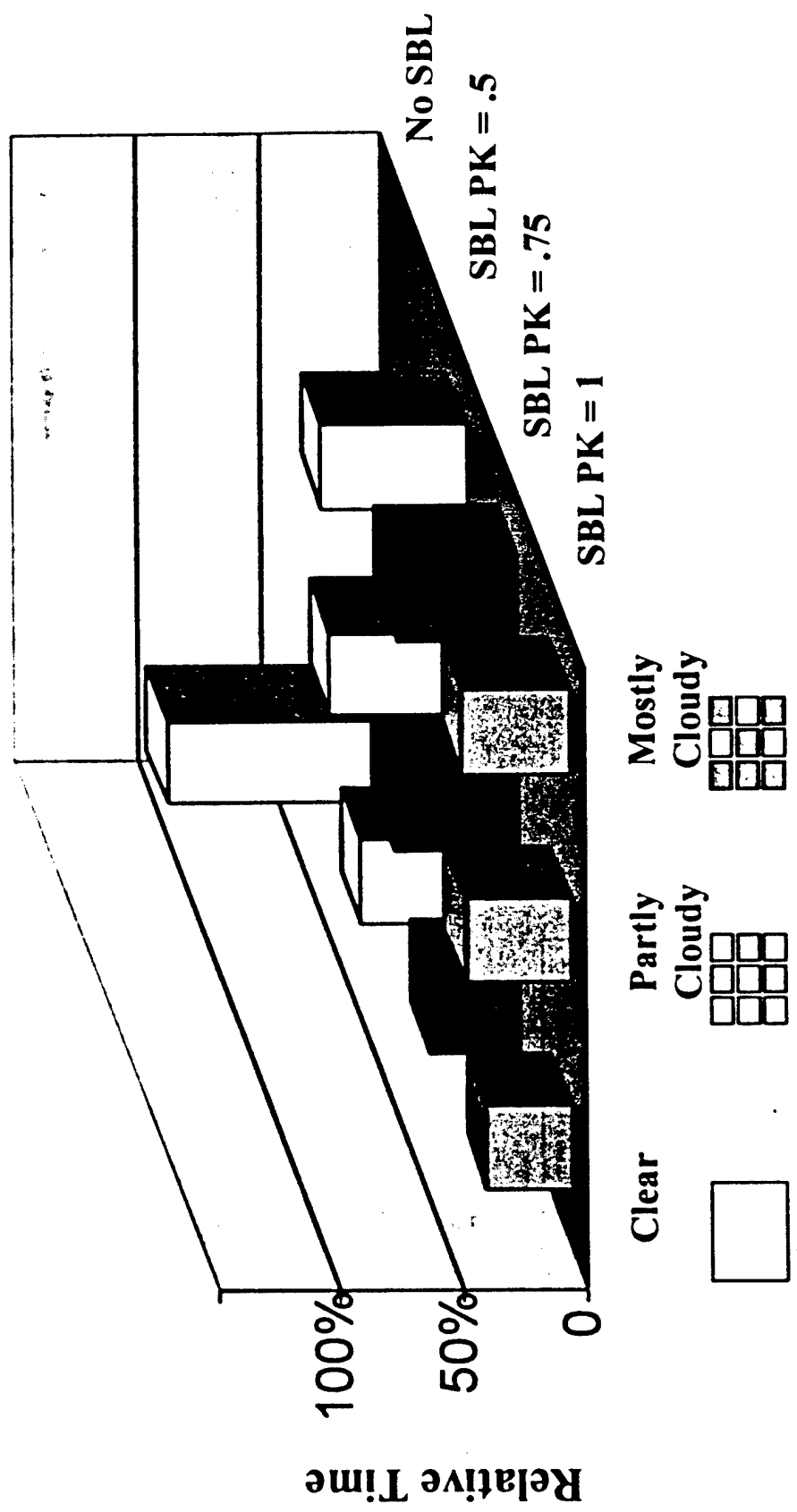


## SBL contributes significantly to the air campaign

3.1-1-65

# SBLs Allow Achievement of Military Objectives With Minimum Casualties and Collateral Damage

- Designator Potential of SBL With Low Power Laser Enables Precision Strike With Dumb Munitions
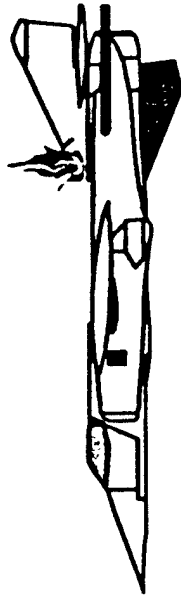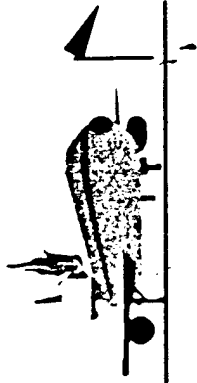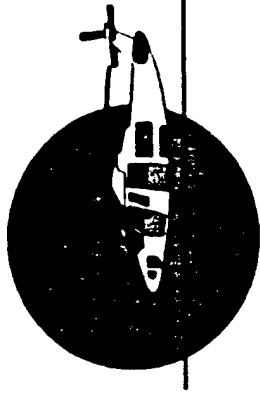
- •Precise Irradiation of Airborne or Ground Objects Disable Threats With Minimum Collateral Damage

- ATTACK CRITICAL FACILITIES FOR DEFENSES SUCH AS COMM ANTENNAS, SAM OR POWER FACILITY
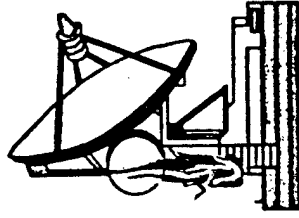
Mission Areas – Attack Ops

# TARGET KILL CRITERIA

- MINIMUM DAMAGE RADIUS -- Heated spot must be large, enough to cause buckling and/or crack size that will propagate and rupture tank

- EDGE INTENSITY (W/cm$^2$) THRESHOLD -- Minimum intensity necessary at edge of damage spot to heat the target and overcome losses such as lateral conduction, reflection, re-radiation, etc (intensity variation over spot must be under ~25%)

- EDGE FLUENCE (J/cm$^2$) THRESHOLD -- Minimum fluence (intensity x dwell time) required to rupture tank

  - Soft targets (metal tanks):          1 - 5  kJ/cm$^2$

  - Hard targets  (composite tanks):   5 - 25 kJ/cm$^2$

Mission Areas -- TMD

# Intensity vs Range



Laser

Beam
Expander

Actual Laser Beam

Diffraction & Aberration
Free Laser Beam

θ

D

R

I

D

I/4

2D

2D

Intensity Pattern

θ

2D

2R
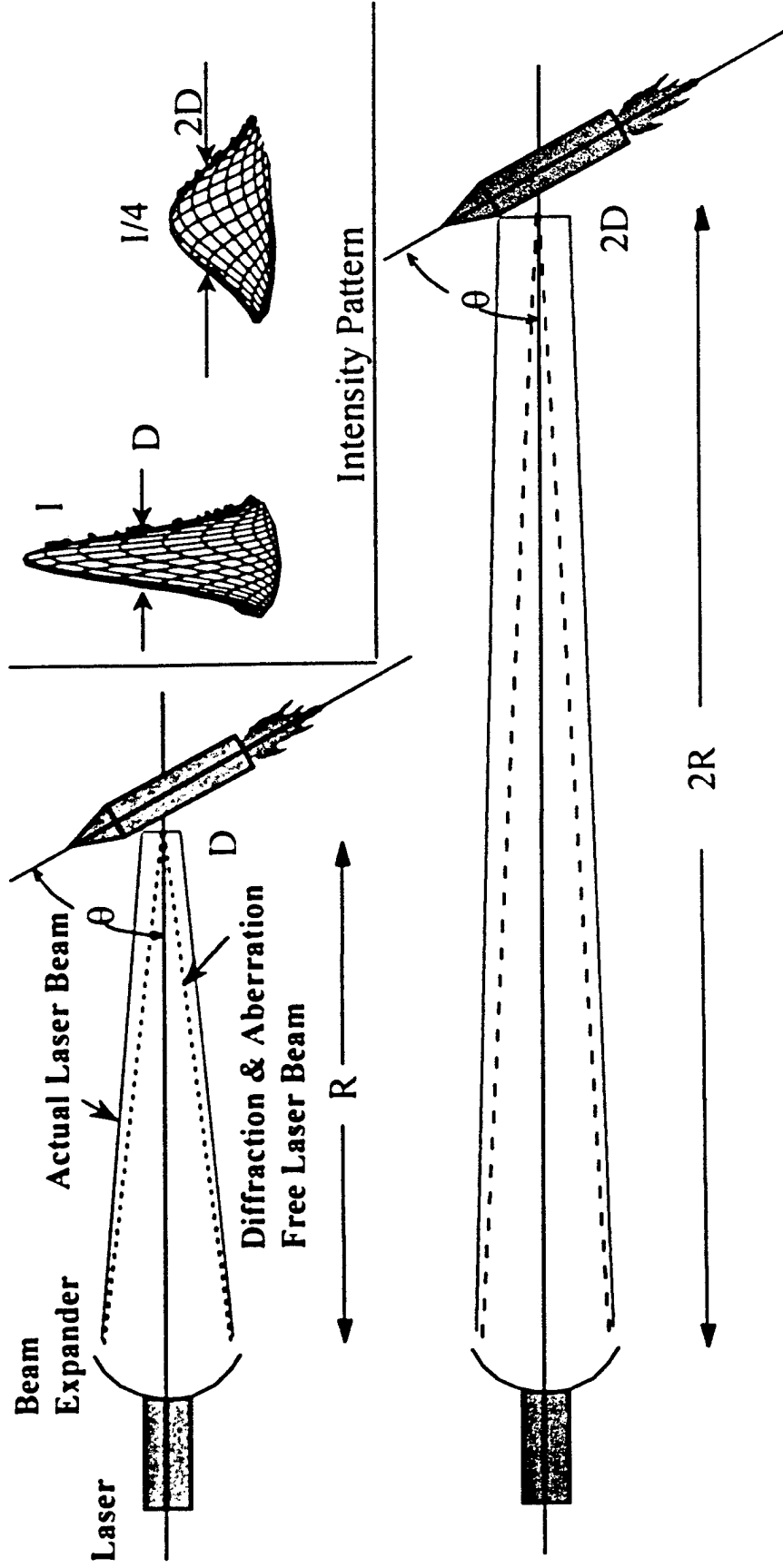
# Beam Spot Diameters

Delivered Beam Spot
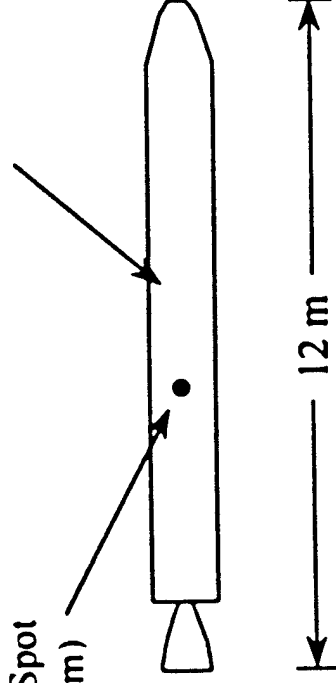
Required Beam Spot
(r = 2 cm, 15 cm)

12 m

- 12 m Aperture
- 1.0 Strehl
- 4000 km Range
- $\lambda = 2.8$ um
- $\sigma_{DIV} = 100$ nrad
- $\sigma_r = 40$ cm
- $I = I_{min}$

**Since Delivered Spot is Larger Than Needed, Intensity Over Required Spot is Maximum**

# Target Vulnerabilities



### Target #6, Fuel Tank Ignition
Time 350 K, h=0.38 cm

— High Confidence. Highly reflective paint
— Medium confidence. TBM white paint

### Target #6, Electronics Failure
High Confidence. Tint = 310 K, h₀ = 0.6 cm, steel electronics box         Medium
confidence. Tint = 310 K, h₀ = 0.6 cm, Al electronics box

### Target #6, Flight Control Surface Melt-Through
— High Confidence. Tint = 350 K, h = 0.254 cm. Highly reflective paint
— Medium confidence. Tint = 350 K, h = 0.13 cm. TBM white paint

# Lethality

## Long History (>20 Years) Validates Ability of Lasers to Destroy Thrusting Missiles

- Extensive Analysis and Laboratory Testing of Thermo-Mechanical Properties of Materials
- MIRACL Laser Demo Against TITAN Stressed and Pressurized to Simulate Launch Loads



Titan Booster With Full Simulated Flight Load Destroyed by MIRACL Laser, September 6, 1985

To kill target, absorbed energy on the target must exceed a minimum level over a minimum area:
(INTENSITY on the target) x (% of energy absorbed) x (DWELL TIME on the target)



Intensity

Spot size

This kills the target

This doesn't kill the target

Lethality requirement
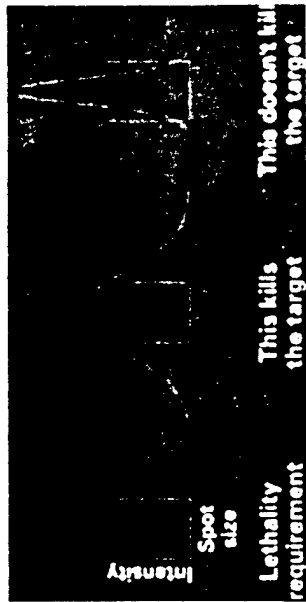
Minimum energy level and minimum area are different for different targets

To kill targets faster (shorter DWELL TIME) or kill harder targets (greater INTENSITY) want shorter RANGE or higher BRIGHTNESS

INTENSITY &
DWELL TIME &
SPOT SIZE &
INCIDENCE ANGLE

BRIGHTNESS

RANGE

## Mission Areas - TMD

# Cruise Missile Detection

Consecutive 0.01 sec Frames

Frame Differencing

Frame Combining

Streak Detection

Detected Target

- Low Flying Cruise Missile
- 3000 km Slant Range
- Clear Line of Sight
- PIXEL IFOV = 1 μrad
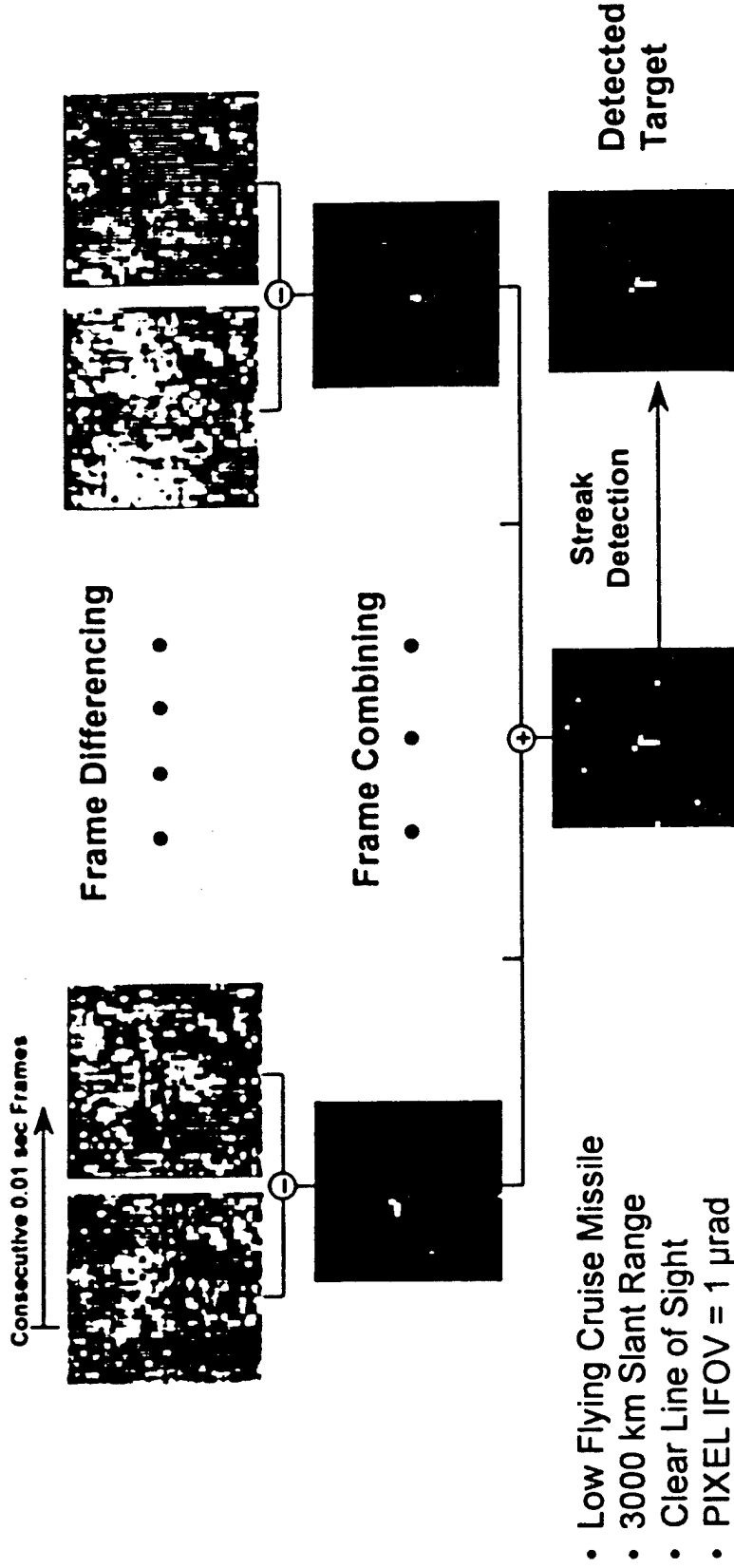
SBL Sensors Can Be Adapted to Detect and Track Low Altitude Targets Within Limited Areas

# ABL and SBL Can Be Synergistic

| | Airborne Laser (ABL) | Space-Based Laser (SBL) |
|---|---|---|
| Missions | TBM Boost-Phase Intercept<br>Potential for Aerospace Control | TBM & ICBM Boost-Phase Intercept<br>Potential for Space, Aerospace Control |
| Availability | Support to multiple theaters<br>Deployed in less than 1 day<br>Easily replenishable shots | Global coverage<br>Instant response<br>Fresh SBLs into theater every 20 min |
| Mutual Supportability of TMD | Against forward based threats<br>Concentrated firepower to select areas | Against deeply based threats<br>Second tier for forward based threats<br>Defends prior to ABL arrival |
| Synergistic Technologies | Atmospheric Propagation — Autonomous Optical Alignment<br>Lethality, Vibration Isolation, Laser Beam Control, Optics & Coatings,<br>Acquisition, Tracking, & Pointing/Fire Control Algorithms,<br>TMD Interfaces, Modeling & Simulation, Processing | |
| Program Status | In PDRR | In early concept definition |
| Schedule | Aircraft with ROC - 2002<br>IOC - 2006, FOC - 2008 | Readiness Demonstrator Flight ~ 2005<br>IOC > 2015 |

# Appendix 3.1-2
## ALI Status

# Alpha LAMP Integration (ALI)

Gary Golnik

# ALI is a Key Stepping Stone in the Path to SBL

Space-Based Laser

Space Demonstration
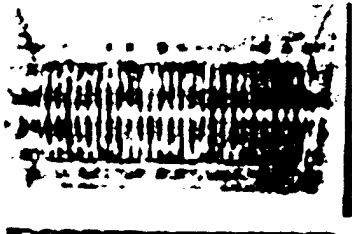
Integrated Ground Test

Alpha Lamp Integration (ALI)

ALPHA (1991)
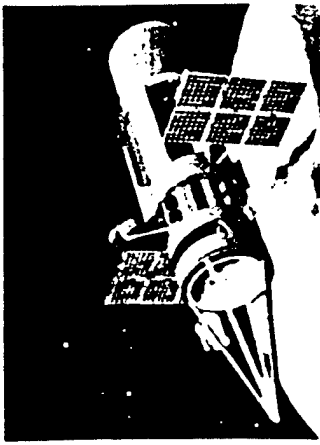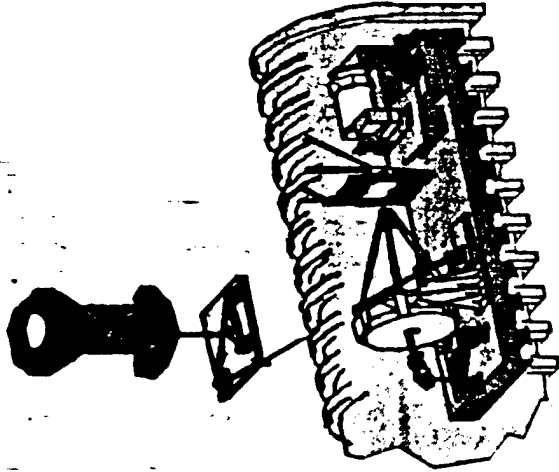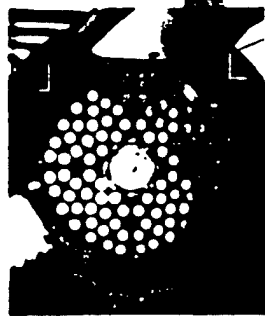
LODE (1987)

Large Optics Demonstration Experiment

LAMP (1989)

Large Advanced Mirror Program
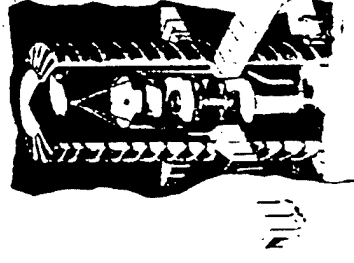
# Briefing Outline

- IRT - 2 Presentation Recap

- Actual Events Since Nov. 97

- Current Near Term Plans

- SOA for SBL Beam Control

# ALL Program Schedule

- Place holder for schedule presented to IRT - 2

3.1-2-5

# ALI Experiment Configuration



Labels in figure:
- High Power Beam from Alpha
- ALPHA Vacuum Chamber
- High Power Beam
- Secondary Mirror / Outgoing Wavefront Sensor
- ALI Vacuum Chamber
- Diagnostic Telescope Assembly
- System Diagnostic Assembly
- High Power Beam Clipper
- LAMP
- Deformable Mirror
- Fast Steering Mirror
- Input Diagnostics Assembly
- Uncooled Turning Flats
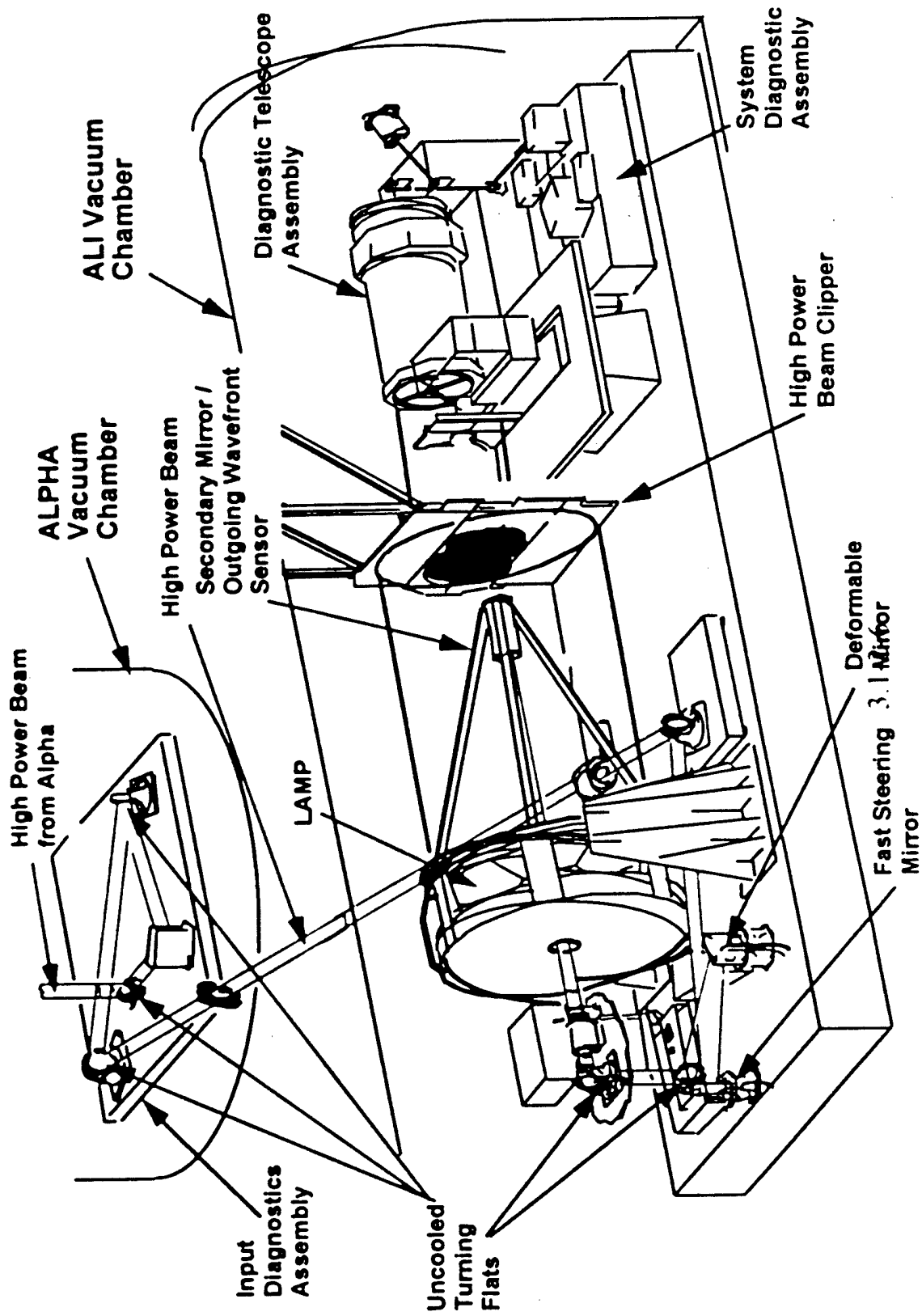
# Data Presented To IRT - 2

- **Preliminary Results from ALI Phase I Test Program**

  – Experiment IIB Data Analysis was in Process

- **Plans to Integrate & Test an Uncooled Deformable Mirror (UDM) @ High Power**

- **Tour Of ALI Hardware**

3.1-2-7

# Alpha/LAMP Integration (ALI) Program Objectives
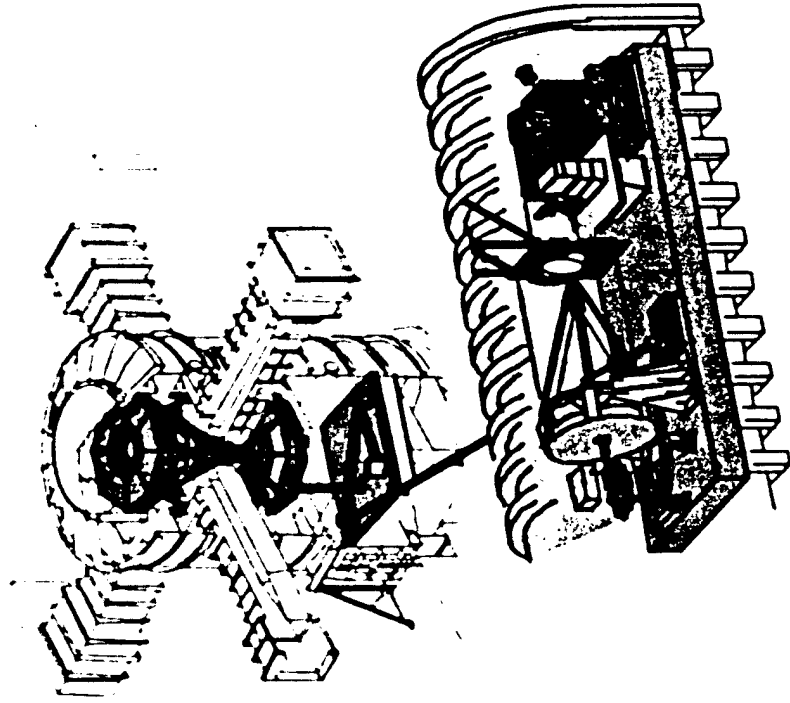
- **Demonstrate Integration of Alpha and High Power Beam Control**

- **Demonstrate Uncooled Optics**

- **Demonstrate High Power Operation of:**

  - **LAMP With HOEs**

  - **OWS Behind Secondary Mirror**

  - **FSM and DM Control Optics**

3.1-2-8

# Experiment I: 1/2 Second Open Loop Test
## 20 February 1997

- Propagate HEL beam safely through the ALI beam train for 1/2 second at nominal power

  - **Successful end-to-end propagation verified by sensors at seven key locations in the ALI beam train**
  - Post-test inspection indicated high power optics and PME in good condition

- Characterize HEL beam and verify beam performance

  - Power, intensity, wavefront and jitter measured by diagnostic sensors at multiple locations in beam train
  - Diagnostics indicate nominal power levels and well filled mode intensity
  - Near & far field measurements verify good beam quality and expected beam jitter
  - Temporal and spatial characteristics of wavefront deduced

- Demonstrate readiness for multi-second closed loop test

  - **Strong P1(7) line measured by system diagnostics**
  - **OWS captured wavefront slopes required for closed loop beam control**
  - Predominance of low temporal and spatial frequencies in wavefront portends effective correction by the ALI Beam Control System

3.1-2-9

# Experiment IIA: 2 Second Closed Loop Test
## 16 July 1997 (Joint ALI/ALO High Power Test)

- Propagate HEL beam safely through the ALI beam train for two seconds at nominal power

  - **Approximately 0.9 second of high power lasing**
  - Test aborted when beam pointing exceeded limits due to pellicle failure in Beam Steering Assembly
  - Diagnostics show well filled mode intensity, power approx. 3/4 of nominal, and P1(7) "dropouts"
  - Post-test inspection indicated high power optics and PME in good condition, minor damage observed in ALPHA GGA secondary array

- Demonstrate stable closed loop performance of the OTS jitter control system

  - **OWS captured wavefront slopes required for closed loop control**
  - **Jitter control loop successfully closed**

- Demonstrate readiness for 2nd multi-second closed loop test (Experiment IIB)

  - Power, intensity, wavefront, and jitter measured by diagnostic sensors at multiple locations in beam train
  - Temporal and spatial characteristics of wavefront measured
  - Predominance of low temporal and spatial frequencies in wavefront portends effective correction by ALI Beam Control System

3.1-2-10

# Experiment IIB: 5 Second Closed Loop Test
## 22 October 1997

- Propagate HEL beam safely through the ALI beam train for five seconds at nominal power

- Demonstrate stable closed loop performance of integrated system at high power

- Collect data necessary to demonstrate feasibility of space-based experiments

3.1-2-11

# Briefing Outline

- IRT - 2 Presentation Recap

→ - Actual Events Since Nov. 97

  - Complete ALI Phase I Data Review

  - Uncooled Deformable Mirror (UDM) High Power Test

  - Beam Control Test

- Current Near Term Plans

- SOA for SBL Beam Control

3.1-2-12

# Experiment IIB: 5 Second Closed Loop Test
## 22 October 1997

- Propagate HEL beam safely through the ALI beam train for five seconds at nominal power

  - **Approximately 1.2 seconds of high power lasing**
  - Out of tolerance signal in the Beam Steering Assembly caused test to abort
  - Diagnostics show well filled mode intensity; wavefront and beam jitter from ALPHA laser nominal; ALPHA beam pointing was stable; ALPHA power low
  - Post-test inspection indicated high power optics and PME in good condition; no GGA damage

- Demonstrate stable closed loop performance of integrated system at high power

  - **Good quality HOE spots detected by the OWS with very few "drop-outs"**
  - OWS captured wavefront slopes required for closed loop control
  - **Jitter and wavefront control loops successfully closed**

- Collect data necessary to demonstrate feasibility of space-based experiments

  - Power, intensity, wavefront, and jitter measured by diagnostic sensors at multiple locations in beam train
  - Temporal and spatial characteristics of wavefront measured
  - Far Field Camera displayed "large spot - small spot," demonstrating wavefront correction by the beam control system

3.1-2-13

# ALI Phase I Conclusions

**Alpha/LAMP Integration (ALI) Program Objectives Were Successfully Completed**

- <u>Successfully Demonstrated</u> Integration of Alpha and High Power Beam Control

- <u>Successfully Demonstrated</u> Uncooled Optics

- <u>Successfully Demonstrated</u> High Power Operation of:
  - LAMP With HOEs
  - OWS Behind Secondary Mirror
  - FSM and DM Control Optics

3.1-2-14
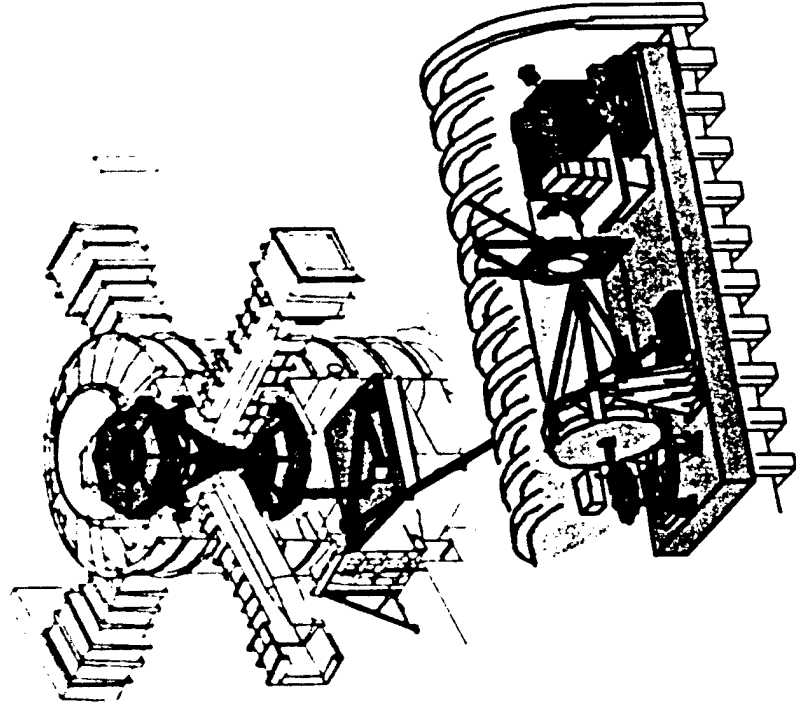
# UDM High Power Test

3.1-2-15

# UDM High Power Test Objectives

- Demonstrate High Power Performance Of UDM

- Demonstrate Beam Control System Performance

  At Full Bandwidth

- Demonstrate ALPHA Jitter Reduction

3.1-2-16

# Test Operations Ran Smoothly

- **Pretest Alignment and Checkout Efficiently Completed**

- **Pump-Down Procedures Accomplished Effectively**

- **Alignments in Vacuum Completed Smoothly**

- **Revised MCC Operating Procedures for OTS Ran Effectively**
  - Maintaining Lamp Segment Pointing and Figure
  - Remote Operation of All Insertion and Retraction Stages
  - AAA Beams Used to Verify Lamp Center Segment Pointing

- **Timeline Operations**
  - Beam Control System's Null Taking Was Timely
  - Lamp Pointing Control Switched From CoCFS Control to Eddy Current Control Just Prior to Start of Automated Timeline as Required
  - PRA Start-up and Operation Nominal
  - Automated Timeline Ran Nominally
  - Optical Test System Automated Timeline Activated on Command
    - Collected ~.5 Seconds Open Loop Data
    - Loops Closed After ~.5 Seconds of Lasing

3.1-2-17

# UDM Test Results Lessons Learned

- Could Have Used More Open Loop Data For Correlation And Other Analysis Functions (1 sec. Rather Than 1/2 sec.)

- Lack Of Common Reference Between OWS And SDA Precluded Good Correlation Of Subaperture Data (BCT Series Will Establish A Common Reference)

- Post Pump-Down Problems With LAMP Fine Figuring

3.1-2-18

# Beam Control Test

3.1-2-19

# ALI BCT Program Schedule
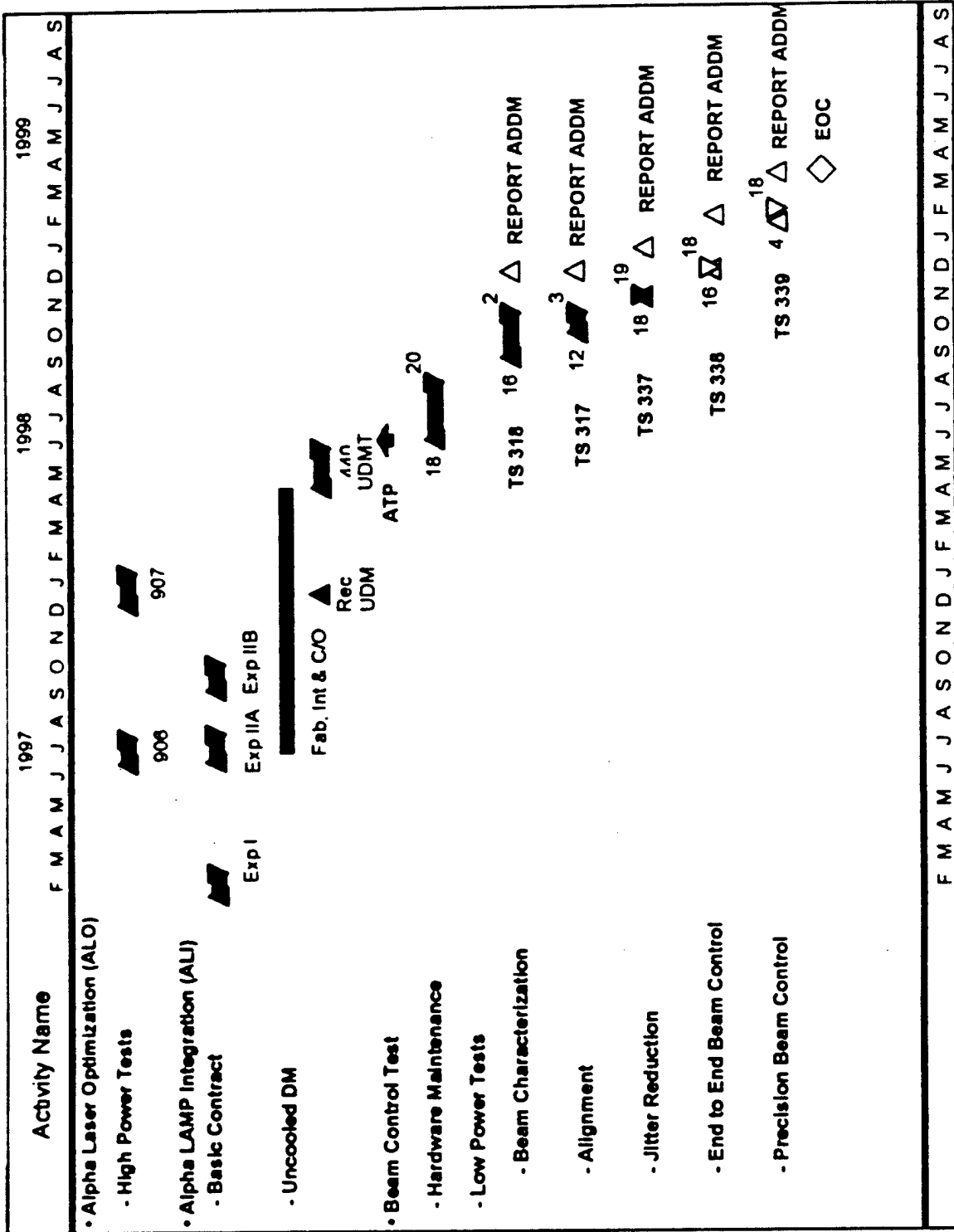


R. Nefzger Mgr.
as of: 12-15-98 Rev. A

# BCT Test Sequence

```
                                                    ┌──────────────┐
                                                    │ PROCEED TO   │
                                                    │ NEXT TEST    │
                                                    └──────────────┘
                                                          ▲
                                                          │ GO
┌──────────────┐                                    ┌──────────────┐      ┌──────────────┐
│ Trouble Shoot│                            NO-GO    │ GO / NO-GO   │      │ TEST         │
│ Fix / Modify │◄───────────────────────────────────│ DECISION     │      │ REPORT       │
└──────────────┘                                    └──────────────┘      └──────────────┘
      ┊                                                    ▲                     ▲
      ┊                                                    │                     │
┌──────────────┐      ┌──────────────┐      ┌──────────────┐
│ PREDICTIONS &│      │ TEST         │      │ RESULTS      │      │ EXPLANATION  │
│ EXIT CRITERIA│      │              │      │              │      │ OF DIFFERENCES│
└──────────────┘      └──────────────┘      └──────────────┘      └──────────────┘
```

3.1-2-21

# Beam Control Test Configuration



Star Sources

Metrology Enhancements

Hartmann Sensor

ALI Vacuum Chamber

ALPHA Vacuum Chamber

High Power Beam

Diagnostic Telescope Assembly

System Diagnostic Assembly

Secondary Mirror / Outgoing Wavefront Sensor

High Power Beam Clipper

High Power Beam from Alpha

LAMP

Uncooled Deformable Mirror

Fast Steering 3.1-Mirror Mirror

Input Diagnostics Assembly

Uncooled Turning Flats

# Beam Control Test Configuration

Star Sources

Diagnostic Telescope Assembly

System Diagnostic Assembly

ALI Vacuum Chamber

High Power Beam Clipper

ALPHA Vacuum Chamber

High Power Beam
Secondary Mirror / Outgoing Wavefront Sensor

High Power Beam from Alpha

Metrology Enhancements

LAMP

Input Diagnostics Assembly

Uncooled Turning Flats

Uncooled Deformable Mirror

Fast Steering Mirror

Hartmann Sensor

3.1-912br

# BCT Hardware Enhancements

- Upgrade Centroid Processor Algorithm To Include Smoothing For Missing HOE Spots (TS 338)

- Refine OWS Internal Alignment To Improve Beam Control System Performance (TS 318)

- Improve Beam Quality Of FFRB Into SDA To Assist In Pre-Test Alignments And Provide A Common Jitter Reference During Testing (TS 317)

- Minimize Spot Of Arago To Improve AAA Spots On OWS Including Increasing AAA Beam Power , Improving Pretest Alignments (TS 338)

- Add Visible And Infrared Hartman Sensors To CAA To Provide More Robust Calibration And Alignment (TS338 7 339)

- Add Simulated Star Sources In SDA To Allow Subaperture Alignment Of Beam Train And Validate SBL Approach For Wavefront Calibration(TS 338)

- Use SDA Far Field Camera Data and WaveFront Sensor With CAA To Provide Improved Pre-Test Calibration(TS 317)

- Improve Pointing Stability Of TAA Laser To Improve Pre-Test Alignments (TS 338)

- Improve SMA And OWSA Actuators And Gravity Offloads (TS 317)

- Improve Visibility Of INTF1 And INTF2 (TS 317)

- Add UDM Diagnostics (TS 318)

3.1-2-24

# BCT Test Series Description

- **Alignment Tests (TS 317) - Complete (3 Nov 98)**
  - Implements Alignment Enhancements
  - Demonstrates Improved Alignment Capabilities
  - Multiple Test Runs Using ALI Alignment Lasers To Achieve Good Statistical Sample Of Beam Alignment

- **Beam Control Characterization Tests (TS 318) - Complete (2 Nov 98)**
  - Implements Beam Control Enhancements
  - Determines Limits Of Correctability Of FSM & UDM
  - Utilizes Aberration Generators To Induce Controlled Jitter & Aberrations On Low Power Beam
  - Multiple Test Runs To Achieve Good Statistical Sample Of Beam Control Performance

- **LAMP Characterization Tests (TS 302) - Deferred**
  - Characterizes LAMP Performance During Steam Generator (PRA) Operation
  - Piggy Backs On ALO Testing On Non-Interference Basis

3.1-2-25

# BCT Test Series Description (Cont.)

- **Low Power Jitter Reduction Tests (TS 337) - Complete (19 Nov 98)**

  - Characterizes Jitter From Both Power Management Equipment (PME) & Optics Coolant Circuits

  - Identifies Jitter Reduction Enhancements

  - Multiple Test Runs At Different Flow Rates

    - Determine Flow Rate That Simulates Observed UDM High Power Test Jitter Condition

    - Determine Best Flow Rate For Low Power End-To-End Simulation Tests and High Power Tests

- **End-To-End Simulation Tests At Low Power (TS 338) - In Process**

  - Provides End-To-End Verification Of System Performance At Low Power Under Simulated High Power Conditions

  - Multiple Test Runs At PME And Optics Coolant Flow Rates Determined In Prior BCT Tests To Achieve Good Statistical Sample Of Beam Control Performance

# BCT Test Series Description (Cont.)

- **Precision Beam Control Test (TS 339) - Schedule (18 Jan 99)**

  - Implements Final System Enhancements Prior To High Power Test

  - Demonstrate Improved End-To-End Alignment

  - Demonstrate Enhanced Beam Control Performance

  - Demonstrate Integrated Flight eXperiment (IFX) Low Power Simulation

  - Demonstrate Common Reference For System Diagnostics And Outgoing Wavefront Sensor

3.1-2-27

# BCT Preliminary Results & Lessons Learned

- Data Review in Process

- Need Clean Beam and Controlled Aberrations to Explore Envelope of Beam Control Performance

- Jitter (on Input Beam) has Major Effect on Beam Control Performance

- Common Reference is Critical to Quantifying System Performance

- Experienced Hardware Limitations

  - Far Field Reference Beam (FFRB)

  - Low Energy Laser / Alpha Probe Laser (LEL / APL)

  - System Diagnostic Assembly Wavefront Sensor (SDA WFS)

3.1-2-28

# Briefing Outline

- IRT - 2 Presentation Recap

- Actual Events Since Nov. 97

→ • Current Near Term Plans

  – Beam Profile Generator Fabrication & Test

- SOA for SBL Beam Control

3.1-2-29

# Near Term Plans Purpose

- Simulate the High Power Laser at Low Power in a Representative Beam Control System to Quantify Design Parameters

- Determine the Limits of the Beam Control System by Providing Controlled Repeatable Inputs

# Beam Profile Generator Configuration

Diagnostic Telescope Assembly

System Diagnostic Assembly

ALI Vacuum Chamber

High Power Beam

Secondary Mirror / Outgoing Wavefront Sensor

ALPHA Vacuum Chamber

High Power Beam Clipper

High Power Beam from Alpha

LAMP

Uncooled Deformable 3.1-Mirror

Fast Steering Mirror

Input Diagnostics Assembly

Uncooled Turning Flats

Beam Profile Generator

# Beam Profile Generator Schematic

- **Spatial Beam Modulator**
- **Jitter Simulator**
- **Deformable Mirror**



**Intensity Monitor**

3.1-2-32

# Beam Profile Generator Layout



3.1-2-33
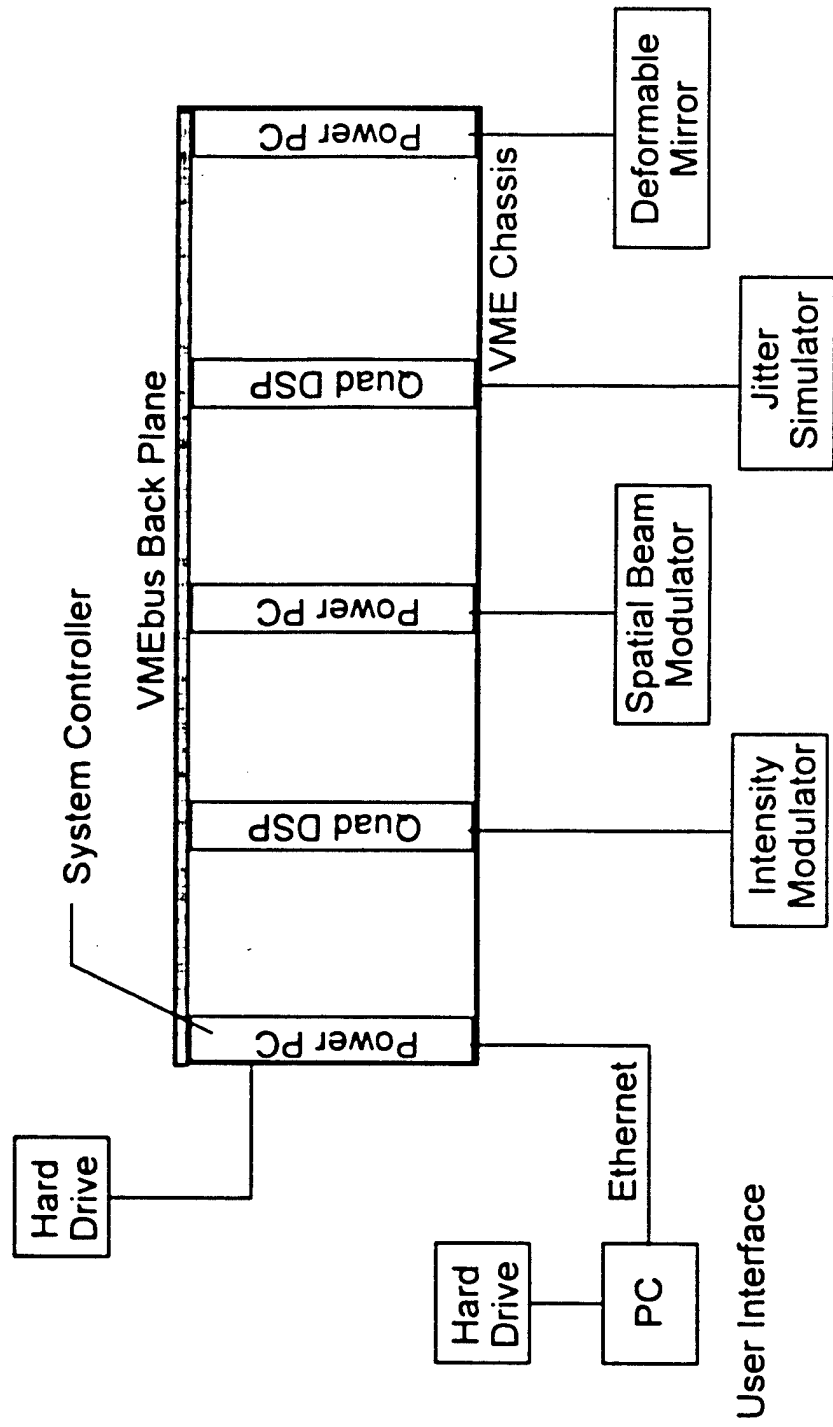
# Beam Profile Generator Test Features

- Uses Results of High Power Test Data to Drive Generator Elements

- Performs Parametric Studies Using Sine Wave Input To Test Limits/Predicted Performance of Beam Control Systems

- Performs Repeatable Tests With Identical Inputs

    - Develops Statistics of Beam Performance

- Simulates Predicted Beam Errors/Disturbances in Future High Power Tests and Flight Systems

- Provides Enhanced Capability Over Alpha Probe Laser Through the Resonater Simulated HEL Input

# Beam Profile Generator Test Features

- **Controls the Dynamic Range and Resolution of Input Errors/Disturbances**
- **Simulates Multiple Laser Types**
  - Provided by Software Implementation
  - Enhances Test Capabilities
- **Aids in the Design Process of Future Space Based Systems (IFX & Operational Systems) by Determining the Transfer Functions Between Space Vehicle Elements**
- **Allows Shorter Turnaround Between Tests**
  - More Tests Per Day/Week/Year
- **Results in Lower Cost Per Test**

3.1-2-35

# Beam Profile Generator Schedule

| Activity Name | 1998 | 1999 | 2000 |
|---|---|---|---|
| | Nov Dec Jan Feb Mar Apr May Jun Jul Aug Sept Oct Nov Dec | Jan Feb Mar Apr May Jun Jul Aug Sept Oct Nov Dec | Jan Feb Mar Apr May |

**System Engineering**
- Preliminary Requirements
- System Design (HW/SW)

- SAIC Analysis of ALO Data
- TRW Reqm'ts & BIM/LEL Layouts

**Systems Integration (Denver)**
- HEL System (LMA Denver)
- Fabricate & Assemble

- Integrate & Test
- Control System Software (LMA)
- Disturbance Sys S/W (TRW/SAIC)
- Hardware Improvements / Characterizations

**System Integration (CTS)**
- Integration

- Acceptance Test
- Test Series 360 UDM (HL 440) Sim.
- Test Series 361 ALO Run Cond (HL 909) Sim.

- High Power Test (HL 450)
- W/Optimal Control System
- End of Contract (EOC)

ATP  CIDR  LL

R. Nefzger Mgr.
as of: 12/16

# Beam Profile Generator Conclusions

- Technically Sound Simulator Concept

- Will Simulate the High Power Laser at Low Power in a Representative Beam Control System to Quantify Design Parameters

- Will Determine the Limits of the Beam Control System by Providing Controlled Repeatable Inputs

3.1-2-37

# ALI Program Summary

- **ALI Beam Control System Operation Demonstrated**
- **UDM Test Ran Full Duration & Achieved Excellent Results**
  - Within 40% of ALI Jitter Goal
  - Within 20% of ALI Wavefront Error Goal
- **Evolved an Efficient Test Operations Approach**
- **BCT Demonstrating Hardware Improvements to Precision Beam Control**
- **Near Term Plans Established**
  - Characterize the Beam Control System
  - Explore Performance Envelope
  - Validate System Performance @ High Power

3.1-2-38

# Appendix 3.1-3
# SBLRD Technology Development

# SBLRD TECHNOLOGY DEVELOPMENT

# CHEMICAL LASER

- Navy Arpa Chemical Laser (NACL) (1975-Present)
  - < MW Class DF
  - Linear
  - Navy
  - Sea Level

- Mid Infrared Advanced Chemical Laser (MIRACL) (1980-Present)
  - MW Class DF
  - Linear
  - Navy
  - Sea Level

- Sigma - Tau (1984)
  - < MW Class
  - Cylindrical
  - Air Force
  - Airborne

- Alpha (1989 to Present)
  - MW Class HF
  - Cylindrical
  - DARPA/SDIO/BMDO/Air Force
  - Space Operation
  - 13 Lasing Tests Performed
  - DARPA/SDIO/BMDO/Air Force

- Tactical High Energy Laser (THEL) (In Fabrication)
  - < MW Class DF
  - Linear
  - Isreal (MOD)/Army
  - Ground
  - Operational System

- Hypersonic Low Temperature (HYLTE) (1992-Present)
  - Module Only (First Test 1998)
  - Advanced High Efficiency Chemical Laser Nozzle
  - Water Cooled, Then Regen Cooled
  - Overtone Laser (In Planning)
  - 3.1μ BMDO/Army/Air Force

# BEAM CONTROL

- Large Optics Demonstration Experiment (LODE) (1987)
    - Brass Board Experiment
    - HOE's On 60 cm Primary
    - 2.7 μm Laser
    - FSM/DM/PM Beam Control
    - Outgoing Wavefront Sensor Control
    - DARPA/AF

- Advanced Beam Control System (ABCS) (1984-Present)
    - Brassboard Experiment
    - Wide Field of View Telescop (3 Mirror)
    - Outgoing Wavefront Sensor Control (OWS)
    - 1.3 μm Laser
    - Rapid Retargeting
    - Automous Alignment
    - SDIO/BMDO/Navy/AF

- ALPHA LAMP Integration (ALI) (1990-Present)
    - Full Scale Integration Of ALPHA/LAMP/LODE Technology
    - 4M LAMP Mirror With HOES
    - Uncooled Beam Control Optics Breakthrough
    - Uncooled FSM and DM
    - 4 High Power (MW Class) Tests Conducted
    - Ongoing-Low Power Beam Control Experiments
    - BMDO/AF

- Advanced Phase Compensation Experiment (APEX) (1992-Present)
    - SBS Flowing Gas Experiment
    - Demonstration of CW HF Phase Conjugation
    - BMDO/Navy/AF

3.1-3-4

# PRIMARY MIRROR

- Local Optical Control System (LOCS) (1982)
  - 60 cm Mirror With Full Aperture Zone Plate Grating
  - AF

- LODE PM Mirror (1985)
  - 60 cm Thin Facesheet segmented Mirror With HOE's
  - DARPA/AF

- Large Advanced Mirror Program (LAMP) (1989)
  - 4m Thin Facesheet Segmented Active Mirror For SBL
  - DARPA SDIO/AF

- Large Optical Segment (LOS) (1992)
  - Thin Facesheet Segments (2) Of 11m Space Weight Mirrors
  - BMDO/AF

3.1-3- 5

# ATP

- Talon Gold (1985)
  - Boresight < 100 nrad
  - Disturbance Rejection & Isolation
  - DARPA/AF

- Alignment Reference Transfer System (ARTS) (1989)
  - Precision Separate Aperture Boresight Transfer
  - SDIO/AF

- Space Active Vibration Isolation (SAVI) (1990)
  - Space Active Vibration Isolation
  - 50 db Isolation
  - SDIO/AF

- Relay Mirror Experiment (RME) (1991)
  - Laser Beam Pointing & Stabilization With Space Relay Mirror
  - SDIO/AF

- Low Power Atmospheric Compensation Experiment (LACE) (1992)
  - Low Power Atmospheric Compensation
  - UV Background Mass
  - BMDO/Navy/AF

- Inertial Pseudo Reference Unit (IPSRU) (1994)
  - Inertial Reference Unit And Isolator (<40 nrad, 90db, 1Hz)
  - BMDO/AF

- Advance Acquisition Pointer Tracker (ADAPT) (1995)
  - ATP Concept Development
  - Design For Star LITE
  - BMDO/AF

- Fire Control Algorithm Development (1997)
  - Plume to Hardbody Hardware
  - Aimpoint Selection
  - BMDO/AF

# ATP (Cont'd)

- Illuminator Laser (1994)
  - Solid State Diode Pumped
  - 40 mj, 60 HZ
  - BMDO/AF
- Space Isolation Control Experiment (SPICE) (1995)
  - Pointing Disturbance Isolation
  - 4m Beam Expander
  - BMDO/AF

## ATP Integration Experiments

- Agile Control Experiment (ACE) (1986)
  - 4m Class Beam Expander In Space
  - Slew/Settling Experiments
  - SDIO/AF
- StarLab (1986)
  - Shuttle ATP Experiment
  - Measurements Of Targets/Background
  - SDIO/AF

- Altair (1987)
  - StarLab Free Flyer Due To Shuttle Disaster
  - SDIO/AF
- High Altitude Balloon Experiment (HABE) (1991-Present)
  - Integrated ATP Test Bed
  - High Resolution Target/Background Imaging
  - Balloon Borne Active Tracking Test
  - BMDO/AF

3.1-3-7

# SPACE EXPERIMENT DESIGN

- **SBL Concept Definition Studies (1980)**
  - Concept Definition Of SBL System
  - AF

- **System Level Validation Demonstration (SLVD) (1985)**
  - Boeing, Rockwell, Lockheed, Martin Marietta
  - SDIO/SMC

- **Independent Research & Development Announcement (IRDA) For Directed Energy Technology Demonstration (1986)**
  - Space Shuttle Compatible
  - Starlab (ATP In Space)/Lockheed
  - ACE (4m BEX In Space)/Martin Marietta
  - SDIO/SMC

- **Zenith Star Competition (1986)**
  - Initially Special Access Program (S.A.P.)
  - Fly ALPHA/LAMP/LODE
  - Competitors: Lockheed, Martin Marietta, Rockwell
  - SDIO

- **Zenith Star Award (1987)**
  - MM Prime (SEIT & SCE)
  - Lockheed-Optical Payload Element Sub
  - TRW-Laser Payload Element Sub
  - Conceptual Design June 1987
  - System Definition Dec 1988
  - Design, Fabrication, In-Orbit, Test - Planned Dec 1995
  - SDIO

3.1-3- 8

# SPACE EXPERIMENT DESIGN (Cont'd)

- Zenith Star - Redirection (1989)
  - ALI Ground Experiment
  - Design Of Complementary Space Experiment (CSE) Subscale (1.2 m) Zenith Star

- StarLITE Space Experiment Design (1994-1996)
  - Uncooled Optics Breakthrough On ALI
  - ALPHA Uncooled Resonator
  - LAMP/Beam Expander
  - LODE Beam Control
  - Single TIVB Launch
  - Conceptual Design Completed
  - BMDO

- SBLRD And EMD Studies (1996)
  - Evolved StarLITE Design
  - Definition Of Op System
  - BMDO

- Concept Definition Studies (1998)
  - Advanced Technology SBLRD
  - LMA & TRW Competitors
  - BMDO/AF

3.1-3-9

# SBL DEVELOPMENT PATH SUMMARY

| | 1975 | 1980 | 1985 | 1990 | 1995 | 2000 | 2005 | 2010 |
|---|---|---|---|---|---|---|---|---|

**LASER**

NACL — MIRACL — SIGMA TAU — ALPHA — THIEL

HYLTE → OVERTONE

**BEAM CONTROL**

LODE — ABCS → ALI

APEX

LOCS — LAMP → LOS

**LARGE OPTICS**

DEPLOYABLE OPTICS

**ATP**

TALON GOLD — STAR LAB / ALTAIR — HABE

RME — LACE — ADAPT

**SPACE EXP. DESIGN**

CDS — SLVD — ZENITH STAR → CDS

SBLRD

3.1-3-10

# CHEMICAL LASER



Timeline (1975–2010):

**SBLRD**

**Navy Argon Chemical Laser (NACL)** (1975-Present)
- MW Class DF
- Linear
- Navy
- Sea Level

**Sigma-Tau (1984)**
- MW Class
- Cylindrical
- Air Force
- Airborne

**Mid Infrared Advanced Chemical Laser (MIRACL) (1980-Present)**
- MW Class DF
- Linear
- Navy
- Sea Level

**Tactical High Energy Laser (THEL)** (In Fabrication)
- MW Class DF
- Linear
- Israel (MIND) Army
- Ground
- Operational System

**Hypersonic Low Temperature (HYLTE)** (1992-Present)
- Module Only (First Test 1998)
- Advanced High Efficiency Chemical Laser Nozzle
- Water Cooled Then Regen Cooled
- Overtone Laser (In Planning)
- BMIND Army Air Force

**Alpha (1989 to Present)**
- MW Class HF
- Cylindrical
- DARPA SDIO BMIDX Air Force
- Space Operation
- Lasing Tests Performed
- 3. DARPA SDIO BMIDX Air Force

# BEAM CONTROL

1975　1980　1985　1990　1995　2000　2005　2010

- Large Optics Demonstration Experiment
  (LODE) (1198")
  Beam Round Experiment
  18 x 4.0m 00 cm Primary
  2.7 μm Laser
  FSM/DM/PM Beam Control
  Outgoing Wavefront Sensor Control
  DARPA,AF

- Advanced Beam Control System
  (ABCS) (1984–Present)
  Broadboard Experiment
  Wide Field of View Telescope (1 Meter)
  Outgoing Wavefront Sensor Control (OWS)
  1.1 μm Laser
  Rapid Retargeting
  Autonous Alignment
  SDIO/BMDO/Navy,AF

- ALPHA LAMP Integration (ALI) (1990-Present)
  Full Scale Integration Of ALPHA/LAMP/LODE Technology
  4M LAMP Mirror With HOES
  Uncooled Beam Control Optics Breakthrough
  Uncooled FSM and DM
  4 High Power (MW Class) Tests Conducted
  Ongoing Low Power Beam Control Experiments
  BMDO,AF

- Advanced Phase Compensation Experiment (APEX)
  (1992-Present)
  SBS Flowing Gas Experiment
  Demonstration of CW HF Phase Conjugation
  BMDO Navy,AF

  3.1-3- 12

SBLRD

# PRIMARY MIRROR



1975   1980   1985   1990   1995   2000   2005   2010

- Local Optical Control System (LOCS) (1982)
  60 cm Mirror With Full Aperture Zone Plate Gating
  AF

- LODE PM Mirror (1985)
  60 cm Thin Facesheet Segmented Mirror With DM
  DARPA AF

- Large Advanced Mirror Program (LAMP) (1989)
  4m Thin Facesheet Segmented Active Mirror For SBL
  DARPA SDIO AF

- Large Optical Segment (LOS) (1992)
  Thin Faceshect Segment (2) Of 11m Space Weight
  Mirrors
  BMDO AF

SBLRD

Deployable Optics

3.1-3- 13

# ATP

1975    1980    1985    1990    1995    2000    2005    2010

SBLRD

- Talonted (1983)
  Beought Internal
  Disturbance Reaction & Isolation
  DARPA AF

- SeaLab (1986)
  Shuttle ATP Experiment
  Measurement Of Target Background
  SDIO AF

- Altair (1987)
  SeaLab Lost Due To Shuttle Disaster
  SDIO AF

- High Altitude Balloon Experiment (HABE) (1991-Present)
  Integrated ATP Test Bed
  High Resolution Target/Background Imaging
  Balloon Borne Active Tracking Test
  BMDO/AF

- Relay Mirror Experiment (RME) (1991)
  Laser Beam Pointing & Stabilization With
  Space Relay Mirror
  - SDIO/AF

- Advance Acquisition Pointer Tracker (ADAPT)
  (1994)
  ATP Concept Development
  Design For Star LITE
  - BMDO/AF

3.1-3-14

# SPACE EXPERIMENT DESIGN

1975    1980    1985    1990    1995    2000    2005    2010

**SBLRD**

- SRI Concept Definition Studies (1980)
  Concept Definition Of SRI System
  AF

- System Level Validation Demonstration (SLVD) (1985)
  Boeing Rockwell Lockheed Martin Marietta
  SDIO SMC

- Zenith Star Award (1990)
  MM Prime (SDIO & SCI)
  Lockheed Optical Payload Element Sub
  TRW Laser Payload Element Sub
  Conceptual Design June 1987
  System Definition Dec 1988
  Design Fabrication In Orbit Test - Planned Dec 1991
  SDIO

- Start HT Space Experiment Design (1994-1996)
  Uncooled Optics Breakthrough On ALI
  ALI PIIA Uncooled Resonator
  LAMP Beam Expander
  LODE Beam Control
  Single ITVB Launch
  Conceptual Design Completed
  BMDO

- SBLRD And LMD Studies (1996)
  Evolved Start HT Design
  Definition Of Op System
  BMDO

- Concept Definition Studies (1998)
  Advanced Technology SBLRD
  LMA & TRW Competitors
  BMDO AF

3.1-3- 15

# Appendix 3.1-4
# Zenith Star History

# History of Zenith Star

- **1985 SBL System Level Validation Demonstration (SLVD) Down Select**

  - SMC Executing Agent

  - Contractors

    - Boeing Did Not Submit BAFO
    - Rockwell          Won SLVD Phase I Contract
    - Lockheed         Won SLVD Phase I Contract
    - Martin Marietta   Won SLVD Phase I Contract

  - Contracts Not Negotiated or Definitized Due to Lack of Funding

- **1986 Several Space Experiment Studies Assessed**

  - Lower Cost

  - Martin Marietta    SBL SX (center segment of LAMP, 500K cylindrical laser (alt. Linear Laser)

  - Lockheed  ???

  - Rockwell  ???

3.1-4-2

# History of Zenith Star

- **1986 SDIO Issued Innovative Research and Development Announcement (IRDA) for Directed Energy (SBL?) Technology Demonstration**

  – Space Shuttle Mission (1987 and 1988)

  – SMC Executing Agent

  – Contractors

    - **Lockheed     Won StarLab Contract**

      – Demonstrate ATP in Space

    - **Martin Marietta  Won Agile Control Experiment (ACE) Contract**

      – Demonstrate 4 Meter Beam Expander in Space

- **1987 Challenger Disaster**

  – ACE Design Changed to ELV Configuration

  – StarLab Design Changed to ELV Configuration

3.1-4-3

# History of Zenith Star

- 1987 SDIO Initiated Competitive Classified Program in Parallel to ACE Contract to Integrated HEL and Demonstrate in Space

  - Unclassified Name Zenith Star

  - TRW Directed Subcontractor to Provide Alpha Laser

  - Competitors

    - **Lockheed**
    - **Martin Marietta**
    - **Rockwell**

  - SDIO Orchestrated "Shotgun" Wedding Martin Marietta / Lockheed

    - **Martin Marietta  Prime**

      - System Engineering / Integration & Test
      - Spacecraft Element

    - **Lockheed        Subcontractor**

      - Optical Payload Element

    - **TRW   Subcontractor**

      - Laser Payload Element

# History of Zenith Star

- **12/88    Zenith Star Phase IIIA Contract Awarded to Martin Marietta**

  - Three Phase Program

    - **Phase I - Conceptual Phase - Completed June 1987**
    - **Phase II / IIA - System Definition Phase - Completed Dec. 1988**
    - **Phase III - Design, Fabricate, Test and Demonstrate SBL on Orbit**

      - Phase IIIA - Design Phase - Planned Completion Jun 1991
      - Phase IIIB- Ground Validation / Integrated Test (GV/IT) Phase - Planned Completion - Apr 1994
      - Phase IIIC - Flight Experiment Phase - Planned Completion Dec 1995

  - Phase IIIA - $347M
  - Zenith Star System Requirements Review Completed - June1989

    - **Cooled Molybdenum Optics**
    - **Megawatt Class Alpha Derived Laser**
    - **LAMP Derived Beam Expander**
    - **Dual Titan IV Launch**

# History of Zenith Star

- **10/89    Zenith Star Program Redirected:**

  - Conduct Integrated Ground Experiment of Alpha, LAMP and LODE Technology

  - Design Complimentary Space Experiment (CSE)

    - **Significantly Lower Cost Experiment**

    - **Conclusion from Exhaustive Set of Low Cost Space Experiments Analyzed**

      - Experiment Cost Driven by Launch Vehicle

      - Megawatt Class Laser Demonstration Most Cost Effective, Meaningful Experiment

- **12/89    ZS / Alpha LAMP Integration (ALI) Program Initiated**

  - Design Phase - Completed Oct. 1990

    - **Established Experiment Design Baseline**

    - **Cooled Molybdenum Optics**

# History of Zenith Star

- **12/90      ALI Fabrication and Operations Phase Initiated**

  - Uncooled Optics Technological Breakthrough Demonstrated at High Power in 1992

  - Funding Driven Replans Conducted in FY 93, 94,95

  - Three Successful High Power Experiments Completed 1997

- **1992 - 1996  Major Technical Advancements Demonstrated**

  - Holographic Optical Elements Application on Large, Segmented Primary Mirror

  - Large PtSi Focal Plane Array

  - Uncooled Fast Steering Mirror

  - Uncooled Secondary Mirror

  - Uncooled Resonator Optics

  - High Density Actuator Deformable Mirror

3.1-4-7

# History of Zenith Star

- **??/93**    **StarLITE Space Experiment Designed**
  - Uncooled Optics
  - Alpha Derived Uncooled Resonator
  - LAMP Derived Beam Expander
  - LODE Derived Beam Control System
  - Single Titan IV Launch

- **??/96**    **SBL RD and EMD Special Study Initiated**
  - Evolved StarLITE Configuration
  - Define Operational System

- **??/98**    **SBL RD Incremental Design Review Terminated**
  - On Track for 2005 Launch
  - IRT Endorsed??

- **6/98 ALI Uncooled Deformable Mirror Successfully Tested**
  - Technical Goals Established in 1991 Demonstrated at Full Laser Power

3.1-4-8

# Appendix 3.1-5
# Technology Progress
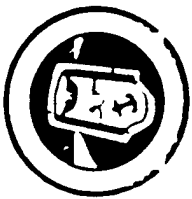
# Space Based Chemical Laser Beam Generator



Goals

Power: Megawatts @ 2.7 µm
Beam Quality: (corr)
Run Time: sec

Alpha Ground Tests
Mw @ 2.7 µm
Beam Quality (corr)

High Power Tests

Rear Cone Alignment Scan

Run Conditions Tests

Alpha Nominal Run Cond.

Alpha Ready for ALI

ALI Tests

Alpha Maintenance "Mode"

Re-establish Capability

Alpha Characterized
Uncooled Mirror

Alpha "First Light"

Alpha Hot Flow Test

Alpha Verification Module
- Hundreds Of Tests

ABL 50 kW Coil Demo

ABL Supersonic Coil

HYLTE Demo Subscale

Sigma-Tau Cylindrical
Laser Operates - Good Mode Control

HYLTE Nozzle Technology Development

High-power HYWND Tests
(MADS - 100 kW)

HYWND (ALpha) Technology Developed

MIRCAL Mid-IR Advanced Chem Laser Mw, Beam Qual

Overtone Complete

Advanced Nozzle Tests

HF Overtone

Fiscal Year

| 79 | 80 | 81 | 82 | 83 | 84 | 85 | 86 | 87 | 88 | 89 | 90 | 91 | 92 | 93 | 94 | 95 | 96 | 97 | 98 | 99 |
|----|----|----|----|----|----|----|----|----|----|----|----|----|----|----|----|----|----|----|----|----|

3.1-5-2

# Space Based Laser
# Beam Control



**Goals**

Retarget:
Wavefront Aberration: $\lambda/18$
Jitter:

LODE - Large Optics
Demo Expts
- $\lambda/15$, 100 nrad
- 150,000 Lines Comp Code

HOE Feasibility
- LAMP Center Segment

Optical Retarget Expts
(Dynamic)

Optical Retargeting
Expts (Static)

HOE Complete
on LAMP

BES

ALI
Expl

ALI
SBSCW
HF

ALI
UDM Test

ALI
ExpIIA ExpIIB

4m Beam Expander

Alignment
Experiments

Wide FOV Retargeting
Telescope Tests

Wide FOV Wave Front Sensor
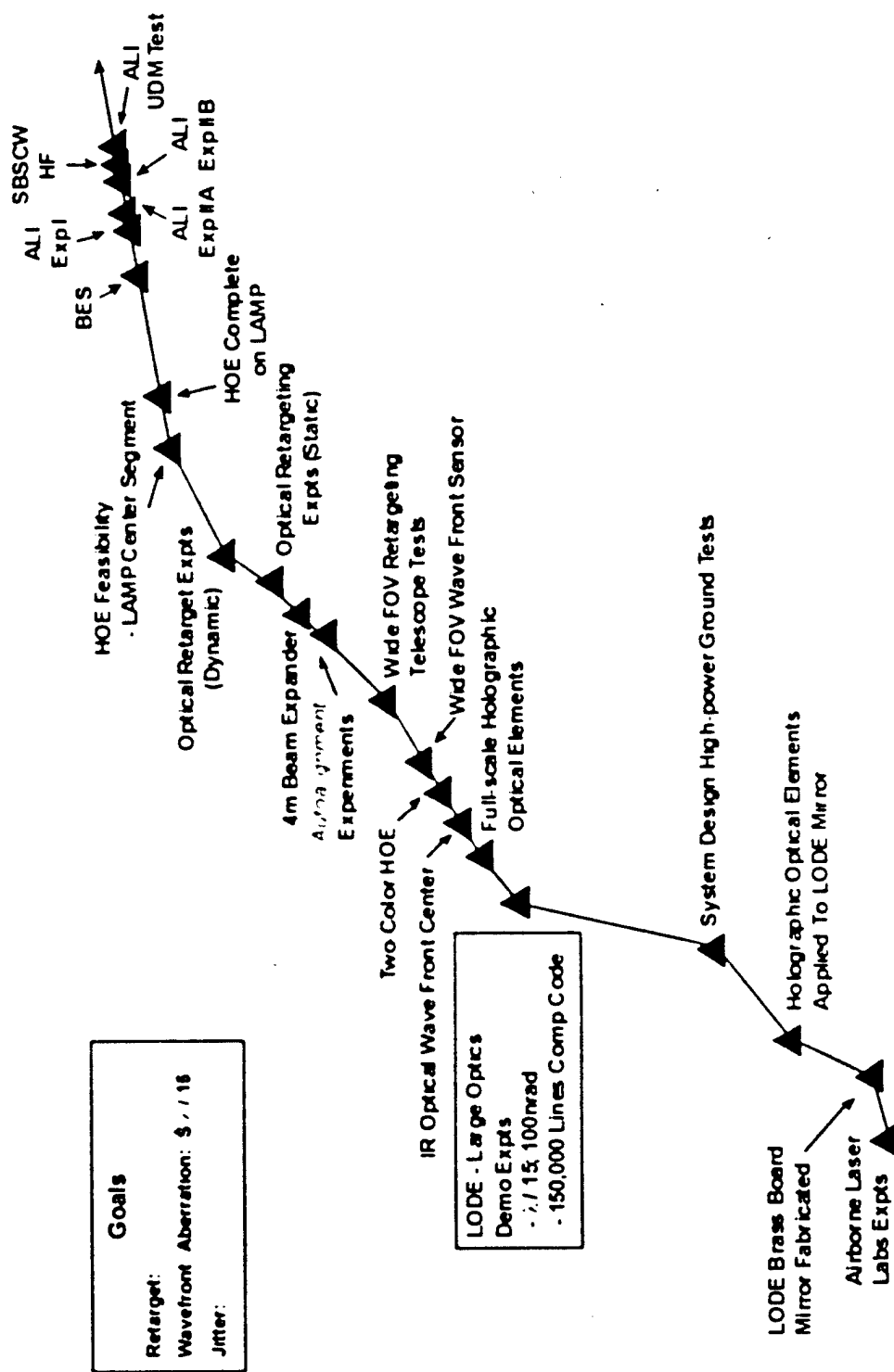
Two Color HOE

IR Optical Wave Front Center

Full-scale Holographic
Optical Elements

System Design High-power Ground Tests

Holographic Optical Elements
Applied To LODE Mirror

LODE Brass Board
Mirror Fabricated

Airborne Laser
Labs Expts

**Fiscal Year**

| 79 | 80 | 81 | 82 | 83 | 84 | 85 | 86 | 87 | 88 | 89 | 90 | 91 | 92 | 93 | 94 | 95 | 96 | 97 | 98 | 99 |
|----|----|----|----|----|----|----|----|----|----|----|----|----|----|----|----|----|----|----|----|----|

3.1-5-3
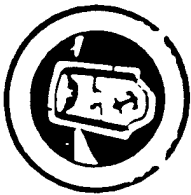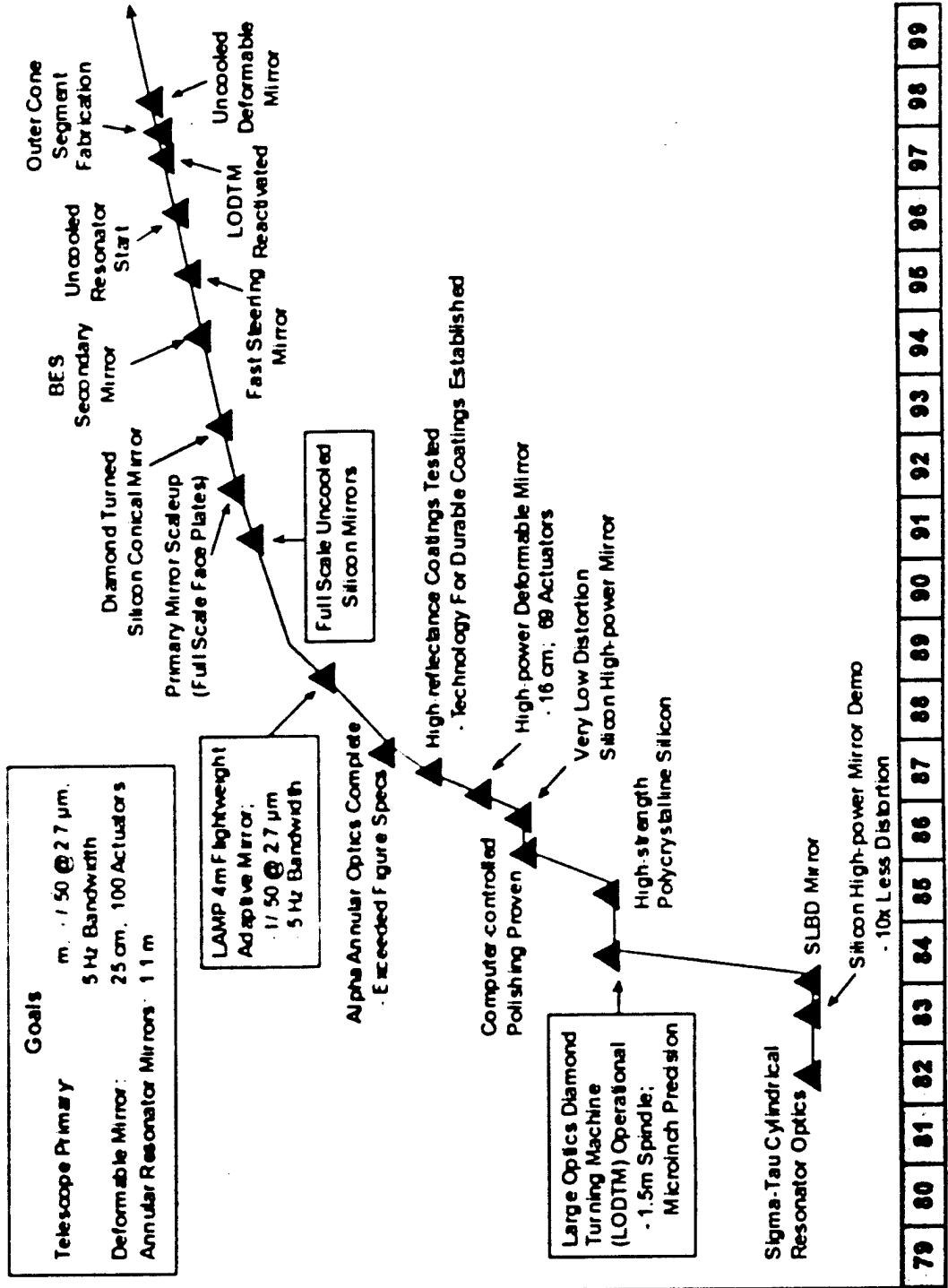
# Appendix 3.1-6

# SBL Industrial  Base Support

Summary of Critical Components for the SBL

by

Louis Morine, Lyn Skolnik, and David Loomis

Schafer Corporation

12 June 1998

# INTRODUCTION

This report responds to a request from IDA to SMC for data relating to key SBL components and the industrial base developed by DOD to fabricate and to manufacture those critical components. The items identified all involve critical hardware manufacturing capabilities that must be available in order to maintain a production base for the SBL. We discuss the critical items in terms of function, critical issues and available suppliers. Table 1 lists a rough estimate of the government investment in these components to date. The WBS shown in Figure 1 is only notional and is intended to show the relationship of space vehicle payload-elements. Figure 2 shows the location of the critical components in the space vehicle.

The uncooled optics comprise several critical individual components of the SBL. These components are listed separately in the WBS, the SBL diagram, and in the cost table. Much of the uncooled optics technology was developed under the LMA ALI contract with (TRW as a subcontractor) and was later transitioned to the TRW ALO contract, under the uncooled resonator effort.

## TABLE 1.

### INDUSTRIAL BASE CRITICAL COMPONENTS
### (ROUGH ESTIMATED GOVERNMENT INVESTMENT TO DATE)

| INDUSTRIAL COMPONENT | COST |
|---|---|
| IPSRU | 10.5M |
| ILLUMINATOR | 6.0M |
| FINE TRACK CAMERA | 0.5M |
| FAST STEERING MIRRORS | 2.5M |
| OWS FOCAL PLANES | 2.0M |
| HOLOGRAPHIC OPTICAL ELEMENTS (HOE's) | 12.0M |
| LARGE SPACE WEIGHT PRIMARY MIRROR | 30.0M |
| DEFORMABLE MIRROR (DM) | 1.5M |
| HIGH ENERGY HF LASERS/ADVANCED NOZZLES | 20.0M |
| UNCOOLED RESONATOR OPTICS | 20.0M |
| UNCOOLED SECONDARY MIRROR | 0.5M |
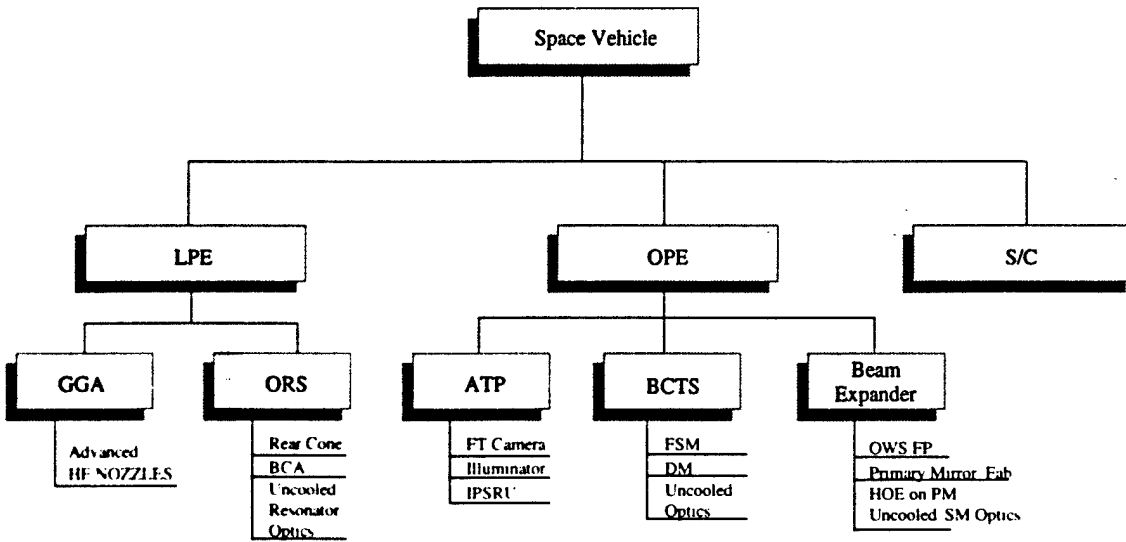
Figure 1. Critical Component WBS.
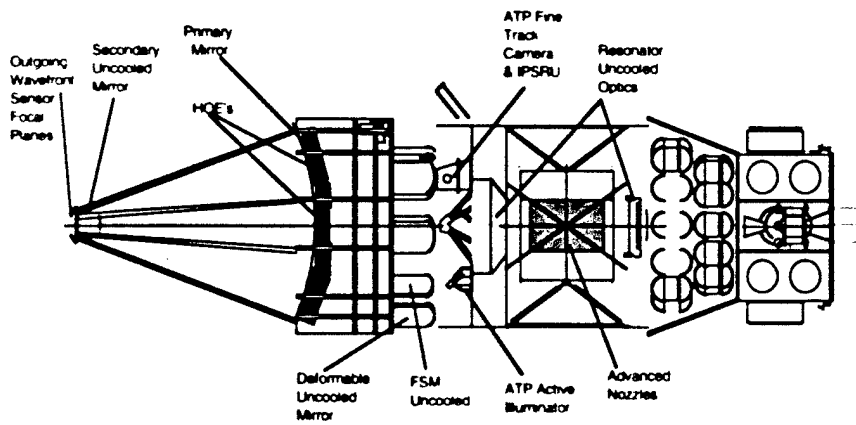


Note Uncooled Optics Include:
Secondary Mirror, Resonator Optics.
All High Power Flats, Deformable Mirror, FSM

Figure 2. Locations of the critical components.

## SBL INDUSTRIAL BASE DISCUSSION

## INERTIAL PSEUDOSTELLAR REFERENCE UNIT (IPSRU)

### DESCRIPTION

The IPSRU is an inertially stabilized platform that has very low friction gimbal suspension and very low jitter. The unit was designed, built, and tested by the Charles Stark Draper Laboratory (CSDL) for the Phillips Lab. The developmental unit is currently used by the HABE program and the same design has been baselined in the SBL concept. In both HABE and SBL, the stabilized element houses a low power alignment laser that is used to stabilize the fine tracker and the beam control system to an inertial reference.

The IPSRU unit uses the Kearfott two axis, dry-tuned gryo. This gyro is probably the quietist inertial reference on the market. This gyro is currently in production for numerous operational programs. In fact, the IPSRU gyro was taken from the gyro production line.

### CRITICAL ISSUES

- CSDL does not build production equipment so the SBL production units would be fabricated by other suppliers. The most obvious choice would be Kearfott and Teledyne since they make the same generic type of gyros.
  - CSDL could build another IPSRU for the SBLRD
  - Jitter performance is to be < 35 nr rms
  - Fine Tracker and beam control stabilization

### POTENTIAL SUPPLIERS

- Kearfott Corp.
- Teledyne
- Allied Signal
- Honeywell
- SSI
- Left Hand Design

## ILLUMINATOR LASER

### DESCRIPTION

The illuminator laser provides signal-to-noise- improvement of the target signature for precision pointing. The system incorporates range measurements, range gating and off-axis steering. Fibertech is currently supplying this type of illuminator for the HABE program. Development of illuminator for the SBL will require an increase in output power and reliability.

### CRITICAL ISSUES

- Output power and coherence length

- Beam quality
- Power efficiency
- Reliability
- Thermal management

POTENTIAL SUPPLIERS
- Fibertech
- HRL
- TRW
- Boeing (Rockwell)
- Rocketdyne


## FINE TRACK CAMERA

### DESCRIPTION
The fine track camera is the primary sensor for directing the HEL to the target. This tracker camera must take a handover from the intermediate IR camera and provide sufficient resolution and signal-to-noise ratio to meet the required pointing command to the beam control system.

### CRITICAL ISSUES
- Pixel field of view
- Pixel sensitivity
- Low Image distortion

### POTENTIAL SUPPLIERS
- ROSI
- Boeing (Rockwell)
- Lockheed Martin Imaging Systems
- Ball Aerospace
- TRW


## FAST STEERING MIRRORS ACTUATORS

### DESCRIPTION
Fast steering mirrors (FSMs) are used to control the line-of-sight and jitter in the beam control system. Typical diameters of the FSM for HEL and LEL control are 30cm.

CRITICAL ISSUES
- Jitter control
- Boresight alignment
- Bandwidth
- Field-of-regard
- VLA Coatings

POTENTIAL SUPPLIERS
- LLMS
- Ball Aerospace
- ROSI
- Left Hand Design
- TRW

## OUTGOING WAVEFRONT SENSOR (OWS) FOCAL PLANES

### DESCRIPTION
The OWS focal planes are designed to sense the jitter and wavefront error of the sampled HEL beam from the primary mirror HOE patches. Current focal planes are fabricated with platinum silicide high yield arrays. The outputs of these arrays are used to control both HEL beam tilt and wavefront control.

### CRITICAL ISSUES
- Read out rate
- Pixel to pixel uniformity
- Wide dynamic range
- Large area array
- High charge transfer efficiency

### POTENTIAL SUPPLIERS
- Lockheed Martin Imaging Systems
- EG&G

## HOLOGRAPHIC OPTICAL ELEMENTS (HOE's)

### DESCRIPTION
Holographic optical elements are produced by etching gratings into the coatings of the primary mirror. The diffracted laser beam from these HOE's are focused on to the OWS focal plane assembly mounted behind the secondary mirror. The sampled HEL beam can then be sensed to determine the jitter and wavefront error, which are corrected by the fast steering mirror and the deformable mirror.

CRITICAL ISSUES
- Accuracy of the HOE patch location on the primary mirror
- Orientation of each HOE patch
- Optical quality of the patches
- Efficiency and uniformity
- Registration

POTENTIAL SUPPLIERS
- ROSI


**LARGE SPACE WEIGHT OPTICS**

**DESCRIPTION**
The primary mirror is made of thin ULE or Zerodur face sheets and uses a monolithic or segmented configuration. The face sheets are attached to actuators to allow corrections after the system is placed in orbit, and for possible wavefront control.

CRITICAL ISSUES
- Fabrication and polishing
- Figure Correction
- Figure maintenance in presence of physical disturbances
- Phase ambiguities

POTENTIAL SUPPLIERS
- ROSI formerly (ITEK, HDOS and Perkin-Elmer)
- Eastman Kodak


**DEFORMABLE MIRROR (DM)**

**DESCRIPTION**
The deformable mirror is composed of a single thin face sheet of single crystal silicon. The face sheet is supported by densely spaced actuators to control the mirror face figure and to correct errors in the HEL wavefront.

CRITICAL ISSUES
- Actuator location on face sheet
- Bonding of actuators to face sheet and backing
- Actuator Coupling
- Surface polishing
- VLA coatings

POTENTIAL SUPPLIERS
- Xinetics
- ROSI


## HIGH ENERGY HF LASERS/ADVANCED NOZZLES

### DESCRIPTION
Combustion of reactants injected into the cavity generates the excited gain medium for the chemical laser. The efficiency of the injection process has a direct affect on the laser output power for a given weight system. An advanced nozzle-design (HYLTE) offers this high efficiency while allowing the nozzle to be regeneratively cooled.

### CRITICAL ISSUES
- Nozzle Efficiency
- Continuous power output
- Regenerative cooling

### POTENTIAL SUPPLIERS
- TRW
- Boeing (Rockwell)

## UNCOOLED HIGH POWER OPTICS

### DESCRIPTION
The fabrication of uncooled high power optics involves several suppliers to produce the completed optic. Uncooled optics are required throughout the high power beam train including resonator turning flats, fast steering mirror, deformable mirrors, resonator optics and secondary mirror. The optical fabrication steps for an uncooled resonator requires the following materials and processes.

- *Large Diameter Silicon Boules*: Large (10 to 20 inches diameter) silicon boules are the basic material used in the production of SBL high power optics.

- *Silicon Brazing*: The shape of the laser resonator optics is accomplished by the brazing individual silicon bricks to form the rough optics shape. This process must not produce voids at the braze joints.

- *Silicon Precision Machining*: The machining process must be very precise. After the brazing process is performed, precision machining provides surfaces accurate enough for diamond turning and final polishing of the optical structure.

- *Large Optics Diamond Turning Machine (LODTM)/Post Polishing*: The final shape and figure control for the laser resonator optics and beam expander secondary mirror are accomplished with the LODTM diamond turning machine at Lawrence

Livermore National Laboratory (LLNL).  The shape is complex and must be extremely accurate (microinches).

- *Low Absorption Coatings*: The multi-layer coatings are deposited on all of the high power optics to provide very high reflectivity, low absorption and low scatter at HEL and visible wavelength.

- *Silicon Carbide Integrating Structures*: The high power optics must be supported by a low coefficient of expansion material in order to minimize distortion of the optical surfaces. Thermal changes may arise from the HEL beam as well as the local thermal environment.

CRITICAL ISSUES
- Large Boules:
  - High purity
  - Single crystal fabrication
- Brazing:
  - Mounting inserts
  - No voids or discontinuities at braze joints
- Silicon Precision Machining
  - Preparation of the optical components for diamond turning
  - Secondary mirror center hole tolerances
- LODTM/Post Polishing
  - Optics figure control
  - Diamond tool wear
- Low Absorption Coatings
  - Multi-layer dielectric coatings for high reflectivity and low absorption
  - Deposition uniformity on large mirrors
- Silicon Carbide Integrating Structures
  - Matching integrating structure CTE with single crystal silicon optic
  - Providing a low stress mounting design

OTHER POSSIBLE SUPPLIERS
- Boules
  - Silicon Castings
- Brazing
  - Scarrott Metallurgical
- Silicon Precision Machining
  - McCarter Machining Company
- LODTM/Post Polishing
  - Lawrence Livermore National Laboratory
- Low Absorption Coatings
  - Laser Power Optics
  - Star Optics
  - Lohn Star Optics
- Silicon Carbide Integrating Structures
  - Xinetics

# Appendix 3.2-1
# Site Selection Screening Criteria

# Laser Test Facility (LTF) Site Selection
## Screening Criteria

Site selection for the Laser Test Facility (LTF) is a structured process that will provide the government with the data necessary to make an informed decision. Although the final siting decision will be based on environmental impact, economic factors, and Executive and Congressional guidance, the siting analysis provides a comprehensive assessment and quantitative ranking of viable sites. The Space-Based Laser Program Office initially provided technical and operational guidelines for the site selection. From these, exclusionary criteria were developed and applied to potential DoD, NASA, and DOE facilities. At the end of this phase, approximately 100 sites still remained under consideration. It was not considered feasible, within the schedule and funding constraints, to visit all sites that passed the exclusionary criteria - nor was it considered necessary. Site Screening Criteria were developed that allowed an evaluation of the sites based on information from available data bases. The highest scoring four sites were then visited to gather data for the final evaluation.

## 1.0 Program Guidelines

1.1     The SBL Readiness Demonstrator (SBLRD) and Engineering and Manufacturing Demonstrator (EMD) space vehicles will be integrated and tested at the same site.

Rationale: Preliminary estimates developed during the SBL Readiness Demonstrator Concept Definition Special Study indicate the cost of the LTF will range from approximately $165 to $185 M. This includes the laser performance test chamber, the space vehicle integration and test areas, and administrative and support buildings. The cost estimate includes the capability to test both the SBLRD and the EMD space vehicles. Cost estimates developed in 1991 for a facility to test an SBLRD-equivalent space vehicle ranged from $80 to $100 M. Thus, the total cost to build a facility to test an SBLRD, and then move the to a new site capable of transporting the EMD space vehicle to the launch site would range from $245 to $285 M. These cost estimates are highly preliminary in nature, but the cost delta between the two options would not be expected to change dramatically.

1.2     Both the SBLRD and EMD space vehicles will be launched from Cape Canaveral/Kennedy Space Center.

Rationale: The baseline launch vehicle for the Space-Based Laser Readiness Demonstrator (SBLRD) is the Titan IVB, while the Engineering and Manufacturing Development (EMD) Space Vehicle will be launched on a new heavy-lift launch vehicle - designated the Stellaris.

Only two sites in the United States are currently capable of launching the Titan IVB, Cape Kennedy and Vandenberg AFB. Upgrading other launch sites, such as Wallops Island, would be a multibillion dollar effort, and the launch sites would not be available in the time frame needed for the SBLRD launch date. The Stellaris will require

extensive launch pad modifications, but the infrastructure to support this launch capability also exists only at Kennedy and Vandenberg.

Due to ground overflight safety restrictions, space vehicles launched from Vandenberg are constrained to initial trajectories ranging from approximately due north (polar orbits) to approximately 63-degrees retrograde (south-southwest). Flights launched from Kennedy can be launched at 28-degees inclination (due east from Kennedy) to maximize on-orbit payload capability. There is an approximately 10% increase in on-orbit payload weight capability for flights launched from Kennedy when compared to Vandenberg - this is due to being able to take advantage of the earth's rotation to add to the velocity required to achieve on-orbit conditions.

The current weight estimate for the SBLRD is 40,037 lbs., of which 1,356 lbs. is laser reactants. A 10% reduction is weight capability that would be dictated by a launch from Vandenberg would require approximately 4,000 lbs. to be off-loaded. This would account for the entire laser reactant allocation. None of the experiments could be performed. An alternate approach would be to substantially decrease the power or primary mirror diameter of the SBLRD. However, the SBLRD would then be unable to perform its primary mission.

The current weight estimate for the EMD space vehicle is 70,000 lbs., of which approximately 12,000 lbs. is laser reactants. A 10% reduction is weight capability that would be dictated by a launch from Vandenberg would require approximately 7,000 lbs. to be off-loaded (approximately 60% of the reactant allocation). To perform the currently defined SBL mission, the on-orbit constellation would have to be increased from 20 to 48 space vehicles. This approach is cost-prohibitive.

Based on the above considerations, the only feasible launch site for the SBLRD or the EMD space vehicles is Cape Kennedy.

1.3     Both the SBLRD and EMD space vehicles will be transported to the launch site by barge.

Rationale:     Maximum launch vehicle performance; technical feasibility; cost

## 2.0     Site Screening Evaluative Criteria

Eight quantitative screening criteria were applied to the list of government sites remaining following the application of the exclusionary criteria. These criteria were selected based on criticality to site selection, construction, and operation; and to availability of information from readily accessed data bases. The criteria and their relative weightings are shown in Table 1.

## Table 1. LTF Site Screening Criteria

| Criteria | Weight (%) |
|---|---|
| 1. Similarity of installation mission | 23 |
| 2. Total population within 80 km | 19 |
| 3. Total installation size | 16 |
| 4. Distance to launch site | 15 |
| 5. Area cost factor | 9 |
| 6. Transportation route availability | 8 |
| 7. Seismic zone | 7 |
| 8. Distance to commercial airport | 3 |

## 2.1 Similarity of Installation Mission

In the 1992 Space Test Site Selection Report listed similarity of installation mission with the mission of the test facility as an exclusionary criteria. Mission similarity strongly implies an existing trained, or readily re-trainable, work force. Maximizing the mission compatibility will also help to minimize the possibility of conflicts between the LTF and other programs at the proposed installation. Support mechanisms and similarities in research/testing projects at the site could conceivably prove to be beneficial to the program through an exchange of technical insights and expertise.

Scoring System:

| 1. Existing/recent projects involving high-energy laser testing | 4 pts* |
|---|---|
| 2. Existing/recent projects involving rocket engine testing | 3 pts |
| 3. Projects/facilities supporting space vehicle integration and test | 2 pts |
| 4. Existing/recent projects involving general military research and development | 1 Pt |

NOTE: In this category, points are additive.

## 2.2 Total population within 80 km

Total population within 80 km - roughly one hour transit time - provides an indication of

available work force. The larger the population, the greater pool available for construction and operation of the LTF. Larger populations also infer the existence of a community infrastructure, an educational system, an general amenities associated with a higher quality of life. Although an indirect measure of these factors, total population is quantifiable.

Scoring System:

| | | |
|---|---|---|
| 1. | Population greater than 500,00 | 10 pts |
| 2. | Population between 250,000 and 500,000 | 7 pts |
| 3. | Population between 100,000 and 250,000 | 4 pts |
| 4. | Population less than 100,000 | 1 pt |

## 2.3  Total Installation Size

Although an exclusionary criteria of a minimum size of 1,300 acres was applied to the initial data base, it would be highly advantageous to site the LTF at a significantly larger location. This would imply a lower probability of conflict with existing facility operations and a higher probability of an existing base infrastructure. Also, the LTF could be sited at a more remote location within the installation, increasing overall operational safety. Finally, a larger site offers greater potential for growth, both for the SBL program and other new projects that could share LTF assets.

Scoring System:

| | | |
|---|---|---|
| 1. | Site Size greater than 20,000 acres | 10 pts |
| 2. | Site size between 15,000 and 20,000 acres | 8 pts |
| 3. | Site size between 10,000 and 15,000 acres | 6 pts |
| 4. | Site size between 5,000 and 10,000 acres | 4 pts |
| 5. | Site size between 2,000 and 5,000 acres | 2 pts |
| 6. | Site size between 1,300 and 2,000 acres | 1 pt |

## 2.4  Distance to Launch Site

Based on the size and weight of the SBLRD and EMD vehicles encapsulated within shipping containers, barge transport is required. The exception to this is if the LTF were co-located with the launch site (Cape Canaveral). Longer transportation

distances imply greater risk to the flight hardware and increased operational costs to the program. Transportation distances less than 25 km imply only ground transportation will be required. Distances ranging from 25 km to 100 km can be routinely traversed in a single day. The distance to Michoud, site of the NASA Shuttle External Tank fabrication, is also considered a bench-mark, as NASA routinely barge transports the external tank from this facility to the Kennedy Space Center.

### Scoring System:

| | |
|---|---|
| 1. Transport distance less than 25 km | 10 pts |
| 2. Transport distance between 25 and 100 km | 7 pts |
| 3. Transport distance between 100 km and 1000 km | 5 pts |
| 4. Transport distance greater than 1000 km | 3 pts |

## 2.5    Area Cost Factor

The area cost factor (ACF) is the index by which the Army Corps of Engineers relates the cost of typical construction projects in any particular area of the country to a standard cost.  The lower the ACF, the lower the cost.

### Scoring System

| | | |
|---|---|---|
| 1. | ACF less than 0.79 | 10 pts |
| 2. | 0.80 < ACF < 0.89 | 9 pts |
| 3. | 0.90 < ACF < 0.99 | 8 pts |
| 4. | 1.00 < ACF < 1.09 | 7 pts |
| 5. | 1.10 < ACF < 1.19 | 6 pts |
| 6. | 1.20 < ACF < 1.29 | 5 pts |
| 7. | 1.30 < ACF < 1.39 | 4 pts |
| 8. | 1.40 < ACF < 1.49 | 3 pts |
| 9. | ACF greater than 1.50 | 2 pts |

## 2.6    Transportation Route Availability

This measure accounts for the availability of the route required in transporting the SBL system by barge from its test and assembly facility to the launch complex at Kennedy Space Center.  Some transit routes may become closed due to inclement weather, flooding, freezing or man-made obstacles and circumstances.

### Scoring System

| | | |
|---|---|---|
| 1. | Along Coast | 10 pts* |
| 2. | Inland Rivers | -3 pts |
| 3. | Above 42 deg. North Latitude | -3 pts |
| 4. | Through Panama Canal | -8 pts |

## 2.7   Seismic Zone

Integration and test of the SBLRD and EMD space vehicles will require extensive alignment and calibration of complex and extremely sensitive optical components and subsystems.  These optical elements  are particularly sensitive to dynamic disturbances.  Also, construction of the LTF will include integration buildings with heights of greater than 75 meters, in which case construction costs could be significantly higher in active seismic zones.

## Scoring System

| | | |
|---|---|---|
| 1. | Zone 0 | 10 pts |
| 2. | Zone 1 | 8 pts |
| 3. | Zone 2a | 5 pts |
| 4. | Zone 2b | 4 pts |
| 5. | Zone 3 | 3 pts |
| 6. | Zone 4 | 0 pts |

## 2.8   Distance to Commercial Airport

Operations at the LTF will require the continuous support of commercial air services, both for personnel and materials.  Therefore the close proximity of a commercial airfield will enhance the effectiveness of any site.

## Scoring System

| | | |
|---|---|---|
| 1. | Less than 25 miles | 10 pts |
| 2. | 26 to 50 miles | 7 pts |
| 3. | 51 to 100 miles | 4 pts |
| 4. | Greater than 100 miles | 0 pts |

# Appendix 3.2-2

# Summary LTF Data Input for Environmental Assessment Analysis

| | | Description of Proposed Action and Alternatives | |
|---|---|---|---|
| **ID #** | **Phase** | **Data Need** | **Source** |
| D-1 | | Where are the manufacturing locations for GSE equipment ( such as the Chamber and PRS)? Are they COTS or similar? | |
| | SBLRD | The GSE manufacturer has not been selected, however since proximity to site will be an important criterion for selection. The equipment will not be commercial-off-the-shelf, however even though the GSE is custom built, it will employ standard commercial practice and design. It is not expected that this will equipment will constitute a special product or process. The manufacturing locations for the GSE will likely be in the Southeast US, as there are several qualified steel plate shops in Texas, Mississippi and Alabama that could support this requirement. | 1 |
| | EMD | Same | 1 |
| | Prod | Same | 1 |
| | | | |
| D-2 | | *Provide details on the reactant (NF₃, D2, H2,F2, He, hydrazine) holding areas (e.g., size of tanks, piping required, fire protection systems, safety distances).* | |
| | SBLRD | The reactants (Helium, fluorine, deuterium, NF₃, and hydrogen)will be stored in tank trailers parked in holding areas nearby the performance test chamber building. The parking area for the storage trailers will be approximately 8000 sq. ft. Separation of the trailers will consist of berms or walls adequate to ensure safety in the event of reactant leakage. These materials will be piped from their trailer tanks into the performance test chamber as required for testing. Manual transfers will be performed by trained personnel with appropriate personnel protection equipment (PPE). Non-essential personnel will be evacuated to a safe distance dependent upon the material be handled, typically 200-300 feet.<br><br>The size of the reactant storage tanks are estimated to be:<br><br>Helium          300 kg<br>Fluorine          50 kg<br>Deuterium          10 kg<br>NF₃          1000 kg<br>Hydrogen          200 kg<br><br>All valving for bringing reactants into the test chamber will be remote and transfer operations will be accomplished after personnel have been evacuated from the area. The area will be monitored by UV, smoke and leak detectors. Fire protection in the reactants storage area will consist of NFPA and DoD dictated fire mains and hydrants. No halon or other overhead systems will be employed in the storage areas.<br><br>Fluorine will be stored as a gas in the outdoor storage area in the same manner as the other reactants. At the time of laser testing, the gas will be pumped to equipment for its liquification and used in its liquid state in quantities required for the test.<br><br>The parking areas will be made of impervious material, e.g. concrete or blacktop pavement. | 5, 6, 2 |

| | EMD | The size of the reactant storage tanks are estimated to be:<br><br>Helium         900 kg<br>Fluorine       150 kg<br>Deuterium   30 kg<br>NF₃          3000 kg<br>Hydrogen   600 kg<br><br>Otherwise the information remains the same. | 5, 6, 2 |
|---|---|---|---|
| | Prod | Parking area will be increased to 15,000 sq. ft.<br><br>The size of the reactant storage tanks are estimated to be:<br><br>Helium         1800 kg<br>Fluorine       300 kg<br>Deuterium   60 kg<br>NF₃          6000 kg<br>Hydrogen   1200 kg<br><br>Otherwise the information remains the same. | 5, 6, 2 |
| | | | |
| D-3 | | *Provide the size of reactants holding area containment devices in case of a spill.* | |
| | SBLRD | The only reactant which is stored in liquid state is fluorine. Only a small amount (not more than 50 kg.) of liquid fluorine will made for each test. It will be contained in an appropriate storage vessel, and located in a pit capable of containing at least 110 percent of the maximum amount of stored material. In cases where the stored material is in a gaseous state, containment berms will not be required. | 5 |
| | EMD | Fluorine storage for 150 kg will be provided, other information remains the same. | 5 |
| | Prod | Fluorine storage for 300 kg will be provided, other information remains the same. | 5 |
| | | | |
| D-4 | | *How much water will be used during testing? How many test will be conducted annually?* | |
| | SBLRD | The primary use of water at the LTF will be for steam generation and the condenser and scrubbers in the pressure recover system (PRS). Most of the water will be recycled and reused. The PRS will be run for 120 to 200 seconds for each laser test. This results in water usage of about 45,000 to 75,000 gallons per test. There may be up to 8 tests per year for the 2 year period of SBLRD testing at the LTF, for a total of 16 tests. This gives a total of 360 kgal to 600 kgal annually. Assuming as little as 50 percent recycling of the water, 180 kgal to 300 kgal would have to be replenished on an annual basis.<br><br>The water would be stored in tanks near the performance test chamber. Water from the scrubbers and condensers would be captured and re-conditioned to typical industrial water composition levels for pH balance and contaminants. Residues will be retained in a sludge tank and disposed of in a manner consistent with HAZMAT disposal requirements. Relatively small amounts of sludge are expected to be accumulated (less than 100 kg) which may contain material which cannot be safely drained into the common sewage disposal system, (e.g. heavy metals, corrosives, etc.) but which nonetheless do not pose significant risk to the environment.<br><br>Peak flow rate for the site would be less than 5,000 gallons per day.<br><br>The domestic water consumption on the site would add an additional 8 kgal to 12 kgal per year. | 1, 4 |
| | EMD | Total water consumption would increase to not more than 1,000 to 1,800 kgal per year, with peak flows less than 15 kgal per day. | 1, 4 |
| | Prod | Total water consumption would increase to not more than 2,000 to 3,600 kgal per year, with peak flows less than 30 kgal per day. | 1, 4 |

| | | | |
|---|---|---|---|
| D-5 | | # When are construction activities scheduled to begin and end for each phase? | |
| | SBLRD | Begin construction 2Q FY01, complete construction 3Q FY03 | 7 |
| | EMD | The construction of LTF modifications and additional facilities is expected to begin one year after the initiation of the EMD phase and will continue for up to two and a half years. There is no certain date for the beginning of EMD, but for planning purposes it may be assumed to be 3Q FY11 | 7 |
| | Prod | The construction of LTF modifications and additional facilities is expected to begin one year after the initiation of the production phase and will continue for up to three years. There is no certain date for the beginning of production, but for planning purposes it may be assumed to be 1Q FY12 | 7 |
| | | | |
| D-6 | | *Please provide a general facility layout of the LTF complex including safety areas. What is the expected total acreage of the LTF complex?* | |
| | SBLRD | The total acreage for the SBLRD complex is 20 acres, including reactant storage and the remote operations building. | 3, 6 |
| | EMD | The acreage for the EMD phase will include the same 20 acres from SBLRD, plus 35 for additional buildings. Only a rough layout of the EMD facilities is available. | 3, 6 |
| | Prod | Acreage for production will increase by an additional 20 acres for an another performance test chamber building, making a total of 75 acres. | 3, 6 |
| | | | |
| D-7 | | *What are the total number of acres to be disturbed by construction (e.g., facilities, utility corridors, roadways, etc.) activities for each year of construction by each phase?* | |
| | SBLRD | The estimated disturbed area for construction in this phase is 2 to 3 times the area of the construction itself, i.e.: 40 to 60 acres. These estimates are both consistent with construction projects of similar scope and have undergone preliminary review in the context of the four candidate sites for the LTF. | 3 |
| | EMD | The estimated disturbed area for construction in this phase is 2 to 3 times the area of the additional construction itself, i.e.: 70 to 105 acres. These estimates are both consistent with construction projects of similar scope and have undergone preliminary review in the context of the four candidate sites for the LTF. | 3 |
| | Prod | The estimated disturbed area for construction in this phase is 2 to 3 times the area of the additional construction itself, i.e.: 40 to 60 acres. These estimates are both consistent with construction projects of similar scope and have undergone preliminary review in the context of the four candidate sites for the LTF. | 3 |
| | | | |
| D-8 | | *How many cubic yards of fill material will be required for each phase of construction?* | |
| | SBLRD | It was estimated that the fill material would not be more than one foot over the building site area. Thus the total fill would be some 35,000 cubic yards. This fill material may come in part from excavation material resulting from the digging of the foundations. The exact amount cannot be determined until a site-specific foundation and drainage design has been accomplished. | 3 |
| | EMD | EMD construction is estimated to require 60,000 cubic yards of fill material in addition to that used in the SBLRD phase. | 3 |
| | Prod | Production facilities construction is estimated to require 35,000 cubic yards of fill material in addition to that used for the SBLRD and EMD construction phases. | 3 |

| | | | |
|------|--------|------------------------------------------------------------------------------------------------------------|---|
| D-9 | | *How many cubic yards of earth will be moved during each phase of construction?* | |
| | SBLRD | (Assume this refers to the amount of "cut" on the site) The amount of earth to be moved will be about half of the "fill", or 18,000 cubic yards. | 3 |
| | EMD | (Assume this refers to the amount of "cut" on the site) The amount of earth to be moved will be about half of the "fill", or 30,000 cubic yards. | 3 |
| | Prod | An additional 18,000 cubic yards will be moved. | 3 |
| | | | |
| D-10 | | *Would a temporary concrete batch plant and truck washdown area be used during construction? If so, where would this area be located and would the washdown area have an impoundment to contain collected water?* | |
| | SBLRD | A temporary concrete batch plant would be erected within ¼ mile of the site for wash-down of concrete mixing, handling and transport equipment. Water from the plant would be captured and collected in an retainment or detainment pond (depending upon the requirements at the specific site). Waste water would be treated and disposed of in accordance with existing permit limitations. | 3 |
| | EMD | Same | 3 |
| | Prod | Same | 3 |
| | | | |

| D-11 | | Would topsoil be removed, stored, and re-spread after completion of construction activities? | |
|------|-------|------------------------------------------------------------------------------------------------|---|
| | SBLRD | The construction site areas where landscaping design dictated the use of top soil would be scalped to a depth of 8 in., with the resulting topsoil relocated, covered and re-spread. | 3 |
| | EMD | Same | 3 |
| | Prod | Same | 3 |
| | | | |
| D-12 | | Where would construction laydown, parking, and temporary mobile office areas be located? Size of area | |
| | SBLRD | The temporary construction, parking, laydown, and office areas are estimated to be less than 10 acres. This area would be located within a ¼ mile of the site. Considerable flexibility exists in the exact placement of these areas and whether they need to be contiguous. | 3 |
| | EMD | Same | 3 |
| | Prod | Same | 3 |
| | | | |
| D-13 | | How much solid waste (construction debris) will be generated during construction activities? What percentage and types of construction debris will be recycled? | |
| | SBLRD | Various types of solid waste and construction debris will be generated in the construction process. The greatest of this material estimated to be 100 – 150 tons per month during peak construction activity. The total waste is estimated 1,000 – 1,500 tons over the course of the construction. No re-cycling of this material is anticipated. | 3 |
| | EMD | In this phase the waste may reach a total of 1,500 to 2,200 tons, with a peak of 150 to 225 tons per month. | 3 |
| | Prod | Same as SBLRD | 3 |
| | | | |
| D-14 | | How much water is anticipated to be used during construction (e.g., site washdown, cement mixing, personnel requirements) by phase? | |
| | SBLRD | Construction water consumption for this phase is estimated at 110 – 150 kgal/month (for a total of 3300 – 4200 kgal), with the peak consumption occurring during the first 6 months, at 250 kgal per month. | 3 |
| | EMD | Total 5,800 to 7,400 kgal. Peak: 440 kgal per month for first 10 months. | 3 |
| | Prod | Same as SBLRD | 3 |
| | | | |
| D-15 | | Provide wastewater generation figures for construction activities. | |
| | SBLRD | Domestic waste water generation estimated at 60 to 120 kgal for project. | 3 |
| | EMD | Domestic waste water generation estimated at 90 to 180 kgal for project. | 3 |
| | Prod | Same as SBLRD | 3 |
| | | | |
| D-16 | | How will storm water runoff, collection, and treatment be handled? Are there any special requirements? | |

| | SBLRD | NPDS permit will be required. Anticipated that the existing permits will cover construction activities for LTF. Storm water will necessitate retention pond. Water treatment will be done according to applicable local regulations. Any demolition on site will require additional consideration to account for possibility of special treatment requirements for existing materials (e.g. asbestos, lead-based paint) | 3 |
|---|---|---|---|
| | EMD | Same | 3 |
| | Prod | Same | 3 |
| | | | |
| | | **Socioeconomics** | |
| | | | |
| S-1 | | *What is the estimated number of construction personnel required during each phase, and the expected time frame for construction activities? What is the phasing of construction personnel? What is the expected cost of construction?* | |
| | SBLRD | Construction personnel are estimated at 400 people on average over the course of the construction period. The peak number is estimated at 600 during the first 6 months of construction. <br><br> Construction Cost: <br> Year 1 Labor $28M Material $65M Total $93M <br> Year 2 Labor $14M Material $33M Total $47M <br> Total $42M $98 Total $140M | 7 |
| | EMD | Construction personnel are estimated at 1000 people on average over the course of the construction period. The peak number is estimated at 1500 during the first 6 months of construction. <br><br> Construction Cost: <br> Year 1 Labor $49M Material $114M Total $163M <br> Year 2 Labor $24M Material $58M Total $82M <br> Total $73M $172M Total $245M | 7 |
| | Prod | Same as SBLRD | 7 |
| | | | |
| S-2 | | *How many full-time operational personnel by pay grade (e.g., manager, engineer, technician, etc.) will be required to support LTF activities? When is full staffing expected to occur? What is the expected annual payroll and operating cost for the LTF program by phase?* | |
| | SBLRD | Total number of operation staff:<br><br> Category        Number      Total Annual Salary <br><br> Managers        8          1.6 M <br> Engineers       46        5.5 M <br> Technicians     71        5.0 M <br> Support         40        1.4 M <br><br> SUBTOTAL    160      $ 13.5 M <br><br> Other Ops Cost          $ 30 M <br><br> Total Cost             $ 41.5 M <br><br> Full staffing will occur in 1Q05 | 6 (with modifications based on more recent discussions with LMA and TRW planners) |

| | | | |
|---|---|---|---|
| | EMD | Total number of operation staff:<br><br>| Category | Number | Total Annual Salary |<br>| Managers | 15 | 3.0 M |<br>| Engineers | 88 | 10.5 M |<br>| Technicians | 135 | 9.5 M |<br>| Support | 67 | 2.5 M |<br>| SUBTOTAL | | 25.5 M |<br>| Other Ops Cost | | 50 M |<br>| Total Cost | | 75.5 M |<br><br>Full staffing will occur in 1Q12 | 6 (with modifications based on more recent discussions with LMA and TRW planners) |
| | Prod | Total number of operation staff:<br><br>| Category | Number | Total Annual Salary |<br>| Managers | 35 | 7.0 M |<br>| Engineers | 40 | 5.0 M |<br>| Technicians | 315 | 22.0 M |<br>| Support | 320 | 16.0 M |<br>| SUBTOTAL | | 50.0 M |<br>| Other Ops Cost | | 100.0 M |<br>| Total Cost | | 150 M |<br><br>Full staffing will occur in | 6 (with modifications based on more recent discussions with LMA and TRW planners) |
| | | | |
| | | **Transportation** | |
| | | | |
| T-1 | | *What are the estimated average daily vehicle and truck trips during construction and operations by phase?* | |
| | SBLRD | Construction: 800 vehicle trips/day (2 x 400 workers), 8 – 10 truck trips/day, peak: 50 truck trips/day<br><br>Operation: 240 vehicle trips/day, 1 truck trip/day | 3 |
| | EMD | Construction: 1400 vehicle trips/day (2 x 700 workers), 15 – 20 truck trips/day, peak: 80 truck trips/day<br><br>Operation: 420 vehicle trips/day, 2 truck trip/day | 3 |
| | Prod | Same as SBLRD | 3 |
| | | | |
| | | **Utilities** | |
| | | | |
| U-1 | | *Please provide the projected monthly utility (e.g., water, wastewater, solid waste, electricity, natural gas) consumption/generation numbers for LTF operations.* | |

| | SBLRD | Utility Consumption:<br><br>Water          100 – 150 kgal/mo.<br>Wastewater    72 kgal/mo.<br>Solid Waste    50 T / mo.<br>Electricity    250,000 kwh<br>Natural Gas    1000 Therms / mo. | 1, 4 |
|---|---|---|---|
| | EMD | Utility Consumption:<br><br>Water          180 – 270 kgal/mo.<br>Wastewater    125 kgal/mo.<br>Solid Waste    80 T / mo.<br>Electricity    450,000 kwh<br>Natural Gas    1800 Therms / mo. | 1, 4 |
| | Prod | Utility Consumption:<br><br>Water          360 - 540 kgal/mo.<br>Wastewater    250 kgal/mo.<br>Solid Waste    160 T / mo.<br>Electricity    250,000 kwh<br>Natural Gas    3600 Therms / mo. | 1, 4 |
| | | | |
| | | **Hazardous Materials and Hazardous Waste Management** | |
| | | | |
| HZ-1 | | *Provide the types and annual amounts of all hazardous materials to be used for each major process.* | |
| | SBLRD | The hazardous materials used in the laser tests are NF3, hydrogen, and deuterium. The usage of these materials is:<br><br>Material    Mass/Test    # Tests/Year    Total Usage<br><br>Deuterium    3 kg    8    32kg<br>NF₁    600 kg    8    4800 kg<br>Hydrogen    12 kg    8    96 kg | 5, 8 |
| | EMD | The hazardous materials used in the laser tests are NF3, hydrogen, and deuterium. The usage of these materials is:<br><br>Material    Mass/Test    # Tests/Year    Total Usage<br><br>Deuterium    9 kg    8    72kg<br>NF₁    1800 kg    8    14400 kg<br>Hydrogen    36 kg    8    288 kg | 5, 8 |
| | Prod | The hazardous materials used in the laser tests are NF3, hydrogen, and deuterium. The usage of these materials is:<br><br>Material    Mass/Test    # Tests/Year    Total Usage<br><br>Deuterium    9 kg    16    144kg<br>NF₁    1800 kg    16    9600 kg<br>Hydrogen    36 kg    16    576 kg | 5, 8 |

| | | | |
|---|---|---|---|
| HZ-2 | | *Can propylene glycol or other DOD approved substance replace ethylene glycol?* | |
| | SBLRD | Yes | 5 |
| | EMD | Yes | 5 |
| | Prod | Yes | 5 |
| | | | |
| HZ-3 | | *Are there any special handling procedures for any of the hazardous materials proposed for use?* | |
| | SBLRD | Special handling procedures will be developed for the LTF using the approved practices and procedures now in place at the HELSTF and CTS. These procedures are documented and managed by the contractors with site operation responsibility and will be transitioned from current practice to the specifics of the LTF as the details of the LTF design are finalized. No operations are planned for the LTF which do not have a direct counterpart in current operations at either the HELSTF and/or CTS | 2, 9 |
| | EMD | Special handling procedures will be developed for the LTF using the approved practices and procedures now in place at the HELSTF and CTS. These procedures are documented and managed by the contractors with site operation responsibility and will be transitioned from current practice to the specifics of the LTF as the details of the LTF design are finalized. No operations are planned for the LTF which do not have a direct counterpart in current operations at either the HELSTF and/or CTS | 2, 9 |
| | Prod | Special handling procedures will be developed for the LTF using the approved practices and procedures now in place at the HELSTF and CTS. These procedures are documented and managed by the contractors with site operation responsibility and will be transitioned from current practice to the specifics of the LTF as the details of the LTF design are finalized. No operations are planned for the LTF which do not have a direct counterpart in current operations at either the HELSTF and/or CTS | 2, 9 |
| | | | |
| HZ-4 | | *Will any ozone-depleting chemicals (ODCs) be utilized during testing or cleaning? If so, provide types and amounts?* | |
| | SBLRD | Not for building mechanical equipment, but ODC freon (Type CFC113) may be used for reactant purge since the compatibility of non-ODC refrigerants and fluorine has not been established and may be contentious. This freon usage is limited to >20 kg per test, 90 percent of which is captured in post-test procedures | 5 |
| | EMD | Not for building mechanical equipment, but ODC freon (Type CFC113) may be used for reactant purge since the compatibility of non-ODC refrigerants and fluorine has not been established and may be contentious. This freon usage is limited to >20 kg per test, 90 percent of which is captured in post-test procedures | 5 |
| | Prod | Not for building mechanical equipment, but ODC freon (Type CFC113) may be used for reactant purge since the compatibility of non-ODC refrigerants and fluorine has not been established and may be contentious. This freon usage is limited to >20 kg per test, 90 percent of which is captured in post-test procedures | 5 |
| | | | |
| HZ-5 | | *Provide the types and annual amounts of hazardous waste that will be generated by LTF activities.* | |

| | | | | |
|---|---|---|---|---|
| | SBLRD | The hazardous materials used in the laser tests are NF3, hydrogen, and deuterium. The usage of these materials is:<br><br>| Material | Mass/Test | # Tests/Year | Total Usage/year | Released/year |<br>| Deuterium | 3 kg | 8 | 32kg | 2 kg |<br>| NF$_3$ | 600 kg | 8 | 4800 kg | 240 |<br>| Hydrogen | 12 kg | 8 | 96 kg | 6 kg | | | 5, 8 |
| | EMD | The hazardous materials used in the laser tests are NF3, hydrogen, and deuterium. The usage of these materials is:<br><br>| Material | Mass/Test | # Tests/Year | Total Usage/year | Released/year |<br>| Deuterium | 9 kg | 8 | 72kg | 4 kg |<br>| NF$_3$ | 1800 kg | 8 | 14400 kg | 500 kg |<br>| Hydrogen | 36 kg | 8 | 288 kg | 12 kg | | | 5, 8 |
| | Prod | The hazardous materials used in the laser tests are NF3, hydrogen, and deuterium. The usage of these materials is:<br><br>| Material | Mass/Test | # Tests/Year | Total Usage/year | Released/year |<br>| Deuterium | 9 kg | 16 | 144kg | 8 kg |<br>| NF$_3$ | 1800 kg | 16 | 28800 kg | 1500 kg |<br>| Hydrogen | 36 kg | 16 | 576 kg | 24 kg | | | 5, 8 |
| | | | | |
| HZ-6 | | *Where will hazardous materials (e.g., reactant manufacturing location) be transported from (if from more than one location, please specify).* | | |
| | SBLRD | Kelly AFB, TX | | 5 |
| | EMD | Kelly AFB, TX | | 5 |
| | Prod | Kelly AFB, TX | | 5 |
| | | | | |

| HZ-7 | | *Please describe any pollution prevention plans proposed for LTF operations.* | |
|---|---|---|---|
| | SBLRD | Pollution prevention procedures will be developed for the LTF using the approved practices and procedures now in place at the HELSTF and CTS. These procedures have been reviewed and approved by federal, state and local environmental authorities and are documented and managed by the contractors with site operation responsibility. They will be adapted from current practice to the specifics of the LTF as the details of the LTF design are finalized. No operations are planned for the LTF which do not have a direct counterpart in current operations at either the HELSTF and/or CTS | 4, 5, 9 |
| | EMD | Pollution prevention procedures will be developed for the LTF using the approved practices and procedures now in place at the HELSTF and CTS. These procedures have been reviewed and approved by federal, state and local environmental authorities and are documented and managed by the contractors with site operation responsibility. They will be adapted from current practice to the specifics of the LTF as the details of the LTF design are finalized. No operations are planned for the LTF which do not have a direct counterpart in current operations at either the HELSTF and/or CTS | 4, 5, 9 |
| | Prod | Pollution prevention procedures will be developed for the LTF using the approved practices and procedures now in place at the HELSTF and CTS. These procedures have been reviewed and approved by federal, state and local environmental authorities and are documented and managed by the contractors with site operation responsibility. They will be adapted from current practice to the specifics of the LTF as the details of the LTF design are finalized. No operations are planned for the LTF which do not have a direct counterpart in current operations at either the HELSTF and/or CTS | 4, 5, 9 |
| | | | |
| | | **Health and Safety** | |
| | | | |
| HS-1 | | *Please provide a description of the safety procedures used for handling hazardous materials (e.g., reactants) and during hazardous operations (e.g., reactant transfer).* | |
| | SBLRD | See answer to HZ-7, above | 4, 5, 9 |
| | EMD | See answer to HZ-7, above | 4, 5, 9 |
| | Prod | See answer to HZ-7, above | 4, 5, 9 |
| | | | - |
| HS-2 | | *Please provide a description of any safety equipment required (e.g., fire suppression system, eye wash, flame detectors) and the locations of this equipment.* | |
| | SBLRD | Information is contained in the Black and Veatch 65% design documents | 3 |
| | EMD | Additional equipment consistent with the increased size and operational procedures of the EMD facility will be provided employing the same design practices as used in the SBLRD design. | 3 |
| | Prod | Additional equipment consistent with the increased size and operational procedures of the production facility will be provided employing the same design practices as used in the SBLRD design. | 3 |
| | | | |
| HS-3 | | *What is the explosive safety-quantity distance (ESQD) for inhabited buildings and uncontrolled public roadways for each facility that will require the storage or handling of explosive materials?* | |
| | SBLRD | TBD (This information to be provided by the Army Corps of Engineers) | |
| | EMD | TBD (This information to be provided by the Army Corps of Engineers) | |
| | Prod | TBD (This information to be provided by the Army Corps of Engineers) | |

|  |  | | |
|---|---|---|---|
|  |  | **Noise** | |
|  |  | | |
| N-1 |  | *What is the expected maximum noise level and duration for LTF testing?  How many test at this noise level will be conducted annually? (3 tests annually)* | |
|  | SBLRD | Current estimates are 120 db at the source.  Duration 100 – 200 seconds.  Up to 8 tests annually | 4 |
|  | EMD | Current estimates are 125 db at the source.  Duration 100 – 200 seconds.  Up to 8 tests annually | 4 |
|  | Prod | Current estimates are 125 db at the source.  Duration 100 – 200 seconds.  Up to 16 tests annually | 4 |
|  |  | | |
|  |  | **Air Quality** | |
|  |  | | |
| A-1 |  | *Please provide a list of construction equipment required and the amount of time the equipment is expected to operate annually by phase.* | |
|  | SBLRD | The following equipment is expected to operate 20 days per month for the 30 month construction period<br><br>Diesel:<br><br>2ea. 50T cranes<br>2  3 yard earth movers<br>2  D8 Caterpillars<br>4  1 yard back hoe loaders<br>1 water truck<br>1 concrete pump<br>3 2T flatbed trucks<br>2  2 yard back hoes<br><br>Gasoline<br><br>12 pickup trucks<br>Gensets<br>Air Compressors<br>Misc. small motor equipment (Compactors, drills, saws, trimmers, mowers, etc) | 3 |

| | | | |
|---|---|---|---|
| | EMD | The following equipment is expected to operate 20 days per month for the 42 month construction period<br><br>Diesel:<br><br>3ea. 50T cranes<br>4  3 yard earth movers<br>4  D8 Caterpillars<br>8  1 yard back hoe loaders<br>1 water truck<br>2 concrete pump<br>6 2T flatbed trucks<br>4  2 yard back hoes<br><br>Gasoline:<br><br>24 pickup trucks<br>Gensets<br>Air Compressors<br>Misc. small motor equipment (Compactors. drills, saws, trimmers, mowers, etc) | 3 |
| | Prod | The following equipment is expected to operate 20 days per month for the 36 month construction period<br><br>Diesel:<br><br>2ea. 50T cranes<br>2  3 yard earth movers<br>2  D8 Caterpillars<br>4  1 yard back hoe loaders<br>1 water truck<br>1 concrete pump<br>3 2T flatbed trucks<br>2  2 yard back hoes<br><br>Gasoline.<br><br>12 pickup trucks<br>Gensets<br>Air Compressors<br>Misc. small motor equipment (Compactors. drills. saws. trimmers. mowers, etc) | 3 |
| | | | |
| A-2 | | *Provide a list of diesel generators required and annual hours of operation expected for LTF activities.* | |
| | SBLRD | 3 diesel generators for back-up power, 750 kw each. Operation dominated by tests runs for reliability and maintenance estimated to be four 4 hour test per year. | 4, 5 |
| | EMD | 3 diesel generators for back-up power, 750 kw each. Operation dominated by tests runs for reliability and maintenance estimated to be four 4 hour test per year. | 4, 5 |
| | Prod | 6 diesel generators for back-up power, 750 kw each. Operation dominated by tests runs for reliability and maintenance estimated to be four 4 hour test per year. | 4, 5 |
| | | | |
| A-3 | | *Provide inventory of mobile vehicles dedicated for use by the program. Provide weight class, fuel type, and annual miles used.* | |

| | | | | | |
|---|---|---|---|---|---|
| | SBLRD | 1 diesel integrated vehicle transporter<br>1 2T diesel flatbed truck<br>4 gasoline-powered vans<br>6 gasoline-powered automobiles | 500 hp<br>300 hp<br>200 hp<br>150 hp | 100 hrs/year<br>500 hrs/year<br>500 hrs/year<br>500 hrs/year | |
| | EMD | SBLRD Vehicles, plus:<br><br>1 diesel integrated vehicle transporter<br>1 2T diesel flatbed truck<br>4 gasoline-powered vans<br>6 gasoline-powered automobiles | 500 hp<br>300 hp<br>200 hp<br>150 hp | 100 hrs/year<br>500 hrs/year<br>500 hrs/year<br>500 hrs/year | |
| | Prod | SBLRD, EMD vehicles plus:<br><br>1 diesel integrated vehicle transporter<br>1 2T diesel flatbed truck<br>4 gasoline-powered vans<br>6 gasoline-powered automobiles | 500 hp<br>300 hp<br>200 hp<br>150 hp | 100 hrs/year<br>500 hrs/year<br>500 hrs/year<br>500 hrs/yea | |
| | | | | | |
| A-4 | | *Describe any equipment using fuels (e.g., annual hours of usage, horsepower rating, load factors).* | | | |
| | SBLRD | TBD | | | |
| | EMD | TBD | | | |
| | Prod | TBD | | | |
| | | | | | |
| A-5 | | *Describe the potential air emissions and processing rates at any battery charging shop.* | | | |
| | SBLRD | Battery charging is not expected to be centralized, but rather accomplished at the location of the battery. Gas emissions allowed to escape into the air. | | | 4 |
| | EMD | Battery charging is not expected to be centralized, but rather accomplished at the location of the battery. Gas emissions allowed to escape into the air. | | | 4 |
| | Prod | Battery charging is not expected to be centralized, but rather accomplished at the location of the battery. Gas emissions allowed to escape into the air. | | | 4 |
| | | | | | |
| A-6 | | *Describe any other processing functions using volatiles and other air emission sources, such as coatings and solvents. Describe process, types and quantities of materials used, and any control devices to be used.* | | | |
| | SBLRD | Ethyl alcohol used for mirror cleaning<br>Aqueous phosphoric acid used in cleaning solutions<br>Nitric- and hydrochloric acids solutions used for passivation and pickling<br>Others TBD | | | 5 |
| | EMD | Ethyl alcohol used for mirror cleaning<br>Aqueous phosphoric acid used in cleaning solutions<br>Nitric- and hydrochloric acids solutions used for passivation and pickling<br>Others TBD | | | 5 |
| | Prod | Ethyl alcohol used for mirror cleaning<br>Aqueous phosphoric acid used in cleaning solutions<br>Nitric- and hydrochloric acids solutions used for passivation and pickling<br>Others TBD | | | 5 |
| | | | | | |

| A-7 | | Describe actual chain of events regarding a nominal test event. Specifically include how PRS is integrated into the operation. Does is begin before the laser-generation reaction is initiated? If so, how long does the PRS purge last? | |
|---|---|---|---|
| | SBLRD | The steam generators are started at the beginning of the test sequence and are exhausted through the PRS approximately 100 seconds before laser operation begins. Operation of both the high and low power lasers commences at nearly the same time and continues for the duration of the test cycle, nominally sixty seconds. The PRS continues to operate after laser shut-down for an additional 40 seconds. | 5 |
| | EMD | The steam generators are started at the beginning of the test sequence and are exhausted through the PRS approximately 100 seconds before laser operation begins. Operation of both the high and low power lasers commences at nearly the same time and continues for the duration of the test cycle, nominally sixty seconds. The PRS continues to operate after laser shut-down for an additional 40 seconds. | 5 |
| | Prod | The steam generators are started at the beginning of the test sequence and are exhausted through the PRS approximately 100 seconds before laser operation begins. Operation of both the high and low power lasers commences at nearly the same time and continues for the duration of the test cycle, nominally sixty seconds. The PRS continues to operate after laser shut-down for an additional 40 seconds. | 5 |
| | | | |
| A-8 | | Description of Low Energy laser operation (i.e. 10 minutes). Are emissions scrubbed? Does the PRS operate during all ten minutes? If not, quantify emissions and emission rates. | |
| | SBLRD | See A-7 above | 5 |
| | EMD | See A-7 above | 5 |
| | Prod | See A-7 above | 5 |
| | | | |
| A-9 | | Is Nitrogen Trifluoride both the fuel and the oxidizer? | |
| | SBLRD | NF₃ is an oxidizer | 5 |
| | EMD | NF₃ is an oxidizer | 5 |
| | Prod | NF₃ is an oxidizer | 5 |
| | | | |

| A-10 | | Confirm the reactant storage levels and flow rates, and pollutant emission rates developed or derived by EDAW, Inc. | |
|------|--------|-----------------------------------------------------------------------------------------------------------------------|-----|
| | SBLRD | Reactant storage levels and flow rates are estimated based on the best available information from plans, current designs and test experience. They should be considered an upper limit on the levels and rates for the LTF, and not treated as a specific point design solution. The scope of this report does not warrant the detailed calculations to improve the precision of the values presented. | 5 |
| | EMD | Reactant storage levels and flow rates are estimated based on the best available information from plans, current designs and test experience. They should be considered an upper limit on the levels and rates for the LTF, and not treated as a specific point design solution. The scope of this report does not warrant the detailed calculations to improve the precision of the values presented. | 5 |
| | Prod | Reactant storage levels and flow rates are estimated based on the best available information from plans, current designs and test experience. They should be considered an upper limit on the levels and rates for the LTF, and not treated as a specific point design solution. The scope of this report does not warrant the detailed calculations to improve the precision of the values presented. | 5 |
| | | | |
| A-11 | | Describe projected paint shop or abrasive blasting shop activity levels and emissions controls | |
| | SBLRD | No paint shop nor abrasive blasting activity is anticipated at the LTF | 6 |
| | EMD | No paint shop nor abrasive blasting activity is anticipated at the LTF | 6 |
| | Prod | No paint shop nor abrasive blasting activity is anticipated at the LTF | 6 |
| | | | |
| A-12 | | Quantify maximum amounts of reactants that would be discharged into the atmosphere at the end of a test. | |
| | SBLRD | See HZ-5 above | 5, 8 |
| | EMD | See HZ-5 above | 5, 8 |
| | Prod | See HZ-5 above | 5, 8 |
| | | | |
| A-13 | | Describe method of discharging residual reactants. | |
| | SBLRD | Residual reactants are purged with helium. The resulting combination is vented to the atmosphere. Less than 1 kg of fluorine is present in the purge product. | 5 |
| | EMD | Residual reactants are purged with helium. The resulting combination is vented to the atmosphere. Less than 1 kg of fluorine is present in the purge product. | 5 |
| | Prod | Residual reactants are purged with helium. The resulting combination is vented to the atmosphere. Less than 1 kg of fluorine is present in the purge product. | 5 |

Sources

1.      Informal Memorandum from Ed Slattery, FSEC, June 29,1998

2.      LMA Space Based Laser Program Environmental/Safety Responses Memo,
        Lockheed Martin Astronautics, August 26, 1997

3.      Notes from meeting and discussion with Black and Veatch technical staff, July 8,
        1998

4.      Meeting Notes from meeting with Rick Asher, TRW Capistrano Test Site July 7,
        1998

5.      Discussions with Lyn Skolnik, Dave Loomis and Larry Zajac, July 28, 1998

6.      STF Facilities Requirement Document, Lockheed Martin Astronautics, Jan 17,
        1997

7.      Discussions with Air Force SMC planning staff, August 1998

8.      Engineering Memo: Exhaust Conditions for STF, Special Study 1, July 1991,
        Martin Marietta Astronautics

9.      Meeting Notes from HELSTF Site Visit and Survey, June 1998

# Appendix 3.2.3
# Cost Analysis Support

The principal activity in support of cost analysis was the development and application of a top-level cost model of SBL systems. This model was used to investigate the architectural implications of large aperture, low jitter beam expander design solutions. Such designs have been put forward as beneficial in increasing laser brightness and thus improving overall architecture performance. While this result is certainly a desirable consequence, there was a concern that the benefit might come only at the expense of a significantly higher overall system cost. This analysis was undertaken to quantify both the performance and cost of a variety of large aperture SBL systems.

In addition to the analysis described above, numerous quick reaction efforts were accomplished in support of program office requirements. These efforts comprised such topics as budget reviews, identification of funding limit effects, and other rapid turnaround tasks. These efforts have been previously documented in monthly activity reports. This section will therefore focus on the cost and performance modeling work.

**Objectives and Approach**

The objective of this analysis was the development and application of a parametric cost model of an SBL system architecture to be used in identifying cost trends and preferred system designs.

The approach taken for this effort was to begin with the establishment of architecture performance levels, identify a set of SBL designs which met performance thresholds and then find the lowest cost system from among the suitable designs. In this way the lowest cost architecture for a given level of performance was found. By starting with the assessment of performance, the analysis assured that all systems under consideration met minimum levels of capability as measured by their kill effectiveness against defined threats. Thus the results of the cost analysis are presented in terms of cost as a function of design parameters for given levels of effectiveness. This enables the identification of the most affordable system designs. It also allows an assessment of preferred design trends.

A further objective of the work was to serve as a demonstration of the utility of parametric cost analysis in the search for an affordable SBL architecture. It is expected that the analysis will be extended and expanded to refine the results and to mprove the fidelity and validity of the estimating methods employed.

The cost estimating process began with the establishment of a cost baseline obtained from previous estimates of systems of the same general design as those under consideration. Since such systems have been the object of considerable cost reseaarch, their use as a starting point takes advantage of a significant amount of existing cost estimating experience and data. Cost excursions from this baseline were made based on previous experience with design trends and engineering judgements about the expected cost impact of design choices. Thus the estimate started with a known baseline cost and followed parametric excursions in design parameters such as: aperture diameter, jitter, wave front error and power. Also varied in the analysis was the level of performance (percent threat objects killed) and target hardness, expressed as the lethality of the SBL against the threat missile.

**Cost Estimating Baseline**

To come to meaningful conclusion about the affordability of a given SBL system, it is necessary to consider all the costs associated with its development, production, deployment and operation. In short, the estimate must be of the entire system life cycle. The life cycle cost (LCC) estimate

began with the research and development phase of the program. The demonstration and validation (Dem/Val) costs for the baseline were based on a large body of analysis of the SBL Readiness Demonstrator program. These cost had been estimated by BMDO and had been through a thorough review for accuracy and completeness. However, these costs did not include all the functions and activities associated with a Dem/Val program, so the added costs were estimated to form the basis for a total Dem/Val phase.

The next phase in the life cycle is Engineering and Manufacturing Development (EMD). The cost of this phase was estimated based on the theoretical first unit cost (T1), which will be discussed in detail subsequently, and estimating factors from the Dem/Val estimate. The estimating factors were derived from previous BMDO experience of similar programs and have widely applied for estimates of this type.

The production cost of the system is also based primarily on the T1 cost. In this phase, T1 is defined to be the cost of the first production model of the operational system. It is used as a peg-point for the sum of all production units, taking account of the "learning" effect of multiple quantity production runs. T1 cost is the principal means by which the design parameters are reflected in the overall LCC. The breakdown of T1 costs into subsystem constituents comprises the heart of the design-related analysis. It will be discussed later.

The non-recurring production costs were estimated from previous BMDO analyses of an operational SBL system and reported in the 1997 time frame as part of a DoD mandated Cost and Operational Effectiveness Analysis (COEA). No additional effort to refine or update this estimate was mead in the current task.

Recurring costs, those incurred in the actual production of the operational units, were estimated using standard cost-quantity learning rate methods. In this case a simple 90 percent learning rate was assumed for the production run. This rate is typical of complex missile program experience, however its application to SBL systems deserves further study. The learning rate refers to the amount of average unit cost reduction which occurs with each doubling of the total quantity produced. Thus a 90 percent learning rate means that if the average cost of producing 10 units is $100, then the average cost of producing 20 units will be $90.

Also included in the production cost for the system is the cost of launching the constellation of platforms. In the analysis, it was assumed that the Evolved Expendable Launch Vehicle (EELV) system will be used for launching the platforms. No independent analysis was conducted to estimate these costs. Rather, the estimate provided by the EELV program office was taken at face value and applied.

Operating and Support (O&S) costs for the system consisted in small part of the ground support system and its operation, which were estimated using the Air Force Unmanned Spacecraft Cost Model (USCM). The preponderance f the O&S costs were those associated with on-orbit replenishment and platform replacement at the end of their operational life. Both estimates were developed in the same manner as the production cost estimates discussed previously.

This then comprises the means by which the baseline cost was estimated. It is based on a known design and established cost estimating methods. It s from this baseline that other variations in design and cost will be made. The attributes of the baseline system are shown in Table 3.2.3-1.

Table 3.2.3-1

Nominal SBL System Attributes

| Number of platform | 35 |
|---|---|
| Number of rings | 5 |
| Learning Rate | 0.9 |
| Power | (Classified) |
| Aperture diameter | 8 M |
| Jitter | (Classified) |
| Strehl ratio | 0.18 |
| Lasing Time | 300 Sec. |

The breakdown of the baseline cost is shown in Table 3.2.3-1.

Table 3.2.3-2

SBL Life Cycle Cost Breakdown

(FY97$M)

| SBL Readiness Demonstrator | 1,709 |
|---|---|
| Dem/Val Add-ons | 424 |
| Total Dem/Val | 2,133 |
| Total EMD | 5,377 |
| T1 | 383 |
| Production (Contractor) | 11,206 |
| Production (Govt & Other) | 3,362 |
| Total Acquisition | 22,078 |
| Launch | 10,861 |
| Ground Segment | 83 |
| Total Cost to FOC | 33,022 |
| Operations | 750 |
| On-Orbit Sustainment | 2,882 |
| Platform Replacements | 20,975 |
| Total O&S | 23,975 |
| Total LCC | 56,997 |

It is important to note the role and influence that the T1 cost plays in the overall development of the LCC cost. It is the means by which the design of the system becomes reflected in the EMD, the production and the O&S cost. In this analysis, the T1 estimate was made in detail only for the baseline system. In order to assess cost trends, it was necessary to develop a means to vary the T1 with key design parameters. This was done by starting with a breakdown of the baseline T1 and then estimating the cost variation in its constituent parts for design changes in the related subsystem. Is These variations in cost will be estimated based on the weight of the subsystem involved. Thus the baseline weight as well as cost is necessary to make this connection. The first step in the process is illustrated in Table 3.2.3-3, a breakdown of the baseline system T1 cost and weight. It is from these values that the scaling for power, aperture, jitter (and related wave front error) are made. Note the asterisk in the last column. This denotes those system elements that are assumed to scale with variations in system jitter.

The scaling in cost and weight was derived from an assessment of the effect of variation in independent parameters and the result such variations would have either on weight or cost. For example, the aperture of the beam expander directly controls the size of the primary mirror (the costliest element in the beam expander). The assumption made was that the size of the primary scaled as the 2.5 power of the diameter. The reasoning was that scaling only by the area (diameter to the $2^{nd}$ power) did not account for the need to increase the thickness of the primary as the diameter increased. Although it has been observed that the thickness does not need to increase directly with diameter (which would be diameter to the $3^{rd}$ power). Thus the compromise position was taken half way between the two. This is one of several areas that should be re-examined using more rigorous study and additional related design data. It was further assumed that the cost of the beam expander scaled directly with the size as reflected by the weight.

Jitter scaling was handled in a slightly different manner. There is no compelling reason to believe that a system with better jitter performance wold weigh more than one of lesser performance. However there is a great body of empirical and anecdotal evidence to suggest that improved jitter does come at a cost penalty. Just what that penalty will be should become the subject of a detailed cost and technology study effort. However, to accomplish the immediate goals of this study, it was assumed that deviations from a nominal level of jitter performance followed a quadratic variation in cost. In other words, if jitter performance increased by a factor of two, cost was assumed to increase by two-squared, or four. This assumption is not entirely arbitrary. There are several pint designs for high energy laser systems with jitter performance which has varied by factors of two and four or so. It is the informed opinion of engineers who have worked on these systems that something like exponential variations fairly reflect the difficulties encountered and overcome in the building of these systems. But again, considerably more study is warranted in this area before definitive results can be asserted.

Power scaling affecting the laser payload was based on numerous cost studies done on SBL design of this class. The conclusion has been that variations in output power are accomplished by corresponding increases in the length of the laser gain generator cavity. This translates directly to additional rings in the combustion stack and therefore, additional cost. But since the rings are, to a first order, all the same, the cost varies linearly with added rings and thus with added power.

In summary, we find a system cost variation that behaves as follows:

Power subsystem element cost varies linearly with laser power.

Beam expander subsystem element cost varies to the 2.5 power with aperture diameter.

Jitter-related subsystem element cost varies as the square of changes in jitter performance.

Using these cost relationships, the analysis was continued based on the results of performance calculations over a range of system design parameters. The results of this work begin to give insight into the nature of the design trades and their effect on the affordability of various SBL conceptual architectures.

| System Component | Weight (Kg) | Cost (FY97$M) | Jitter Related* |
|---|---|---|---|
| Space Vehicle Int & Assy | | 16 | * |
| Spacecraft | 11,930 | 183 | |
| Structure | 6,550 | 45 | |
| GN&C | 700 | 29 | |
| Thermal | 220 | 6 | |
| Power | 2,000 | 25 | |
| TT&C | 310 | 13 | |
| ACS | 1,950 | 13 | |
| Comm/DSP | 200 | 51 | |
| RSFS | 7,680 | 41 | |
| Tankage | 3,810 | | |
| Reactants | 3,870 | | |
| Laser Payload Element | 16,550 | 57 | |
| Gain Generator Assy | 11,610 | 48 | |
| Energy Magmnt Assy | 680 | 2 | |
| Optical Resonator Assy | 4,260 | 8 | * |
| Optical Payload Element | 20,390 | 85 | |
| Beam Expander | 13,220 | 42 | * |
| Beam Control System | 6,610 | 11 | * |
| Acq., Pointing & Tracking | 560 | 32 | * |
| Total | 56,550 | 383 | |

**Cost Sensitivities and Trends**

The first trades investigated in this task were those associated with power and jitter for constant performance. Recent conjecture within the high energy laser community has led some to the conclusion that the optimal means of increasing laser brightness is through the mechanism of large optical apertures. To test this hypothesis, a range of values for the power and diameter were studied. In all cases the resulting brightness and corresponding system performance was held constant by adjusting the size of the constellation required to achieve a given kill capability. The trade thus becomes one of finding whether a large number of platforms with less brightness

(a measure of individual platform performance) are more or less costly than a constellation with a smaller number of more capable platforms. The figure below illustrates the result.
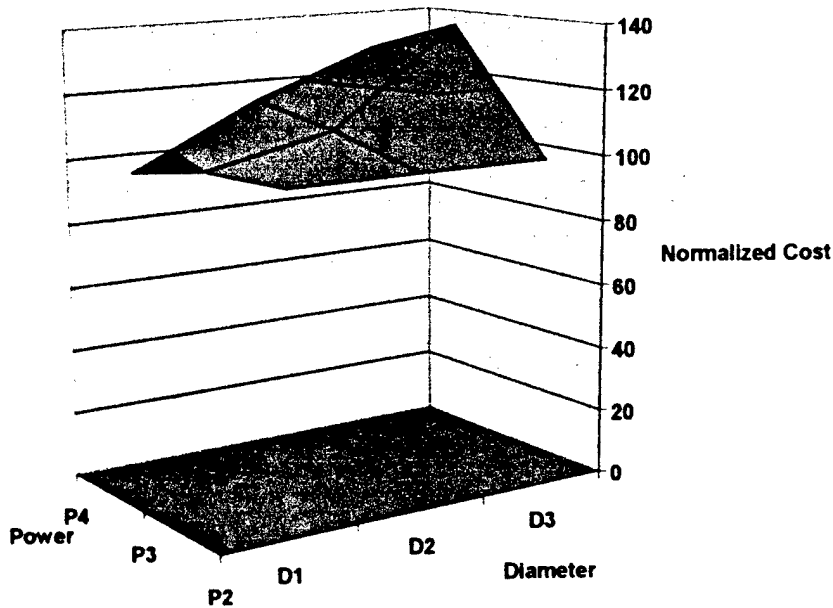


**Figure 3.2.3-1**

**LCC Variations with Power and Diameter**

This figure shows that at relatively low power levels (P2 is the low end of the range), there is almost no variation in cost with diameter. However, as the power goes up, so does the effect of diameter on the system cost. In fact, for large diameter systems, there can be as much as a 40 percent increase in cost for constant effectiveness. Clearly, it is not the case that larger diameters are always better.

The foregoing results were derived for a single value of system jitter. If instead we take a system with a constant power level and examine the trade between diameter and jitter, the result is as shown in Figure 3.2.3-2, below. This figure shows that regardless of diameter there is a sharp break in the cost as the jitter value exceeds the nominal value. In part, this is an artifact of the analysis and the choice of quadratic scaling of jitter-related costs. However it is also a true reflection of a design feature of low jitter systems. The assumed relationship for jitter is felt to be an accurate representation of manufacturing difficulty associated with low jitter. Thus any design which pushes the state of the engineering art involved in the system's construction can and will have a pronounced effect on cost. This is borne out by the results shown in the figure. However, it should also be stated that the result is preliminary at best. Considerably more detailed study is justified based on these results
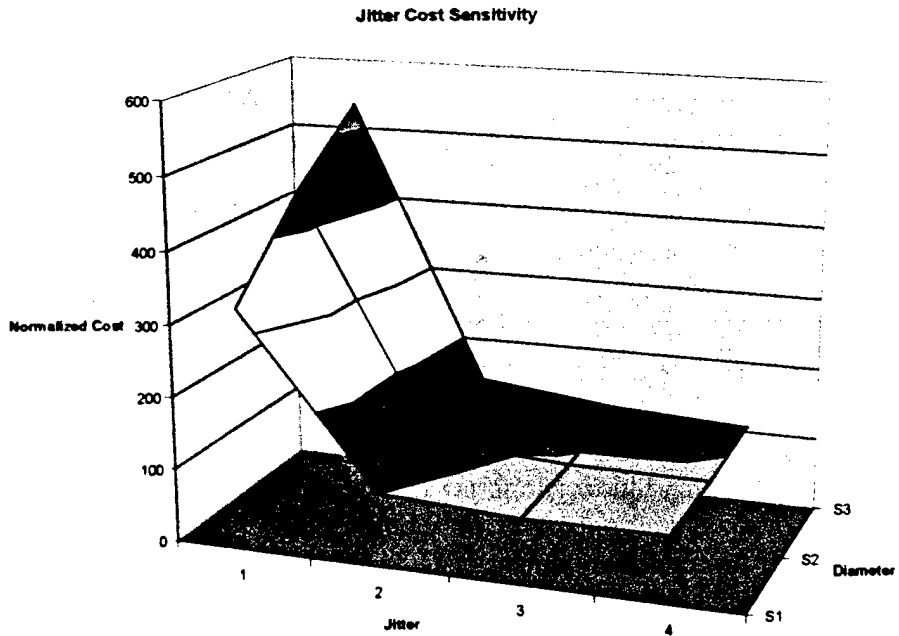
**Cost as a Function of Jitter**

**Figure 3.2.3-2**

Another set of cost results is shown in Figure 3.2.3-3 below, which shows the effect of increased threat missile hardness (or SBL lethality) on the cost of the required constellation.
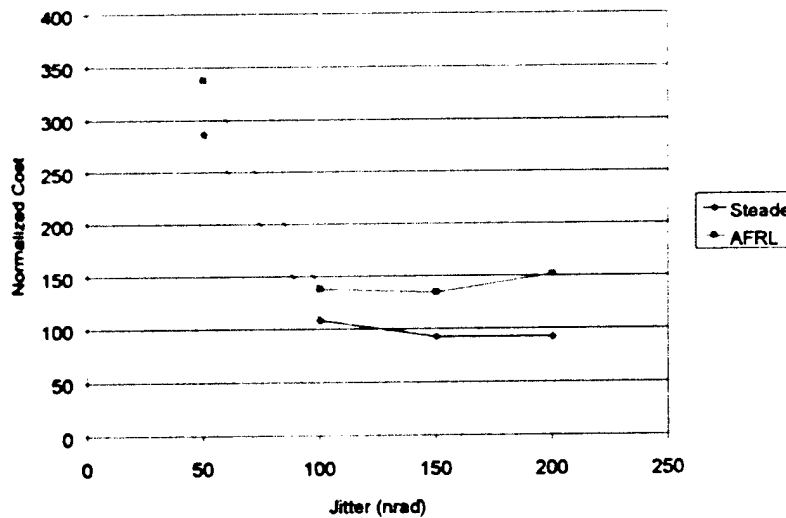


**Cost for Two Levels of SBL Lethality**
**Figure 3.2.3-3**

As can be seen from these results, the lethality of the system against the threat can have a significant impact of the overall cost. Based on this observation, it seems reasonable to assume that careful attention to the lethality requirement is justified.

## Conclusions

In conclusion, the study has shown that commonly held beliefs about the efficacy of certain design choices are not always reliable. Obtaining high brightness through the employment of large optics can result in systems that are unnecessarily costly. Although the results are based on simplistic models, they are interestingly suggestive of important underlying cost trends. In becomes important therefore, to consider expanding this research and developing a better and more exhaustive set of cost model with which to study these design options.

# Appendix 3.3-1
# SBL Growth Path

# SBL Growth Path

Jim Vieceli

Schafer Corp.

Prepared for SMC/ADE

Steve Brown

23 Feb. 1998

Schafer

3.3-1-2

# Schafer

## Agenda

- Threat countermeasure assumptions

- Technology counter-countermeasure assumptions

- SBL growth path assumptions

- SBL growth path approach

- SBL growth path results

# Schafer  Threat countermeasure assumptions

- Ballistic missile technology will proliferate
  - The threat issues we now see as part of NMD will become part of TMD
    - Hardened/composite materials
    - Fast burn/depressed/maneuvering trajectories
- Early release submunition implementation as a countermeasure to midcourse and terminal intercept will make boost phase intercept more critical

3.3-1-4

# Technology counter- countermeasure assumptions

**Schafer**

- From a technology standpoint, the TMD/NMD distinction is irrelevant

  – It is all BMD and the deployed system will counter both

- Constellation inclination will cover polar regions

- Platform brightness/platforms in the battle will counter high launch rate/short burn time associated with hardened TMD threats

3.3-1-5

# Schafer SBL Growth Path Assumptions

- The deployed system is 15-20 years away

- Many technologies will advance for other reasons without SBL implementation /funding

  - Large erectable, possibly deployable apertures
    - IR space telescope, space based radar
  - Line-of-sight stabilization
    - Telescopes, weapon guidance, surveillance
  - Shorter wavelength lasers
    - Diode pumped solid state laser, shorter wavelength chemical laser

3.3-1-6

**Schafer** SBL Growth Path Approach

- Focus near term(RD) activities on essential technical and operational issues

  - Facility simulation of space environment

  - Boresight tracker/laser and aimpoint maintenance in nonquiescent environment

    • Monolithic primary provides most stable approach

      – Combustion

      – Slew/settle

  – Lethality

  – Cost, risk

  – Missions, BMC$^3$, interoperability

3.3-1-7

# Schafer

## SBL Growth Path Approach
### (continued)

- Focus far term activities on growth path

  – Coordination of large constellations and interoperability with other BMD assets

  – Response to countermeasures

    • Larger constellations(20 → 36 → 40)

      – More platforms in battle/shorter average range/shorter kill time/fixed kill time at higher hardness

    • Lower altitude(1300 → 700km)

      – Shorter average range/shorter kill time/fixed kill time at higher hardness

    • Higher brightness(1 → 20x) at 2x power

      – Shorter kill time/fixed kill time at higher hardness

# SBL Growth Path Results

**Schafer**

- Near term theater(10/1)
  - 24/8/8/2.7/1.22/16/100

- Near term strategic(10/2.5)
  - same as above

- Mid term theater, conservative(10/25)
  - 36/16/20/2.7/1.22/16/40

- Mid term theater, aggressive(10/15)
  - 24/12/12/1.3/1.22/16/25(option at 1300km)
  - 32/8/12/1.3/1.22/16/25(option at 1000km)
  - 24/8/16/1.3/1.22/16/25(option at 1300km)

- Far term theater(10/50)
  - 40/8/20/1.3/1.22/16/25

# *Schafer*

# Cost/Near term



RELATIVE POWER

RELATIVE CC

D=4    D=8    D=12    D=16    D=20    D=24

3.3-1-10

# Platform number/Near term



3.3-1-11

# Schafer

## Altitude/Near term



3.3-1-12
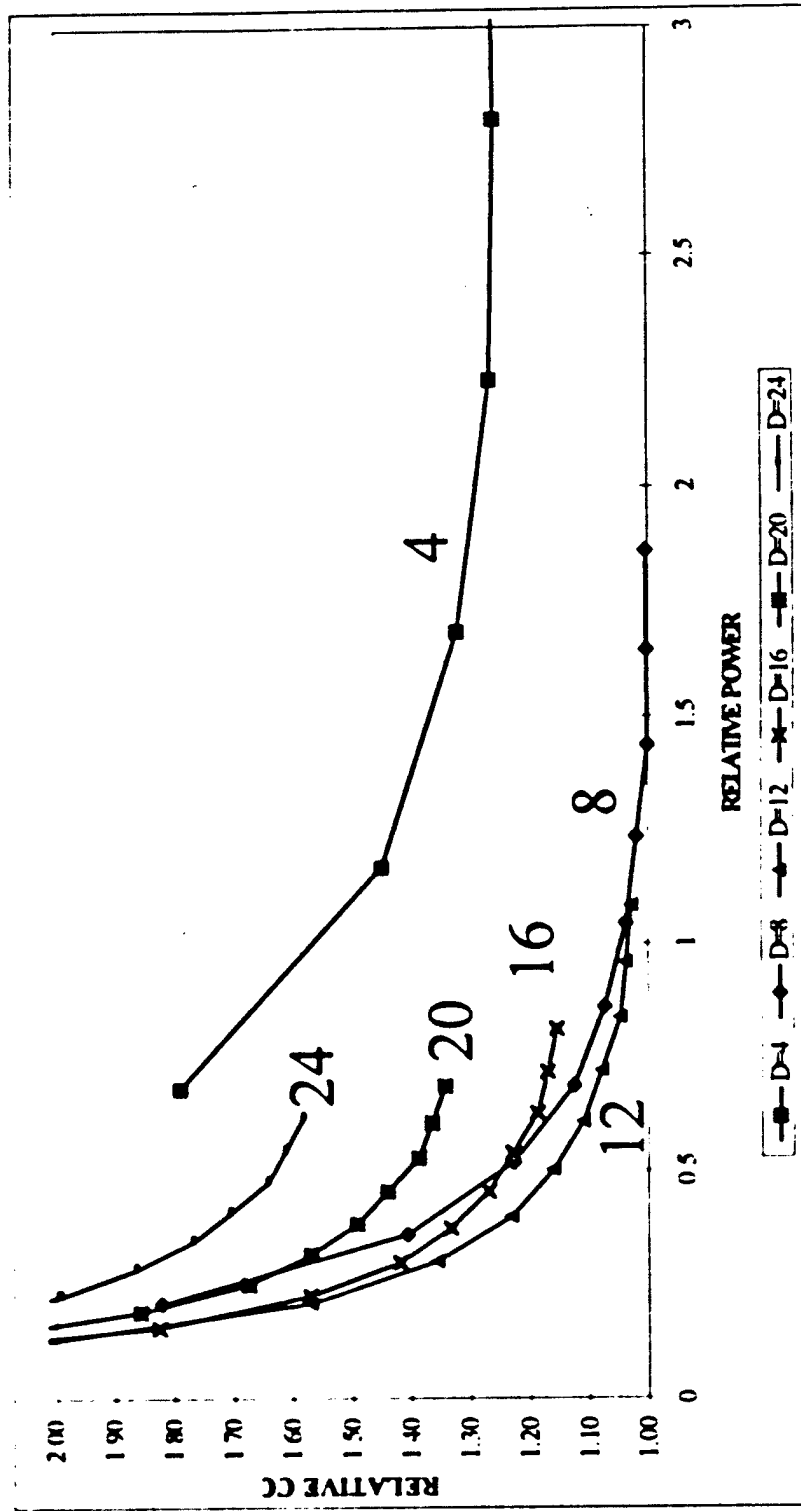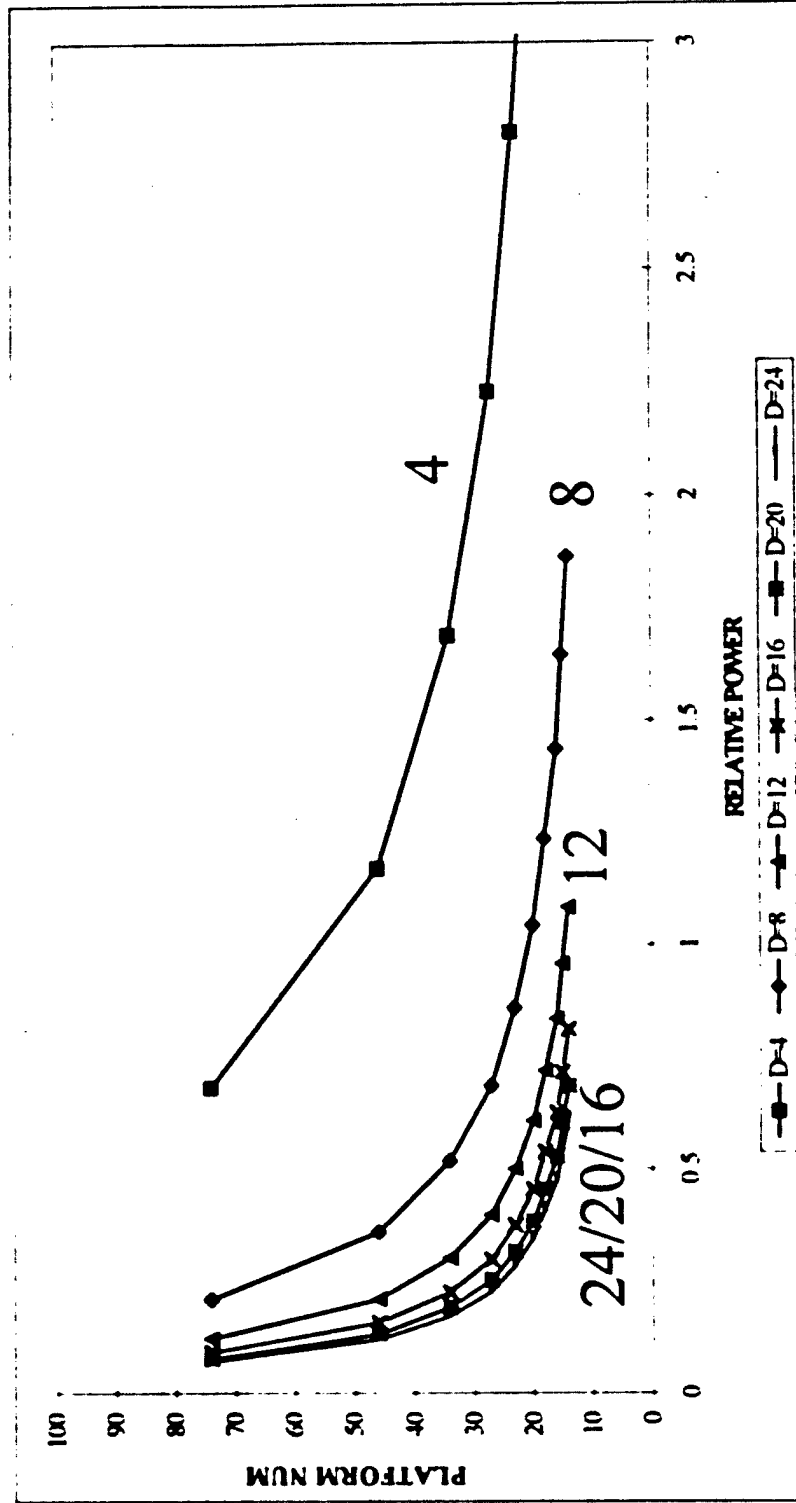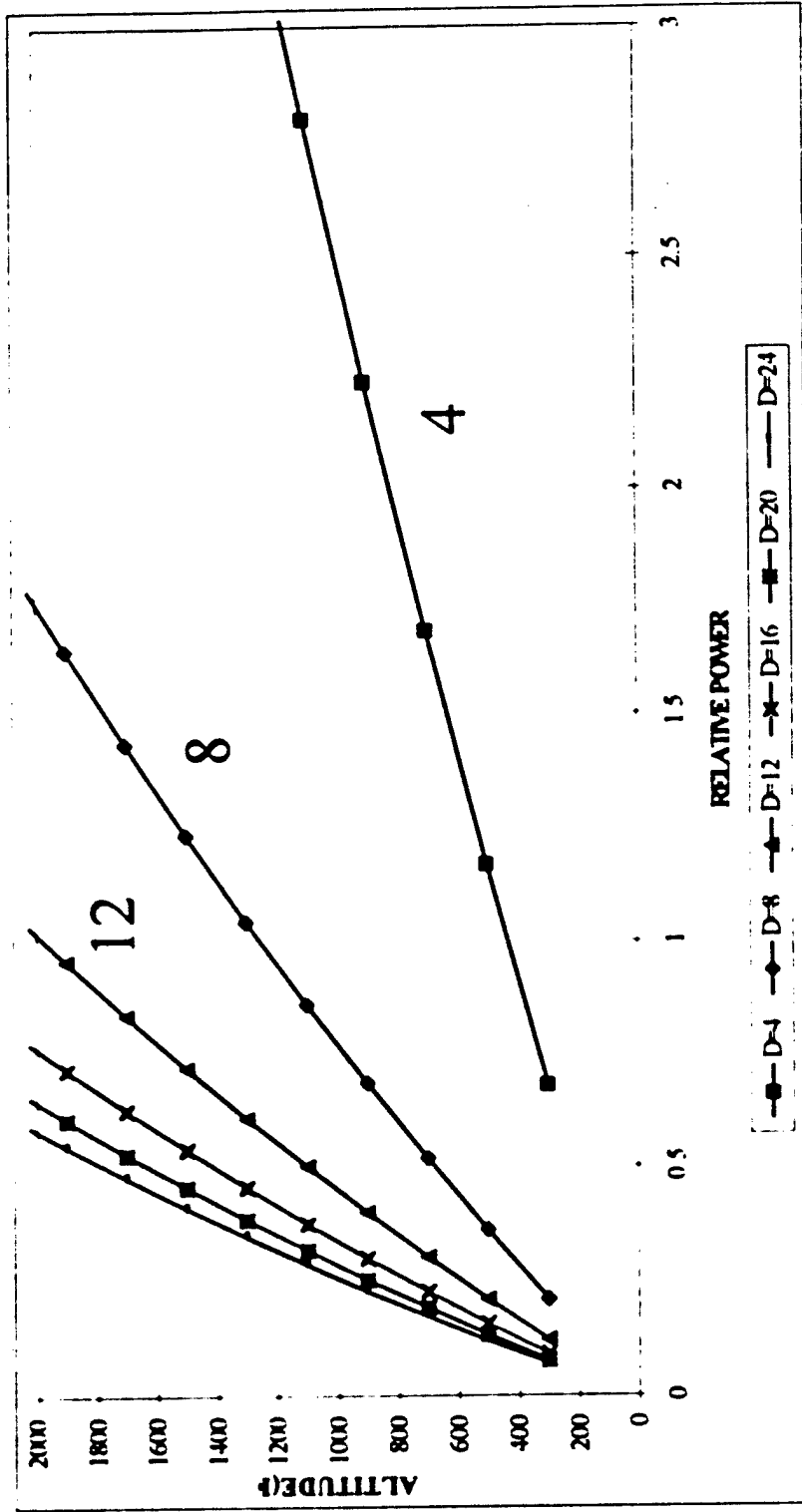
# Schafer

## Cost/Mid term(conservative)



3.3-1-13

Platform number/Midterm
(conservative)

*Schafer*

3.3-1-14

# Schafer

# Altitude/Mid term
# (conservative)



3.3-1-15

Schafer

Cost/Mid term(aggressive)

RELATIVE POWER

RELATIVE COST

D=4   D=8   D=12   D=16   D=20   D=24

3.3-1-16
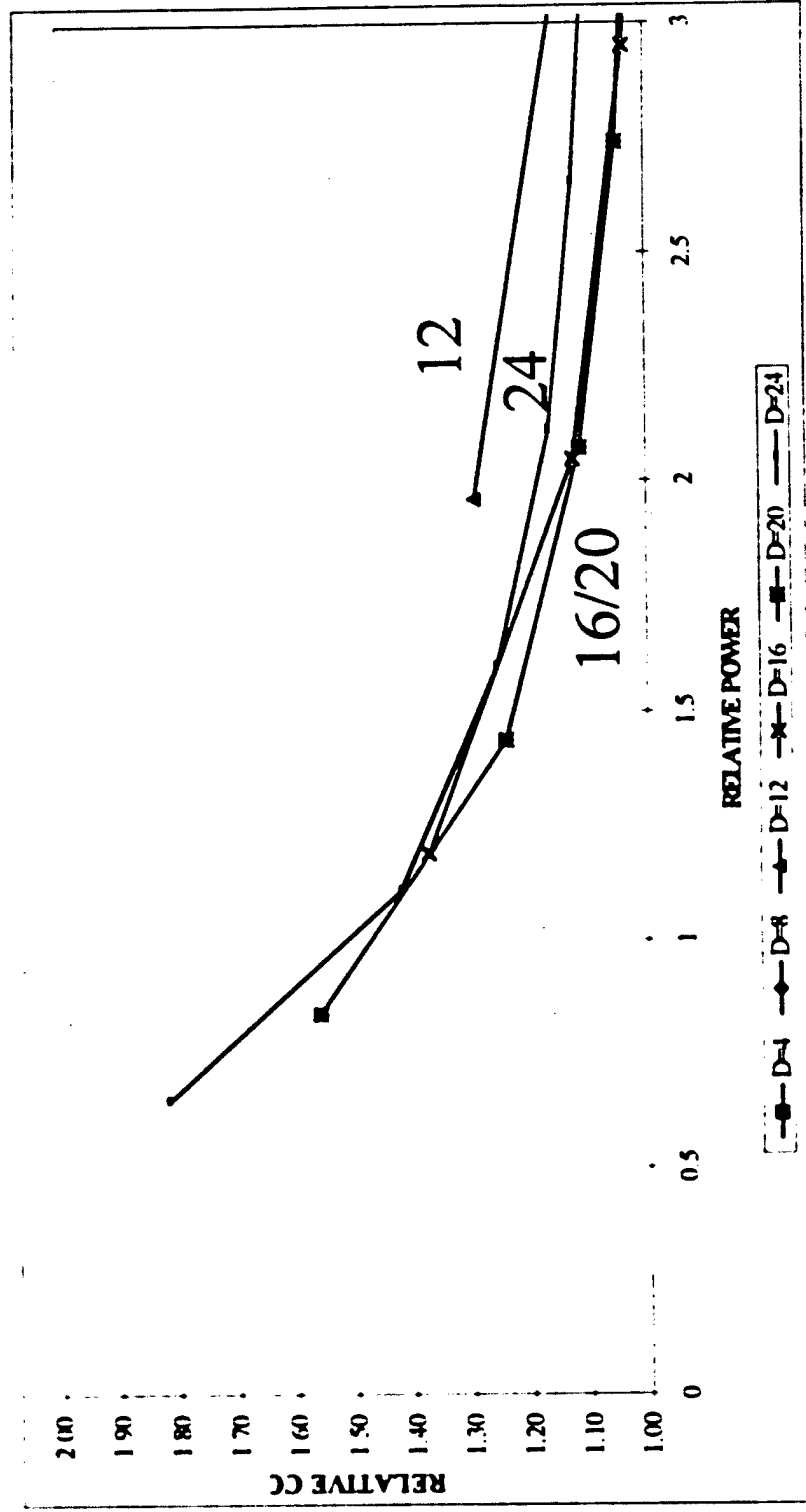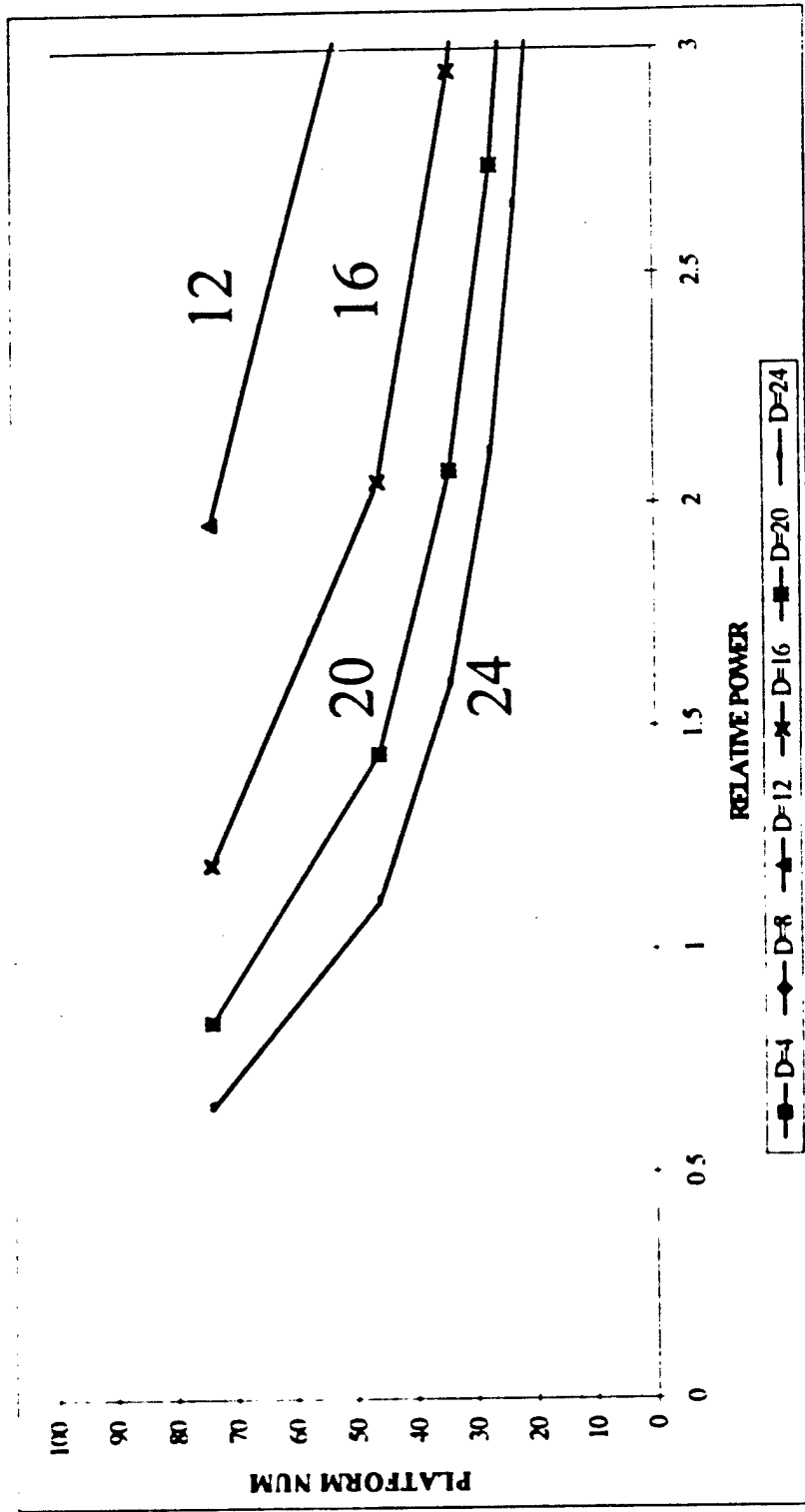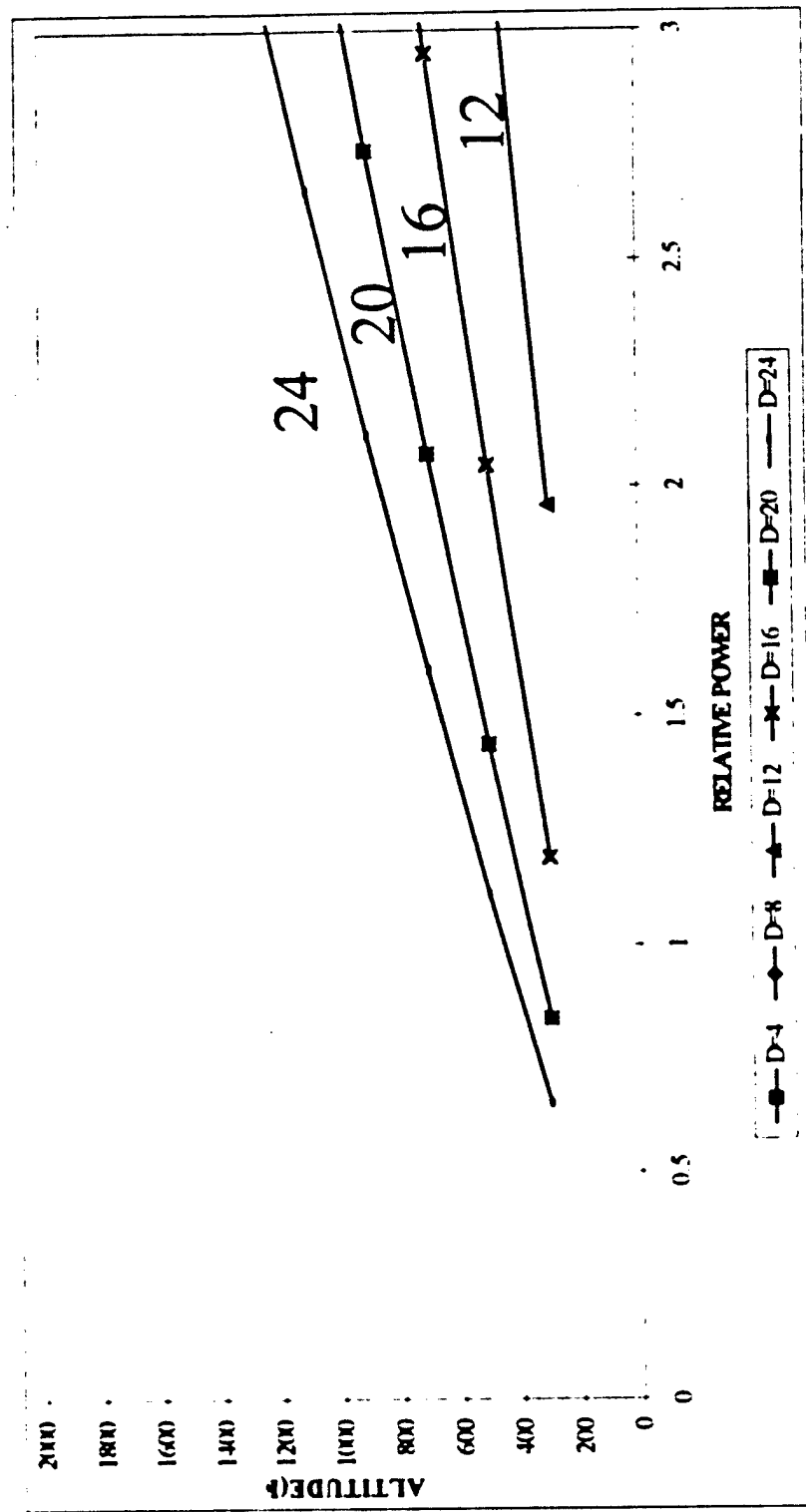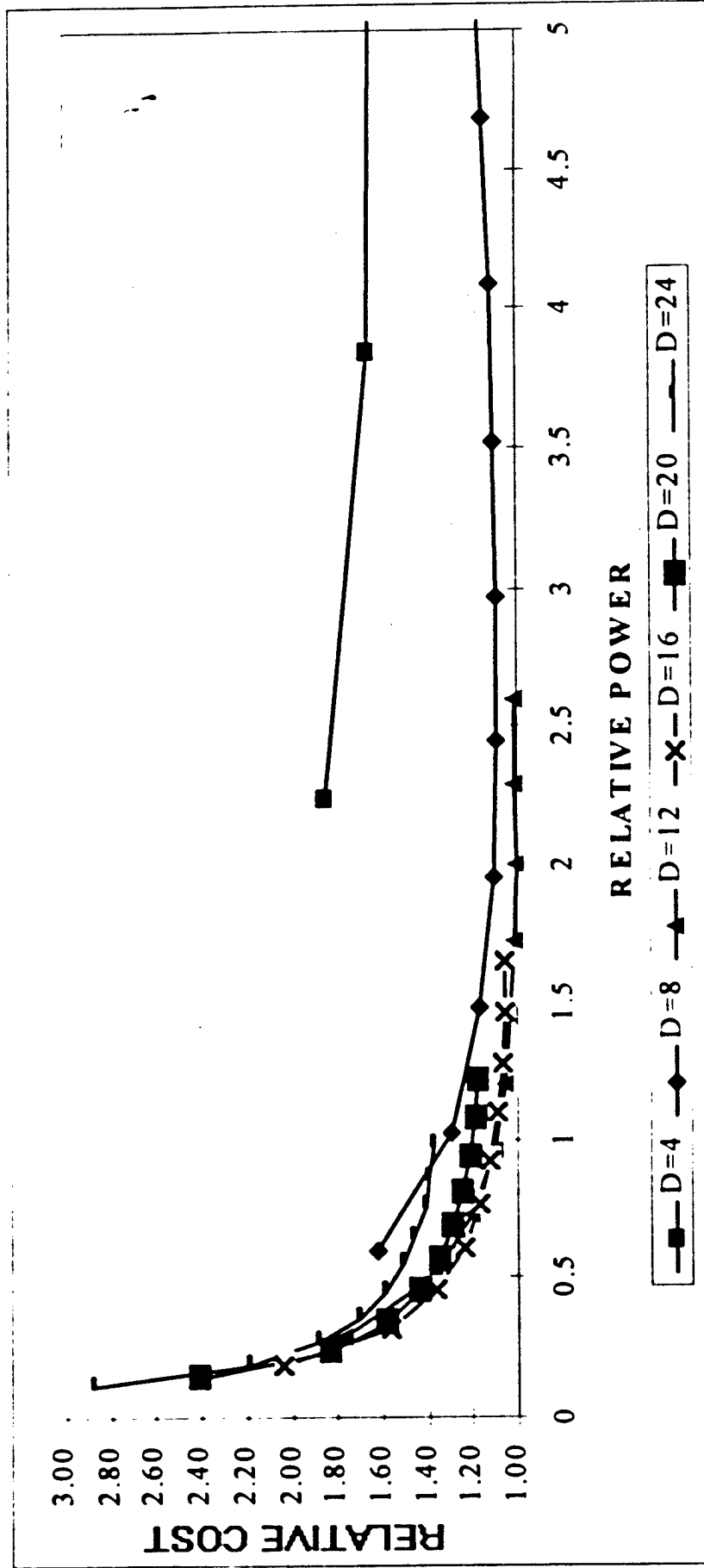
Platform number/Midterm (aggressive)

PLATFORM NUMBER

RELATIVE POWER

D=4
D=8
D=12
D=16
D=20
D=24

3.3-1-17

# Schafer
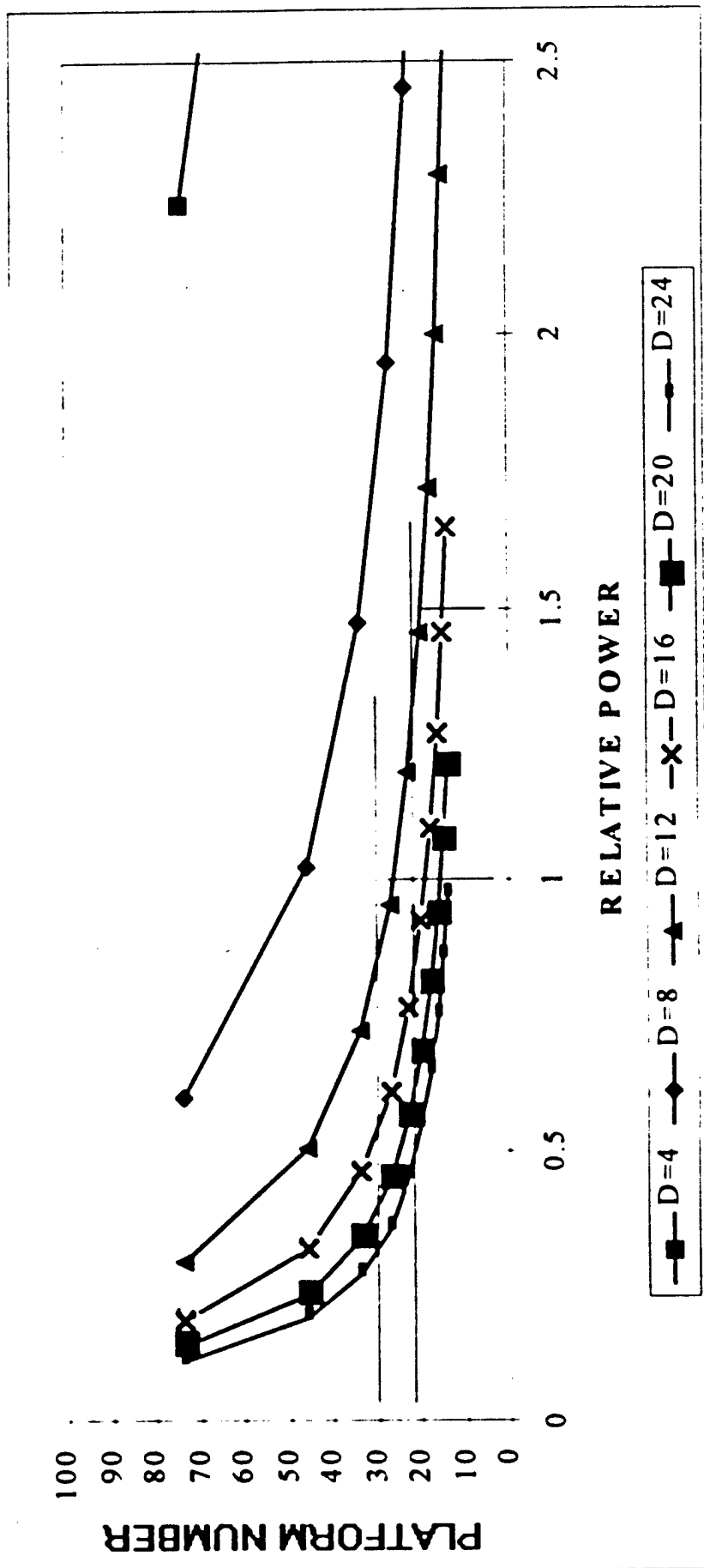
## Altitude/Mid term
## (aggressive)



Chart: ALTITUDE(KM) vs RELATIVE POWER

Legend: D=4, D=8, D=12, D=16, D=20, D=24
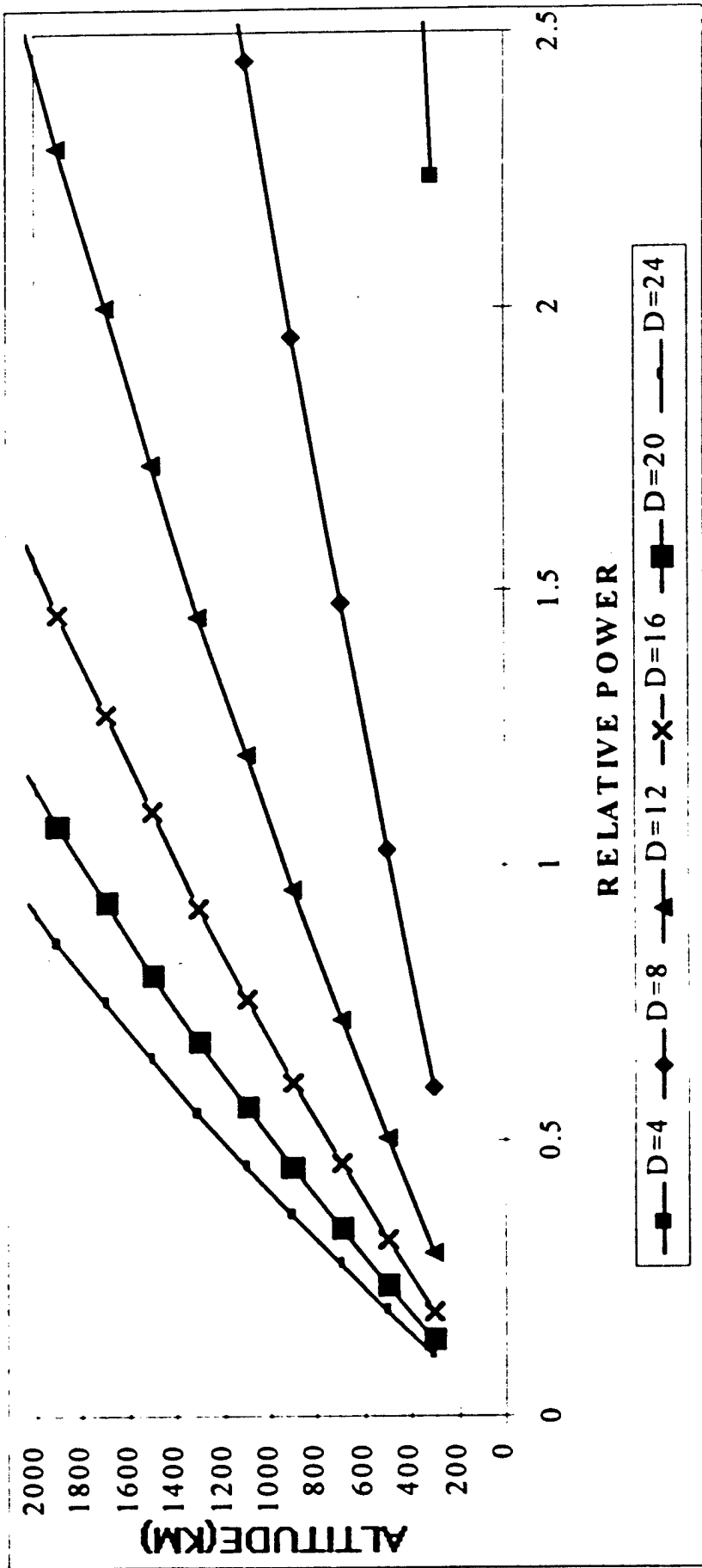
# Schafer

Coverage for 24 platform option
at 1300km/60deg



LATITUDE(DEG.)

LONGITUDE(DEG.)

3.3-1-19
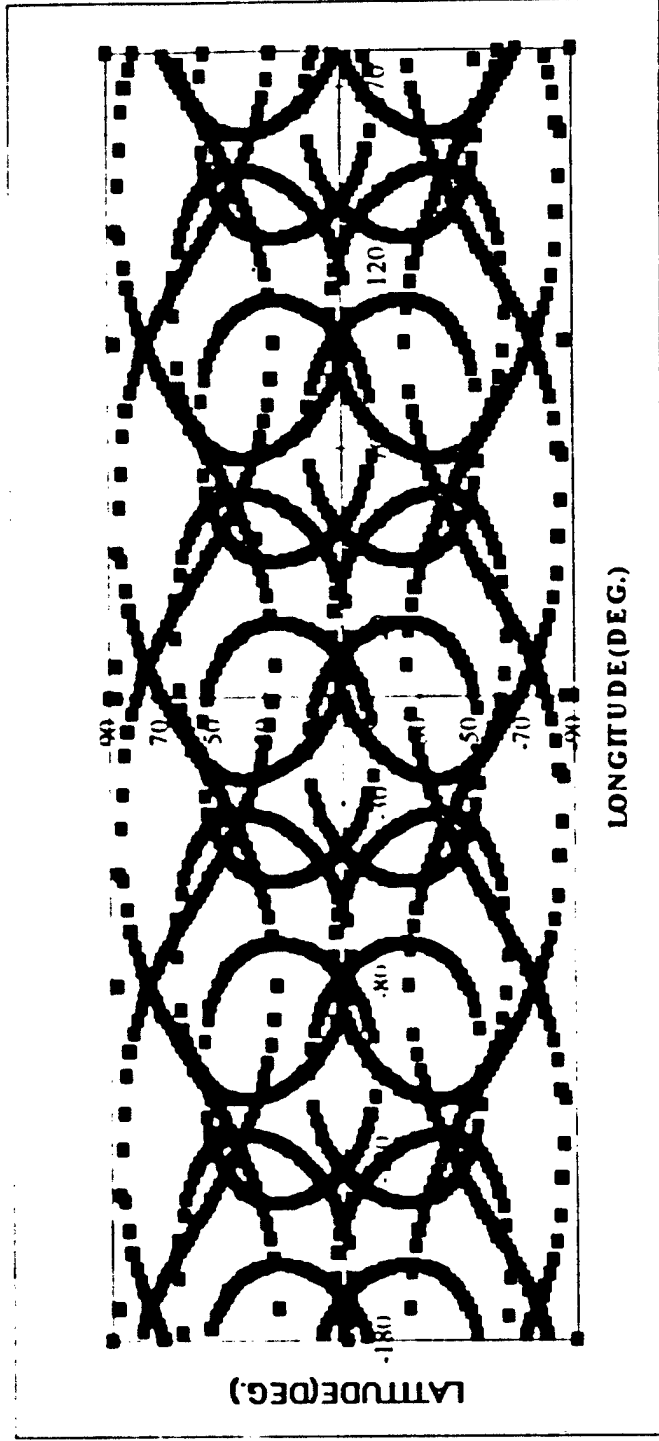
# Coverage for 32 platform option
## at 1000km/60deg



**LONGITUDE(DEG.)**

**LATITUDE(DEG.)**

*Schafer*

3.3-1-20

# Cost/Far term



**Schafer**

3.3-1-21

# Schafer

## Platform number/Far term



PLATFORM NUM

RELATIVE POWER

D=4   D=8   D=12   D=16   D=20   D=24

3.3-1-22

Altitude/Far Term



ALTITUDE

RELATIVE POWER

D=4    D=8    D=12    D=16    D=20    D=24

3.3-1-23

# Schafer

## Summary
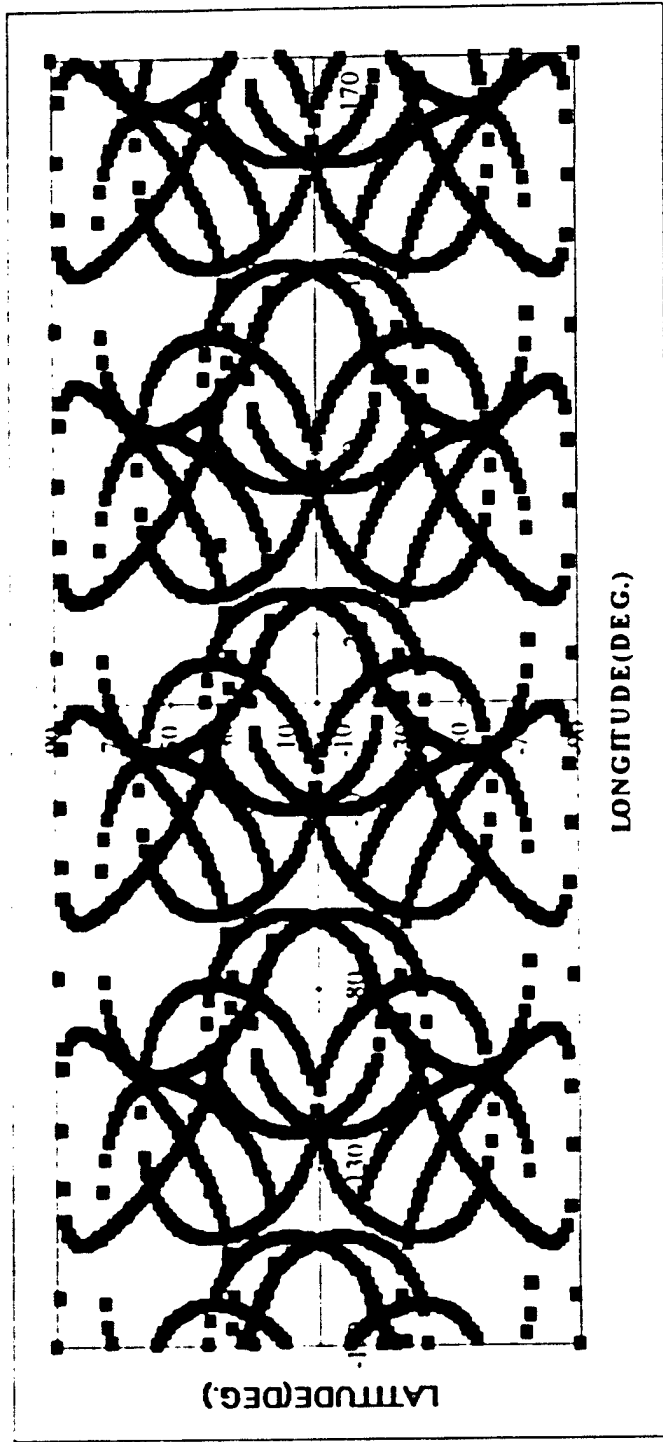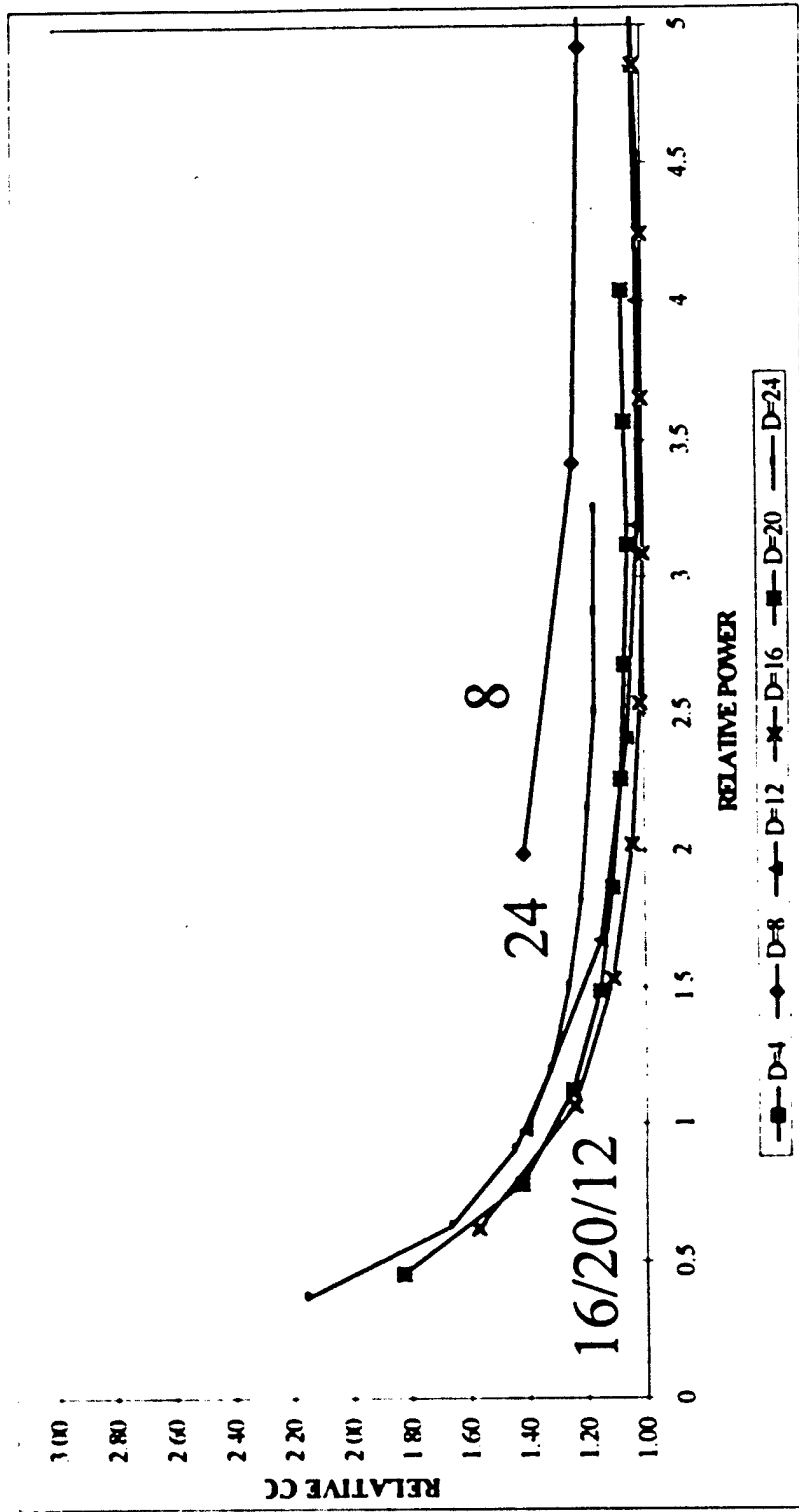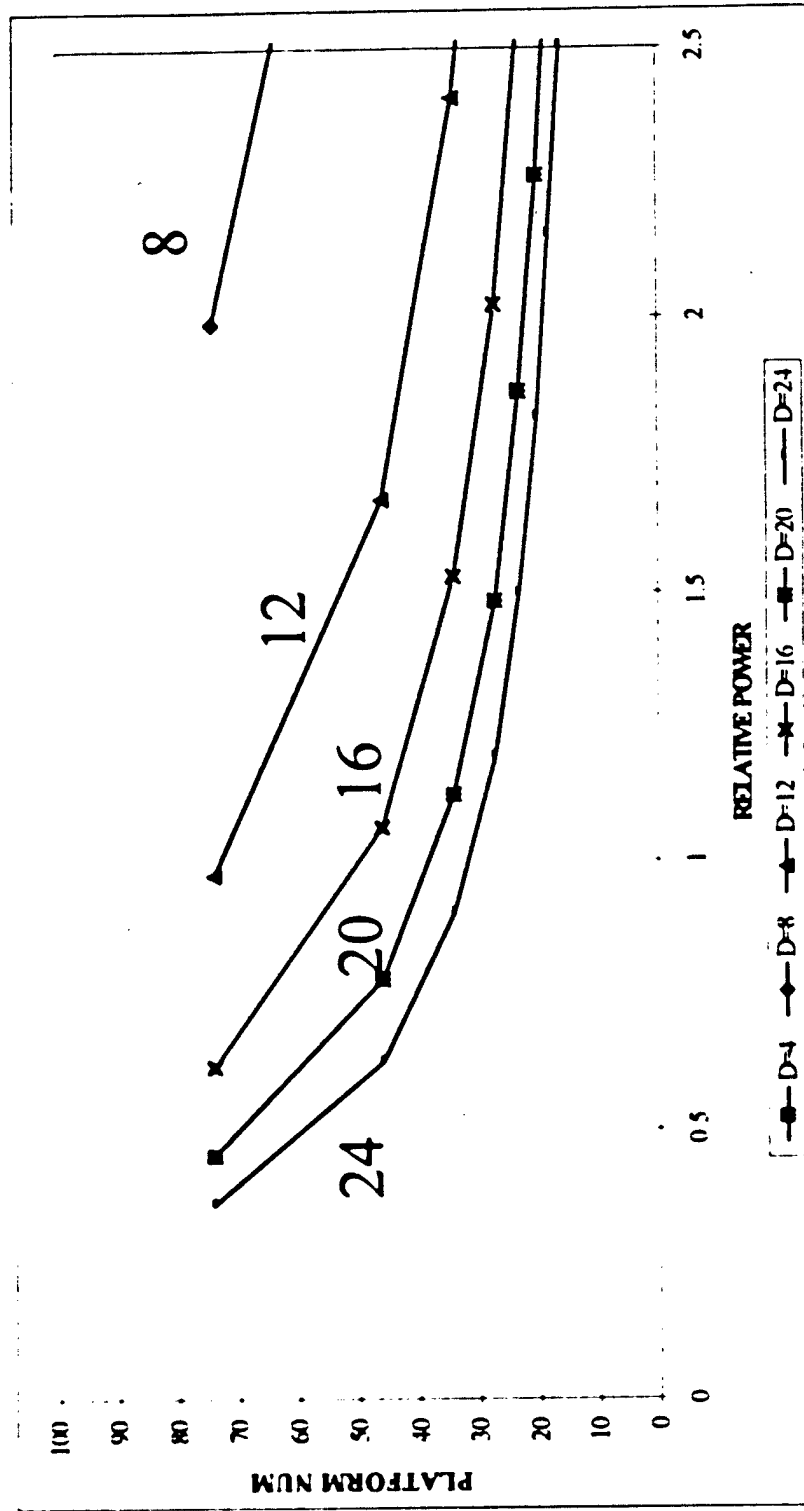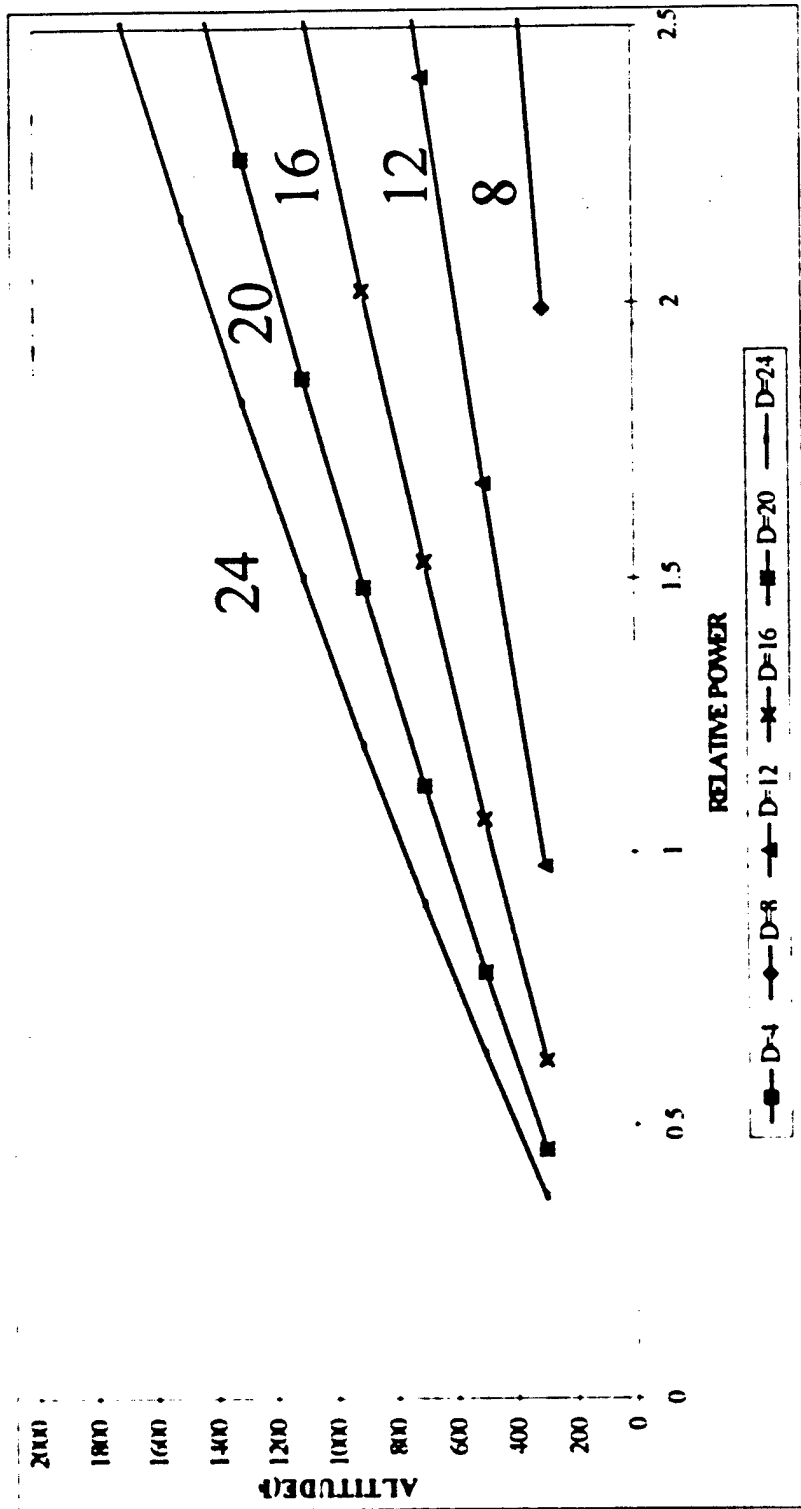
- Preliminary results indicate growth potential to counter worst case threat countermeasure

  – Detailed ISAAC analysis required to confirm

  – Update of cost optimization required

3.3-1- 24

# Appendix 3.3-2
# Far Term SBL Lethality Assessment

# Far-term SBL Lethality Assessment

**Prepared by Schafer Corp.**

Jim Vieceli

Larrene Harada

**Prepared for SMC/ADE**

Steve Brown

1 Sept. 98

3.3-2-2

# Agenda/Introduction

- Analysis approach

- TMD threat

  - Current threat/Near term SBL system

  - Advanced threat/Far term SBL system requires large apertures

- Advanced NMD threat requires large apertures

  - Near-term jitter and fundamental wavelength lead to large platform number

  - Far-term jitter, overtone improve platform number

- Simple model and detailed model(ISAAC) are in good agreement

- Using large apertures to achieve high brightness raises spot size issues re: lethality

  - Vent versus structural failure

  - Still need to be resolved

# Pre-CDS Baseline

- Threat expectations(harder) and deployment plans(later) make this system less supportable

| | Analytic TMD Baseline | Analytic Advanced TMD | Analytic NMD Baseline | AFRL ISAAC NMD Baseline | Howie ISAAC NMD Baseline | Analytic Advanced NMD |
|---|---|---|---|---|---|---|
| | 10 | 10 | 5 | 5 | 5 | 5 |
| | 40 | 40 | 200 | 200 | 200 | 200 |
| | 100 | 40 | 100 | 100 | 100 | 40 |
| | 2.7 | 1.3 | 2.7 | 2.7 | 2.7 | 1.3 |
| | 1000 | 15000 | 15000 | 15000 | 15000 | 15000 |
| System 1 | 8 | 12 | 12 | 12 | 12 | 6 |
| | 8 | 12 | 12 | 12 | 12 | 12 |
| | 20 | 24 | 40 | 38 | 28 | 20 |
| | 1300 | 1100 | 600 | 500 | - | 1350 |
| System 2 | 8 | 8 | 8 | 8 | 8 | 4 |
| | 16 | 16 | 16 | 16 | 16 | 16 |
| | 24 | 24 | 45 | 40 | 30 | 20 |
| | 1000 | 1000 | 500 | 500 | - | 1250 |

3.3-2-4

# SBL Responsive to Far-term TMD Threat

- Far-term TMD threat requires large apertures, short wavelength and advanced jitter control

- Not officially recognized as a threat, but proliferation is inevitable

| | Analytic TMD Baseline | Analytic Advanced TMD | Analytic NMD Baseline | AFRL ISAAC NMD Baseline | Howie ISAAC NMD Baseline | Analytic NMD Baseline | Analytic Advanced NMD |
|---|---|---|---|---|---|---|---|
| | 10 | 10 | 5 | 5 | 5 | 5 | 5 |
| | 40 | 40 | 200 | 200 | 200 | 200 | 200 |
| | 100 | 40 | 100 | 100 | 100 | 100 | 40 |
| | 2.7 | 1.3 | 2.7 | 2.7 | 2.7 | 2.7 | 1.3 |
| | 1000 | 15000 | 15000 | 15000 | 15000 | 15000 | 15000 |
| System 1 | 8 | 12 | 12 | 12 | 12 | 12 | 6 |
| | 8 | 12 | 12 | 12 | 12 | 12 | 12 |
| | 20 | 24 | 40 | 38 | 28 | | 20 |
| | 1300 | 1100 | 600 | 500 | 500 | | 1350 |
| System 2 | 8 | | 8 | 8 | 8 | 8 | 4 |
| | 16 | | 16 | 16 | 16 | 16 | 16 |
| | 24 | | 45 | 40 | 30 | | 20 |
| | 1000 | | 500 | 500 | 500 | | 1250 |

3.3-2-5

# Advanced NMD Threat
## Fundamental wavelength and near-term jitter

- Large number of platforms not desirable from cost standpoint

|  | Analytic<br>TMD Baseline | Analytic<br>Advanced TMD | AFRL<br>Analytic<br>NMD Baseline | ISAAC<br>NMD Baseline | Howie<br>ISAAC<br>NMD Baseline | Analytic<br>Advanced NMD |
|---|---|---|---|---|---|---|
|  | 10 | 10 | 5 | 5 | 5 | 5 |
|  | 40 | 40 | 200 | 200 | 200 | 200 |
|  | 100 | 40 | 100 | 100 | 100 | 40 |
|  | 2.7 | 1.3 | 2.7 | 2.7 | 2.7 | 1.3 |
|  | 1000 | 15000 | 15000 | | | 15000 |
| System 1 | 8 | 12 | 12 | 12 | 12 | 6 |
|  | 8 | 12 | 12 | 12 | 12 | 12 |
|  | 20 | 24 | 40 | 38 | 28 | 20 |
|  | 1300 | 1100 | 600 | 500 | - | 1350 |
| System 2 | | 8 | 8 | 8 | 8 | 4 |
|  | | 16 | 16 | 16 | 16 | 16 |
|  | | 24 | 45 | 40 | 30 | 20 |
|  | | 1000 | 500 | 500 | - | 1250 |

# Advanced NMD Threat
## Fundamental wavelength and near-term jitter

- Analytic model and detailed model(ISAAC) are in good agreement

| | Analytic TMD Baseline | Analytic Advanced TMD | Analytic NMD Baseline | AFRL ISAAC NMD Baseline | Howie ISAAC NMD Baseline | Analytic Advanced NMD |
|---|---|---|---|---|---|---|
| | 10 | 10 | 5 | 5 | 5 | 5 |
| | 40 | 40 | 200 | 200 | 200 | 200 |
| | 100 | 40 | 100 | 100 | 100 | 40 |
| | 2.7 | 1.3 | 2.7 | 2.7 | 2.7 | 1.3 |
| | 1000 | 15000 | 15000 | 15000 | 15000 | 15000 |
| System 1 | 8 | 12 | 12 | 12 | 12 | 6 |
| | 8 | 12 | 12 | 12 | 12 | 12 |
| | 20 | 24 | 40 | 38 | 28 | 20 |
| | 1300 | 1100 | 600 | 500 | 500 | 1350 |
| System 2 | 8 | 8 | 8 | 8 | 8 | 4 |
| | 16 | 16 | 16 | 16 | 16 | 16 |
| | 24 | 45 | 40 | 40 | 30 | 20 |
| | 1000 | 500 | 500 | 500 | 500 | 1250 |

## Advanced NMD Threat
## Fundamental wavelength and near-term jitter

- Impact of lethality assumption(AFRL/Howie) is platform number
- Contingent on lethality independent of spot size

| | Analytic TMD Baseline | Analytic Advanced TMD | Analytic NMD Baseline | AFRL ISAAC NMD Baseline | Howie ISAAC NMD Baseline | Analytic Advanced NMD |
|---|---|---|---|---|---|---|
| | 10 | 10 | 5 | 5 | 5 | 5 |
| | 40 | 40 | 200 | 200 | 200 | 200 |
| | 100 | 40 | 100 | 100 | 100 | 40 |
| | 2.7 | 1.3 | 2.7 | 2.7 | 2.7 | 1.3 |
| | 1000 | 15000 | 15000 | 15000 | 15000 | 15000 |
| **System 1** | 8 | 12 | 12 | 12 | 12 | 6 |
| | 8 | 12 | 12 | 12 | 12 | 12 |
| | 20 | 24 | 40 | 38 | 28 | 20 |
| | 1300 | 1100 | 600 | 500 | - | 1350 |
| **System 2** | 8 | 8 | 8 | 8 | 8 | 4 |
| | 16 | 16 | 16 | 16 | 16 | 16 |
| | 24 | 24 | 45 | 40 | 30 | 20 |
| | 1000 | 1000 | 500 | 500 | - | 1250 |

3.3-2-8

# Advanced NMD Threat

## Overtone wavelength and far-term jitter

- Baseline far-term systems are responsive to advanced NMD threat
- Advanced NMD and TMD systems are compatible

|  | Analytic TMD Baseline | Analytic Advanced TMD | Analytic NMD Baseline | AFRL ISAAC NMD Baseline | Howie ISAAC NMD Baseline | Analytic Advanced NMD |
|---|---|---|---|---|---|---|
|  | 10 | 10 | 5 | 5 | 5 | 5 |
|  | 40 | 40 | 200 | 200 | 200 | 200 |
|  | 100 | 40 | 100 | 100 | 100 | 40 |
|  | 27 | 1.3 | 2.7 | 2.7 | 2.7 | 1.3 |
|  | 1000 | 15000 | 15000 | 15000 | 15000 | 15000 |

**System 1**

|  | Analytic Advanced TMD | Analytic NMD Baseline | AFRL ISAAC NMD Baseline | Howie ISAAC NMD Baseline | Analytic Advanced NMD |
|---|---|---|---|---|---|
|  | 8 | 12 | 12 | 12 | 6 |
|  | 8 | 12 | 12 | 12 | 12 |
|  | 20 | 24 | 40 | 38 | 28 | 20 |
|  | 1300 | 1100 | 600 | 500 | - | 1350 |

**System 2**

|  | Analytic Advanced TMD | Analytic NMD Baseline | AFRL ISAAC NMD Baseline | Howie ISAAC NMD Baseline | Analytic Advanced NMD |
|---|---|---|---|---|---|
|  | 8 | 8 | 8 | 8 | 4 |
|  | 16 | 16 | 16 | 16 | 16 |
|  | 24 | 45 | 40 | 30 | 20 |
|  | 1000 | 500 | 500 | - | 1250 |

3.3-2-9

# Summary

- Top level platform parameters(power/diameter/jitter/wavefront error/altitude) are less sensitive to lethality assumptions
  - Lethality differences accounted for with platform number
  - Spot size effects for advanced threat are TBD

3.3-2-10

# Appendix 3.3-3
# TMD Analysis

Review of

TMD Feasibility White-paper

Prepared for Steve Brown

M&S TIM

9-10 September 1998

Presented by: Jim Vieceli

Based on work performed by:

SAIC, Schafer, Sparta

3.3-3-2

# Agenda

- Why is there an issue?
  - Short battle time between cloud break and burn out
  - Long BMC$^3$ time delay characteristic of existing systems

- Time-line analysis suggests 10s BMC$^3$ time delay is conservative

- Several analyses support high level of SBL TMD performance

- Baseline TMD system(pre-CDS)

- CDS class systems also have high TMD performance

3.3-3-3

# Roadmap

- SBL has addressed TMD since early 90s

  – SU collapse

  – GPALS defined many potential theater threats

  – BMDO baseline designed for near-term TMD threat

- SBL TMD performance analysis results validated as part of AF COEA in April 1996(EADSim, ISAAC, PLASTR)

- CDS NMD threat more stressing than near-term TMD threat(15-20 x harder but only 5-6 x battle time)

  – CDS designs will be near-term TMD capable

  – Growth path to far-term TMD capability defined

# Kill number is a linear function of time delay (in a simple analytic approximation)

$$N_{kill} = (t_{bat} - t_{delay}) \frac{BN_{sat-in-bat}}{hR_e H}$$

$$B = P / 2\pi\sigma^2$$

$$\sigma^2 = \sigma_D^2 + \sigma_J^2$$

$$\sigma_D = \sqrt{2\lambda_s} / \pi D$$

# SBL TMD Timeline - Current Best Estimate

Continuous Surveillance

TBMs Launched

TBM visible
- Cloud free -28 -42sec
- cloud 10 km -39 - 42sec

Search revisit rate 0.3 - 2.5 sec

Body & BEX Slew 0.5 - 3.0 sec

Activate HEL 3.0 - 15 sec

Track & ID Target 0.1-0.2 sec

Plan engagement -.3 sec

Slew mirrors - 0.1 - 0.3 sec

Select aimpoint 0.1 -0.2 sec

Release weapon 1 -10 sec

Ignite laser 2.75 sec

Lase Target ave. 2.0 sec
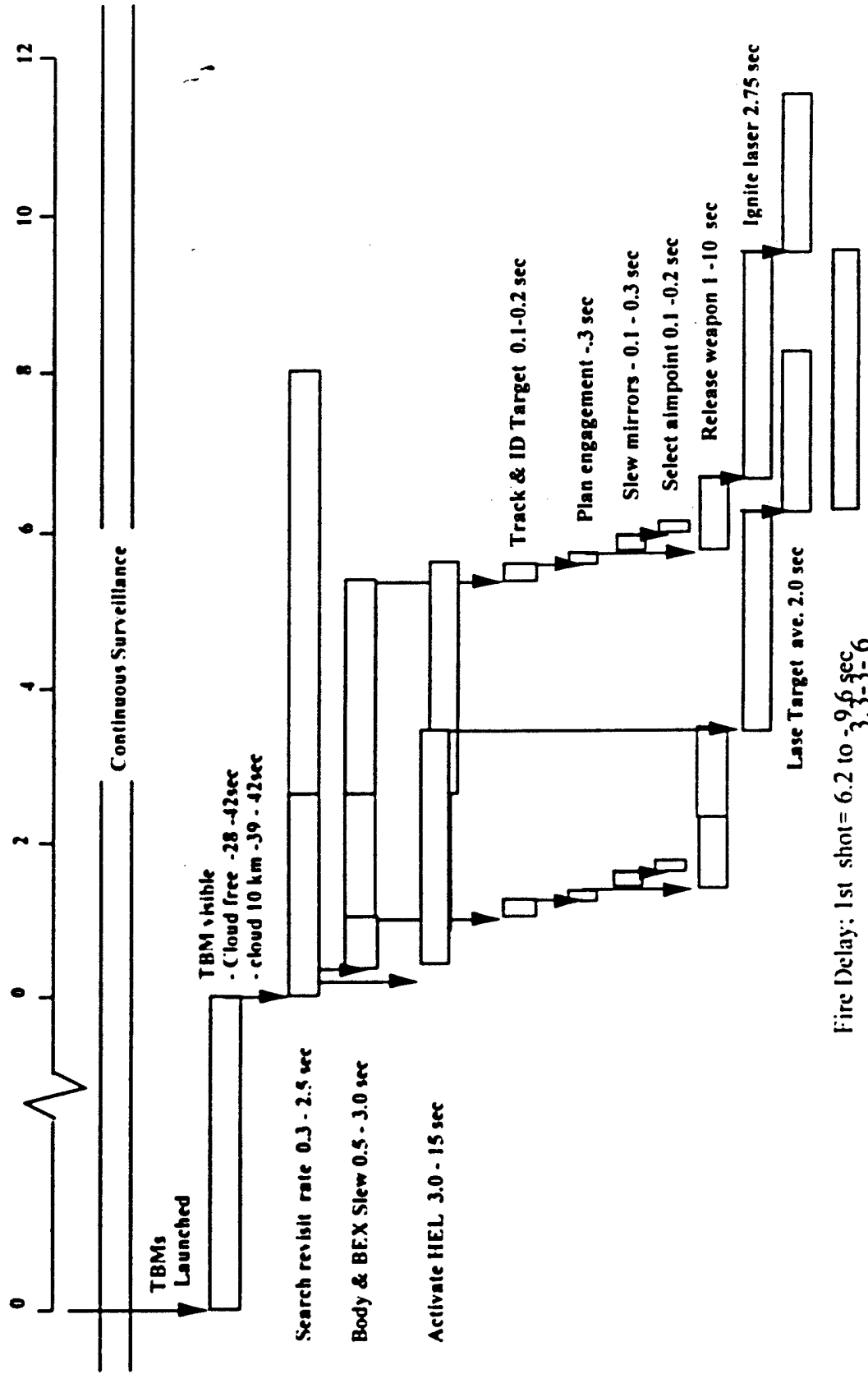
Fire Delay: 1st shot= 6.2 to 9.6 sec

3.3-3-6

# 10 s time delay based on time line analysis

- Laser in standby mode
- Laser on-board surveillance assets assigned geographically
- Weapon release pre-authorized

Table 1. Timeline analysis.

| Function | Minimum time(s) | Maximum time(s) |
|---|---|---|
| **Pre-engagement, one time only** | | |
| Activate HEL | 3.0 | 15.0 |
| Ignite laser | 2.75 | 2.75 |
| Weapon release | 1.0 | 10.0 |
| Search revisit | 0.3 | 2.5 |
| **Pre-engagement total** | **7.05** | **30.25** |
| **Each engagement** | | |
| Track&ID target | 0.1 | 0.2 |
| Plan engagement | 0.3 | 0.3 |
| Select aimpoint | 0.1 | 0.2 |
| Kill assessment | 0.1 | 0.1 |
| **Each engagement total** | 0.6 3- 7 | 0.8 |

# Simple analytic model

- 8 simultaneous kills(average) for short range TMD threat

Table 2. Kill number as a function of range

| Nominal Range(Km) | Time to 10 Km(s) | Burn time(s) | Maximum Battle time(s) | Kill Number for 10s Delay |
|---|---|---|---|---|
| 50 | 37.56 | 41.73 | 4.17 | 0 |
| 100 | 37.66 | 48.29 | 10.63 | 0 |
| 150 | 37.72 | 53.12 | 15.40 | 2 |
| 200 | 39.59 | 59.09 | 19.50 | 4 |
| 300 | 40.37 | 68.42 | 28.05 | 8 |
| 600 | 50.16 | 98.35 | 48.19 | 17 |
| 1000 | 49.55 | 110.11 | 60.56 | 22 |

3.3-3- 8

# SBLs Provide Overlapping Theater Global Coverage

**Single Platform Capability from 20 Satellite Constellation At 1300 Km with a 40 Degree Inclination**
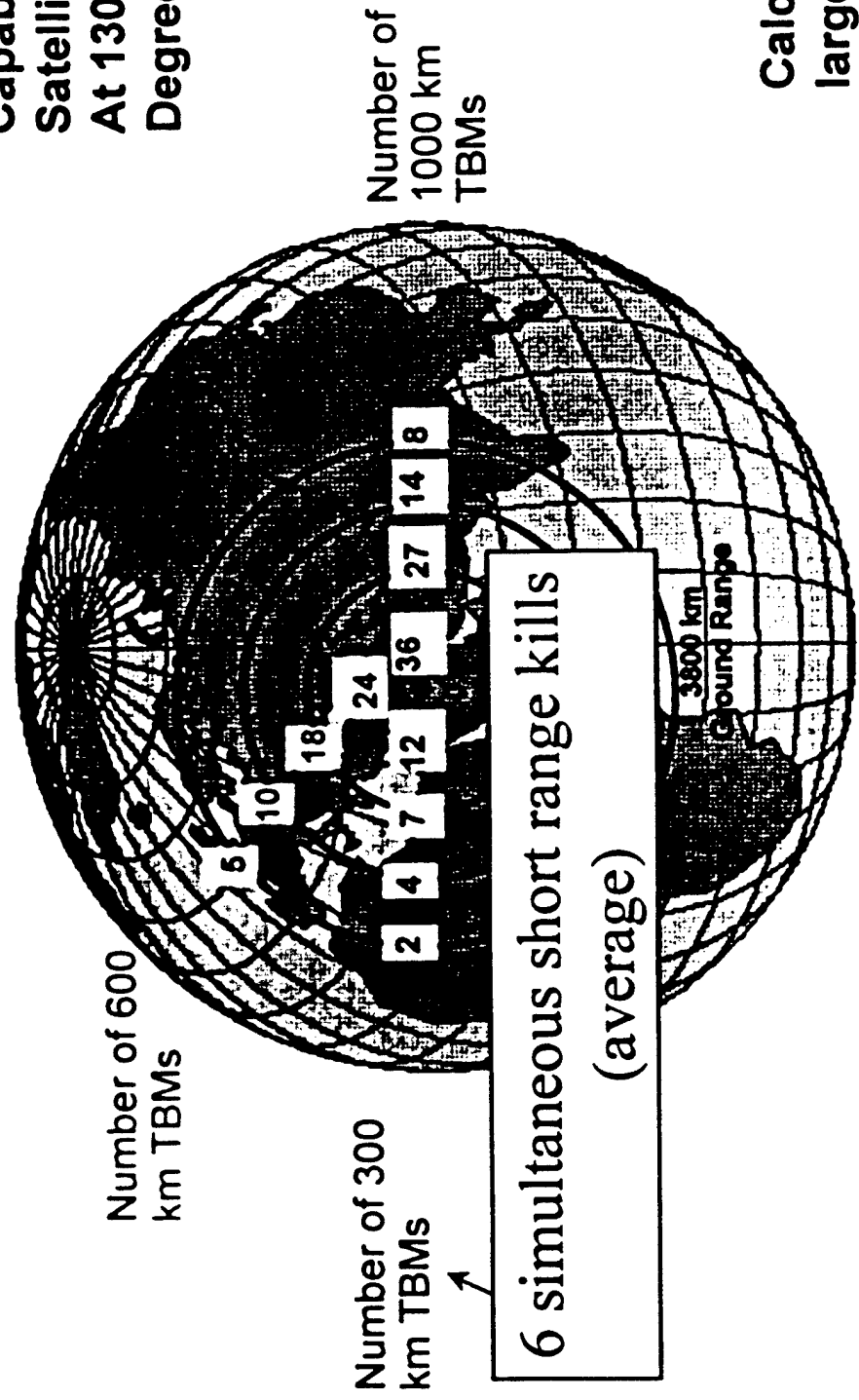
**Calculated using a large number of ISAAC runs**

Number of 1000 km TBMs

Number of 600 km TBMs

Number of 300 km TBMs

6 simultaneous short range kills (average)

3.3-3-9

72036

- Linear decrease with time delay confirmed
- 10 simultaneous kills for short range TMD

## Effectiveness Tied to Early Weapons Release Authority

**NMD**

Russia → US



Missiles Negated

50 40 30 20 10

5 45 85 125 165 205

Seconds after cloud break engagement initiated

**TMD**

N. Korea → Japan



Missiles Negated

50 40 30 20 10

5 25 45 65

Seconds after cloud break engagement initiated

N. Korea → S. Korea



Missiles Negated

50 40 30 20 10

5 15 25
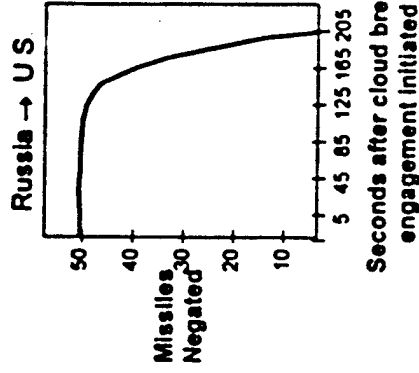
Seconds after cloud break engagement initiated
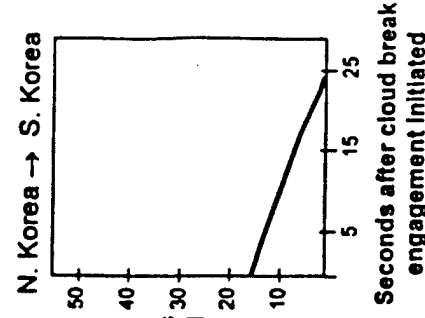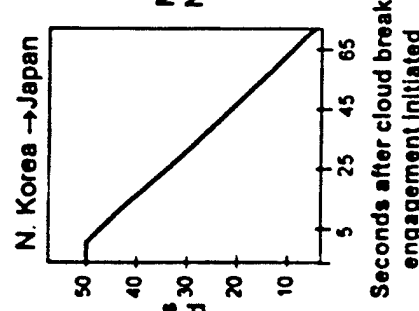
- **Centralized battle management of platforms to maximize effectiveness**
- **Maximum allowed lasing time ~ 15 s per shot, boost-only kills**
- **50 simultaneously launched missiles (at randomly selected time point)**
- **24 Satellites for NMD, 4 rings of 6, 1300 km altitude, 58° inclination**

34

# TMD Baseline
# Cost Optimum

**Original TMD Baseline**



RELATIVE POWER

3.3-3-11
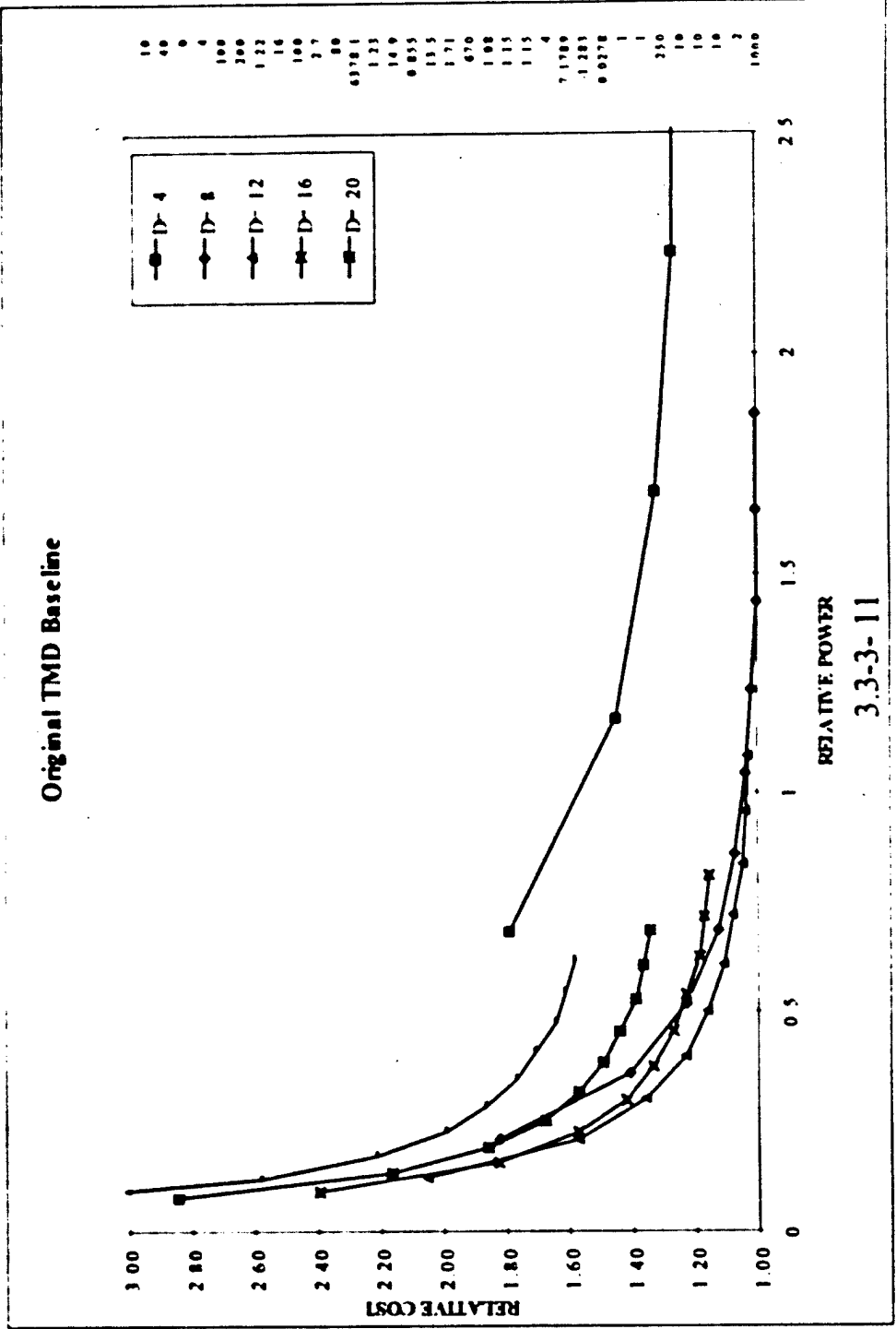
# TMD Baseline
# Platform Number
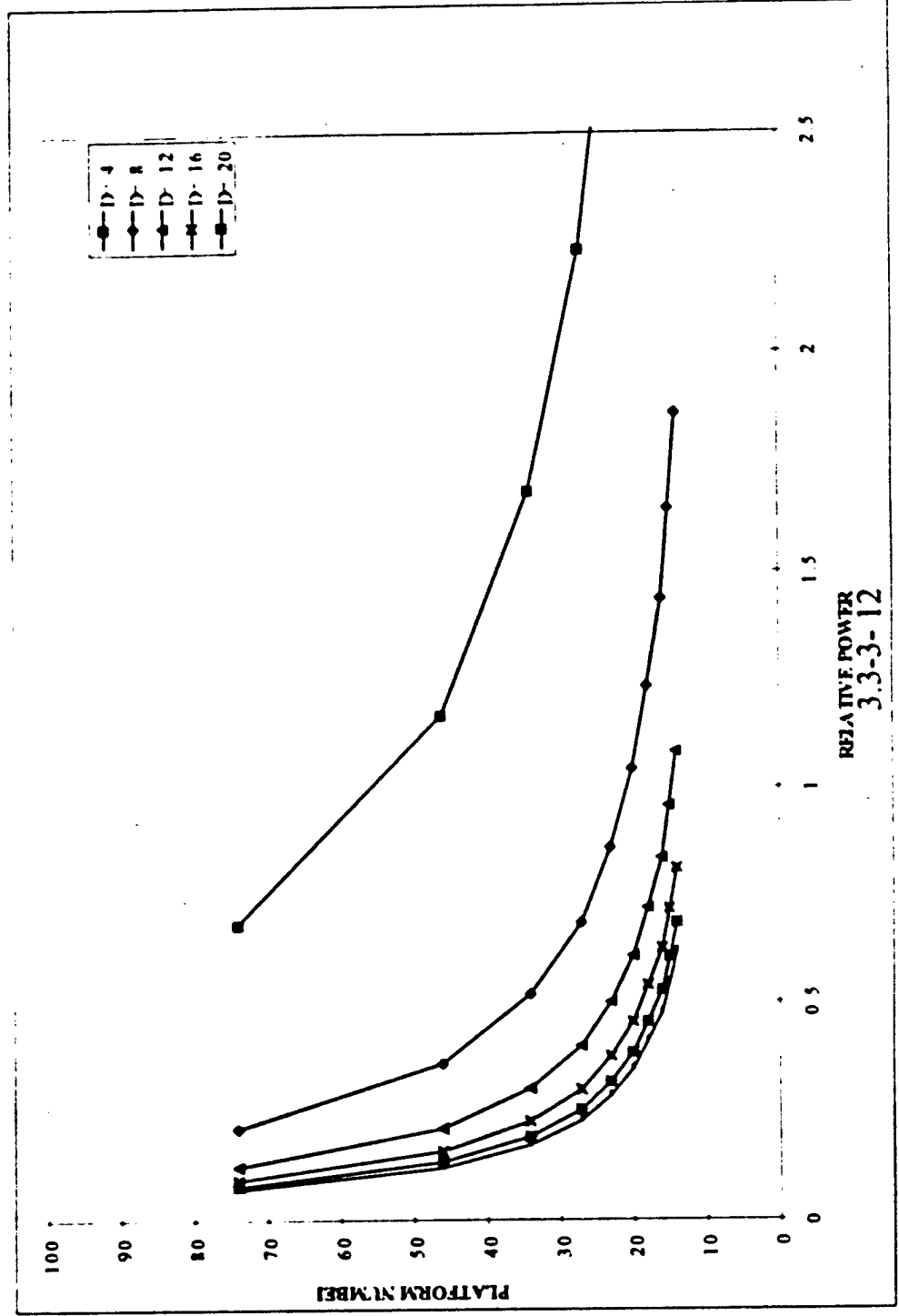
# TMD Baseline
# Deployment Altitude
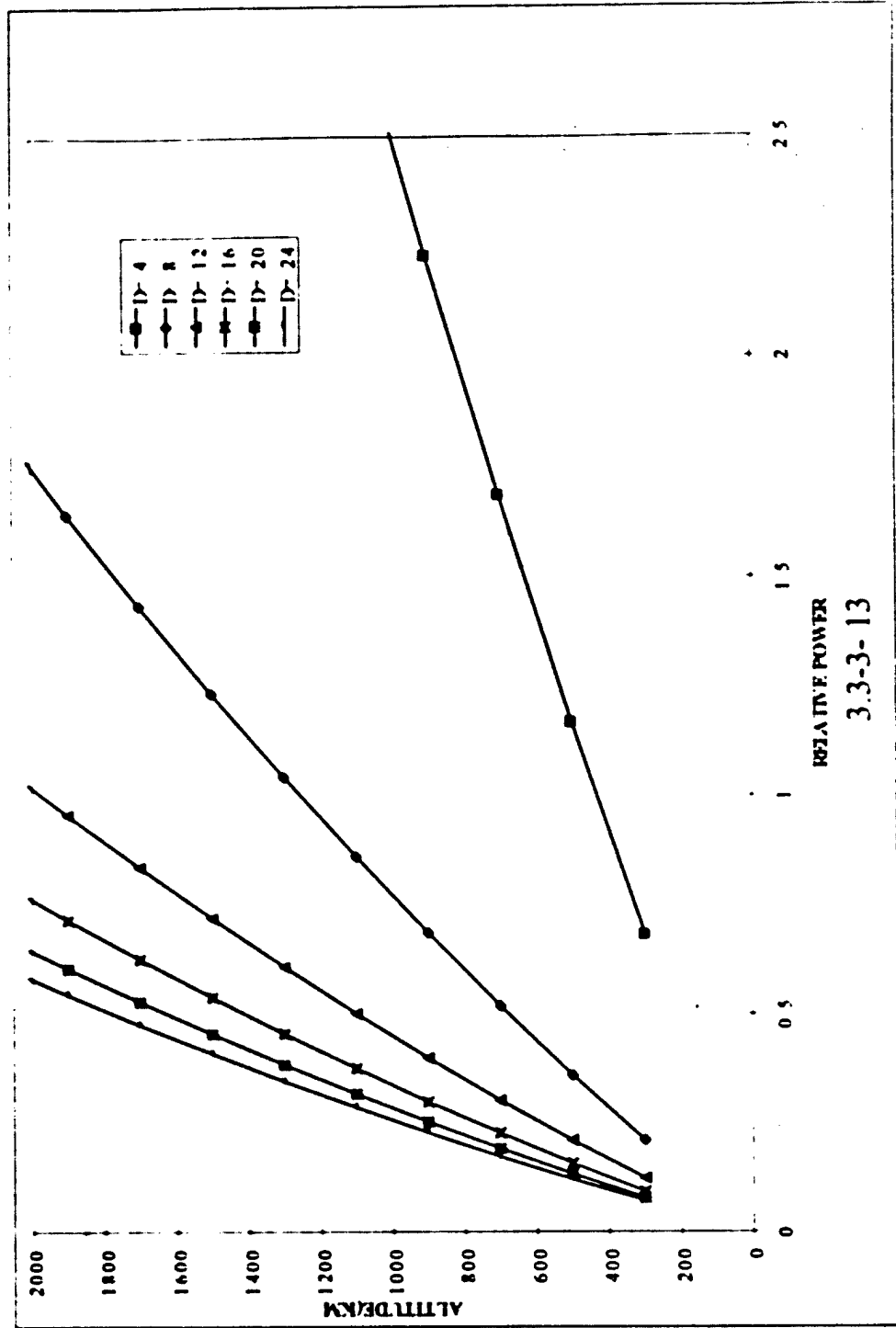


RELATIVE POWER

3.3-3-13

13

# Classified charts

- High performance levels for SWAN and NEA

3.3-3- 14

# Lethality Assumptions

## AFRL estimate



## S. Howie estimate
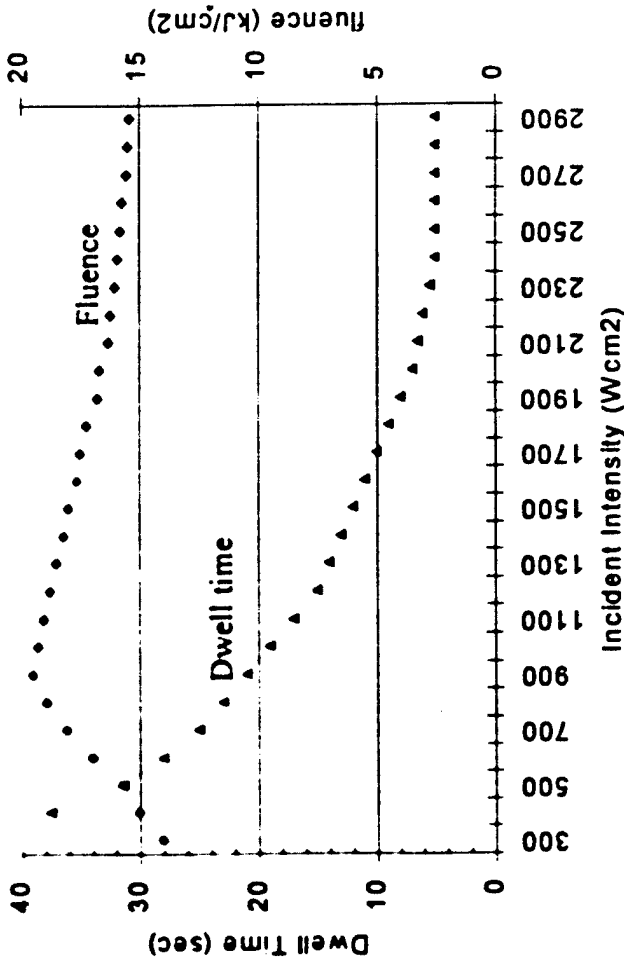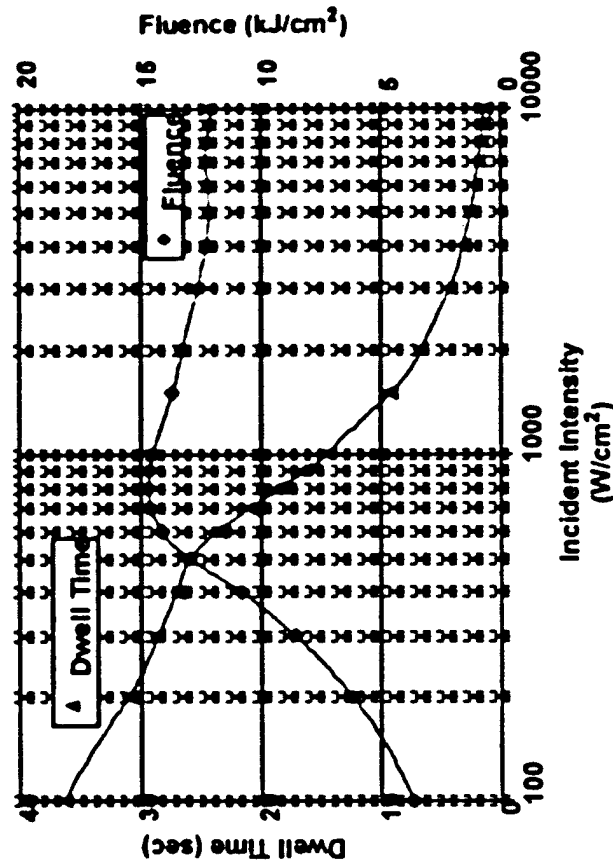


The intensity regime between 100-500 W/cm$^2$ drives the constellation sizing problem.

3.3-3-15

15

# Far-term TMD
# Cost Optimum

Advanced TMD
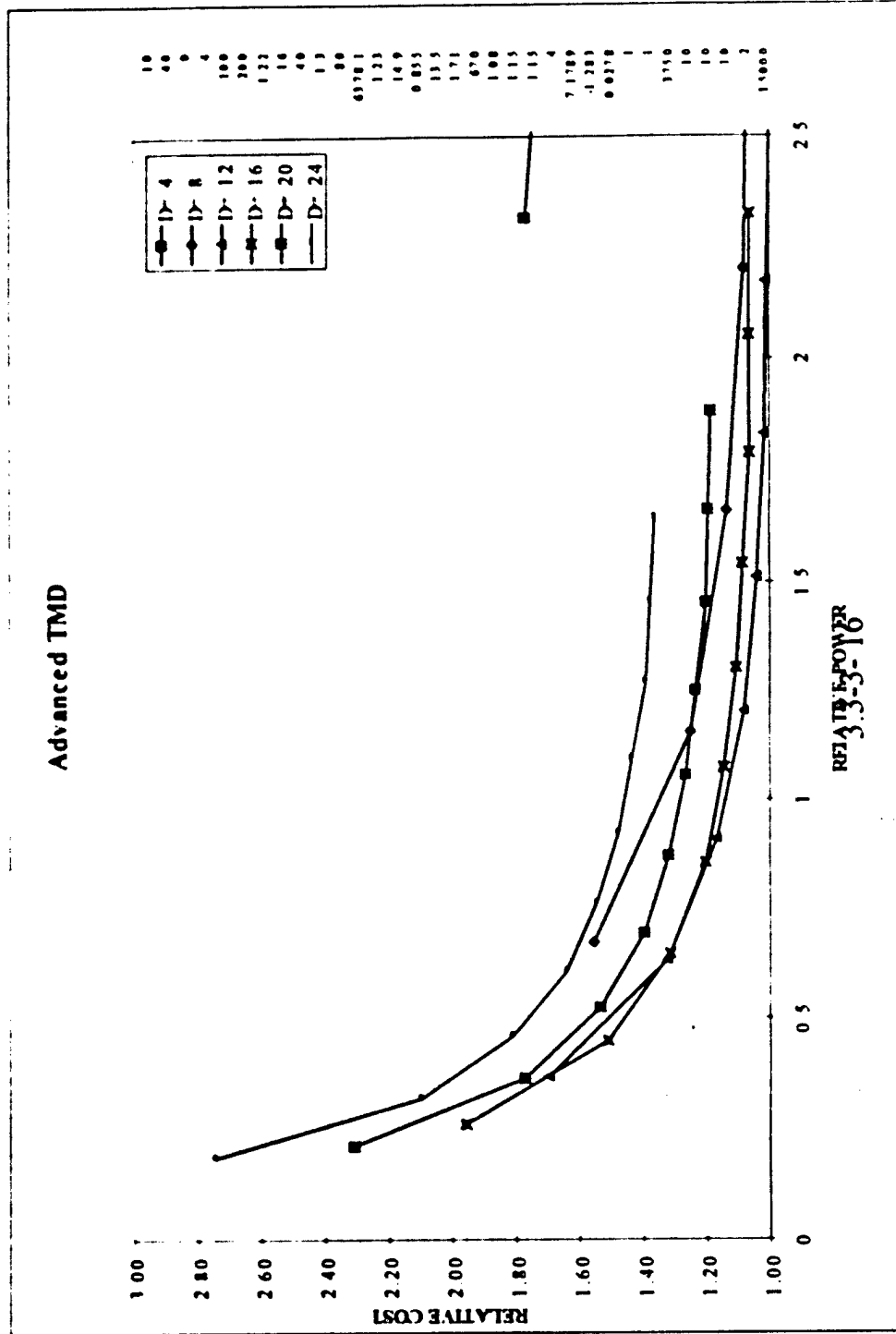
# Far-term TMD
# Platform Number
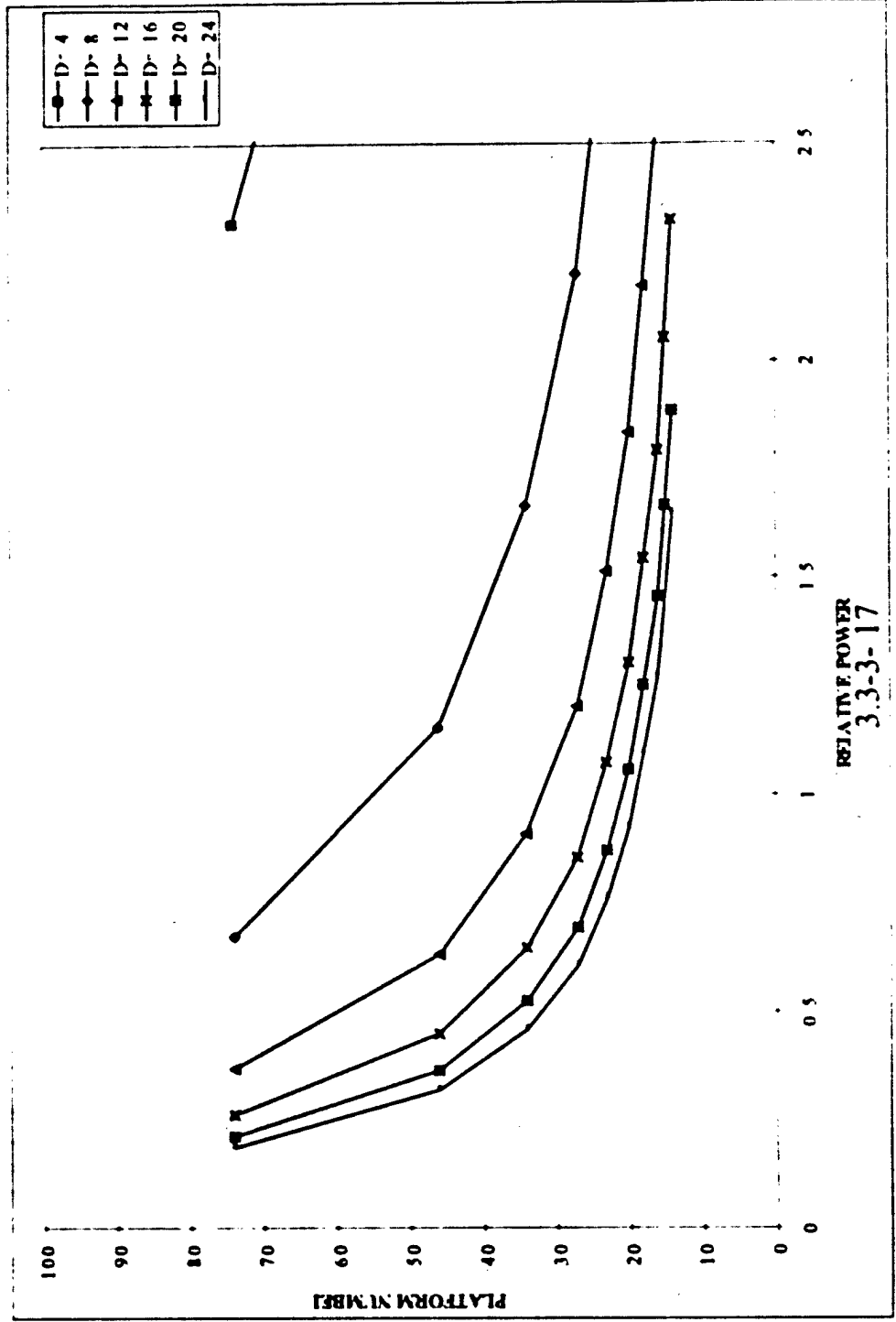
# Far-term TMD
# Deployment Altitude
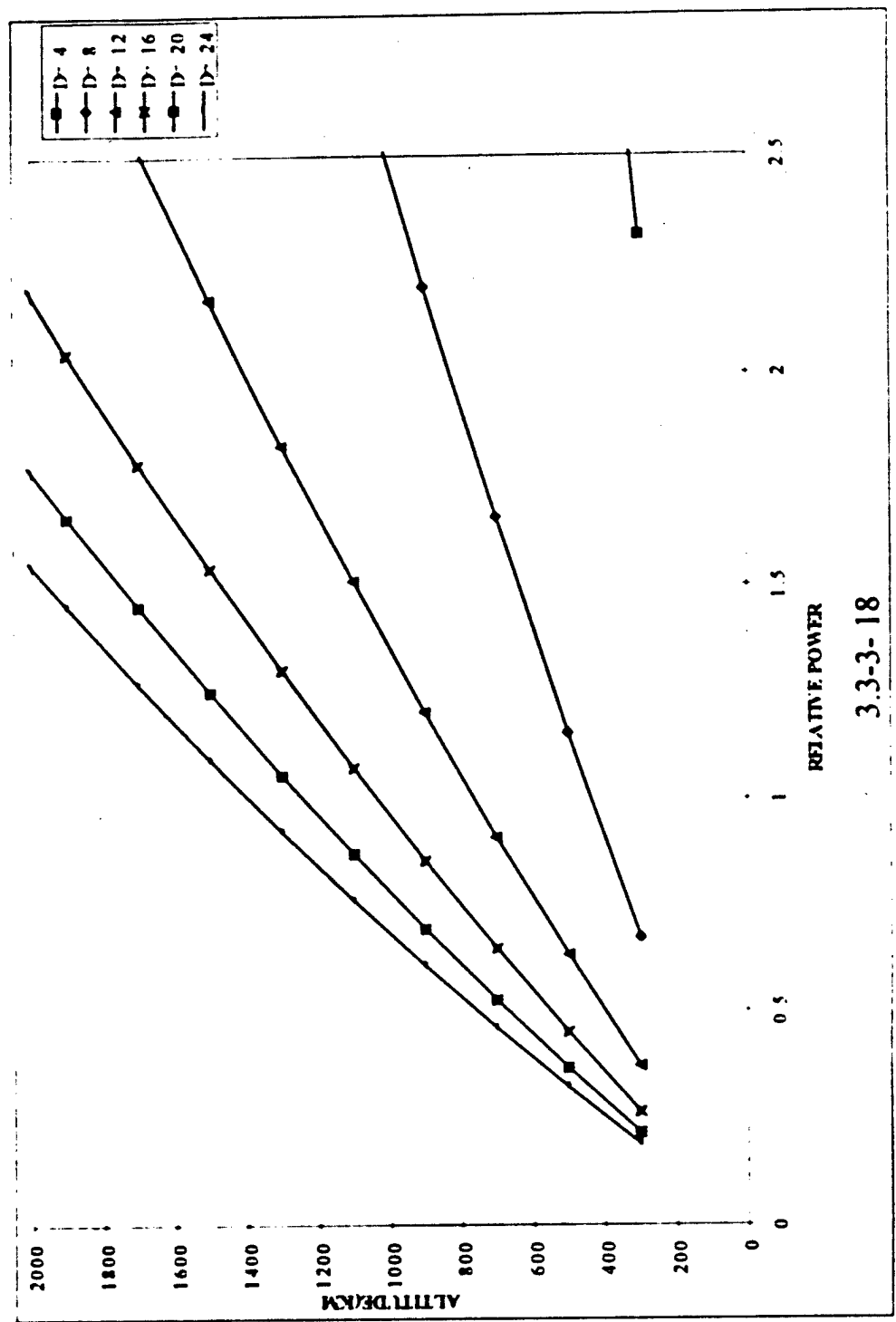
3.3-3-18

**Appendix 3.3-4**

**Technical Presentations**

*Schafer*

# Bifocal Comments/Suggestions

Gary Golnik
Schafer Corporation
1 June 1998

3.3-4-2

*Schafer*

## Design Drivers

- Power losses to receiver mirror (absorption, scintillation, phase errors)

- Beam size at receiver

- Receiver-side beacon correction

- On-board beam control

- CMG et al noise (large torques required)

- Two-body pointing (two precise LOS at once)

- Off-axis (unobscured) telescope design

- Tracker integration with fighting mirror LOS

- Dual DM control separation (residuals tend to be at same frequencies)

3.3-4-3

# Schafer

## Comments continued

- Bifocal is not "less glass in space" but ~2x SBL

- Gimbal flats missing

- Concept shows no tie between front and back end beam control (ASE?)

- Comparing cost of a heavy monolith with a light deployable makes no sense. Showing deployables at 10-15 kg/m2 is grossly optimistic.

- Leonard-SBL at 5200 km with only 20% more power than at 1200 km makes no sense.

- Small high power mirrors not an issue– first two briefings both claim they are.

3.3-44

# Schafer

## Paradigm Shifts

- Large optics real costs must fall to small fraction of laser costs.

- Beam control systems must achieve near-perfection.

- Very-high-stiffness, high-damping structures needed to get adequate resonant frequency to solve two-body pointing stability in face of large torques required.

- Low absorptivity coatings on large optics.

# Schafer

# Electric vs. Chemical Laser Status Update

Richard T. Demers

Douglas M. Allen

Gary Golnik

Schafer Corporation

7 July 1998

3.3-4-6

# Outline

**Schafer**

- Laser Concepts
- Power Generation Concepts
- HF / COIL / Electric Comparisons
- Plans

3.3-4-7

**Schafer**

Laser Concepts

3.3-4-8

# Device Architectures

1. Heat capacity solid-state laser concept

   • Advantages
      • No aberrations due to cooling gradients
      • Lower power demand-sequential lasing and cooling cycles
   • Materials development required (GGG)
      • Improved quality and larger crystal size
   • Gain medium mass is proportional to output power
   • LLNL's GPOW - Global Precision Optical Weapon
      • >100 kW average pwr, 4 MJ burst energy, 20 m aperture

# Device Architectures (cont'd)

## 2. Conventional DPSSLs

- Power oscillators
  - Hughes, LLNL Yb:YAG lasers 1 kw lasers
  - Scale to 100 kW using moving media
    - Rotating discs
    - Linear motion slabs

- MOPAs
  - LLNL's Mercury Laser - power amp
    - 100 Joule @ 10 Hz in 2000 A.D.
    - Scale to Mjoule for IFE-Inertial Fusion Energy System
    - Electrical/Optical efficiency goal of 10%
  - TRW's ATLAS 1 kw, $M^2 < 1.1 \times DL$

3.3-4-10

# Device Architectures (cont'd)

3. Power scaled diode-pumped fiber lasers

- MDA's HPFOL (High Power Fiber Optic Laser)
  - Phase modulation of $\sim 10^7$ 100-watt fiber amps using adaptive wavefront control
  - ~70% optical conversion efficiency of fiber amp at low power

4. Diode-pumped gas lasers

- Boeing/Rocketdyne patented concept for coherent pumping of gases was previously demonstrated in low power devices under a ONR/IST program. There is no ongoing program to demonstrate and develop diode-pumped gases.

# Light Source Heat Generation

*Schafer*

Diode laser generated heat

- Electrical dissipative - diodes are ~ 40-50% wall-plug efficient

- Unabsorbed pump light ~ 5-30% of pump

Gain medium quantum defect

- Yb:YAG - 8 %

- Nd:YAG - 24%

- GGG (for GPOW) ?

3.3-4-12

# Diode Laser Characteristics

**Schafer**

- Diode lasers require low voltage, high current

- Diode laser performance under continuous improvement

  - Typical lifetimes ~ $10^5$ hours@ 20% output reduction

  - Aluminum free devices last longer

  - Electrical efficiencies

    - Currently 50% for commercial devices

    - Research trendline extrapolates to >65% in 2000 A.D.

  - Cost of ownership

    - Currently ~ $20/cw watt for commercial devices

    - Historic trendline extrapolates to well under $1/cw watt in 2000 A.D.

3.3-4-13

**Schafer**

# Power Generator Concepts

3.3-4-14

**Schafer**

# Power Source for Electric SBL

- Background

- History

- System Requirements

- Technology Options

- Task Plan

3.3-4-15

## Background

**Schafer**

- BMDO working on HF chemical laser system

- AFRL presentation on "Power Generation for Electric Weapons"

  - Possible new alternatives for an electric SBL

  - Technology derived from other BMDO and AF programs

  - AFRL has new power technology budget starting in FY00 for high power space systems

  - Presented opportunity for cooperative program

- Previous SDIO/BMDO work on FEL, NPB, CPB is still relevant

  - Power system design work

  - Some components have been improved

  - Most of the work done in the 1983-1992 timeframe

3.3-4-16

# History

**Schafer**

- Mid to late 80s - SDI Space Power Architecture Study
  - SDIO funded, managed jointly by NASA LeRC & Sandia National Laboratory
  - TRW, GE, Martin Marietta were prime contractors
  - Evaluated 20 alternative system approaches to providing multiple MW in space
  - Recommended most promising technologies for development
  - Basis for >$100M SDIO investment in technology development in late 80s-early 90s
  - Schafer has all of the system spreadsheets used for technology comparisons

- Late 80s - early 90s - SDIO power technology component development
  - Baseload and burst power technologies
  - Nuclear and non-nuclear technologies
  - Power generation, storage, conversion, distribution
  - Many technologies funded
  - Many breakthroughs achieved, many problems uncovered
  - Primary SDIO agent for power technology was what is now AFRL (Wright-Patterson)

- Early 90s - BMDO Dewpoint program to develop system demonstration
  - Directed Energy Weapons Power Integration
  - Power system for an NPB
  - Managed by Sandia with participation from SMDC and AFRL
  - System engineering and pulse forming network were key development items
  - Program terminated in 1993 due to declining interest at BMDO in electric powered weapons

3.3-4-17

# *Schafer*

## History (continued)

- Mid - late 90s - AFRL development of More Electric Aircraft (MEA)
  - Goal was improved reliability and O&M costs
  - Eliminate gear boxes, replace hydraulic lines with fault tolerant electric systems
  - Technology transitioned to C-141, F-16, others
  - Increasing power generator size on aircraft

- Mid - late 90s - BMDO optimally cooled GBR technology program
  - IS&T program to improve range and Pd of future TMD GBR systems
  - Agents are SMDC for radar and AFRL for power
  - Includes development of a MW HTSC generator and 99% efficient cooled DC/DC converters

- Late 90s - AFRL electric airborne laser studies
  - Recent development, part of reason for briefing to BMDO on electric SBL possibility
  - Also recent AFRL decision to increase spending on space power for SBR, weapons starting in FY00 ($1-3M/yr)

3.3-4-18

## References

*Schafer*

- M. Edenburn and J. Smith, Summary and Evaluation of the Strategic Defense Initiative Space Power Architecture Study, NASA Technical Memorandum 102012, March 1989

- R. Wiley, Scaling of Space Based Prime Power Power Systems for SDIO-Type Applications, Auburn University Space Power Institute, May 1989

- J. Gavin, et. al., Advanced Power Sources for Space Missions, National Research Council Report, National Academy Press, 1989

- J. Beam, "Power Generation for Electric Weapons," Presentation to BMDO/TOD, March, 1998

- G. Morr, "Comparison of COIL and HF Lasers for Space Applications," SAIC presentation, 1998

- Various program review materials from the Optimally Cooled GBR program, More Electric Aircraft program, Li-ion program, Dewpoint program,and others, 1989 - 1998

3.3-4-19

# Power System Requirements

**Schafer**

- Keys to selecting best technology are power level and voltage
- Analysis to date is based on solid state lasers
  - MW class lasers
  - Low voltage -- means high current source
- For space based application, key considerations are:
  - System size and mass
    - Due to launch vehicle constraints and costs
  - Component recurring costs
  - Reliability
    - Could be in place for years before needed, then must work
  - Efficiency
    - Effects size and mass of reactants or energy storage system required
  - Impact on other spacecraft systems
    - Effluent exhaust and rotating machinery torquesmust be designed to have little impact on laser pointing
  - Technology maturity
    - Is it feasible for a near term demonstration
  - Required run time
    - Both per engagement and total - effects reactant/tankage requirements and technology trades

3.3-4-20

*Schafer*

# Technology Options

- Power generation

  - Turbine/generator (as proposed by AFRL)
    - SOTA is AFRL programs for MEA and Optimally cooled GBR
    - 70% turbine efficiency appears possible with high delta-T (radiator size an issue)
    - 99.5% generator is designed - appears feasible
    - System engineering for use on spacecraft is not trivial - cooling, spacecraft interactions need to be analyzed

  - Fuel cells
    - 70 to 80% efficiency possible with latest electric vehicle and Army technologies
    - Size and mass are the biggest issue
    - Biggest advantage is can design stack to deliver exactly the current and voltage required by the laser, plus no moving parts

  - Solar arrays (charging an energy storage device to power the laser)
    - Rechargeable batteries are getting lighter (but still tend to be heavy)
    - Time between engagements could be an issue (to charge batteries)
    - Solar power is nearly free - may have to increase size a little from baseload, but no reactants required
    - No moving parts

  - Primary lithium batteries
    - Available now, but tend to be heavier than other options
    - No moving parts

  - MHD
    - Usually best for very high power (10s of MW)

3.3-4-21

**Schafer**

# Technology Options (cont.)

- Energy storage
  - Rechargeable batteries (Li - ion, Na-S, others)
    - Large DoD/NASA program for Li-ion development at 100 Whr/kg starting
    - Na-S demonstrated in flight recently, also 100 Whr/kg, operates at 350°C
    - Electric vehicle programs have driven technology for last decade
  - Flywheels
    - AFRL/NASA LeRC program for dual mode flywheel/attitude control system
    - Probably heavy for this application
  - Superconducting magnetic energy storage
    - Has been very heavy in past comparisons - needs to be reevaluated with HTSC advancements

- Cooling
  - Thermal energy storage
    - Past Electric SBL studies showed this to be lowest mass approach - collect heat in phase change material, then dissipate through heat pipes to small radiator over time
    - Minimum time between engagements drives system mass
    - Phase change medium selected based on temperature of heat rejected from power generation system
  - Radiators
    - Carbon-carbon is SOTA, BMDO/AFRL white coatings developed for radiation tolerance
    - Flexible heat pipes developed in late 80s to allow deployable radiators for large heat loads

3.3-4-22

# *Schafer*     Technology Options (Cont.)

- Power conversion/power conditioning
  - Refrigerated DC/DC converters (as proposed by AFRL)
    - Product of BMDO funded SBIR program - 50V to 8V conversion at >99% operating at 240K to be demonstrated this year
    - Also working on 200V to 50V converters at same efficiency
    - System issue is cooling required vs. higher efficiency of higher temp converters .
  - Pulse forming networks (for pulsed lasers or particle beams)
    - Dewpoint designs are still SOTA
    - Most work is on high voltage systems (kVs)
  - Advanced capacitor technology (ultracaps, ceramic capacitors)
    - Again, doesn't apply directly to CW systems
    - Ultracaps good for seconds, ceramics for fractions of a second
- Nuclear reactors
  - Not a realistic option for technical, cost, and political reasons

3.3-4-23

# Schafer

## Concept for Comparison of Chemical Lasers

•Energetic Species Generation, $e_1$

•Optical Power Extraction, $e_4$

•Energetic Species Transport, $e_2$

Output Beam

Exhaust Gas to Space

•Inject Cavity Gas and Generate Excited Species, $e_3$

Reactants and Carrier Gas

Cavity Gas

Reactant Storage and Feed
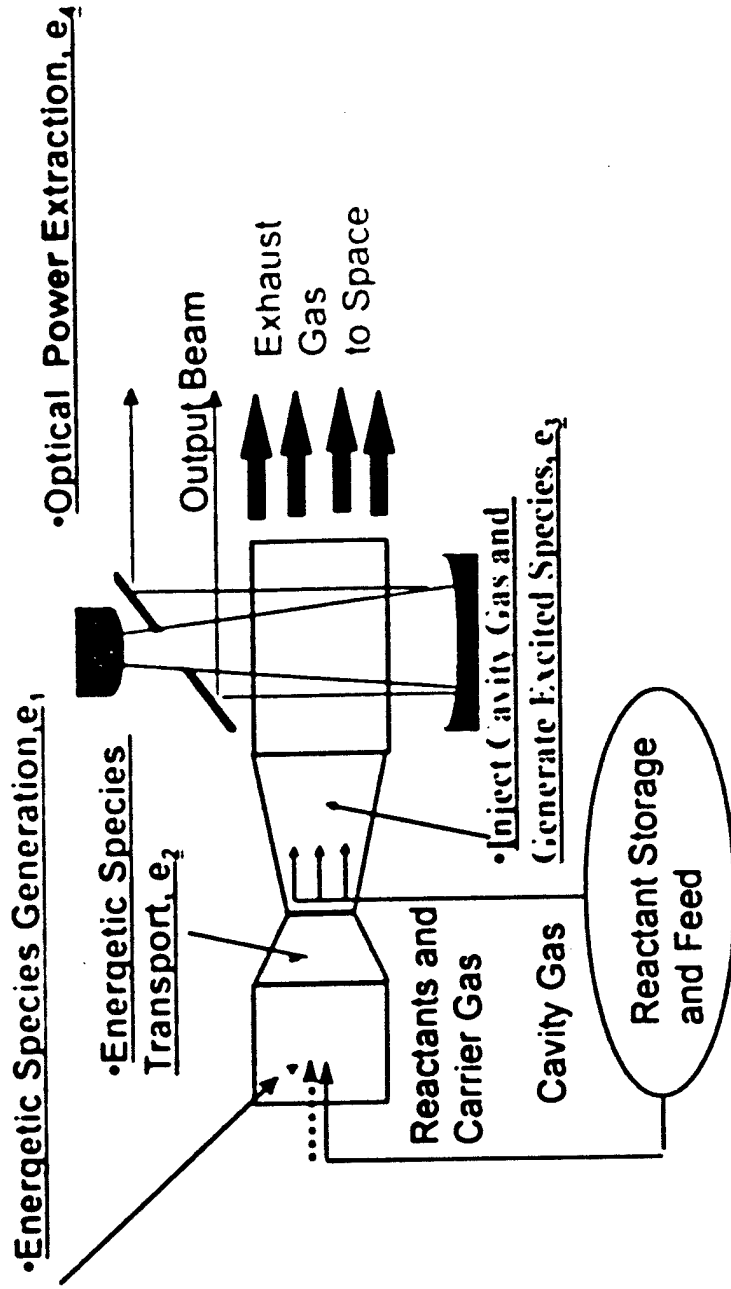
•Identify Key Processes
•Define Efficiency Factors
•Compare Efficiencies for COIL and HF

3.3-4-24

# Schafer — Concepts for Comparison of Electric Lasers

•Energetic Species Generation, $e_1$

•Optical Power Extraction, $e_4$

Output Beam

Thermal energy removal system

Laser medium

•Electrical energy pumping diodes

•Diode energy pumps disks or fibers or gas

Diodes

Reactant Storage or Batteries/Flywheel

Power conditioning

Turbo generator or solar cells
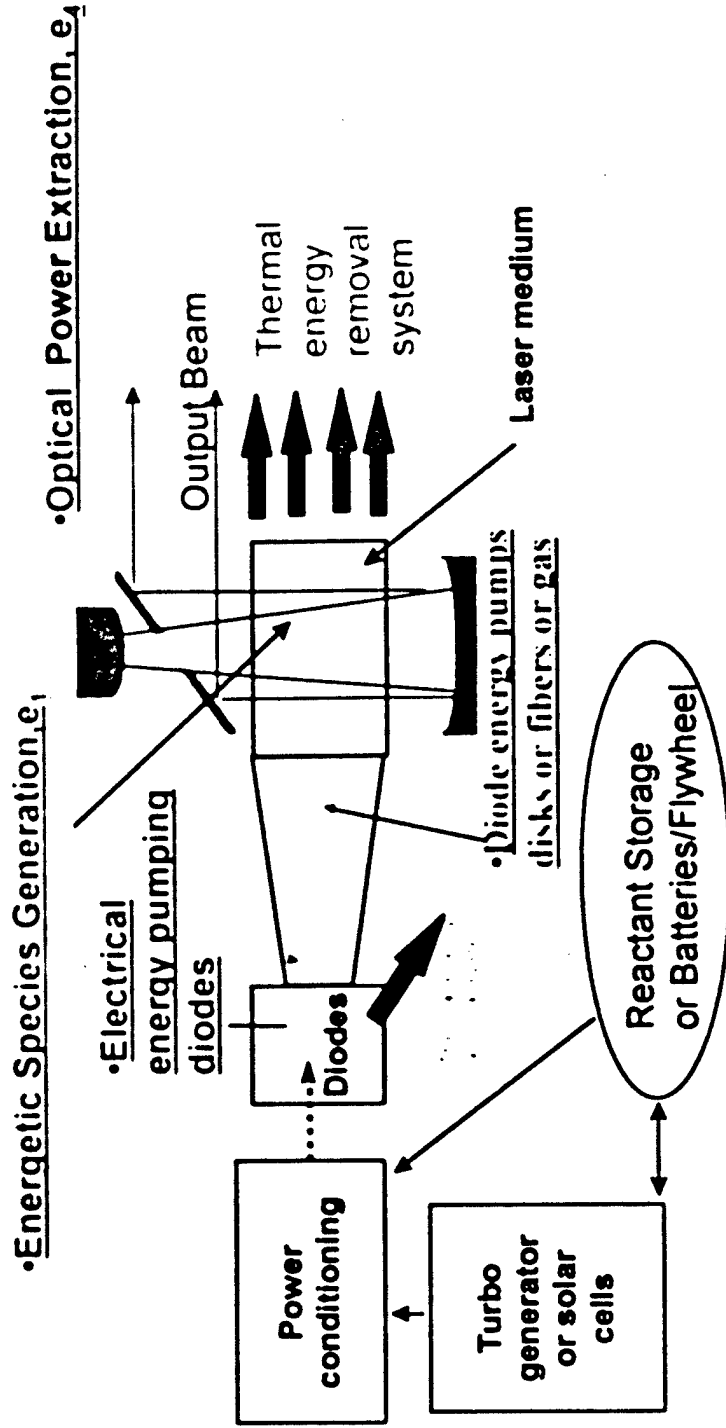
•Identify Key Processes
•Define Efficiency Factors
•Compare Efficiencies for Chemical and Electrical

3.3-4-25

# System Concept for COIL

**Schafer**



Exhaust

Exhaust Assembly

Optical Cavity

Optical Resonator

Cavity Injector

Iodine-Helium

Counterflow Spray Generator

BHP

Chlorine-Helium

Spray Cooler

Vapor

BHP Conditioner

Reactant Storage and Feed Assembly

3.3-4-26
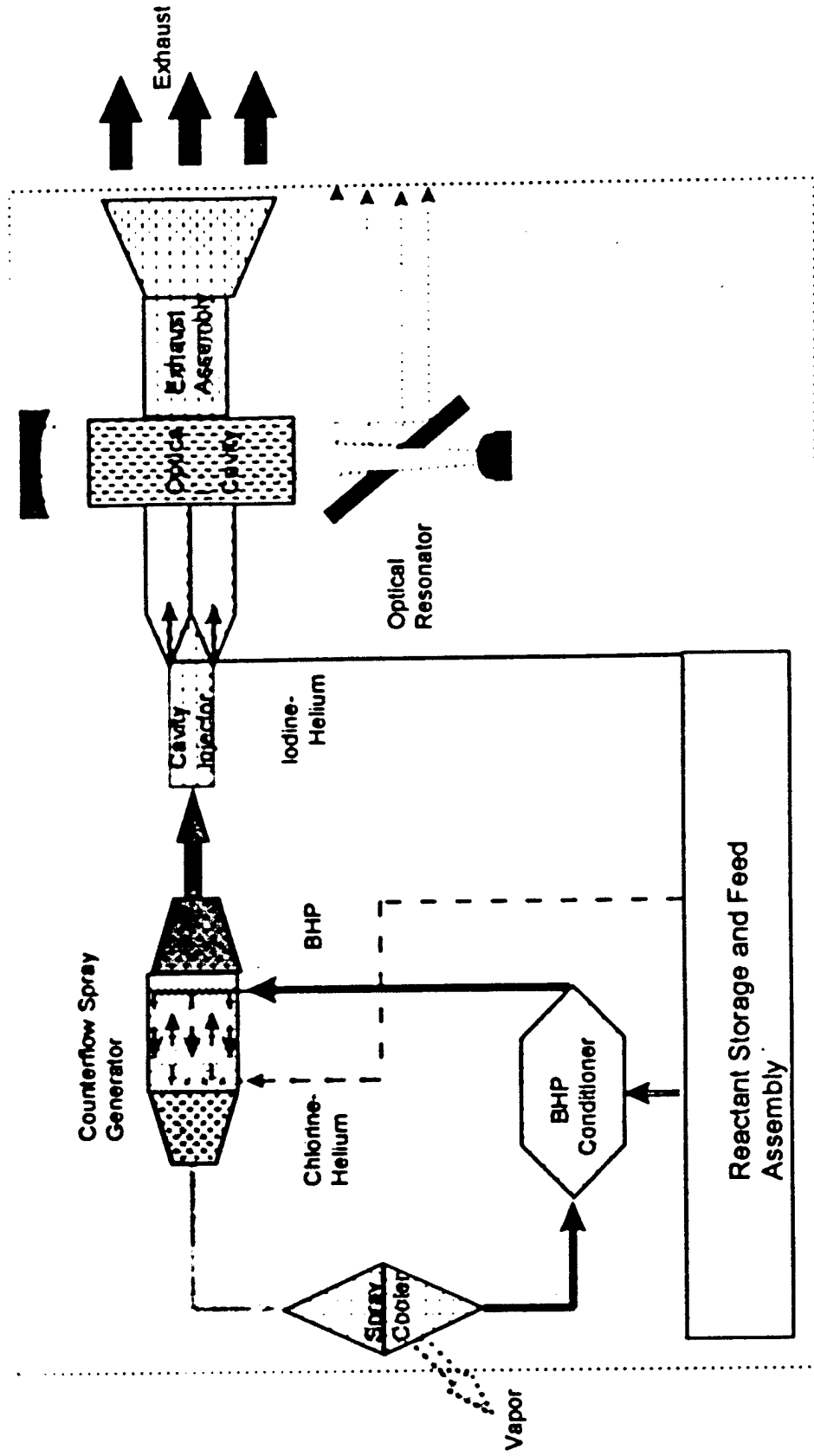
# Schafer System Concept for Electric (Turbo/heat capacity)



Exhaust or radiators

Heat removal

Optical Cavity

Optical Resonator

Diode lasers

Power conditioning

Turbogenerator

Exhaust gas

Reactant Storage

Thermal cycle time may require multiple laser cavities

3.3-4-27
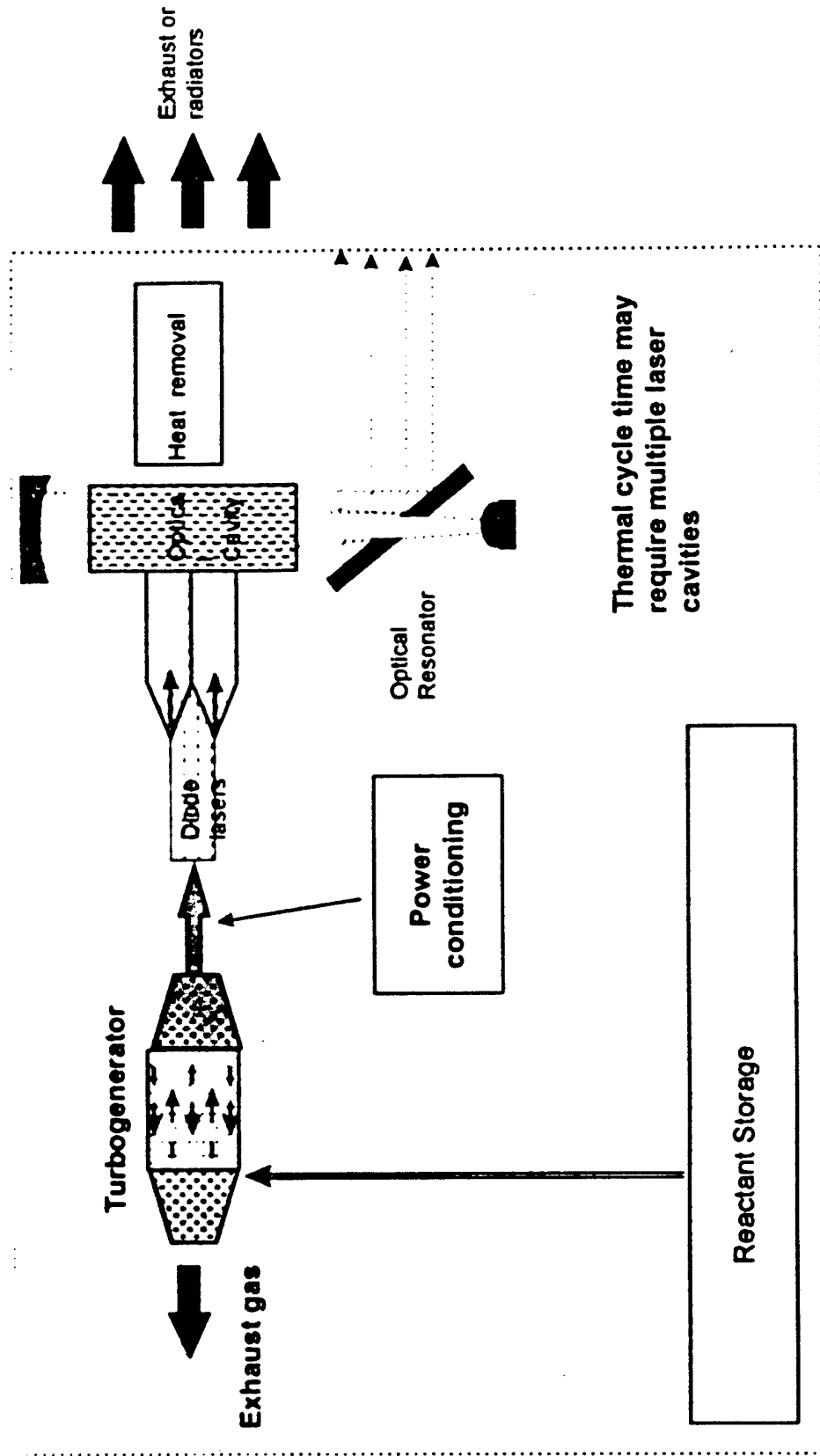
# *Schafer* System Concept for Electric (solar/heat capacity)

Exhaust or radiators

Heat removal

Optical Cavity

Optical Resonator

Diode lasers

Thermal cycle time may require multiple laser cavities

Power conditioning

Flywheel

Batteries

Solar cells

3.3-4-28
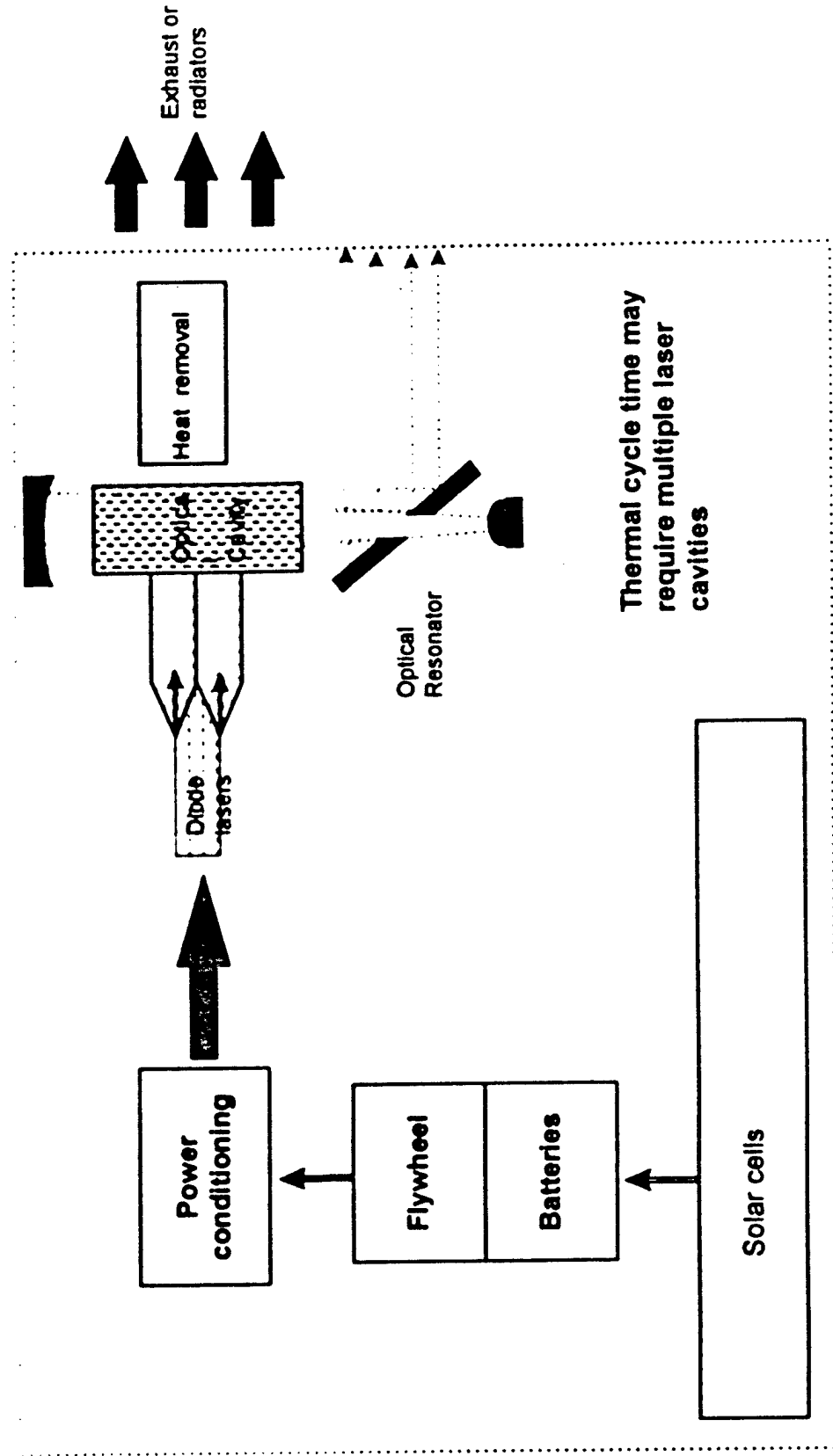
# Key Chemical and Electrical Laser Processes

| Process | COIL | HF Laser | Electric |
|---------|------|----------|----------|
| Generate Energetic Species, $e_1$ | Mix $H_2O_2$ and KOH to Form BHP (Exothermic)<br>Inject $Cl_2$ to Generate $O_2(^1\Delta)$ (Exothermic) | Inject and Burn Fluorinated Oxidizer and Deuterium to Generate Atomic Fluorine | Chem   Solar<br>Burn $H_2O_2$   Solar cells<br>hot gas   feed batteries<br>turbine gen- or flywheel erates electricity |
| Transport Energetic Species, $e_2$ | Transport $O_2(^1\Delta)$ to Cavity Injector (Ducting and Cold Trap), $Y_c$ | Transport Atomic Fluorine to Cavity Injector, C9 | Condition power and transport to diodes |
| Inject Cavity Gas and Generate Excited Species, $e_3$ | Inject Iodine-Helium Gas Mixture<br>Dissociate Iodine<br>Transfer $O_2(^1\Delta)$ Energy to Generate I* | Inject and Mix Atomic Fluorine and Hydrogen<br>Produce HF* by F+$H_2$ Cold Reaction | Diodes pump amplifier, generating excited species and heat |
| Extract Power with Optical Resonator, $e_4$ | Deplete $O_2(^1\Delta)$ by I* Energy Extraction and Repetitive pumping with $O_2(^1\Delta)$ | Deplete Gain for all HF* by Extraction by Optical Resonator | Deplete gain, cool or let temp rise to limit |

3.3-4-29

# Schafer    Definition of Figures of Merit

- Thermal Efficiency, $\eta_t$

  – $\eta_t$=(Output Beam Energy)/(Energy Released by Chemical Processes)

  – $\eta_t=e_1 \cdot e_2 \cdot e_3 \cdot e_4$

- Specific Energy, $\sigma$

  – $\sigma$=(Output Beam Energy)/(Mass of Reactants Supplied)

- Auxiliary Heat Rejection Ratio, HRR

  HRR=(Energy Rejected by Auxiliary Heat Exchanger)/(Output Beam Energy)

- Electric Laser Figures of merit more complex and dependent on type

3.3-4-30

# Electric Laser Figures of Merit

- Thermal Efficiency
    - $\eta_e$ = Output beam energy / total available energy dissipated ($1-\eta_e$ = heat which must be handled)

    - $\eta_e = E_1 \, E_2 \, E_3 \ldots$

- Specific Energy
    - $\sigma_e$ = output beam energy / non-common mass of electrical generation and storage (can be defined by reactants in turbogenerator concept)

- HRR
    - $1-\eta_e$

- Different processes limit run time, depth of magazine, etc.

# Definition of Efficiency Factors

## Efficiency Factor for Energetic Species Generation, $e_1$

- $e_1 =$ (Energy of "Energetic Species")/(Energy Released by Chemical Processes)

- **COIL**

  - $e_1 =$ (Energy of $O_2(^1\Delta)$)/(Heat of $BHP$ Formation+Heat of Chlorine Reaction+ Energy of $O_2(^1\Delta)$)

  - $e_1 = 22.54$ kCal/(11.95+26.29+22.54) kCal

- **HF**

  - $e'_1 =$ (Energy of F+H$_2$ Cold Reaction)/(Energy of Combustion to Produce Atomic Fluorine+ Energy of F+H$_2$ Cold Reaction)

  - $e'_1 = 31.7$ kCal/(Combustion Energy+31.7 kCal), Where Combustion Energy is Dependent on Reactants, Carrier Gas, Combustion Temperature and Pressure

- **Electric**

  - $E_1 =$ Total Energy Created by Solar Cells, Stored in Storage Divided by Total Energy Dissipated

  - $E'_1 =$ Electrical Energy / (Energy of Combustion to Form H$_2$O + hot H$_2$)(Turbogenerator Efficiency)

3.3-4-32

**Schafer** Definition of Efficiency Factors (cont.)

- Efficiency Factor for Transport of Energetic Species, $e_2$
  - $e_2$=(Moles Energetic Species at Cavity Injector)/(Moles Energetic species Generated)

- COIL
  - $e_2$=(Moles $O_2(^1\Delta)$ at Cavity Injector)/(Moles $O_2(^1\Delta)$ at Generator)
  - $e_2 = Y_c$, Oxygen Yield at Generator

- HF
  - $e'_2$=(Mass of Atomic Fluorine)/(Mass of Total Fluorine)
  - $e'_2=\alpha$ , Fluorine Dissociation Fraction at Cavity Injector

- Electric
  - $E_2$ = Electrical Energy Lost in Transport, Power Conditioning, and net optical power out of diodes
  - = Product of Efficiencies

3.3-4-33

# *Schafer* Definition of Efficiency Factors (cont.)

- Factor for Production of Excited State Species, $e_3$

  - $e_3$=(Energy Available for Lasing)/(Total Energy of Energetic Species)

- COIL

  - $e_3$=(Energy Available for Lasing with no Deactivation)/(Energy of $O_2(^1)$)

  - $e_3$=(Moles $O_2(^1)$ After Iodine Dissociation)/( Moles $O_2(^1)$ at Cavity Injector) $*(-H_{I*}/-H_{O_2(^1)})$

  - $e_3$=$(1-N_c(n_{I_2,Cl_2}/U)/Y_c) *(-H_{I*}/-H_{O_2(^1)})$, Where Nc is Number of $O_2(^1)$ Deactivations Required to Dissociate Iodine, $n_{I_2/Cl_2}$ is Molar Ratio of Iodine to Chlorine, and U is Mole Fraction of Chlorine Reacted

- HF

  - $e_3$=(Energy Available for Lasing with no Deactivation)/(Energy of $F+H_2$ Cold Reaction)

- Electric

  - $E_3$ = Energy Available for Lasing After Diode Pumping

  - = Efficiency of Diode Pump Process

3.3.4-34

**Schafer** Definition of Efficiency Factors (cont.)

Efficiency Factor for Energy Extraction, $e_4$

- $e_4$=(Laser Energy Extracted)/(Laser Energy Available with no Deactivation)

• COIL

- $e_4$=(Laser Energy Extracted(With Specified Losses))/(Laser Energy Available with no Deactivation)

• HF

- $e_4$=(Laser Energy Extracted(With Specified Losses))/(Laser Energy Available with no Deactivation)

• Electric

- $E_4$ = Laser Energy Extracted / Laser Energy Available (May Vary With Time and Temperature)

3.3-4-35

# Theoretical HF Power Extraction

*schafer*



POST-LASING POPULATION DISTRIBUTIONS
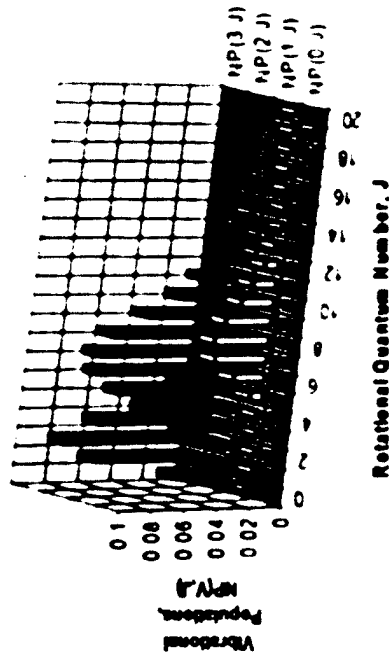
PRE-LASING POPULATION DISTRIBUTIONS
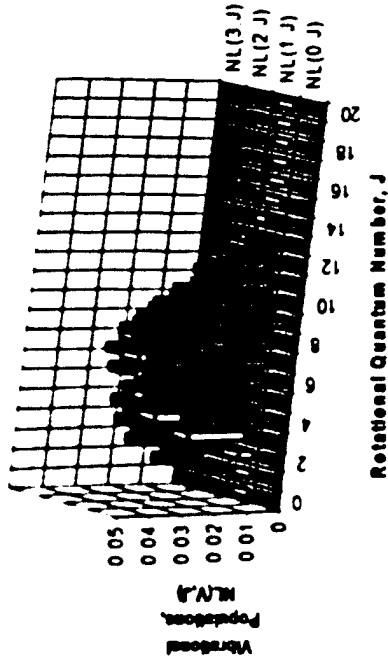
SPECTRAL INTENSITY DISTRIBUTIONS
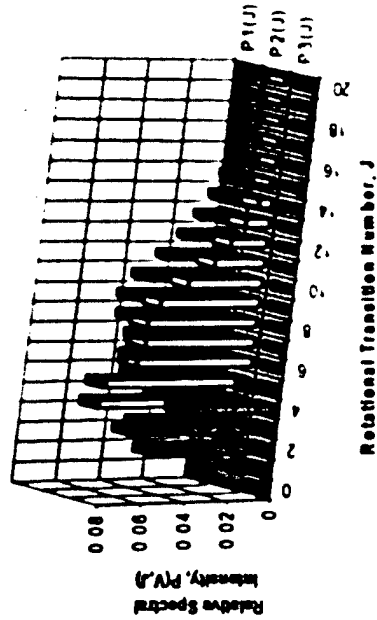
| Relative Pumping Rates | | |
|---|---|---|
| k1 | k2 | k3 |
| 0.3 | 1 | 0.5 |

| | E32(tot) | E21(tot) | E10(tot) | Esum |
|---|---|---|---|---|
| Molecular Transitions | 0.187602 | 0.48508 | 0.348471 | |
| Transitions Energy (Cal) | 1942.809 | 5255.843 | 3947.137 | 11145.79 |
| Fraction Total | 0.174309 | 0.471554 | 0.354137 | |
| Eta-chem (J/g-F) | | | | 2454.42 |

3.3-4-36

# Specific Energy and Heat Rejection Ratio

- Specific Energy, $\sigma$
  - $\sigma$=(Output Beam Energy)/(Mass of Reactants Supplied)
- COIL
  - $\sigma = U \cdot e_2 \cdot e_3 \cdot e_4 \cdot 94352$/(Mass of Reactants per g·Mole Chlorine)
  - $\sigma = U \cdot Y_c \cdot \eta \cdot 91000 \cdot (1 - N_c \cdot n_{I2/Cl2}/(U \cdot Y_c))/$   $(70.9 + 262.2 \cdot U + 253.8 \cdot n_{I2/Cl2} + 4 \cdot n_{He/Cl2})$ kJ/kg
- HF
  - $\sigma = e'_2 \cdot e'_3 \cdot e'_4 \cdot 132700$/(Mass of Reactants per g·Mole-F) kJ/kg, Where Mass per g·Mol-F=39.1, 92.8, and 72.2 for Theoretical, Demonstrated, and Projected Technologies
- COIL Heat Rejection Ratio
  - HRR=(Heats of BHP Formation+Chlorine Reaction+$O_2(^1\Delta)$ Quenching Energy+Sensible Heat of Peroxide and Hydroxide Solutions)/(Output Beam Energy)
  - HRR=$(11.95 + 26.29 + 22.54 \cdot (1-Y_c) + 13.11)/(22.54 \cdot e_2 \cdot e_3 \cdot e_4)$
- Electric

| Efficiency Factors | COIL | | | HF | | |
|---|---|---|---|---|---|---|
| | Theory | Current | Projected | Theory | Current | Projected |
| (1) Energetic Species Generation, $e_1$ | 0.37 | 0.37 | 0.37 | 0.72 | 0.36 | 0.48 |
| (1) Energetic Species Transport, $e_2$ | 0.80 | ~0.40 | 0.50 | 1.00 | 1.00 | 1.00 |
| (1) Energetic Species Production, $e_3$ | 0.93 | ~0.87 | 0.91 | 0.35 | 0.35 | 0.35 |
| (1) Laser Energy Extraction, $e_4$ | 1.00 | ~0.75 | 0.80 | 1.00 | 0.52 | 0.65 |
| Thermal Efficiency, $\eta_T$ | 0.27 | 0.10 | 0.13 | 0.25 | 0.07 | 0.11 |
| Specific Energy, * | 196 | 69 | 96 | 1194 | 262 | 421 |
| Auxiliary Heat-X Ratio | 3.34 | 11.04 | 7.65 | 0 | 0 | 0 |

# 𝒮𝒸𝒽𝒶𝒻𝑒𝓇  Electric Weight Comparisons

| Subsystem | Chem (CARD) | Laser Heat Capacity Turbo | Solar battery | Solar flywheel |
|---|---|---|---|---|
| Tanks, etc. | 13353 | 8000-? | NA | NA |
| Fuels | 11865 | inc. in above | NA | NA |
| Cabling | | ? | ? | ? |
| Solar array | | NA | ? | ? |
| Flywheel/battery | | NA | 44000-115000 | 70000 |
| Heat management | | ? | ? | ? |
| GGA | 7780 | 7500-? | | |
| Resonator | 6528 | ? | | |
| Total of relevant systems (about 50% of SBL) | 39496 | ? | ? | ? |

All systems scaled to CARD power and approximate run time.  Duty cycle of electric systems questionable for run times.  Electric lasers are shown as a range, the low estimate being the projected state of the art after development, the higher estimate the current values.  All current numbers are gross estimates which need considerable refinement.

Notes on assumptions:  The turbogenerator weights assume that the laser is net 50% efficient and that no additional power is needed for cooling.  Thermal balance of the turbogenerator is assumed; i.e., no additional power is needed to cool the superconducting devices or to remove waste heat from the system.  No thermal control mass (insulation, etc. is included.  The heat capacity laser is assumed to need three banks to maintain equivalent duty cycle.

3.3-4-39

# Comparison Results

*(Major Update Needed, Probably Several Charts)*

**Schafer**

- COIL and HF Thermal Efficiencies Nearly Equal, Electric are TBD but vary widely with assumptions
  - Theoretical Values of 25 to 27%(HF/COIL)
  - Demonstrated Values of 7 to 10%(HF/COIL)
  - Projected Values of 11 to 13%(HF/COIL)

- HF Specific Energy 3 to 5 Times Higher Than for COIL

- Thermal Control of COIL More Complex Than for HF
  - Auxiliary Heat-X to Reject Heat at Rates of ~10 Times Output Beam Power
  - Thermal Conditioning of Device Required
    - Low Temperature (~245 K) for Generator, Ducts and Cold Traps
    - High Temperatures (~400 K) for Iodine Supply and Cavity Injector

- Current COIL Technology Requires Liquid Transport, Spray, and Recovery Processes in Space

- Electric Lasers Thermal Control More Complex that COIL. Theoretical and Projected Efficiencies are TBD

# Plan

**Schafer**

- The objective is to evaluate leading electric laser architectures to determine the weight per output power ratios and weight per brightness ratios for each architecture

- The payload consists of
  - Laser device
  - Power generator
  - Cooling system for laser and power generator

- Compare with HF and COIL ratios
- Prepare Updated Briefing

3.3-4-41

# *Schafer*

## Where do we go from here?

- Validate laser power input requirements (power, voltage)

- Develop system mass estimates
  - For most likely options
    - Turbine/generator/cooled converters
    - Fuel cells
    - Solar array/energy storage
  - Update SPAS spreadsheets with latest technology figures of merit to reduce effort required for mass estimates
  - Some items parametric (i.e. - system mass vs. time between engagements)

- Identify issues for each option
  - Technical issues - maturity, spacecraft integration, etc.
  - Synergism with other government ongoing programs
  - Alternatives for improved integration with the laser options
  - System efficiency parameters - from reactant heating values to energy into the laser

- Provide results to BMDO
  - Provide size and mass estimates for best system option
  - Allow comparison with IIF laser systems

3.3.4-42

# SBL Status for NRL

Gary Golnik
Schafer Corporation
21 October 1998

3.3-4-43

# SBL Overview

*Schafer*

- "CARD" System defined 1997

- Program transferred to SMC

- Program redefined to fit smaller vehicle, harder targets, advanced technology inserted immediately

- Program emphasized competition between two contractor teams (split old team)

- Plan for award of TSA contract for RD based on "process" not design

- Program recently redefined as "technology for ten years" followed by eventual decision on space experiment

3.3-4-44

*Schafer*

## SETA structure

- Common BMDO "master" contract included team of Schafer, SAIC, GRC, GFG, U of I; also ABL support

- BMDO reduced contract to SBL only and awarded to ANSER, SMC added Aerospace and several "local" SETAs; SAIC dropped SETA and works for hardware contractors; other SETA contractors fragmented to various vehicles

3.3-4-45

# Schafer

## Key Technologies

- Beam Control (conventional and SBS)

- Uncooled cylindrical resonator

- Large lightweight deployable optics

- Autoalignment

- Laser Device (HYLTE / other)

- Lightweight reactant storage and supply

- ATP testing at range

- Ground test methods

- Heavy lift launch vehicle

3.3-4-46

# Schafer

# SBL Constellation Sizing
## AFRL Lethalities



**Jitter=100nrad**

Number of Satellites

**Jitter=50nrad**

Number of satellites

Average Percent of Kills

Legend: p4d3, p3d3, p4d2, c1best-jorge, p3d2, p2d3, p4d1, c2best-jorge, p2d2, p3d1, c2-jorge, p1d3, p2d1, p1d2
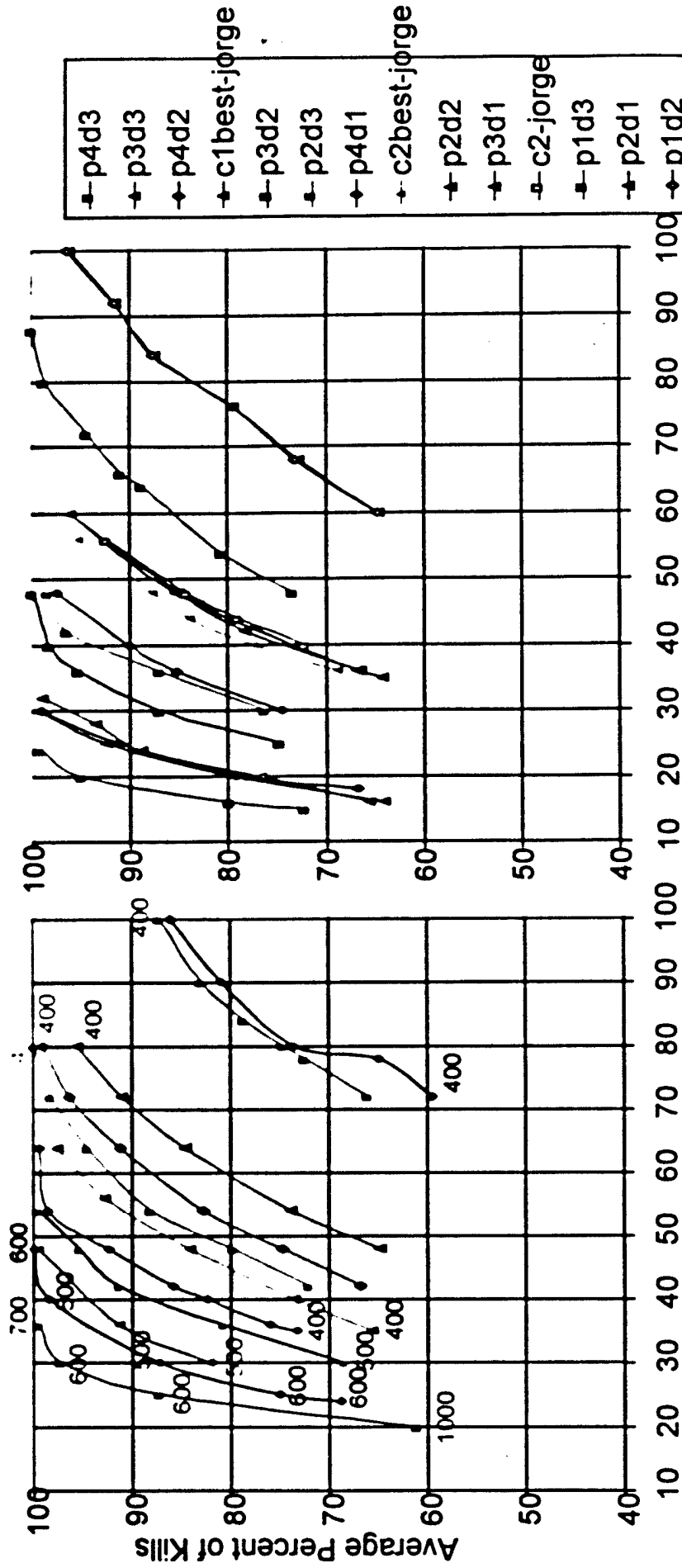
zonal coverage

3.3-4-47

# Schafer

# Brightness Scaling



**Brightness Scaling
(Diameter, Wavelength, Power all vary)**
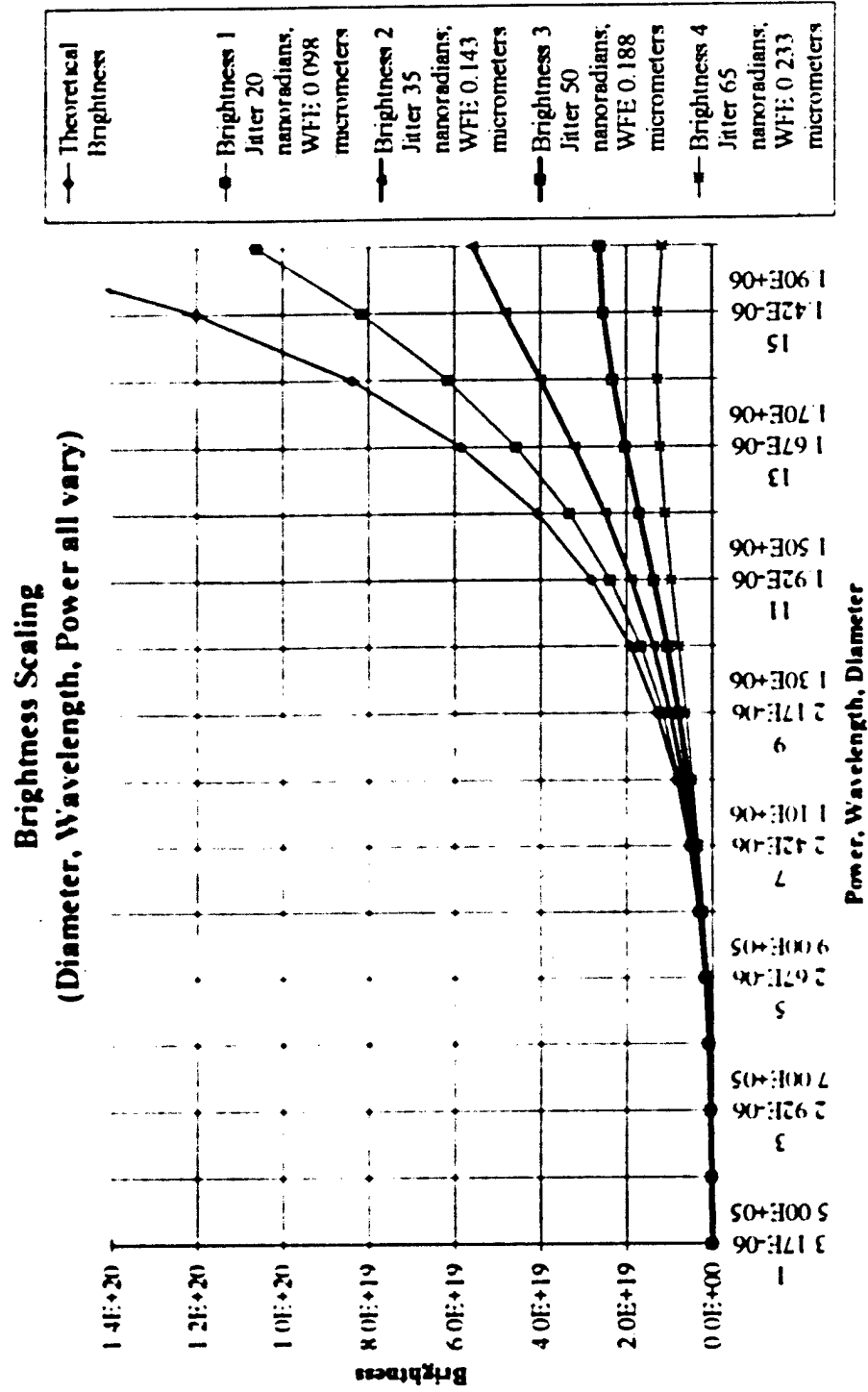
# Summary of 1986 Bifocal Concept Studies

G. Golnik

Schafer Corporation

18 December 1998

# GBL/Bifocal Concept

**Schafer**

Monocle Relay
(elliptical orbit)

40,000 km

Bifocal Fighting Mirror

Target

3.3-4-50

# Bifocal Program

**Schafer**
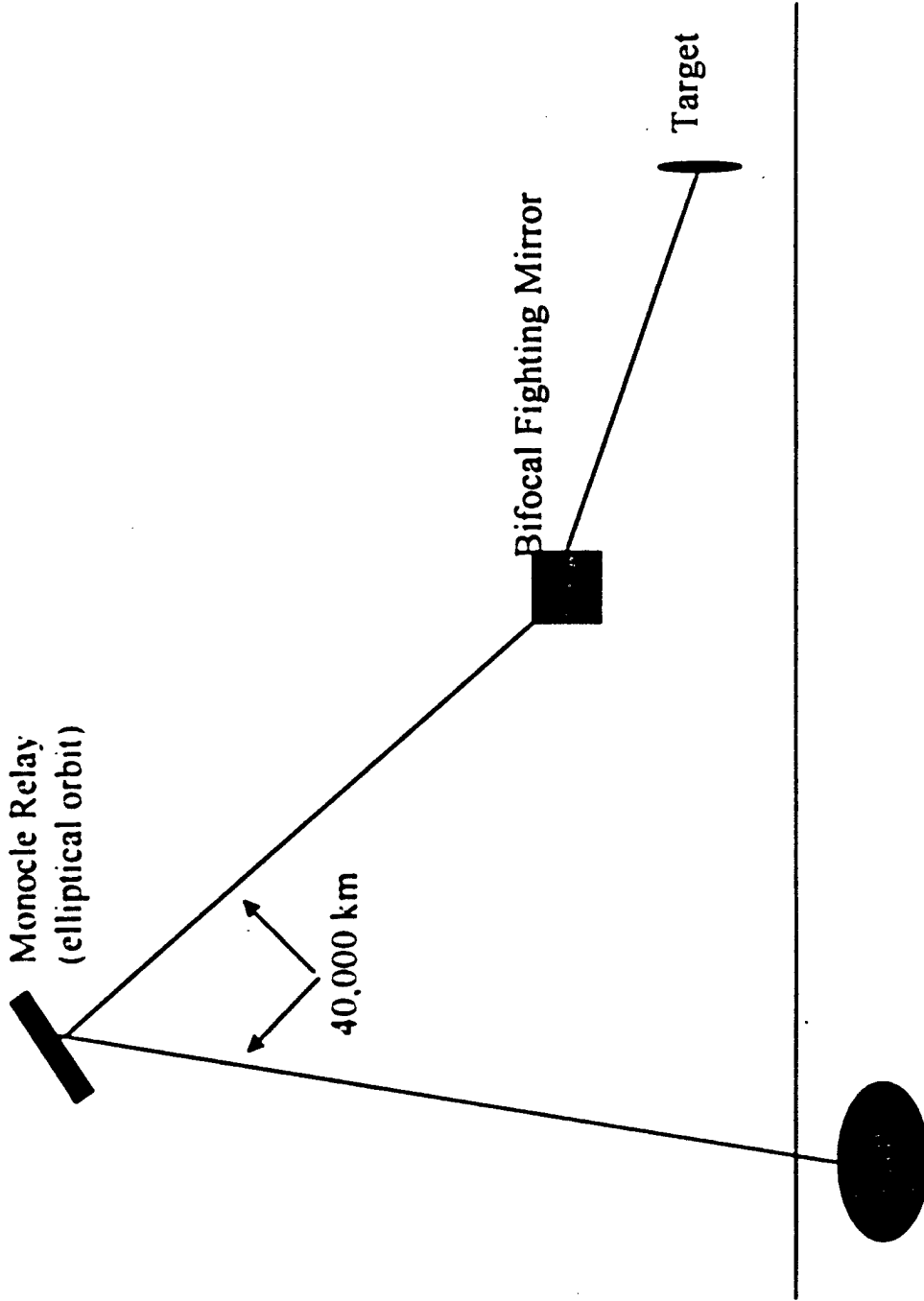
- Two Parallel Concept Studies June-Dec 1986 (~$1M each)

- Each Effort Included:
  - Operational System Concept Study
  - Space Experiment (SPEX) Study
  - Risk Reduction Plan Development

- Risk Reduction Experiments (~$2-3M each)
  - Perkin Elmer (HDOS) brassboard and HOE
  - LMSC ARTS

3.3-4-51

**Schafer**

## Bifocal Reports

- AFWL-TR-86-153 March 1988 Perkin Elmer Concept Study
- AFWL-TR-86-154 August 1988 LMSC Concept Study
- AFWL-TR-89-67 February 1990 LMSC ARTS
- 51 Other Documents in the Unclassified Library

# *Schafer* General "Conclusions" from Concept Studies

- Studies of many mirror design forms

- Studies of many "gimbal" options

- Some error budgets (but all verge on the absurd)

- Much study of wavefront/jitter sensing and control

- Off-axis designs (driven by unobscured beam from FEL)

- Significant concerns about structures, CMGs

  - CMG weight 20,000 kg

- Input and output mirrors of comparable size (input ~75% of output; input driven by diffractive beam size from long propagation)

3.3-4-53

# Schafer

## Slides from Final Reports

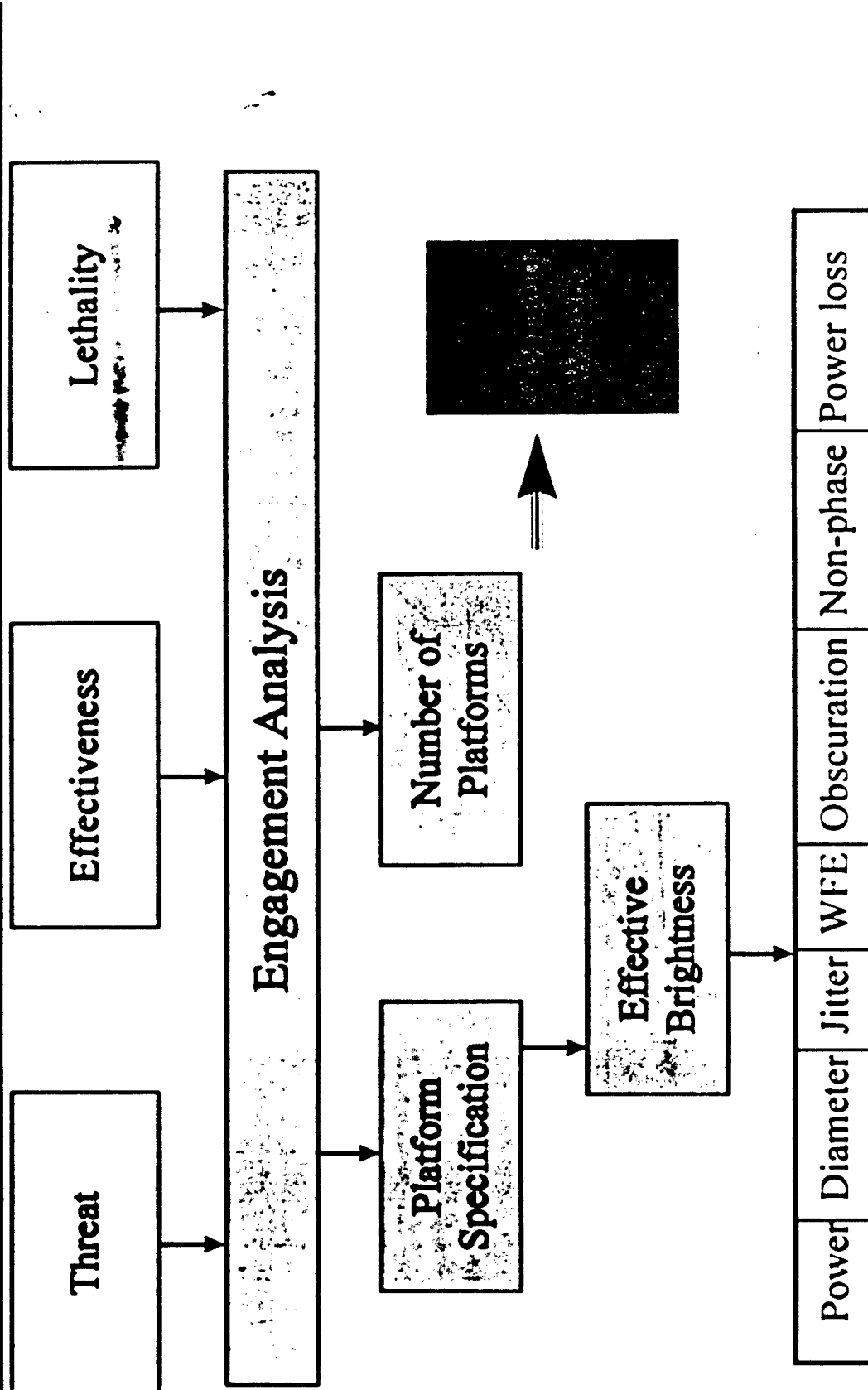- Perkin Elmer (HDOS)
- LMSC

3.3-4-54

**Schafer**

## Summary

- Considerable concept work has been done
- Contractors and Government team should be encouraged to review reports
- Other reports from early SMC architecture studies should also be assembled and "mined" for information

3.3-4-55

# SBL Requirements Definition

G. Golnik

Schafer Corporation

18 December 1998

# Schafer   SBL Requirement Development

```
┌──────────┐   ┌───────────────┐   ┌──────────┐
│  Threat  │   │ Effectiveness │   │ Lethality│
│          │   │               │   │          │
└────┬─────┘   └───────┬───────┘   └────┬─────┘
     │                 │                │
     ▼                 ▼                ▼
┌─────────────────────────────────────────────┐
│           Engagement Analysis               │
└──────┬──────────────────────────────┬───────┘
       │                              │
       ▼                              ▼
┌─────────────┐              ┌──────────────┐
│  Platform   │              │  Number of   │
│ Specification│              │  Platforms   │
└──────┬──────┘              └──────────────┘
       │
       ▼
┌──────────────┐
│  Effective   │
│  Brightness  │
└──────┬───────┘
       │
       ▼
```

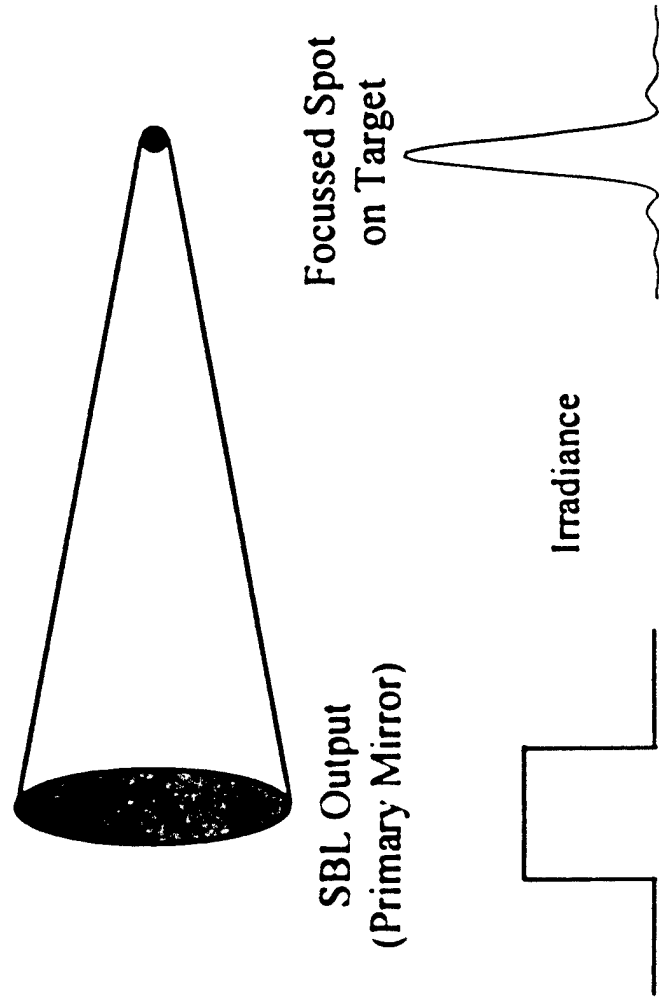| Power | Diameter | Jitter | WFE | Obscuration | Non-phase | Power loss |
|-------|----------|--------|-----|-------------|-----------|------------|

3.3-4-57

# schafer

## Brightness

• Brightness (W/steradian) is a convenient simplification to describe the diffraction and aberration properties of the SBL

SBL Output
(Primary Mirror)

Focussed Spot
on Target

Irradiance

Spot is not a perfect point
Spreads due to diffraction and aberrations

3.3-4-58

# Irradiance Kills the Target

- When the beam leaves the laser, we know its power and the exit diameter, the wavelength, the aberrations, and the range to target

  - We need to know the irradiance at the target, for that is what kills

From diffraction theory:

$$I_{peak} = \frac{\pi\, PD^2}{4\lambda^2 R^2} S$$

S the reduction in peak irradiance due to aberrations

Redefining terms for convenience:

$$I_{peak} = \frac{B}{R^2}$$

Brightness (simple version):

$$B = \frac{\pi\, PD^2}{4\lambda^2} S$$
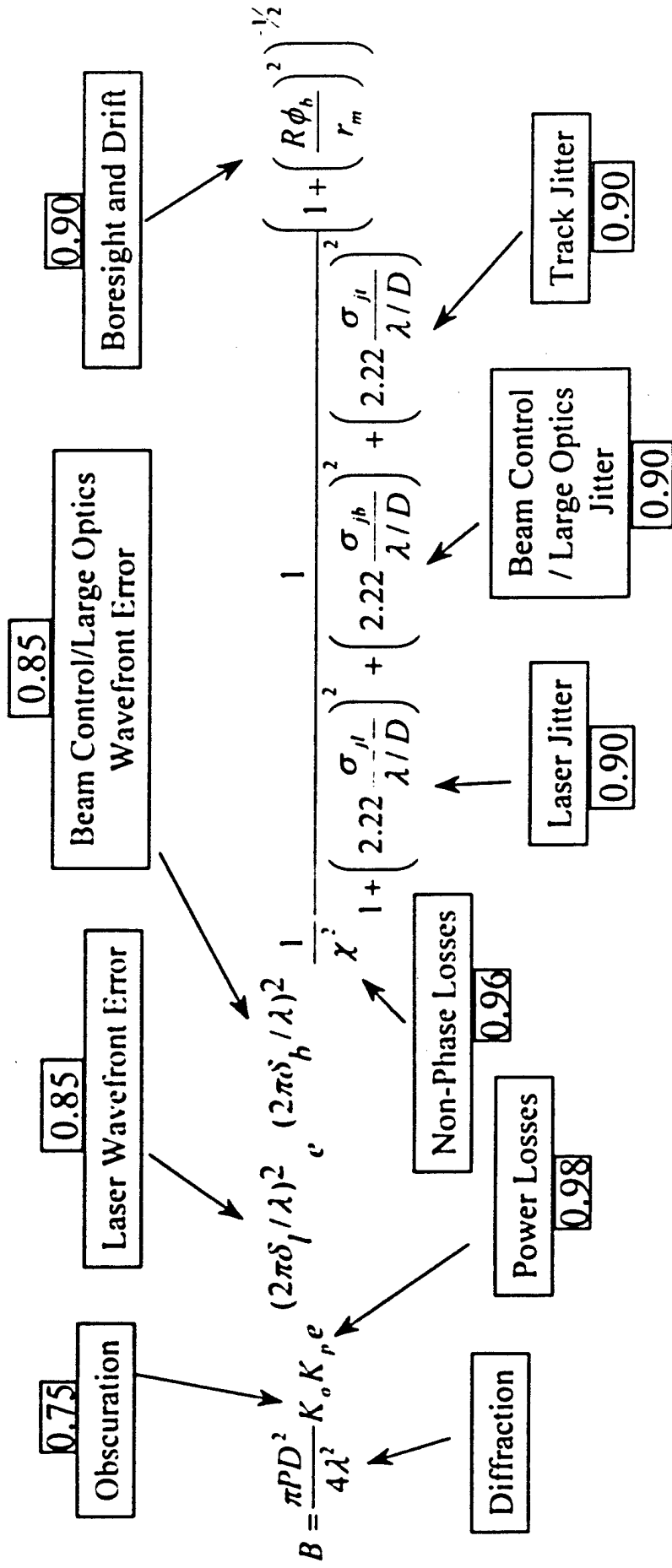
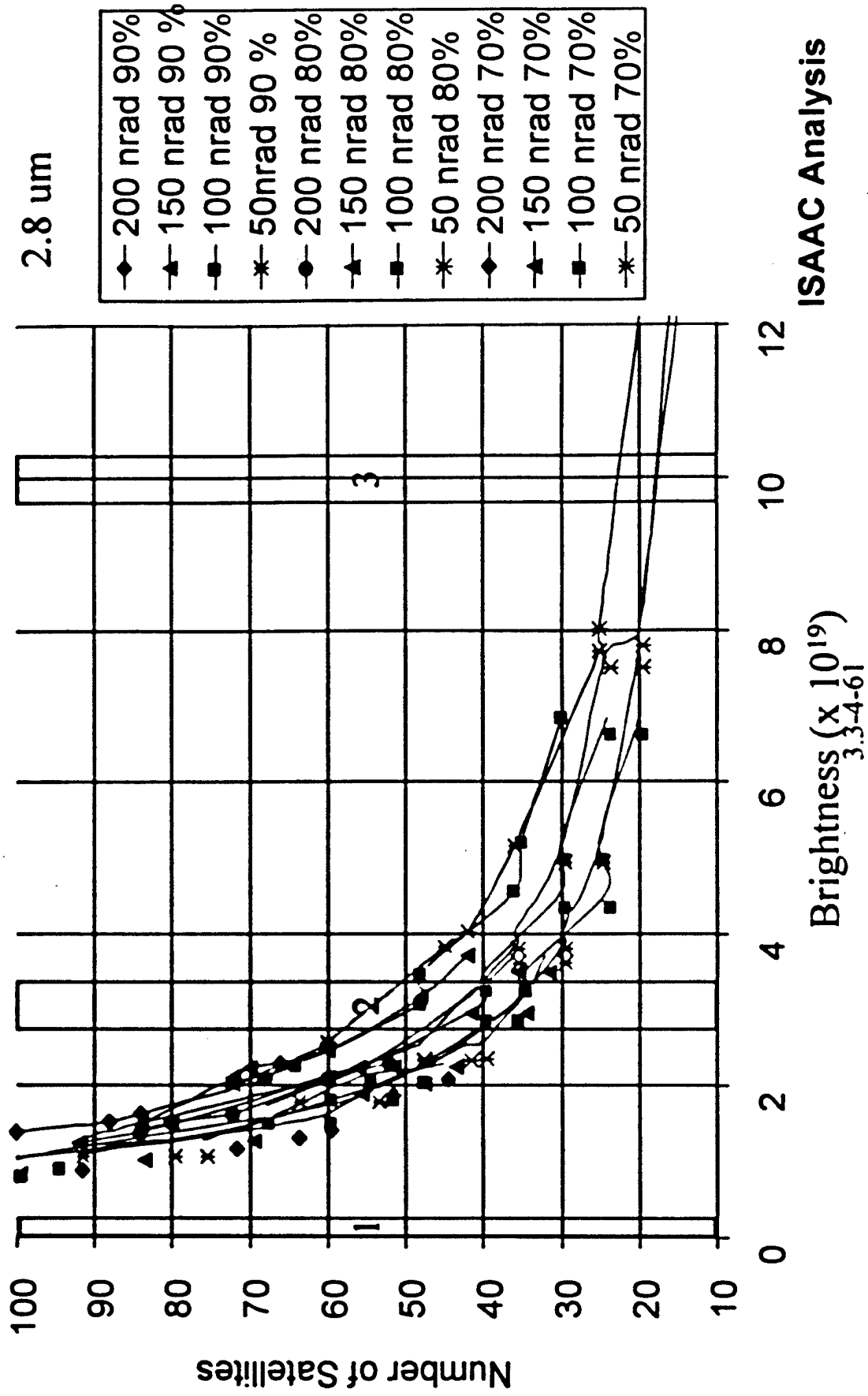But beware!! **S** is a function of power, wavelength, and diameter!

Other effects such as edge irradiance, angle of incidence, coupling to target, lethality, etc. are considered after the "incident energy" is calculated, but are included in lethality models

3.3-4-59

**Schafer**

# Brightness Equation (not so simple version)

$S$ (all terms but diffraction) typically <0.5 (sometimes much less)

Boresight and Drift — 0.90

Beam Control/Large Optics Wavefront Error — 0.85

Laser Wavefront Error — 0.85

Obscuration — 0.75

Track Jitter — 0.90

Beam Control / Large Optics Jitter — 0.90

Laser Jitter — 0.90

Non-Phase Losses — 0.96

Power Losses — 0.98

Diffraction

$$B = \frac{\pi P D^2}{4\lambda^2} K_o K_r \, e^{-(2\pi\delta_l/\lambda)^2} \, e^{-(2\pi\delta_h/\lambda)^2} \frac{1}{\chi^2} \left[ 1 + \left(2.22\frac{\sigma_{jl}}{\lambda/D}\right)^2 + \left(2.22\frac{\sigma_{jb}}{\lambda/D}\right)^2 + \left(2.22\frac{\sigma_{jt}}{\lambda/D}\right)^2 \right] \left[ 1 + \left(\frac{R\phi_h}{r_m}\right)^2 \right]^{-1/2}$$
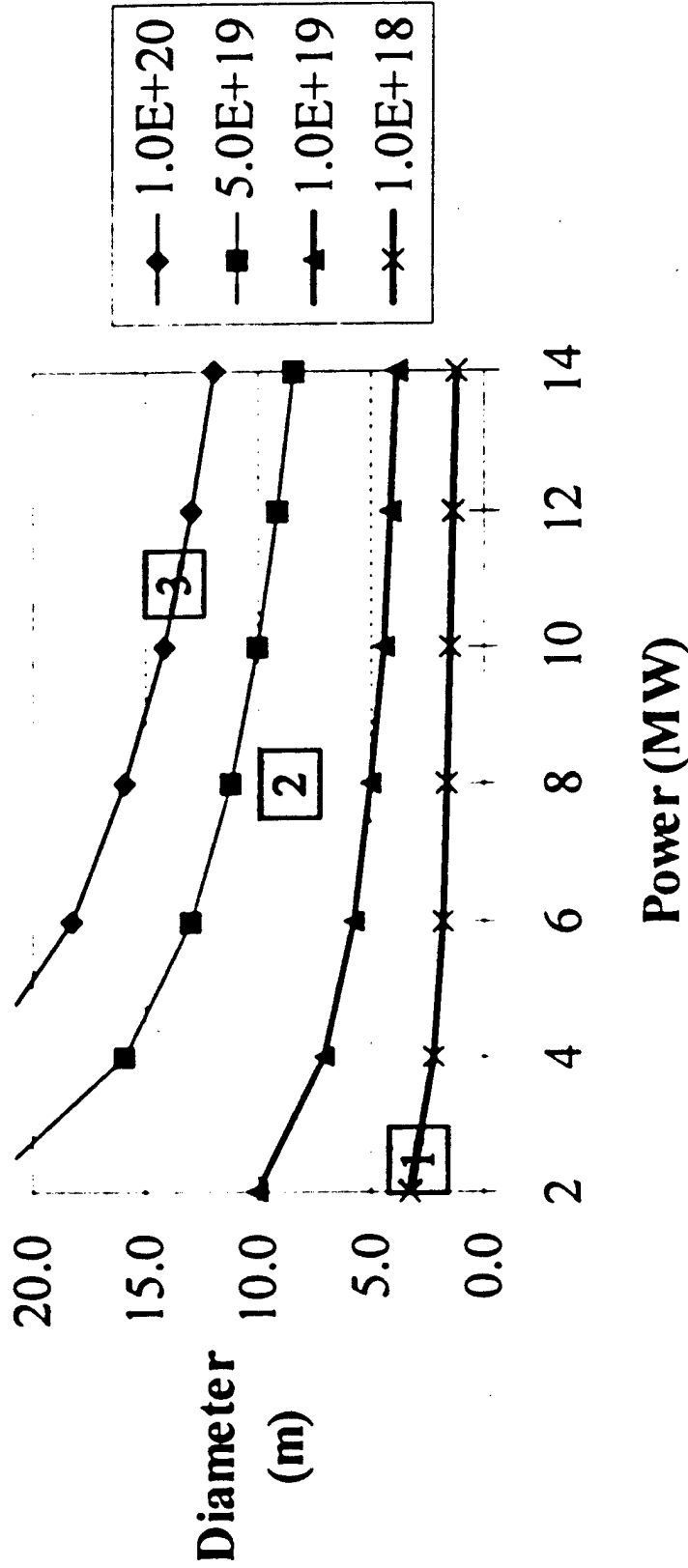
Valid only for small aberrations but within ranges currently carried in error budgets
Values shown for illustration only

3.3-4-60

# Engagement Analysis

*Schafer*

## 2.8 um



Legend:
- 200 nrad 90%
- 150 nrad 90 %
- 100 nrad 90%
- 50nrad 90 %
- 200 nrad 80%
- 150 nrad 80%
- 100 nrad 80%
- 50 nrad 80%
- 200 nrad 70%
- 150 nrad 70%
- 100 nrad 70%
- 50 nrad 70%

X-axis: Brightness (x $10^{19}$)
3.3-4-61

Y-axis: Number of Satellites

ISAAC Analysis

# Schafer System Power and Diameter Required for Given Brightness (Excellent Performance)

## S=0.5  2.8um



Legend:
- ◆ 1.0E+20
- ■ 5.0E+19
- ▲ 1.0E+19
- ✕ 1.0E+18

Y-axis: Diameter (m) — 0.0, 5.0, 10.0, 15.0, 20.0
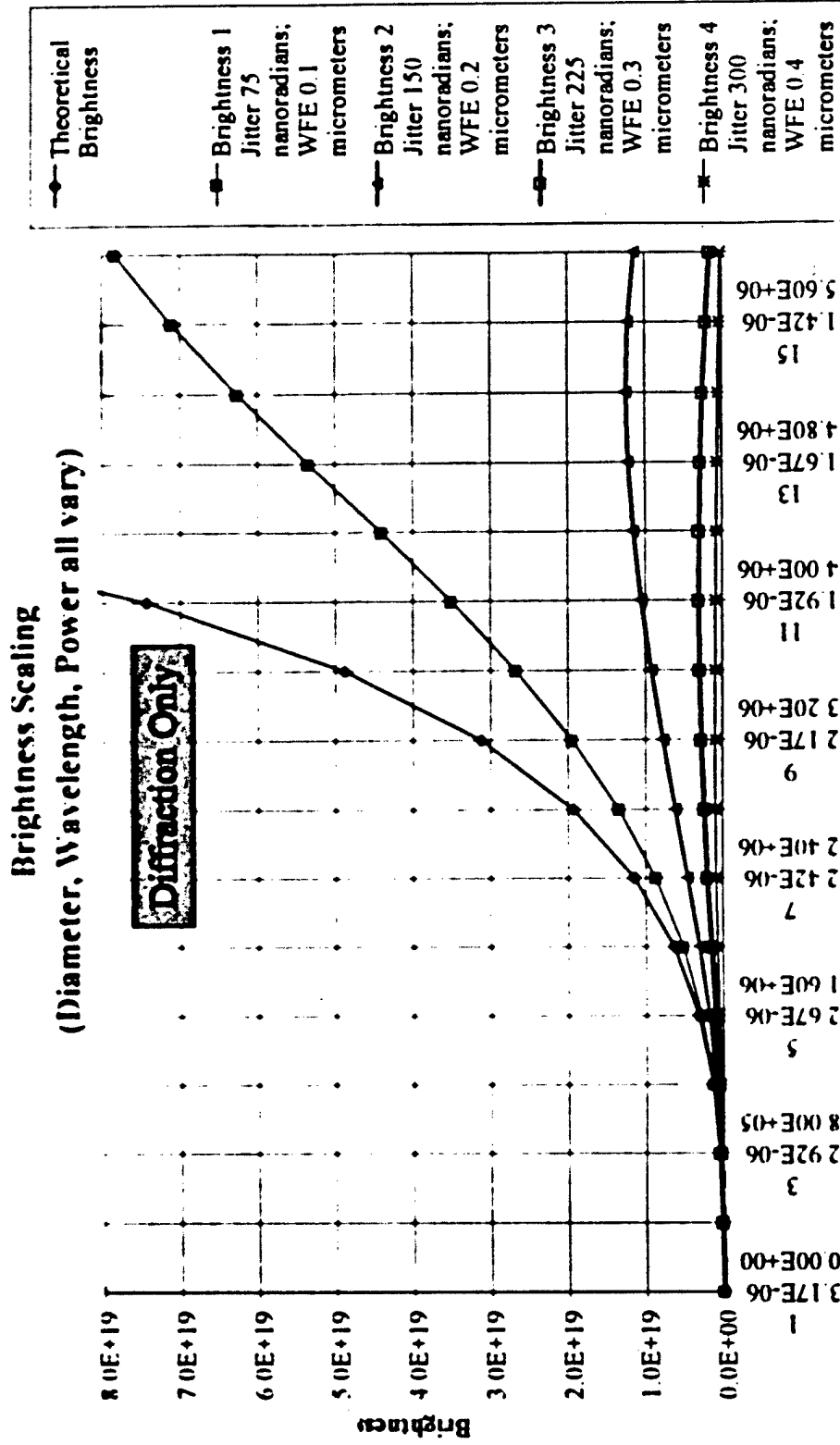
X-axis: Power (MW) — 2, 4, 6, 8, 10, 12, 14

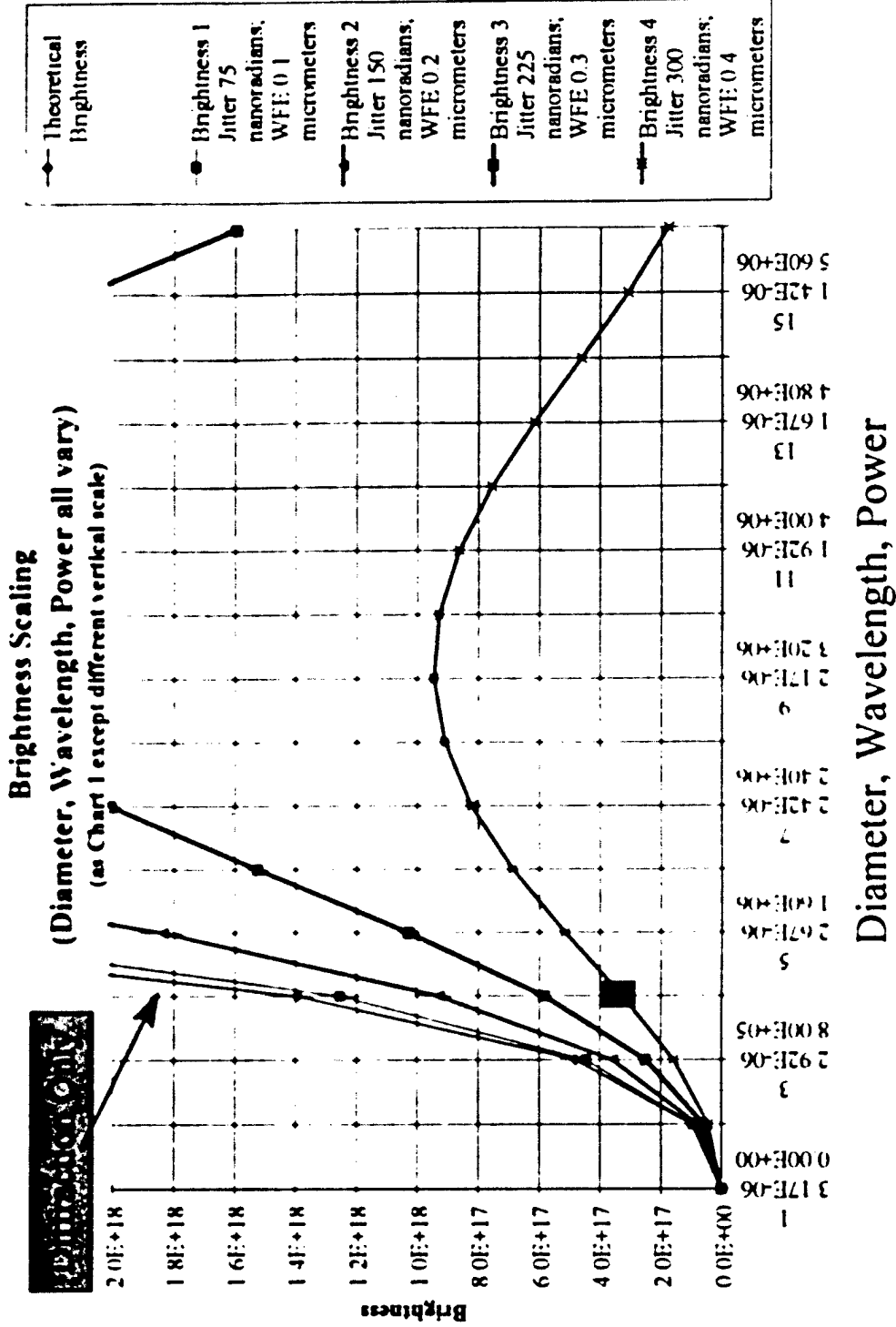Caveat: As Diameter Increases, Achieving the Same System Quality (S) Becomes Much More Difficult

# Brightness Scaling Including Shorter Wavelengths
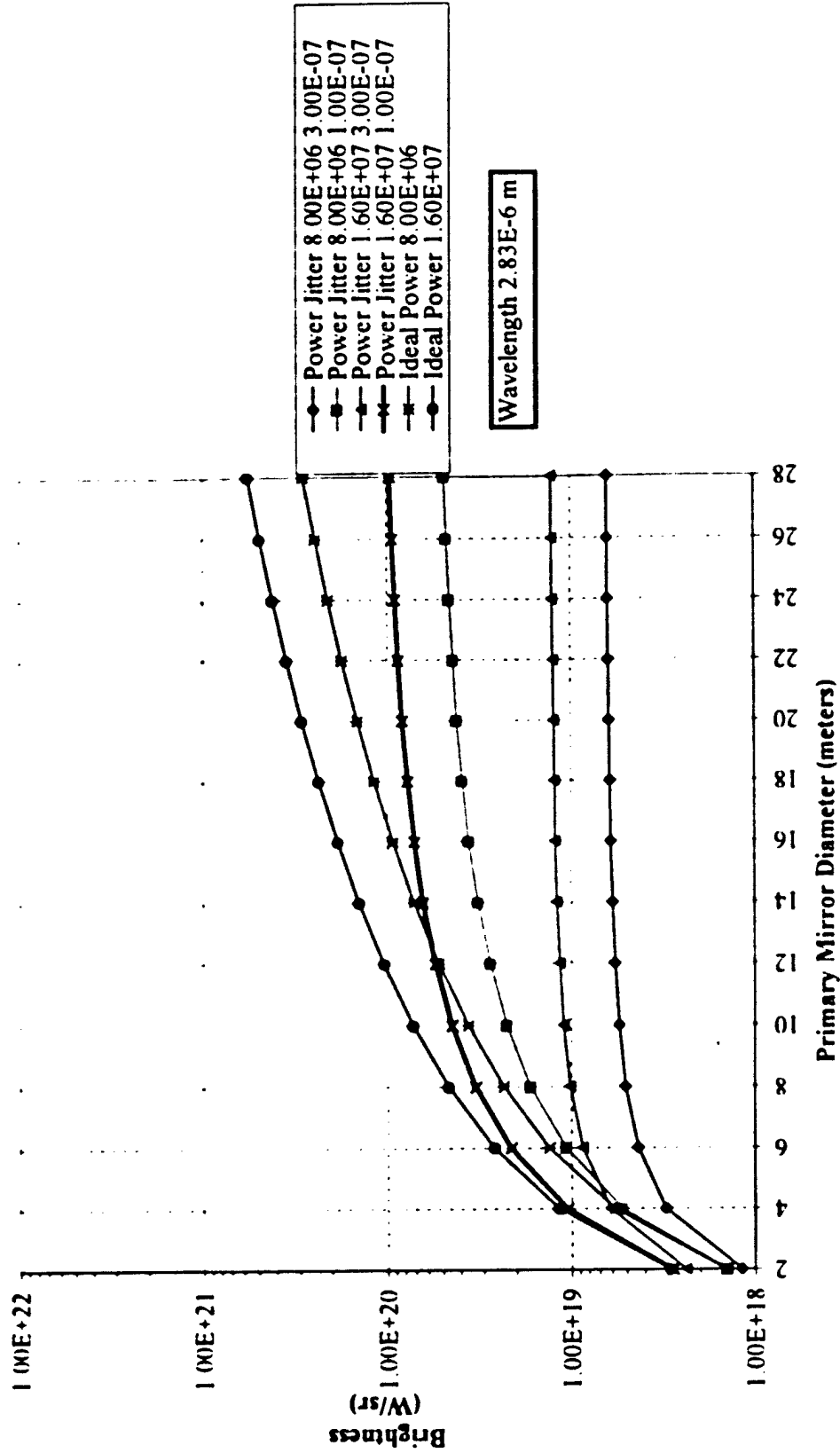
~~(showing brightness saturation)~~



Diameter, Wavelength, Power

# Expanded Scale

**Brightness Scaling**
**(Diameter, Wavelength, Power all vary)**
(as Chart 1 except different vertical scale)



Diameter, Wavelength, Power

Legend:
- Theoretical Brightness
- Brightness 1 Jitter 75 nanoradians, WFE 0.1 micrometers
- Brightness 2 Jitter 150 nanoradians, WFE 0.2 micrometers
- Brightness 3 Jitter 225 nanoradians, WFE 0.3 micrometers
- Brightness 4 Jitter 300 nanoradians, WFE 0.4 micrometers

*Schafer*

3.3-4-64

# SBL Requirements Summary

- ALO/ALI Technology (Brightness) Nearly Comparable to Initial Flight Experiment (IFX/RD) Although Not Flight-Weight

- IFX-Class Confirms Space Operation and Provides ASAT Capability

- EMD-Class Makes Substantial Improvement and Provides TMD and NMD Capability Against TMD-Class Targets

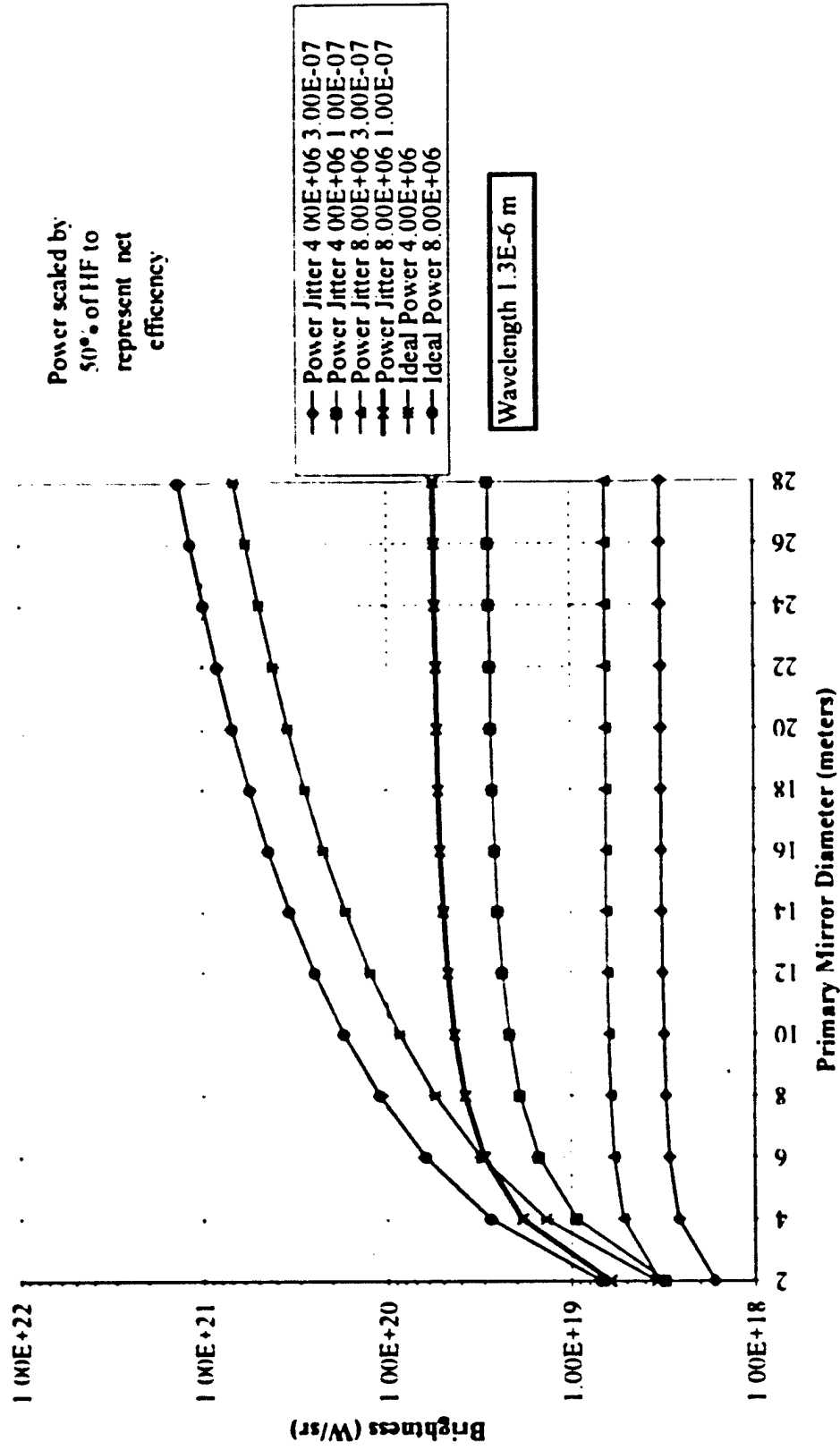- Advanced-Class Makes Further Improvement and Provides Robust NMD Capability

*Schafer*

3.3-4-65

# Schafer Brightness vs. Jitter (nominal errors) HF

## Brightness and Diameter Scaling
### (critically dependent on jitter)



Legend:
- Power Jitter 8.00E+06 3.00E-07
- Power Jitter 8.00E+06 1.00E-07
- Power Jitter 1.60E+07 3.00E-07
- Power Jitter 1.60E+07 1.00E-07
- Ideal Power 8.00E+06
- Ideal Power 1.60E+07

Wavelength 2.83E-6 m

X-axis: Primary Mirror Diameter (meters)
Y-axis: Brightness (W/sr)

3.3-4-66

# Brightness vs. Jitter (nominal errors) HF
## Overtone

**Schafer**

**Brightness and Diameter Scaling**
**(critically dependent on jitter)**

Power scaled by
50% of HF to
represent net
efficiency

- Power Jitter 4.00E+06 3.00E-07
- Power Jitter 4.00E+06 1.00E-07
- Power Jitter 8.00E+06 3.00E-07
- Power Jitter 8.00E+06 1.00E-07
- Ideal Power 4.00E+06
- Ideal Power 8.00E+06

Wavelength 1.3E-6 m

Primary Mirror Diameter (meters)

Brightness (W/sr)

3.3-4-67

# Combined HF and HF OT

**Schafer**

**Brightness Vs. Diameter (HF and HF OT combined)**



Legend:
- —■— OT Ideal
- —■— OT Ideal Lower Power
- —■— HF Ideal
- —□— HF Ideal Lower Power
- —■— HF High Power 100 nrad
- —■— HF OT High Power 100 nrad
- —◆— HF High Power 300 nrad
- —+— HF OT High Power 300 nrad

X-axis: Primary Mirror Diameter (m) — 2, 4, 6, 8, 10, 12, 14, 16, 18, 20, 22, 24, 26, 28

Y-axis: Brightness — 1.00E+18, 1.00E+19, 1.00E+20, 1.00E+21, 1.00E+22

3.3-4-68

# Schafer
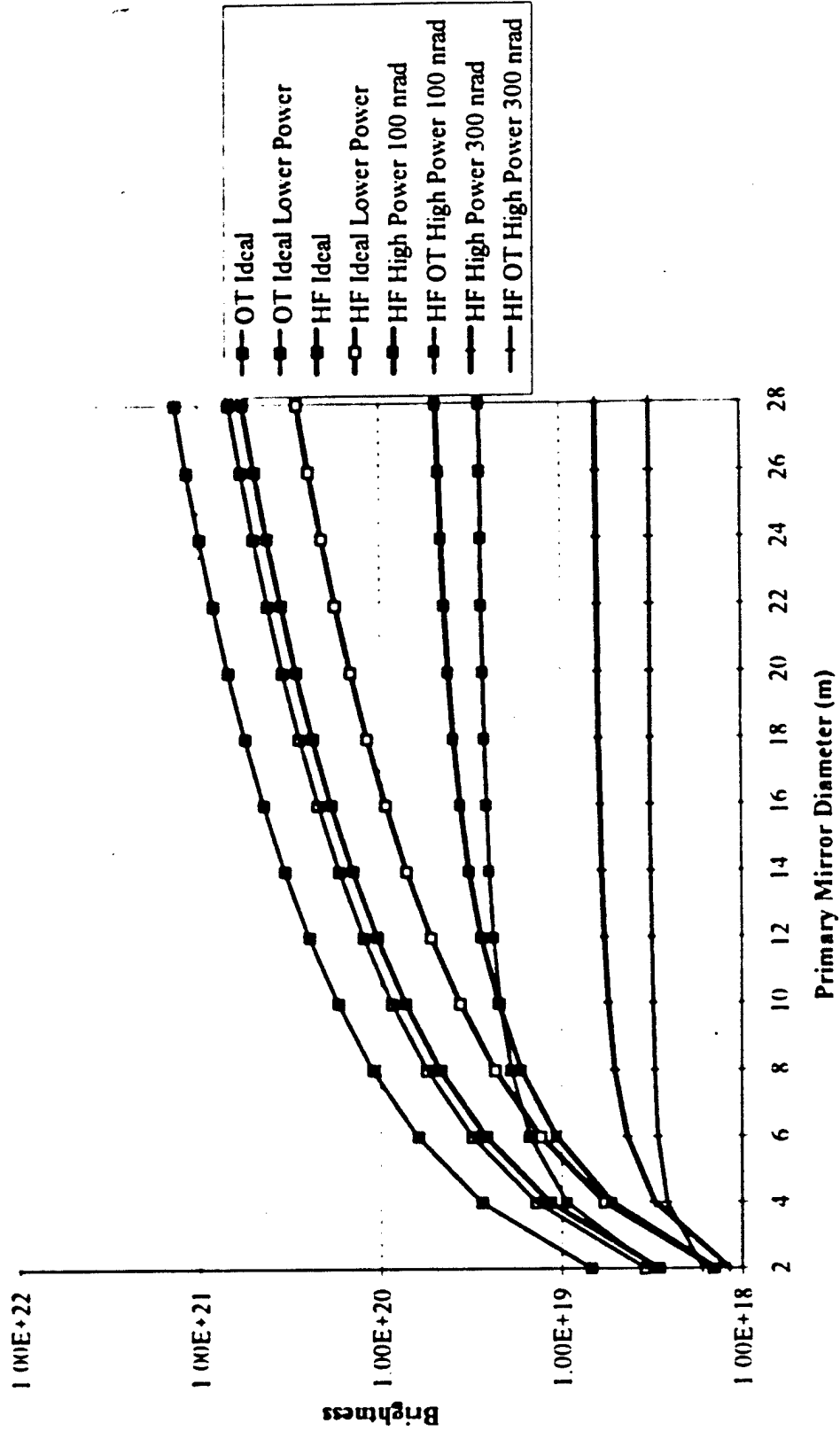
## Overtone or Other Short Wavelength Devices Require Low Jitter Technology for Larger Diameters

### HF vs. HF OT Crossover Due to Jitter



Legend:
- HF High Power 100 nrad
- HF OT High Power 100 nrad

Y-axis: Brightness (1.00E+18, 1.00E+19, 1.00E+20)

X-axis: Primary Mirror Diameter (m) (2, 4, 6, 8, 10, 12, 14, 16, 18, 20, 22, 24, 26, 28)
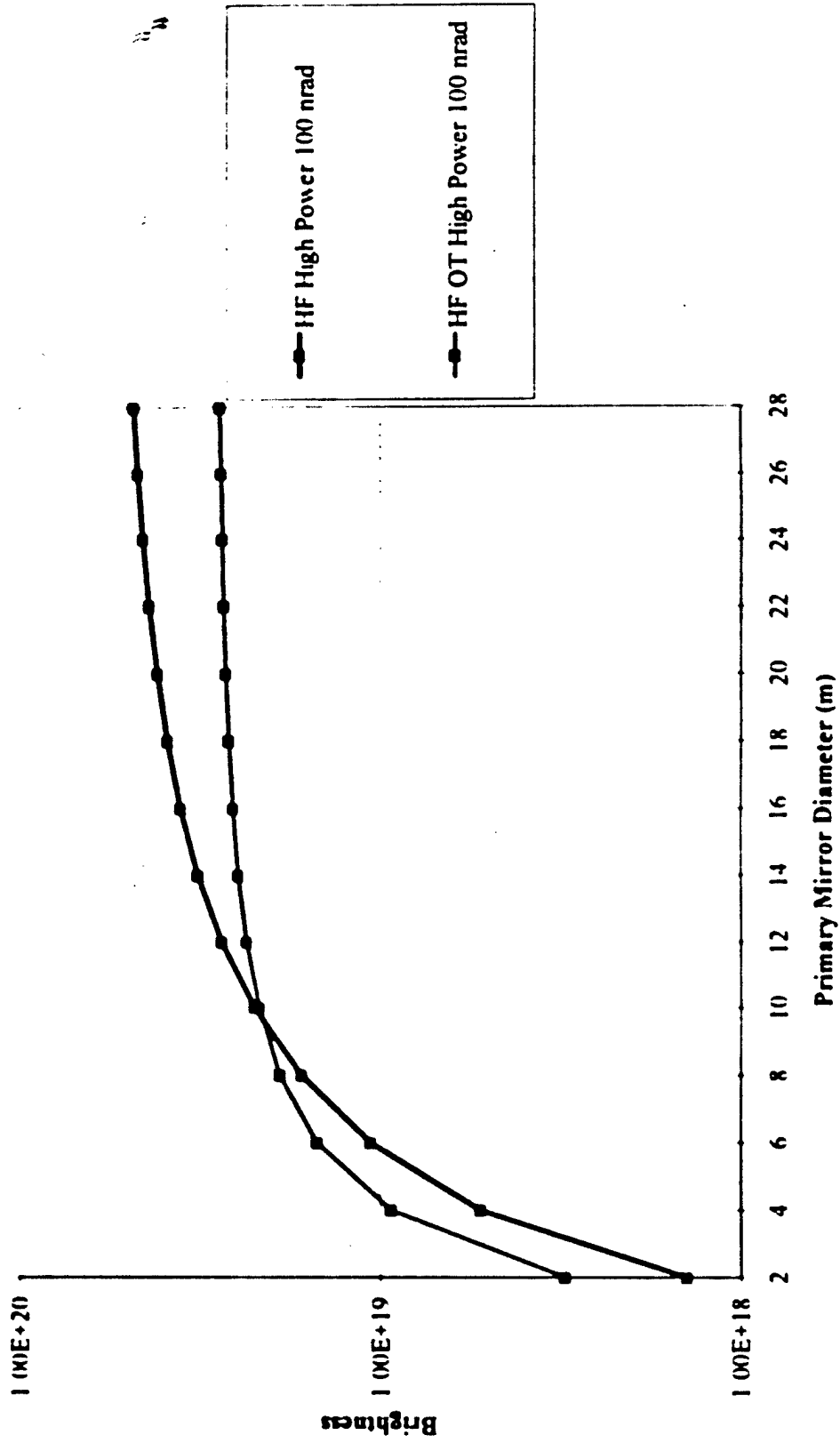
3.3-4-69

# Appendix 3.3-5
# Large Deployable Primary Mirror Study

## SUMMARY:

· ·· · . The objective of this study was to determine the pointing errors incurred when a large beam expander primary mirror is rapidly re-targeted. For the sake of this study, it was assumed that the mirror had to be re-targeted 0.100 radian and be ready for use after 2.1 seconds. (Mirror figure responses also have to be correctable after 2.1 seconds. A previous study indicated that a re-targeting time of 1.75 seconds with a settling time of 0.35 seconds provided the best compromise between the higher energy inputs for shorter re-targeting times and the time it takes for the mirror response to attenuate sufficiently for use. This approach was not re-visited in this study (which used a higher rigidity faceplate) because of limited time. Responses were calculated for 8.0, 12.0 & 16.0 meter diameter primary mirrors. The resulting pointing error estimates for the 1% and 5% modal damping are shown in Figures 1 & 2, respectively. The "corrected" pointing error was calculated assuming that 80% of the difference between the temporal response of the outer portion of the mirror (2.0 meters to the outside diameter) and the core structure (0.5 to 2.0 meters), on which the deformable mirror is assumed to be mounted, can be corrected. The corrected pointing errors at the x-axis support and 22.5 ° mid-point between supports are shown in Table 1 for 1% and 5% modal damping. They vary from approximately 5 nano-radians for the 8.0 meter primary mirror at the x-axis support (with 5% damping), to approximately 130 nano-radians for the 16 meter primary mirror at the 22.5 ° mid-point between supports (with 1% damping).

### Table 1: Summary of The Mirror Corrected Pointing Errors

| DAMPING | LOCATION | 8.0 METER | 12.0 METER | 16.0 METER |
|---------|----------|-----------|------------|------------|
| 1% | X-Axis | 12 nano-radian | 29 nano-radian | 76 nano-radian |
| | 22.5 ° | 25 nano-radian | 55 nano-radian | 130 nano-radian |
| 5% | X-Axis | 5 nano-radian | 12 nano-radian | 33 nano-radian |
| | 22.5 ° | 13 nano-radian | 42 nano-radian | 75 nano-radian |

## DEPLOYABLE MIRROR STRUCTURAL CONCEPT:

This study utilized a Schafer developed deployable space truss mirror structure. ·The mirror is shown in the deployed configuration in Figure 3 and stowed for launch in Figure 4. This approach was developed because the existing concepts in the community were neither sufficiently rigid to provide the required pointing accuracy, nor do they provide a full aperture mirror. The mirror panels utilize a 95 mm "honeycomb" core (5% core density) with 0.9 mm silicon face plates. The areal density of the panels alone was 15 kg/m². The design utilizes a fixed 4.0 meter "core structure", as shown in Figures 2 & 3. (It was assumed that a 5.0 meter inside diameter shroud would be available by the time the device is launched.) The core structure supports the deployable outer panel. (Figure 4) that fold like an umbrella and are stowed between the radial core support trusses at 45°. Two, four & six meter radial length supports are used with the four meter diameter core to form 8.0, 12.0 & 16.0 meter diameter primary mirrors. To accommodate the folded panels, the height of the core structure is varied from 2.0 meters for the 8.0 meter diameter primary mirror to 6.0 meters for the 16.0 meter diameter primary mirror. The support structure was designed using carbon fiber reinforced silicon carbide (C/SiC). The C/SiC material is ideally suited for optical space structures because of its very high Young's Modulus to density ratio (comparable to graphite epoxy). In addition, neither moisture absorption in the atmosphere nor out-gassing in space are a problem with the C/SiC material. Because of high strength to density of the C/SiC material, theoretical areal densities of 17.9, 18.4 & 19.0 kg/m² were obtained for the 8.0, 12.0 & 16.0 meter diameter primary mirrors, respectively. These weights were obtained directly from the models. For this reason, additional weights for actuators, joints and other mechanisms; however, from these theoretical results it appears **areal densities of 20 kg/m² are realistic.**

Truss supports for the "honeycomb" mirror panels are provided under alternate segment junctions at 45°. Both the radial and diagonal members shown in the figure are provided at each of these locations. (Of course, any number of segments can be used to form the mirror. The configuration using 45° between supports was arbitrarily selected for this study. In fact, the larger diameter mirrors will require smaller angle segments for

storage during launch.) Panel support and positioning members are also utilized across the I. D. & O.D. cords of each panel. The support members are hinged at both ends. The diagonal supports are attached to the vehicle attach ring. Deployment and storage are achieved by synchronized translation of the ends of the diagonal struts in the vertical direction. (The diagonal members are stored in the vehicle structure optical bay outer wall during launch.) The panels are also hinged around the two parallel axes on either side of the 22.5 $^{\circ}$ segment. At the support truss locations, the hinge axis is at the bottom of the support panel, while at the along the radial line at the mid-point of the segments between the support trusses, the hinge axis is slightly above the mirror face. This placement allows the mirror segments to "fold" toward one another. In the fully retracted position, each "pair" of segments is folded inwardly and stowed in the wedge shaped (45 $^{\circ}$) space between support trusses. The radial support members rotate about their hinge axes attached to the top of the core structure. Their hinge axes are tangential and are placed below the center of the radial members to allow the outer petals to rotate away from the inner core mirror. In the deployed position, the panels and support struts are precision indexed relative to one another and locked into pre-determined positions after deployment. These would be preset before launch to minimize the additional alignment required in space. However, as part of this pre-alignment system and for correction for any changes that occur during launch and/or over time in space, precision stepper motors (with very high gear ratios) arranged in a three-point bipod provide a kinematic mount of each mirror segment panel. Thus, the segment-to-segment mis-registrations can be adjusted during operation.

Although the secondary mirror was not considered in this study, their support struts can also be attached to the ends of the support members (four at 90 $^{\circ}$) and deployed with the primary mirror. If Axial length is a problem, these struts can also be telescoped during launch.

## DEPLOYABLE MIRROR STUDY SUMMARY:

The study utilized "Modal Time History" analyses to determine the pointing error incurred due to the dynamic response of the mirror after rapid re-targeting. In this type analysis, the natural frequencies of the structure are determined and stored. The

frequency data is then used in the modal time history analysis to determine the response during a input acceleration time and the settling time after re-targeting.

The study was performed for 8, 12 & 16 meter primary mirror sizes. The overall model of the twelve-meter mirror is shown in Figure 5. The plan view shown in Figure 6 shows the mirror petal segments to be similar in plan view for all mirror petals. Each two meter annulus employs identical petals. With the exception of the core mirror petals, the inside diameter cord length of the petal is equal to half the length of the outside diameter cord length of the petal in the previous bay. Thus, all petals are two meters in radial span with an inner chord length of 0.78 meter and an outer chord length of 1.56 meters, only the sides at different angles in each radial bay. (The core petals are simply truncated at the 0.5 meter diameter.) Of course, the mirror figure (curvature) and the angle of the panel sides are different in each bay. If this full mirror model had been used in the study, too many more modes would have been required and the solution time would have increased to unsatisfactory levels. For this reason, the 90° segment indicated in Figure 6 and shown in Figure 7 was employed.

For the twelve meter mirror, one hundred frequencies were calculated, as shown in Table 2. A majority of these modes are "support modes" or "primarily support modes". The "real modes of the primary mirror" are indicated in the table as "Plot" modes. A sampling of the mirror modes are shown in Figures 8-18. All modes are included in the modal time history analyses; however, the majority of the response is a result of the "real modes".

Typical normal responses at the 6, 4, 2 & 0.5 meter locations along the support truss on the X-axis are shown in Figures 19-22. The temporal normal response data (recorded when these curves are plotted) is then used to calculate the angular responses between stations on the mirror (difference between the normal responses divided by the radial distance between points). Typical resulting angular response "reduced data" is shown in Figures 23 & 24. Figure 25 shows this type of data for the twelve meter mirror between 4.0 and 6.0 meter and between 2.0 and 4.0 meter Radius stations. The fact that the "responses" between 6.0 and 4.0 meters are 180° out of phase with the responses between 4.0 and 2.0 meters indicates that the radial support is bending. Since this effect

would be corrected by the deformable mirror, these deflections do not represent a "pointing error". For this reason, only the difference in deflections between the outside radius of 6.0 meters and the deflections at the 2.0 meter radius are considered in the pointing error calculation.

## Table 2: Twelve Meter Segment Frequencies

| Frequency# | Frequency, hertz | Type |
|---|---|---|
| 1 | 8.29 | Supports--Plot |
| 2 to 6 | 8.7,9.01,13.19,13.23,13.27 | Supports |
| 7 | 16.84 | Plot |
| 8 | 17.72 | Supports--Plot |
| 9 to 12 | 17.88,17.94,18.02,18.10 | Supports |
| 13 to 14 | 18.14, 18.21 | Primarily Supports--Plot |
| 15 | 18.28 | Supports |
| 16 to 18 | 18.96,18.98,19.45 | Primarily Supports |
| 19 to 31 | 19.64, 23.07, 23.16, 23.22, 23.46, 23.68, 24.20, 26.13, 26.19, 26.22, 26.55, 26.78, 26.99 | Supports |
| 32 | 34.88 | Plot |
| 33 | 36.54 | Plot--Boundary Petals |
| 34 | 37.87 | Primarily Supports--Plot |
| 35 | 38.04 | Supports |
| 36 | 38.12 | Primarily Supports--Plot |
| 37 to 41 | 38.13, 41.63, 42.20, 42.66, 49.46 | Supports |
| 42 | 49.62 | Primarily Supports--Plot |
| 43 to 47 | 49.86, 49.98, 50.16, 50.28, 50.48 | Supports |
| 48 | 50.51 | Primarily Supports--Plot |
| 49 | 51.38 | Plot |
| 50 to 55 | 64.1, 64.43, 64.63, 64.96, 65.62, 66.72 | Supports |
| 56 | 67.35 | Plot |
| 57 | 69.15 | Primarily Supports--Plot |
| 58 to 59 | 69.5, 70.17 | Supports |
| 60 | 70.64 | Primarily Supports--Plot |
| 61 | 71.82 | Primarily Supports--Plot |
| 62 to 70 | 73.63, 73.99, 74.06, 75.73, 76.35, 76.94, 78.93, 78.97, 79.08 | Supports |
| 71 | 80.33 | Plot |
| 72 | 81.00 | Plot |
| 73 | 83.16 | Plot |
| 74 | 84.36 | Plot |
| 75 | 89.50 | Plot |
| 76 | 92.20 | Plot |
| 77 | 93.74 | Plot |
| 78 | 96.57 | Plot |
| 79 to 84 | 98.09, 98.18, 98.28, 98.50, 98.63, 98.98 | Supports |
| 85 | 102.25 | Plot |
| 86 | 104.76 | Plot |
| 87 | 108.17 | Plot |
| 88 | 112.66 | Plot |
| 89 | 114.04 | Plot |
| 90 | 116.01 | Plot |
| 91 to 96 | 116.17, 118.08, 119.00, 119.25, 119.42, 120.14 | Supports |
| 97 | 121.74 | Plot |
| 98 | 123.17 | Plot |

| 99 to 100 | 126.5, 126.71 | Primarily Supports |

# Figure 1: Mirror Response With 1% Damping



Corrected Mirror Pointing Error At 2.10 Seconds, X-Axis
(After Re-Targeting 0.100 Radian in 1.75 Seconds, 1% Damping)



Corrected Mirror Pointing Error At 2.10 Seconds, Mid-Point At 22.5°
(After Re-Targeting 0.100 Radian in 1.75 Seconds, 1% Damping)



Mirror Pointing Error At 2.10 Seconds, X-Axis
(After Re-Targeting 0.100 Radian in 1.75 Seconds, 1% Damping)



Mirror Pointing Error At 2.10 Seconds, Mid-Point Between Frames At 22.5°
(After Re-Targeting 0.100 Radian in 1.75 Seconds, 1% Damping)

# Figure 2: Mirror Response With 5% Damping



Corrected Mirror Pointing Error At 2.10 Seconds, X-Axis
(After Re-Targeting 0.100 Radian in 1.75 Seconds, 5% Damping)



Corrected Mirror Pointing Error At 2.10 Seconds, Mid-Point Between Frames At 22.5°
(After Re-Targeting 0.100 Radian in 1.75 Seconds, 5% Damping)



Mirror Pointing Error At 2.10 Seconds, X-Axis
(After Re-Targeting 0.100 Radian in 1.75 Seconds, 5% Damping)



Mirror Pointing Error At 2.1 Seconds, Mid-Point Between Frames At 22.5°
(After Re-Targeting 0.100 Radian in 1.75 Seconds, 5% Damping)

## Figure3:  Deployed Mirror Structure
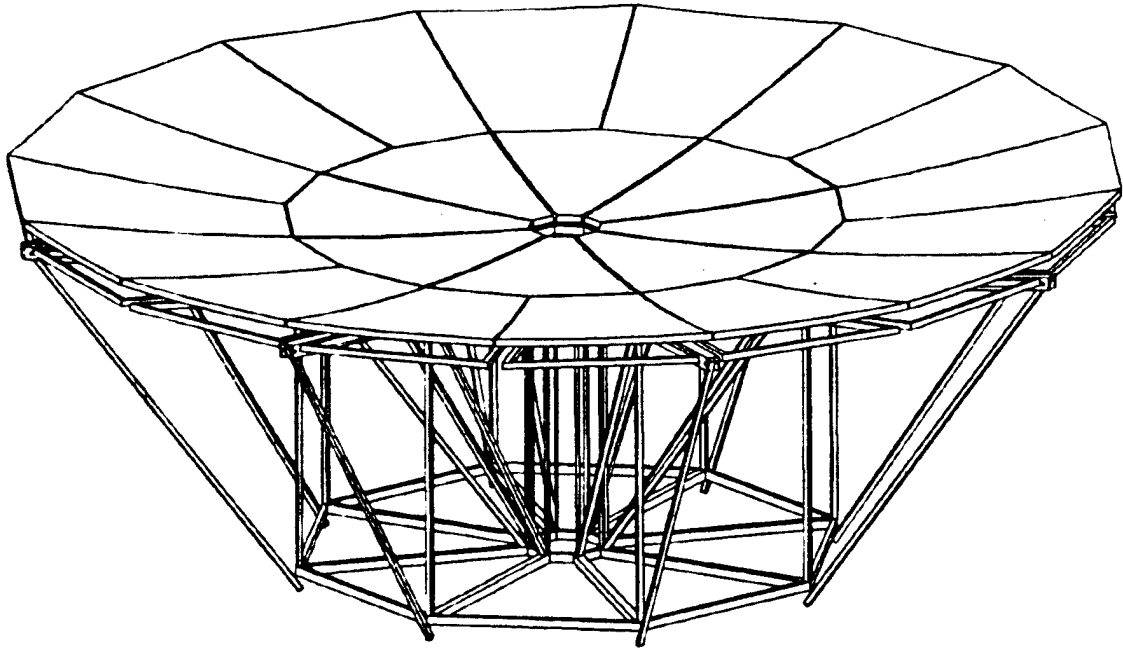


## Figure 4: Mirror Stowed For Launch
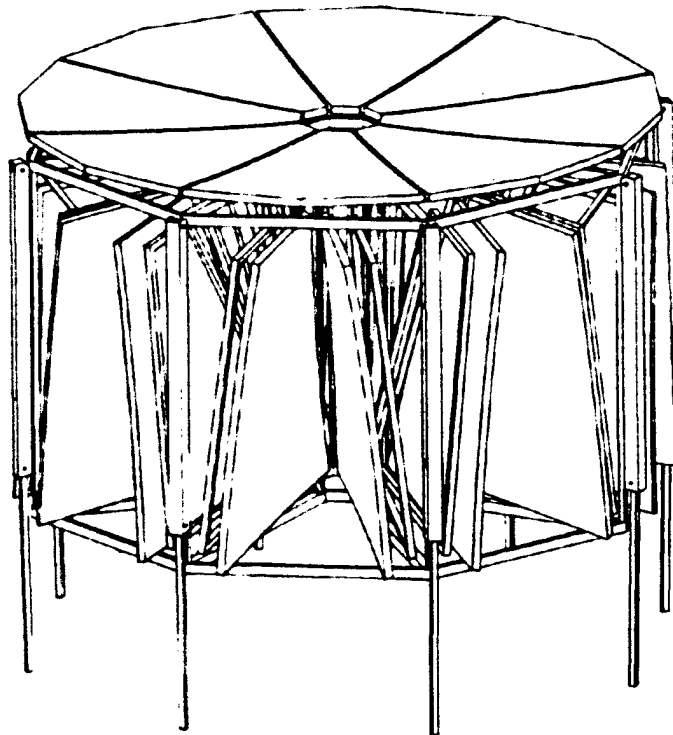
## Figure 5: Overall Model, Twelve-Meter Primary Mirror
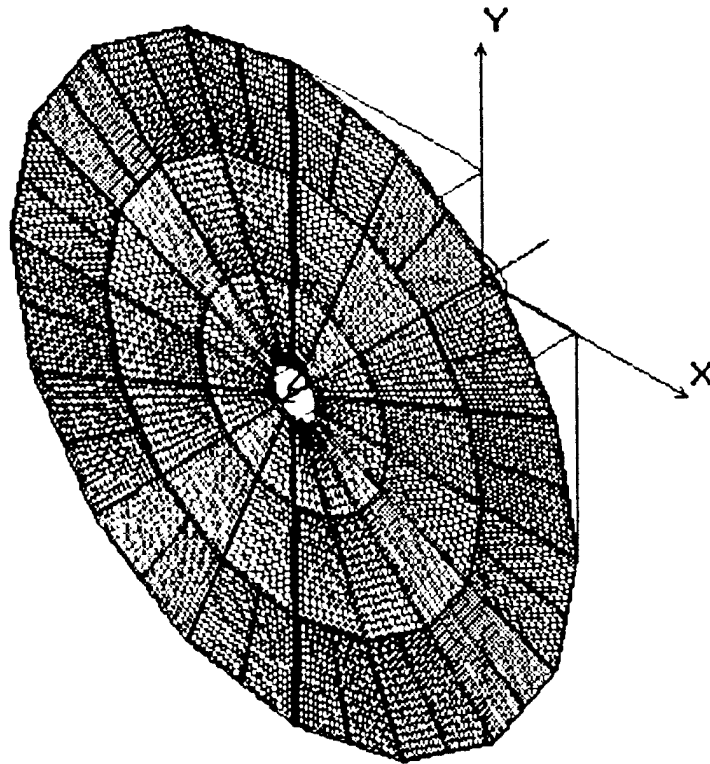


## Figure 6: Twelve Meter Primary Mirror Plan View & Study Segment
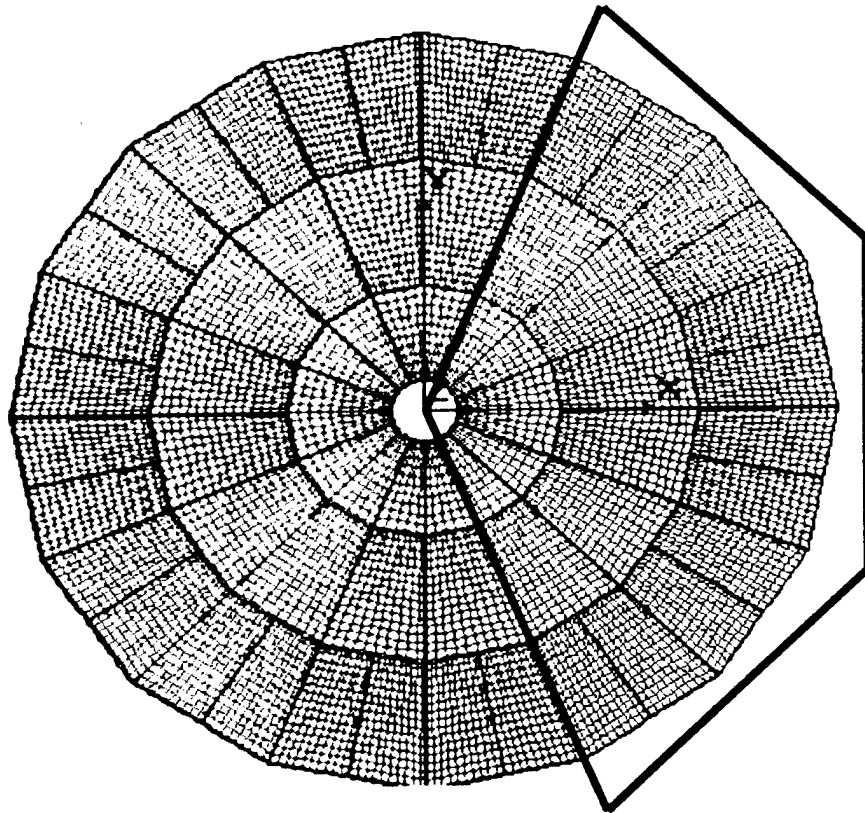
# Figure 7: Twelve Meter Primary Mirror Segment
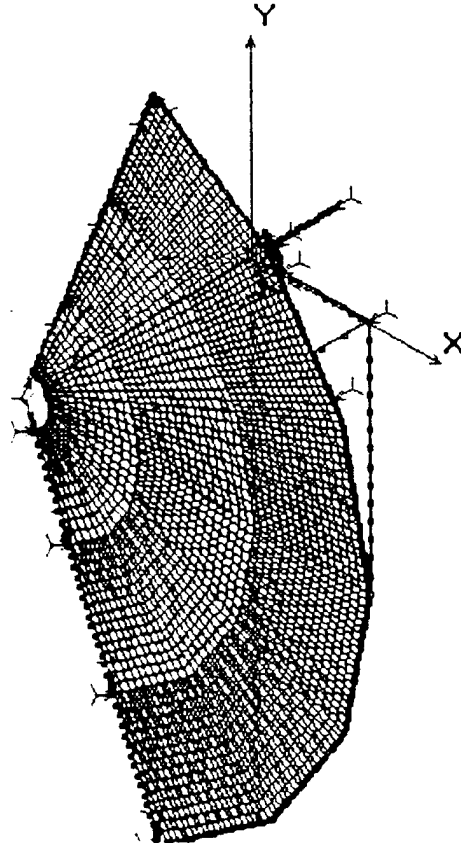


# Figure 8: Twelve Meter Primary Mirror, Mode 7

_Mode=7   16.8431        Hz



Disp_Z

| | |
|---|---|
| ■ | 0.767190 |
| ▓ | 0.621880 |
| ▒ | 0.476570 |
| ░ | 0.331260 |
| ▓ | 0.185950 |
| ▒ | 0.040636 |
| ░ | -0.10467 |
| ▓ | -0.24999 |
| ■ | -0.39530 |
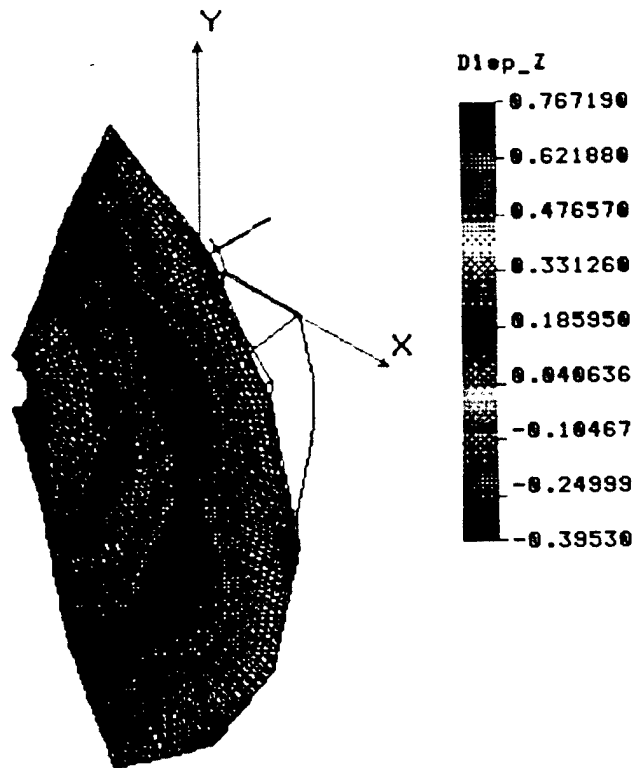
## Figure 9: Twelve Meter Primary Mirror Typical Support Frequency

Mode=8   17.7217      Hz

Disp_Res

6.780800000
5.933200000
5.085600000
4.238000000
3.390400000
2.542800000
1.695200000
0.847600000
6.2563E-008
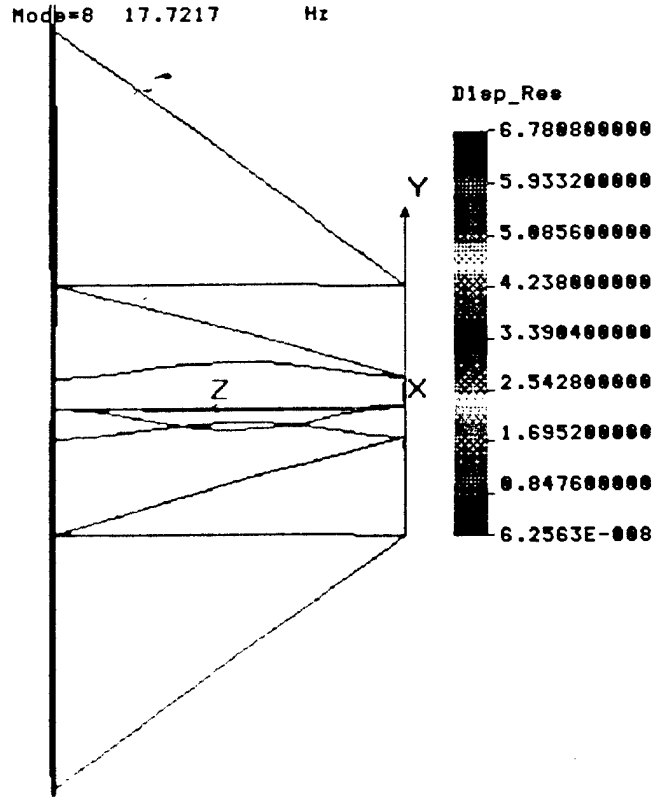
## Figure 10: Twelve-Meter Primary Mirror, Mode 32

Mode=32  34.8769      Hz

Disp_Z

0.912270
0.644990
0.377710
0.110430
-0.15686
-0.42414
-0.69142
-0.95870
-1.22600
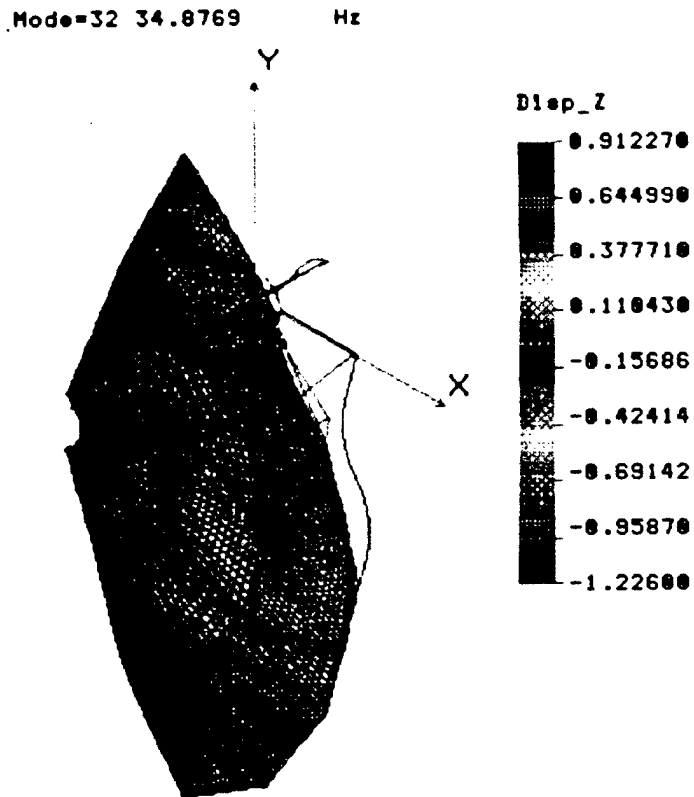
## Figure 11: Twelve-Meter Primary Mirror, Mode 42

Mode=42 49.6298        Y  Hz

Disp_Z

1.080700
0.837260
0.593850
0.350440
0.107040
-0.13637
-0.37978
-0.62319
-0.86660
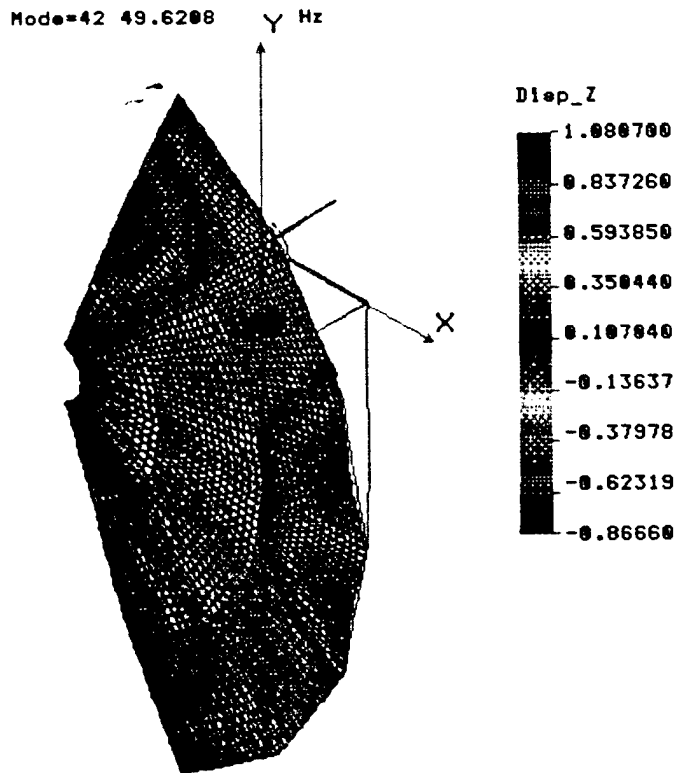


## Figure 12: Twelve-Meter Primary Mirror, Mode 49

_Mode=49 51.3825        Hz

Disp_Z

1.497500
1.123100
0.748730
0.374370
0.000000
-0.37437
-0.74873
-1.12310
-1.49750
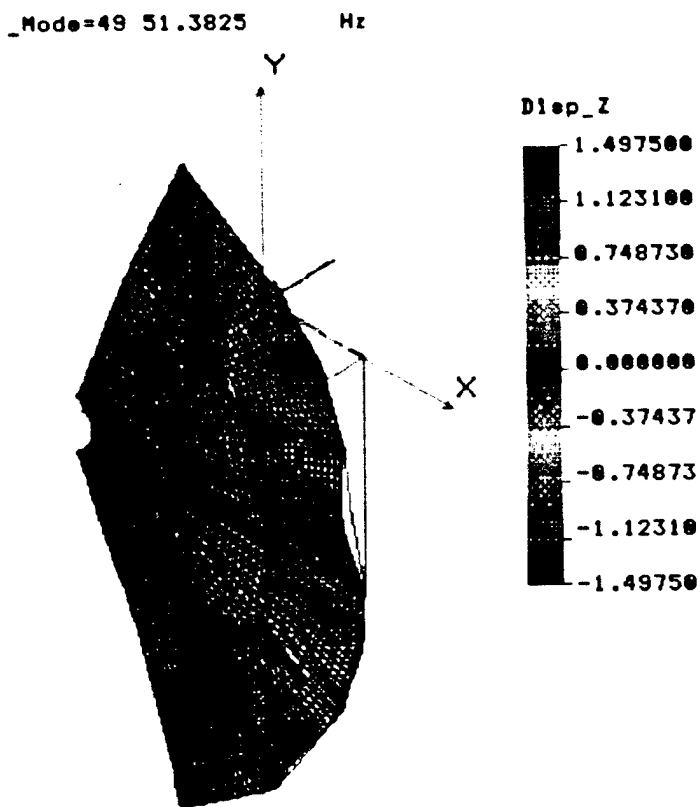
## Figure 13: Twelve-Meter Primary Mirror, Mode 56

_Mode=56  67.3499     Y  Hz

Disp_Z

- 0.950550
- 0.716270
- 0.481990
- 0.247710
- 0.013426
- -0.22085
- -0.45514
- -0.68942
- -0.92370
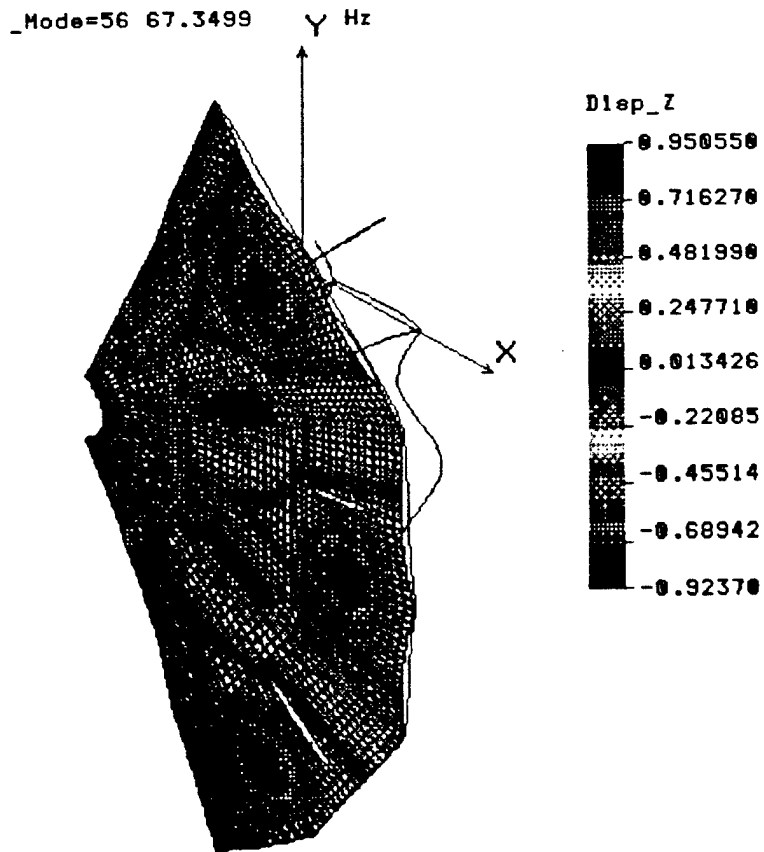
## Figure 14: Twelve Meter Primary Mirror, Mode 71

_Mode=71  80.328        Hz

Disp_Z

- 1.241800
- 0.931360
- 0.620910
- 0.310450
- 0.000000
- -0.31045
- -0.62091
- -0.93136
- -1.24180
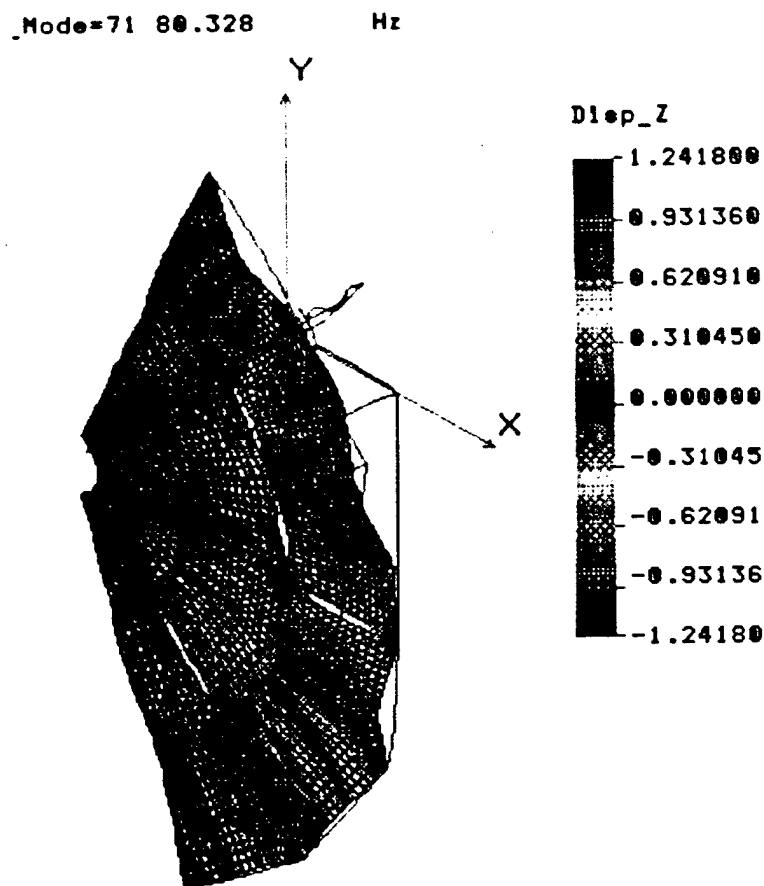
## Figure 15: Twelve Meter Primary Mirror, Mode 73

_Mode=73 83.1631      Hz



Disp_Z

| |
|---|
| 0.837230 |
| 0.577190 |
| 0.317150 |
| 0.057114 |
| -0.20292 |
| -0.46296 |
| -0.72300 |
| -0.98383 |
| -1.24310 |
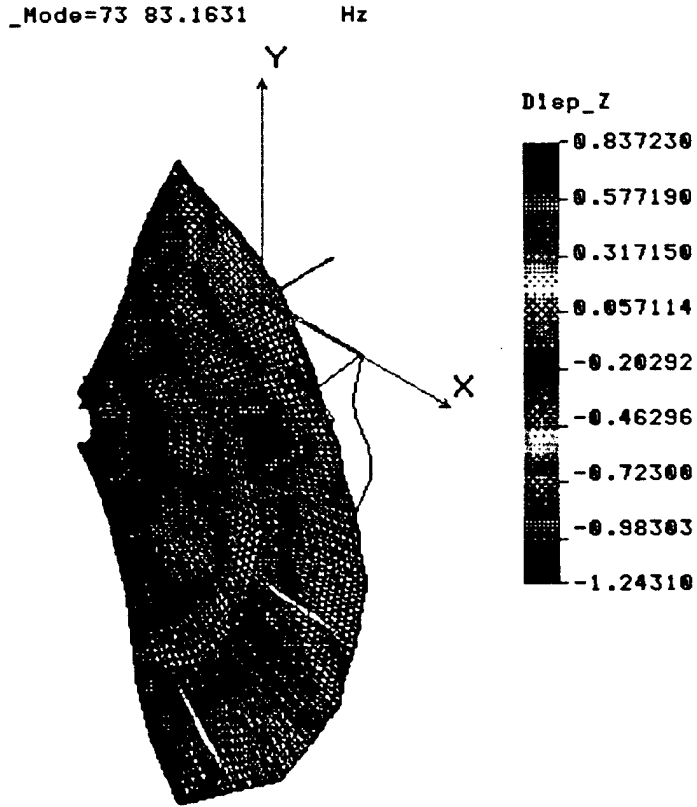
## Figure 16: Twelve Meter Primary Mirror, Mode 78

_Mode=78 96.5721      Hz



Disp_Z

| |
|---|
| 1.076900 |
| 0.807670 |
| 0.538440 |
| 0.269220 |
| 0.000000 |
| -0.26922 |
| -0.53844 |
| -0.80767 |
| -1.07690 |
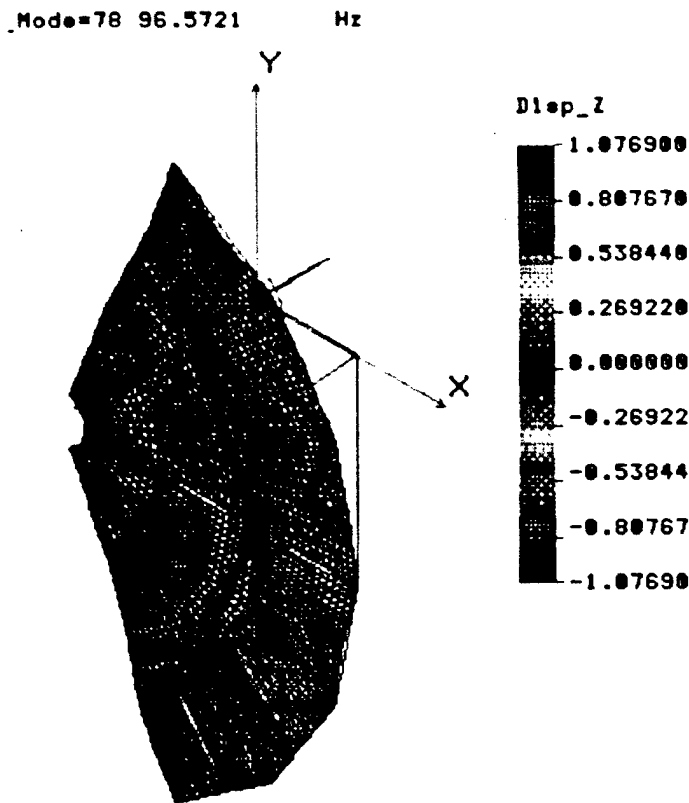
## Figure 17: Twelve Meter Primary Mirror, Mode 85

_Mode=85 102.254   Hz



Disp_Z

1.37190
1.03670
0.701540
0.366380
0.031220
-0.30394
-0.63910
-0.97426
-1.30940
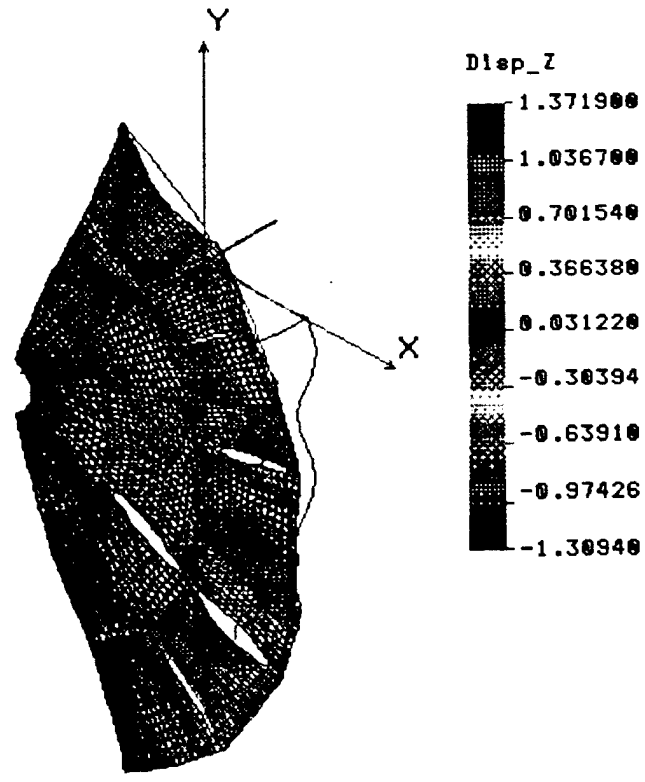
## Figure 18: Twelve Meter Primary Mirror, Mode 87

_Mode=87 108.174   Hz



Disp_Z

1.05080
0.788090
0.525390
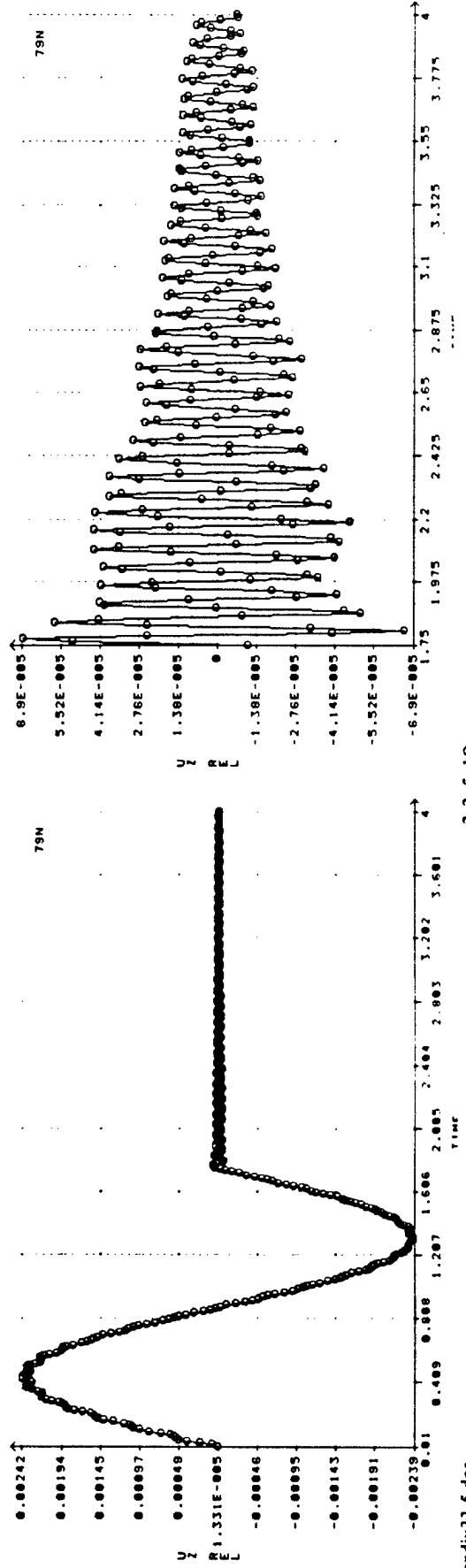0.262700
0.000000
-0.26270
-0.52539
-0.78809
-1.05080
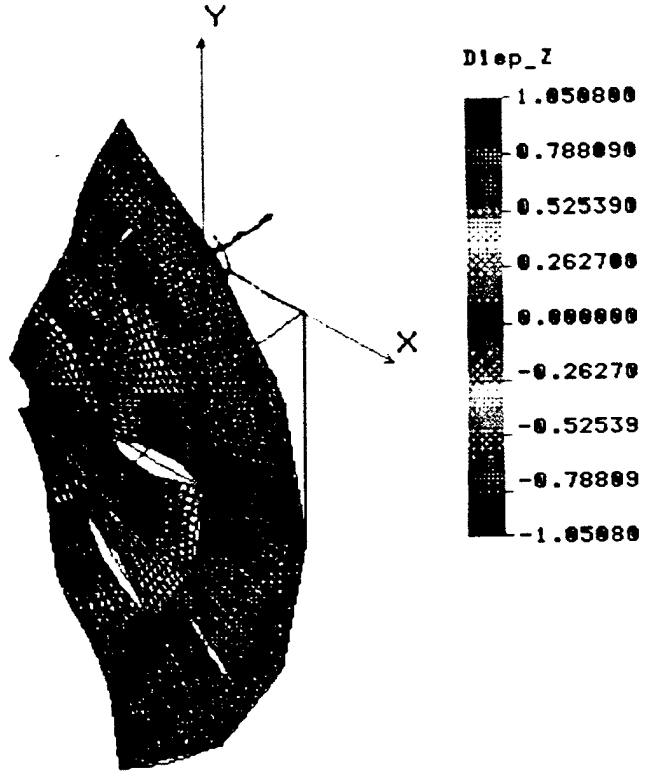
# Figure 19: Response along the X-Axis at the 6.0 Meter Radius after Re-Targeting 0.100 Radian in 1.75 Seconds
## (1% Modal Damping)
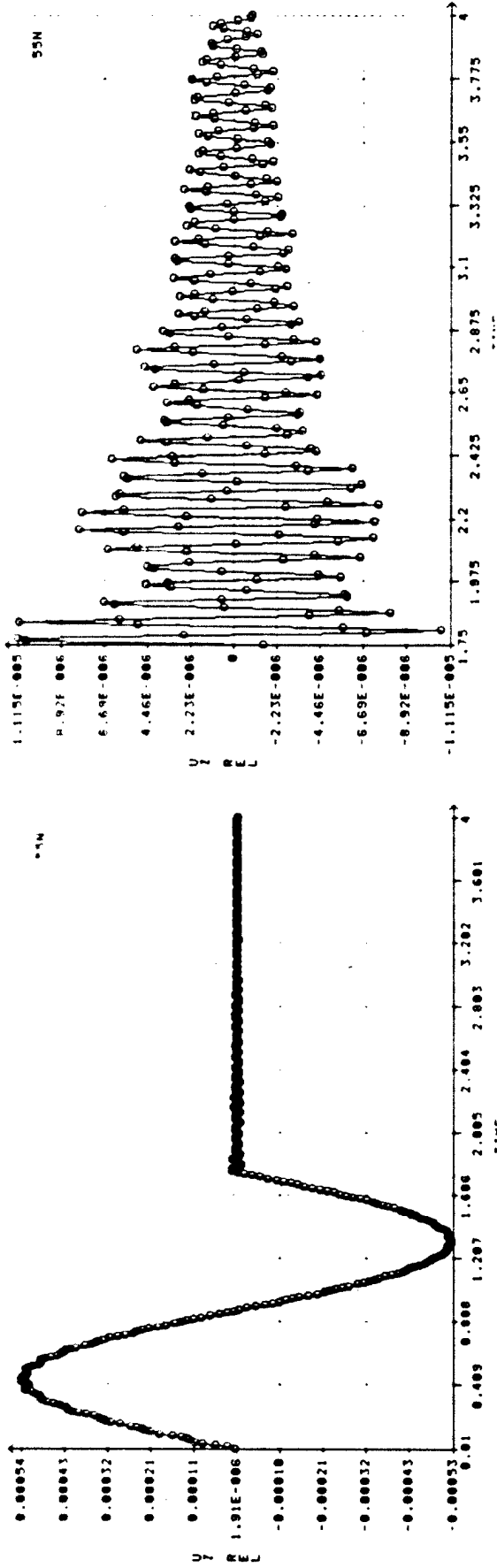


# Figure 20: Response along the X-Axis at the 4.0 Meter Radius after Re-Targeting 0.100 Radian in 1.75 Seconds
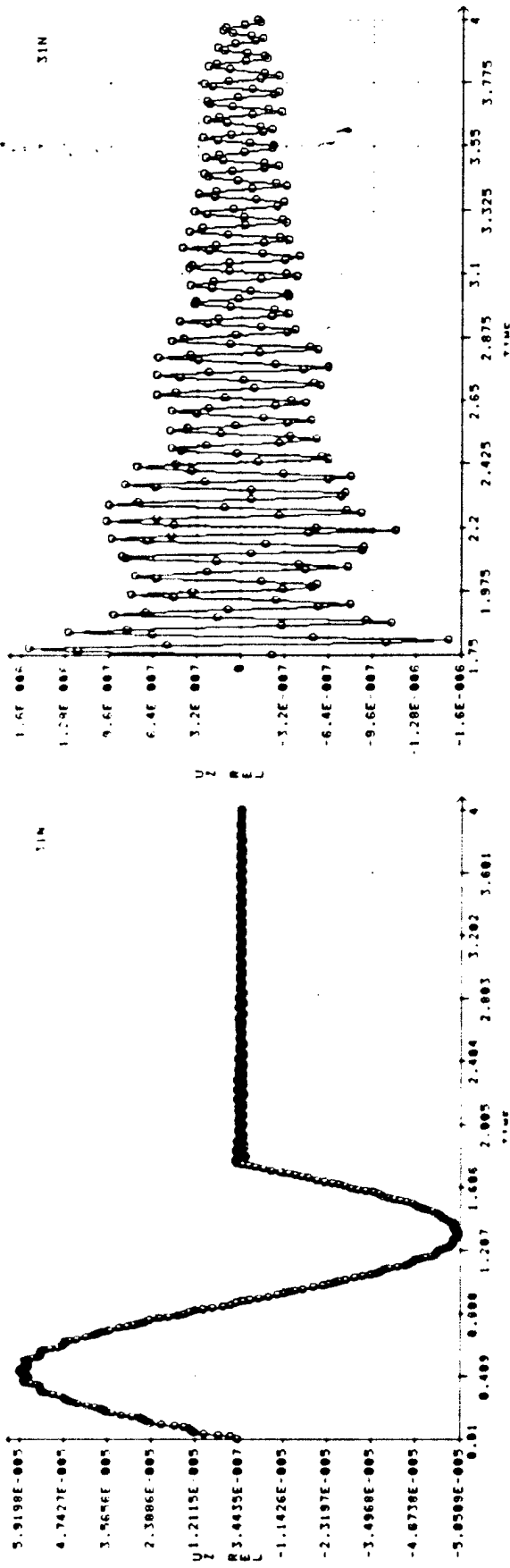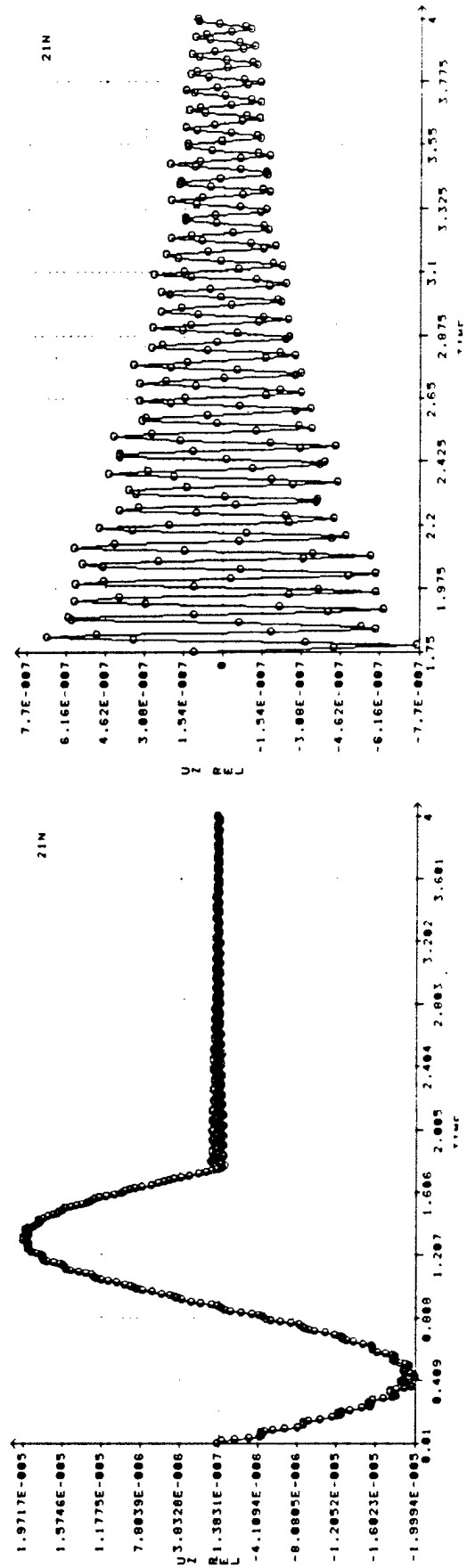## (1% Modal Damping)



3.3-5-19

Figure 21: Response Along The X-Axis At The 2.0 Meter Radius After Re-Targeting 0.100 Radian In 1.75 Seconds
(1% Modal Damping)

Figure 22: Response Along The X-Axis At The 0.5 Meter Radius After Re-Targeting 0.100 Radian In 1.75 Seconds
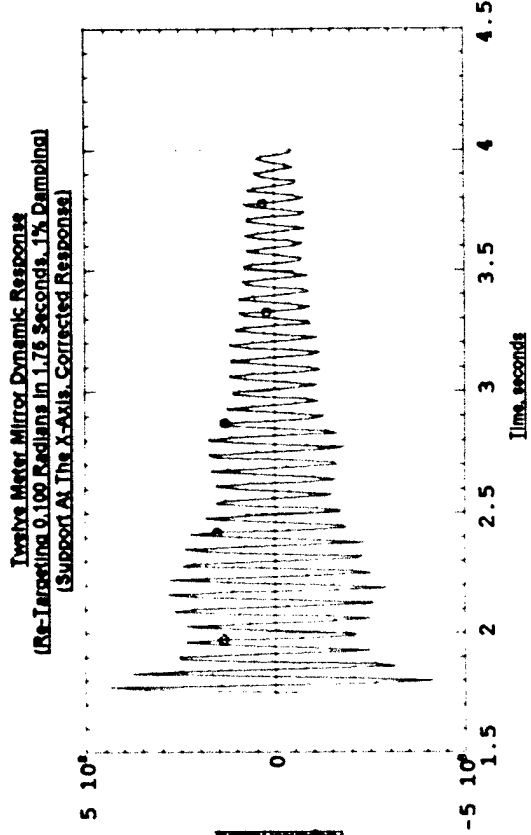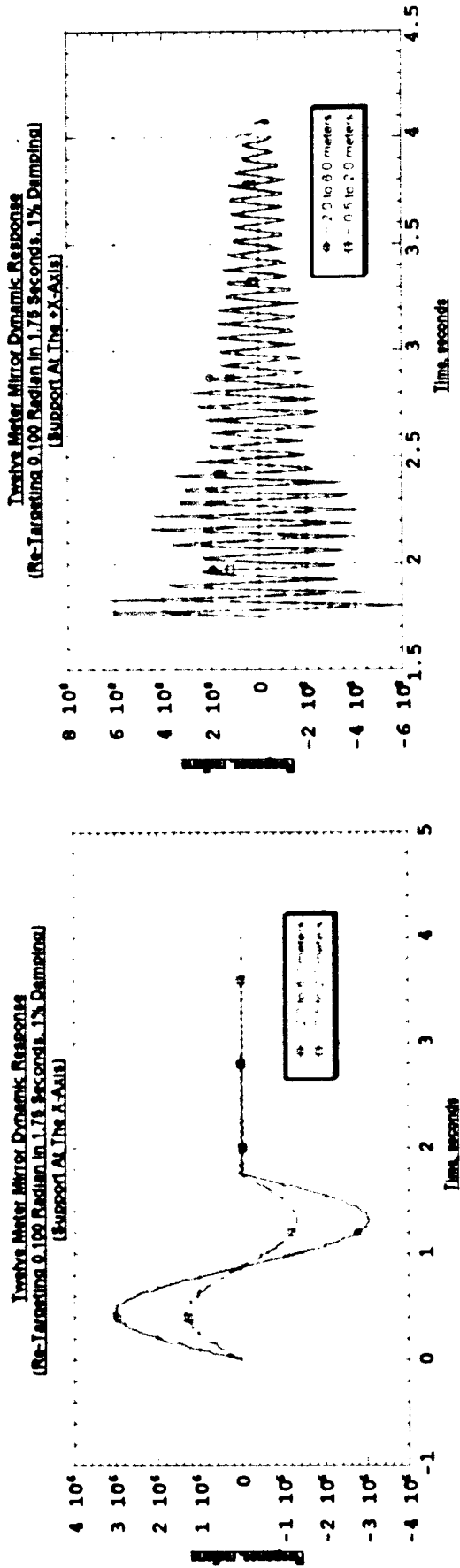(1% Modal Damping)

3.3-5-20

# Figure 23: Response Along The X-Axis Re-Targeting 0.100 Radian In 1.75 Seconds
## (1% Modal Damping)



Twelve Meter Mirror Dynamic Response
(Re-Targeting 0.100 Radian In 1.75 Seconds, 1% Damping)
(Support At The +X-Axis)

Twelve Meter Mirror Dynamic Response
(Re-Targeting 0.100 Radian In 1.75 Seconds, 1% Damping)
(Support At The X-Axis)

Twelve Meter Mirror Dynamic Response
(Re-Targeting 0.100 Radian In 1.75 Seconds, 1% Damping)
(Support At The X-Axis, Corrected Response)

# Figure 24: Response Along The X-Axis Re-Targeting 0.100 Radian In 1.75 Seconds (5% Modal Damping)
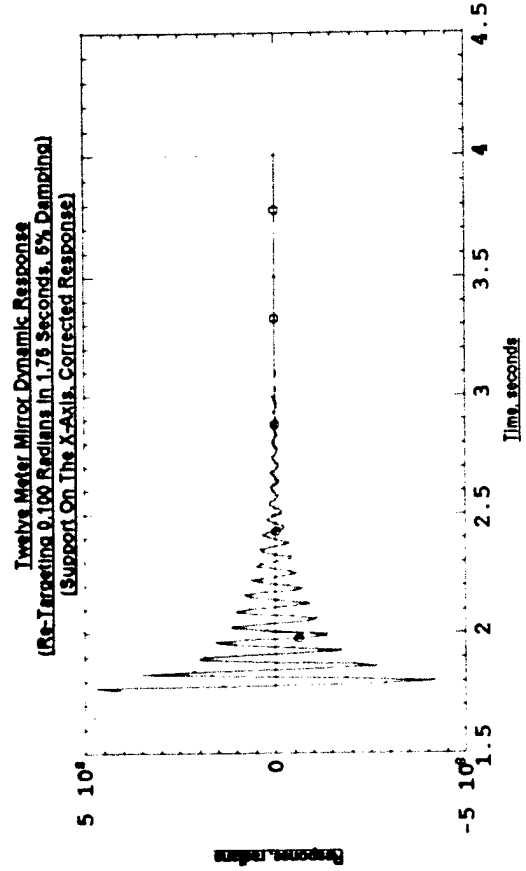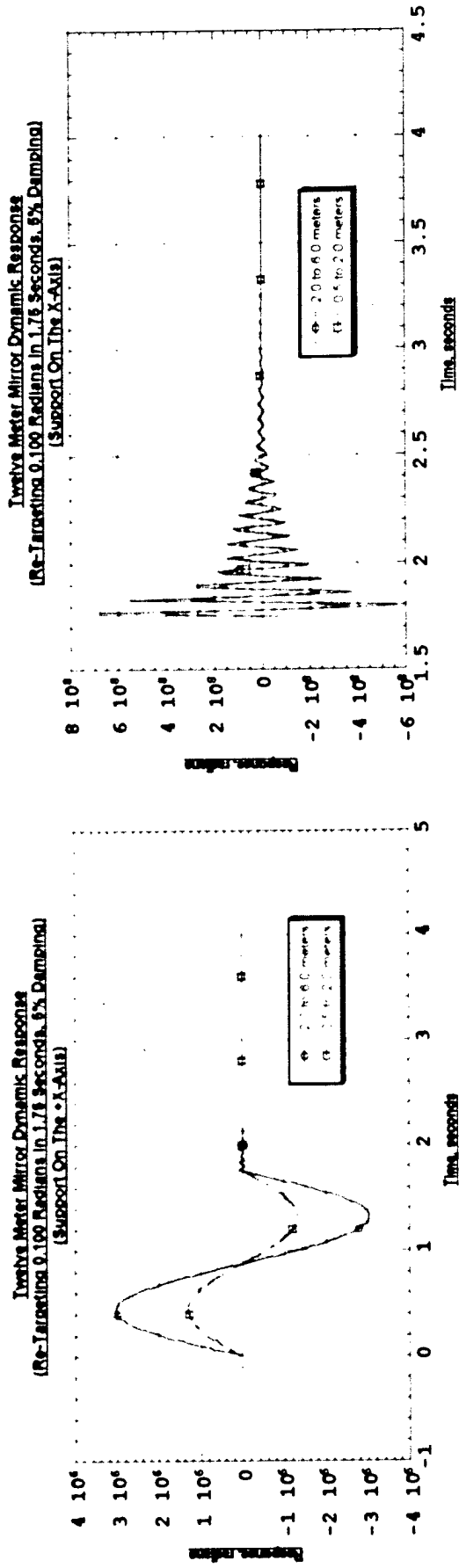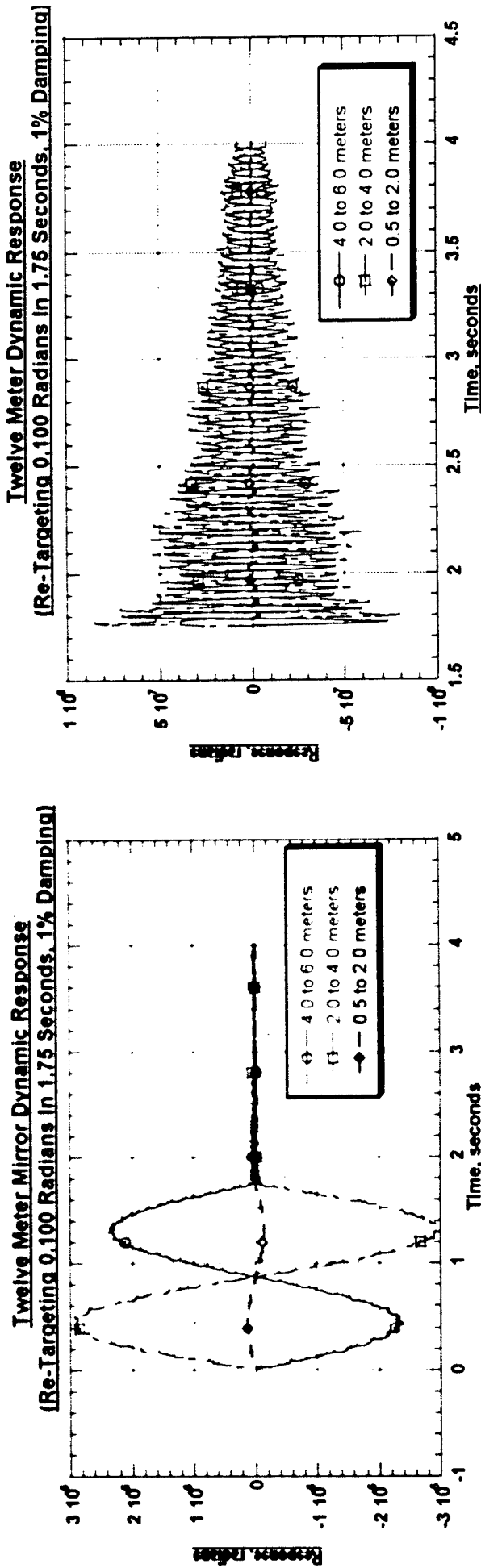
# Figure 25: Response Along The X-Axis After Re-Targeting 0.100 Radian In 1.75 Seconds
## (Responses Calculated For 6.0 to 4.0 , 4.0 to 2.0 & 2.0 to 0.5 Meters)
### (1% Modal Damping)



Twelve Meter Dynamic Response
(Re-Targeting 0.100 Radians In 1.75 Seconds, 1% Damping)

Twelve Meter Mirror Dynamic Response
(Re-Targeting 0.100 Radians In 1.75 Seconds, 1% Damping)

**Note:**   The fact that the "responses" between 6.0 and 4.0 meters are 180° out of phase with the responses between 4.0 and 2.0 meters indicates that the radial support is bending.  Since this effect would be corrected by the deformable mirror, these deflections do not represent a "pointing error".   For this reason, only the difference in deflections between the outside radius of 6.0 meters and the deflections at the 2.0 meter radius are considered in the pointing error calculation.

# Appendix 3.3-6
## GBL Implementation

# ISAAC Upgrades: GBL Implementation

## Schafer

27 January 1999
D. Gettman
A. Pruessner

- GBL entity state variables

- GBL design parameters

- Additional functions added to ISAAC for GBL simulation

- Mods to existing ISAAC functions for GBL simulation

- Loss models (GBL to RM, RM to RM, RM to target)

- Sample input and output files

- Sample ESAU output

# GBL State Variables

- Position (ECI)

- Velocity (rot. of earth)

- Status: idle, engaged

- pointing direction (initial: straight up)

**Schafer**

- Jitter (scraper, beam control, tracker)

- Constellation parameters (No. ground sites, positions)

- Uplink parameters (max. uplink distance, max. uplink zenith angle, etc.)

- Deployment parameters (output aperture diameter, power, wavelength, etc.)

- Retarget Parameters

# GBL Functions Added

- Find uplink routine

- GBL position updates

- Find GBL ops (similar to find RM ops)

- Uplink propagation table initialization

- Strehl value lookup and associated routines

- GBL input file reads

- Graphics file output: GBL position and engagements

- GBL slew time routine

- Visibility check at end of dwell (for entire path)

*Schafer*

3.3-6-6

# Modifications to Existing ISAAC Routines

- StoreOp - added uplink information

- InitHEL - initialize GBL parameters and state info.

- Find GBL ops (modified SBL/RM path finding routine)

- GBL Target - uses RM loss model with uplink strehl

- ProcessShots - include GBL mirror ops

- FindPaths

- THELvis - RM visibility used as before for path finding

- Capture efficiency function - updated using new brightness eq.

# GBL to RM Uplink Loss Model

**The equations used are derived from GG-96B-06:**

$$RM_{cut} = \alpha_{obsc}\, \alpha_{insmt}\, \alpha_{other}\, f_{capture}\left(\lambda, D_{GBL}, D_{Uplink}, R_{GBL \to Uplink}, \sigma^2_{jt}\right)$$

$$f_{capture}\left(\lambda, D_{GBL}, D_{Uplink}, R_{GBL \to Uplink}, \sigma^2_{jt}\right) = \min\left\{1 - e^{-\left(\frac{\pi^2 \cdot D_{GBL}^2 \cdot D_{Uplink}^2 \cdot \sigma_d^2}{16\,\lambda^2 \cdot R^2_{GBL \to Uplink} \cdot \left(\sigma_d^2 + (2.22)^2 \cdot \sigma^2_{jt}\right)}\right)},\ 1 - e^{-2}\right\}$$

$$\sigma^2_{jt} = \sigma^2_{scraper} + \sigma^2_{tracker} + \sigma^2_{beam}$$

$$\sigma_d = \frac{\lambda}{D_{GBL}}$$

$$P_{in,Uplink} = P_{out,GBL} \cdot \alpha_{strehl}$$

$$P_{out,Uplink} = P_{in,Uplink} \cdot RM_{cut}$$

# RM to RM Crosslink Loss Model

**The equations used are derived from GG-96B-06:**

$$RM_{cut} = \alpha_{obsc} \, \alpha_{insm} \, \alpha_{other} \, f_{capture}\left(\lambda, D_{RM1}, D_{RM2}, R_{RM1 \to RM2}, \sigma^2_{jt}\right)$$

$$f_{capture}\left(\lambda, D_{RM1}, D_{RM2}, R_{RM1 \to RM2}, \sigma^2_{jt}\right) = \min\left\{ 1 - e^{-\left[\frac{\pi^2 \cdot D^2_{RM1} \cdot D_{RM2}{}^2 \cdot \sigma_d^2}{16 \lambda^2 \cdot R^2_{RM1 \cdot RM2}\left[\sigma_d{}^2 + (2.22)^2 \cdot \sigma^2_{jt}\right]}\right]}, 1 - e^{-2} \right.$$

$$\sigma^2_{jt} = \sigma^2_{scraper} + \sigma^2_{tracker} + \sigma^2_{beam}$$

$$\sigma_d = \frac{\lambda}{D_{RM1}}$$

$$P_{out,RM2} = P_{Out,RM1} \cdot RM_{cut}$$

*Schafer*

# *RM to Target Intensity Model*

The equations for the following calculations are the same as for the SBL only model. (See GG-96B-06a)

- Brightness
- Lethal Intensity
- Dwell Time

# Sample ISAAC Output (.trs)

| Kr | ITT | IPH | Tvis | TSTRT | TSLW | TOWL | TEND | RANG | LmtO | RVs | SIAng | Spot | ALOS |
|---|---|---|---|---|---|---|---|---|---|---|---|---|---|
| 2 | 41 | 0 | 48 | 48 | 0 | 6.73 | 55.23 | 3049.17 | 163.83 | 10 | 0 | 263.19 | 36.86 |
| 1 | 42 | 0 | 48 | 48 | 6.9 | 8.09 | 61.49 | 2361.29 | 180.5 | 10 | 0 | 203.81 | 6.75 |
| 7 | 10 | 0 | 48 | 48 | 10.877 | 3.88 | 63.26 | 2736.28 | 281.27 | 8 | 0 | 66.77 | 44.02 |
| 2 | 45 | 0 | 48 | 55.23 | 0.976 | 8.59 | 63.29 | 3021.66 | 167.2 | 10 | 0.2 | 280.81 | 36.7 |
| | 6 | 0 | 48 | 63.26 | 1.1 | 3.41 | 68.26 | 2855.28 | 320.16 | 8 | 0 | 64.79 | 39.37 |
| | 44 | 0 | 48 | 81.49 | 1.1 | 5.82 | 68.91 | 2312.9 | 188.4 | 10 | 0 | 199.64 | 1.31 |
| 2 | 49 | 0 | 48 | 63.29 | 1.143 | 6.46 | 71.39 | 2995.89 | 170.46 | 10 | 0.42 | 258.57 | 36.56 |
| | 4 | 0 | 48 | 88.28 | 1.1 | 3.3 | 73.16 | 2847.81 | 330.58 | 8 | 0 | 64.61 | 37.35 |
| 1 | 48 | 0 | 48 | 68.91 | 1.1 | 5.85 | 76.36 | 2316.32 | 187.5 | 10 | 0 | 199.93 | 1.87 |
| | 3 | 0 | 48 | 73.16 | 1.1 | 3.22 | 77.99 | 2626.05 | 338.76 | 8 | 0 | 64.08 | 36.72 |
| 2 | 46 | 0 | 48 | 71.39 | 1.217 | 6.36 | 79.47 | 2989.68 | 172.95 | 10 | 0.55 | 258.05 | 35.7 |
| | 9 | 0 | 48 | 77.99 | 1.1 | 3.12 | 82.7 | 2592.63 | 350.48 | 6 | 0 | 63.26 | 36.02 |
| | 50 | 0 | 48 | 76.36 | 1.1 | 5.84 | 83.81 | 2308.65 | 187.78 | 10 | 0 | 199.27 | 5.01 |
| 2 | 47 | 0 | 48 | 79.47 | 1.002 | 6.22 | 87.19 | 2970.98 | 176.68 | 10 | 0.23 | 256.44 | 34.97 |

| AllS | AllD | AllK | PL | TWstrt | Bounces | RM1 | RM2 | RM3 | Uplink |
|---|---|---|---|---|---|---|---|---|---|
| 10.1 | 10.1 | 13.06 | 1 | 0 | 0 | 0 | 0 | 0 | -1 |
| 10.15 | 13.19 | 16.18 | 1 | 0 | 1 | 2 | 0 | 0 | -1 |
| 10.13 | 15.09 | 17.07 | 1 | 0 | 2 | 8 | 0 | 0 | 14 |
| 13.35 | 13.81 | 17.12 | 1 | 0 | 0 | 0 | 0 | 0 | -1 |
| 17.27 | 17.86 | 19.74 | 1 | 0 | 2 | 8 | 0 | 0 | 14 |
| 16.44 | 17.02 | 20.22 | 1 | 0 | 1 | 2 | 0 | 0 | -1 |
| 17.41 | 18.03 | 21.68 | 1 | 0 | 2 | 8 | 0 | 0 | -1 |
| 20.05 | 20.68 | 22.62 | 1 | 0 | 2 | 8 | 0 | 0 | 14 |
| 20.48 | 21.12 | 24.66 | 1 | 0 | 1 | 2 | 0 | 0 | -1 |
| 22.94 | 23.61 | 25.63 | 1 | 0 | 2 | 8 | 0 | 0 | 14 |
| 21.99 | 22.71 | 26.7 | 1 | 0 | 0 | 0 | 0 | 0 | -1 |
| 26.01 | 26.72 | 28.78 | 1 | 0 | 2 | 8 | 0 | 0 | 14 |
| 24.96 | 25.66 | 29.52 | 1 | 0 | 1 | 2 | 0 | 0 | -1 |
| 26.98 | 27.64 | 31.89 | 1 | 0 | 0 | 0 | 0 | 0 | -1 |

## Output parameters added:

- Bounces: No. bounces from HEL
- RM1/RM2/RM3 : RM ID number
- Uplink: ID of uplink RM (-1 if an
  SBL or SBL/RM engagement)

3.3-6-11

# Sample ISAAC Input (.dat)

**Schafer**

| Sample Situation Parameters | | RMs | 6x4 |
|---|---|---|---|
| GBL diam | 10 m | RM phase | 0.66 |
| GBL power | 20 MW | RM incl | 60 |
| Wavelength | 1.2 | RM alt. | 800 |
| Max.zenith | 35 | RM loss | 0.92 |
| Max bounces | 3 | RM jitter | 30 |
| Max Uplink dist. | 10000 km | RM WFE | 0.06 |
| No. GBLs | 1 | RM in | 4m |
| GBL 1 lat. | 40 | RM out | 10m |
| GBL 1 lon. | -100 | Threats | 70 |
| GBL 2 lat. | 50 | Hardness | 5kj/cm2 |
| GBL 2 lon. | -55 | | |

3.3-6-12

# Sample ESAU Output (View from North Pole)

# Appendix 3.3-7
# ESAU

# ESAU 3D - flowchart

```
Documentation ──────────────────────────────▶ Manual

AVI Capture ──▶ Determine          ──▶ Purchase and
(done)          Software to be          Install
                Used
                (done)

Create JAVA ──▶ Determine and      ──▶ Install JAVA
Control         add the                Control
                functions

                                       Design the ──▶ Consolidate
                                       HTML            ALL. files and
                                       Interface       software
                                       (done)          (done)

Add Formulas ──▶ Consolidate    ──▶ Install VRML
to Code          VRML files          main.wrl
(done)           (done)              (done)
```

3.3-7-2
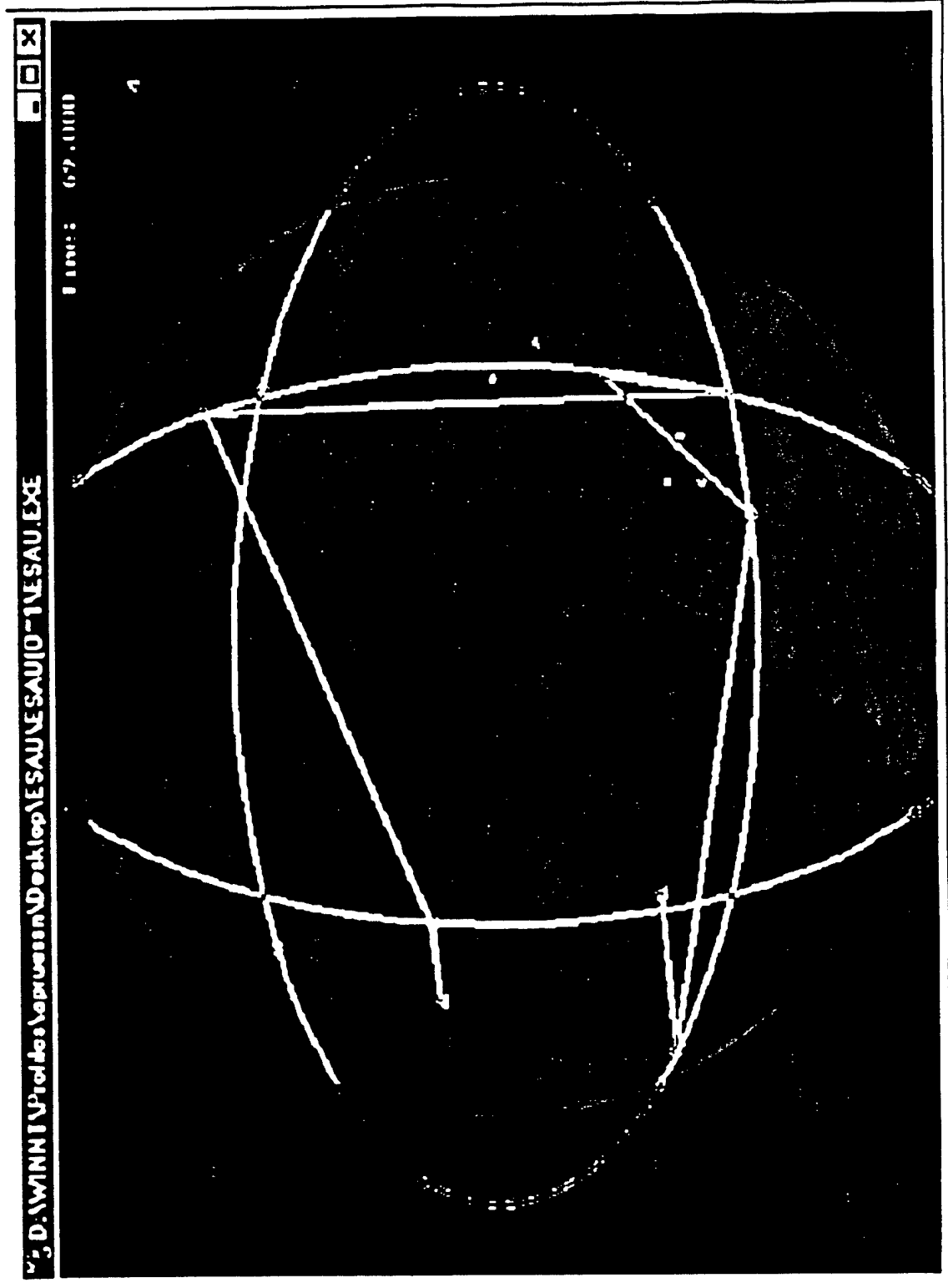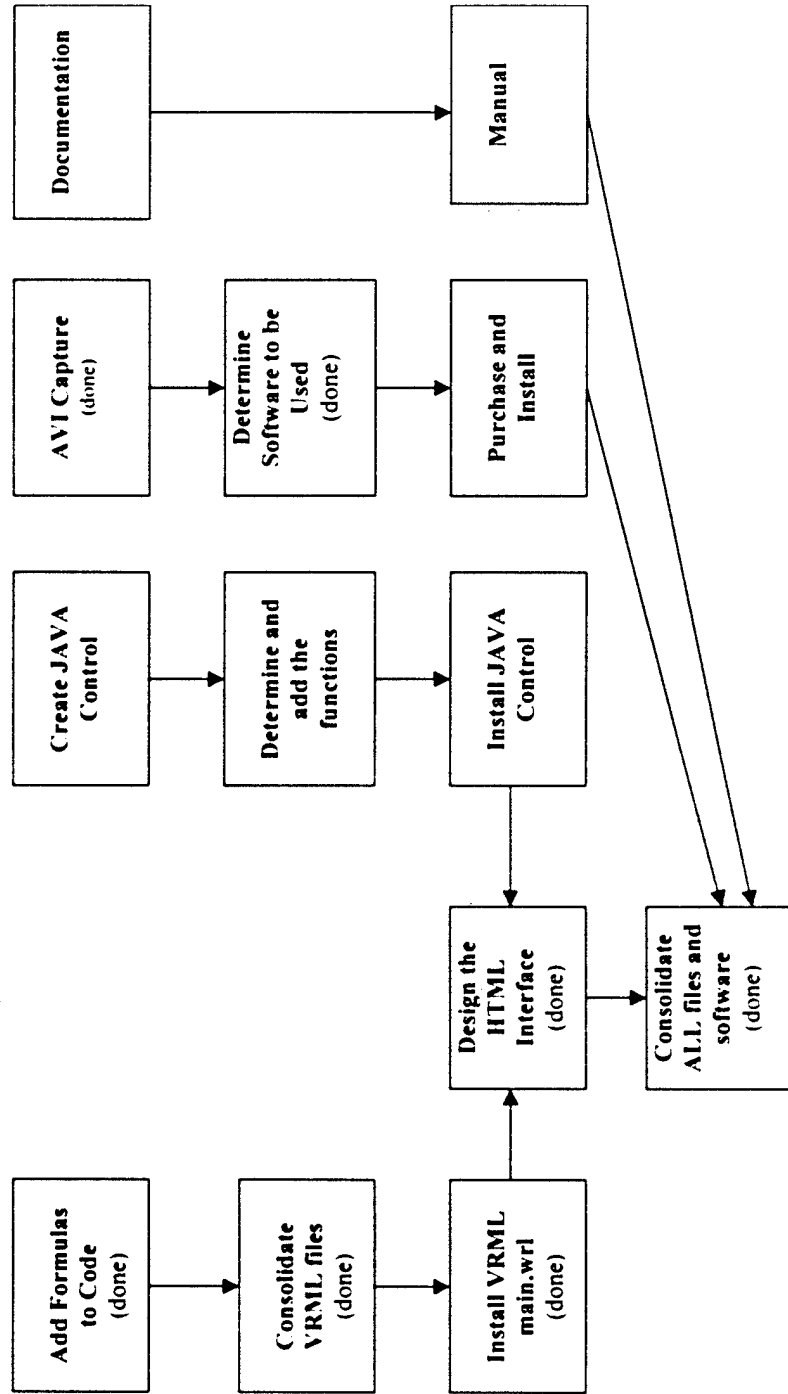
# ESAU 3D - sample screen capture
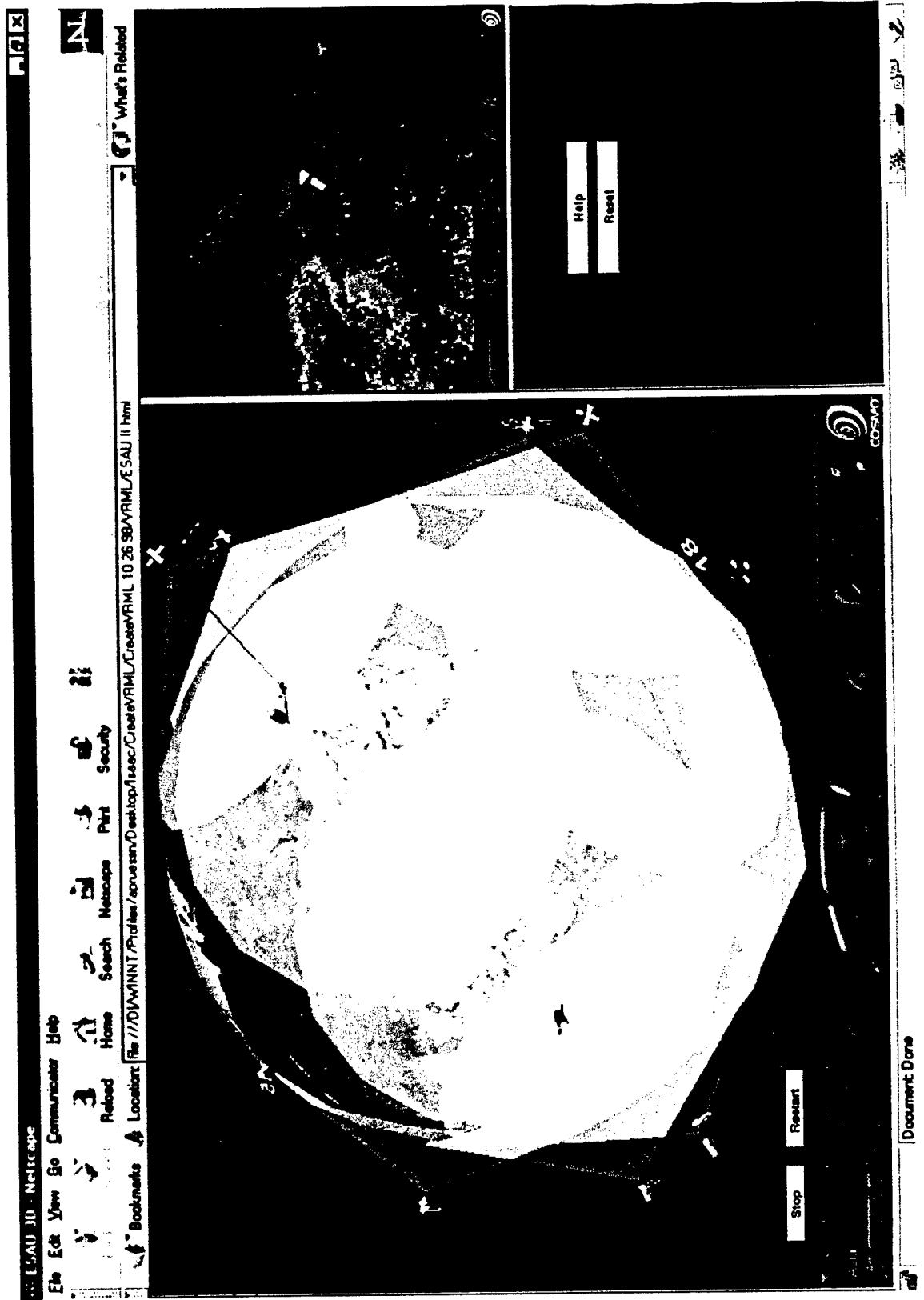
# Appendix 3.3-8
# ISAAC Analysis

# ISAAC Analysis

Work was done on the following codes associated with the ISAAC (Integrated Strategic Architecture Analysis Code) family of programs.

1)      ETA-T

2)      ESAU-3D

3)      ISAAC

In each section a brief overview of the code and a list of upgrades/modifications are included. Furthermore, some future work is outlined as well.


## 1. ETA-T

**Overview:**

ETA-T (Engagement Timeline Analysis) is a software code written in FORTRAN which simulates the flight of a ballistic missile from launch-point to an aim-point on a spherical, rotating earth. Optional outputs include trajectory curve fits, flight statistic summary information and trajectory state vectors. The trajectory curve fits are used in ISAAC for satellite constellation design and analysis.


**Work Performed:**

1)      modified to accommodate long range missiles
2)      corrected bug for fixed burn time and fixed flight path angle options
3)      created a set of threat files (missile files, scenarios, trajectory files)


**Descriptions:**

The code did not run very efficiently for long range missiles. The problem was traced to an optimization function which was changed to accommodate for the different ranges.

Corrections to the "fixed" options (burn time and flight path angle) were mostly associated with parameters not being stored properly in memory. Work performed included testing and debugging for other minor errors.

Work done in creating the set of threat files included research for the proper missile parameters and scenarios, debugging the program for each missile input file and creating the actual missile trajectory files.

**Possible Future Work:**

1)   Lofted and depressed trajectory capability
2)   Output of state data after each missile stage

## 2. ESAU-3D

**Overview:**

ESAU-3D (Engagement Simulation Animation Utility 3D) is a graphics tool for animating the output of ISAAC, JACOB or other ISAAC suite programs. It is written in VRML (Virtual Reality Markup Language) and can be interpreted by any web browser (such as Netscape's Navigator or Microsoft's Internet Explorer), provided one has a VRML browser plug-in. Some of its features include the ability for the user to navigate and view the animation from different viewpoints.

**Work Performed:**

1)   Consolidated VRML files previously created
2)   Designed and created HTML interface (includes menu and help files)
3)   Added various features including different viewpoints and stop/restart capability
4)   Wrote filter program to create VRML animation files from ISAAC output (.GRF files)
5)   Debug and testing

**Descriptions:**

The project was inherited from another Schafer employee who had already created some of the components to be used. The first task was to sort through the routines to see which parts could be used and how to fit them together. After consolidating the VRML files various new features were added, including different viewpoints (from the major continents and each SBL) and rotational effects of the earth. Also, software for image and video (.AVI) capture were determined.

The second task entailed creating an HTML interface to control the VRML world. This also included creating menus and help files. Furthermore, testing and debugging was done of the VRML animation itself to ensure that it portrayed the scenario evaluated in ISAAC.

The final task was to write a filter program (in FORTRAN) which reads in the .GRF files created by ISAAC and write the VRML animation files automatically. Again, testing and debugging was done to ensure that the output was accurate.

**Possible Future Work:**

1) addition of GBLs, ABLs, and relay mirrors
2) more detailed animation of threat trajectories and kills
3) more animation control capability (stop, start, slow motion, reverse motion, etc.)

# 3. ISAAC

## Overview:

ISAAC (Integrated Strategic Architecture Analysis Code) is intended as a tool for architecture and system level analysis of SBLs or ABLs against threats. It models an M-on-N simulation and gives performance statistics such as time to kill, altitude of kill, requirements of major weapons subsystems (e.g. aperture jitter, threat analysis) and overall effectiveness.

## Work Performed:

1) added multiple constellation capability (i.e. multiple inclinations and/or altitudes)
2) Began GBL and relay mirror addition
   - research and testing of path finding algorithms
   - GBL specific routines

## Descriptions:

Upgrades for multiple constellation capability were begun mainly by modifying the SBL orbit propagation routine. Work is not yet complete.

GBL upgrades were complicated because of the inefficiency of most path-finding algorithms. In order to get a thorough list of all possible paths visibility checks must be done between all objects (all SBLs to all RMs, all RMs to all RMs). Because the visibility checks employ trigonometric functions this takes a lot of time. Some work was done testing alternate path-finding routines. While some were faster than the brute-force approach, the more efficient algorithms only calculated one possible path. This is impractical for scenarios where GBLs and SBLs are both simultaneously in play.

# Appendix 3.3-9
# Improving ETA-T Efficiency

# IMPROVING ETA-T EFFICIENCY

Various simulation runs using short, medium, and long range missiles show that Eta-T does not always converge to an accurate solution in a reasonable amount of time. Since the program runs well with short range, but not as well with long range missiles, it was suggested by Larry Carlson that a new optimization function be used. Several functions were developed and tested. The most promising is one in which parameters depend on the range of the scenario. Results of simulation runs so far are encouraging. The following information shows some of the solution attempts and their results, as well as some observed bugs.

## Overview

The purpose of the optimization routine (POWELL) in Eta-T is to minimize the burn time of the miss distance. The original function used is:

$$f = missdist + 1,000 \cdot \Delta burntime + 100 \tag{1}$$

The function was chosen such that the absolute values of the miss distance (in meters) and of the change in burn time (in seconds) are roughly equal. This ensures that the optimization routine minimizes both parameters equally fast. For short range missiles this works quite well. For long range missiles the initial miss distance is far greater than the change in burn time so that initial variations have no effect on the function. Several attempts were made to improve the accuracy and efficiency for longer range missiles. The following is a brief description of these attempts and their results.

## I.    Changing the Variational Matrix

Presently, the initial suggested variations in burn time, course heading, and flight path angle are independent of one another. The current variation matrix (in the subroutine POWELL) is:

$$\begin{bmatrix} 0.1 & 0 & 0 \\ 0 & 0.01 & 0 \\ 0 & 0 & 0.01 \end{bmatrix} \tag{2}$$

Where the first value in each column represents the variation in the cutoff time, the second the variation in course heading, and the third the variation in the flight path angle. Several variation matrices in which changes in the parameters happen simultaneously were tested. None of them improved the accuracy or efficiency of the program.

## II.  Changing the Flight Path Angle Rollover Constant

Simulation runs using different flight path angle rollover constants suggest that the parameter needs to be adjusted according to the range of the scenario. Different parameter values resulted in different altitudes and ranges at burn out.

| FPA at burn out (deg) | FPA Rollover Constant | $T_{burn}$ out (sec) | Altitude at $t_{bo}$ (m) | Range at $t_{bo}$ (m) |
|---|---|---|---|---|
| Auto | 10.0 | 122.862 | 120,049.54 | 274,227.18 |
| Auto | 6.0 | 123.046 | 132,959.71 | 267,484.44 |
| 21.18 | 10.0 | 122.862 | 132,409.57 | 266,387.28 |
| 21.18 | 6.0 | 123.610 | 134,665.68 | 270,884.67 |

## III.  Using a Piece-Wise Defined Optimization Function

In order to improve efficiency for long range missiles, a piece-wise defined optimization function was tested.

$$f = missdist + \alpha \cdot \Delta burntime \qquad \alpha = \begin{cases} 1,000 \rightarrow missdist < 100km \\ 10,000 \rightarrow 100km < missdist < 1,000km \\ 100,000 \rightarrow 1,000km < missdist \end{cases} \qquad (3)$$

Since the optimization subroutine (POWELL) does not converge continuously to the minimum miss distance (POWELL bounces back and forth between values), a piece-wise defined function is impractical. As soon as the miss distance is within acceptable range, POWELL might iterate to a very large miss distance and hence use a different parameter $\alpha$. The subroutine bounces between different optimization functions and cannot complete enough iterations with one function to converge.

## IV.  Using a Continuous Optimization Function

Several optimization functions using constant factors $\alpha$ were tested. None significantly improved the current program. Finally, a continuous, miss distance dependent function was developed.

$$f = missdist + \frac{missdit}{1,000} \cdot \Delta burntme \qquad (4)$$

This function ensures that even for long range missiles, where the initial miss distance is greatest, the absolute values of the miss distance (in meters) and of the change in burn time (in seconds) remain roughly equal. Throughout preliminary tests the new function

converged to a more accurate result in the same amount of time (or less). Specifically, for long range missiles the function appears to be much more efficient.

The following simulation data was compiled using a Pentium 233 MHz PC with 128 MB or memory. Different tolerance factors, which determine the actual cutoff point for the program were used for each of the functions. For the original function (1), a tolerance which depends on the variation of the functional value was used (ftol = 0.1). For the new function a tolerance which depends on the actual functional value was implemented (fret < 150).

## Short Range Data

Aim Point:     35 N    128 E   -  1 stage missile

| Function | Static Range (km) | Launch Position | Simulation Time (min) | Number of Iterations | Miss Distance (m) |
|---|---|---|---|---|---|
| Old (1) | 45.59 | 35N,    127E | 1 | 93 | 10.50 |
| New (4) | 45.59 | 35N,    127E | 1 | 68 | 10.84 |
| Old (1) | 106.59 | 35.5N, 127E | 1 | 98 | 21.61 |
| New (4) | 106.59 | 35.5N, 127E | 1 | 98 | 21.61 |
| Old (1) | 120.19 | 36N,    127E | 2 | 125 | 19.22 |
| New (4) | 120.19 | 36N,    127E | 1 | 106 | 43.32 |
| Old (1) | 172.98 | 36.5N, 127E | 2 | 146 | 12.79 |
| New (4) | 172.98 | 36.5N, 127E | 1 | 113 | 17.31 |
| Old (1) | 281.89 | 37.5N, 127E | 2 | 112 | 37.08 |
| New (4) | 281.89 | 37.5N, 127E | 2 | 97 | 22.94 |

## Medium Range Data

Aim Point:     34:04 N    118:15 E    -  3 stage missile

| Function | Static Range (km) | Launch Position | Simulation Time (min) | Number of Iterations | Miss Distance (m) |
|---|---|---|---|---|---|
| Old (1) | 5,252.38 | 80N,    145W | 6 | 125 | 1,287.26 |
| New (4) | 5,252.38 | 80N,    145W | 6 | 115 | 888.58 |
| Old (1) | 4,711.74 | 0N,    145W | 7 | 134 | 1,239.16 |
| New (4) | 4,711.74 | 0N,    145W | 5 | 85 | 1,224.58 |
| Old (1) | 3,484.55 | 60N,    145W | 6 | 125 | 516.25 |
| New (4) | 3,484.55 | 60N,    145W | 5 | 109 | 526.49 |
| Old (1) | 3,072.69 | 20N,    145W | 6 | 136 | 481.72 |
| New (4) | 3,072.69 | 20N,    145W | 4 | 72 | 501.19 |
| Old (1) | 2,466.35 | 40N,    145W | 4 | 80 | 319.48 |
| New (4) | 2,466.35 | 40N,    145W | 6 | 115 | 381.52 |

## Long Range Data

Aim Point:     34:04 N   118:15 E     - 3 stage missile

| Function | Static Range (km) | Launch Position | Simulation Time (min) | Number of Iterations | Miss Distance (m) |
|---|---|---|---|---|---|
| Old (1) | 8,353.35 | 0N,   170E | 12 | 200 | 2,958.22 |
| New (4) | 8,353.35 | 0N,   170E | 7 | 110 | 2,945.98 |
| Old (1) | 7,870.80 | 10N,   170E | 11 | 151 | 2,271.04 |
| New (4) | 7,870.80 | 10N,   170E | 8 | 115 | 1,944.81 |
| Old (1) | 7,155.18 | 20N,   170E | 9 | 145 | 1,680.60 |
| New (4) | 7,155.18 | 20N,   170E | 6 | 91 | 1,705.99 |
| Old (1) | 6,246.38 | 40N,   170E | 8 | 144 | 1,398.10 |
| New (4) | 6,246.38 | 40N,   170E | 5 | 80 | 1,304.98 |
| Old (1) | 5,945.41 | 80N,   170E | 7 | 114 | 1,615.37 |
| New (4) | 5,945.41 | 80N,   170E | 5 | 104 | 1,085.25 |
| Old (1) | 5,803.22 | 60N,   170E | 8 | 155 | 1,646.21 |
| New (4) | 5,803.22 | 60N,   170E | 6 | 117 | 1,526.33 |

## Evaluating Efficiency

In order to compare the results (run time and miss distance) of the two functions an efficiency formula had to be developed. The general formula is:

$$Efficiency := \frac{1}{\alpha \cdot time + missdist} \qquad (5)$$

Where the parameter $\alpha$ depends on the range of the scenario (short, medium or long). This is done to ensure that the run time and the miss distance are weighed equally in determining the efficiency. One should note that the units of the efficiency formula are not in percentage and that the efficiencies for one range cannot be compared to those in another range. The formula only shows the efficiency of the original function with respect to the new one. According to the developed efficiency rating, a higher efficiency value is to be interpreted as a higher effective efficiency.

**Short range:**

$$Efficiency := \frac{1}{25 \cdot time + missdist}$$

**Efficiency for Short Ranges**
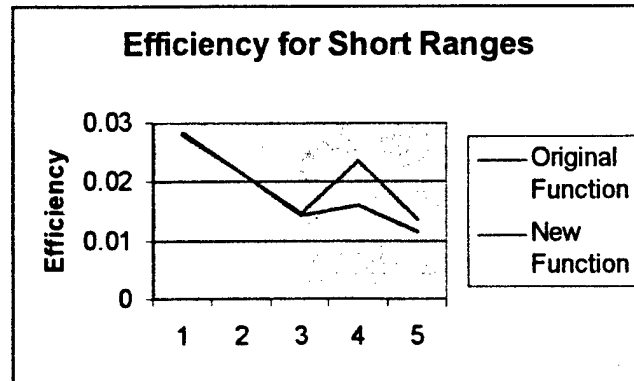
**Medium Range:**

$$Efficiency := \frac{1}{150 \cdot time + missdist}$$



**Efficiency for Medium Ranges**
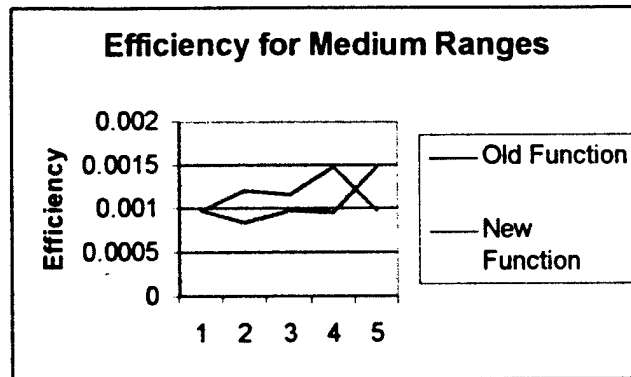
**Long Ranges:**

$$Efficiency := \frac{1}{150 \cdot time + missdist}$$

## Efficiency for Long Ranges
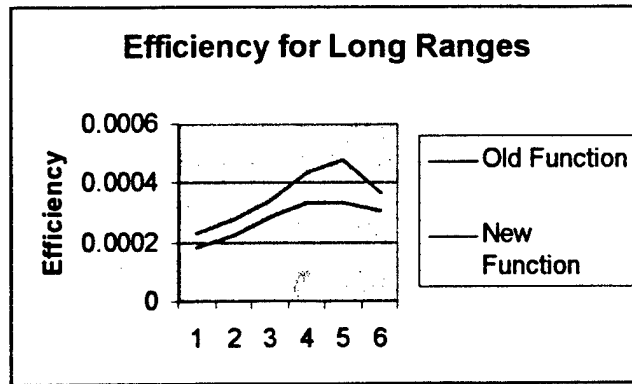
## Summary

As the graphs of the respective efficiencies show, Eta-T runs faster with the new optimization function (4). For short range scenarios this change is not very significant, but for long range scenarios the computation time is between two and four minutes less (total computation time for long range scenarios is between six and twelve minutes). Furthermore, the accuracy of the computation is comparable to that of the original function, if not better.

## Bugs

1) For long range scenarios (using the original function) Eta-T was sometimes not able to compute a satisfactory result ('SUBSTANTIAL FLYOUT ERROR' displayed when the miss distance is greater than 4,000m). This problem seems to have been resolved using the new optimization function.

2) For long range scenarios the integration subroutine (RKDRIVE2) sometimes stops and displays an error message stating that more than 100,000 integrations have been performed. The optimization subroutine (POWELL) then appears to disregard the result due to integration and proceeds with minimization. This does not seem to have any adverse effects on the final results.

3) The fixed flight path angle, fixed burn time, and lofted/ depressed trajectory options do not work. For the fixed flight path angle option the angle remains fixed for the first twenty or so iterations and then fluctuates as in the 'automatic' setting. The code for this option will need to be inspected further.

# Appendix 3.4-1

# University of Illinois

# UNIVERSITY OF ILLINOIS
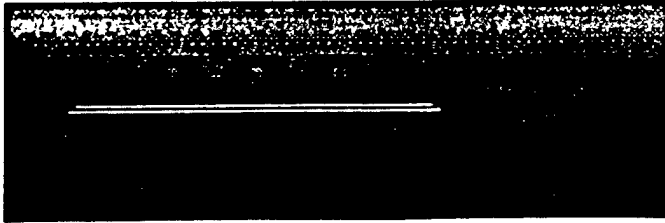
# FINAL REPORT

for the period

28 April 1998 to 28 January 1999

Contract Number:  N00014-97-D-2014

**Laser and Electro-Optical Engineering and Technical Support Program**

Work Performed By  Lee H  Sentman
Aeronautical and Astronautical
Engineering Department
University of Illinois
306 Talbot Laboratory
104 S. Wright St.
Urbana, IL 61801

This report is unclassified

## EXECUTIVE SUMMARY

One of the designs under consideration by TRW for the regeneratively cooled HYLTE nozzle employs a film of Helium injected on the upstream subsonic portion of the HYLTE primary nozzle walls. This raises the question of what effect injecting He along the walls of the subsonic part of the nozzle will have on laser performance. In an attempt to answer this question, the design of the UIUC HYLTE Simulating nozzle (HYSIM) was modified to inject a film of Helium as close to the upstream tip of the nozzle blade as possible. A separate plenum for the film He (FHe) was provided to allow independent control of the flow rates of the FHe and secondary He.

The He Film nozzle bank maximum fundamental performance, 71.3 Watts, which occurred for flow rates different than those for the HYSIM nozzle bank, was 10 Watts less than that of the HYSIM nozzle bank independent of reflectivity. The effect of the film Helium flow rate on power and blade temperatures was measured. The He film flow rate for maximum performance was 0.040 g/s ($\dot{n}Y_{molar\ FILM\ He}$ / $\dot{n}Y_{molar\ total\ no\ FILM\ He}$ = 0.11). Increasing the Helium film flow rate beyond this value reduced the power of the laser. At 0.140 gm/s of He film ($\dot{n}Y_{molar\ FILM\ He}$ / $\dot{n}Y_{molar\ total\ no\ FILM\ He}$ = 0.385), the performance decreased by 12%. At high He film flow rates, reoptimization of the $SF_6$, $H_2$, and secondary He flow rates recovered 49% of the lost power.

Bell Aerospace Textron data showed that notching the exit of the $H_2$ injection tubes of their Star nozzle increased the mixing. This suggested the possibility that notching the exit of the $H_2$ orifices in the side wall of the HYLTE nozzle might increase laser performance. To investigate this possibility, a duplicate of the UIUC HYSIM (HYLTE simulating) nozzle was constructed. For the initial tests, only the $H_2$ injectors were notched. Comparison of the performance of the Notched $H_2$ Injector and HYSIM nozzles showed that notching the $H_2$ injectors did not result in an increase in performance. Since one of the purposes of the Helium injectors is to shield the Hydrogen from the F atoms in the primary flow until the Hydrogen has reached the nozzle exit plane, maybe there was no increase in performance with the Notched $H_2$ Injector nozzle because the Helium injectors were not notched. To investigate this possibility, the Helium injectors were notched the same way the $H_2$ injectors were notched. Comparison of the Notched

3.4-1-3

H$_2$ and Helium Injector nozzle performance with that of the HYSIM and Notched H$_2$ Injector nozzles showed that there was no increase in performance. Thus, notching the H$_2$ and/or Helium side wall injectors did not result in increased laser performance.

In previous UIUC studies of line selected performance, the grating degraded due to the intracavity flux generated in the laser resonator. This problem was solved by coating the copper substrate with silver, polishing the silver, machining the grooves into the silver and then coating the silver with gold. The grating manufactured this way is denoted Grating 4.

The highly efficient Grating 4 put 80.4% to 99.99% of the total power in the useful outcoupled beam and increased performance on peak power lines by at least 30%.

Multiple line selected performance was measured for 18 line combinations, 5 cascade pairs, 8 non-cascade pairs, and 5 triplets. The peak performance cascade pairs were [P$_2$,I(6), P$_{1,OL}$(7)], [P$_2$,L(7), P$_{1,OL}$(8)], and [P$_2$,L(8), P$_{1,OL}$(9)]. [P$_2$,L(7) P$_{1,OL}$(8)] was the highest performing cascade pair at 51.1% of the multiline power. The peak performance non-cascade pairs were [P$_2$,L(7), P$_{1,OL}$(7)] and [P$_2$,L(8), P$_{1,OL}$(7)], with [P$_2$,I(7), P$_{1,OL}$(7)] achieving 41.4% of the multiline power. The peak performance triplets were [P$_2$,L(8), P$_{2,OL}$(7), P$_{1,OL}$(8)] and [P$_2$,L(8), P$_{1,OL}$(9), P$_{1,OL}$(8)]. The triplet [P$_2$,I(8), P$_{1,OL}$(9), P$_{1,OL}$(8)] achieved 52.1% of the multiline power which was the highest performing line combination

The data showed that the angle between the incident radiation on the grating and the direction of the first order diffracted beam must be less than or equal to $9°$ for efficient off-Littrow operation.

Data showed that grating efficiency is independent of Blaze wave length. The rapid decrease in efficiency at the Blaze wave length was due to the fact that, at that wave length, the incident angle became larger than $57°$ for the 600 lines/mm grating. First order grating efficiency decreases sharply beyond $\theta_i = 57°$ because the grating surface begins to behave as a grazing optic This means that the incident radiation becomes increasingly *reflected* along the angle of the zero order diffraction, which is the angle for specular reflection, as the incident angle increases. In the limit of $\theta_i = 90°$, also known as the *critical grazing angle* for a surface opaque to the wavelength range of interest, the incident radiation will be completely reflected into the zero order.

A 550 lines/mm grating will have all incident angles less than 57° for the wave length range $P(3)$ to $P(11)$, which would avoid the fall off in efficiency for the wave length range of interest. It is recommended that a 550 lines/mm grating be obtained to see if high grating efficiencies can be maintained across the entire wave length range of interest

## Table of Contents

# I. Introduction

The studies completed during the period 4/28/98 to 1/28/99 are summarized. In Section II, the effect of injection of a film of He on the upstream, subsonic walls of the primary nozzles of a cw HF laser is presented. Based on Bell Aerospace Textron data[1], the possibility of increasing laser performance by putting notches at the exit of the $H_2$ and/or He injection ports of the UIUC HYLTE simulating (HYSIM) nozzle was studied. The results are summarized in Section III.

Previous UIUC line selected studies of cw HF laser performance[2] suggested a new manufacturing process would result in a grating that would survive the intracavity flux in the laser resonator. The line selected performance obtained with this new grating, denoted Grating 4, is summarized in Section IV.

## II. The Effect of Injecting He on the Upstream, Subsonic Walls of an HF Laser

One of the designs under consideration by TRW for the regeneratively cooled HYLTE nozzle employs a film of Helium injected on the upstream subsonic portion of the HYLTE primary nozzle walls. This raises the question of what effect injecting He along the walls of the subsonic part of the nozzle will have on laser performance. In an attempt to answer this question, the design of the UIUC HYLTE Simulating nozzle (HYSIM) was modified to inject a film of Helium as close to the upstream tip of the nozzle blade as possible. A separate plenum for the film He (FHe) was provided to allow independent control of the flow rates of the FHe and secondary He.

Since the UIUC laser is an arc driven device while the TRW laser is a combustion driven device, these experiments will not be able to determine the cooling effectiveness of the injected He. Never the less, nozzle blade temperatures were measured to obtain qualitative data on the cooling effect of the He film on the nozzle blades. Two thermocouples, one close to the He film injection slit and one close to the upstream edge of the primary nozzle throat, were installed on two adjacent nozzle blades. The thermocouples are located at the center of the blade height. Laser performance and nozzle blade temperatures were measured as a function of He film mass flow rate.

## Design of He Film Injected Nozzle Blades

The HYSIM and He Film nozzle blades are compared in Fig. 2.1. The first difference in the nozzle blades is the modification of the blade tip to inject He tangential to the nozzle blade wall. The nozzle blades were machined in two pieces. The leading edge of the nozzle blade is machined into the top half of the nozzle bank, Fig. 2.2. The rest of the blade is machined into the bottom half, Fig. 2.3. The Helium film slit is formed by the relative positions of these two pieces when the top and bottom halves of the nozzle bank are assembled. Fig. 2.1.

The second difference was a decision made by the machinist without our knowledge to ease the manufacturing process. The secondary Helium and secondary Hydrogen injection holes are 0.020" in diameter at an angle of 35° from the surface of the blade. Approaching the blade surface at this angle with such a small drill bit will cause the drill bit to bend and break rather than penetrate the surface. Each injection hole was started with a 0.025" diameter end mill. This provides a small surface normal to the drill bit which makes it easier to penetrate the surface without bending or breaking. The result is an injection hole where the diameter steps from 0.020" to 0.025" near the exit. Fig 2.1. This gives the injection hole a diverging section similar to the HYLTE nozzle rather than a constant cross section like the HYSIM.

The He Film nozzle bank requires an additional plenum to feed film Helium to each of the nozzle blades. The FHe plenum was machined into the top half of the nozzle bank parallel to the secondary He plenum. Separate plenums for the film Helium and secondary Helium allow for independant control of the respective Helium flow rates.

Two thermocouples, one close to the FHe injection slit and one close to the upstream edge of the primary nozzle throat, were installed on two adjacent nozzle blades. The thermocouples are located at the center of the blade height.

Grooves were machined into the top surfaces of two adjacent nozzle blades to route the thermocouples from the secondary Helium feed hole to the appropriate position near the He film slit and near the throat on each of these two nozzle blades. Each thermocouple is identified by a number (1 or 2) and a letter (S or T). The number indicates in which blade the thermocouple is placed. The letter indicates whether the thermocouple is near the slit (S) or near the throat (T). These are shown in the

photograph, Fig. 2.3. The thermocouple near the throat on blade 1 (thermocouple 1T) was broken during assembly. There are no temperature data from this thermocouple.
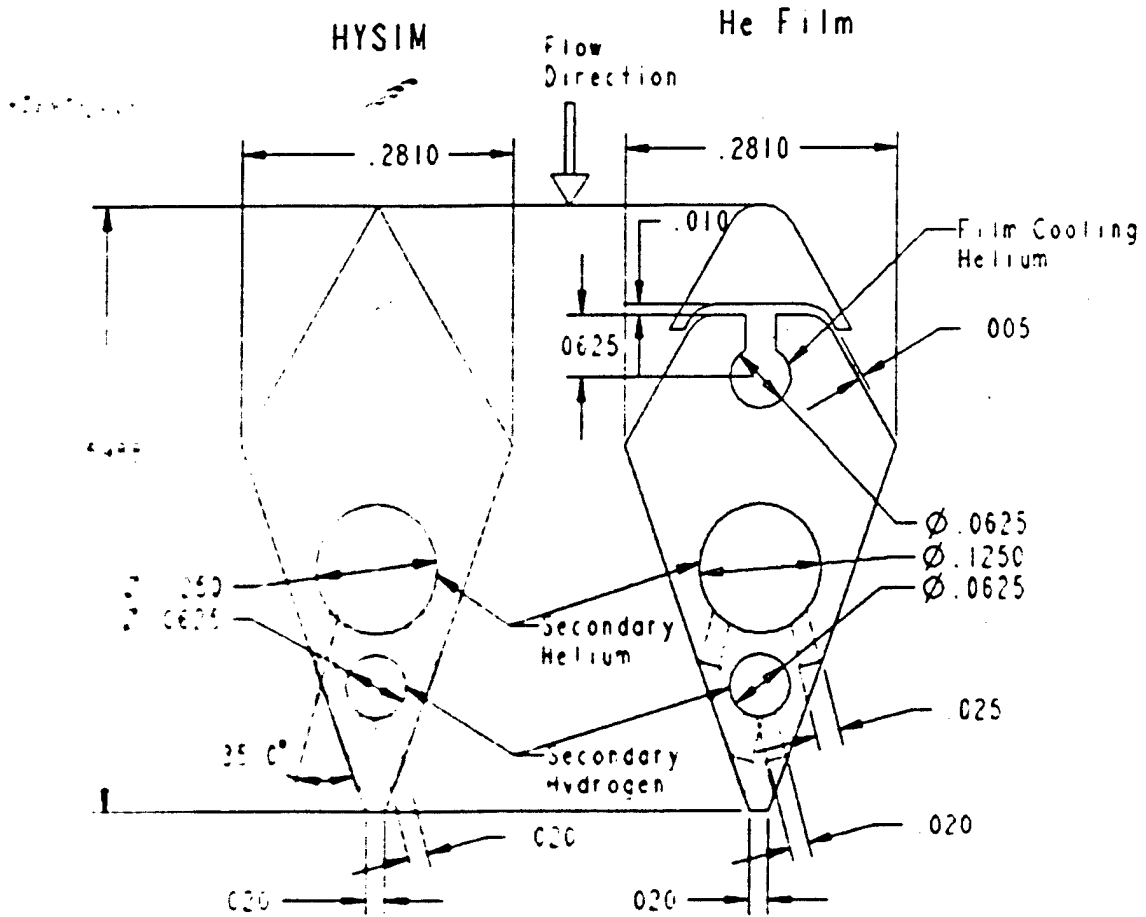
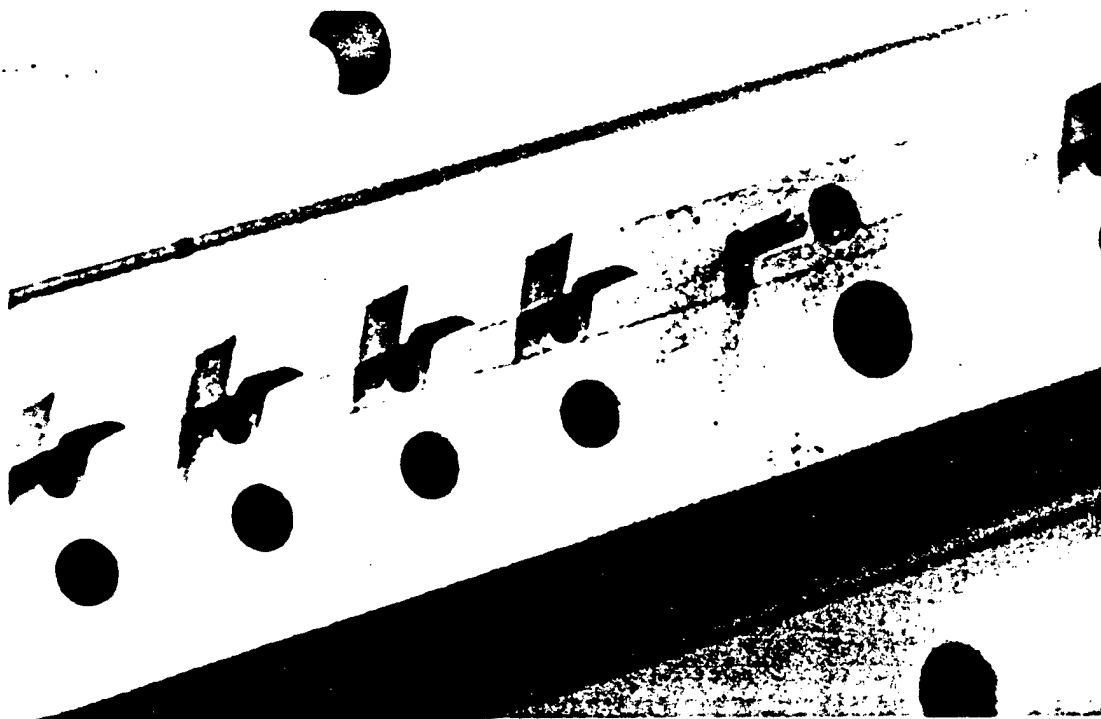Figure 2.1 Comparison of HYSIM and He Film nozzle blades.

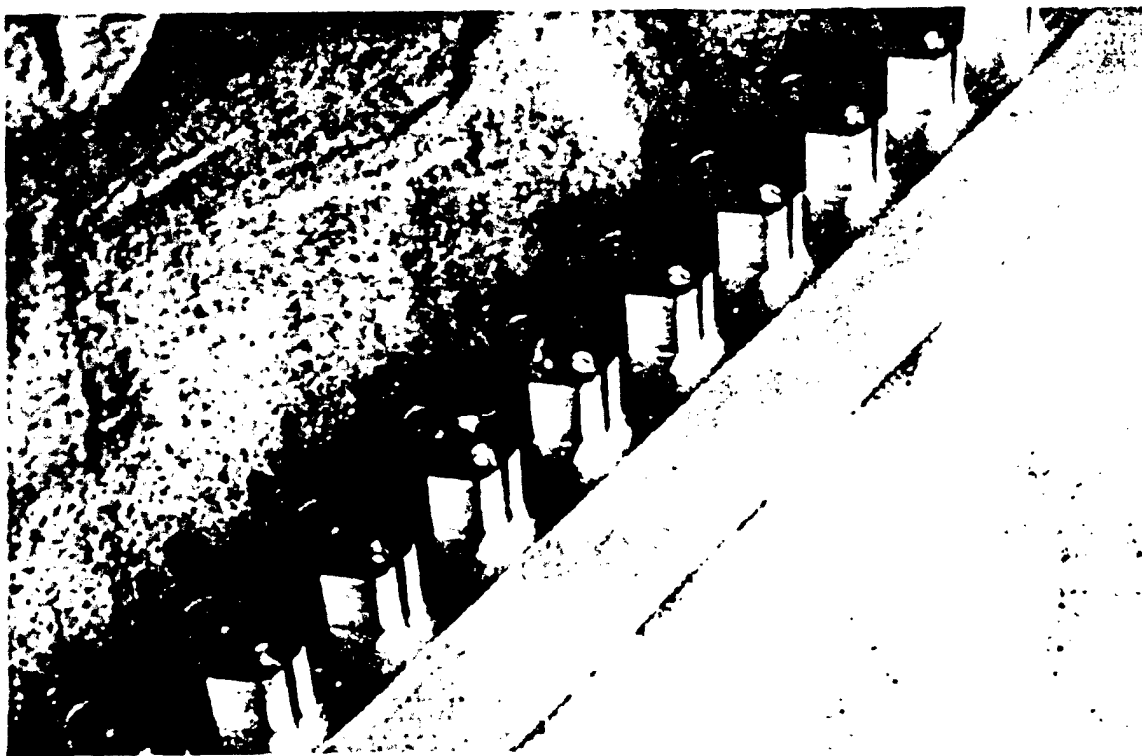Figure 2 2   Close up view of the upstream tips of the He film nozzle blades



Figure 2 3   Close up view of the downstream part of He film nozzle blades

## He Film Nozzle Performance

The He Film nozzle bank maximum fundamental performance, 71.3 Watts, occurred for flow rates different than those for the HYSIM nozzle bank[1]. The fundamental performance of the He Film nozzle bank was 10 Watts less than that of the HYSIM nozzle bank independent of reflectivity, Fig. 2.4.

There are two differences between the shapes of the nozzle blades of the He Film and HYSIM nozzle banks. Either or both could account for the difference in performance. The first difference is the rounded leading edge and film He slits near the leading edge of the He Film nozzle blade. The second difference is a step change in diameter near the exit of the secondary Helium and secondary Hydrogen injection holes.

The effect of notches on the HYSIM secondary Helium and secondary Hydrogen injection holes was investigated, Section 3. Since it was found that such notches have no effect on the fundamental performance of the nozzle bank, it is unlikely that the step change in diameter near the exit of the secondary Helium and secondary Hydrogen injection holes of the He Film nozzle bank is responsible for the decreased performance. Thus, it is more likely that the decreased performance is due to the rounded leading edge and film Helium injection slits on the subsonic portion of the nozzle blades.

The effect of the film Helium flow rate on power and blade temperatures was measured, Fig. 2.5. The He film flow rate for maximum performance was 0.040 g/s $(\dot{m}_{molar\ FILM\ He} / \dot{m}_{molar\ total\ no\ FILM\ He} = 0.11)$. Increasing the Helium film flow rate beyond this value reduced the power of the laser. At 0.140 gm/s of He film $(\dot{m}_{molar\ FILM\ He} / \dot{m}_{molar\ total\ no\ FILM\ He} = 0.385)$, the performance decreased by 12%. At high He film flow rates, reoptimization of the $SF_6$, $H_2$, and secondary He flow rates recovered 49% of the lost power.
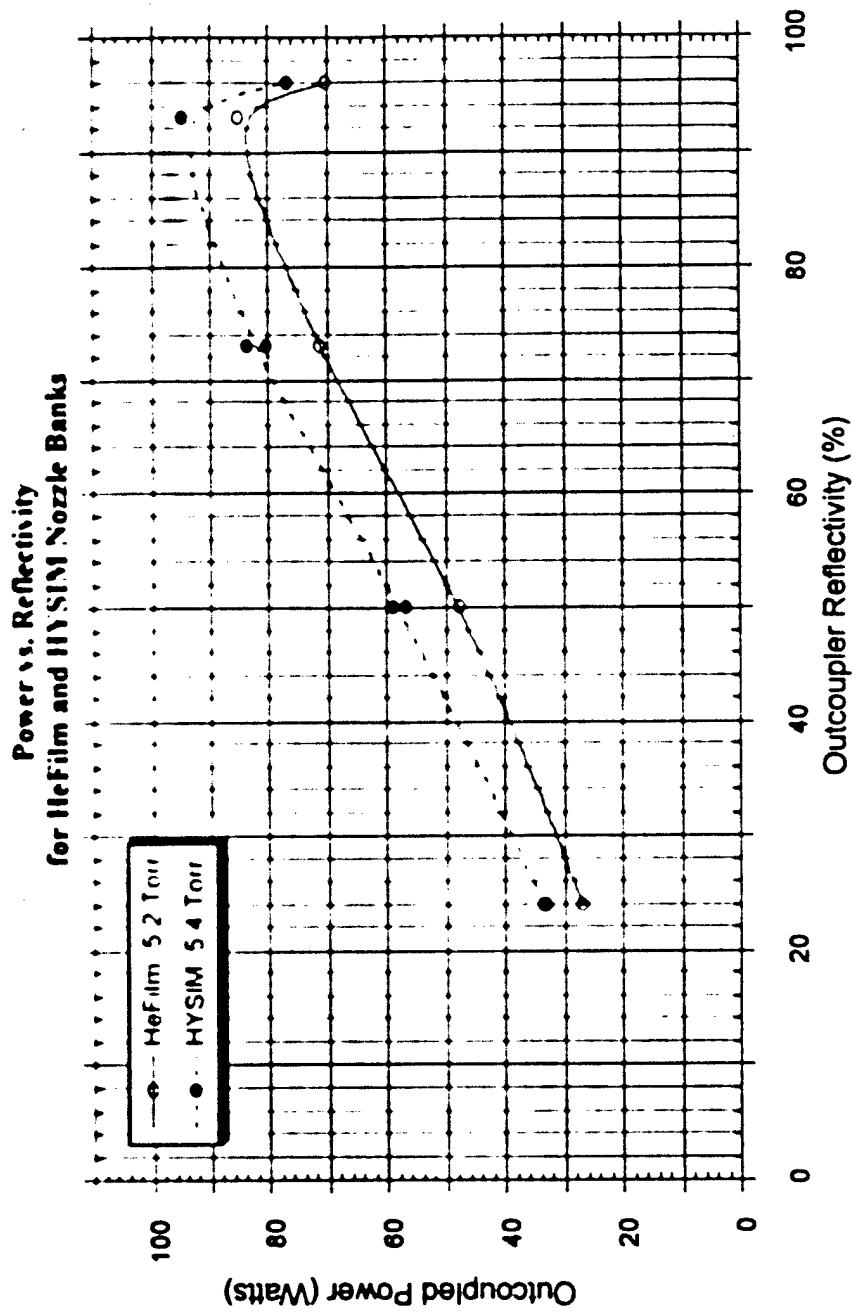
Figure 2.4.    He Film and HYSIM power versus outcoupler reflectivity.  He Film data were measured at the flow rates for optimum performance.  HYSIM data were measured at the flow rates for optimum performance.

3.4-1-13

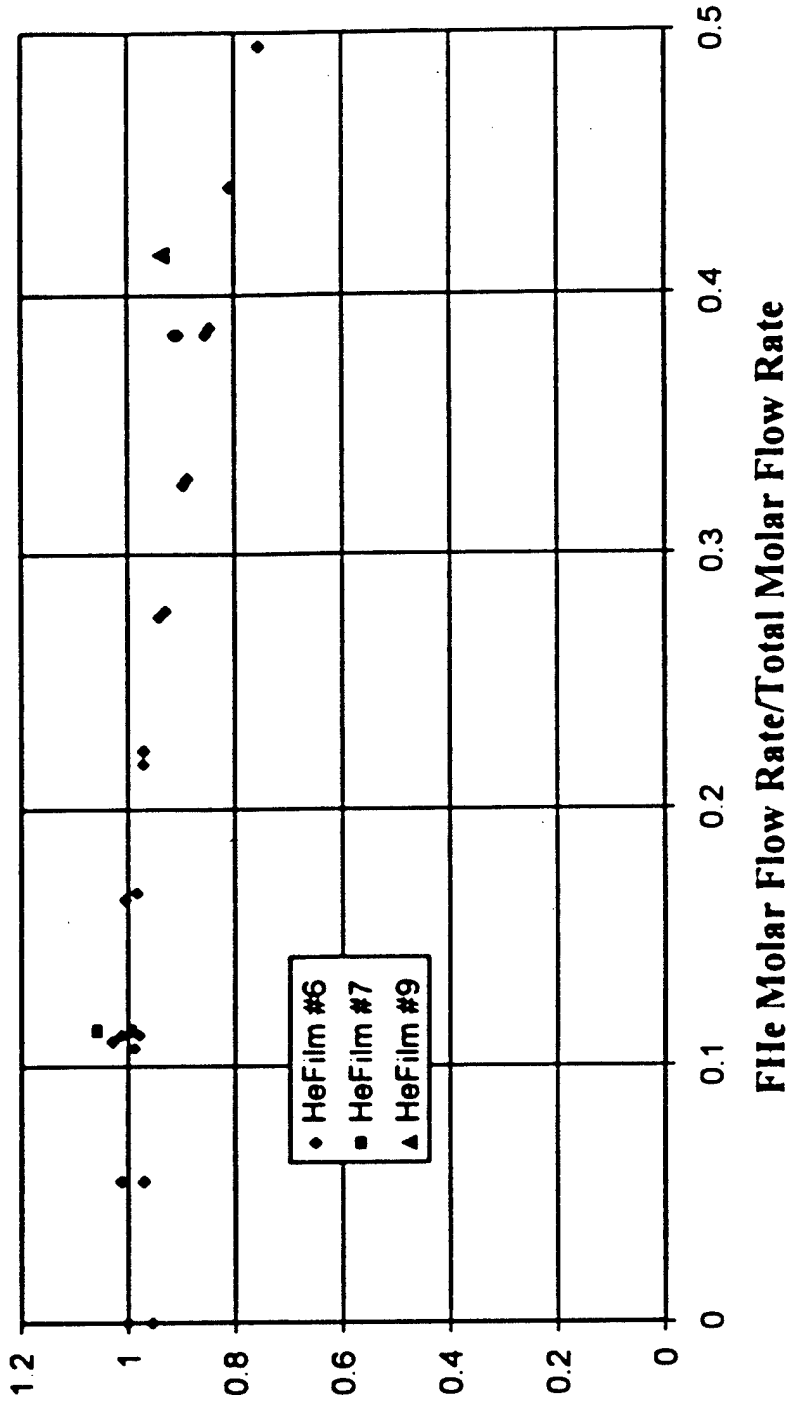# Power/P ref as a function of
# FHe Molar Flow Rate/Total Molar Flow Rate



**FHe Molar Flow Rate/Total Molar Flow Rate**

Legend:
- ♦ HeFilm #6
- ■ HeFilm #7
- ▲ HeFilm #9

Figure 2.5  Normalized power as a function of film Helium molar flow rate divided by the total (primary + secondary) molar flow rate. $P_{ref} = 70$ watts

3.4.1-14

Blade temperatures decreased monotonically with increasing film Helium flow rate · up to $\dot{m}_{FHe} = 0.120$ gm/s, Fig. 2.6. Blade temperatures were constant for $\dot{m}_{FHe} = 0.120 - 0.140$ gm/s. Blade temperatures appear to decrease further for film Helium flow rates greater than 0.140 gm/s.

**Blade Temperature versus Helium Film Flow Rate**
**other flows fixed at optimum values for m $_{FHe}$=0**
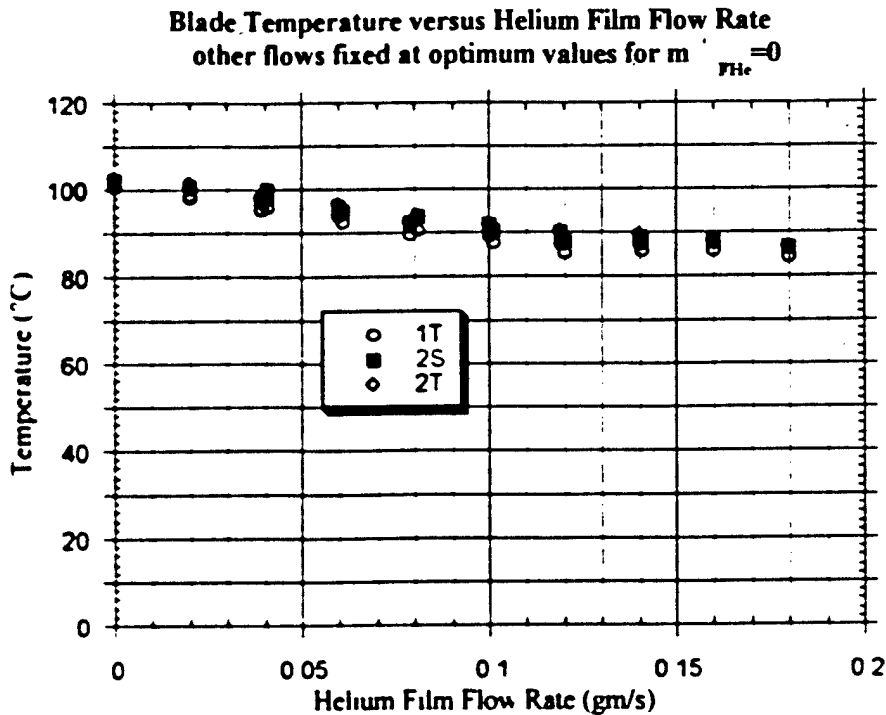


Figure 2 6    Temperature as a function of Helium film flow rate  Other flow rates held fixed at the optimum flow rates for the HeFilm nozzle bank with $\dot{m}_{FHe} = 0$ gm/s

Normalized He Film nozzle performance data as a function of He film flow rate are presented for comparison to other laser devices[.]  The power data are normalized by the 70 Watt performance observed with $\dot{m}_{FHe}$=0  The normalized powers are presented as a function of the He film mass flow rates, molar flow rates, and He film mass and molar flow rates divided by the total primary flow, the secondary $H_2$ flow, the secondary He flow, the total secondary flow, the total (primary + secondary) flow and the total throat area of the nozzle bank

## III. Notched Injector Nozzle

Bell Aerospace Textron data[1] showed that notching the exit of the $H_2$ injection tubes of their Star nozzle increased the mixing. This suggests the possibility that notching the exit of the $H_2$ orifices in the side wall of the HYLTE nozzle might increase laser performance. To investigate this possibility, a duplicate of the UIUC HYSIM (HYLTE simulating) nozzle was constructed. For the initial tests, only the $H_2$ injectors were notched. The notch dimensions were based on ratios of the Star nozzle notch dimensions to injector inside diameters, Table 3.1. The HYSIM notches are shown in Figs. 3.1 and 3.2.

The flow rates that optimized the performance of the notched injector nozzle were the same that maximized the performance of the HYSIM nozzle. Performance was measured as a function of outcoupler reflectivity and cavity pressure. The performance of the Notched $H_2$ Injector and HYSIM nozzles is compared in Fig. 3.3. This comparison showed that notching the $H_2$ injectors did not result in an increase in performance.

Since one of the purposes of the Helium injectors is to shield the Hydrogen from the F atoms in the primary flow until the Hydrogen has reached the nozzle exit plane, maybe there was no increase in performance with the Notched $H_2$ Injector nozzle because the Helium injectors were not notched. To investigate this possibility, the Helium injectors were notched the same way the $H_2$ injectors were notched. The flow rates for optimum performance with both the $H_2$ and Helium injectors notched were the same as for the HYSIM and Notched $H_2$ Injector nozzles. Comparison of the Notched $H_2$ and Helium Injector nozzle performance with that of the HYSIM and Notched $H_2$ Injector nozzles, Fig 3.3, showed that there was no increase in performance. Thus, notching the $H_2$ and/or Helium side wall injectors did not result in increased laser performance.

| Star Nozzle Notch Geometry | Ratios (Geometry/I.D.) | HYSIM Injector I.D. | HYSIM |
|---|---|---|---|
| Groove Depth=0.020 in. | GD/I.D.=0.465 | | Groove Depth=0.009 in. |
| Groove Width=0.016 in | GW/I.D.=0.372 | 0.02 in. | Grove Width=0.007 in. |
| Wall Thickness=0.01 in. | WT/I.D.=0.233 | | Grove Length=0.004 in. |
| I.D. of Tube=0.043 in. | | | |

Table 3.1    Notch dimensions and ratios of notch dimensions to injector inside
diameter
             For the Bell Aerospace Star Nozzle and the HYSIM nozzle.

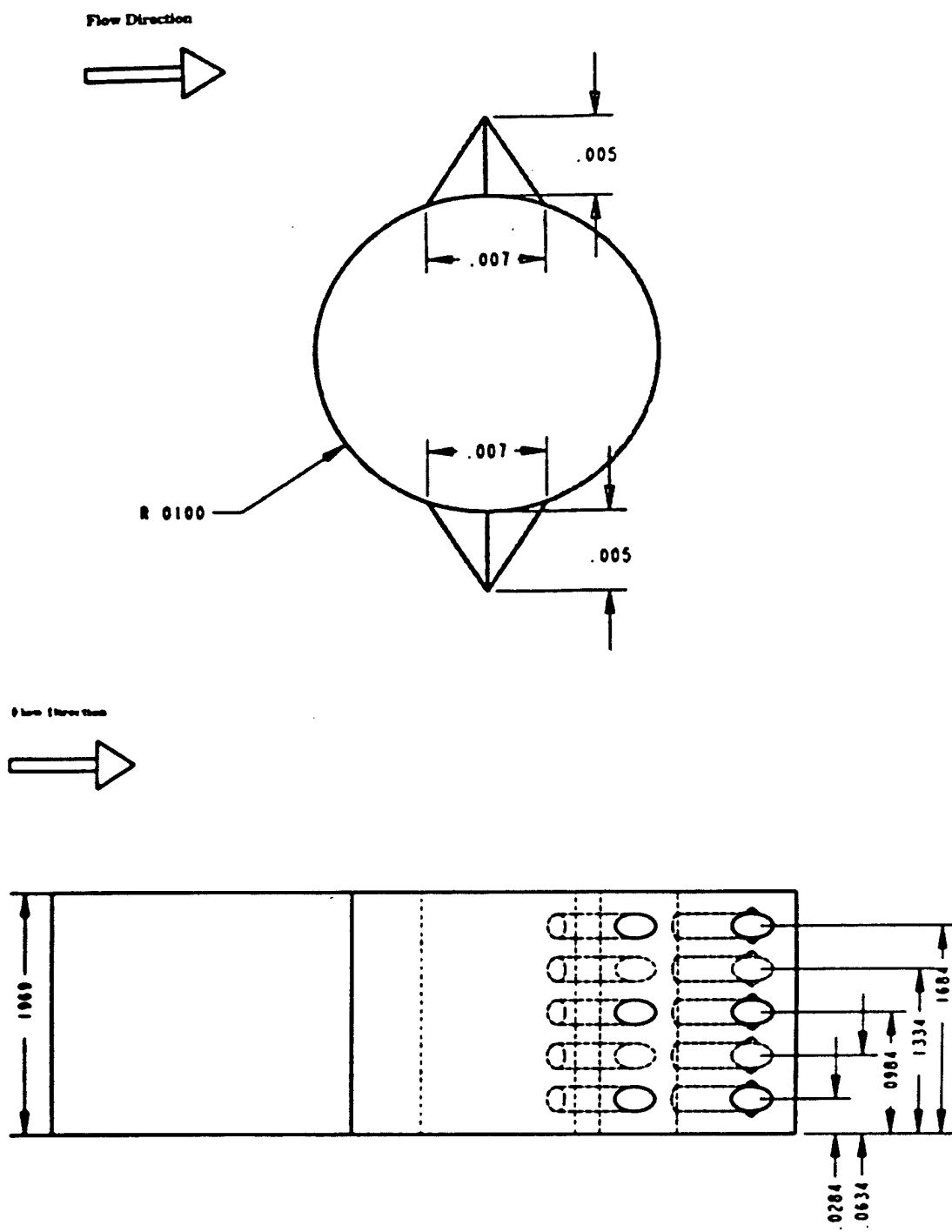Figure 3.1 Close-up and side view of the the notches on the hydrogen injectors of the Notched H₂ Injector nozzle.

Figure 3.2  Close up of notched $H_2$ injectors.

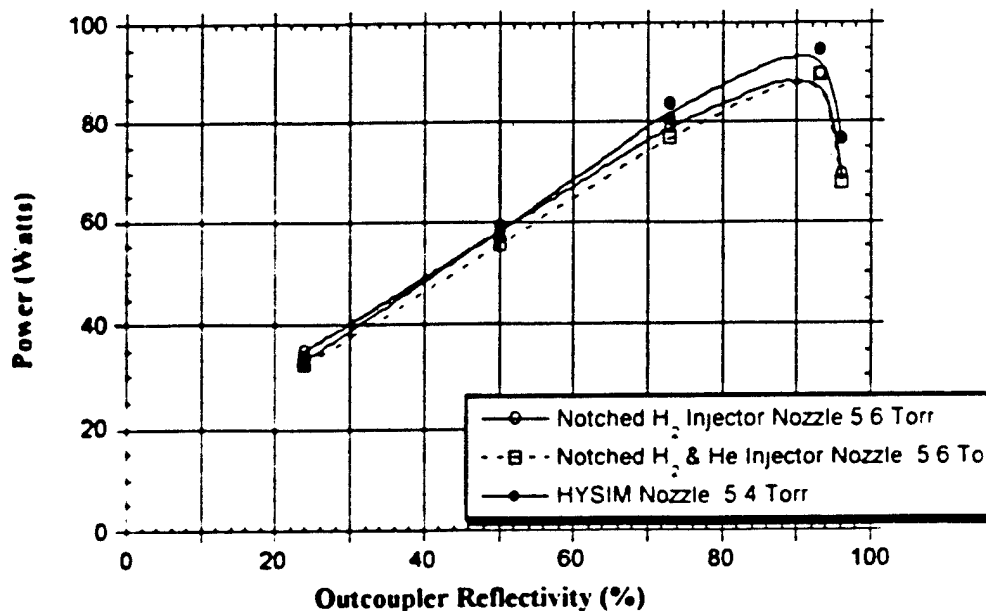**Power vs. Reflectivity for the Notched H $_2$ Injector, Notched H $_2$ & He Injector, and HYSIM Nozzle Banks**



Figure 3 3 Notched H$_2$ and He Injector, Notched H$_2$ Injector and HYSIM power versus outcoupler reflectivity

## IV. Grating 4 Line Selected Performance

In previous UIUC studies of line selected performance[2], the grating degraded due to the intracavity flux generated in the laser resonator. The grating manufacturer suggested that this problem could be solved by coating the copper substrate with silver, polishing the silver, machining the grooves into the silver and then coating the silver with gold. The grating manufactured this way is denoted Grating 4. The line selected performance obtained with this grating is summarized.

Grating 4 Littrow data were obtained for the 73% reflective outcoupler. The highly efficient Grating 4 put 84.2% to 99.99% of the total power (outcoupled + primary zero order) in the outcoupled beam. Grating 3 put 68.9% to 99.8% of the total power in the outcoupled beam. The less efficient Grating 2 placed 15% to 84% of the total power

in the outcoupled beam. The outcoupled power for Grating 4 was higher on all lines than for Gratings 2 and 3. On most lines, the total power for Grating 4 was higher than the total powers for Gratings 2 and 3.

Single line off-Littrow performance was measured for Grating 4. The highly efficient Grating 4 put 80.4% to 99.99% of the total power (outcoupled + secondary zero order + primary zero order) in the outcoupled beam. The less efficient Grating 2 placed 45.0% to 51.8% of the total power in the outcoupled beam.

Multiple line selected performance was measured for 18 line combinations, 5 cascade pairs, 8 non-cascade pairs, and 5 triplets. The best performing cascade pairs were $[P_2(6), P_3(7)]$, $[P_3(7), P_4(8)]$ and $[P_4(8), P_5(9)]$ with $[P_2(7), P_3(8)]$ giving almost 25% more power than the other two pairs, 26.3 watts. The best performing non-cascade pair was $[P_3(7), P_4(7)]$, which gave as much power, about 21 watts, as the cascade pairs $[P_2(6), P_3(7)]$ and $[P_4(8), P_5(9)]$. The only other non-cascade pair that came close to cascade pair performance was $[P_3(8), P_4(7)]$ at 18 watts. The triplet performance was rather interesting. When the line $P_4(7)$ was added to the non-cascade pair $[P_3(8), P_3(7)]$, the triplet performance was 21.6% larger than the pair performance. However, when the line $P_5(8)$ was added to this same pair, the triplet performance was 58% larger than the pair performance. This suggests that multiple line selected performance is a strong function of the lines that can be lased simultaneously. The possibilities are limited by the grating equation. When $P_4(8)$ was added to the cascade pair $[P_3(8), P_4(9)]$, the triplet perfromance was 14.7% larger than the pair performance. Adding $P_3(6)$ to the pair $[P_3(8), P_4(7)]$ increased performance by only 6.1%. Adding $P_4(7)$ to the pair $[P_4(9), P_4(8)]$ decreased performance by 2%.

Comparison of the zero order, outcoupled and total (outcoupled + zero order + secondary zero order) powers of the line selected combinations that were measured for both Grating 2 and 4 show that Grating 4 outcoupled power is significantly larger and the zero order power is significantly smaller than that for Grating 2.

Grating efficiencies were determined from Littrow and off-Littrow single line data. Because Grating 4 is a very good grating, it was necessary to take into account the transmission and absorption/scattering losses of the feedback mirror when grating efficiencies were deduced from the off-Littrow data. For lines whose wave length is shorter than the Blaze wave length of the grating, the efficiency is greater than 99.8%.

For lines whose wave length is longer than the Blaze wave length of the grating, the efficiency falls off rapidly the farther the wave length is from the Blaze wave length. The efficiencies deduced from the Littrow and off-Littrow data agree within 0.15% for lines whose wave length is less than the Blaze wave length of the grating. The differences between the Littrow and off-Littrow efficiencies increase the longer the wave length is compared to the Blaze wave length.

A plot of grating efficiency versus wavelength, Fig. 4.1, for Grating 4 single line Littrow, single line off-Littrow, and line combination efficiencies shows that all the deduced efficiencies decreased sharply as wave length increased beyond the Blaze wavelength. The Littrow line combination efficiencies are slightly larger than the single line Littrow efficiencies, which may be due to better alignment. For $\alpha_1^\lambda < 5°$, the off-Littrow line combination efficiencies are as high as the Littrow line combination efficiencies. For $5° < \alpha_1^\lambda < 7°$ and $7° < \alpha_1^\lambda < 9°$, the off-Littrow line combination efficiencies are the same as the single line off-Littrow efficiencies for $\alpha_1^\lambda = 6°$. For $\alpha_1^\lambda > 9°$, the off-Littrow line combination efficiencies are considerably lower than the off-Littrow efficiencies for $\alpha_1^\lambda < 9°$. These data show that to optimize line selected performance in the off-Littrow resonator, $\alpha_1^\lambda$ should be less than 5° if possible. Acceptable efficiencies are obtained for $5° = \alpha_1^\lambda = 9°$. If $\alpha_1^\lambda > 9°$, the decrease in efficiency is unacceptable. The angle $\alpha_1^\lambda$ is the angle between the incident radiation on the grating and the direction of the first order diffracted beam of wave length $\lambda$.

Grating 4 achieved 28.2% to 34.7% of the multiline power in the peak Littrow lines and 20.3% to 21.4% of the multiline power in the peak off-Littrow lines. The efficient Grating 4 gives a significant increase in the fraction of multiline power over that obtained by Gratings 2 and 3 on most lines for both Littrow and off-Littrow data.

The peak performance cascade pairs were [$P_{2,L}(6)$, $P_{1,OL}(7)$], [$P_{2,L}(7)$, $P_{1,OL}(8)$], and [$P_{2,L}(8)$, $P_{1,OL}(9)$]. [$P_{2,L}(7)$ $P_{1,OL}(8)$] was the highest performing cascade pair at 51.1% of the multiline power. The peak performance non-cascade pairs were [$P_{2,L}(7)$, $P_{1,OL}(7)$] and [$P_{2,L}(8)$, $P_{1,OL}(7)$], with [$P_{2,L}(7)$, $P_{1,OL}(7)$] achieving 41.4% of the multiline power. The peak performance triplets were [$P_{2,L}(8)$, $P_{2,OL}(7)$, $P_{1,OL}(8)$] and

$[P_{2,L}(8), P_{1,OL}(9), P_{1,OL}(8)]$.  The triplet $[P_{2,L}(8), P_{1,OL}(9), P_{1,OL}(8)]$ achieved 52.1% of the multiline power which was the highest performing line combination.
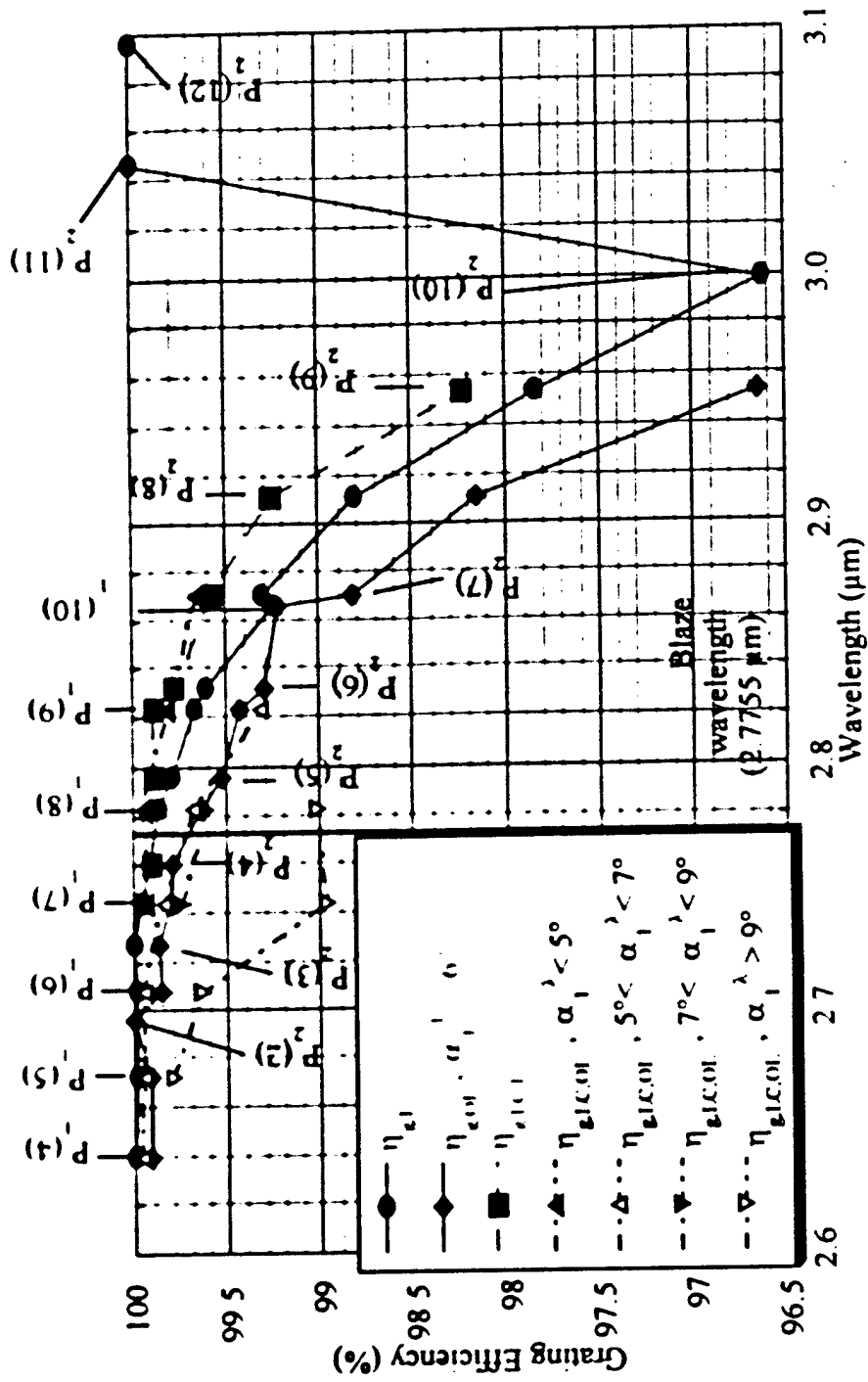
Figure 4.1. Comparison of Grating 4 Littrow, off-Littrow, and line combination efficiencies as a function of wavelength. These efficiencies were deduced from line selected data.

Efficiency data for Gratings 2 and 3 suggested that a grating with a Blaze wavelength shorter than any of the wavelengths of interest may have a higher efficiency than that of a grating with a Blaze wavelength in the center of the wavelength range of interest. The groove spacing and Blaze angle were measured with a HeNe laser for Gratings 2, 3, and 4 for both 0° (right side up) and 180° (upside down) orientation of the grating face. These experiments confirmed that all of the gratings were ruled as specified, 600 lines/mm. The measurements showed that the Blaze angles in the 0° orientation for Gratings 3 and 4 were 56.37°, as specified. For the degraded Grating 2, the 0° orientation Blaze angle was 21°. In the 180° orientation, the Blaze angles for Gratings 2 and 4 were both 33.63° and for Grating 3 was 21°. The corresponding groove vertex angles, which were supposed to be 90°, were 125.37° for Grating 2, 102.63° for Grating 3 and 90° for Grating 4. For the wavelength range of interest, 2.5 to 3.1μm, diffracting into the first order, a Blaze angle of 33.63° corresponds to a blaze wavelength of 1.85μm. Since Grating 4 is Blazed at 1.85 μm in the 180° position, which is shorter than all wavelengths of interest, single line Littrow performance was measured with Grating 4 in the 180° position to test the efficiency hypothesis.

The grating efficiency ranged from 100.0% to 98.13% for the grating in the 180° orientation and from 99.98% to 98.96% for the grating in the 0° orientation. Fig. 4.2. Efficiencies for the two orientations for the same line never differed by more than 0.11%. For the grating in the 180° orientation, the efficiency decreased as wave length increased, and the efficiency decreased sharply beyond the Blaze wavelength. This was the same trend observed for all the Grating 4 line selected efficiencies for the grating in the 0° orientation. Thus, Grating 4 efficiency was independent of grating orientation about the optical axis. This result supports the reciprocity theorem[4] for diffraction gratings. This theorem states that *the efficiency in the zero order does not change when the grating is rotated by 180° about an axis which is perpendicular to the plane on which it has been ruled.* Zero order efficiency is the zero order power divided by the incident power. Since zero order efficiency is independent of grating orientation, first order efficiency should also be independent of grating orientation if only first and zero order diffractions are

possible. Based on the reciprocity theorem and the calculated line selected efficiencies, the Blaze angle has no effect on Grating 4 efficiency for the HF laser.

A plot of grating efficiency versus $\lambda/d^5$ shows that first order efficiency decreases sharply beyond $\lambda/d = 1.68$. For $\lambda/d = 1.68$, the angle of incidence is about 57°. For all
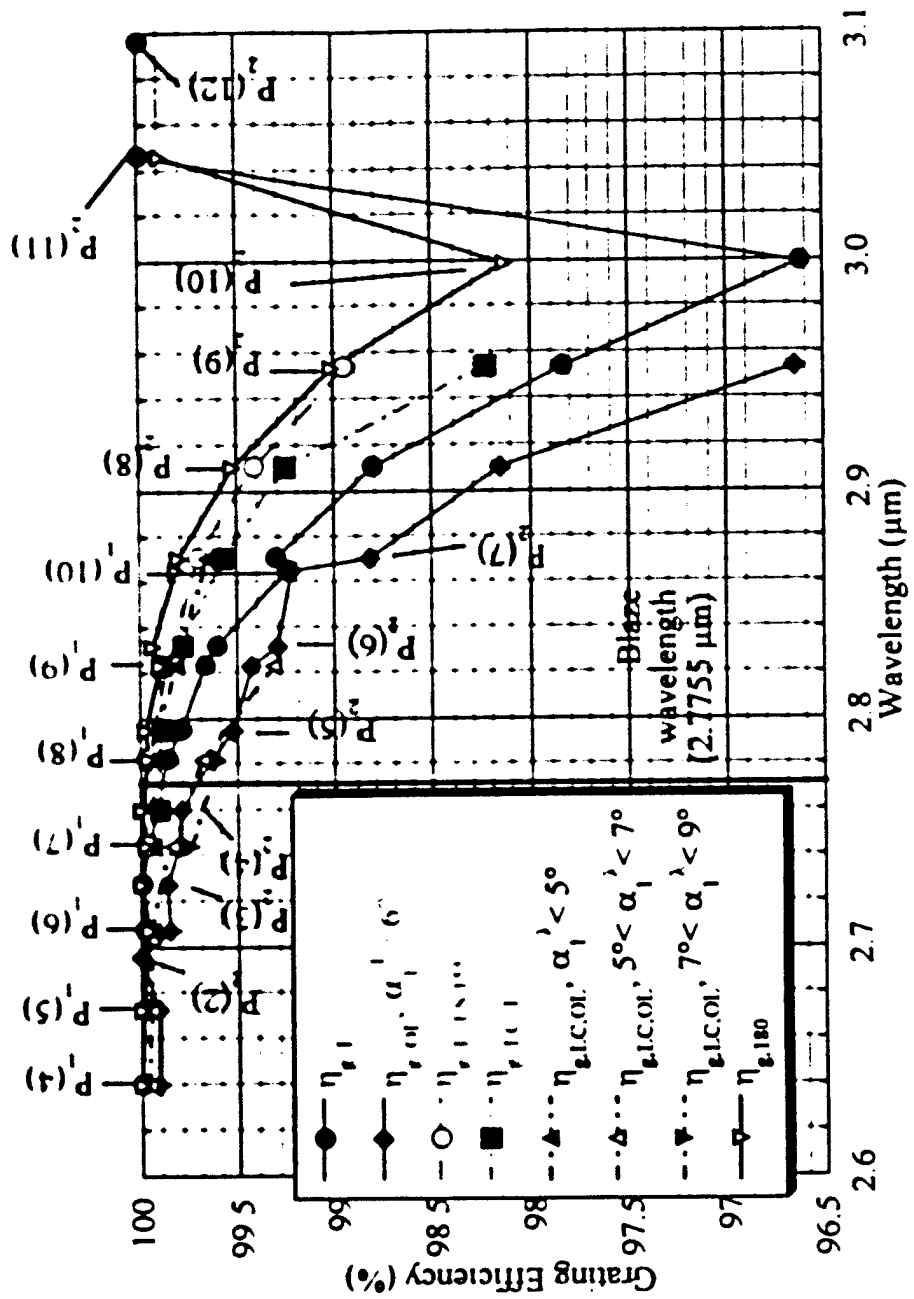
Figure 4.2. Efficiency versus wavelength for Grating 4 line selected data. The efficiency data for the most recent single line Littrow data is denoted $\eta_{g, L, LS, 155}$. The efficiency data for the Grating in the 180° orientation is denoted $\eta_{g, 180}$.

3.4-1-27

the line selected data for Grating 4, efficiency decreased as wave length increased. Efficiency decreased sharply beyond $\theta_i > 57°$, where $\theta_L = 56.99°$ is the incident angle for $P_2(5)$ in the Littrow configuration. Thus, Grating 4 efficiency results are in agreement with the first order efficiency versus $\lambda/d$ plot given in Ref. (4). First order grating efficiency decreases sharply beyond $\theta_i = 57°$ because the grating surface begins to behave as a grazing optic[4]. This means that the incident radiation becomes increasingly *reflected* along the angle of the zero order diffraction, which is the angle for specular reflection, as the incident angle increases. In the limit of $\theta_i = 90°$, also known as the *critical grazing angle* for a surface opaque to the wavelength range of interest, the incident radiation will be completely reflected into the zero order[5].

The shortest wavelength for which consistent single line Littrow lasing was obtained was $P_1(3)$ ($\lambda = 2.6084$ μm). The longest wavelength for which consistent single line Littrow lasing was achieved for Grating 4 was $P_2(11)$ ($\lambda = 3.0462$ μm). The grating equation predicts that only a first order diffraction is possible for a 550 lines/mm grating over the wavelength range $2.6084$ μm $\leq \lambda \leq 3.0462$ μm. Since there are no higher order diffractions, grating anomalies are avoided for a 550 lines/mm grating over the wavelength range of interest..

Given the wavelength range $2.6084$ μm $\leq \lambda \leq 3.0462$ μm and 550 lines/mm, the grating equation gives the incident angle range as $45.8° < \theta_i < 56.9°$. By comparison, over the same wavelength range, a 600 lines/mm grating has the incident angle range $51.5° < \theta_i < 66.0°$. The angular separation for 550 lines/mm is a little narrower than for 600 lines/mm. However, a 550 lines/mm grating has smaller zero order diffraction angles. In order for the zero order diffracted beams to pass through the calcium flouride window to outside the line selected vacuum box where the powers of the beams are measured, a 550 lines/mm grating will have to be moved 3" farther away from the laser cavity than the 600 lines/mm grating. The effects of smaller angular separation with a 550 lines/mm grating are offset by the additional 3" of moment arm.

It is recommended that a 550 lines/mm grating be obtained to see if high grating efficiencies can be maintained across the entire wave length range of interest. Single line

Littrow and off-Littrow performance should be measured with this new grating. Multiple line combination performance should be measured for the peak line combinations obtained with Grating 4. Additional line combination experiments should be performed with Grating 4 to gain a more comprehensive understanding of line combination performance before specific line combination experiments are planned for the new grating.

## References

1. Bell Aerospace Textron, "Advanced Gain Generator Technology Program," Report No D9309-953001, June 1982.

2. S J Gordon, L. H. Sentman, D. S. Jenkins and A. J. Eyre, "A Study of Line Selection in CW HF Lasers," AAE TR 97-02, UILU Eng 97-0502, Aeronautical and Astronautical Engineering Department, University of Illinois, Urbana, IL, March, 1997.

3. L. H Sentman, A. J. Eyre, J. T. Cassibry and B. P. Wootton, "Studies of CW HF Chemical Laser Performance," AAE TR 99-01, UILU Eng 99-0501, Aeronautical and Astronautical Engineering Department, University of Illinois, Urbana, IL, January, 1999.

4. R Petit, Electromagnetic Theory of Gratings, Springer-Verlag Berlin Heidelberg, New York, 1980, pp. 13, 164, 165.

5. M C Hutley, Diffraction Gratings, Academic Press, London, 1982, pp. 175-178, 263-265.